

Springer Tracts in Civil Engineering

Sašo Medved
Suzana Domjan
Ciril Arkar

Sustainable Technologies for Nearly Zero Energy Buildings

Design and Evaluation Methods

 Springer

Springer Tracts in Civil Engineering

Springer Tracts in Civil Engineering (STCE) publishes the latest developments in Civil Engineering—quickly, informally and in top quality. The series scope includes monographs, professional books, graduate textbooks and edited volumes, as well as outstanding Ph.D. theses. Its goal is to cover all the main branches of civil engineering, both theoretical and applied, including:

Construction and Structural Mechanics
Building Materials
Concrete, Steel and Timber Structures
Geotechnical Engineering
Earthquake Engineering
Coastal Engineering
Hydraulics, Hydrology and Water Resources Engineering
Environmental Engineering and Sustainability
Structural Health and Monitoring
Surveying and Geographical Information Systems
Heating, Ventilation and Air Conditioning (HVAC)
Transportation and Traffic
Risk Analysis
Safety and Security

To submit a proposal or request further information, please contact: Pierpaolo Riva at Pierpaolo.Riva@springer.com, or Li Shen at Li.Shen@springer.com

More information about this series at <http://www.springer.com/series/15088>

Sašo Medved · Suzana Domjan
Ciril Arkar

Sustainable Technologies for Nearly Zero Energy Buildings

Design and Evaluation Methods

 Springer

Sašo Medved
Faculty of Mechanical Engineering
University of Ljubljana
Ljubljana, Slovenia

Ciril Arkar
Faculty of Mechanical Engineering
University of Ljubljana
Ljubljana, Slovenia

Suzana Domjan
Faculty of Mechanical Engineering
University of Ljubljana
Ljubljana, Slovenia

ISSN 2366-259X ISSN 2366-2603 (electronic)
Springer Tracts in Civil Engineering
ISBN 978-3-030-02821-3 ISBN 978-3-030-02822-0 (eBook)
<https://doi.org/10.1007/978-3-030-02822-0>

Library of Congress Control Number: 2018959255

© Springer Nature Switzerland AG 2019

This work is subject to copyright. All rights are reserved by the Publisher, whether the whole or part of the material is concerned, specifically the rights of translation, reprinting, reuse of illustrations, recitation, broadcasting, reproduction on microfilms or in any other physical way, and transmission or information storage and retrieval, electronic adaptation, computer software, or by similar or dissimilar methodology now known or hereafter developed.

The use of general descriptive names, registered names, trademarks, service marks, etc. in this publication does not imply, even in the absence of a specific statement, that such names are exempt from the relevant protective laws and regulations and therefore free for general use.

The publisher, the authors and the editors are safe to assume that the advice and information in this book are believed to be true and accurate at the date of publication. Neither the publisher nor the authors or the editors give a warranty, express or implied, with respect to the material contained herein or for any errors or omissions that may have been made. The publisher remains neutral with regard to jurisdictional claims in published maps and institutional affiliations.

This Springer imprint is published by the registered company Springer Nature Switzerland AG
The registered company address is: Gewerbestrasse 11, 6330 Cham, Switzerland

Preface

In the past decades, the energy performance of buildings has increased by a factor of 10, which is significantly higher than in other energy use sectors. At that time, the EU's energy and environment policy led to the creation of regulatory requirements, standards and technologies for the implementation of complex systems such as passive buildings or sustainable buildings. European Union expressed commitment to develop sustainable, competitive, secure and decarbonized energy system, by adopting Directive on the Energy Performance of Buildings (EPBD), including requirements for nearly Zero-Energy Buildings (nZEB). Since energy efficiency and environmental sustainability requirements are becoming more and more complex, the knowledge of building designers must be more comprehensive too—from understanding of physical principles, have an overview of legal framework, to be familiar with advanced building service technologies and finally to have a knowledge of using methods for comprehensive verification of the 'final product': nZEB. Awareness that deep interdisciplinary knowledge is the only guarantee that this task will be fulfilled has been a guide to the design of the contents and the scope of this book.

Through 14 chapters, the book leads the reader through basics of planning and evaluation of living comfort in the indoor environment, basics of building physics, instructions for determination of thermal response of building structures, explanations and evaluation of nZEB requirements and design, energy efficiency evaluation of buildings' service systems, presentation of methods for planning and evaluation of buildings' energy performance and the environmental impacts caused by lifelong use of energy and materials in buildings. Students of architecture, civil and mechanical engineering and students of other engineering professions, as well as professional building planners, will get acquainted with modern technologies for 'in-situ' and 'near-by' production of heat, cold and electricity in nearly zero-energy buildings including energy-efficient measures and renewable energy technologies utilization. Theoretical content is supported by in-situ experiments results, numerical examples and case studies, which were developed by colleges of Laboratory for Sustainable Technologies in Buildings (LOTZ), Faculty of Mechanical Engineering, University of Ljubljana.

The book is an upgraded teaching material developed in the frame of ERASMUS+ Project EduLabFrame (2014-1-RO01-KA203-002986) and we would like to thank the colleagues involved in the project. The authors would also like to thank Viessmann Werke GmbH & Co. KG for extended picture material. We would like to thank all other cited authors and sources. Finally, we would like to thank company TRIMO d.o.o. to enable TRIMOExpert software for downloading from www.TRIMO.eu.

Ljubljana, Slovenia

Sašo Medved
Suzana Domjan
Ciril Arkar

Contents

1	Indoor Comfort Requirements	1
1.1	Indoor Thermal Comfort	2
1.1.1	Criteria for Indoor Environment Thermal Comfort Global Parameters	5
1.1.2	Integral Indicators of Indoor Thermal Comfort: PMV and PPD	11
1.1.3	Adaptive Model of Thermal Comfort	13
1.1.4	Local Indoor Thermal Comfort Indicators	14
1.2	Indoor Air Quality (IAQ)	15
1.2.1	Required Ventilation for IAQ	15
1.3	Visual Comfort	20
1.3.1	Criteria of Visual Comfort Parameters	21
1.4	Acoustic Comfort	24
1.4.1	Sound Recognition and Noise Protection	25
	References	27
2	Energy Sources	29
2.1	Renewable Energy Sources (RES)	31
2.1.1	Solar Energy	33
2.1.2	Geothermal Energy	37
2.1.3	Tidal Energy	39
2.2	Fuels as Energy Carriers	40
2.2.1	Non-renewable Fossil Fuels	43
2.2.2	Renewable Fuels Made from Biomass	46
2.3	Electricity	51
	References	57
3	Introduction to Building Physics	59
3.1	Heat Transfer in Building Structures	59
3.1.1	Thermal Transmittance of Building Structures (U-Value)	60

3.1.2	Thermal Transmittance of Homogeneous Structures . . .	61
3.1.3	Thermal Transmittance of Structures with Closed Air Gap or Ventilated Air Layer	63
3.1.4	Thermal Transmittance of Green Building Structures	64
3.1.5	Thermal Transmittance of Building Structures in Contact with the Ground	66
3.1.6	Thermal Transmittance of Windows (and Doors)	67
3.1.7	Thermal Bridges	69
3.1.8	Specific Transmission Heat Transfer Coefficient (Average Thermal Transmittance of Building Envelope)	74
3.1.9	Total Solar Energy Transmittance of Windows (and Transparent Envelope Structures)	75
3.1.10	Heat Accumulation in Building Structures	76
3.2	Psychrometrics	81
	References	83
4	Experimental Evaluation of Buildings' Envelope Thermal Properties	85
4.1	Semi-professional Tools and Applications for Evaluation of Indoor Comfort	85
4.2	In-Situ Determination of Heat Transfer Coefficient U of Building Structures	87
4.3	In-Situ Determination of Glazing Total Solar Energy Transmittance g	92
4.4	In-Situ Determination of the Building Envelope Thermal Insulation with Thermography	93
4.5	In-Situ Determination of Building Airtightness	96
4.6	In-Situ Determination of Overall Building Thermal Properties	99
	Reference	103
5	Global Climate and Energy Performance of the Building	105
5.1	Energy Performance of Building Directive (EPBD) and Nearly Zero Energy Buildings (NZEB)	107
5.2	Determination of Energy Performance of the Buildings	109
5.2.1	Time Step Intervals and Calculation Period	111
5.3	Determination of Building Energy Needs	112
5.3.1	Energy Need for Heating Q_{NH}	112
5.3.2	Energy Need for Cooling Q_{NC} : Monthly Calculation Period	116
5.3.3	Energy Need for Heating Q_{NH} and Cooling Q_{HC} : Hourly Calculation Method	118

5.3.4	Energy Need for Ventilation Q_V	121
5.3.5	Energy Need for Domestic Hot Water Q_W	121
5.3.6	Energy Need for Humidification Q_{HU} and Dehumidification Q_{DHU} of Indoor Air	122
5.3.7	Energy Need for Lighting Q_L	123
5.4	Delivered Energy for the Building Operation Q_f	124
5.5	Primary Energy Needed for the Building Operation	127
	References	129
6	Best Available Technologies (BAT) for On-Site and Near-by Generation of Heat for NZEB	131
6.1	Local or Decentralized Heat Generators for Residential Buildings	132
6.1.1	Biomass Stoves and Furnaces	132
6.1.2	Electrical Heaters	135
6.2	Heat Generators for Central Heating Systems	136
6.2.1	Combustion Boilers	136
6.2.2	Heat Pumps	143
6.3	Solar Thermal Collectors	152
6.3.1	Thermal Efficiency of Solar Thermal Collectors	154
6.3.2	Production of Heat: Rule of Thumb	157
6.4	District Heating	158
6.5	Other Heat Generators	159
	References	160
7	Best Available Technologies (BAT) for On-Site Electricity Generation for nZEB	161
7.1	Photovoltaic (PV) Systems	162
7.1.1	Types of PV Cells	165
7.1.2	PV Modules	169
7.1.3	Building Integrated PV Modules	171
7.1.4	PV Systems	173
7.1.5	Production of Electricity: Rule of Thumb	174
7.1.6	Environmental Impacts of PV Cells	175
7.2	Small Scale Cogeneration	175
7.2.1	Cost Effectiveness	178
7.2.2	Environmental Benefits of mCHP	179
7.3	Wind Turbines	179
7.3.1	Wind Energy Potential	180
7.3.2	Rated Power and Efficiency of Wind Turbines	182
7.3.3	Types of Wind Turbines	184
7.3.4	Production of Electricity: Rule of Thumb	186
7.3.5	Environmental Impacts	186

7.4	Fuel Cells (FC)	187
7.4.1	Types of Fuel Cells	188
	References	189
8	Space Heating of nZEB	191
8.1	Heat Load of the Building	191
8.1.1	Rule of Thumb	193
8.1.2	Steady State Heat Load	193
8.1.3	Heat Load Determination by Dynamic Simulations	196
8.2	Central Space Heating Systems	198
8.2.1	Comparative Advantages and Disadvantages of Hydronic and Hot Air Space Heating Systems	198
8.2.2	Sub-systems of Space Heating System	201
8.2.3	Basic Elements of Space Heating System	203
8.3	Heat Storage	203
8.4	Distribution Systems	206
8.4.1	Hydronic Systems	207
8.5	End Heat Exchangers/Heat Emitters	210
8.5.1	Radiators	210
8.5.2	Convectors and Fan-Coils	212
8.5.3	Active Beams	214
8.5.4	Floor and Ceiling Radiant Heat Emitters	215
8.5.5	Thermally Activated Building Structures	218
8.5.6	Other Applications of Floor Heating	219
8.6	Control of Space Heating Systems	220
8.7	Energy Needs and Delivered Energy for Space Heating	223
8.8	Principles of Rational Use of Energy for Space Heating	228
	References	230
9	Space Cooling of nZEB	231
9.1	Cooling Load of Buildings	232
9.1.1	Rule of Thumb	232
9.1.2	Steady State Cooling Load	232
9.1.3	Cooling Load Determination by Dynamic Simulations	238
9.2	Techniques for Cooling of the Buildings	238
9.3	Mechanical Cooling of nZEB	240
9.4	Mechanical Space Cooling Systems for nZEB	246
9.4.1	Direct Evaporation (DX) Cooling Systems	246
9.4.2	Chilled Water Space Cooling Systems	247
9.5	Environmental Impacts of Space Cooling	255
9.6	Energy Needs and Delivered Energy for Space Cooling	255
9.7	Principles of Rational Use of Energy for Space Cooling	258

9.7.1	Architecture Design	258
9.7.2	Natural Cooling and Free Cooling of the Buildings ...	262
9.7.3	Free Cooling	262
9.7.4	Solar Cooling	264
9.7.5	Other Measures for Increasing Energy Efficiency of Space Cooling Systems	267
References	268
10	Domestic Hot Water Heating in nZEB	269
10.1	Demand for DHW	269
10.2	DHW Heating Load	271
10.3	Energy Needs and Delivered Energy for DHW	276
10.4	Principles of Rational Use of Energy for DHW Heating	279
10.4.1	DHW Solar Heating	279
10.4.2	Waste Heat Recovery from Drain-Water	283
10.4.3	Heat Recovery from Utility Sewage Systems	283
10.5	Treatment of DHW for Reliable and Healthy Operation of DHW Heating System	284
10.6	Avoiding the Presence of Harmful Microorganisms in Domestic Hot Water	287
References	288
11	Ventilation of nZEB	289
11.1	Natural Ventilation	290
11.1.1	Advantages and Disadvantages of Natural Ventilation	290
11.1.2	How Natural Ventilation Works	291
11.1.3	Determination of Ventilation Air Flow Rate in Case of Natural Ventilation	294
11.1.4	Controlling of Natural Ventilation	298
11.2	Mechanical Ventilation	298
11.2.1	Advantages and Disadvantages of Mechanical Ventilation	298
11.2.2	Mechanical Ventilation Systems	300
11.2.3	Types of Heat Recovery Units (HRU) in Air Handling Units (AHU)	301
11.2.4	Fans	307
11.2.5	Filters in AHU	308
11.2.6	Design of Mechanical Systems with Balanced Ventilation and Heat Recovery	309
11.3	Energy Efficiency Indicators of Mechanical Ventilation Systems with HRU	315
11.3.1	Energy Needs and Delivered Energy for Mechanical Ventilation	319

11.4	Techniques for Improving Energy Efficiency of Ventilation	320
11.4.1	Increasing Heat Recovery Efficiency by Ground Heat Exchanger (GHX)	320
11.4.2	Increasing Energy Efficiency of Buildings with Passive Cooling with Night-Time Natural Ventilation	323
11.4.3	Increasing Energy Efficiency of Buildings with Integration of Building Service Systems	324
	References	326
12	Energy Efficient Lighting of nZEB	327
12.1	Light	327
12.2	Visual Comfort	329
12.3	Sources of Light	329
12.3.1	Daylight	329
12.3.2	The Luminance of the Clear Sky	332
12.3.3	The Luminance of the Overcast Sky and the CIE Overcast Sky	333
12.3.4	Luminous Efficacy of the Direct and the Diffuse Solar Radiation	334
12.3.5	Availability of Daylight	335
12.4	Artificial Sources of Light	335
12.5	Requirements and Criteria of Visual Comfort	338
12.5.1	Illuminance	338
12.5.2	Daylight Factor	339
12.6	Principles of Rational Use of Energy for Lighting	341
12.6.1	Energy Needs and Delivered Energy for Lighting of nZEB	342
	References	347
13	Energy Labelling of Buildings	349
13.1	Energy Performance Certificates of Buildings	350
13.1.1	Calculated Energy Performance Certificate of Building (cEPC)	351
13.1.2	Measured Energy Performance Certificate (mEPC)	353
	Reference	356
14	Environmental Labelling of Buildings	357
14.1	Sustainable Development and Environmental Impacts of Buildings	357
14.2	Ecodesign and Energy Labelling of Energy Related Products	359
14.3	Environmental Labels	361
14.4	Environment Product Declaration—EPD	364

- 14.4.1 Single Issue Type III Environmental Declarations 366
- 14.5 Life Cycle Impact Assessment (LCIA) 368
 - 14.5.1 Classification, Characterization, Normalization,
and Weighting in LCIA Methodologies 369
- 14.6 Environmental Impact Assessment of Buildings 379
 - 14.6.1 BREEAM 380
 - 14.6.2 LEED 381
 - 14.6.3 DGNB 384
 - 14.6.4 Level(s) 387
- References 387

About the Authors

Sašo Medved, Ph.D. is a Full Professor at the University of Ljubljana, Faculty of Mechanical Engineering. He also lectures at the Faculty of Architecture (Building Physics and Utility Technologies) and at the Faculty of Health Sciences (Energy and the Environment). He is the holder of the several subjects in the Doctoral studies in the field of energy-efficient buildings and environmental impact assessment. He is the author of several educational books, multimedia packages and computer software codes for industrial companies in the field of solar energy and heat and mass transfer in buildings. His research areas include renewable energy sources, environmental engineering, heat and mass transfer in buildings, heat and mass transfer in urban environments and mitigation of climate change.

Suzana Domjan, M.Sc. is a researcher at the University of Ljubljana, Faculty of Mechanical Engineering. She is involved in the education of students of architecture and health science. Her area of expertise is heat transfer in buildings, building energy survey and project management. She is an expert in the field of sustainability assessment and energy labelling of buildings.

Ciril Arkar, Ph.D. is an Associate Professor at the University of Ljubljana, Faculty of Mechanical Engineering and Faculty of Architecture. His pedagogical activities include lecturing courses on Renewable Energy Sources. His area of expertise is solar energy utilization in buildings, modelling of heat transfer in components and systems for solar energy utilization, latent heat thermal energy storages and systems, thermal environment in buildings. His professional work includes in-situ verification of the buildings' elements and systems performance, and development of software tools for buildings' energy performance indicators.

Chapter 1

Indoor Comfort Requirements

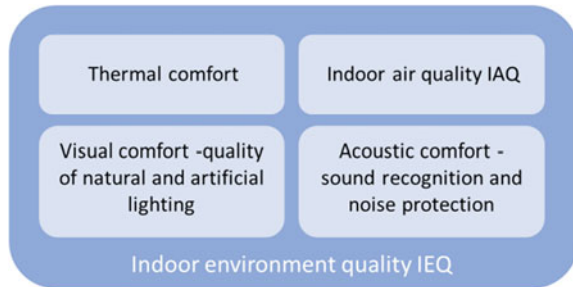


Abstract In this chapter, the design and assessment of indoor living comfort conditions are presented from an engineering perspective. This means that perceived physical process that occur in the indoor environment and influence the response of the residents' bodies and ability to perform work are transferred into several groups of physical indicators and ranges of acceptable values to ensure a pleasant, healthy, and productive environment. Indicators are used in the process of building design as well as in the process of the in situ assessment of indoor environment quality, (IEQ, also called 'building ergonomics' or 'building ecology') during the operation of the buildings.

An overview of human history shows that development has been deeply related to the use of energy. Technologies for energy conversion that were available at a point in history influence how the shelters and later buildings that protect us from severe environment conditions were built. The use of locally available materials and consideration of bionic principles, which characterized the pre-fossil fuels period, have recently gain much attention again, but with significant differences in the requirements of living conditions, because nowadays we spend the majority of our lives inside buildings, and providing a wellbeing is an essential function of contemporary buildings.

The assessment of indoor living comfort is based on multiple physical variables that influence how indoor environment is perceived by individuals according to their psychological and physiological responses. In this chapter, we will focus on requirements of physical conditions and on engineering approaches to IEQ assessment. Thermal comfort, indoor air quality, lighting, and acoustic comfort will be discussed. Incorporating the requirements of energy efficiency means that the designers of buildings must ensure IEQ with the lowest possible use of energy (Fig. 1.1).

Fig. 1.1 From the engineering point of view, IEQ can be achieved with adequate thermal comfort, indoor air quality, visual and acoustic comfort



Note:

- please be aware that IEQ must not be sacrificed due to desired decreasing of energy use in buildings
- all aspects of indoor design are equally important and must be considered
- segments such as aesthetics, urban architecture, or traditional principles like Feng Shui will not be discussed; nevertheless contemporary design and assessment methods are based on the traditional knowledge.

1.1 Indoor Thermal Comfort

Human beings are warm-blooded. Our bodies provide constant internal temperature ($37\text{ °C} \pm 0.8\text{ °C}$), regardless of the ambient temperature or activity of the muscles. Heat is produced in the internal organs with process of combustion (oxidation) of proteins and fats. This process is called ‘metabolism’ which is regulated so that body is in thermal equilibrium with its surroundings.

Our body is a type of heat engine that converts only a small fraction of the supplied energy into internal heat and mechanical work. Similar to power plants, the surplus of energy must be transferred to the surroundings using different mechanisms of heat transfer. If the processes of heat transfer from or to our bodies are not perceived as annoying, the condition of thermal comfort is achieved (Fig. 1.2).

The heat response of the body greatly depends on its internal heat generation and thermal insulation. Heat generation depends on peoples’ physical activities. For design purposes, it is assumed that the reference person was a physically active average adult (30 years old, weight 70 kg, 1.7 m tall with surface area of 1.8 m^2) seated and emitting heat flux of 58 W per m^2 of skin, as stated in the standard EN ISO 8996.¹ Instead of watts, heat flux of reference person can be expressed with

¹EN ISO 8996:2004 Ergonomics of the thermal environment—Determination of metabolic rate.

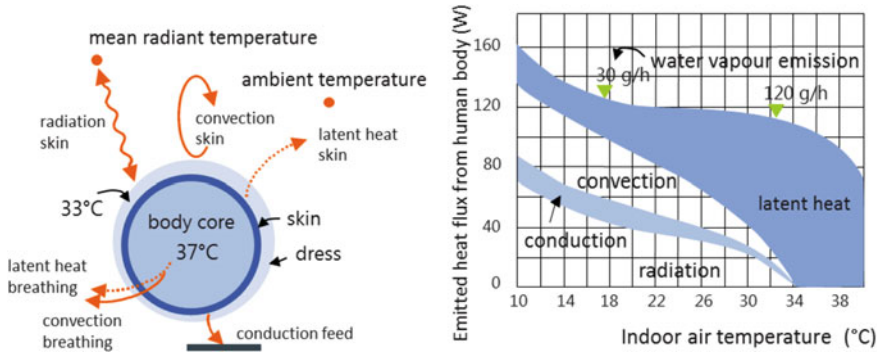


Fig. 1.2 Our body needs energy in form of the food to maintain its internal temperature at constant value and to do the required mechanical work. As with other heat engines, the efficiency of work production of our body is limited by Carnot efficiency. Mechanical work cannot be performed without transfer of heat from the body to the environment using all available sensible and latent heat transfer mechanisms. The share of each mechanism depends predominantly (but not only) on indoor temperature; at a temperature equal to the skin’s temperature, the body can cool down only by emitting latent heat with sweating

metabolism rate M of 1 “met”. A more physically active person emits more than one met, as shown in Table 1.1: Specific heat flux emitted by 1 m^2 of skin of reference adult person at different physical activities; for the purposes of thermal comfort design, total emitted heat flux is expressed as metabolic rate in met (EN ISO 8996).

Note: Several methods were developed for determination of metabolism rate for “non-reference” persons, for example on the basis of heart rate or oxygen consumption.

People dress for thermal insulation. Similar to building structures, the thermal resistance of clothing can be expressed by heat transferred resistance R or by I_{cl} , the value of the clothing factor in the unit “clo”. One clo represents a thermal resistance of $0.155 \text{ m}^2\text{K/W}$. The clothing factor is defined by the sum of clo of each clothes that person wears. Values of clo for typically dressed persons are presented in Table 1.2.

Beside intermediary conditions included by met and clo, four global physical parameters define indoor thermal comfort conditions: indoor air temperature (θ_i), mean radiant temperature of the interior surfaces (θ_{mrt}), indoor air velocity (v), indoor air relative humidity (ϕ) (Fig. 1.3).

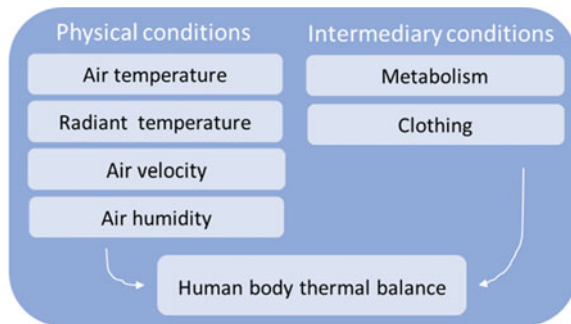
Table 1.1 Specific heat flux emitted by 1 m^2 of skin of reference adult person at different physical activities; for the purposes of thermal comfort design, total emitted heat flux is expressed as metabolic rate in met (EN ISO 8996)

	Emitted heat flux (W/m^2)	M metabolic rate (met)
Sitting	58–70	1.0–1.2
Housework	116–198	2.0–3.4
Walking	116–267	2.0–4.6
Dancing	140–256	2.4–4.4

Table 1.2 Cloths factor I_{cl} is defined by the sum of each part of cloths that person wears in particular room and is expressed in units of clo (EN ISO 8996)

	I_{cl} (clo)
Naked body	0
Light clothing	0.3
Business suit	1
Winter clothing	1.5

Fig. 1.3 Six parameters are used for global assessment of indoor thermal comfort



The range of global indoor comfort parameters values are defined in the standard EN 15251² in form of categories. The minimum category that must be fulfilled is defined in national legislation, but the most common is at least Category III is required. For vulnerable groups (children or elderly people), category I is recommended (Table 1.3).

²EN 15251:2007 Indoor environmental input parameters for design and assessment of energy performance of buildings addressing indoor air quality, thermal environment, lighting and acoustics.

Table 1.3 According to standard EN 15251 IEQ, the quality of indoor living comfort is defined by category is categorized in four classes. The most common at least class III is required

Category	Explanation
I	High level of expectation and is recommended for spaces occupied by very sensitive persons (very young children, sick, elderly persons, etc.)
II	Normal level of expectation for new buildings and renovations
III	An acceptable, moderate level of expectation, for existing buildings
IV	Acceptable for a limited part of the year

Note:

- according to EN 15251 not only thermal comfort, but all aspects of IEQ are categorized in categories I–IV,
- standard EN ISO 7730³ categories indoor environment quality in classes A, B and C.

Indoor thermal comfort parameters can be determined or evaluated numerically (by empirical equations or computer modelling during the design phase), by in situ measurements (on existing buildings), or by questioner (on already used buildings). In the case of in situ evaluation, parameters are measured in the centre of the living zone, a virtual part of the room defined by following dimensions: 1 m from exterior walls, 0.5 m from internal walls, and in-between 0.1 and 1.8 m above the floor and for representative period (~10 days) during the coldest and warmest months.

1.1.1 Criteria for Indoor Environment Thermal Comfort Global Parameters

Indoor air temperature or dry bulb temperature (θ_i) should be lower in the rooms in which persons are more active or have heavier clothing:

- 20 °C in residential space (1 clo), 18 °C in bedrooms, and 24 °C bathrooms (0 clo) during winter and up to 26 °C during summer (0.5 clo),
- 20–22 °C in offices (1 clo) during the winter and up to 26 °C during summer (0.5 clo),
- up to 16 °C during the winter in spaces where heavy work (5 met) is performed.

³EN ISO 7730:2005 Ergonomics of the thermal environment—Analytical determination and interpretation of thermal comfort using calculation of the PMV and PPD indices and local thermal comfort criteria.

Fig. 1.4 Vernon globe thermometer with diameter of 152.4 mm is commonly used for in situ determination of mean radiant temperature



Mean radiant temperature (θ_{mrt}) is the mean temperature of all visible (from a person's point of view) surfaces within the room. Mean radiant temperature can be calculated analytically if the geometry of areas, surface temperatures and emissivity of all surfaces that form closed space are known. It can be measured in situ using a Vernon globe thermometer, shown in Fig. 1.4. The following equation can be used to calculate θ_{mrt} in Kelvin:

$$T_{\text{mrs}} = \sqrt[4]{T_g^4 + 1.3 \cdot 10^8 \cdot (T_g - T_i) \cdot \frac{v^{0.6}}{d^{0.4}}} \quad (\text{K})$$

↑ air velocity (m/s)
↑ temperature of air inside the Vernon globe thermometer (K)
↑ air temperature (K)
↑ globe diameter (m)

Case study: Calculate mean radiant temperature from data obtained by Vernon globe thermometer with diameter of 152 mm ($T_g = 301$ K (28 °C)), air velocity sensor ($v = 0.5$ m/s) and air temperature sensor ($T_i = 293$ K (20 °C)).

$$T_{\text{mrs}} = \sqrt[4]{301^4 + 1.3 \cdot 10^8 \cdot (301 - 293) \cdot \frac{0.5^{0.6}}{0.152^{0.4}}} = 313.6 \text{ K (40.5}^\circ\text{C)}$$

Operative temperature θ_o combines the effects of the air temperature θ_i and mean radiant temperature θ_{mrt} on perceived indoor temperature. θ_o is used for design of the thermal comfort and as well as for energy demand calculation. In the simplest way, operative temperature is determined by air and mean radiant temperatures, as follows:

$$\theta_o = 0.5 \cdot \theta_i + 0.5 \cdot \theta_{mrt} \text{ (}^\circ\text{C)}$$

↙ for natural ventilated buildings, $v \sim 0.2$ m/s

$$\theta_o = 0.6 \cdot \theta_i + 0.4 \cdot \theta_{mrt} \text{ (}^\circ\text{C)}$$

↙ for mechanical ventilated buildings, $v \sim 0.6$ m/s

Case study: Operative temperature θ_o is used as a set-point temperature for regulation of heating and cooling systems as well as for calculation of needed energy for heating and cooling (see Sect. 5.3). According to building envelope thermal properties, there can be significant difference between air and operative temperature. As an example, the graph shows difference between indoor air temperature and operative indoor temperature in the residential and technical unit of the Virtual Lab (Figs. 1.5 and 1.6).

Data were calculated with hourly meteorological data for city of Ljubljana, Slovenia. The differences between operative and air temperatures are noticeable. The difference would be even higher in the case of a poorly thermally insulated building. Required higher air temperature during the heating period and lower air temperatures during the cooling period increase the energy needs for heating and cooling.

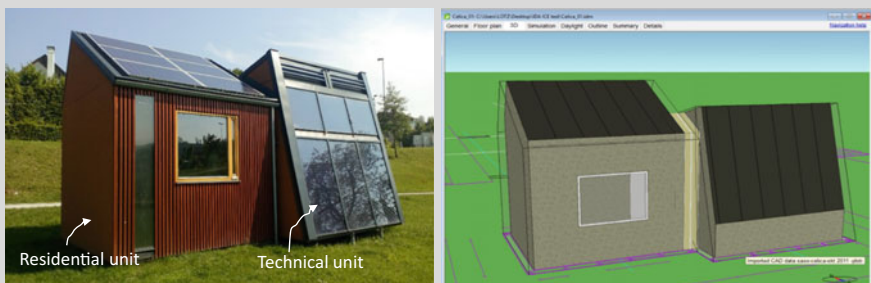


Fig. 1.5 Photo of Virtual Lab building with living (residential) and technical unit (left), Virtual Lab building in computer simulation tool IDA-ICE (IDA Indoor Climate and Energy, Version: 4.8, EQUA Simulation AB, Stockholm, Sweden) (right)

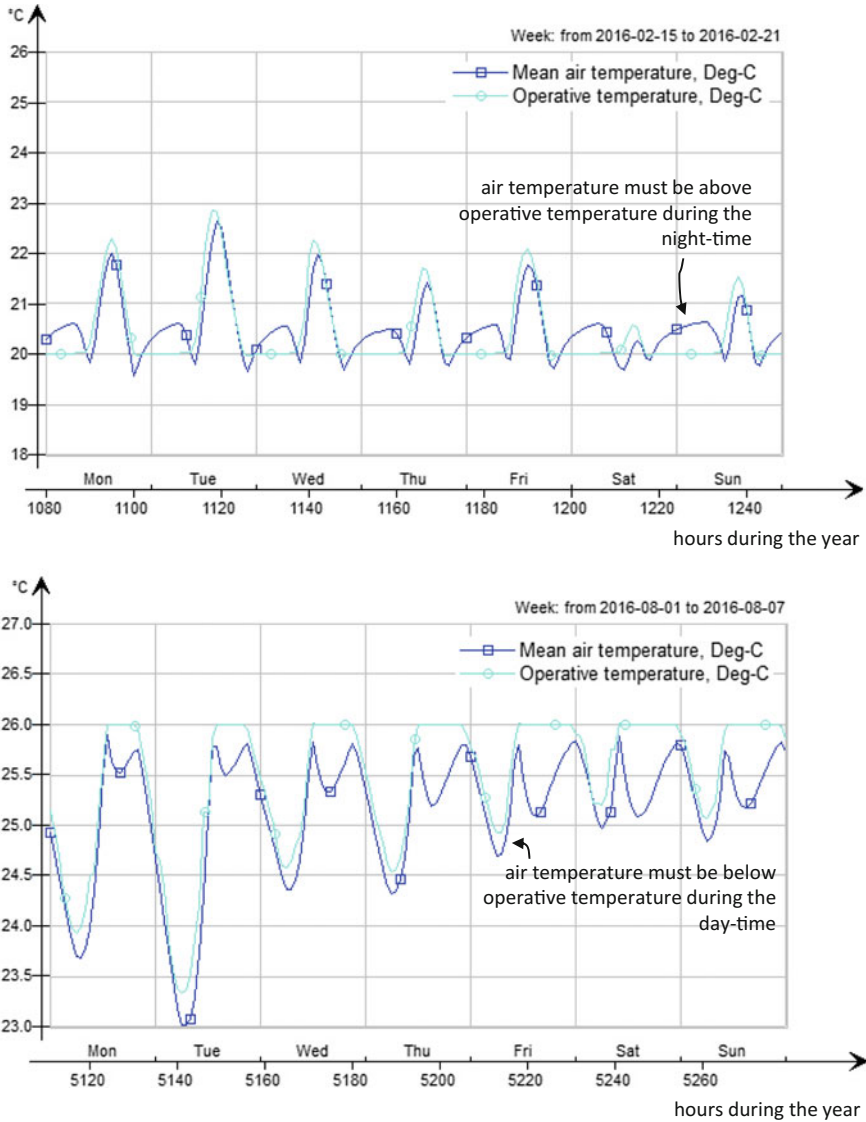


Fig. 1.6 Operative and indoor air temperature in living unit of Virtual Lab during one week in February (top) and in August (bottom) (IDA-ICE)

Air velocity in indoor environment (v); as movement of the air in indoor environment impacts convective heat losses and water evaporation from our body, air velocity should be (at θ_i 20 °C) maintained below 0.15 m/s in the heating season; it can be up to 0.65 m/s during the cooling season (at θ_i 26 °C) (Fig. 1.7).



Fig. 1.7 During the cooling season, a ceiling fan blows air downwards and because of higher air velocity residents perceive lower indoor temperature (at 1 m/s a decrease of ~ 3 °C); if the tilt of the blades is changed during the heating season, the fan draws air up and reduces temperature stratification without the feeling of an unpleasant draught (www.powerhousefan.com)

For the modelling of building energy performance, it is assumed that periodic indoor temperature swing (for example, caused during the heating period because of intermediate heating, internal heat gains, and solar heating) decreases energy demand because heat and cold are stored in the building constructions in this way. The resulting range of suitable temperatures according to the category of indoor environment is shown in Table 1.4. As indoor temperatures and air velocity interact, a higher category of indoor comfort also requires lower air velocity.

Air humidity (ϕ) has a minor influence on thermal comfort, if the relative air humidity is within the range of 35–70% at air temperatures between 20 and 26 °C. In spaces with higher temperatures, the humidity should be lower, in order to enable the body to dissipate heat with evaporation. At relative humidity lower than 35%, particles stay airborne for a longer time, which irritates mucosa. Meanwhile, at relative humidity above 70%, in wintertime, there is greater chance of condensation of water vapour on cool surfaces of the building envelope. Nevertheless, air conditioning could significantly increase the energy needs for operation of the building because cold must be provided for dehumidification of the air (for cooling the air below the dew point temperature) and to create water vapour molecules for humidification of the air.

Note: Definition of water vapour partial pressure, absolute and relative air humidity is presented in Sect. 3.2.

Table 1.4 Indoor comfort category versus operative temperature θ_o and air velocity v (EN 15251)

Type of building, Space	Clothing, winter (clo)	Activity (met)	Category of indoor environment	Operative temperature winter (1 clo) (°C)	Operative temperature summer (0.5 clo) (°C)	Mean air velocity winter (m/s)	Mean air velocity summer (m/s)
Residential buildings	1.0	1.2	I	21.0–25.0	23.5–25.5	0.15	0.18
			II	20.0–25.0	23.0–26.0	0.18	0.22
			III	18.0–25.0	22.0–27.0	0.21	0.25
Open space office	1.0	1.2	I	21.0–23.0	23.5–25.5	0.15	0.18
			II	20.0–24.0	23.0–26.0	0.18	0.22
			III	19.0–25.0	22.0–27.0	0.21	0.25
Kindergarten	1.0	1.4	I	19.0–21.0	22.5–24.5	0.13	0.16
			II	17.5–22.5	21.5–25.5	0.16	0.20
			III	16.5–23.5	21.0–26.0	0.19	0.24
Shopping centre	1.0	1.6	I	17.5–20.5	22.0–24.0	0.13	0.16
			II	16.0–22.0	21.0–25.0	0.15	0.20
			III	15.0–23.0	20.0–26.0	0.18	0.23

Table 1.5 Recommended criteria for humidification and de-humidification of indoor air in buildings in which humans are a major source of water vapour (EN 15251 and CEN/TR 16798-2⁴)

Category of indoor thermal environment	Dehumidification relative air humidity (%)	Humidification relative air humidity (%)
I	50	30
II	60	25
III	70	20
IV (only accepted for limited part of the year)	>70	<20

If a building has an air conditioning system to control air humidity by humidification and de-humidification of indoor air, the following recommended criteria shown in Table 1.5 could be implemented as design values.

1.1.2 Integral Indicators of Indoor Thermal Comfort: PMV and PPD

By comparing the votes on the perceived thermal comfort by a large number of persons exposed to various indoor conditions, in 1982, Professor Fanger established a method for combining the effects of different physical parameters on the overall thermal comfort in the form of the so-called Predicted Mean (PMV). Fanger defined the scale of PMV between cold (mark -3) and hot (mark +3). The ideal thermal comfort conditions are fulfilled at value of PMV equal to zero.

The percentage of dissatisfied persons with indoor thermal conditions was also proposed by Professor Fanger. The so-called Predicted Percentage of Dissatisfied or PPD is expressed as the percentage of dissatisfied persons in a given indoor thermal environment conditions. The relationship between PMV and PPD is shown in Fig. 1.8. PMV and PPD values are used for design and in situ validation indoor thermal comfort. The limit values are proposed in standard CEN/TR 16798-2 and presented in Table 1.6.

⁴CEN/TR 16798-2:2017 Energy performance of buildings—Ventilation for buildings—Part 2: Interpretation of the requirements in EN 16798-1—Indoor environmental input parameters for design and assessment of energy performance of buildings addressing indoor air quality, thermal environment, lighting and acoustics (Module M1-6)

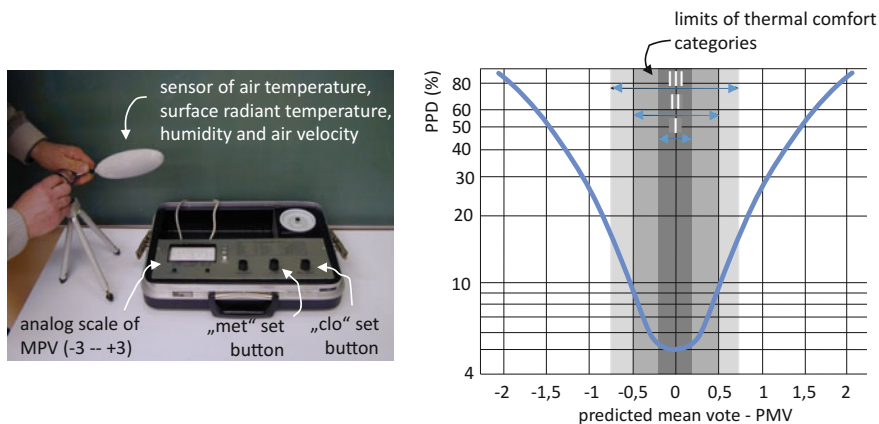


Fig. 1.8 Instrument for measuring θ_i , θ_{mrt} , v , φ with one multiple sensor. Met and clo are set according to aim of the room (e.g. bedroom, office, bathroom) (left); Fanger’s scale of predicted mean vote (right)

Table 1.6 Categories of thermal environment as defined in standards EN 15251 and CEN/TR 16798-2 for design of heated and cooled buildings

Category of indoor thermal environment	Thermal state of the body as a whole	
	PPD (%)	PMV
I (A)	<6	-0.2 < PMV < +0.2
II (B)	<10	-0.5 < PMV < +0.5
III (C) ^a	<15	-0.7 < PMV < +0.7
IV (only accepted for limited part of the year)	<25	-1.0 < PMV < +1.0

^aCategories as defined in EN ISO 7730:2005 Ergonomics of the thermal environment—Analytical determination and interpretation of thermal comfort using calculation of the PMV and PPD indices and local thermal comfort criteria

Case study: Computer simulation tools for the modelling of the thermal response of the buildings usually enable the determination of Fanger’s indoor thermal comfort indicators (PMV, PPD). An example is shown in this case study. PMV and PPD indoor thermal comfort indicators were calculated on an hourly scale for the living unit of Virtual Lab building with the IDA-ICE computer simulation tool. Hourly meteorological data for the city of Ljubljana, Slovenia were used for calculation. It can be concluded that indoor thermal comfort Category III can be provided in the living unit (-0.7 < PMV < 0.7) (Fig. 1.9).

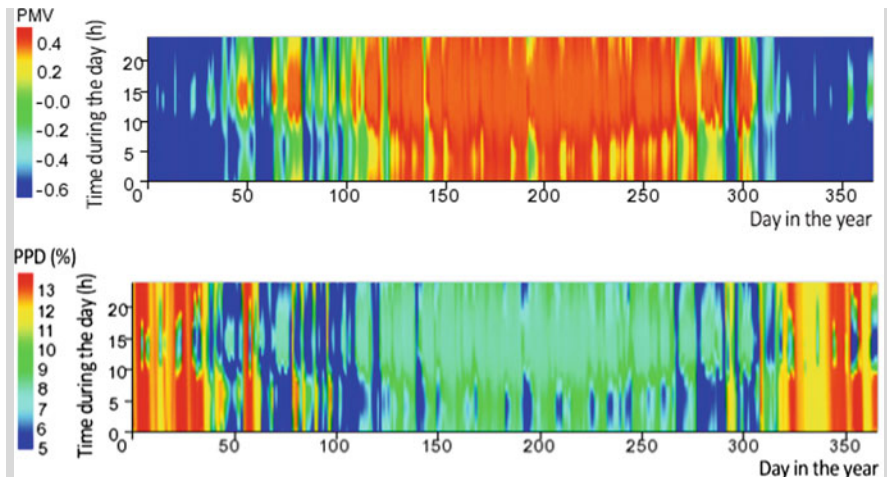


Fig. 1.9 PMV and PPD indoor thermal comfort indicators calculated for living unit of Virtual Lab building (IDA-ICE)

1.1.3 Adaptive Model of Thermal Comfort

Fanger's scale of thermal comfort is defined for steady state conditions and for 'ordinary' (young and healthy) persons. However even vulnerable groups adapt to some extent to indoor conditions. This adaptation can result from:

- personal adjustment (adjusting to the surroundings by changing personal behaviour, such as clothing, activity, moving to a different location),
- technological adjustment (modifying the surroundings themselves, when control is available, such as opening/closing windows or shades, turning on fans or heating, blocking air diffusers),
- cultural adjustments which include scheduling activities, dress codes,
- outdoor climate conditions.

Most commonly, the adaptive thermal comfort model is used for adaptation of operative indoor temperature for a building without a mechanical cooling system. The model is presented in standard CEN/TR 16798-2 and defines the range of acceptable indoor operative temperature according to external running mean temperature. If the daily average of the outdoor temperature is known for the previous seven days, the following equation for the determination of the running mean outdoor air temperature is proposed:

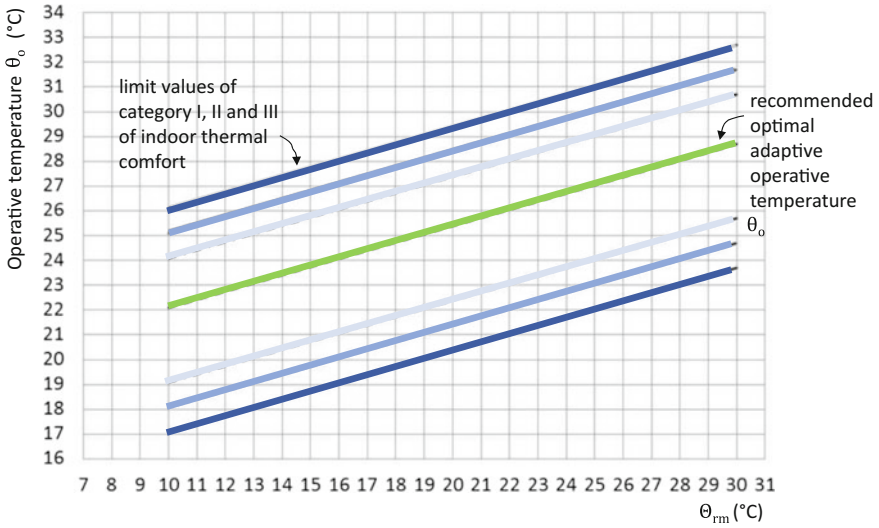


Fig. 1.10 Limits of comfortable adaptive operative temperature as a function of the mean running outdoor air running temperature according to standard CEN/TR 16789-2

$$\theta_{rm} = \frac{\overset{\text{average daily air temperature day before (}^\circ\text{C)}}{\theta_{ed-1}} + 0.8 \cdot \overset{\text{average daily air temperature two days before (}^\circ\text{C)}}{\theta_{ed-2}} + 0.6 \cdot \theta_{ed-3} + 0.5 \cdot \theta_{ed-4} + 0.4 \cdot \theta_{ed-5} + 0.3 \cdot \theta_{ed-6} + 0.2 \cdot \theta_{ed-7}}{3.8} \text{ (}^\circ\text{C)}$$

Once the running mean temperature is known, the recommended operative indoor temperature θ_o can be calculated with the equation:

$$\theta_o = 18.8 + 0.33 \cdot \overset{\text{running mean outdoor air temperature (}^\circ\text{C)}}{\theta_{rm}} \text{ (}^\circ\text{C)}$$

The optimal adaptive operative temperature θ_o and range of θ_o for different categories of indoor thermal comfort are shown in Fig. 1.10.

1.1.4 Local Indoor Thermal Comfort Indicators

The presented indicators are so-called global indoor thermal comfort indicators. They are used for the design of building and building services, and are, as already mentioned, measured in the middle of the living zone. To address a particular part of the space, for example the working space in a large office, indicators including the vertical temperature gradient, radiant temperature asymmetry, floor temperature, and draught rating are used. For all those indicators, ranges of values are defined

according to the category of indoor environment as well as the influence on PMV and PPD values. Please use other sources to study local indoor thermal indicators.

1.2 Indoor Air Quality (IAQ)

Inadequate indoor environments in all the segments presented in Fig. 1.1 can lead to minor or more serious health problems. In the previous decade, health issues of the indoor environment related to indoor air quality have been a topic of interest. The fact is that we spend most of our time in buildings and that indoor air is as a rule more polluted than outdoor air. Because of poor indoor air quality two phenomena arise:

- sick building syndrome (SBS): sick building syndrome is a phenomenon related to health problems, such as headache, problems with concentration, dry throat, irritation of the mucous membranes or nausea. SBS affects people while staying in the building. The exact cause of SBS is difficult to discover, and symptoms disappear soon after the afflicted people leave the building;
- building-related illness or BRI: in the case of long-term exposure to the pollutants in the building, a cluster of several diseases appears including respiratory infections, as well as viral and bacterial diseases. Links between polluted indoor air and cardiovascular diseases and cancer have also been found. BRIs indicate permanent loss of health.

Ventilation is a common technique for the dilution of pollutants in the indoor air with the supply of outdoor air. As a rule, outdoor air is less polluted than the air in buildings. Ventilation of buildings can be natural or forced (mechanical). Regardless of which ventilation is implemented, the air flow results from the difference in the air pressure between indoor and outdoor environments.

1.2.1 Required Ventilation for IAQ

Several methods are used for the determination of the design value of fresh air flow rate q_{vent} for diluting emissions from people, appliances, and building materials:

- air exchanges per hour (ACH) (h^{-1} , read per hour) is most often used for residential building ventilation; ACH represents how many times air in the building (or in the room) is replaced by fresh air from outdoors in one hour. ACH is determined by the standard CEN/TR 16789-2 and in the national regulations. For example, in Slovenia, the minimal ACH for residential building is 0.2 h^{-1} when the building is empty (to dilute emissions from building materials) and 0.5 h^{-1} when it is occupied. In case of the absence of national requirements, a minimum ventilation rate of 0.1 L/s per m^2 of residential building and 0.2 L/s

per m^2 of non-residential building is recommended during non-occupied hours in CEN/TR 16798-2. When the required ACH is known, the required air flow rate is given by equation⁵:

$$q_{\text{vent}} = n \cdot V_{\text{bui}} \quad (\text{m}^3/\text{h})$$

↙ net volume of building (m^3)
↖ air exchange rate (h^{-1})

- method based on perceived air quality; in this case, the air flow rate is designed regarding to the bio effluents emitted by persons and emissions from building (building materials and appliances). The standard CEN/TR 16798-2 defines minimal air flow rates per person for diluting body emissions (bio effluents) as well as the category of air quality (from I to IV) and expected percentage of people who will perceive the air quality as dissatisfying. The ventilation air flow rate needed for diluting emissions from building depends on the characterization of the building emission category. Buildings can be very low, low, or non-low polluting.

Note: categories of polluting buildings are based on concentration of total volatile organic compound (TVOC), ammonia, formaldehyde and carcinogenic pollutants and evaluated using a 28-day test of the concentration emitted from a material sample in a ventilated chamber (see Chap. 14).

Required ventilation rate q_{vent} is defined by equation:

$$q_{\text{vent}} = (n_p \cdot q_p + A_f \cdot q_{\text{bui}}) \cdot \frac{3600}{1000} \quad (\text{m}^3/\text{h})$$

↙ number of persons (-)
↖ ventilation rate for diluting bio effluents (l/s/pers)
↘ floor area of building (m^2)
↗ ventilation rate for diluting emission from building (l/s/m^2)

Ventilation rates for diluting bio effluents q_p and emissions from building q_{bui} are designed regarding the selected IAQ category, as shown in Tables 1.7 and 1.8.

The amount of air flow rate designed according to perceived air quality is defined by odour emitted by persons and building expressed in ‘olfs’ (from the Latin word for ‘smell’). It is assumed that an average sitting person emits 1 olf of odour and a list of emitted olfs has been developed for more active persons and building materials (in olfs per m^2) as presented in Table 1.9. The ventilation air flow rate is defined regarding to the number of decipols (dp). One decipol corresponds to ventilation air flow rate 10 L/s per one olf of odours. The required ventilation rate q_{vent} is then defined by equation:

⁵Pravilnik o učinkoviti rabi energije v stavbah (Rules on efficient use of energy in buildings with a technical guideline) (Uradni list RS, št. 52/10 in 61/17—GZ).

Table 1.7 Ventilation rate q_p for diluting emissions from people (bio effluents) to provide a certain IAQ category (CEN/TR 16798-2)

Category	Expected percentage of dissatisfied PD (%)	Airflow per non-adapted person (l/s/person)	Airflow per adapted person (l/s/person)
I	15	10	3.5
II	20	7	2.5
III	30	4	1.5
IV	40	2.5	1.0

Note Adapted person is person that stays in building (room) for longer time and because of that person adapt to bio effluents (odour)

Table 1.8 Ventilation rate q_{bui} for diluting emissions from building to provide a certain IAQ category (CEN/TR 16798-2)

Category	Very low polluting building (l/sm ²)	Low polluting building (l/sm ²)	Non low-polluting building (l/sm ²)
I	0.5	1.0	2.0
II	0.35	0.7	1.4
III	0.2	0.4	0.8
IV	0.15	0.3	0.6

Table 1.9 Emissions of odours expressed with olfs per person according to their physical activity and per square metre of floor lining materials (Hausladen et al. 2005)

Sitting person 1–1.2 met	1 olf/pers
Sitting person, smoker	5 olf/pers
Smoker, continuously	25 olf/pers
Athlete	30 olf/pers
Wool carpet	0.2 olf/m ²
Synthetic carpet	0.4 olf/m ²
PVC	0.2 olf/m ²
Granite	0.01 olf/m ²
Rubber	0.6 olf/m ²

$$q_{vent} = \left(\sum n_{pers} \cdot \text{olf}_{pers} + \sum A_f \cdot \text{olf}_{bui} \right) \cdot dp \cdot \frac{3600}{1000} \text{ (m}^3\text{/h)}$$

number of persons (-) personal olfs (olf) decipol (l/s/olf)
 floor area (m²) building material olfs (olf)

- method based on limit values of pollutant gas concentration. Amount of air flow rate regarding the maximum concentration of gasses; to calculate the ventilation air flow rate, the following quantities must be known;
- source of each pollutant gas \dot{S} (kg/h) emitted by pollution sources (inhabitan-cies, appliances or systems);

- maximum concentration of each pollutant gas in the air $C_{i,max}$ (kg/m^3) that is not harmful to the health or does not have a negative impact on the well-being of occupants; these values are commonly defined by the World Health Organization (WHO);
- concentration of each pollutant gas in outdoor air C_e (kg/m^3).

$$q_{\text{vent}} = \frac{\dot{S}}{C_{i,max} - C_e} \quad (\text{m}^3/\text{h})$$

source of each pollutant gas (kg/h)
↙ \dot{S} ↘
↖ $C_{i,max}$ ↗ C_e
↖ maximum concentration of each pollutant gas in indoor air (kg/m^3) ↗ concentration of each pollutant gas in outdoor air (kg/m^3)

The concentration of CO_2 is a commonly used indicator of indoor air quality. The difference in concentrations of CO_2 in indoor and outdoor air is used to define the IAQ category, as shown in Table 1.10. Values are defined in ‘parts per million’ or ppm as a volumetric unit of pollutant concentration.

For controlling mechanical ventilation systems and for the purposes of energy demand assessment, the EN 15251 standard recommends that the maximum ventilation rate has to be designed to correspond to the maximum indoor CO_2 concentration above outdoor concentration, as shown in Table 1.11.

Table 1.10 IAQ is divided into categories and levels of indoor air pollution according to maximal difference between concentrations of CO_2 in indoor and outdoor air (CEN/TR 16798-2)

Type of building or space	Category	Occupancy (pers./ m^2)	Indoor concentration above the outdoor value ΔCO_2 (ppm)		
			Very low-polluting	Low-polluting	Not low-polluting
Single office	I	0.1	370	278	185
	II	0.1	529	397	265
	III	0.1	926	694	463
	IV	0.1	1389	1010	654
Open plan office	I	0.07	317	222	139
	II	0.07	454	317	198
	III	0.07	741	556	347
	IV	0.07	1235	794	483
Conference room	I	0.5	505	463	397
	II	0.5	722	661	567
	III	0.5	1263	1157	992
	IV	0.5	1462	1389	1502

Table 1.11 Recommended CO₂ concentrations above the outdoor concentrations for energy demand calculations (EN 15251)

Category of IAQ	Concentration of CO ₂ above the outdoor values (ppm)
I	350
II	500
III	800
IV	>800

Case study: Person exhales approximate 55 L of CO₂ per hour when performing work while seated. Density of CO₂ is 1.98 kg/m³. Concentration of CO₂ in outdoor air is 1080 mg/m³. Determine required ventilation air flow rate q_{vent} (i) so that the CO₂ concentration does not exceed WHO limit value of CO₂ concentrations in indoor air of 3000 mg/m³ and (ii) assuming that a person emits 1.5 olf of bio effluents and that the room is ventilated with 1 decipol.

$$q_{vent,a} = \frac{\dot{S}}{C_{i,max} - C_e} = \frac{55 \cdot 10^{-3} \cdot 1.98}{3000 \cdot 10^{-6} - 1080 \cdot 10^{-6}} = 57 \left(\frac{m^3 \cdot kg \cdot m^3}{h \cdot m^3 \cdot kg} = \frac{m^3}{h} \right)$$

$$q_{vent,b} = \left(\sum n_{pers} \cdot olf_{pers} \right) \cdot dp \cdot \frac{3600}{1000} = (1 \cdot 1.5) \cdot 10 \cdot \frac{3600}{1000} = 54 \left(\frac{olf \cdot l \cdot s \cdot m^3}{s \cdot olf \cdot h \cdot l} = \frac{m^3}{h} \right)$$

The efficiency of pollutant dilution is defined by the way that fresh air is supplied and dirty air extracted from the building (room). In Fig. 1.11, three typical conditions that differ in the efficiency of the dilution of pollutants in the indoor air are shown. Supply air can cause short cut, mixing or displacement ventilation.

The quantity of fresh supply air presented in Tables 1.7 and 1.8 are determined assuming mixed air flow characterised by dilution efficiency $\epsilon_v = 1$. If ventilation is provided by short cut air movement. The dilution of pollutants is less effective, and the quantity of supply air must be enlarged to maintain same indoor air quality.

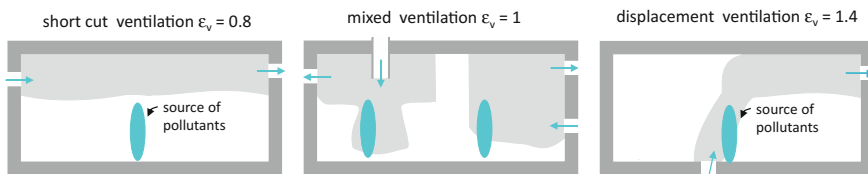


Fig. 1.11 Efficiency of dilution according to position of air inlet and outlet openings in the ventilated zone

If the ventilation system is designed as displacement ventilation, the dilution of pollutants is more effective, and a smaller quantity of supply fresh air must be provided in the zone. This decreases the energy demand for fan operation. Taking into account the efficiency of pollutant dilution, the ventilation air flow that must be supplied into the zone is determined by the following equation:

$$q_{\text{vent, supply}} = q_{\text{vent}} \cdot \frac{1}{\epsilon_v} \left(\frac{\text{m}^3}{\text{h}} \right)$$

nominal ventilation air flow rate (m³/h)
pollutant dilution efficiency (-)

1.3 Visual Comfort

People receive more than 80% of information from their environment by vision. The human eye perceives electromagnetic radiation with wavelengths in the range between 380 nm (violet light) and 760 nm (red light). From an engineering point of view, visual comfort is ensured if a person can efficiently perform tasks for which vision is the most important source of information. Visual comfort can be provided by natural (daylight) lighting, artificial (electric) lighting, or a combination of both. Visual performance can be accomplished by three fundamental measures:

Fig. 1.12 Improving (left to right) visual performance with different measures



- enlarging the size of observed detail; the size of the detail is measured in degrees of space angle and defined by the size of the detail and the distance of observer (Fig. 1.12, top);
- increasing the contrast between the observed detail and its immediate surroundings (Fig. 1.12, middle);
- increasing the illuminance of the detail; illuminance is defined by the luminous flux on the area of the surface of the observed detail (Fig. 1.12, bottom).

Visual comfort is extremely important for various reasons that are even more important than energy efficiency requirements. From the health aspect, it is necessary that suitable daylighting of indoor spaces in buildings provides well-being, mental health and vitality, enhances our satisfaction, optimism and trust, and enhances the production of vitamin D in our skin. It has been proven that a lack of daylight results in psychosomatic illnesses, such as depression, concentration disorders, and insomnia. From the psychological aspect, adequate natural or electrical lighting is needed to guide people in motion and orientation in space, to help distinguish important information, to provide people with feelings of intimacy by designing different illuminated areas in large spaces, to eliminate fear where danger is expected (e.g. at the end of long hallways). Daylight enhances our internal sense of time, and studies have shown that the duration of sunlight is one of the most important factors when buying a new apartment.

1.3.1 Criteria of Visual Comfort Parameters

Design of natural and artificial lighting and visual comfort assessment is based on several indicators including:

- duration of sunshine; describes the number of hours in a day when the sun's rays (direct solar radiation) is entering in room; this requirements deals with healthy aspects of sunlight and is not directly connected to the energy efficiency of the buildings;
- Illuminance of the surfaces in the room; illuminance (E) is defined by density of light flux in lumens (lm) per unit of illuminated area (m^2) and measured in lux (lm/m^2); required illuminance level is defined by the complexity of work performed; the range is between 50 lux for low-demand visual tasks (walking in a corridor) to 1000 lux if small details with low contrast must be recognized or precise colour detection is required. In living spaces, illumination of a virtual plane 0.8 m above the floor between 200 and 300 lux is required.
- daylight factor (DF) is a benchmark of daylight quality; it is expressed as a percentage of the indoor and outdoor illuminance of a horizontal unshaded plane under overcast sky; minimum DF and room average DF must be verified; if average DF is lower than 2%, the room will be perceived as to dark meanwhile rooms having average DF higher than 5% will be perceived as a bright space; however, only if average room DF is higher than 10% will daylight significantly affect electricity demand for artificial lighting.

Case study: Lighting of the buildings must be analysed in the procedure of evaluation of a building's energy efficiency indicators. Especially in non-residential buildings, lighting is related to high electricity demand, which can be lowered by the smart adaptation of electrical lighting to daylight. Computer simulation tools for modelling of thermal response of the buildings commonly enable determination of daylight level by daylight factors (DF) (Figs. 1.13 and 1.14).



Fig. 1.13 Photo of Virtual Lab building (left), Virtual Lab building in computer simulation tool IDA-ICE (right)

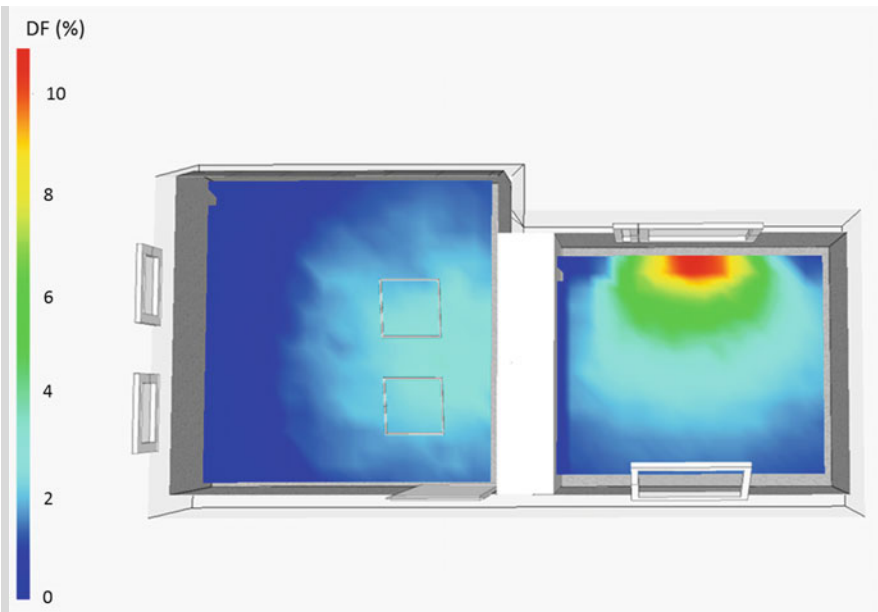


Fig. 1.14 Daylight analyses by computer tool IDA-ICE; daylight factor DF in living cell of Virtual Lab on 21st September at 12:00; CIE overcast sky condition (see Chap. 12)

- uniformity of illuminance is defined by the difference in illuminance of the worst and the best illuminated working spaces in a room; this ratio should not be greater than 1:6 (in case of simple visual task) to 1:3 in residential buildings or schools, uniformity of illuminance could be problematic in cases of deep rooms with windows on one side; several techniques can be used for improving daylight uniformity;
- rearranging the windows on opposite walls or installing daylight tubes;
- reflecting daylight into the back of the room with reflective jalousies, window shelves, prismatic elements and holographic optical elements;
- preventing the glare disturbance; high luminance (measured in cd/m^2) area of lamps, bright walls, reflective floor covers, or glazing areas can be disturbing if such surfaces are located in the centre of the view and have luminance over $2000 \text{ cd}/\text{m}^2$. For luminaries, the UGR (unified glare rate index) in scale 10–30 is used for rating. It can be expected that light sources will not be disturbing if UGR is lower than 16 and will cause a distraction if UGR higher than 28; with diffuse surfaces and shading of windows and appropriate choice of lamps, housing glare can be avoid (Fig. 1.15).
- temperature of colour of artificial light source regarding the required illuminance of working space; warmer colour temperature ($T < 3500 \text{ K}$) is suitable if lower illuminance is required and cold colour temperatures ($T > 5000 \text{ K}$) if the required illuminance level of work space is high ($E > 1000 \text{ lux}$).
- colour rendering index Ra, which defines how well the colour of the object will be recognized when it is illuminated by the luminaire; the scale of Ra is in the range between 1 and 100. Ra 1 means that luminaire emits monochromatic light, meanwhile Ra 100 is characteristic for natural light at clear sky conditions at sun noon. A minimum value of 80 is required for residential, office, and education buildings.



Fig. 1.15 Uniformity of illuminance in day-lit rooms can be improved by skylights and prismatic elements for guiding light toward the ceiling of the room (left: www.solatube.si; right: www.okalux.com)

1.4 Acoustic Comfort

Sound propagates through medium as mechanical waves causing the periodic formation of areas with high and low pressure relative to a reference atmospheric pressure (10^5 Pa). The distance between neighbouring compressions is called wavelength λ (m); frequency f (1/s) describes the number of compressions per second. The local air pressure deviation from the reference atmospheric pressure is called sound pressure (measured in Pa). Humans can sense sound pressure larger than 2×10^{-5} Pa, while sound pressure above 20 Pa causes pain. Due to the wide span, a sound pressure level (L_p) was introduced. Sound pressure level has a logarithmic scale, and it is measured in decibels (dB). The minimum sound pressure that people can sense corresponds to L_p 0 dB and sound pressure of 20 Pa corresponds to L_p 120 dB. Sound pressure level L_p changes rapidly; therefore, it is averaged in short time intervals. The method of averaging is a property of sound level meters. By agreement, 'F' and 'S' stand for fast and slow, while for impulsive sounds 'I' time averaging is used. Consequently, the sound pressure level is marked as $L_{p,F}$, $L_{p,S}$ or $L_{p,I}$ (dB) (Fig. 1.16).

The sound spectrum combines sound level pressure and sound frequency. Considering the typical sound spectrum, we distinguish between tune, sound, and noise (white noise, pink noise). Noise is defined as unpleasant sound that cause a decrease in concentration as well as a number of diseases.

In general, humans can hear sound with frequencies between 16 and 20,000 Hz but our hearing was adapted to hear best the frequencies that are typical for speech: in the range between 200 and 5500 Hz. We can hear speech if the sound pressure level is between 30 and 75 dB.

Introducing sound weighting curves sound pressure level L_p as the physical quantity can be transformed into the physiological quantity of sound level, which takes into account the dependence of sound intensity and frequency. Weighting

Fig. 1.16 Sound meter offer different methods for averaging of sound pressure level. Most common are 'F' (fast) or 'I' (impulsive) averaging



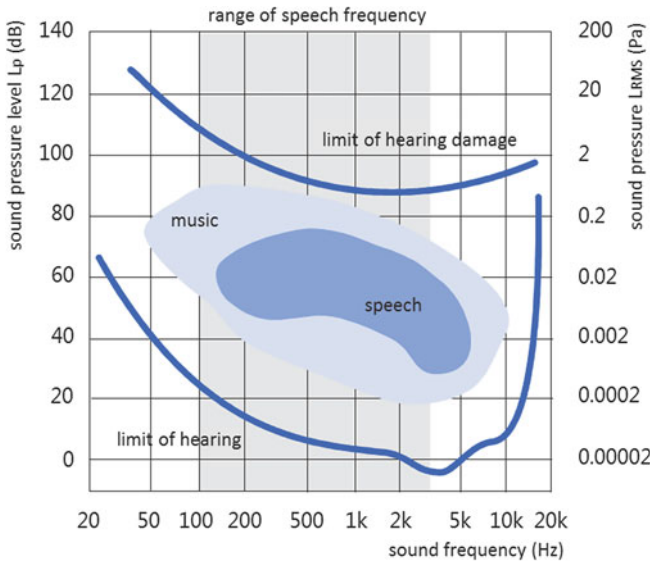


Fig. 1.17 Human hearing is adapted to the perception of speech; consequently, we can hear much quieter sounds if sound frequencies are in the range between 200 and 5000 Hz. From the figure, it can be seen that we can hear sound at different frequencies at different minimum sound pressure values

curve A is most commonly used in acoustics. In respect to the weighting curve used, sound pressure level is marked as $L_{p,A}$ in dB (A) or as $L_{p,F,A}$ in dB (A) if it is measured using fast averaging (Fig. 1.17).

1.4.1 Sound Recognition and Noise Protection

Requirements of acoustic comfort are related to two main tasks that must be taken into consideration by designers:

- adequate room acoustics, which is described by reverberation time, which is the time between the moment that the listener in the room detects the sound coming directly from the source and the moment that he detects the sound from the same source that is reflected from the surrounding surfaces in the room; reverberation time should be between 50 and 100 ms for good sound recognition because long reverberation times can cause undesirable echo; in engineering practice, the Sabin reverberation time method is used for design and in situ assessment of room acoustics. Sabin reverberation time corresponds to the time interval in which sound pressure level decrease for 60 dB after the source of white or pink sound is switched off. Typical design (and requested) values of Sabin reverberation time are between 0.8 s for smaller rooms to 2+ s for large concert halls;

- protection from high noise level; noise is transmitted through the air (as so-called air-born sound) or solid bodies (as structure-born or impact sound); low sound pressure level in the buildings can be achieved with the appropriate sound reduction index (R) of building construction and adequate impact sound insulation; the R index indicates to what extent air-born sound from outdoors or from neighbouring rooms is absorbed in building constructions; typical requested minimum R values for outer and separate walls are between 50 and 62 dB; impact sound insulation is measured by sound pressure level L_n that occurs in the room as consequences of impact sound transmission caused by a standardized tapping machine; typical allowed maximal L_n values are between 40 and 55 dB (Figs. 1.18, 1.19 and 1.20).

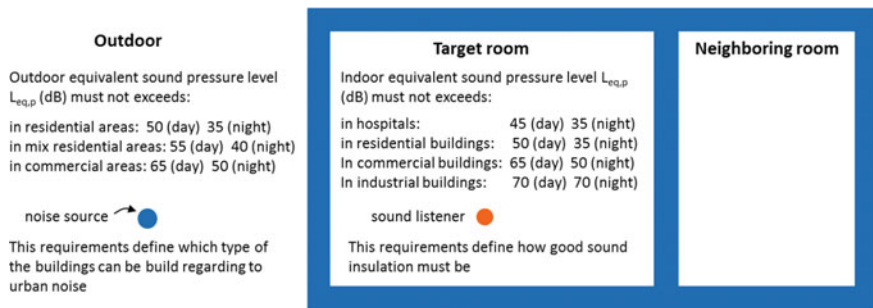


Fig. 1.18 General requirements regarding equivalent sound pressure level; equivalent sound pressure level is the (virtual) average constant sound pressure level during a long interval (e.g., the “day” interval is between 6 a.m. and 10 p.m.) with the same sound energy as actual sound; outdoor equivalent sound pressure level defined (i) which type of the building could be constructed in such a neighbourhood and (ii) if sound protection measures should be taken according to the type of building in the neighbourhood

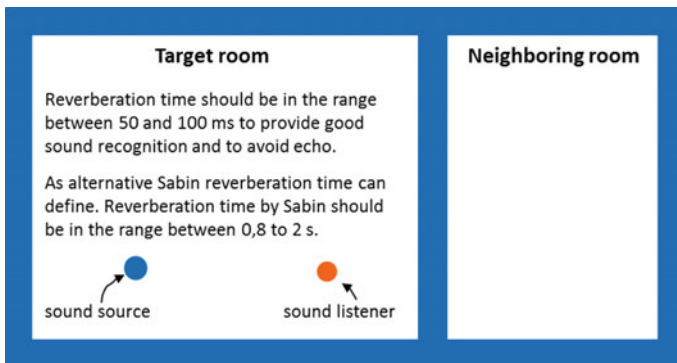


Fig. 1.19 Requirements regarding sound recognition; note the difference between physical and Sabine reverberation time

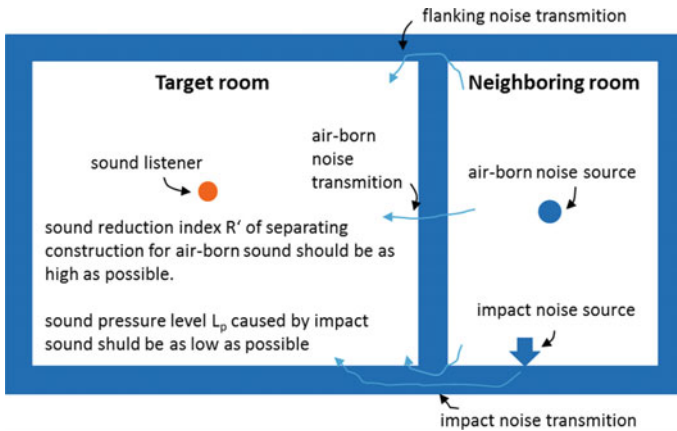


Fig. 1.20 Requirements regarding sound insulation from air-born and impact sound; in situ sound reduction index R' of building constructions between 50 and 62 dB is commonly required for homogeneous façade and interior walls and 35–45 for windows and doors for neighbourhood where equivalent sound pressure level is below 65 dB; flanking noise transmission reduce R by 2–5 dB; sound pressure level L_p caused by standardised impact noise machine should be lower than 45–55 dB

References

- Čudina M (2001) Tehnična akustika (Engineering acoustics). Faculty of Mechanical Engineering, University of Ljubljana, Ljubljana
- Fanger PO (1982) In Robert E Thermal comfort. Krieger Publishing Company, Malabar, FL
- Giedraityte L, Holmér I, Gavhed D (2001) Validation of methods for determination of metabolic rate in the Edholm Scale and ISO 8996. *Int J Occup Saf Ergon* 7(2):135–148
- Hausladen G et al (2005) *Clima Design Lösungen für Gebäude, die mit weniger Technik mehr können*. Verlag Georg D.W. Callwey GmbH, Germany
- Lenz B et al (2011) *Sustainable building services—principles, system, concepts*. Detail Green Books
- Medved S (2014) *Gradbena fizika II (Building physics II)*. Faculty of Architecture, University of Ljubljana, Ljubljana
- Mommertz E (2008) *Acoustics and sound insulation—principles, planning, examples*. Detail Practice

Chapter 2

Energy Sources



Abstract The development of societies depends now more than ever on reliable energy supplies. We are in the century in which there will be a transition from the dominance of non-renewable fossil fuels to low carbon societies that will be based on the use of renewable energy sources. Nevertheless, it is expected that non-renewable sources will remain significant energy carriers in the coming decades. In this chapter, natural energy sources as primary energy sources are presented. The chapter starts with a presentation of solar, tidal, and geothermal energy sources, followed by a presentation of the energy and environmental properties of renewable and non-renewable fuels. The chapter ends with descriptions of technologies that are used for on-site, near-by, and distant production of electricity.

Increased energy consumption in the past century was deeply related to the prosperity of humankind. Thus, one of the most important tasks of the modern societies is to ensure reliable energy supplies. Energy supply systems comprises many processes that are driven by politicians, corporations, experts, non-governmental organizations and users. These processes can be divided into three stages:

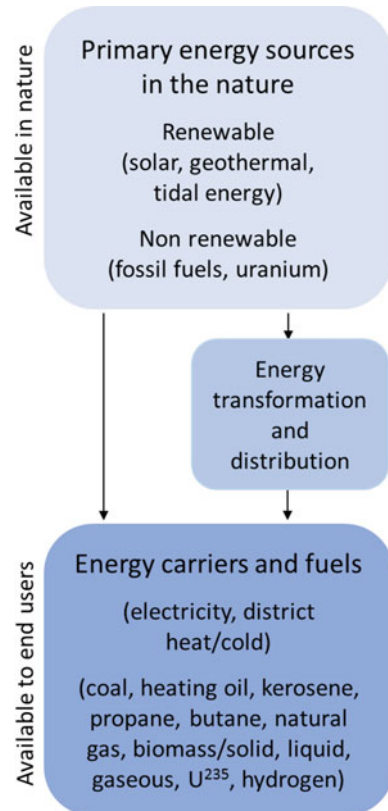
- harvesting of natural energy sources, called primary energy sources; primary energy sources are most commonly characterized as renewable or non-renewable energy sources;
- transformation of primary energy sources into different forms of energy carriers (such as electricity or district heat) or fuels (such as natural gas or biomass fuels); some primary energy sources that can be found in nature are in forms that can be directly used without transformation (solar heat, geothermal water); energy transformation is always related to energy losses; the term “energy carrier” is used for any matter or process that contains energy that can be transformed into other form on-site; meanwhile, fuels are materials that contain chemical or nuclear energy that can be converted on-site at specific conditions into the heat by combustion or nuclear decay;

- distribution of energy carriers or fuels to the end users by infrastructure systems (pipelines, high voltage electricity grid, roads); distribution is always related to the energy losses.

Warnings from climatologists about global climate changes and social studies that show that the prosperity of society can be achieved simultaneously with decreased energy use confront modern society with two challenges: more efficient use of energy and intensive utilization of renewable energy sources, which are locally available and which causes much less environmental pollution in comparison to non-renewable energy sources (Fig. 2.1).

Following use of primary energy sources through the history of human race, the short period of fossil fuels dominance in which we live today can be observed. It starts less than 200 years ago at the beginning of Industrial Revolution, symbolized by invention of steam engine and use of coal. The dominance of non-renewable energy sources will end in this century, not only because shortage of reserves of non-renewable fossil fuels, but because of the development of renewable energy technologies, driven by global and regional environment protection policies, will enable cheaper and more sustainable energy supplies (Fig. 2.2).

Fig. 2.1 Conversion of primary energy into final energy that is available to end users



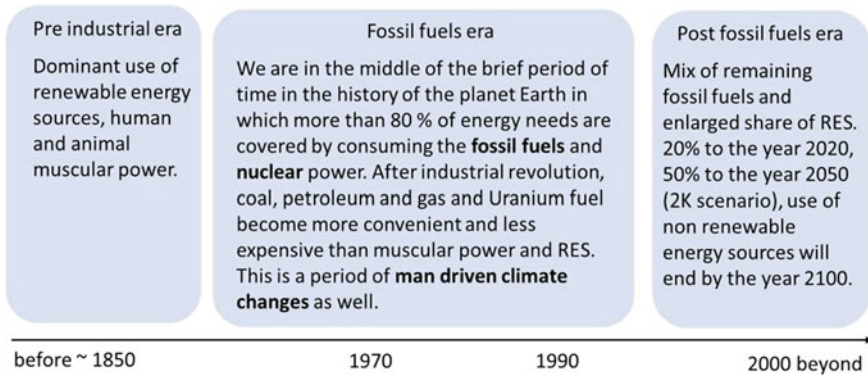


Fig. 2.2 Role of renewable and renewable energy sources in energy supply in the last 200 years

2.1 Renewable Energy Sources (RES)

Renewable energy sources are constantly generated in the environment by natural processes and contain different forms of energy as the results of the transformations of the following primary energy sources:

- solar energy that arrives on the Earth surface in form of electromagnetic radiant flux that is emitted by the photosphere of the Sun; in nature, solar energy it is transformed into environmental heat, wind, waves, hydro energy, grove of biomass;
- planetary or gravitational energy which results from the interaction of gravitational and centrifugal forces between the Earth, Moon and Sun, causing periodical changing of potential and kinetic energy in water reservoirs as tidal energy;
- geothermal energy is heat that is transferred from the hot core of the Earth, where it is constantly generated as geothermal energy by the nuclear decay of radioactive chemical elements, such as uranium and thorium.

Renewable energy sources will be generated for the next 5–10 billion years; consequently, they are treated unlimited and thus sustainable energy sources (Fig. 2.3).

Renewable energy sources have some distinct advantages because they are time unlimited, have a potential that is much greater than current energy demand; they are fairly evenly distributed throughout the planet and have no geo-political barriers. The transformation of renewable energy sources into other forms of final energy has, in general, little or no impact on environment. The disadvantages of renewable energy, such as low energy density or inconsistency, will be overcome in the future with intensive research and new technical solutions and especially with the transition to a sustainable, circular economy (Fig. 2.4).



Fig. 2.3 Solar energy, gravitational planetary energy, and geothermal heat are natural energy sources that will be available for humans for the next 10 billion years. Several energy forms called “renewable energy sources” available in nature, like wind, tidal or hydro energy, are generated from these sources (left: National Aeronautic and Space Administration www.nasa.gov); (middle: National Aeronautic and Space Administration www.earthobservatory.nasa.gov); (right: blog.hawaiiinilvi.blogspot.si)



Fig. 2.4 Low energy density is one of the drawbacks of RES; one turbine presented on the picture with rotor diameter of 70 m, has power of electricity generator comparable with mechanical power of the motor of F1 racing car; despite that, electricity production by wind turbines is cost effective especially with off shore applications because of the higher wind speeds in comparison to those on the land (<http://wonderfulengineering.com/38-high-def-wind-turbine-pictures-from-around-the-world/>)

2.1.1 Solar Energy

Solar radiation is transformed in nature into the different forms of energy. The majority of these forms are transient; only in the form of biomass and heat stored in oceans is solar energy stored in nature. Solar energy is the most important energy source for the Planet Earth (Fig. 2.5).

Solar energy is generated in sun core by the fusion of hydrogen atoms into helium atoms. The reduced mass of the matter as a result of this nuclear reaction is transformed into energy. With different mechanisms, energy is transferred from the sun core to the photosphere from which the sun emits thermal radiation in form of electromagnetic radiation. The temperature of the photosphere (~5760 K) and fact that the sun is a black body, define the wavelength of electromagnetic radiation; it is in the range between 0.1×10^{-6} m (100 nm) and $+1000 \times 10^{-6}$ m. The total emitted radiation of the photosphere is determined by Stefan-Boltzmann law for black body emitters (Fig. 2.6).

Solar radiation reaches the outer surface of the atmosphere of Earth as extraterrestrial radiation. The rate of extra-terrestrial solar irradiation per unit or the area perpendicular to sun rays is called the “solar constant” G_{ex} , which is defined as

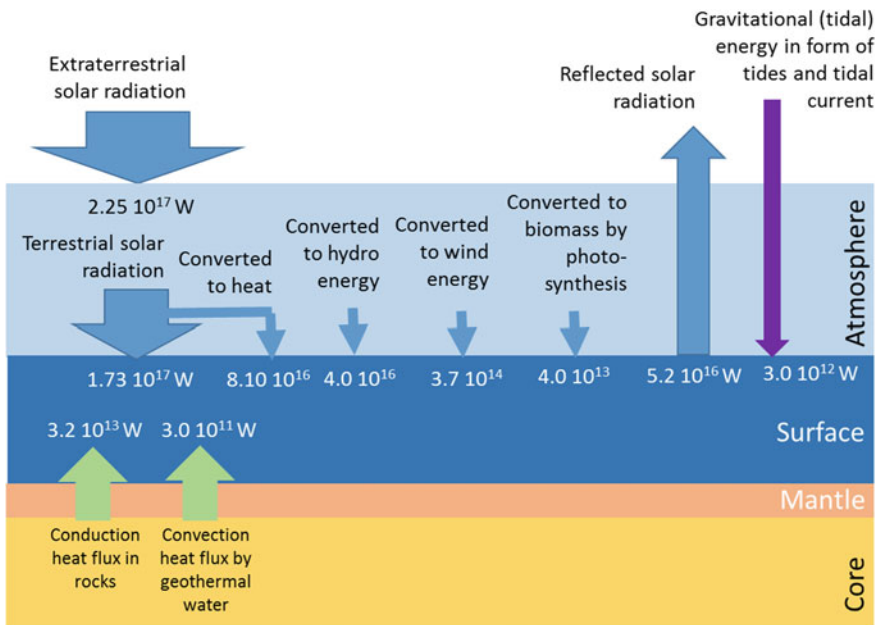


Fig. 2.5 Average annual energy flows on the Earth in W; around 70% of extraterrestrial solar radiation is available on the planet, most in form of sensible heat of environment and latent heat of water vapour in the natural water cycle; only a minority of terrestrial solar radiation is used by plants for photosynthesis; geothermal and tidal energy flows are much smaller in comparison to solar energy but much higher than the energy currently needed by human race in form of non-renewable energy sources

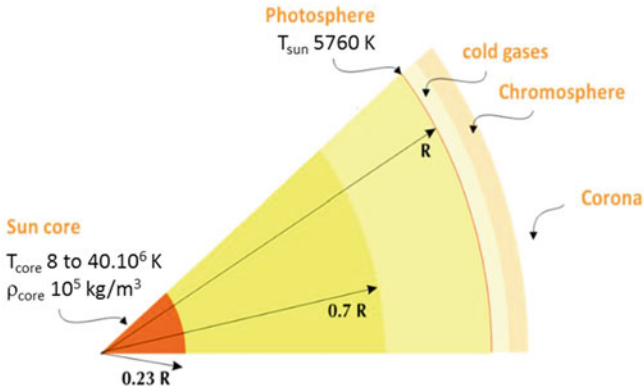


Fig. 2.6 Energy generated in the Sun’s core by nuclear fusion is emitted by the photosphere as electromagnetic radiation; the photosphere has a quite low temperature and consequently emits radiation with wavelength in the range between 0.1×10^{-6} m (100 nm) and $+1000 \times 10^{-6}$ m

the ratio between total radiation flux emitted by sun’s photosphere and the area of the sphere with diameter equal to the Sun-Earth distance (Duffie and Beckman, 1991). Considering the Sun’s radius ($r \sim 0.695 \times 10^9$ m), the temperature of the photosphere ($T_{sun} \sim 5760$ K), and the distance between the Sun and Earth ($R \sim 1.498 \times 10^{11}$ m), the solar constant is equal to:

Stefan-Boltzmann's law expression

$$G_{ex} = \frac{\dot{Q}_{sun}}{A_R} = \frac{A_{sun} \cdot \sigma \cdot T_{sun}^4}{A_R} = \frac{4 \cdot \pi \cdot r^2 \cdot \sigma \cdot T_{sun}^4}{4 \cdot \pi \cdot R^2} \quad (W/m^2)$$

area of sphere with radian equal to distance between Sun and Earth (m²)

$$G_{ex} = \frac{4 \cdot \pi \cdot (0.695 \cdot 10^9)^2 \cdot 5.67 \cdot 10^{-8} \cdot 5760^4}{4 \cdot \pi \cdot (1.498 \cdot 10^{11})^2} = \sim 1350 \text{ W/m}^2$$

Note: The term “radiation” is used for radiation emitted from the emitter surface, the term “irradiation” for radiation on the receiver surface. Both are

measured in watts (W) as total heat flux or in W per m² of emitted/received area as rate (density) of heat flux.

Solar constant is measured on the plane that is perpendicular to the sun rays and, as such, represents the maximum solar irradiation. Because the Earth’s path around the Sun is not circular, the solar constant varies through the year. In simplified forms, the day-by-day value can be determined with the equation (Hsieh, 1986)

$$G_{ex,N} = G_{ex} \left[1 + 0.033 \cdot \cos \left(\frac{360 \cdot N}{365} \right) \right]$$

yearly average value of extraterrestrial solar irradiation (W/m²)
day of the year (-)

When passing the atmosphere, part of solar irradiation is absorbed and dispersed on the molecules of gases and on the particles. As result, solar irradiation on the surface of the Earth (G_o) is lower in comparison to extra-terrestrial irradiation (G_{ex}). The attenuation of solar radiation traveling through the atmosphere can be expressed by “air-mass” (m), which depends on the length of sun rays’ path through the atmosphere and the optical condition (pollution) of the atmosphere. In geometric form, air mass is defined by the sun’s altitude angle α_s or zenith angle z (EN ISO 52010-1,¹ for α_s > 10 °C) (Fig. 2.7):

$$m = \frac{1}{\sin \alpha_s} = \frac{1}{\cos z} \quad (-)$$

sun altitude angle (°)
sun zenith angle (°)

Air mass is equal to 1 if Sun is in the zenith (α_s = 90°) and increases with the decreasing of the sun’s altitude angle. According to air-mass, spectral terrestrial solar irradiation can be defined for specific wavelengths and as integral tp spectral irradiation over the range of wavelengths as total terrestrial solar irradiation (Fig. 2.8).

Note: In engineering practice, wavelengths of solar radiation are limited to range between 0.3 and 3 μm despite the fact that photosphere emits radiation in wavelengths range between 0.10 μm and up to 1000 μm. Wavelengths below 0.3 μm are absorbed by stratospheric ozone; wavelengths above 3 μm are not transmitted through ordinary glass. This wavelength range includes 97% of solar radiation power.

¹EN ISO 52010-1:2017 Energy performance of buildings—External climatic conditions—Part 1: Conversion of climatic data for energy calculations

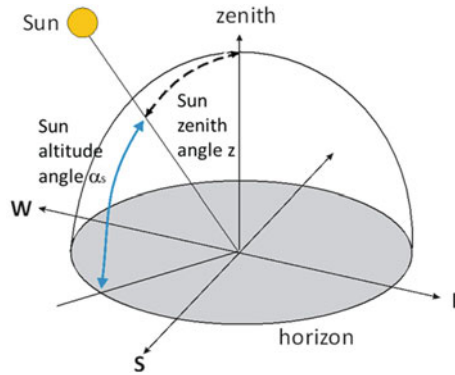


Fig. 2.7 Sun’s altitude angle α_s is the angle between sun ray and horizontal plane; the sun’s altitude angle is maximum during the day at solar noon and equal to zero at sunrise and sunset

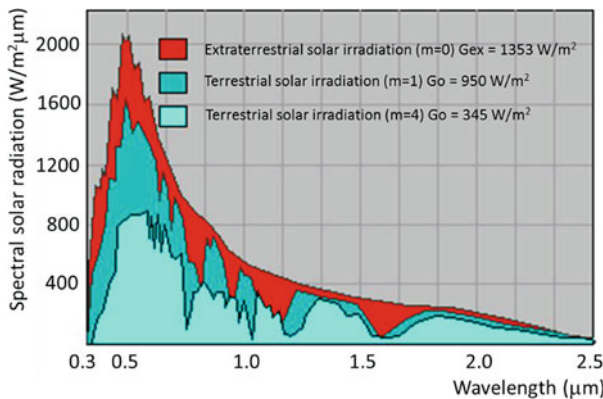


Fig. 2.8 Spectral solar radiation on the outer surface of the atmosphere known as extraterrestrial solar irradiation can be compared to theoretical blackbody emitted radiation; on the path through atmosphere, solar radiation is absorbed by molecules of gasses and particles and, as result, total terrestrial solar irradiation (area below spectral radiation curve) decreases with increased air mass

Solar terrestrial irradiation that comes directly from the sun as beam radiation is maximal on the surface that is perpendicular to the sun beams (G_b). Solar beam irradiation on a horizontal surface is lower (unless the sun is in the zenith), and it is called direct horizontal solar irradiation ($G_{dir,o}$). Direct solar irradiation on a tilted surface ($G_{dir,\beta}$) at a particular position of the sun during the year is defined by current zenith angle z , incident angle I (angle between of sun beams and normal of receiving surface), as shown in Fig. 2.9.

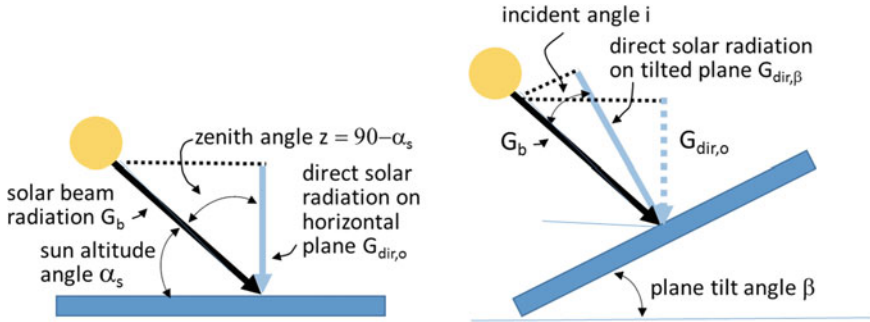


Fig. 2.9 Direct solar irradiation on tilted surface $G_{dir,\beta}$ is determined by direct solar irradiation on the horizontal plane, the sun’s zenith angle (z) and the incident angle (i)

$$G_b = \frac{G_{dir,o}}{\cos z} = \frac{G_{dir,\beta}}{\cos i} \rightarrow G_{dir,\beta} = G_{dir,o} \frac{\cos z}{\cos i} \quad (W/m^2)$$

↑ zenith angle (°) ↑ incident angle (°)

In addition to direct solar irradiation, the surface receives diffuse irradiation from the sky. The amount of diffuse irradiation depends on the cloudiness of the sky and the part of the sky exposed to the receiving surface. Empirical extensions (e.g. Liu-Jordan correlation or Rabl correlation) are used for the calculation of diffuse solar radiation. If the plane is tilted, it receives solar irradiation that is reflected from its surroundings. Therefore, global solar radiation on the tilted plane $G_{glob,\beta}$ is the sum of direct, diffuse, and reflected solar radiation.

By integration of global solar irradiation on particular surface through time frame (hour, day, month or year), energy of solar radiation can be determine. Annual solar radiation is common used for presenting the potential of solar energy for specific location as it is shown in Fig. 2.10 in case of Slovenia.

2.1.2 Geothermal Energy

Heat in the core of the Earth arises from yet another nuclear reaction – energy fission (decay) of heavy natural radioactive chemical isotopes, such as uranium (U^{238}), thorium (Th^{232}) and potassium (K^{40}). Total energy flux is constantly generated in the Earth’s interior. Geologists estimate that over the next 10 billion years, 44 TW including contribution of 20 TW from decay of U^{238} and Th^{232} and 4 TW from decal of K^{40} will be generated (Ragheb 2017). Heat is generated from the kinetic energy of high-speed isotopes particles that collide with surrounding materials in the Earth core, which heats up to 5000–6000 K.

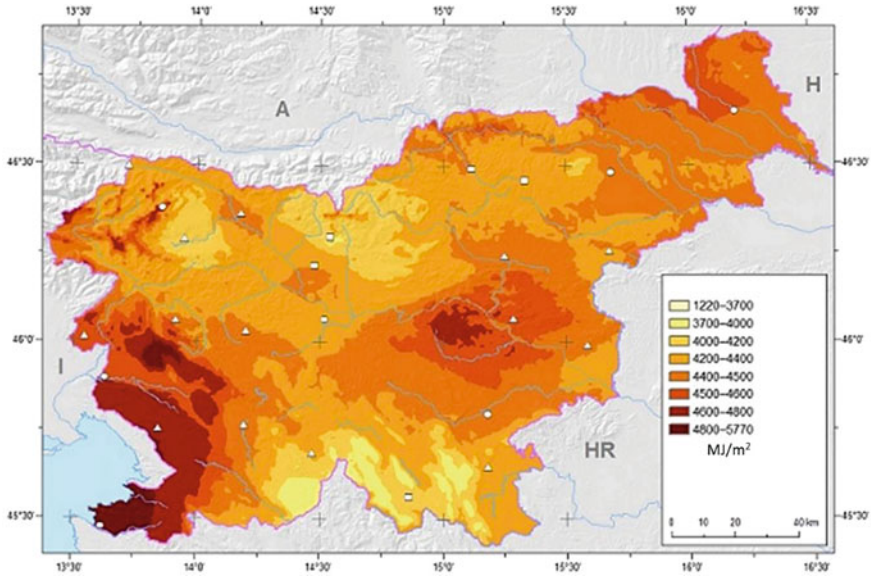


Fig. 2.10 Long-term average annual solar radiation on horizontal plane for the period between the year 1994 and 2010, expressed in kWh/m² on the territory of Slovenia (Kastelec et al. 2007)

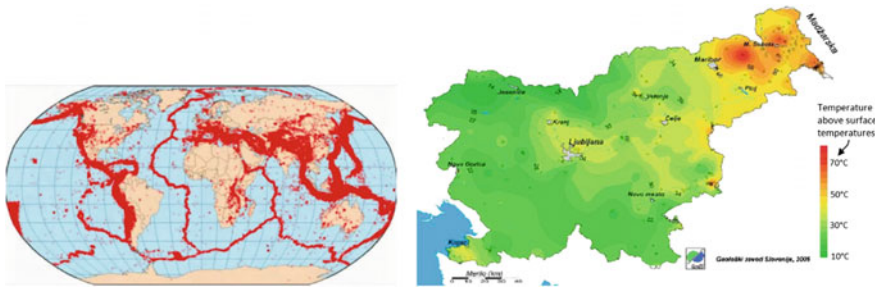


Fig. 2.11 Areas along boundaries of tectonic plates have the largest geothermal potential (left; Ragheb 2017); temperatures 1 km beneath the surface on Slovenian territory indicate significant geothermal potential in the north-eastern region (right) (Geothermal potential in Slovenia, Geološki zavod Slovenije, 2008)

Geothermal heat is transferred towards the surface by conduction and convection heat transfer. Conduction heat flux through impermeable mantle and crust occurs because of temperature gradient; nevertheless, the heat flux is rather low because of the low thermal conductivity of rocks ($\sim 1\text{--}3 \text{ W/mK}$). Heat transfer via the convection of geothermal water enables much more intense heat transfer. Geothermal water, as part of the Earth’s water cycle, heats up in deep permeable aquifers to up to 250 °C. The geothermal energy potential is higher at locations along the tectonic plate boundaries, as shown in Fig. 2.11, because the magma layer is shallow.

Geothermal water rises in the form of natural geothermal springs or it can be pumped into utilization systems for agriculture, heating, and electricity production. Geothermal energy potential is commonly expressed as the temperature gradient of soil temperatures on the surface and at the depth of 1 km. Areas with geothermal temperature gradient above 80 K per km have great geothermal energy potential, while moderate geothermal potential is characteristic for areas where geothermal the temperature gradient is at least 50 K/km.

2.1.3 Tidal Energy

Tidal energy results mostly from gravitational attraction between Moon and Earth; even the Sun contributes to tidal phenomena because of its large mass. Tides in oceans are quite low (~ 0.5 m) but can be much higher (up to ~ 15 m) in some parts of the world at the shore due to coastal contours and estuaries. Tidal energy can be utilized in two ways:

- by utilization of potential energy of periodic changing of water column level. and
- by utilization of kinetic energy of tidal flow which can reach up to 5 m/s on some coastal areas (Figs. 2.12 and 2.13).

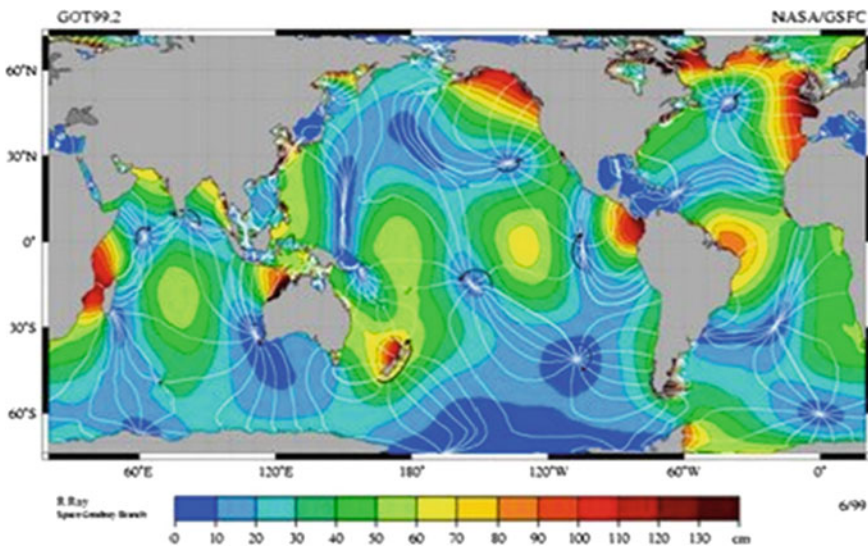


Fig. 2.12 Tidal energy potential depends significantly on geographic location; unlike most of renewable energy sources, it can be precisely predicted regarding its time of appearance (www.nasa.gov)



Fig. 2.13 Tidal current can be utilized by underwater turbines (Whole Building Design Guide, www.wbdg.org/resources/oceanenergy.php)

Utilization of tidal-related energy forms is possible only in limited areas along the coasts of seas and oceans and in general cannot be used for on-site and near-by energy production as required for nearly Zero Energy Buildings.

2.2 Fuels as Energy Carriers

At specific conditions, fuel can release chemical energy, which binds atoms in the molecules of the fuel in the form of heat in the process called combustion. Combustion is a thermochemical reaction. In addition to the fuel, the presence of air (oxygen) and high temperatures of the fuel and air mixture must be provided. The amount of air needed for complete combustion is called a stoichiometric quantity. Complete combustion results in maximum realisation of heat at the lowest environmental pollution. In the practice, combustion can only be close to the complete. Beside heat, the combustion process generates flue gasses and possible solid unburned particles. Because biomass fuels can contain a high share of water and non-combustible material, the process of the combustion of these fuels is the most complex.

The combustion of biomass consists of several phases, starting with drying that occurs at the temperature up to 150 °C in two phases—by evaporation of surface

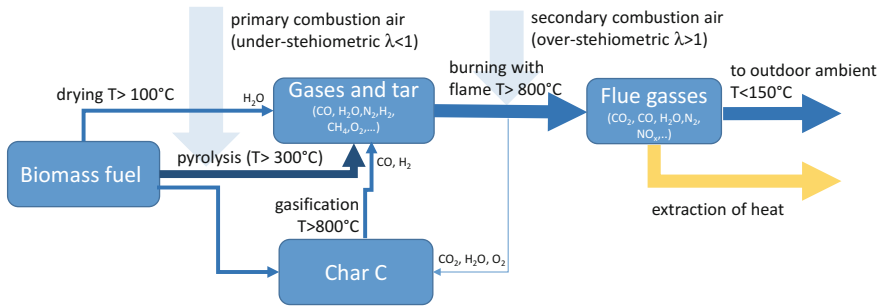
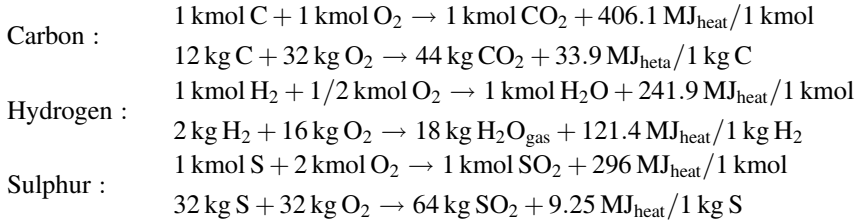


Fig. 2.14 Thermo-chemical reaction of biomass fuel combustion (adopted from Nussbaumer 2003)

moisture and evaporation of inherent moisture at higher temperatures. Only after moisture is removed from the biomass fuel, does pyrolysis as process of decomposition of biomass fuel into volatile components in form of gases (CO, CO₂, H₂ and H₂O) and tar start at temperatures 200–300 °C. Primary combustion air (below the stoichiometric amount) is supplied during this phase to control the amount of the fuel to decomposition. In this phase, 70% of biomass fuel decomposes and, as result of supply of additional amount of air (secondary combustion air), the burning of volatile compounds starts at temperatures higher than 800 °C. During the pyrolysis and combustion phase some fuel remain solids in the form of char (carbon). At higher temperatures (>800 °C) and with the presence of gasses like CO₂, H₂O and O₂, gasification of carbon starts, and the results are combustible gasses CO and H₂. Oxidation of those gasses increases amount of produced heat (Fig. 2.14).

The described process is called “direct combustion”. The process of pyrolysis and gasification can be used for the production of gaseous and liquid fuels. If combustible gasses are the main product of pyrolysis, such process is called “gasification”. Biofuels can also be produced with bio-chemical reactions; for example, with the alcoholic fermentation of sugars, ethanol can be produced or with anaerobic digestion in an oxygen-free environment, where microorganisms use carbon compounds to produce biogas, a mixture of CO₂, CH₄ and some other combustible gasses.

The quantity of realized heat can be determined theoretically by stoichiometric equations, which are mass-weighted chemical balance equations. This equations indicate the amount of reactants, the amount of products, and the quantity of realized heat. For three combustible elements in fuels, the following stoichiometric equations are valid:



Note: 1 kmol is 1 kg molecular weight, which is a mass equivalent to the sum of the atomic weights, expressed in kg; 1 kmol of hydrogen gas has a mass of 2 kg, because the hydrogen molecule consists of two atoms; molecular weight of C is 12 kg/kmol, O 16 kg/kmol and S 32 kg/kmol.

In practice, the combustion process is only near to complete and the amount of heat realized is lower than the stehiometric value. In engineering practice, combustion heat realised by fuel burning is express as:

- lower calorific value LCV (lower heating value, net calorific value, H_i) or
- gross calorific value GCV (higher heating value, H_s).

In the case of LCV, it is assumed that the water vapour from the drying of the fuel and the oxidation of hydrogen remain in the fuel gases in gaseous form, and heat is gained only from the combustion process. If flue gasses are cooled below the dew point temperature of water vapour, the condensation or latent heat of water vapour is gained. The sum of sensible heat released by burning and latent heat of water vapour is expressed as gross calorific value. The difference between lower and gross calorific value of the fuel is greater if the amount of hydrogen in fuel is higher. The difference is app. +5% in the case of heating oil, and +11% in the case of methane (natural gas).

Case Study How much is the difference between LCV and GCV for hydrogen. LCV is equal to 121.4 MJ/kg and 9 kg of water vapour occurs from 1 kg of hydrogen. Condensation heat r of water vapour is 2.5 MJ/kg H_2O .

$$\text{GCV} = \text{LCV} + w_{\text{H}_2\text{O}} \cdot r \rightarrow 121.4 + 9 \frac{\text{kg}}{\text{kg}} \cdot 2.5 \frac{\text{MJ}}{\text{kg}} = 143.9 \frac{\text{MJ}}{\text{kg}}$$

Note: Mass weights are rounded.

If the quantity of chemical elements in fuel are not known, calorific value is determinate by experiment—burning a small amount of the fuel in oxygen

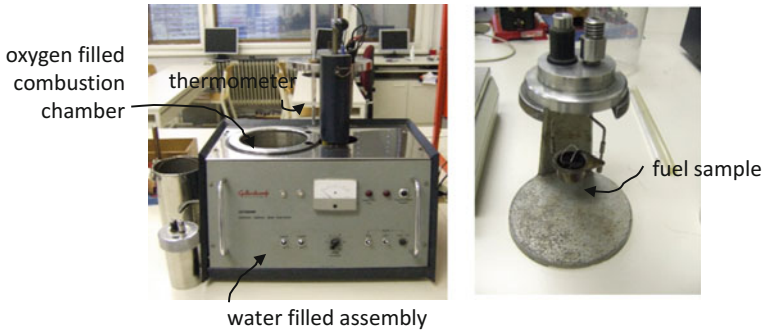


Fig. 2.15 LCV and GCV calorific values of fuel could be determined experimentally by burning a small amount of the fuel in oxygen atmosphere using a “bomb calorimeter”

atmosphere using a “bomb calorimeter”. After the fuel and oxygen react, heat is transferred to the water in container. Since the mass of water is known, the realized heat can be calculated on the basis of the temperature differences of the cooling water. If fuel gases are cooled below 150 °C, the gross calorific value of the fuel is measured (Fig. 2.15).

2.2.1 Non-renewable Fossil Fuels

Fossil fuels, as natural but non-renewable sources, are composed of various compounds of Hydrogen and carbon, and other chemical compounds (S, O, N, water). The oldest fossil fuels are about 500 million years old. They originate from organisms deposited on the bottom of the oceans and decomposed by bacteria. It is very slow process, taking between 3000 and 10,000 year or longer. Therefore, fossil fuels are not renewable energy sources and the supply is based solely on existing reserves.

The physical state of fossil fuels depends on number of carbon atoms in fuel molecule. They are solid if molecules consist more than 20 carbon atoms; they are liquid if number of carbon atoms are between 4 and 20, and gaseous if the number of carbon atoms is less than 4. As organic matter, fossil fuels consist other organic elements, including oxygen, sulphur, nitrogen, and minerals.

For heat production in buildings, the following fossil fuels are commonly used.

2.2.1.1 Natural Gas

Natural gas (NG) is gaseous hydrocarbon fuels extracted from underground deposits in porous formation. Natural gas consist of 93% of methane (CH_4), small amounts of ethane (C_2H_6), propane (C_3H_8), butane (C_4H_{10}) and some nitrogen, but no sulphur. Consequently, slightly higher levels of nitrogen oxides (NO_x) are present in flue gasses,

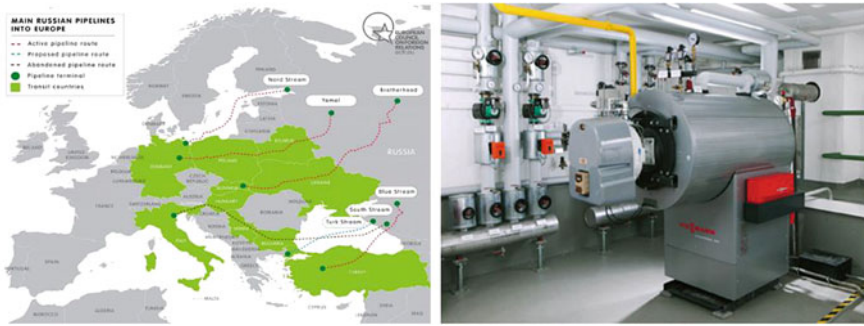


Fig. 2.16 Several new pipelines are currently being built to secure supply of EU by Russian natural gas (left: www.ecfr.eu); natural gas is transported in buildings in yellow pipes (right: www.viesmann.com)

but without the emission of sulphur oxides. Because the highest ratio between hydrogen and carbon atoms is in the methane molecule, emissions of greenhouse CO_2 per kWh of realized heat are the lowest among fossil fuels ($\sim 200 \text{ g/kWh}_t$). Natural gas is transported in gaseous form in pipelines. With compression, methane can be liquefied (LNG), but a large amount of energy is needed for liquidification, and such a supply is economical on long distance by tankers and for storing. Natural gas is about 40% lighter than air, so should it ever leak, it can dissipate into the air. Other positive attributes of natural gas are a high ignition temperature and a narrow flammability range, meaning natural gas will ignite at temperatures above 1100° and burn at a mix of 4–15% volume in air (Fig. 2.16).

The LCV of natural gas (content 93% of methane) is 35.14 MJ/m^3 ($\sim 9.8 \text{ kWh/m}^3$), GCV is 38.96 MJ/kg ; (at 0°C and 1013 mbar).

Note: Caloric values can defer regarding to local conditions at the place of pumping.

2.2.1.2 Liquefied Petroleum Gas

Liquefied petroleum gas (LPG) is mixture of propane (C_3H_8) and butane (C_4H_{10}) and some other gases. These gases are produced by distillation of petroleum in a fractionating column. As the temperature of the column decreases from bottom to top, more volatile components (gaseous) are condensed towards the top of the column. Propane and butane can be liquefied at high pressure (propane 22 bar, butane at 2 bars) or at low temperature (propane -45°C , butane $\sim 0^\circ \text{C}$). As a liquid, the volume decreases to $1/270$. As such, it can be easily transported by trucks



Fig. 2.17 Transportation of LPG. LPG is stored in the external or underground reservoirs. Environment heat is used for the evaporation of LPG into gas before entering the distribution pipeline in building

and stored on site in reservoirs. In cold climates and when reservoirs are located outdoor, LPG contains mostly propane because it vaporizes at a lower temperature than butane. When the reservoir is placed underground and indoors, LPG is commonly a mixture of 35% of propane and 65% of butane. Unlike methane, propane and butane are heavier than air and remain at the bottom of the room in case of leaking. With small units, the external surface of reservoir is large enough to transfer the heat to vaporize the LPG; for larger units, additional vaporizer is needed.

Like NG, LPG is sulphur-free but emissions of CO_2 are slightly higher (210 g CO_2 per kWh_T). The LCV of propane is 92.9 MJ/m^3 or 46.3 MJ/kg ($\sim 12.9 \text{ kWh/kg}$), GCV is 50.3 MJ/kg ; LCV of butane is 121.9 MJ/m^3 or 45.8 MJ/kg ($\sim 12.7 \text{ kWh/kg}$) and GCV 132 MJ/m^3 or 49.5 MJ/kg (at 0°C and 1013 mbar) (Fig. 2.17).

2.2.1.3 Lightweight Heating Oil

Heating oil is produced similarly to LPG from crude oil. Molecules of heating oil have 15–18 atoms of carbon; consequently, their emissions of CO_2 are larger (260 g CO_2 per kWh_T). Because part of the carbon in the fuel not oxidized, emissions of solid particles (PM) are problematic. As lightweight heating oil has a relatively high content of sulphur, emissions of sulphur-dioxide that cause acidification of precipitation also affect the environment. In buildings, heating oil is stored in reservoirs made from steel, PVC, or PC. The floor of the room with reservoir must be water tight to prevent leakages of oil into underground water. An alternative solution is double-wall reservoirs with leaking sensors in the space between the walls. Only such reservoirs can be buried directly into the ground.

The GCV of heating oil is in the range between 38.1 and 42.6 MJ/l (10.58–11.8 kWh per litre) and LCV is assumed as 40.0 MJ/l (11.12 kWh per litre) (Fig. 2.18).



Fig. 2.18 Reservoirs for lightweight heating oil must be placed in a watertight pool to prevent the leakage of oil into ground water or must be made as double wall tanks with integrated leakage sensors

2.2.2 Renewable Fuels Made from Biomass

Most renewable fuels are produced from biomass, which is organic matter produced by plants by photosynthesis. Organic matter is produced by converting sun light, absorbing CO_2 from air and using nutrients that plants receive from soil. It is assumed that only 0.1% of solar energy is transformed into organic mass by photosynthesis worldwide on a yearly average. In forests, photosynthetic efficiency is $\sim 1\%$. The highest photosynthesis efficiency is in so-called C4 plants, such as corn and sugar cane (the first product of photosynthesis is a 4-carbon sugar). In nature, C3 plants (wheat, soybeans, trees; the first product of photosynthesis is 3-carbon sugar) prevail.

The environment efficiency of biomass growth could be measured by water-use efficiency (WUE). This is ratio between amounts of CO_2 absorbed by plant normalized to 1 g of water transferred by plant from the soil. In addition to the type of the plant, WUE depends on the concentration of CO_2 in the air. The most efficient plant is soya (WUE 15 mg $\text{CO}_2/\text{g H}_2\text{O}$) at a concentration of 900 ppm CO_2 in the air (Fig. 2.19).

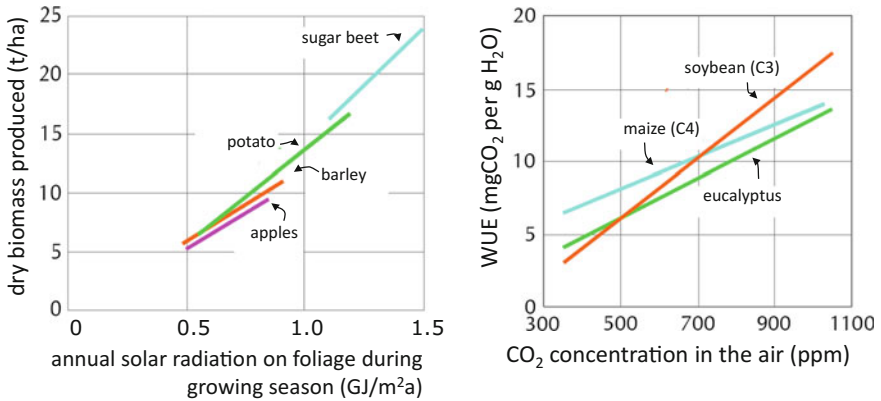


Fig. 2.19 The quantity of produced dry biomass is related to solar radiation on the foliage surface during the growing period (left); the WUE (water-use-efficiency) of plant is defined by the mass of water that plant uses for the transportation of nutrients from the soil, and it mostly evaporates on the surfaces of the leaves or needles to the mass of CO₂ fixed in the plant by photosynthesis; average planetary concentration of CO₂ in the air is ~360 ppm; it can be seen that at such CO₂ concentration in the air, plants on average need 300–1000 tonne of water to produce 1 tonne of dry biomass (right) (adopted from Johansson et al. 1993)

Case Study Determine the amount of CO₂ fixed by photosynthesis in 1 m³ of soft wood. Use an equation from standard EN 16449.² How much water does a plant need for the fixation of CO₂ from the air if WUE is equal to 5 mg CO₂/g H₂O?

$$P_{CO_2} = \frac{44}{12} \cdot C_f \cdot \frac{\rho_{wood} \cdot V_{wood}}{1 + \frac{\psi_{wood}}{100}}$$

Labels for the equation above:
 - 44: molecular weight of CO₂ (g/mol)
 - 12: molecular weight of C (g/mol)
 - C_f: share of carbon in wood (-/typical 0,5)
 - ρ_{wood}: wood density (kg/m³)
 - V_{wood}: wood volume (m³)
 - ψ_{wood}: volume of moister in dry wood (%); (typical 10-12%)

$$P_{CO_2} = \frac{44}{12} \cdot 0.5 \cdot \frac{550 \cdot 1}{1 + \frac{12}{100}} = 900 \text{ kg/m}^3$$

For the fixation of 900 kg of CO₂ from the air, 180 tonnes of water is used by tree.

²EN 16449:2014 Wood and wood-based products - Calculation of sequestration of atmospheric carbon dioxide

The combustion heat of biomass fuels can be calculated if the composition of fuel is known from measurement or empirical data regarding to the type of the wood. In this case, the LCV in GCV of biomass fuels can be calculated, taking into account the mass share of carbon, hydrogen, sulphur, oxygen, and water by empirical expressions (AEBIOM 2008):

$$\begin{aligned}
 \text{LCV} &= 33.9 \cdot w_C + 121.4 \cdot \left(w_H - \frac{w_O}{8} \right) + 9.25 \cdot w_S - 2.5 \cdot w_{H_2O} \quad \left(\frac{\text{MJ}}{\text{kg}} \right) \\
 &\quad \begin{array}{l} \text{mass share of carbon (kg/kg)} \\ \text{mass share of hydrogen (kg/kg)} \end{array} \quad \begin{array}{l} \text{mass share of oxygen (kg/kg)} \\ \text{mass share of sulphur (kg/kg)} \end{array} \quad \begin{array}{l} \text{mass share of water (kg/kg)} \end{array}
 \end{aligned}$$

$$\begin{aligned}
 \text{GCV} &= \text{LCV} + 2.5 \cdot (w_{H_2O} + 9 \cdot w_H) \quad \left(\frac{\text{MJ}}{\text{kg}} \right) \\
 &\quad \begin{array}{l} \text{by burning 9 g of water vapour is} \\ \text{released from 1 g of hydrogen} \end{array}
 \end{aligned}$$

Case Study Calculate LCV and GCV of biomass fuel produced from a coniferous tree that consists of 0.457 kg of carbon per kg of fuel, 0.063 kg/kg of hydrogen, 0.350 kg/kg of oxygen, 0.02 kg/kg sulphur and 0.06 kg/kg of water and 0.05 kg/kg of ash.

$$\begin{aligned}
 \text{LCV} &= 33.9 \cdot 0.457 + 121.4 \cdot \left(0.063 - \frac{0.35}{8} \right) + 9.25 \cdot 0.02 - 2.5 \cdot 0.06 = \\
 &= 17.87 \frac{\text{MJ}}{\text{kg}} = 4.96 \frac{\text{kWh}}{\text{kg}}
 \end{aligned}$$

$$\text{GCV} = \text{LCV} + 2.5 \cdot (0.06 + 9 \cdot 0.063) = 21.00 \frac{\text{MJ}}{\text{kg}} = 5.833 \frac{\text{kWh}}{\text{kg}}$$

Note: Values are stated for the sample of commercial product. If mass shares refer to dry fuel, the content of water will be 0 kg/kg. Ash is not combustible.

2.2.2.1 Solid Biomass Fuels

The most commonly used biomass fuel is solid logwood. The combustion heat of logwood depends predominately on water content:

- freshly cut wood (with humidity around 60% for coniferous trees and 50% for deciduous) has average low caloric value (LCV) 7–8 MJ/kg,



Fig. 2.20 Solid wood biomass fuels in form of grafted wood, woodchips, pellets and briquettes (from left to right; Malamateinios et al. 2017)

- fire wood should have humidity less than 30%; freshly cut wood has such content of water after one year of drying in open space, LCV is around 12.2 MJ/kg,
- dry wood (heated to 105 °C for few days) has LCV equal to 19 MJ/kg.

Note: Values differ depending on type of wood and meteorological conditions.

Solid biomass fuels can also be produced from waste wood and farm crops in the form of:

- dry or moist wood chips (LCV ~ 12 MJ/kg);
- pellets or briquettes made of dry biomass (LCV ~ 18 MJ/kg); because these types biofuels are made of preselected dry raw biomass, these are the only biomass fuels whose quality is standardized. EN 14961-2 defines three quality classes of pellets: A1, A2, and B. The classification is done regarding water content (should be less than 10%, bulk density (>600 kg/m³), mechanical stability, ash content (<0.7%) and LCV. Classes differ mainly on the basis of ash content;
- hay bales and other waste farm crops (LCV ~ 14 MJ/kg). (EN 14961-2³) (Fig. 2.20)

While logwood and chips are stored outside and protected against moisture, pellets must be stored in water vapour tight reservoirs. Reservoirs are connected to a mechanical or pneumatic transportation system that transports the pellets (or wood chips) into the biomass boiler (Fig. 2.21).

2.2.2.2 Liquid Biomass Fuels

Biodiesel and bioethanol (C₂H₅OH) are the most common liquid fuels that are produced from biomass. Biodiesel is produced from refined vegetable oil and

³EN 14961-2:2011 Solid biofuels—Fuel specifications and classes—Part 2: Wood pellets for non-industrial use.



Fig. 2.21 Outdoor storage for wood chips (left); outdoor silos for pellets (right) (www.mywoodpelletsolution.com)

animal fat. Bio-oils could be used as fuels but their gasses are toxic, and the fuel solidifies at winter temperatures. In reaction with methanol and potassium hydroxide (KOH), called transesterification, oils are transformed into volatile esters (crude biodiesel), and glycerine is the by-product. After refining, methanol is recovered, and biodiesel is the end product. Up to 1000 L per hectare per year of biodiesel can be produced from sunflowers or rapeseed and up to 5000 L per hectare per year from palm oil (Twidell and Weir 1986).

Bioethanol is produced by microorganisms in the process of alcoholic fermentation under acidic conditions (pH 4–5). Plants that contain sugar (e.g. sugarcane or sugar beet) are conventionally used as feedstock (1st generation bioethanol). Bioethanol is separated from water mixture by distillation. Cellulose biomass can also be used as feedstock material, but an additional process of decomposition of lignocellulose in sugars by hydrolysis by enzymes is needed (2nd generation). Up to 3500 l of ethanol can be produced from sugarcane per hectare per year.

Liquid biofuels are mostly used for the replacement of fossil diesel and petrol fuels in the transportation sector. Due to high prices and lifecycle environmental impacts that include farming and fuel extraction, this fuels are not commonly used as energy carriers for building energy supply.

2.2.2.3 Gaseous Biomass Fuels

Gaseous biofuels are produced by the decomposition of carbohydrate material by bacteria in wet, warm and dark environments without the presence of oxygen, in a process called anaerobic digestion. It occurs in a closed environment called a ‘biomass digester’ or in landfills where municipal waste is treated. Carbohydrate material (generally in the form of a $C_cH_hO_o$ molecule) is decays into CO_2 (by the oxidation of carbon) and into CH_4 (by the reduction of biomass molecules).

Digesters are often used at the mid-stage of a waste-water treatment system, in which soluble organic pollutants are converted into biogas by bacteria. Cleaned water is free of biodegradable materials and can be used for irrigation or drain down to the surface watercourse. The amount of produced biogas and contents of the combustible gases depends on the temperature and pH of the sludge. Temperatures in the range 35–37 °C are ideal, and the pH value of the sludge must be in the range between 6.5 and 7.5. In such conditions, decomposition of organic material takes 1–3 weeks and the produced biogas consists of 50–70% of methane (CH₄), 25–40% of CO₂, some N₂, H₂, O₂ as well as volatile organic compounds.

Landfill disposal of municipality waste has been a commonly used technology for solid waste treatment. Solid waste that contains a high portion of organic waste is compacted on landfill fields. This leads to an oxygen-free environment and organic wastes are processed by anaerobic bacteria and converted to the landfill gas. The anaerobic decomposition of solid organic material is a very slow process, and landfill gas is produced for 30 years and beyond after disposal. Landfill gas contains 45–60% methane, 40–50% CO₂, 2–5% N₂, trace amounts of gases, such as O₂, NH₃, H₂, and a non-methane organic compound (NMOC). Approximately 6–8 m³ of landfill gas per tonne of disposed municipal solid waste is produced per year or 150–250 m³ per ton of waste during the lifetime of the landfill site.

The caloric value of biogas and landfill gas depends on the amount of methane. If share of methane is 50%, the caloric value is 18.8 MJ/m³ or 5.2 kWh/m³ (Fig. 2.22).

2.3 Electricity

Electricity is an essential energy carrier in modern societies, not only because electricity demand in the EU has share of 24% in total final energy consumption, but due to the specific characteristics of the electricity. Electricity is pure exergy, meaning that can be transformed completely into other forms of energy but cannot be stored by current technologies on large scale; therefore, the production-supply-demand process must be balanced. This means that the production and demand of electricity must be synchronized, which is done by large inter-state distribution systems, by the optimization of electricity use at the end-user level or by the integration of (large numbers) of decentralized electricity production systems into smart grid infrastructure systems. In this chapter, technologies for large-scale production will be presented; small scale applications for on-site and near-by building electricity production will be discussed in Chap. 7. An overview of the share of electricity production technologies in EU shows that almost three quarters of electricity is produced by non-renewable energy sources (48% by conventional thermal and 26% by nuclear power plants) and only 12% by hydro power plants, 10% by wind turbines and 4% by other renewable technologies (e.g. PV systems). Nevertheless, as shown in Fig. 2.23, a breakdown of electricity production in EU states differs significantly between the countries.



Fig. 2.22 Centre for solid waste treatment of Municipality of Ljubljana that will replace landfills in the future (top, left); landfill ready for municipal solid waste disposal with water-tight membrane and set of degassing shafts (top, right); landfill gas pumping station with open burners where landfill gas is burned if the content of methane in the landfill gas is lower than 40% or during the maintenance (bottom, left); system of landfill gas power plants as cogeneration units; unit can produce electricity and heat if the amount of methane in landfill gas is above half of designed value (bottom, right) (Trivunčević 2016)

From a thermodynamic perspective, the water steam closed loop process is the most common process for electricity production in thermal power plants. Such power plants consist of elements that are shown in Fig. 2.24. It is possible to use a wide range of fuels, including biomass and solid waste. Advanced thermal power plants consist of two-stage sequential production of electricity by gas and water steam processes (Fig. 2.25). High quality and, therefore, expensive fuel must be used in the gas cycle (e.g. natural gas).

Nuclear power plants use nuclear a reactor as a heat generator and a separate heat exchanger as a water steam generator (Fig. 2.26). Because of lower water steam temperatures, the efficiency of nuclear power plants is lower in comparison to fossil thermal power plants.

Thermal power plants can use solar energy or geothermal water for the generation of steam. In solar thermal power plants, solar radiation must be concentrated by parabolic mirrors or heliostats, a group of flat mirrors, equipped with a solar tracking system. High-temperature-resistant oil is used as a heat transfer media for storing heat at temperatures up to 500 °C and producing steam. Because of the low

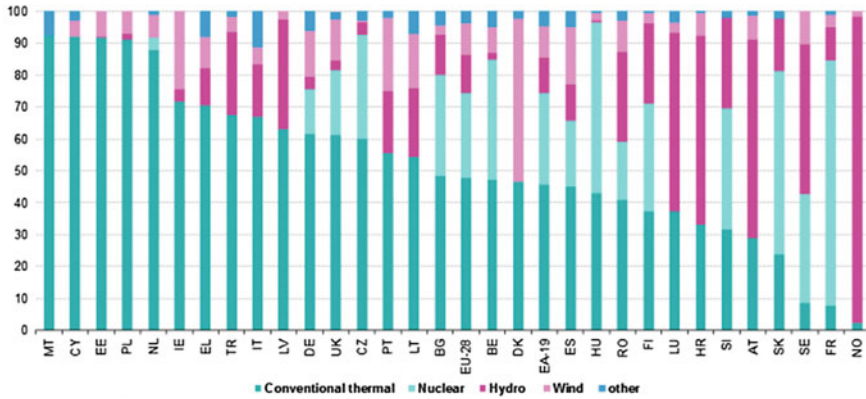


Fig. 2.23 Share of electricity production technologies in EU countries (2015) (www.ec.europa.eu/eurostat)

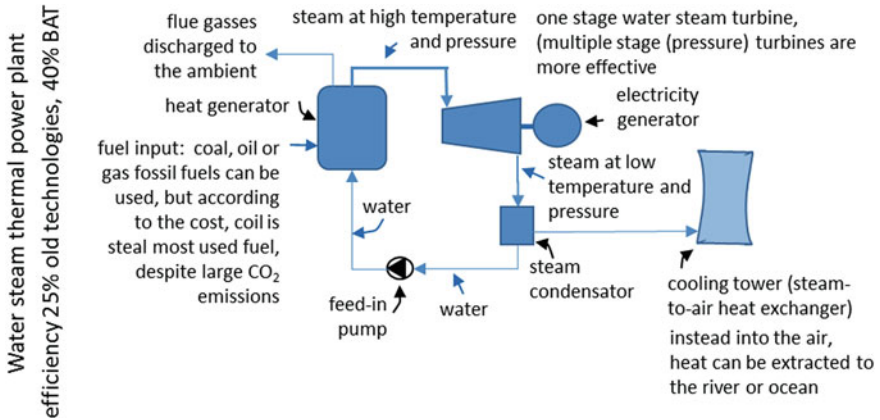


Fig. 2.24 Water steam closed loop process is most commonly used in thermal power plants

steam quality (low temperature and pressure), the efficiency of solar thermal power plants does not exceed 20% (Fig. 2.27).

Where geothermal energy is available on the surface in the form of geothermal water steam, electricity can be produced in dry steam power plants, similar to fossil thermal power plants. Because of the low thermal properties of geothermal steam, electricity production efficiency is low (< 20%), but the overall efficiency of power plant can be increased by using thermal energy for district heating. In areas with lower geothermal potential, the pressure of pumped geothermal water can be decreased in device called a “flasher”, which results in water steam production in so-called “flash steam power plants”. If the temperature of the geothermal water is even lower, water as working fluid must be replaced by organic fluid (e.g.

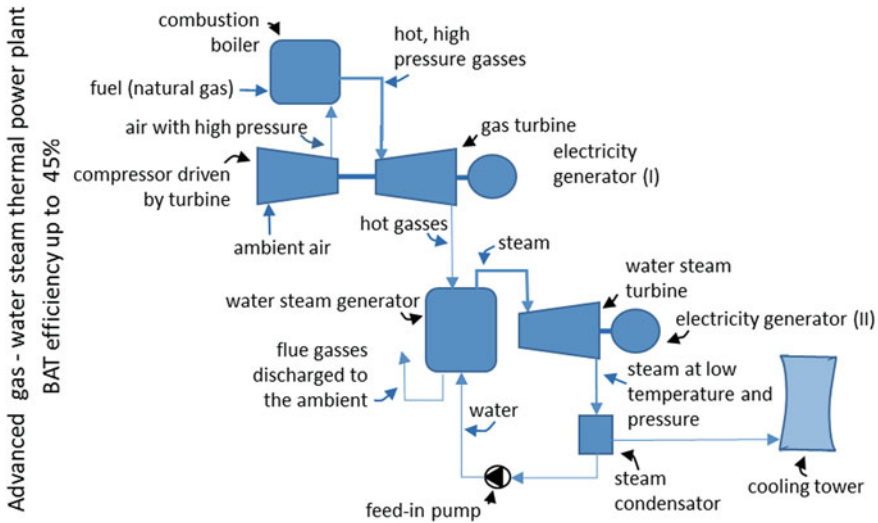


Fig. 2.25 Advanced thermal power plants consist of combined gas (open cycle) and water steam (closed loop cycle) process; hot flue gasses that exit gas turbine boil the water in water steam generator

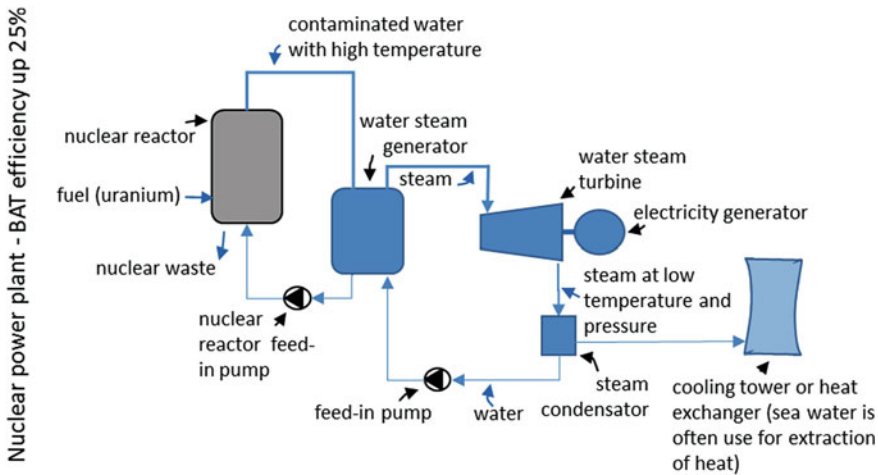


Fig. 2.26 Most nuclear power plants have high-pressure water nuclear reactors and separate heat exchangers (evaporator) for the production of water steam; this ensures the safer operation of nuclear power plants

isobutene) in binary organic cycle (ORC) power plants or by ammonia (NH_3) in so called Kalina process power plants (Fig. 2.28).

Hydro power plants are most used technology that utilized renewable energy for electricity production in EU. Largest units can be build (up to 10.000 MW) and

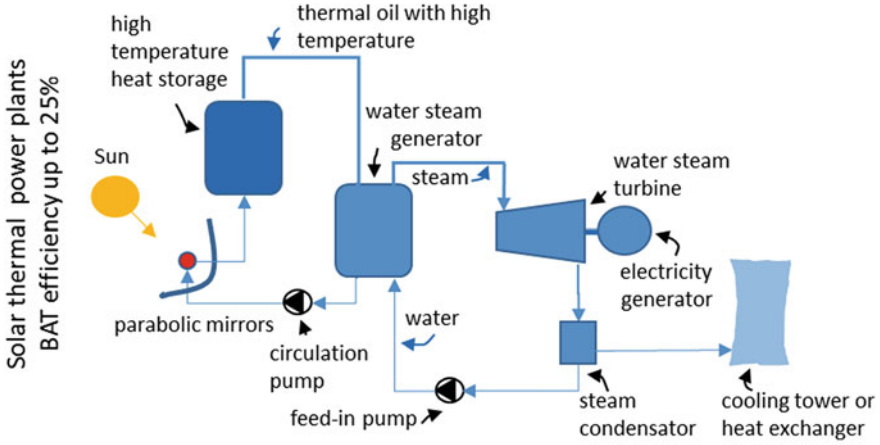


Fig. 2.27 In solar thermal power plants, parabolic mirrors or heliostats with sun tracking systems are used for heating oil to 400–500 °C

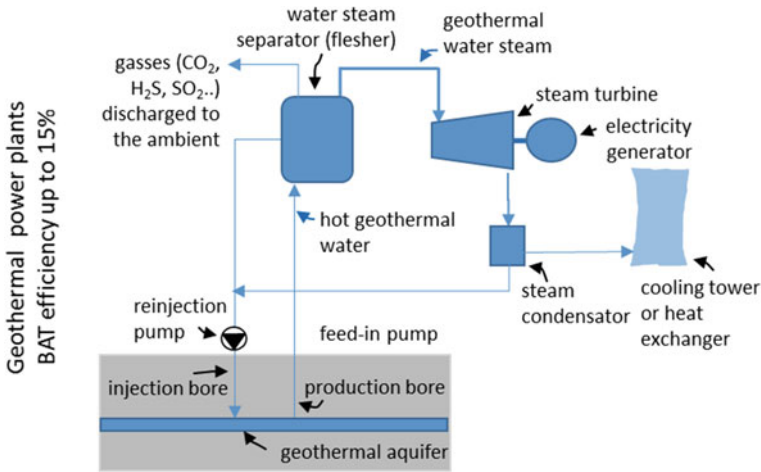


Fig. 2.28 The most efficient geothermal power plants utilize dry geothermal steam; unfortunately, only 10% of geothermal fields worldwide have such potential; at less favourable conditions, flash steam and ORC geothermal power stations can be built

have high overall efficiency (up to 80%). Hydro power plants defer regarding to the amount of the water that is stored behind the dam on accumulation or run-of-river hydropower plants and regarding to the type of the installed turbine regarding to pressure head and water flow rate as it is presented in Fig. 2.29.

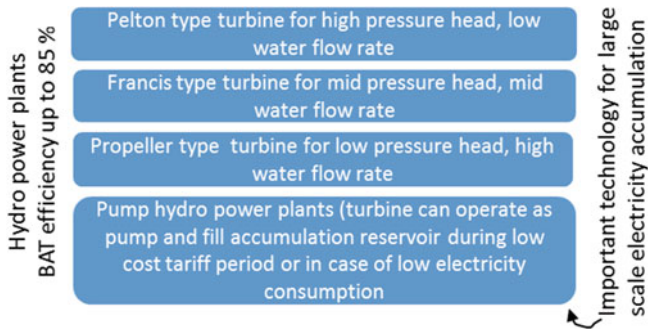
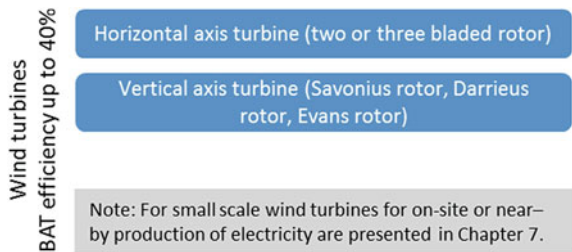


Fig. 2.29 Several types of turbine are used in hydro power plants, and the type is chosen regarding to water pressure head and water flow rate

Fig. 2.30 Two groups of wind turbines, divided according to rotation axe position, are currently used for electricity production



Wind turbines have the second largest share in electricity production in EU. High speed wind turbines with speed ratio larger than 5 (see Chap. 7) with rated power up to 5 MW with efficiency up to 40% are built on locations where average yearly wind speed exceed 6 m/s. Technologies of wind turbines are generally divided regarding the position of the axis of rotor on wind turbines with horizontal or vertical rotation axis. Nowadays wind turbines with horizontal rotation axis prevail because larger units can be built and the higher wind speeds that occur at higher altitudes can be utilized (Fig. 2.30).

Technologies for electricity production differ not only according to size and efficiency, but also according to environmental impact. In Fig. 2.31, different environmental impact indicators for different technologies are shown: emission of greenhouse gasses per kWh of produced electricity during material extraction, construction and operation, land that is occupied by a power plant per one TWh produced electricity in expected operation life time of the power plants, and energy pay-back ratio, which is defined as the ratio of produced and used energy for

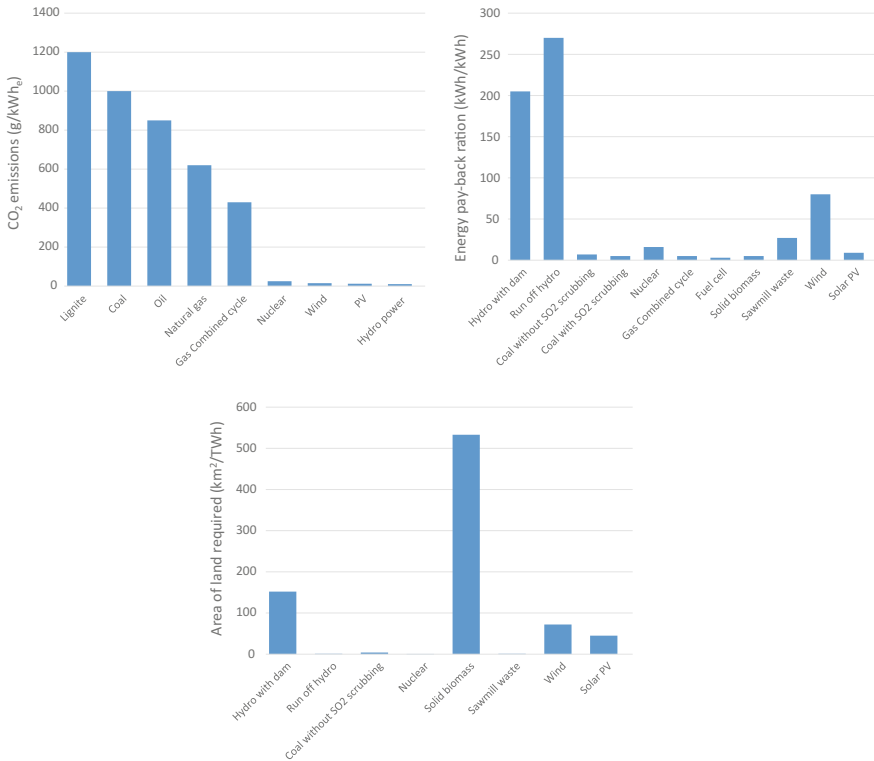


Fig. 2.31 Environmental impact indicators for different technologies for electricity production; CO₂ emissions in g per kWh of produced electricity in the operation time of power plant; ratio between energy produced and energy use for manufacturing, installation and maintenance throughout the life time of operation (top, right); land area required for power plant per TWh of produced electricity (bottom) (adopted from Paul-Scherrer-Institute) (www.psi.ch)

building and operation of the power plant throughout its operation. Advantages of technologies for utilization of renewable energy are obvious in all indicators.

References

AEBIOM (2008) Wood fuels handbook. AEBIOM
 Duffie JA, Beckman WA (1991) Solar engineering of thermal processes. Wiley, New York
 Hsieh JS (1986) Solar energy engineering. Prentice-Hall Inc.
 Johansson TB et al (1993) Renewable energy sources for fuels and electricity. Island Press
 Kastelec D, Rakovec J, Zakšek K (2007) Sončna energija v Sloveniji. SAZU, Ljubljana
 Malamateinios C, Giakoumelos L, Mavron E (2017) Renewable energy sources. Erasmus+ EduLabFrame project
 Nussbaumer T (2003) Combustion and co-combustion of biomass: fundamentals, technologies, and primary measures for emission reduction. Energy & Fuels

- Ragheb M (2017) Terrestrial radioactivity and geothermal energy. Available on: www.ragheb.co
- Trivunčević D (2016) Modelling the generation of landfill gas and a long-term forecast for the Barje landfill site. Diploma work. Faculty of Mechanical Engineering, University of Ljubljana, Ljubljana
- Twidell J and Weir T (1986) Renewable energy resources. E. & F. N. Spon Ltd.

Chapter 3

Introduction to Building Physics

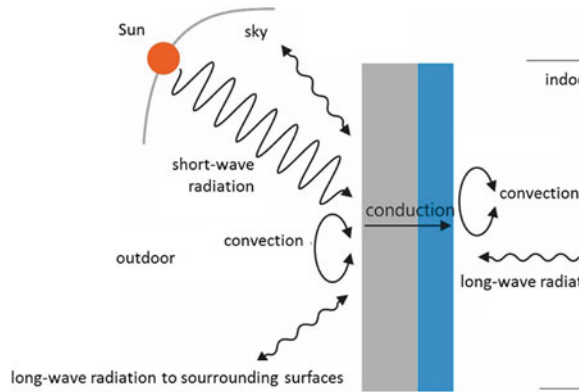


Abstract Building physics study the processes that occurs in the building structures that influence the indoor comfort and safety of inhabitants. A group of building physics professors at European universities, founded by Professor Karl Gertis, defined the following fields of interest: heat transfer in buildings, water and water vapour transfer in building structures including psychrometric process, lighting, building acoustics, fire development and fire protection in buildings, and urban microclimates. In this chapter, heat transfer in buildings and the basic psychrometry of air will be discussed as these process are directly involved in the assessment of the energy performance of a building. Elementary and essential indicators of building structures and buildings will be presented, and dynamic heat transfer in building structures will be discussed briefly.

3.1 Heat Transfer in Building Structures

As is generally the case, heat in building constructions is transferred by heat flux as the consequence of temperature difference. Different forms of heat flux appear in building constructions: as convective and long-wave radiant heat fluxes on inner and outer surfaces and as conduction heat flux in solid layers of the building structure. Convection heat flux is a consequence of moving air molecules, while structural surfaces exchange long-wave (IR) thermal radiation with surroundings and sky on outer surfaces and with inner surfaces and heat sources at the inner surface. In the case of a structure with a closed gap filled by air or noble gasses such as insulated glazing, or ventilated air gap, such as ventilated roofs, the heat is transferred between the surfaces of the gap by convection and by long-wave radiation. The outer surface of a structure also absorbs short-wave (solar) radiation. Because neither outdoor or indoor temperatures nor solar radiation are constant values, conduction heat transfer inside structure caused heat accumulation in the form of sensible heat or in the form of latent heat if phase change materials (PCM) are used. Consequently, heat transfer in building structures is always

Fig. 3.1 In building structures, heat is transferred by convective, radiant, and conductive heat fluxes



dynamic (unsteady in time); nevertheless, the process of heat transfer can be treated as a steady process for the determination of elementary building structures thermal properties (Medved 2014).

Heat flux or rate of heat transfer is expressed in watts or as a specific value in watts per m^2 of building structure area. Physical properties including a material's thermal conductivity λ (W/m K), convective heat transfer coefficient α ($\text{W/m}^2 \text{K}$), long-wave radiation emissivity ε ($-$) of the surfaces in contact with air or gasses and short-wave solar radiation absorptivity α_s ($-$), in addition to geometrical properties such as the thickness of solid layers and the position of a building structure (e.g. vertical wall or horizontal ceiling), define the quantity of heat flux that is transferred through building structure at current indoor and outdoor conditions (Fig. 3.1).

3.1.1 Thermal Transmittance of Building Structures (U-Value)

Heat transfer in building structures is always time-dependent and therefore non-stationary; nevertheless, the determination of the heat transfer in stationary conditions (meaning at assumed constant indoor and outdoor conditions with no solar radiation) is adequate for primary verification of the thermal insulation properties of a building envelope. For this purpose, thermal transmittance or the U-value of a structure is used. The U-value is defined as the rate of heat transfer \dot{q} (W) through 1 m^2 of building structure at a constant air temperature difference of 1 K between both sides of the structure. The unit for thermal transmittance is therefore $\text{W/m}^2 \text{K}$. With respect to the specifics of heat transfer, the building structure may be divided into homogeneous structures with a closed air or gas-filled gaps, structures with an open natural or forced ventilated gaps, greened structures, and structures in contact with the ground.

Regarding the directive on the energy performance of buildings of European Parliament (EPBD¹), the U-values of building structures must be limited in national legislation to the maximum allowed values.

3.1.2 Thermal Transmittance of Homogeneous Structures

Homogeneous building structures are made of homogeneous building materials whose physical properties are constant throughout the whole volume and independent of temperature and moisture content. All the layers in homogeneous structures, as well as the external and internal surfaces of such structures are parallel. The heat flux as a vector quantity passes only in the perpendicular direction to the surface of the structure.

One may reasonably conclude that practically no structures fulfil the requirements of this definition: the brick walls are bound with mortar, the heat conductivity of fibrous insulating materials depends on the orientation of fibres, and so forth. However, these anomalies have a relatively minor impact on the heat transfer, so most building structures can be treated as homogeneous. In such case, the thermal transmittance is determined using the thermal resistances between the temperature nodes, as shown in Fig. 3.2. The thermal resistance R_{λ} of each layer to heat conduction is equal to:

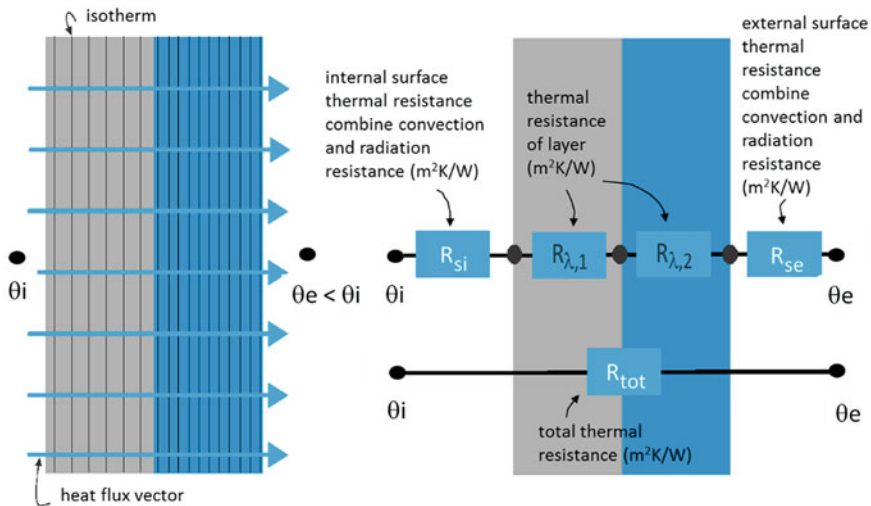


Fig. 3.2 In homogeneous building structures, the direction of the heat flux is perpendicular to the surface of the structure and isotherms are parallel (left); total thermal resistance R_{tot} of a structures is the sum of all thermal resistances (right)

¹Directive 2010/31/EU of the European Parliament and of the Council of 19 May 2010 on the energy performance of buildings (recast) (Official Journal of the European Union, L 153/13).

$$R_{\lambda} = \frac{d}{\lambda} \quad (\text{m}^2 \cdot \text{K}/\text{W})$$

↖ thickness of the layer (m)
↘ thermal conductivity of the layer (W/mK)

The resistances to heat transfer by convection and radiation at the surface of the structure are replaced by the combined surface resistances R_{si} (at “i” inner surface) and R_{se} (at “e” external surface) ($\text{m}^2 \text{K}/\text{W}$). The two are determined according to air velocity at the surface of the construction and direction of heat flux. Typical values are: R_{se} $0.04 \text{ m}^2 \text{K}/\text{W}$ and R_{si} $0.13 \text{ m}^2 \text{K}/\text{W}$ if heat flux direction is horizontal, $0.10 \text{ m}^2 \text{K}/\text{W}$ for up-wards, and $0.17 \text{ m}^2 \text{K}/\text{W}$ for down-wards heat flux. Total thermal transmittance resistance R is the sum of all resistances:²

$$R_{\text{tot}} = R_{si} + \sum_{i=1}^n R_{\lambda,i} + R_{se} \quad (\text{m}^2 \cdot \text{K}/\text{W})$$

↖ internal surface thermal resistance which combine convection and radiation resistance at interior surface ($\text{m}^2\text{K}/\text{W}$)
↘ thermal resistance of the layer i ($\text{m}^2\text{K}/\text{W}$)
↖ total number of layers
↘ external surface thermal resistance which combined convection and radiation resistance at exterior surface ($\text{m}^2\text{K}/\text{W}$)

The building structure thermal transmittance U equals the reciprocal of total thermal resistance:

$$U = \frac{1}{R_{\text{tot}}} \quad (\text{W}/\text{m}^2 \text{K})$$

Case Study 1 Calculate minimum thickness of thermal insulation U of the brick wall with thickness of the brick layer at 19 cm. The thermal conductivity of brick is $0.58 \text{ W}/\text{m K}$ and thermal insulation $0.035 \text{ W}/\text{m K}$. Maximum U -value for walls is $0.28 \text{ W}/\text{m}^2 \text{K}$.

$$U_{\text{max}} = \frac{1}{R_{\text{tot,min}}} \rightarrow R_{\text{min}} = R_{si} + R_{\lambda,\text{brick}} + R_{\lambda,\text{ti}} + R_{se} = \frac{1}{0.28} \text{ m}^2 \cdot \text{K}/\text{W}$$

$$R_{\lambda,\text{ti,min}} = R_{\text{tot,min}} - R_{si} - R_{\lambda,\text{brick}} - R_{se} \rightarrow R_{\lambda,\text{ti,min}} = \frac{1}{0.28} - 0.13 - \frac{0.19}{0.58} - 0.04 = 3.091 \text{ m}^2\text{K}/\text{W}$$

$$R_{\lambda,\text{ti}} = \frac{d_{\text{ti}}}{\lambda_{\text{ti}}} \rightarrow d_{\text{ti}} = R_{\lambda,\text{ti}} \cdot \lambda_{\text{ti}} = 0.108 \rightarrow d_{\text{ti}} = 12 \text{ cm} \quad \leftarrow \begin{array}{l} \text{market available} \\ \text{thickness} \end{array}$$

²EN ISO 6946:2017 Building components and building elements—Thermal resistance and thermal transmittance—Calculation methods.

Case Study 2 Find a list of building structures of Virtual Lab building in the software TRIMO Expert > Project > Virtual Lab and overview thermal transmittance of those structures. Compare these values to the national requirements in your country.

3.1.3 Thermal Transmittance of Structures with Closed Air Gap or Ventilated Air Layer

Building structures with an air gap are quite common. An air gap can be designed as closed or ventilated. Closed air gaps are formed when levelling the differences in the thicknesses of building structure layers. Such closed air gaps improve sound insulation and fire resistance, as well as reducing the structure's thermal transmittance.

The heat flow inside the closed (unventilated) air gap is transferred by convection and radiation. Because of that, the thermal resistance of unventilated air gap is combined into a substitute resistance of a closed air layer R_a . Thermal resistance R_a depends on air gap thickness d_a , gap surfaces long wave emissivity $\epsilon_{IR,a}$ and on direction of heat flow. Typical values are in the range:

- R_a 0.15 m² K/W ($d_a = 5$ cm, $\epsilon_{a,1}, \epsilon_{a,2} = 0.9$ (high IR emissivity, typical value), up-wards heat flow direction) to 0.18 m² K/W (in case of horizontal heat flux direction);
- R_a 0.22 m² K/W (down-wards heat flux) and 0.46 m² K/W ($d_a = 5$ cm, $\epsilon_{a,1}, \epsilon_{a,2} = 0.05$ (low IR emissivity e.g. metal foil), and upwards heat flux direction), 0.68 m² K/W (horizontal heat flux) and 1.37 m² K/W (down-wards heat flux).

The thermal transmittance U equals the reciprocal of total thermal resistance R_{tot} , air layer is treated as one of the solid layers that comprise a building structure, as shown in Fig. 3.3.

Structures with ventilated air layers are designed to enable less hindered transportation of water vapour from interior air to the exterior during the critical winter period and thus minimize the risk of interstitial condensation water vapour. To ensure a sufficient air flow rate through the ventilated air layer, inlet and outlet openings must have an area of at least 1500 mm² per metre of length for vertical constructions or 1500 mm² per m² of surface area in horizontal and tilted structures. The thermal transmittance U of building structures with ventilated layers is calculated by disregarding the thermal resistance of the layers situated between the ventilated air layer and the external environment and equalize surface resistance R_{sc} to R_{si} . From this point on, the determination of U -value is then equal to procedure for homogeneous structures (Fig. 3.4).

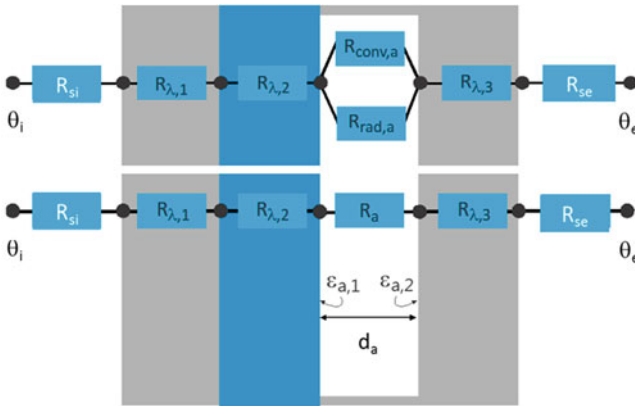
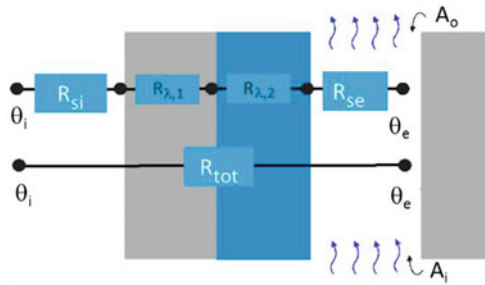


Fig. 3.3 U-value of building constructions with closed air gap is calculated taking into account combined thermal resistance of the air gap R_a

Fig. 3.4 U-values of building structures with well-ventilated air gaps is calculated with the thermal resistance of the layer between the interior and the ventilated air gap and equalized surface thermal resistance R_{se} to R_{si}



Note: According to national regulations in Slovenia, the maximum allowed U-value of walls is $0.28 \text{ W/m}^2 \text{ K}$, a ceiling below an unheated attic $0.20 \text{ W/m}^2 \text{ K}$, roofs $0.20 \text{ W/m}^2 \text{ K}$. U-values are limited for separation walls between neighbours' flats to $0.90 \text{ W/m}^2 \text{ K}$.

3.1.4 Thermal Transmittance of Green Building Structures

A vegetation blanket on green building structures has a significant role in regulating the microclimate in cities and reducing the heat transfer into the building during the summer. Due to their high absorptivity of short-wave solar radiation and high

Fig. 3.5 Green building structures improve the microclimate in urban environments, absorb air pollutants, capture rainwater and reduce heat transfer to building interiors



emissivity of long-wave thermal radiation, the plants act as micro shades, simultaneously keeping themselves cool by the processes of radiative cooling, and especially by evapotranspiration. Evapotranspiration is a process combining the evaporation of the water from the soil and the evaporation of water, transported from the root system from grooving substrate, through the leaf pores (transpiration) (Fig. 3.5).

Despite coupled heat and mass transfer process, the U-value of green structures is calculated similarly to that of homogeneous structures, only without taking into account thermal resistance of all layers that are in contact with rainwater. Therefore, the waterproofing layer (waterproof foil, or as closed-cell thermal insulation (such as XPS), impervious to rainwater) is the last layer towards the exterior; its conductance thermal resistance $R\lambda$ is taken into account. As necessary for all other building structures, the U-value of green structures must be lower than the allowed value.

Note: According to national regulations in Slovenia, the maximum allowed U-value of green roofs is $0.20 \text{ W/m}^2 \text{ K}$.

3.1.5 Thermal Transmittance of Building Structures in Contact with the Ground

In comparison to all other building constructions, heat transfer in building structures in contact with the ground differ because the ground temperature is higher and varies less than the temperature of ambient air and because the ground layer represents an additional thermal resistance to heat transfer from the buildings. Because of that, building structure form factor B' must be defined first as the ratio of the area of construction in contact with the ground and the circumference of construction:

$$B' = \frac{\overset{\text{area of ground construction (m}^2\text{)}}{A}}{0.5 \cdot \underset{\text{circumference of ground construction (m)}}{P}} \text{ (m)}$$

Form factor B' has great influence on heat transfer in this case. Calculation methods for the determination of thermal transmittance U of building structures in contact with the ground differ according to the type. They are divided among horizontal structures with continuous or partial thermal insulation layer, and vertical structures built partially or complete under the ground layer. As an example, in Fig. 3.6, thermal transmittances U for ground floor structures with and without thermal insulation layer as a function of form factor B' is shown (Medved and Černe 2002).

Note: According to national regulations in Slovenia, the maximum allowed U -value of building construction in contact with the ground is $0.35 \text{ W/m}^2 \text{ K}$.

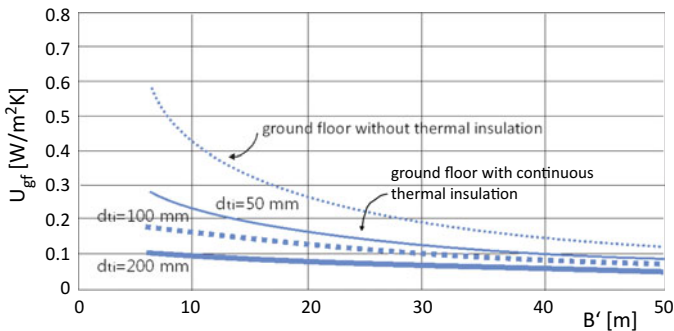


Fig. 3.6 Thermal transmittance U of ground floor structures made by 20 cm thick concrete layer without and with continuous thermal insulation layer (Medved and Černe 2002)

3.1.6 Thermal Transmittance of Windows (and Doors)

Due to their complex geometric shape and the associated heat transfer mechanisms, the thermal transmittance of windows U_w is define by the thermal transmittance of glazing U_g , the thermal transmittance of window frame U_f , and the linear thermal bridge transmittance ψ_s on the glazing spacer:

$$U_w = \frac{U_g \cdot A_g + U_f \cdot A_f + \psi_s \cdot L_s}{A_g + A_f} \quad \left(\frac{W}{m^2 \cdot K} \right)$$

thermal transmittance of glazing (W/m²K) thermal transmittance of frame (W/m²K) linear thermal transmittance of spacer (W/mK)
 ← length of spacer (m)
 area of glazing (m²) area of frame(m²)

The thermal transmittance of window glazing U_g depends above all on the aspect ratio of the gap (the ratio of gap height to width) and the gas inside the gap, which influence the heat transfer between the window panes by convection and the emissivity of glass surfaces enclosing the gap. Nowadays, the window glazing gaps are filled with the noble gases argon or krypton, which are known to have a considerably higher density ρ and smaller thermal conductivity λ than air. The glass is coated with low-emission coatings (long-wave emissivity is decreased in this way from ϵ_{IR} 0.88 of ordinary glass to below 0.05) that significantly decrease radiation heat transfer between the glass panes. The thermal transmittance of window glazing U_g can also be decreased by multiple glass panes. Glazing with up to 4 panes can be found on the marker. Table 3.2 shows thermal transmittance U_g and U_f of contemporary windows.

Window frames are usually made of wood, plastic or metal (aluminium). The selection of materials depends on the mechanical strength, maintenance frequency, cost and required thermal transmittance U_f of the frame. The wooden window frames can be designed to ensure the required thermal transmittance value with a 70–100 mm thick profile (Fig. 3.7).

The thermal transmittance of plastic and metal frames can be reduced by dividing the frame into sections or chambers, and by breaking the thermal bridging formed on the frame profile ribs. Nevertheless in general, the thermal transmittance of plastic and metal frames exceeds the thermal transmittance of wooden frames. Windows ready for installation in energy-efficient buildings have frames packed with layers of thermal insulation or closed air chambers, so that the frame’s thermal transmittance U_f is as low as thermal transmittance of the glazing U_g . For example, the glazing and frame thermal transmittance of windows installed in passive buildings must be under 0.8 W/m² K (Fig. 3.8).

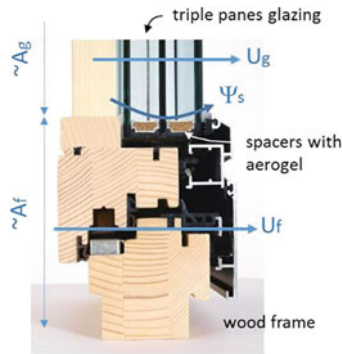


Fig. 3.7 Thermal transmittance of window U_w is defined by size and properties of glazing, frame, and glass spacer

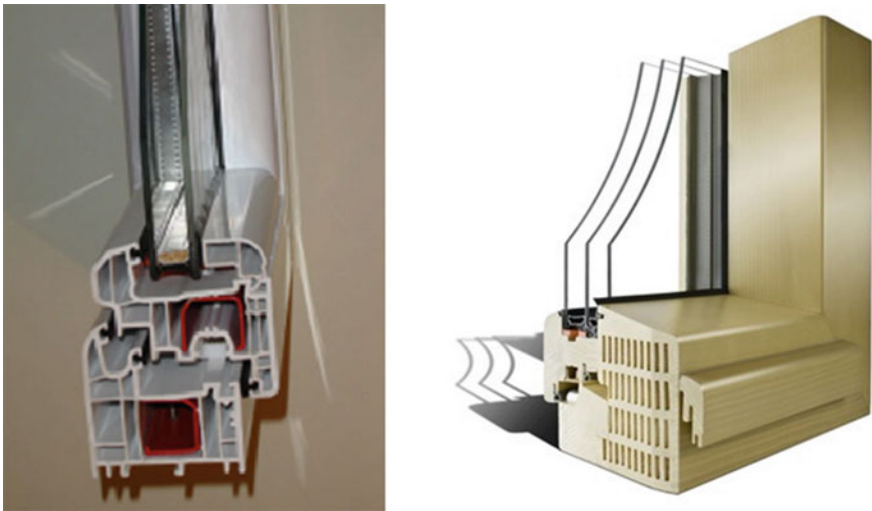


Fig. 3.8 Plastic window frame with 5-chamber profile and heat bridge barrier (left); wood window frame with closed air chambers (right) (M-SORA, www.m-sora.si)

The spacer bar between the window panes seals gaps between the panes. Linear thermal transmittance ψ_s of the thermal bridge caused by the spacer bar depends on the spacer material. For an ordinary Al spacer bar, the linear thermal bridge transmittance ψ_s is approximately 0.10 W/m K, and for a plastic spacer it only in the range of 0.03–0.04 W/m K per m of the length (Fig. 3.9).

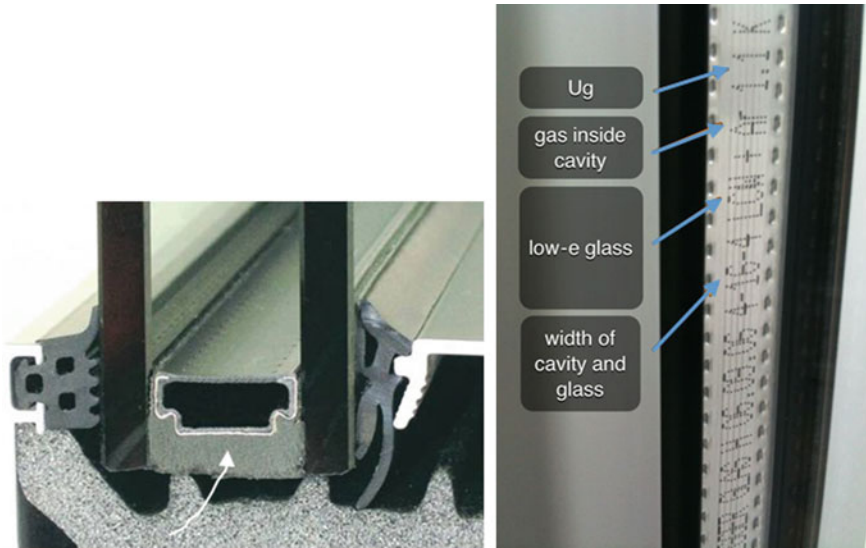


Fig. 3.9 Window glass spacer (left); data of window glazing properties are printed on window spacer (right)

Software could be used for determination of the thermal transmittance of the windows (and doors), for example WINDOW software,³ although it is more common to determine U_w using laboratory experiments. The thermal properties of windows are shown in Table 3.2.

3.1.7 Thermal Bridges

A thermal bridge is virtual part of the building envelope where the heat transfer through the building envelope differs in comparison to homogeneous structures. Thermal bridges occurs in case of:

- full or partial penetration of the structure at the building envelope by an element having a different thermal conductivity (e.g. supporting column, wooden beam);
- a change in the thickness and form of the structure (e.g. edge of window opening in the wall);
- a difference between internal and external surface areas (e.g. wall corners, wall and floor junctions, structures in contact with the ground).

The consequence of thermal bridges is increased heat transfer in building structures. As result, the temperatures at the external surface of a building structures

³WINDOW 7.0, Lawrence Berkeley National Laboratory, University of California, USA.



Fig. 3.10 During the period of low external temperatures and heating period, heat bridges can be detected by thermal imaging; typical thermal bridges in non-thermal insulated buildings are presented on the photos

during the winter are higher and thermal bridges are thus easily detected by thermal imaging (see Sect. 4.4). The temperatures at the indoor surfaces of structures are lower, increasing the risk of surface condensation and creating the conditions for the growth of harmful organisms. As transmission heat losses also increase, the thermal bridges must be avoided to the maximum possible extent (Fig 3.10).

The influence of thermal bridges on the transmittance heat losses of building envelopes is evaluated by correction factors. These factors represent the difference between the heat flux passing through the thermal bridge-affected area of the structure and the theoretical heat flux passing through the same area of the structure without thermal bridges at the same temperature difference between indoor and outdoor environments. The effect of thermal bridges on the isotherms and the heat flow rate in a building structure can be two- or three-dimensional and modelled as two-dimensional thermal bridges by using thermal transmittance ψ (“psi”) or as three-dimensional thermal bridge using point thermal transmittance χ (“chi”). Linear thermal bridges ψ are normalized to 1 m thermal bridge length, for example to 1 m of the junction between a partition wall and an external wall, to 1 m of the circumference of door or window openings, or 1 m length of the balcony slab joined to the external bearing building structure. The impact of point thermal bridges χ is given by the number of point thermal bridges in the building structure. Linear and point thermal transmittance can be determined using customized software (such as Trisco⁴—shown here) or computer fluid dynamics software (CFD tools like Phoenics, Fluent or AVL) or can be found as pre-defined in the catalogues of producer pre-build of building structures. Rules for numerical methods are presented in the standard EN ISO 10211 (Tichelman and Ohl 2005; Medved et al. 2004).⁵

⁴Trisco, version 12.0w, Physibel, Maldegem, Belgium.

⁵EN ISO 10211:2017 Thermal bridges in building construction—Heat flows and surface temperatures—Detailed calculations.



Fig. 3.11 Photo of Virtual Lab building with impact area of analysed thermal bridges

Case Study Procedure for the determination of two linear thermal bridges transmittance at a segment of facade of the Virtual Lab are shown. Using Trisco software, heat flux that passes a selected segment of the build facade was calculated numerically and compared to the reference heat flux that passes through the same part of the facade consisting of homogeneous structures without thermal bridges. In case A, the reference thermal transmittance $U_{1,homog}$ is $0.155 \text{ W/m}^2 \text{ K}$ and reference area A_1 equal to 1.05 m^2 . In case B, reference thermal transmittances $U_{1,homog}$ is $0.139 \text{ W/m}^2 \text{ K}$ and $U_{2,homog}$ is $0.112 \text{ W/m}^2 \text{ K}$ and reference areas are A_1 0.84 m^2 and A_2 0.786 m^2 . In both cases, indoor air temperature θ_i is set to $20 \text{ }^\circ\text{C}$ and outdoor air temperature θ_e $-10 \text{ }^\circ\text{C}$. Calculated heat flux are \dot{Q}_A 5.279 W and \dot{Q}_B 5.126 W .

Note 1: Temperature differences could be chosen arbitrarily and will not affect linear thermal transmittance as long as direction of heat flux is the same (Figs. 3.12 and 3.13).



Fig. 3.12 Students at “learning-by-doing”, i.e. constructing the Virtual Lab building (left); interior of Virtual Lab building (right)

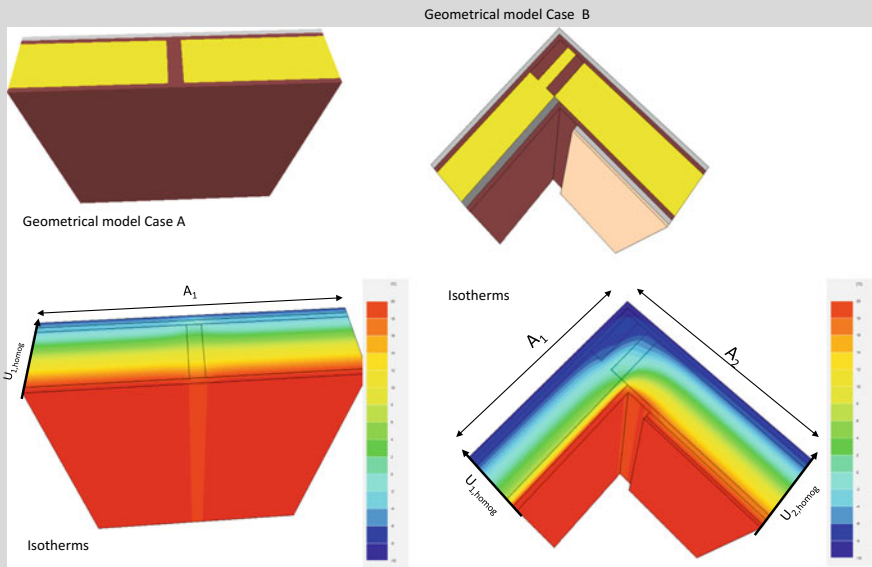


Fig. 3.13 Two examples of numerical calculation of thermal bridges in Virtual Lab building: case A (left) and case B (right) from Fig. 3.11

thermal transmittance of virtual homogeneous building structure (W/m²K) area effected by thermal bridge (m²) length of linear thermal bridge (m)

$$\dot{Q}_{num,A} = \left(\sum_{i=1}^1 (U_{i,homog} \cdot A_i) + \psi_A \cdot l_A \right) (\theta_i - \theta_e) \rightarrow$$

indoor air temperature (°C) outdoor air temperature (°C)

$$\rightarrow \psi_A = \frac{\frac{\dot{Q}_{num,A}}{(\theta_i - \theta_e)} - \sum_{i=1}^1 (U_{i,homog} \cdot A_i)}{l_A} = \psi_A = \frac{5.279}{(20 - (-10))} - 0.155 \cdot 1.05}{1} = 0.013 \text{ W/mK}$$

and similar:

$$\psi_B = \frac{5.126}{(20 - (-10))} - (0.139 \cdot 0.840 + 0.122 \cdot 0.786)}{1} = -0.042 \text{ W/mK}$$

Note 2: Linear thermal transmittance could be negative; the reason is that we take into account the size of areas of the building thermal envelope that are in contact with outdoor air, as is common practice. Because of the thick insulation layer, there is a big differences between indoor surfaces (where heat is transferred from the indoor environment) and outdoor surfaces (where heat is transferred to the outdoor environment).

Note 3: Be aware that several other thermal bridges exist in the building shown; for example, around the windows and door, in contact with the ground or at the edge of roof-wall structure connection.

The procedure for the determination of point thermal transmittance χ is the same, only the length of the linear thermal bridge is replaced by the number of point heat bridges; therefore, point thermal transmittance is measured in W/K per point. In the fact, the influence of all heat bridges on heat transfer through building envelope can be analysed by thermal transmittance and areas of all (assuming) homogeneous building structures that form the building envelope with only one point of thermal transmittance.

3.1.8 Specific Transmission Heat Transfer Coefficient (Average Thermal Transmittance of Building Envelope)

The influence of heat bridges on heat transfer in a building envelope is taken into account by introducing the thermal bridge correction factors (ψ and χ) in the calculation of specific transmission heat transfer coefficient H'_T . H'_T (W/K) is defined as heat flux through 1 m² of the building envelope at temperature differences between indoor and outdoor air temperature 1 K. As such, it represents the average (or overall) heat transfer coefficient of a building envelope (Fig. 3.14):

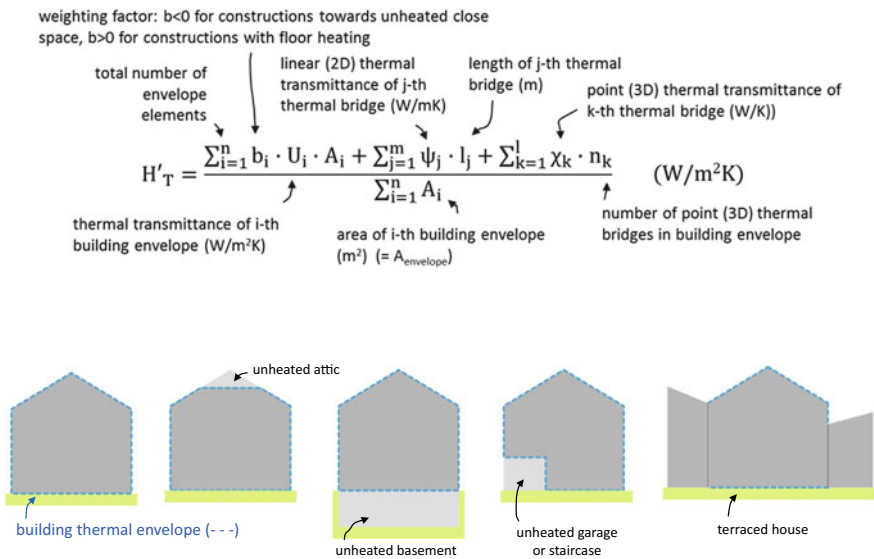


Fig. 3.14 Building thermal envelope (A_{envelope}) is total area of all constructions that divide conditioned space and outdoor environment or unheated spaces. Surface area is measured at the contact with outdoor air or with the air in unheated space; some examples are shown

Note: According to the national regulations, the calculation of specific transmission heat transfer coefficient H'_T could be simplified by introducing a constant overall correction factor. For example, the value of 0.06 W/m² K is prescribed in Slovenia regulations on the energy efficiency of buildings. In this case, H'_T is determined by equation:

$$H'_T = \frac{\sum_{i=1}^n b_i \cdot A_i \cdot U_i + \sum_{j=1}^m \psi_j \cdot I_j + \sum_{k=1}^l \chi_k \cdot n_k}{\sum_{i=1}^n A_i} = \frac{\sum_{i=1}^n b_i \cdot A_i \cdot U_i}{\sum_{i=1}^n A_i} + 0.06 \text{ (W/m}^2\text{K)}$$

3.1.9 Total Solar Energy Transmittance of Windows (and Transparent Envelope Structures)

Solar heat gains through window glazing and other transparent elements on the building envelope depends on optical properties of the glazing. Some incoming global solar radiation is reflected back to the outdoors and some absorbed in the window panes. Consequently, the temperature of the inner glazing surface could be above the indoor air temperature and additional convection and long wave radiation heat flux (\dot{q}_{c+r}) is transferred into the interior space. The ratio of total heat flux that is transferred to indoor environment (as the sum of transmitted short-wave solar irradiance and convection and long-wave radiation from the interior surface of the transparent element) to solar irradiance on the external surface defines the total solar energy transmittance or g-value (Fig. 3.15):

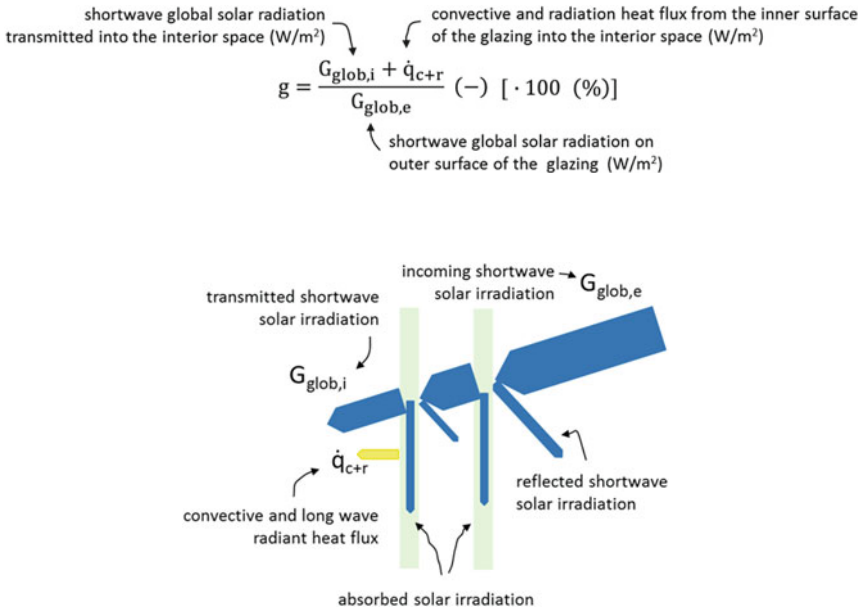


Fig. 3.15 Solar heat gains through transparent elements of the building envelope are determined by the total heat flux that is transferred into the interior space as a consequence of incoming solar irradiation on the outer surface (direct and diffuse $G_{glob,i}$) and convective and long-wave radiation heat flux (q_{c+r}) from the glass surface to the interior space



Fig. 3.16 Examples of adjustable, high solar reflective shading devices; rotating shading louvers with integrated PV modules for electricity production (left), shading roll installed in the way that enable double side convection cooling and daylighting of interior of the building (middle), adjustable reflective shading fins installed 25 cm in front of the facade (right), in presented cases, total solar irradiation transmittance (including shading and window glazing) is below 0.08

Total solar energy transmittance g of contemporary glazing is in the range between 0.15 (15%) (solar protection glazing with multiple absorption micro layers) to 0.75 (75%) (white glass double glazing). The high value of g enables the effective natural solar heating of the buildings and daylighting but can cause overheating during cooling period. Since adaptive or switch glazing is not available yet, windows and glass facades must be equipped with outdoor shading. Some examples of adjustable, high-solar reflective shading devices cooled by both side natural convection are presented in Fig. 3.16.

3.1.10 Heat Accumulation in Building Structures

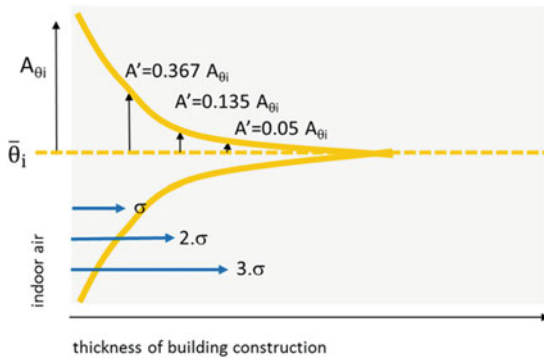
Energy needs for heating and cooling of the buildings depend on the accumulation of heat in building structures. In this way, during the heating period, solar energy can be stored without overheating and building structures can be cooled during the night-time to “store cold” for the next daytime period during the cooling period. To enable such a process, the thermal response of the building must be unsteady and periodical with a typical 24-hour period of changing the indoor air temperature. The indoor air temperature variation can be approximated by a periodic function with daily average indoor air temperature $\bar{\theta}_i$ and air temperature amplitude $A_{\theta i}$ as independent variables:

$$\theta_{i,t} = \bar{\theta}_i + A_{\theta i} \cdot \cos\left(\frac{2 \cdot \pi}{L} \cdot t\right) \text{ (}^\circ\text{C)}$$

amplitude of indoor air temperature (°C)
time of observation (h)

average daily indoor air temperature (°C)
length of period (24 h)

Fig. 3.17 Temperature in building structures oscillate with a 24-hour period as consequences of periodic change of air temperature or heat flux at inner surface



Note: No indoor air temperature swing ($A_{\theta_i} = 0$), and no heat accumulation in the building structures! Temperature swing could results from midday solar gains or intermediate heating or cooling of the building. Acceptable indoor air temperature swing is limited by indoor comfort class (see Chap. 2).

Indoor temperature swing causes temperature variations inside the building structure. Since the process is limited to a 12-hour interval of higher and a 12-hour interval of lower temperatures as daily average values, the temperature variation inside a building can be observed only in a limited depth of the structure. The depth of building structure where the amplitude of the temperature is exactly 36.7% of the daily indoor air temperature A_{θ_i} is called the effective thickness (σ) for heat accumulation. The adequate double effective thickness (2σ) is the depth at which the temperature amplitude is $0.135 A_{\theta_i}$ and at triple effective thickness the temperature amplitude is only $0.05 A_{\theta_i}$. For the short term (daily) accumulation of heat, a depth of construction equal to 2σ is assumed to be optimal (Fig. 3.17).

Effective thickness (σ) of the building structure depends on physical properties: density ρ , thermal conductivity λ and specific heat c_p , which can be combined in thermal diffusivity a (Table 3.1), with the equation:

$$\sigma = \sqrt{\frac{\lambda \cdot L}{\pi \cdot c_p \cdot \rho}} = \sqrt{\frac{L}{\pi}} \cdot \sqrt{a} = 165.8 \cdot \sqrt{a} \text{ (m)}$$

thermal conductivity (W/mK) length of period (24 h) thermal diffusivity (m²/s)
 specific heat capacity (J/kgK) density (kg/m³)

Table 3.1 Thermal properties of selected materials

	Density ρ (kg/m ³)	Thermal conductivity λ (W/m K)	Specific heat c_p (J/kg K)	Thermal diffusivity a (m ² /s)	Thermal effusivity b (kJ/m ² K s ^{0.5})
Aluminium	2700	203	940	8230×10^{-8}	22.5
Air	1.18	0.025	1	2500×10^{-8}	0.01
Thermal insulation (rock wool)	0.04	70	840	167×10^{-8}	0.03
Concrete	2400	2.04	960	68×10^{-8}	2.18
Solid brick	1400	0.58	920	59×10^{-8}	1.17
Aerated concrete	600	0.23	1050	26×10^{-8}	0.25
Water	1000	0.59	4180	14×10^{-8}	1.56
Wood (soft)	550	0.14	2090	14×10^{-8}	0.38

Note: Data on thermal conductivities of materials can be acquired from national lists, producer's datasheets, or from dedicated software tools [TRIMO Expert (TRIMO Expert, Version: 14.5.3.1, trimo-group.com, TRIMO, Trebnje, Slovenia.)]

The quantity of accumulated heat Q_{acc} during the first 12 h of observation is equal to the heat released in the next 12 h and depends on indoor air temperature amplitude A_{θ_i} and the physical properties of the building's construction material (Table 3.1). Q_{acc} per m² of building structure area is defined by the equation (Hagentoft, 2001):

$$Q_{\text{acc}} = 2 \cdot \sqrt{\frac{L \cdot 3600}{2 \cdot \pi}} \cdot \lambda \cdot c_p \cdot \rho \cdot A_{\theta_i} = 2 \cdot \sqrt{\frac{L}{2 \cdot \pi}} b = 234.5 \cdot b \cdot A_{\theta_i} \quad (\text{J/m}^2)$$

Case Study Determine the recommended thickness of a building structure and the amount of daily stored sensible heat in wood and concrete wall. Assume that indoor air temperature amplitude A_{T_i} is 3 K. The physical properties of wood: $a = 14 \times 10^{-8}$ m²/s; $b = 380$ J/m² K s^{0.5} and concrete: $a = 68 \times 10^{-8}$ m²/s; $b = 2180$ J/m² K s^{0.5}.

$$\sigma = 165.8 \cdot \sqrt{a} \rightarrow \sigma_{\text{wood}} = 165.8 \cdot \sqrt{14 \cdot 10^{-8}} = 0.062 \text{ m}$$

$$\sigma_{\text{concrete}} = 165.8 \cdot \sqrt{68 \cdot 10^{-8}} = 0.137 \text{ m}$$

The suitable thickness of the wood building structure (2σ) is 124 mm, of concrete building structure equal to 273 mm. In such building structure thickness, the amount of daily accumulated heat is equal to:

$$Q_{\text{acc,wood}} = 234.5 \cdot b \cdot A_{T_i} = 234.5 \cdot 380 \cdot 3 = 267,000 \left(\frac{\text{J}}{\text{m}^2}\right) = 74.1 \text{ Wh/m}^2$$

$$Q_{\text{acc,concrete}} = 234.5 \cdot b \cdot A_{T_i} = 234.5 \cdot 2180 \cdot 3 = 1,534,000 \left(\frac{\text{J}}{\text{m}^2}\right) = 426.1 \text{ Wh/m}^2$$

It can be concluded that concrete is a much more appropriate material for heat accumulation in comparison to wood, despite the fact that a thicker layer is required for heat accumulation. Note that amount of stored heat is calculated assuming air temperature amplitude A_{θ_i} 3 K.

Table 3.2 Thermal transmittance U_g , total solar irradiation transmittance g and transmittivity of light (τ_{vis}) of different window glazing (including BAT), thermal transmittance of windows (U_w) with different frame materials (U_f), and U_w for windows having different size and glazing thermal transmittance U_g

Glazing	Thermal transmittance U_g (W/m ² K)	Total solar energy transmittance g (-)	Daylight transmittance τ_{vis} (-)
Single	5.80	0.85	0.90
Double	2.80	0.80	0.80
Triple	2.10	0.72	0.65
Double/Ar	1.40	0.78	0.80
Double/Ar/1 low-e	1.00–1.20	0.64	0.78
Double/Kr/1 low-e	0.80–1.20	0.64	0.78
Triple/Kr/2 low-e	0.50	0.5–0.6	0.72
quadruple/Kr/3 low-e	0.30	0.40	0.60
solar control double/Ar/1 low-e	1.10	0.12–0.40	0.40–0.65
Vacuum double/triple (lab value)	0.50/0.30	0.65/0.60	0.70/0.80
Frame (25% area of window), metallic spacer	U_g (W/m ² K)	U_f (W/m ² K)	U_w (W/m ² K)
Wooden	0.80	1.50–0.80	1.23–1.06
Plastic	0.80	1.30–1.10	1.19–1.14
Metallic	0.80	1.50–1.20	1.23–1.16
Window size (m)	U_w (W/m ² K)		
	U_g 1.3 W/m ² K	U_g 0.9 W/m ² K	U_g 0.4 W/m ² K
0.6 × 0.6	1.50	1.15	0.60
1.0 × 1.0	1.45	1.10	0.55
1.0 × 1.2	1.40	1.00	0.45

Note: Typical U_g values are stated for glazing 1.2×1.4 m in size; in case of deviation of this size, the share of glazing area and convective heat flux between window panes is amended due to the different gap aspect ratio

Note: According to national regulations in Slovenia, the maximum allowed glazing thermal transmittance U_g is 1.1 W/m² K, meanwhile U_w for windows with wooden and plastic frames is 1.3 W/m² K and U_w for windows with metal frames 1.60 W/m² K

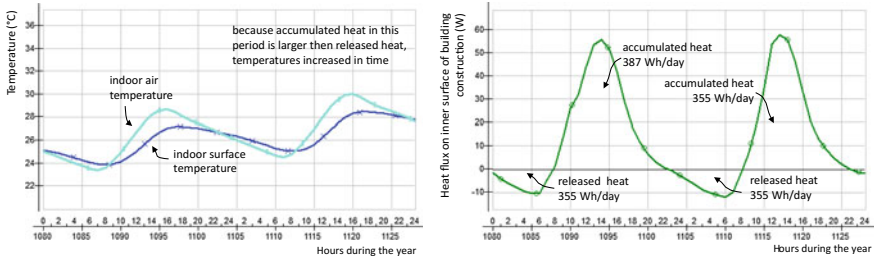


Fig. 3.18 Dynamic thermal response of wall of Virtual Lab (IDA-ICE)

A dynamic thermal response model should be used for the all-year design of heat accumulation mass. The following example shows the thermal response of a wall of the Virtual Lab for two consecutive days (Fig. 3.18).

Heat losses are related to transmission heat transfer through a building’s thermal envelope and ventilation heat losses, because fresh ventilation air should be heated in the winter and cooled during the summer. Heat losses can be expressed by coefficients. Transmission heat transfer coefficient H_T (W/K) is defined as the heat flux that transmits through the building thermal envelope (Fig. 3.14) at temperature differences 1 K between indoor and outdoor air temperatures. H_T is defined by equation:

$$H_T = H'_T \cdot A_{\text{envelope}} = \sum_{i=1}^n b_i \cdot U_i \cdot A_i + \sum_{j=1}^m \psi_j \cdot l_j + \sum_{k=1}^l \chi_{k} \cdot n_k \quad (\text{W/K})$$

The total amount of fresh air that enters the building is the sum of the infiltration air flow rate that enters the building through non-tight openings in the building envelope and the ventilation air flow rate that enters the building. Energy demand caused by ventilation is defined by ventilation heat transfer coefficient H_v (W/K), which represents the specific heat flux transferred by ventilation air flow at temperature differences between indoor and outdoor air temperatures 1 K. For the determination of H_v , air flow rate \dot{q}_{vent} (m^3/h), air density ρ_a (kg/m^3) and heat capacity of air per unit of mass $c_{p,a}$ ($\text{J}/\text{kg K}$) must be known:

$$H_v = \rho_a \cdot c_{p,a} \cdot \dot{q}_{\text{vent}} \cong 0.34 \cdot \dot{q}_{\text{vent}} \quad (\text{W/K})$$

↙ ventilation air flow rate (m^3/h)

In the case of mechanical ventilation, fresh ventilation air is delivered by a controlled fan. It is very likely that a heat exchanger is installed in such a system to enable heat transfer from discarded (from interior) to fresh air. In this case, the ventilation heat transfer coefficient (and ventilation heat losses) is significantly lower. However, no building is completely airtight; therefore, the air flows also into the building because of infiltration. Taking into account the above facts, the

ventilation heat transfer coefficient is defined by equation:

$$H_v \cong 0.34 \cdot (n_{inf} \cdot V + (1 - \eta_{rec}) \cdot \dot{q}_{vent}) \quad (W/K)$$

net building volume (m³)
ventilation rate (m³/h)

infiltration air exchange rate, approximate value n₅₀/10 to n₅₀/20 could be assumed (h⁻¹)
efficiency of heat recovery unit, 0.75 to 0.95 for BAT (-)

Note: See Chap. 4 for an explanation of n₅₀ and Chap. 11 for a description of mechanical ventilation systems.

3.2 Psychrometrics

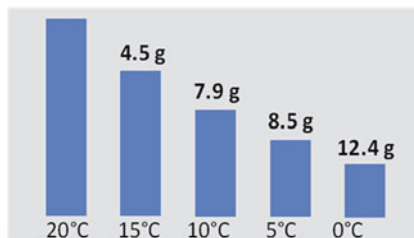
Air is a mixture of gases (N₂ 78%, O₂ 21%, Ar 0.9%, CO₂ 0.035%, with traces of methane, hydrogen, CO, ozone, ammonia, SO₂, VOC (volatile organic compounds) and other gases) and water vapour. The amount of each gas in the air can be expressed by its partial pressure, and the sum of partial gas pressures is equal to the atmospheric air pressure. The study of processes consisting of dry air and water (in vapour, liquid and solid state) is known as psychrometrics. The psychrometrics of indoor and outdoor air will be presented in this chapter. The amount of water vapour that can be present in the air decreases with decreases of the air temperature. If air is saturated with water vapour, the partial pressure of water vapour reaches the maximum value p_{sat, H₂O}, which is called saturated water vapour pressure. Saturated water vapour pressure depends on the air temperature: (Fig. 3.19).

$$p_{sat,H_2O} = e^{(49.27 - \frac{6651}{T} - 4.531 \cdot \ln T)} \quad (kPa)$$

air temperature (K)

The amount of water vapour in the air can be expressed as relative or absolute air humidity. Relative air humidity φ is defined by the ratio of actual partial pressure of water vapour in the air and partial pressure of water vapour in saturated air.

Fig. 3.19 Mass of water vapour extracted by condensation from 1 m³ of air exposed to cooling from 20 °C to zero degrees



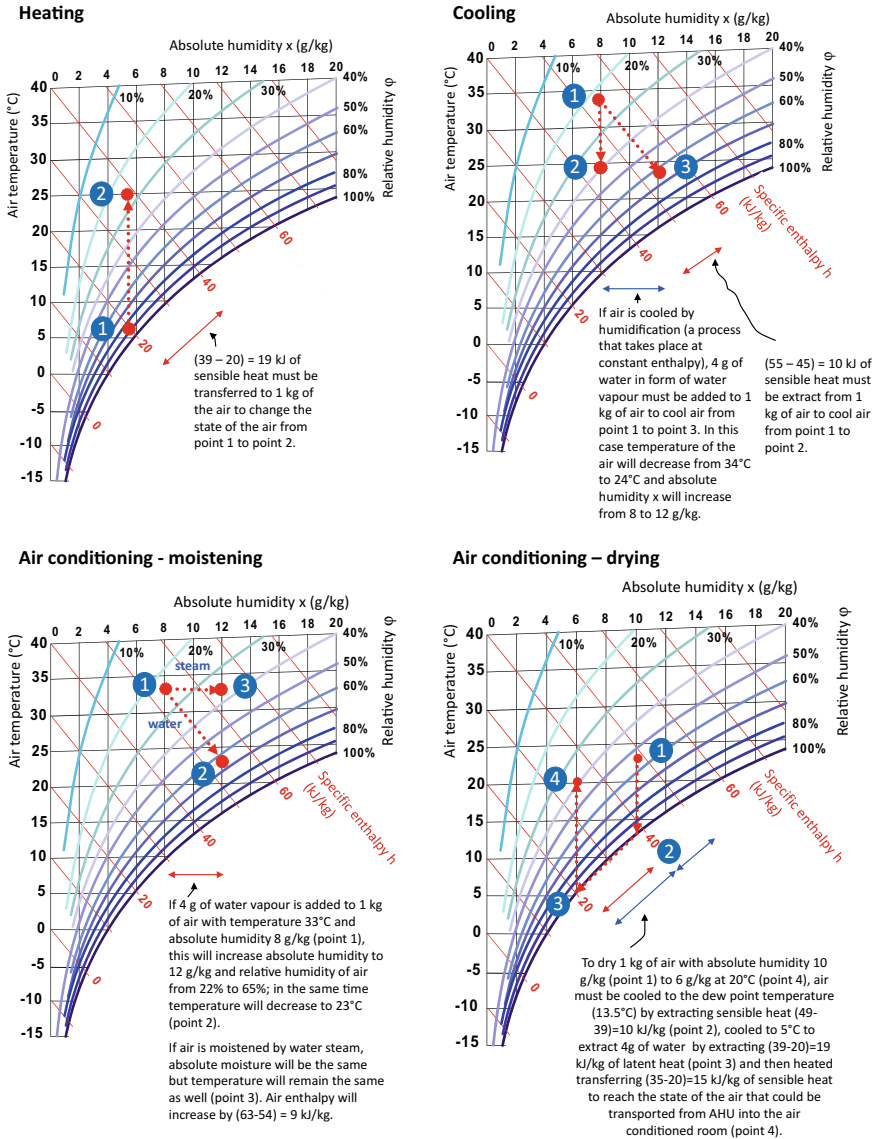


Fig. 3.20 Processes of air-conditioning presented in Mollier's T-x psychrometric diagrams

$$\phi = \frac{P_v}{P_{\text{sat},H_2O}} \quad (-) \quad [\cdot 100 (\%)]$$

When air is saturated with water vapour, the value relative humidity is 1 or 100%. Typical relative humidity of indoor air ranges between 25 and 60%. Air humidity can also be expressed as absolute humidity x . In this case, the amount of water

vapour in the air is defined by the ratio of the mass of water vapour (in kg or g) in 1 kg of dry air. Typical values of absolute humidity of indoor air are between 0.005 and 0.010 kg/kg.

Because air consists of sensible (of dry air and water vapour) and latent heat (of water vapour), the internal energy of the air cannot be expressed only by air temperature. Therefore, enthalpy is used for the determination of moist air's internal energy. The enthalpy of moist air is equal to the sum of the enthalpy of dry air, the enthalpy of water vapour in the air, and the evaporation heat that is required to generate a known quantity of water vapour present in the air (Oprešnik 1987; Moran and Shapiro 1998):

$$H_{\text{air}} = H_{\text{air,dry}} + H_{\text{wv}} + m_{\text{wv}} \cdot r = m_{\text{air,dry}} \cdot c_{p,\text{air}} \cdot \theta + m_{\text{wv}} \cdot c_{p,\text{wv}} \cdot \theta + m_{\text{wv}} \cdot r \quad (\text{J})$$

↑ sensible heat of dry air (J)
 ↑ sensible heat of water vapour (J)
 ↑ latent heat of water vapour (J)
 ↑ temperature of air = temperature of water vapour (°C)
 ↑ evaporation heat of water (J/kg)

↑ mass of dry air (kg)
 ↑ specific heat at constant pressure of dry air (J/kgK)
 ↑ mass of dry air (kg)
 ↑ specific heat at constant pressure of dry air (J/kgK)

It is defined that enthalpy of dry air is 0 J at air temperature 0 °C and increases with temperature and the amount of the water vapour. Enthalpy is property of the state of the air that is used for determination of energy needs for the heating, cooling, humidification, and dehumidification of the air, which are typical processes in air-conditioning systems. These processes are often presented and analysed in psychrometric diagrams. One of the most commonly used forms of such diagrams is the so-called Mollier's T-x diagram of moist air, shown in Fig. 3.20, in which the enthalpy of the air is presented as specific enthalpy h (J/kg) of 1 kg of dry air.

References

- Hagentoft CE (2001) Introduction to building physics. Studentlitteratur, Lund
- Medved S (2014) Gradbena fizika II (Building physics II). Faculty of Architecture, University of Ljubljana, Ljubljana
- Medved S, Černe B (2002) A simplified method for calculating heat losses to the ground according to EN ISO 13370 standard. Energy Build 34(5):523–528
- Medved S, Černe B, Arkar C (2004) Linear and point thermal transmittance of TRIMO lightweight insulation panels (included in TRIMO Expert computer tool)
- Moran, JM, Shapiro NH (1998) Fundamentals of engineering thermodynamics. John Wiley & Sons Ltd
- Oprešnik M (1987) Termodinamika (Thermodynamics). Faculty of Mechanical Engineering, University of Ljubljana, Ljubljana
- Tichelmann K, Ohl R (2005) Wärmebrücken Atlas: Trockenbau, Stahl-Leichtbau, Bauen im Bestand. Müller, Rudolf Verlag

Chapter 4

Experimental Evaluation of Buildings' Envelope Thermal Properties



Abstract In this chapter, methods for the experimental determination of thermal properties of building envelopes are presented. These methods are used for commissioning, the process performed by independent experts prior to handing over the building to the customer, in the process of energy labelling of the buildings or to evaluate the most cost effective measures for the renovation of the buildings. Some semi-professional tools and equipment will also be presented, as they are very useful for the preliminary evaluation of different aspects of living comfort and energy efficiency for students and designers.

Indoor living comfort and the energy efficiency of the buildings after construction and during exploitation can significantly differ from designed values. The reason for this may be in personal adjustment of indoor condition by the users, as well as the specific needs of elderly people or people with disabilities. Regardless, the reasons for deviations between design and in situ values of indoor comfort parameters and energy use are often discrepancies in the properties of materials, the poor quality of building structures, and the poor quality of building services. In order to determine the reasons for the deviations, experimental methods and procedures are used.

4.1 Semi-professional Tools and Applications for Evaluation of Indoor Comfort

Smartphones have several built-in sensors to enable the monitoring of the environment. Built-in cameras can be used for measuring outdoor and indoor illumination, as well as for the evaluation of daylighting and the quality of electrical lightning. The built-in microphone can be used for measuring sound pressure levels and sound spectre.

For example, the built-in camera can be used to evaluate potential of solar heating and daylight influenced by surround natural and built obstacles using the Sun Seeker application (available for iOS and Android), which shows a diagram of

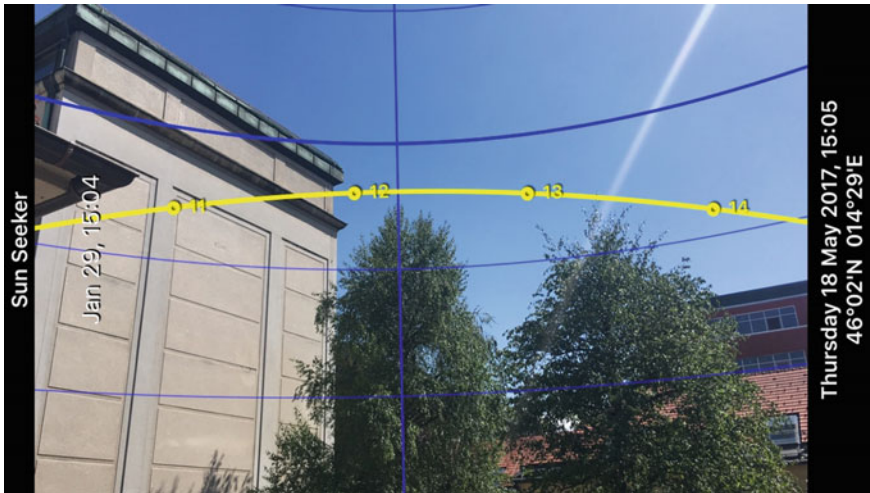


Fig. 4.1 Sun's path shown for specific location using the Sun Seeker app (SunSeeker, v5.6.1, ozPDA, www.ozpda.com), it can be seen that window (point of the stand) will be in shadow on January 29th until 11:55

the sun's path over a photo of an outdoor environment for a selected date, which enables users to define the in-situ shading factor for windows and façade elements when calculating energy demand for heating or cooling or daylighting potential (Fig. 4.1).

Smart phones can be used for the evaluation of indoor comfort, energy demand, and the controlling of appliances and systems. As an example, the Apple HomeKit¹ platform enables the connection of smart devices and a protocol for information exchange for iOS-driven smart devices. Defining scenarios, timers, and rules, some features of smart buildings can be implemented in cost-effective manner (Fig. 4.2).

Thermography, the process of detecting surface temperatures from a distance, is a very common technique for the evaluation of heat transfer in building structures and building service components. The latest developments of thermo-vision devices enable the low-cost yet accurate detection of the thermal properties of buildings and building services. Nowadays, such appliances are available as add-on devices for smart phones (Fig. 4.3).

¹Apple Inc., 2017.

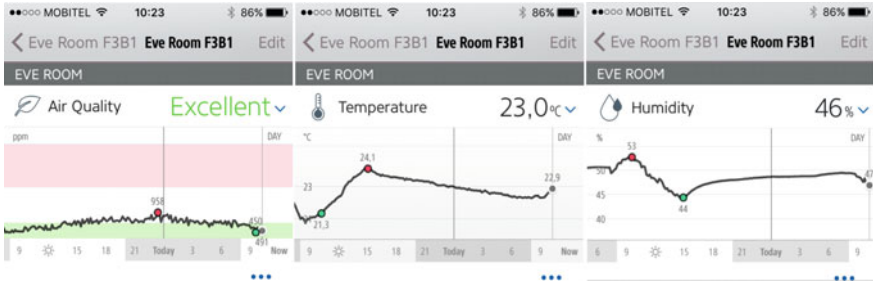


Fig. 4.2 Elgato Eve smart units include Eve Room. Devices can be used for monitoring indoor thermal comfort and IAQ. Data can be sent to actuators that can control, for example, thermostatic valves on heat emission units, fans, or lighting units (Elgato Eve, Eve Systems GmbH, 2016)

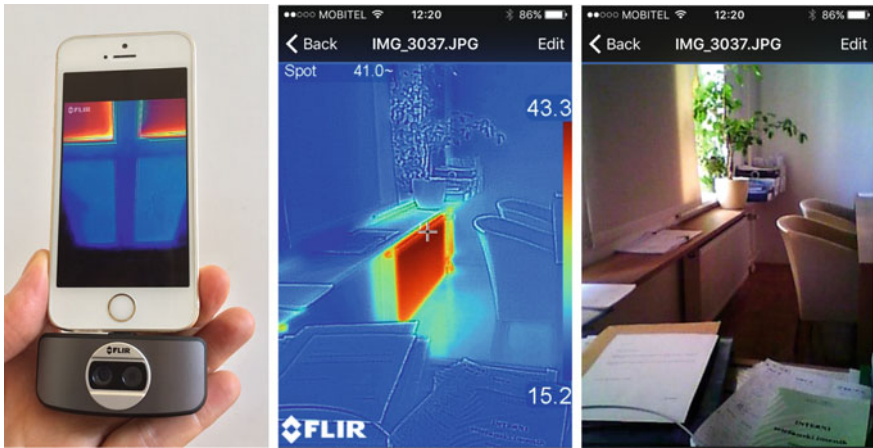
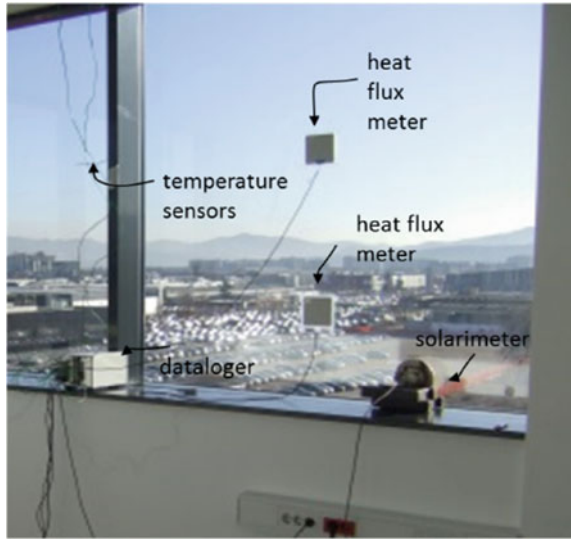


Fig. 4.3 Semi-professional thermal camera as an add-on device for smart phones (left); FLIR One IR camera simultaneously produces IR and visible photo of observed area and offers a large number of tools for data editing (right) (FLIR Systems, Inc., 2005)

4.2 In-Situ Determination of Heat Transfer Coefficient U of Building Structures

Steady state thermal transmittance U can be determined in situ by measuring the heat flux and temperatures of indoor and outdoor air or inner and outer surfaces over a certain period. If the air temperature difference is measured, the $U_{in-situ}$ value of building construction is calculated with the equation (Fig. 4.4):

Fig. 4.4 Thermal transmittance of the glazing is measured in situ with a heat flux meter installed on the window glazing and pair of temperature sensors (note \dot{q} is > 0 when $\theta_i > \theta_e$)



$$U_{in-situ} = \frac{1}{R_{tot}} = \frac{\dot{q}}{(\theta_i - \theta_e)} \quad (W/m^2K)$$

specific heat flux (W/m^2)
 total heat transfer resistance of the building structure (m^2K/W)
 indoor air temperature ($^{\circ}C$)
 outdoor air temperature ($^{\circ}C$)

In this case, the combined convection and radiation heat transfer coefficient of inner and outer surfaces will be included in the experimental value of $U_{in-situ}$ as they reflect the current indoor and outdoor conditions and could differ from values used in the theoretical approach (see Chap. 3). Meanwhile, if the surface temperatures of inner and outer surfaces are measured instead, the combined convection and radiation resistance (R_{si} and R_{se}) must be added as theoretical values:

$$U_{in-situ} = \frac{1}{R} = \frac{1}{R_{si} + \frac{(\theta_{si} - \theta_{se})}{\dot{q}} + R_{se}} \quad (W/m^2K)$$

total heat transfer resistance of the building construction (m^2K/W)
 internal surface thermal resistance which combine convection and radiation resistance at interior surface (m^2K/W)
 external surface thermal resistance which combined convection and radiation resistance at exterior surface (m^2K/W)
 outer surface temperatures ($^{\circ}C$)

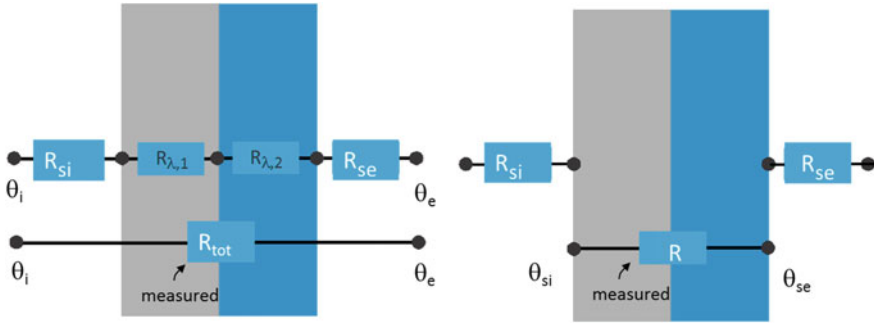


Fig. 4.5 Thermal transmittance U of building structures can be determined in situ by measuring specific heat flux \dot{q} and either air or surface temperature differences

Note: Suggested values of $R_{a,i}$ and $R_{a,e}$ for vertical building structures are $R_{s,i}$ $0.13 \text{ m}^2\text{K/W}$ and $R_{s,e}$ $0.04 \text{ m}^2\text{K/W}$.

Heat transfer in a building envelope is always unsteady because the temperature of outdoor air is time dependent, the surfaces of building elements absorb solar radiation, and the wind’s speed and direction are changing during measurement period. Even indoor temperature is not constant because of solar and internal heat gains. To compensate for heat accumulation in building construction, it first must be defined if the building structure should be treated as lightweight or heavyweight. This is done regarding to thermal capacitance C of the structure, which is defined by equation (Fig. 4.5):

$$C_k = \sum_{i=1}^n d_i \cdot \rho_i \cdot c_i \quad (\text{J/m}^2 \text{K})$$

number of layers \downarrow thickness of the i-th layer (m) \downarrow specific heat of i-th layer (J/kgK) \downarrow
 $C_k = \sum_{i=1}^n d_i \cdot \rho_i \cdot c_i$ density of i-th layer (kg/m³) \uparrow

Lightweight structures are considered to have thermal capacitances lower than $20,000 \text{ J/m}^2\text{K}$. Such structures include window glazing or thinner thermal insulation panels. In the case of lightweight building components, it is assumed that the effect of accumulated heat in the building structure is negligible. Consequently, the thermal transmittance $U_{in-situ}$ is determined as an average value calculated by measured specific heat flux and temperature during measurement intervals, which are limited to night-time only, starting one hour after sunset and finishing at time of sunrise on the following day. The experiment is completed when the $U_{in-situ}$ values in the three consecutive days do not differ by more than $\pm 5\%$.

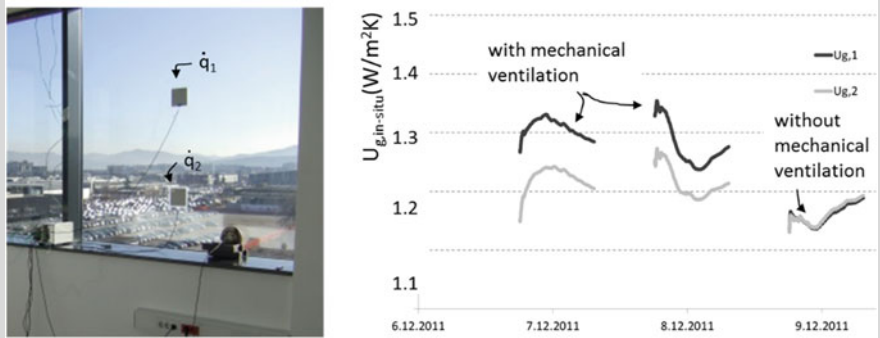


Fig. 4.6 Position of heat flux meter (left); calculated thermal transmittance (right)

Case study Example of in-situ determination of $U_{g,in situ}$ value of double glazing. A heat flux meter was installed in the middle (\dot{q}_1) and on the bottom of the glazing (\dot{q}_2) (see position of heat flux meters in Fig. 4.6). Data on the graph show thermal transmittance U calculated from night-time measurement data. It can be seen that because of higher air velocity in the case of mechanically ventilated space, the surface resistance is lower in comparison to non-ventilated space, resulting in the higher thermal transmittance of the glazing.

Only three consecutive nights were needed to fulfil the criteria of the repeatability of daily (night-time average) $U_{g,in situ}$ values. The in-situ determined value of glazing was $U_{g,in situ}$ 1.28 W/m^2K in the middle and $U_{g,in situ}$ 1.21 W/m^2K at the bottom of the glazing. When the ventilation system was operating, air velocity was higher and internal surface thermal resistance R_{si} difference was lower and dependant on location. When natural convection is present at the internal surface of the glazing, resistance was lower and unified across glazing, resulting in $U_{1,in situ}$ equal to $U_{2,in situ}$. As the producer of the glazing states that the U -value is $1.2 \pm 0.1 W/m^2K$, the manufacturer's data was confirmed.

In the case of the heavyweight building components, measurement is carried out in the same way, but throughout the day. Thermal transmittance is then determined based on the average values of specific heat flux and the difference between indoor and outdoor air temperatures. The duration of the measurement can be shortened with the use of the thermal mass correction factors (F_i determine according to heat accumulation of inner part of construction and F_e determine according to heat accumulation of outer part of building construction), where the stored heat in a building component is taken into account with the correction of the measured specific heat flux. The following equation is used for the determination of the thermal transmittance $U_{in-situ}$ of heavy-weight structures:

$$U_{in-situ} = \frac{\sum_{j=1}^n \dot{q}_j - \frac{F_i \cdot \Delta\theta_i + F_e \cdot \Delta\theta_e}{\Delta t}}{\sum_{j=1}^n (\theta_{i,j} - \theta_{e,j})} \quad (W/m^2K)$$

Annotations for the equation above:

- $\sum_{j=1}^n \dot{q}_j$: heat flux rate (W/m²) multiplied by number of measurements
- F_i and F_e : thermal mass factors (J/m²K)
- $\Delta\theta_i$ and $\Delta\theta_e$: differences in average indoor and outdoor air temperature in the last 24 hours of experiment (°C)
- Δt : time period of the sampling (s)
- $\theta_{i,j}$ and $\theta_{e,j}$: indoor and outdoor air temperatures (°C)

According to the standard ISO 9869,² measurements must take place for at least 4 days. The experiment is completed when the calculated U-value does not differ by more than ±5%, referring to the U-value measured 24–48 h previously.

Case Study Example of in-situ determination of $U_{in-situ}$ value of brick wall. Thermal capacitance C of the structure is equal to 1,224,000 J/m²K and the procedure intended for heavyweight structures must be used. From the figure, it can be seen that duration of experiment could be (much) shorter if thermal mass correction factor is used (Fig. 4.7).

Theoretical (calculated) thermal transmittance U of the wall is equal to 0.91 W/m²K, and measured thermal transmittance of the wall is $U_{in-situ} = 0.95 \pm 0.08$ W/m²K. Interval (±0.08 W/m²K) was determined with error analysis, taking into account the accuracy of each sensor.

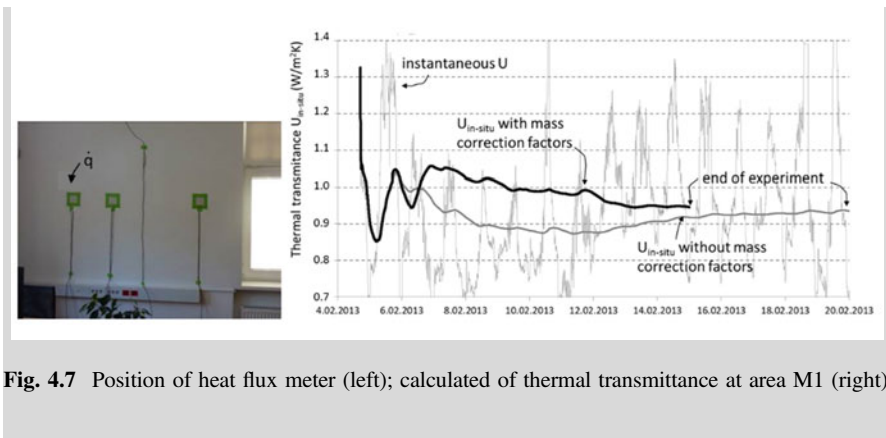


Fig. 4.7 Position of heat flux meter (left); calculated of thermal transmittance at area M1 (right)

²ISO 9869-1:2014 Thermal insulation—Building elements—In situ measurement of thermal resistance and thermal transmittance—Part 1: Heat flow meter method.

4.3 In-Situ Determination of Glazing Total Solar Energy Transmittance g

Total solar energy transmittance g is a property of the glazing that defines solar gains. In addition to laboratory testing and numerical modelling based on optical properties of glass panes and gas filling, it can be evaluated in situ, implementing the following procedure:

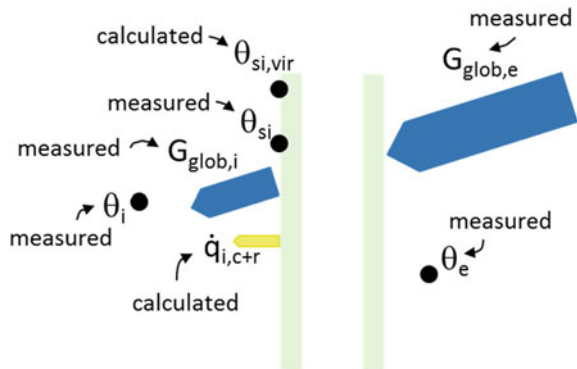
- heat transmittance of glazing U_g must be determined first by measuring specific heat flux and indoor and outdoor air temperature differences, as described in Sect. 4.2.
- virtual surface temperature of indoor glass surface $\theta_{si,vir}$ must be calculated, assuming that glazing is not exposed to solar radiation by equation:

$$\theta_{si,vir} = \theta_i - \frac{U_g \cdot (\theta_i - \theta_e)}{\frac{1}{R_{si}}} \quad (^\circ\text{C})$$

thermal transmittance of glazing ($\text{W}/\text{m}^2\text{K}$) outdoor air temperature ($^\circ\text{C}$)
indoor air temperature ($^\circ\text{C}$) internal surface thermal resistance which combine convection and radiation resistance at interior surface ($\text{m}^2\text{K}/\text{W}$)

- at in situ conditions and when a window is exposed to solar radiation, the actual surface temperature of indoor glass θ_{si} is measured (usually at such conditions θ_{si} is greater than $\theta_{si,vir}$) and heat flux that is transferred by convection and radiation from indoor surfaces of the glazing to the indoor air is defined by equation (Fig. 4.8):

Fig. 4.8 Measured or calculated quantities needed for in-situ determination of total solar energy transmittance g of glazing



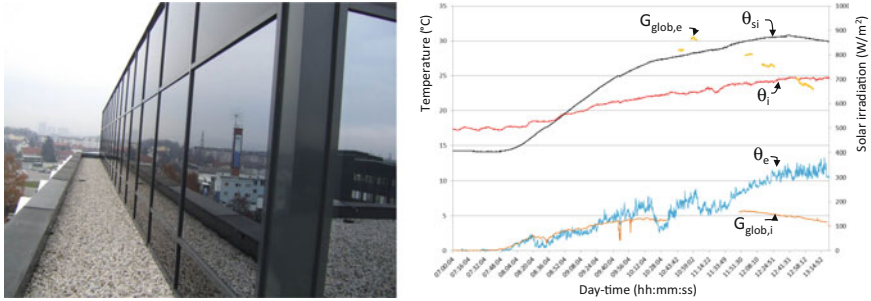


Fig. 4.9 Measured quantities (right) used for the determination of total solar energy transmittance g of glazed façade (left); in-situ-determined g value was equal to 0.28 ± 0.02 , which confirms the manufacturer’s declaration of g 0.26

combine convective and radiation heat
transfer coefficient ($= 1/R_{si}$) (W/m^2K)

$$\dot{q}_{i,c+r} = \alpha_{si} \cdot (\theta_{si} - \theta_{si,vir}) \quad (W/m^2)$$

- using data of measured global (direct and diffuse) solar irradiation on the plane of the outside window glazing and transferred solar irradiation into the interior, the total solar transmittance of the glazing is defined by equation (Fig. 4.9):

$$g = \frac{G_{glob,i} + \dot{q}_{i,c+r}}{G_{glob,e}} \quad (-)$$

total (global) solar irradiation on outer surface of the glazing (W/m^2)
 specific convective and radiation heat flux (W/m^2)
 total (global) solar irradiation towards interior (W/m^2)

4.4 In-Situ Determination of the Building Envelope Thermal Insulation with Thermography

Thermography is a method of remote sensing of the heat flux emitted by the surfaces using a thermal (or infra-red (IR)) camera. Each body with a surface temperature above absolute zero (0 K) emits from its surface heat flux in the form of electromagnetic radiation and is called a thermal emitter. A black body is a

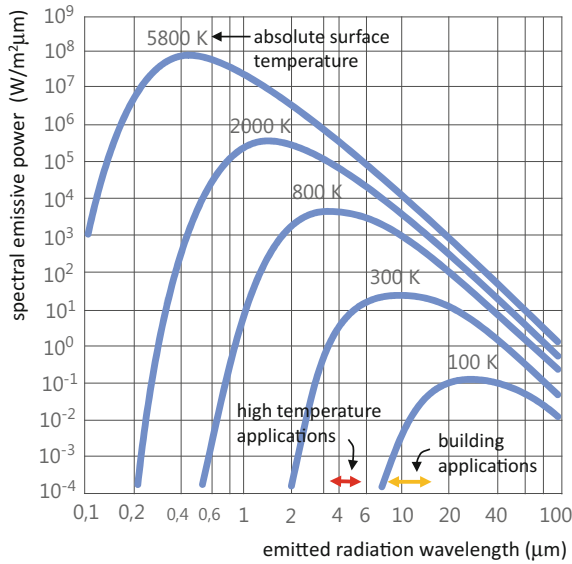


Fig. 4.10 According to the Plank’s law, building structures (treated as blackbodies here) have such a temperature that they emit maximal spectral thermal radiation at wavelengths between 8 and 14 μm. For these wavelengths, the Earth atmosphere is transparent and, therefore, do not disturb remote sensing with thermography. For high-temperature applications, such as furnace inspections, the spectral response of IR sensors in thermal cameras should be in the range of 3–5 μm

thermal emitter that emits at a specific surface temperature T (measured in K) maximum (possible) heat flow. The intensity of the emitted heat flow and the wavelength of emitted radiation heat flow depends on the absolute temperature of the emitter’s surface. At the same time, the increasing of the temperature of thermal emitter causes the emitter to emit larger heat flux, and the wavelength of emitted radiation become shorter and shorter. The range of wavelengths of the thermal radiation and the intensity of the emitted radiation at a certain wavelength is expressed by Planck’s equation for blackbody radiation. This mathematical expression is presented in graphical form in Fig. 4.10 as monochromatic spectral emissive power.

Total emitted radiation heat flux is defined by the integration of monochromatic radiation heat flux over all wavelengths. This integral can be expressed in simple form as the Stefan-Boltzmann law:

$$\dot{Q}_b = \sigma \cdot T^4 \cdot A \quad (\text{W})$$

absolute temperature of emitter surface (K) area of emitter (m²)
↙ ↘
↙ ↘
↙ ↘
 Stefan-Boltzmann constant (W/m²K⁴)

In reality, no emitter is perfect (=black body), and emitted radiation heat flux is lower. The ratio between the actual emitted heat flux and heat flux emitted by a black body at the same absolute temperature is called emissivity; for real emitters, the total emitted heat flux is equal to:

$$\dot{Q} = \sigma \cdot \varepsilon \cdot T^4 \cdot A \quad (\text{W})$$

↑
 thermal emissivity of emitter surface (between 0 and 1)

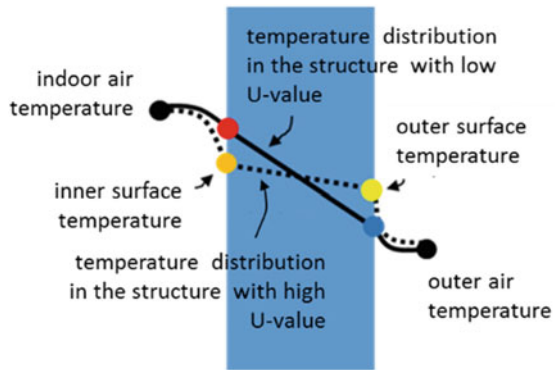
Thermal cameras have integrated calculation routines that convert the measured heat flux to a more representative quantity, the surface temperature, by using the Stefan-Boltzmann law. Before performing thermography measurements, one must adjust the emissivity of observed areas. As most building materials have high emissivity ($\varepsilon \sim 0.9$) and emit radiation as diffuse emitters, thermal imaging is a widely used technique for the evaluation of buildings; nevertheless, exact thermal properties, such as the determination of heat transfer coefficient U or thermal bridge heat transmittance ψ , χ , cannot be evaluated directly. Conditions for the implementation of thermography in the thermal properties evaluation of buildings are defined in standard EN ISO 6781-3.³ The most important requirements are:

- at least 24 h before thermography, the outdoor air temperature should not vary by more than ± 10 °C;
- at least 24 h prior to and during thermography, the temperature difference between indoor and outdoor air temperature should at least $3/U$ (°C) (where U is thermal transmittance of the building envelope) and in any case not less than 5 °C;
- at least 12 h before thermography, the building envelope must not receive direct solar radiation
- during thermography, the indoor air temperature shall not vary by more than ± 2 °C and outdoor temperature by more than ± 5 °C;
- during thermography, the sky must be cloudy.

For the interpretation of thermal images, it is important that during the heating season building structures with lower thermal transmittance U have higher inner and lower outer surface temperatures, as shown on Fig. 4.11. Some examples are presented in a case study below (Fig. 4.12).

³EN ISO 6781-3:2015 Performance of buildings—Detection of heat, air and moisture irregularities in buildings by infrared methods—Part 3: Qualifications of equipment operators, data analysts and report writers.

Fig. 4.11 Temperatures on building structure surfaces indicate if a building structure is lowly and highly thermal insulated or the existence of thermal bridges



4.5 In-Situ Determination of Building Airtightness

The air tightness of buildings is essential to reducing the air infiltration leaky joints in the building envelope. As heat losses increase, cold winter air can cause cooling of the building structure below the dew point which can lead to increased water content in the building structure; air infiltration can cause unpleasant draught and thus thermal discomfort. Consequently, requirements regarding the airtightness of the building are defined in EU regulations on energy efficiency of the buildings.

Airtightness of the building can be tested in two ways:

- by measuring the time-dependent decrease of tracer gas concentration after a specific level of tracer gas was established in the room (building) at the start of the test; the less the building is tight, the quicker the tracer gas concentration reaches the outdoor level;
- by measuring the flow rate of air the passing building envelope at an elevated (positive and negative) pressure difference between the building interior and ambient environment created by a fan; a higher pressure difference is necessary for more accurate measurement of air flow rate and to prevent the impact of natural ventilation; for airtight testing of buildings, this method is required.

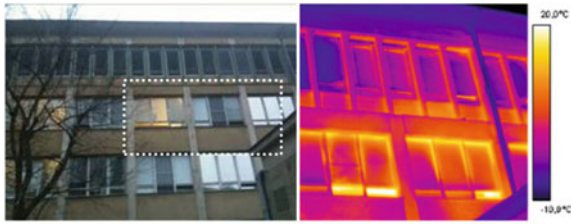
As mentioned, the difference in the air pressure is generated by a fan, which is installed with a tight sheet in an opening in the building envelope, most often on the door opening, as shown in Fig. 4.13. This is why the test is named in engineering practice as “the blower door test”.

The blower door test can be performed by two methods: by Method A (EN ISO 9972⁴) when the building is in full operation regime or by Method B at which all openings are sealed (for example, a channel for supply and exhaust air in the system of mechanical ventilation) and only the airtightness of building envelope is tested.

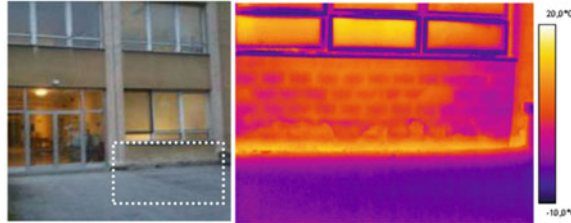
⁴EN ISO 9972:2015 Thermal performance of buildings—Determination of air permeability of buildings—Fan pressurization method.

Case study: Interpretation of thermal images of a building envelope of a non-thermal insulated building taken during the heating season.

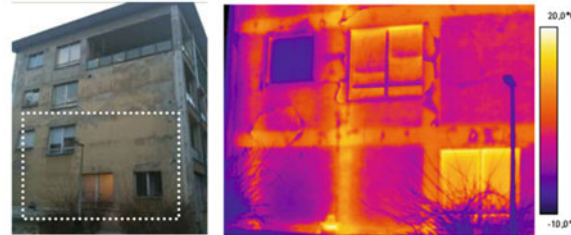
Warm upper and cold lower window frame areas indicate air leakage. As some windows are open, this indicates inadequate ventilation of the rooms.



High surface temperatures indicate that the brick wall is not thermally insulated; even higher temperature above the ground indicates that wall is moist.



Heat bridges on the columns and floor slab can be observed here.



Using thermography, the quality of thermal insulation of heat generators, pipelines and storage tanks can also be checked.



Fig. 4.12 Thermal images of case study building envelope and building service system elements



Fig. 4.13 Blower door equipment installed tightly on the entrance door of building (left); it is common practice that the blower door test is performed in new buildings before finishing to enable the airtightness to be improved with minimum cost (middle, right)

Method B is used most often. Regardless of the method used, the blower door test should be performed under the following conditions:

- the test must be repeated for several steady-state conditions at positive (over pressure) and negative (under pressure) air pressure differences between the building and ambient environment; the pressure difference must range between 20 and 100 Pa;
- the test can be performed if the current value of product of temperature difference between indoor and outdoor air temperature and the height of the building is smaller than $5000 \text{ K} \times \text{m}$;
- at wind speeds lower than 6 m/s to avoid stagnation pressure caused by the wind having any significant influence on air infiltration.

The result of the blower-door test is expressed with a graph with linear approximation of measured air flow rate V (m^3/h) at different pressure differences (Pa). The air exchange rate at pressure difference of 50 Pa is denoted as n_{50} . The n_{50} air exchange rate is defined by equation:

$$n_{50} = \frac{\dot{V}_{50}}{V} \quad (1/\text{h})$$

air flow rate at pressure difference between interior and outdoor 50 Pa (m^3/h)
 net volume of the building (m^3)

Note 1: The maximum air exchange rate n_{50} is limited and prescribed as a building energy efficiency indicator by national regulations. For example, in Slovenia, n_{50} must be less than 3 h^{-1} for naturally ventilated buildings and less than 2 h^{-1} for buildings with mechanical ventilation.

Note 2: For passive buildings (PHPP), n_{50} must not exceed 0.6 air exchanges per hour (Fig. 4.14).

During the blower-door test, an expert verifies if any air leakage is present. A smoke generator and a velocity meter can be used for detection of air leakage in the building envelope or un-tight appliances (Fig. 4.15).

4.6 In-Situ Determination of Overall Building Thermal Properties

In Sect. 3.1.11, methods for the calculation of transmission H_T and ventilation H_V heat transfer coefficient, linear ψ and point thermal transmittance χ of thermal bridges and total solar energy transmittance of glazing g were presented. These parameters have substantial impact on energy needs for heating and cooling of the building; deviation of in situ values from the design can cause significant deviation

Fig. 4.14 Report on blower door test is presented in a log-log diagram as the air flow rate at different over- and under-pressure differences; n_{50} is shown on the diagram

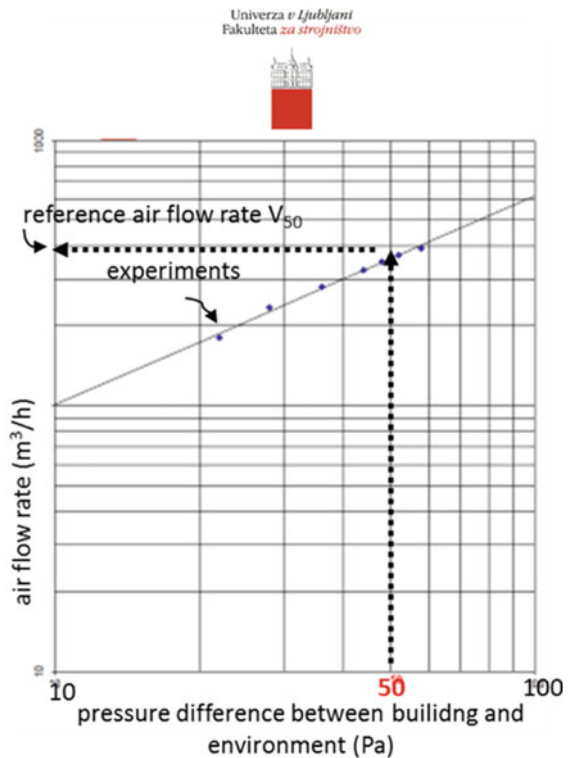




Fig. 4.15 Air velocity at the leaky details on the building envelope is in the range from 2 to 4 m/s and air leaks can be easily detected with air velocity measurement

in the calculated value of energy needs. For the evaluation of those quantities by a single set of experiments, the so-called co-heating method was developed. This is quasi-stationary method based on linear regression analysis of dynamic thermal response of the building. With a co-heating test (i) the total heat loss coefficient HLC (as sum of transmission H_T and ventilation heat transfer coefficient H_v) and (ii) the solar aperture area (product of glazing area and total solar transmittance g of glazing) are estimated. During the test, the interior of the building is heated to a steady-state elevated temperature (e.g. 25 °C) using electrical heaters and ventilators (to ensure minimum temperature gradient). At same time, the outdoor temperature, wind speed, and solar radiation are monitored (Fig. 4.16).



Fig. 4.16 During a co-heating method experiment, the building is maintained at a constant uniform and elevated temperature with electric heaters and fans installed in each thermal zone (space) in the building (Bauwens and Roels 2013)

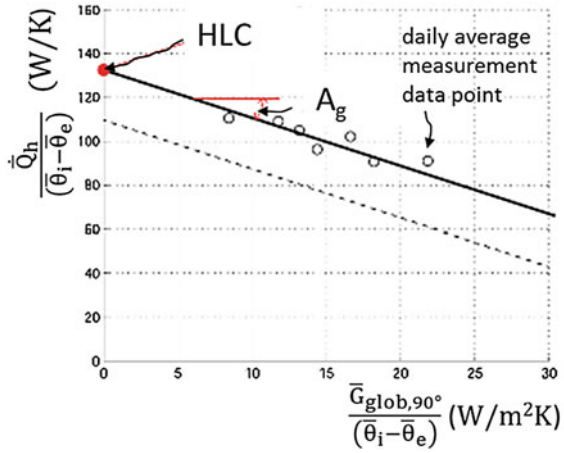
Following heat flux balance is assumed:

$$\dot{Q}_h + \sum_{i=1}^n A_{g,i} \cdot G_{glob,\beta,i} = HLC \cdot (\theta_i - \theta_e) \quad (W)$$

electrical power of heater (W) \rightarrow \dot{Q}_h
 number of windows that affect solar heating \rightarrow n
 global solar radiation on i-th window (W/m²) \rightarrow $G_{glob,\beta,i}$
 indoor air temperature (°C) \rightarrow θ_i
 outdoor air temperature (°C) \rightarrow θ_e
 effective glazing area of glazing (solar aperture) of i-th window (m²) \rightarrow $A_{g,i}$
 total heat loss coefficient (W/K) \rightarrow HLC

Solar aperture area $A_{g,i}$ of i-th window includes properties about the size of the window, the share of the window frame in the window area, the total solar energy transmittance g , and the shading factor of the shades and surrounding object S_f :

Fig. 4.17 In the co-heating method, one to three weeks of daily average experiment data is approximated by the line of the established in-situ total heat transfer coefficient HLC and the total solar aperture area of windows A_g



$$A_{g,i} = A_{w,i} \cdot (1 - f_f) \cdot g_i \cdot S_{f,i} \quad (\text{m}^2)$$

area of i-th window (m²) frame area factor (1)
 total solar energy transmittance of i-th window glazing (1) shading factor of shades and surrounding objects affected i-th window (1)

The total heat loss coefficient HLC is sum of:

$$HLC = H_T + H_v + \sum_{j=1}^n \psi_j \cdot l_j + \sum_{k=1}^m \chi_k \cdot n_k \quad (\text{W/K})$$

transmission heat transfer coefficient (W/K) ventilation heat transfer coefficient (W/K) linear thermal bridge heat transfer factor (W/K) point thermal bridge heat transfer factor (W/K)

The heat flux balance of heat losses and gains could be rearranged taking into account daily average values:

$$\frac{\dot{Q}_h}{(\theta_i - \theta_e)} = HLC - \sum A_{g,i} \cdot \frac{G_{glob,\beta,i}}{(\theta_i - \theta_e)}$$

As proposed by the co-heating method, linear regression is performed over one to three weeks of daily average in situ data to determine the values of HLC (at interception with ordinate) and total solar aperture area $\sum A_{g,i}$ of windows (as slope angle) (Fig. 4.17).

Reference

Bauwens G, Roels S (2013) Co-heating test methodology. Transfer of building physics and CO₂ methodologies to optimize energy efficient competencies across the three sectors (LDV-TOI-18/12). Lifelong learning programme Leonardo da Vinci transfer of innovation

Chapter 5

Global Climate and Energy Performance of the Building



Abstract In this chapter, the link between environmental protection and energy policy on future energy supply and demand is shown. The contents of the Energy Performance of Building Directive (EPBD) as direct results of global warming mitigation policy is presented. Energy performance indicators of nearly Zero Energy Buildings are presented, as they are defined in the recast EPBD. Assessment methods for the determination of building energy needs, primary energy demand, and use of renewable energy carriers for the operation of the buildings are described and explained.

In recent decades, energy policy in the EU has been driven by ecology and environment protection targets. Despite the fact that energy conversion has impact on all environmental spheres, the long-term global climate change as a consequence of anthropogenic emissions of greenhouse gases (GHG) is considered to be the most critical energy use-related environmental problem. While GHG do not affect the short-wave solar irradiation received on and reflected by the Earth's surface, they retain part of the long-wave thermal radiation emitted by Earth's surface towards the space. This property of the atmosphere is called the greenhouse effect. Although the consequence of this effect is a suitable temperature for the development of living beings on our planet, climatologists warn of a rapid change in the greenhouse effect due to anthropogenic greenhouse gas emissions that already causing noticeable global overheating of the planet.

Note: As different pollutants can cause the same environment problem (like changing of greenhouse effect of atmosphere, depletion of stratospheric ozone or acidification of precipitation), it is common that the total emission of pollutants is expressed as a weighted sum of the mass of emitted pollutants. Weighting factors represent the relative influence of individual pollutants to the environment in comparison to reference matter and are determined assuming certain periods of presence in the environment (20, 100 or 500 years). The sum of weighted emissions is expressed as an equivalent of the emissions of the reference matter, for example eq CO₂ (or CO₂eq) for greenhouse gasses or eq CFC-11 for the emission of gasses that cause stratospheric ozone depletion (Fig. 5.1).

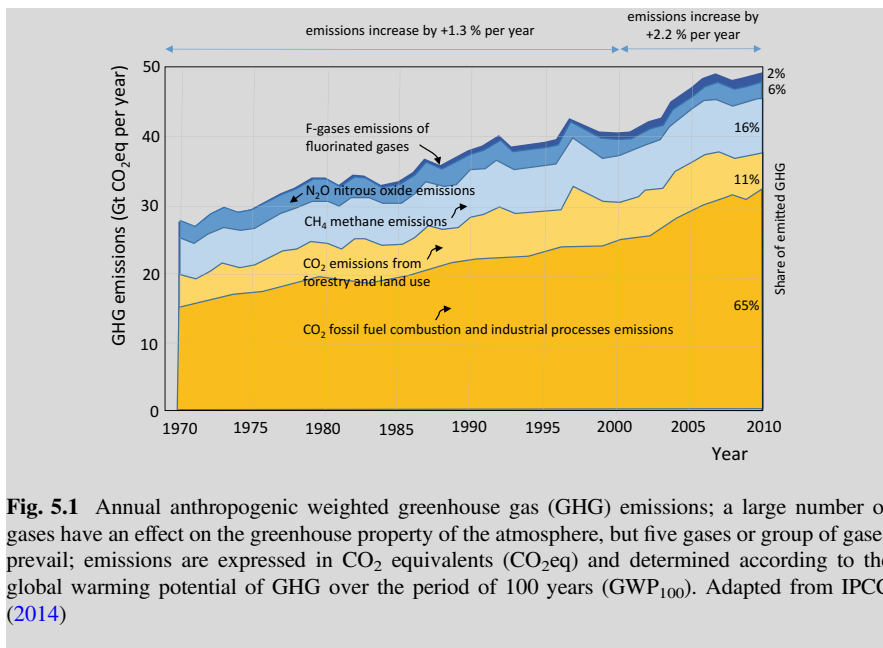


Fig. 5.1 Annual anthropogenic weighted greenhouse gas (GHG) emissions; a large number of gases have an effect on the greenhouse property of the atmosphere, but five gases or group of gases prevail; emissions are expressed in CO₂ equivalents (CO₂eq) and determined according to the global warming potential of GHG over the period of 100 years (GWP₁₀₀). Adapted from IPCC (2014)

Anthropogenic emissions of GHG, expressed as CO₂ equivalent, are used as a typical indicator to analyse the energy consumption-associated environmental impacts and the strategies of energy supply and demand in the future. The most important for the development of climate and energy policy at the global level is the role of the Intergovernmental Panel on Climate Change (IPCC), which was established by the UN Environmental Programme (UNEP) and the World Meteorological Organisation (WMO) in 1988. The objectives and measures of the current global climate and energy policy are mainly based on the results of the Climate Convention in 1992 (United Nations Framework Convention on Climate Change, UNFCCC).

At the climate summit in Copenhagen in 2009, the delegates adopted the non-binding Copenhagen Accord, the aim of which is to reduce the anthropogenic impact on the global climate; it represents a continuation of the Kyoto Protocol. In the document, the climate scenario “2 K” was adopted for establishing the guidelines for supply and use of energy for the period up to 2100. According to this scenario, the total anthropogenic greenhouse gas emissions should be decreased to such extent that in this century an increase in the average global temperature of the atmosphere will likely not exceed 2 °C above the pre-industrial period. According to current knowledge this goal can be achieved if the concentration of greenhouse gasses in the atmosphere expressed by CO₂ equivalent does not exceed ~450 ppm CO₂eq and the average yearly GHG emissions in the period between 2011 and 2100 should not be above 25 Gt CO₂eq comparing to 49 Gt CO₂eq in the year 2010 (Fig. 5.2).

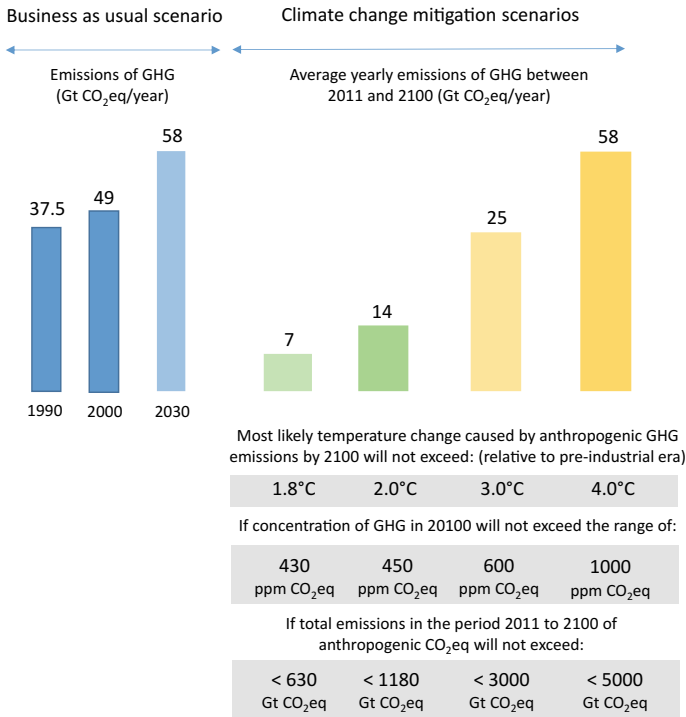


Fig. 5.2 Global emissions of greenhouse gasses in Gt per year in the year 2002 (left); increase in average planet temperature (mean air temperature) as result of yearly anthropogenic emissions of CO₂ equivalent; it can be seen that maintaining of CO₂eq emissions at current level will cause the planet’s temperature to rise by 3 K; to fulfil the “2 K” global climate scenario, yearly emissions of CO₂eq must be decreased to 32 Gt per year (right). Adapted from IPCC (2014)

Two groups of measures are considered in global climate changes mitigation scenarios: (i) wider implementation of energy conservation measures, which leads towards increased energy efficiency and (ii) intense replacement of non-renewable (fossil and nuclear) with renewable energy sources. Measures from both groups are very efficient when implemented in buildings; consequently, requirements for energy efficiency in buildings are very strict nowadays.

5.1 Energy Performance of Building Directive (EPBD) and Nearly Zero Energy Buildings (NZEB)

Energy-related emissions contribute almost 80% of the EU’s total greenhouse gas emissions, and energy use for the operation of the buildings corresponds to 40% of total final energy demand and 36% of total anthropogenic CO₂ emissions. As a

result, the Energy Performance Building Directive (EPBD),¹ key legislation on efficient energy use in buildings in the EU Member States, was adopted. The directive addresses, among other items, the following:

- requires integrated methodology to rate the energy performance of buildings;
- sets minimum performance standards for new and existing buildings that undergo major renovation;
- introduces energy certificates for buildings (see Chap. 13);
- introduces requirements regarding regular inspections of boilers and air-conditioning systems.

The EPBD was implemented in Member States at the end of the year 2010.

In 2010, a new directive was published as the EPBD was recast,² introducing further requirements of energy efficiency for buildings. The most noticeable change is the requirement for nearly Zero Energy Buildings (nZEB). nZEB buildings are buildings that have integrated systems for energy production on or in the building itself or in the vicinity of the building (for example solar collectors, heat pumps, PV system, small scale biomass district heating system) that cover the majority of delivered energy needed for the operation of the building. The term “delivered energy for operation of the building” indicates total quantity of energy delivered to the building with different energy carriers to fulfil indoor living comfort criteria according to thermal comfort, indoor air quality, domestic hot water needs, and lighting (see Chap. 1) through installed building service systems. In the case of public buildings, nZEB requirements should be implemented by the end of 2018 and for all other buildings after 2020. At the moment, three nZEB indicators for new and renovated buildings are defined in national legislation in most cases:

- maximum allowed annual energy needs for heating per unit of the conditioned space (m²);
- maximum allowed annual non-renewable primary energy needed for operation of building per unit of the conditioned space; the assessment must include evaluation of so-called “EPBD systems”, which are systems for heating, domestic hot water heating, cooling, ventilation, air conditioning, and lighting of the buildings;
- minimum share of renewable energy in total primary energy needed for operation of building.

The recast EPBD declares that the limit values of those indicators must be developed on a cost-optimal basis. As a consequence, the most efficient and cost-optimal measures and technologies, known as best market available technologies (BAT), must be implemented.

¹Directive 2002/91/EC of the European Parliament and of the Council of 16 December 2002 on the energy performance of buildings (Official Journal of the European Union, L 001/65).

²Directive 2010/31/EU of the European Parliament and of the Council of 19 May 2010 on the energy performance of buildings (recast) (Official Journal of the European Union, L 153/13).

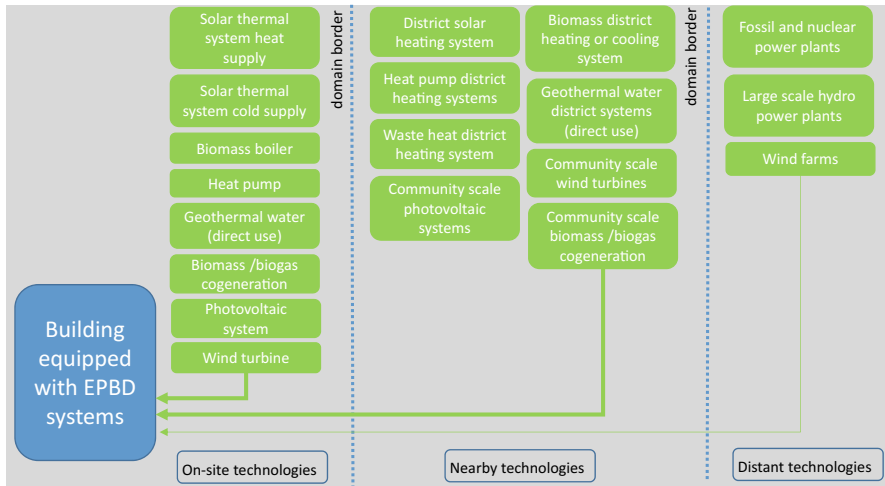


Fig. 5.3 On-site (building integrated), nearby and distant technologies for utilization of RES; as required by nZEB; most of the energy needed for operation of buildings must be produced on-site or nearby from renewable energy sources (EN ISO 52000-1 EN ISO 52000-1:2017 energy performance of buildings—overarching EPB assessment—part 1: general framework and procedures)

Note: As proposed in Slovenia Energy law and the Action Plan for nZEB, the required values of nZEB indicators in Slovenia are: maximum energy need for heating $25 \text{ kWh/m}^2 \text{ a}$, maximum non-renewable primary energy needed for operation of the building $E_{P,nren} 75 \text{ kWh/m}^2 \text{ a}$ is allowed for new residential and $55 \text{ kWh/m}^2 \text{ a}$ for new non-residential buildings. The minimum required share of renewable energy sources RER 50% utilized by on-site or nearby systems is required for all buildings (Fig. 5.3).

5.2 Determination of Energy Performance of the Buildings

Despite the fact that nZEB criteria will come into force in the next couple of years, similar energy efficiency indicators of buildings are already used in EU member states. Indicators are determined by annual energy balance on three computational levels: (i) as energy needs that are defines with respect to indoor living comfort requirements, (ii) as delivered (or final) energy, energy needed for operation of the building service systems, which is defined according to the type and amount of the energy carrier used and (iii) as renewable and non-renewable natural energy sources

(primary energy sources) needed for operation of the building; at this level, the impacts on the environment are a consequence of energy use.

Energy needs for space heating, space cooling, domestic hot water heating, ventilation, and lighting and, if installed, for air conditioning must be determined according to EPBD. Energy needs for heating (Q_{NH}), cooling (Q_{NC}), and ventilation (Q_V) depend on the architecture of the building, the thermal quality and air tightness of building envelope, the type of ventilation and solar and internal heat gains. Energy needs for domestic water heating (Q_W) depend on the usage profile according to the type of the building; energy needs for lighting (W_L) depend on required illumination level and quality of daylighting. Energy needs for humidification (Q_{HU}) and de-humidification (Q_{DHU}) depend on climate conditions and internal water vapour sources. Energy needs are determined taking into account indoor comfort requirements according to the type of the building. Energy needs are presented as specific values expressed per 1 m^2 of building useful floor area ($\text{kWh}/\text{m}^2 \text{ a}$), or, per 1 m^3 of conditioned net volume in case of non-residential buildings. In countries where energy demand for heating prevails, the specific value of energy needs for heating (Q'_{NH} in $\text{kWh}/\text{m}^2 \text{ a}$) is used for defining the buildings energy efficient class (A–G), which is the most recognizable indicator of building energy efficiency in general.

Note: It is important to realise that energy needs are calculated using a pre-selected category of indoor comfort (see Chap. 1) and with the assumption that the energy efficiency of all appliance and technical building systems installed is assumed to be 100% and, therefore, no heat losses are generated and no auxiliary energy is needed for the operation of the systems.

Delivered energy is expressed with the amount and type of consumed energy carriers needed for operation of the building during one year period. Delivered energy is established separately for each of installed building technical service system, taking into account energy needs, energy losses of the generation and the transportation of heat, cold or electricity, controlling of the systems as well as use of auxiliary energy ($W_{f,AUX}$) needed for operation of the building service systems. At this stage, the efficiencies of the building service system components, as stated by the manufacturer on the basis of standardized tests or designer, are taking into account. Delivered energy for space heating ($Q_{f,H}$), space cooling ($Q_{f,C}$), ventilation ($Q_{f,V}$), preparation of domestic hot water ($Q_{f,W}$), lighting ($W_{f,L}$), and air-conditioning ($Q_{f,DHU}$, $Q_{f,HU}$) must be verified. Most often there is no limitation of delivered energy demand in national legislation, but components of systems must fulfil minimum efficiency criteria.

Once the type and amount of each energy carrier needed for building operation is known, primary energy needed for operation of the building and CO_2 emissions can be calculated using pre-defined factors and emission coefficients. Specific values of these two indicators are calculated per 1 m^2 of building useful floor area (in $\text{kWh}/$

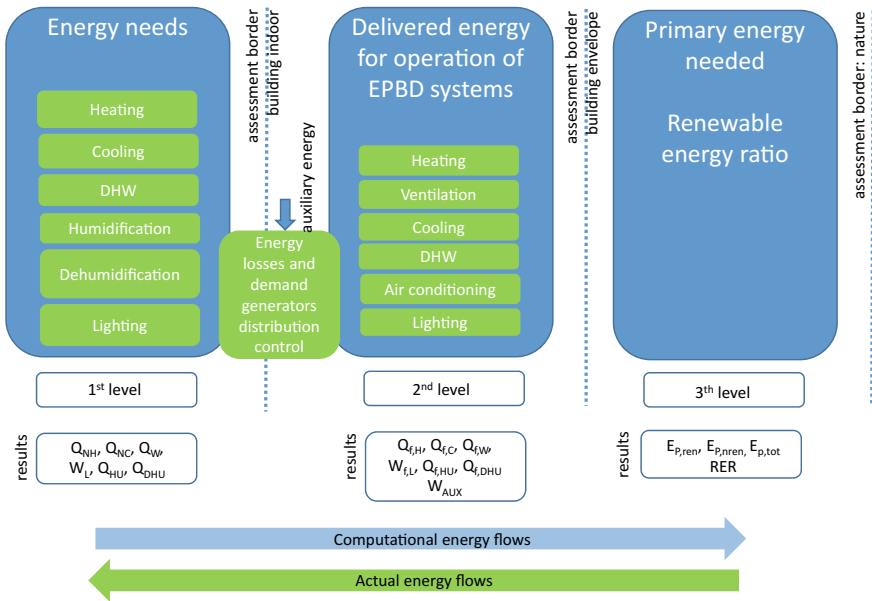


Fig. 5.4 Energy performance of the building is determined on three levels by the energy balance carried out in the opposite direction compared to actual energy flows (EN ISO 52016-1 (EN ISO 52016-1:2017 energy performance of buildings—energy needs for heating and cooling, internal temperatures and sensible and latent heat loads—part 1: calculation procedures))

m^2 a and kg/m^2 a) and tested according to the maximum allowed values stated in national regulations on energy efficient buildings. Primary energy needed for operation of the building is expressed as renewable ($E_{P,ren}$), non-renewable ($E_{P,nren}$), and total ($E_{P,tot} = E_{P,ren} + E_{P,nren}$) primary energy. At this stage, the share of renewable energy sources (RER Renewable Energy Ratio) for the operation of the building is determined as the ratio between renewable and total primary energy needed (Fig. 5.4).

5.2.1 Time Step Intervals and Calculation Period

Two time step intervals are common for the determination of energy balance and the calculation of energy efficiency indicators of the buildings:

- monthly methods: performed using simple calculation tools taking into account average monthly data of (steady) ambient and indoor temperatures and solar radiation; monthly calculation methods are more accurate for evaluation of residential buildings without cooling, with 24/7 occupancy profile and give

better results for high weighted buildings with low and moderate thermal insulation of the building envelope and in the case of lower internal heat gains;

- hourly methods: can be performed using advanced software to enable the evaluation of unsteady heat transfer in building elements and the dynamic thermal response of the building; hourly meteorological data and hourly profiles of operation, occupancy, and internal heat gains must be defined; application of such method is necessary in the case of non-residential buildings with cooling and air-conditioning systems.

Regardless of the selection of the calculation method, energy efficiency indicators are determined in the opposite direction regarding actual energy flows. Because of the interaction between systems (for example, domestic hot water distribution system decrease the use of delivered energy for space heating) or energy transformation (electricity for operation of pump is partly transformed in the form of heat, which increases the heat supplied by heat transfer media), delivered energy demand and primary energy needed must be calculated in iterative loops.

As a rule, calculation period is one (calendar) year. Regardless of the time step interval of calculation, energy demand is reported as monthly values.

5.3 Determination of Building Energy Needs

5.3.1 Energy Need for Heating Q_{NH}

Energy need for heating Q_{NH} is determined on the basis of the monthly (in kWh/m) or hourly (in kWh/h) balance of heat loss and weighted heat gains. Heat losses are a consequence of heat transfer through the building envelope that separate the building's interior and the ambient environment (transmission heat losses) and the supply of fresh air needed to maintain appropriate indoor air quality (ventilation heat loss). Transmission and ventilation heat losses depend on transmission H_T and ventilation H_V heat transfer coefficients, which are explained in Sect. 3.1.11. Monthly heat losses are defined by equation:

$$Q_{T,m} = (H_T + H_V) \cdot (\theta_{i,h} - \bar{\theta}_{e,m}) \frac{24 \cdot n_m}{1000} \quad (\text{kWh/m})$$

transmission heat transfer coefficient (W/K) ventilation heat transfer coefficient (W/K) set-point indoor temperature for heating (°C) hours per day (h/day) number of days per month (day/m)

average monthly outdoor air temperature (°C) constant (Wh/kWh)

The heat gains are result of natural heating by solar irradiation transmitted through transparent envelope and internal heat gains emitted by human bodies and appliances. Internal heat gains $Q_{i,m}$ include heat produced by human bodies and appliance that are not part of building service systems. For residential buildings, constant heat flux in the range 2–4 W per m^2 of useful floor area is most often taking into account. For non-residential buildings, internal gains during building occupancy are higher and differ significantly regarding to type of the buildings and category of space (ISO 18523-1³).

Natural solar heating gains are calculated as the sum of the contributions of all transparent building structures (most often windows) and depend on the size of the transparent part of the window, total solar energy transmittance (see Sect. 3.1.9), global solar monthly radiation on the outer surface of window glazing, and correction factors. The factor is defined according the ratio between the glazed area and the total area of window, decreased transmittance of glazing at average incident angles regarding the window slope and orientation and decreased monthly solar radiation because of shading of surrounding objects (always present), and shading devices on windows, which can be static or movable. Monthly solar heat gains are determined with the equation:

$$Q_{S,m} = \sum_{i=1}^n (g_{i,l} \cdot F_{w,i} \cdot (1 - F_{f,i}) \cdot A_{w,i}) \cdot H_{glob,m,i} \cdot F_{SH,m,i} \quad (\text{kWh/a})$$

total solar transmittance measured perpendicular to glazing (-)
window area (m^2)
global (direct, diffuse and reflected) monthly solar radiation on window (kWh/m^2m)

correction factor, includes solar incident angle, dirt on glazing), typical value 0,9 (-)
window frame factor
shading factor of surrounding object and shading devices on window (-)

The calculation method for the determination of energy needs is defined in standard EN ISO 13790⁴ which was recently replaced with standard EN ISO 52016-1. As mentioned before, technical systems have no influence on energy needs for heating, and it is assumed that infinite heat flux can be provided by heat generators.

The assessment boundary between buildings and their surroundings is defined as a building’s thermal envelope. It is assumed that inside the envelope, the required thermal comfort parameters are ensured without limitations. Section 3.1.8 shows

³ISO 18523-1:2016 Energy performance of buildings—Schedule and condition of building, zone and space usage for energy calculation—Part 1: Non-residential buildings.

⁴EN ISO 13790:2008 Energy performance of buildings—Calculation of energy use for space heating and cooling.

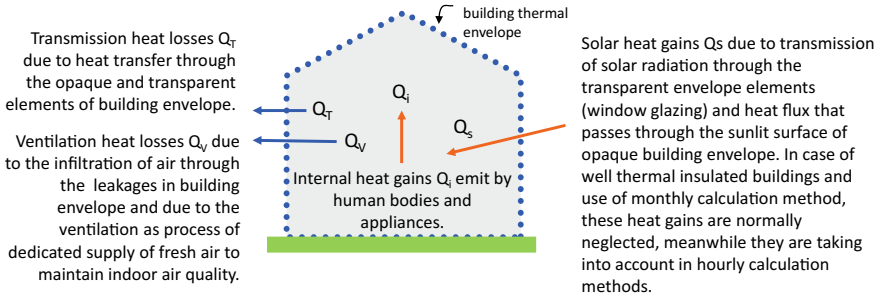


Fig. 5.5 Building thermal envelope is the physical and thermodynamic border between the conditioned interior and outdoor air, ground or unheated spaces; the envelope defined the assessment domain for determination of energy needs; transfer and ventilation heat losses as well as solar and internal heat gains are considered in the evaluation of energy needs for heating and cooling

how to determine the area of the building’s thermal envelope regarding the architecture of the building (Fig. 5.5).

In the case of the monthly calculation method, the energy balance is made for each month of the year and the sum of monthly values for months in which $Q_{NH,m} > 0$ (kWh/m) represent annual energy needs for heating. In the calculation procedure, it is foreseen that only part of heat gains (solar and internal) can be utilized (solar and internal) to decrease energy demand for heating $Q_{NH,m}$ because of potential overheating during the months of low heat losses. Yearly energy needs for heating are defined by equation:

$$Q_{NH} = \sum_{m=1}^{12} Q_{NH,m} = \sum_{m=1}^{12} [(Q_{T,m} + Q_{V,m}) - \eta_{H,gn,m} \cdot (Q_s + Q_i)] \quad (\text{kWh/a})$$

gain utilization factor (-)

$$Q_{NH,m} < 0 \rightarrow Q_{NH,m} = 0$$

Heat gain utilization factor $\eta_{H,gn,m}$ is calculated for each month and depends on the gain ratio $\gamma_{H,m}$ between the total monthly heat gains ($Q_s + Q_i$) and total heat losses ($Q_T + Q_V$) and the thermal capacity of indoor environment. The thermal capacity of the building can be determined numerically using detailed data about building materials or simplified as an aggregated quantity as proposed in standard EN ISO 52016-1 if the monthly calculation method is implemented. In this case, buildings are classified into one of the mass categories as extremely light, light, moderate, heavy, or extra heavy regarding the time constant of the building’s

thermal response. Thermal capacity C in kJ per K of the building is approximated according to useful floor area A_u as $(80 \times A_u)$ for very light building to $(370 \times A_u)$ kJ per K in the case of extra heavy construction. Thermal capacity influences the accumulation of solar energy and internal heat gains; consequently, the energy needed for heating is lower in a heavy-weight building than a light-weight building of the same size. The value of $\eta_{H,gn,m}$ is between 1 (needed heat for heating in this month is reduced by total amount of heat gains) and 0.3 (typical for passive solar heated building in the mid-season months).

Case Study 1 If gain ratio $\gamma_{H,m}$ is equal to 0.80 gain utilization factor $\eta_{H,gn,m}$ will be equal to 0.62 in the case of an extremely light building and 0.99 in the case of a heavy building.

Case Study 2 Determine energy needs for heating of Virtual Lab building using the TRIMO Expert tool.

Start the software, select Virtual Lab as working project (> PROJECT). Check on-site meteorological parameters (> Meteorological data). The Virtual Lab building is divided in two thermal zones: living unit (LU) and technical unit (TU). Check (> THERMAL ZONE) sizes, temperature set points, infiltration and ventilation rates for each zone. Check areas and composition of building structures and windows (> BUILDING and > ANALYSIS > Building constructions). Visit www.ee.fs.uni-lj.si/cell (> technologies) for detailed overview of building structures. Check energy needs for heating (> ANALYSIS > Thermal Zones) (Fig. 5.6).

Yearly energy needs for heating of Virtual Lab building (> REPORT > Building) is equal to 763 kWh/a the living unit and 1217 kWh/a for the technical unit, in total 1980 kWh/a. As the total useful area of Virtual Lab is 29 m², specific energy need for heating of Virtual Lab building is equal to 68.3 kWh/m² a (Fig. 5.7).

Note 1: The Virtual Lab building is divided into two thermal zones because the use profiles are different, and the heating and ventilation systems are separated.

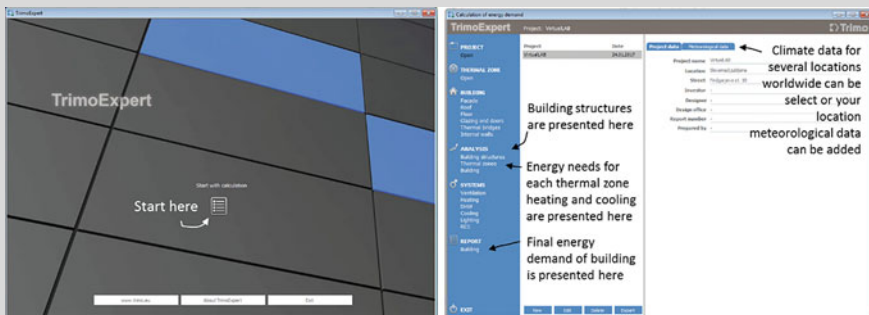


Fig. 5.6 TRIMO Expert computer tool user interface

Heating		Cooling													
Heating	Jan kWh	Feb kWh	Mar kWh	Apr kWh	May kWh	Jun kWh	Jul kWh	Aug kWh	Sep kWh	Oct kWh	Nov kWh	Dec kWh	Total kWh/a		
Transmission heat losses	209	170	136	88						94	152	188	1037		
Ventilation heat losses	32	26	21	14	← ventilation heat losses are small because unit is ventilated with mechanical system with heat recovery							15	24	29	161
Internal heat gains	21	19	21	20						21	20	21	142		
Solar heat gains	35	49	61	62						48	29	26	310		
Gain utilization factor	1,00	0,99	0,97	0,89						0,94	1,00	1,00			
Energy for heating (Q _{NH})	186	129	77	30						44	126	171	763		
Number of heating days	31	28	31	29	↑ Living unit needs heating only 29 days in April							31	30	31	211
													energy needs for heating of Living unit (kWh/year)		

Heating		Cooling												
Heating	Jan kWh	Feb kWh	Mar kWh	Apr kWh	May kWh	Jun kWh	Jul kWh	Aug kWh	Sep kWh	Oct kWh	Nov kWh	Dec kWh	Total kWh/a	
Transmission heat losses	224	192	156	108	51				54	112	173	212	1292	
Ventilation heat losses	30	24	20	14	7				7	14	22	27	165	
Internal heat gains	0	0	0	0	0				0	0	0	0	0	
Solar heat gains	10	17	34	51	60	gain utilization factor is lower because heat losses are much lower than in winter months				40	23	11	8	254
Gain utilization factor	1,00	1,00	1,00	0,99	0,80				0,94	1,00	1,00	1,00		
Energy for heating (Q _{NH})	254	199	142	72	10				23	103	183	231	1217	
Number of heating days	31	28	31	30	28				30	31	30	31	270	
													energy needs for heating of Technical unit (kWh/year)	

Fig. 5.7 Monthly energy needs for heating Q_{NH} of Virtual Lab building (TRIMO Expert)

Note 2: Specific energy need for heating is much above the nZEB criteria. The reason is that Virtual Lab is a quite small building and that the architectural concept was adapted to enable installation of on-site systems for the utilization of solar energy for heating, cooling and electricity production.

5.3.2 Energy Need for Cooling Q_{NC}: Monthly Calculation Period

The energy need for cooling Q_{NC} is equal to the heat that must be removed from the building to maintain user-defined set-point temperature in observed month. It is determined by a similar energy balance to Q_{NH} but the opposite regarding to heat gains and losses. Internal and solar heat gains increase the energy needs for cooling, while heat transfer through the building envelope and ventilation heat transfer when the ambient temperature is lower than the set-point temperature decrease energy needs for cooling as the heat losses increase. The heat transfer utilization factor $\eta_{C,gn,m}$ is determined for each month and depends on the ratio between the heat gains by solar radiation and interior heat (Q_S + Q_i) and heat sinks or gains by transmission and ventilation (Q_T + Q_V). The heat transfer utilization factor indicates to what extent a building is cooled by night-time ventilation and heat transfer through its envelope to enable the accumulation of heat from internal heat sources and solar radiation during the next day. Values of $\eta_{C,gn,m}$ are between 0.25 and 1 (in the case of transmission and ventilation heat losses in this particular month are quite large in comparison to heat gains). Q_{NC} is determined with the equation:

$$Q_{NC} = \sum_{m=1}^{12} Q_{NC,m} = \sum_{m=1}^{12} [(Q_{S,m} + Q_{i,m}) - \eta_{C,gn,m} \cdot (Q_{T,m} + Q_{V,m})] \quad (\text{kWh/a})$$

$Q_{NC,m} < 0 \rightarrow Q_{NC,m} = 0$

monthly energy need for cooling (kWh/m) solar heat gains (kWh/m) internal heat gains (kWh/m) monthly heat transmitted through thermal envelope (kWh/m) (+ if heat is transferred from interior to exterior) heat transfer by infiltration and ventilation (kWh/m) (+ if heat is transferred from interior to exterior)

heat transfer utilization (-)

Case Study 1 If gain ratio $\gamma_{C,m}$ is equal to 1, heat transfer utilization factor $\eta_{C,gn,m}$ will be equal to 0.62 in the case of an extremely light building and 1 in the case of extra heavy building.

Case Study 2 Determine energy needs for cooling of Virtual Lab building using the TRIMO Expert tool.

Yearly energy needs for heating of Virtual Lab building (> REPORT > Building) is equal to 29 kWh/a living unit and 15 kWh/a for Technical unit, in total 44 kWh/a. This is because of the rather small window areas and internal gains but especially because of local climate data.

Results of monthly calculations are shown in Fig. 5.8.

Heating		Cooling													
Cooling		Jan kWh	Feb kWh	Mar kWh	Apr kWh	May kWh	Jun kWh	Jul kWh	Aug kWh	Sep kWh	Oct kWh	Nov kWh	Dec kWh	Total kWh/a	
Transmission heat losses						69	81	63	73	56				342	
Ventilation heat losses						33	39	30	35	27				165	
Internal heat gains						25	40	42	42	20				169	
Solar heat gains						20	35	35	34	15				138	
Loss utilization factor						0,43	0,57	0,70	0,62	0,41					
Energy for cooling (QNC)						2	6	12	8	1				29	
Number of cooling days						19	30	31	31	15				126	
energy needs for cooling of Living unit (kWh/year)															
Heating		Cooling													
Cooling		Jan kWh	Feb kWh	Mar kWh	Apr kWh	May kWh	Jun kWh	Jul kWh	Aug kWh	Sep kWh	Oct kWh	Nov kWh	Dec kWh	Total kWh/a	
Transmission heat losses							86	67	78					232	
Ventilation heat losses							44	34	40					118	
Internal heat gains							0	0	0					0	
Solar heat gains							68	72	61					200	
Loss utilization factor							0,49	0,63	0,49						
Energy for cooling (QNC)							4	8	3					15	
Number of cooling days							30	31	31					92	
energy needs for cooling of Technical unit (kWh/year)															

Fig. 5.8 Monthly energy needs for cooling Q_{NC} of Virtual Lab building (TRIMO Expert)

5.3.3 Energy Need for Heating Q_{NH} and Cooling Q_{HC} : Hourly Calculation Method

The hourly calculation method is based on the balance of average heat fluxes repeated in hourly intervals. In this way, the impact of dynamic boundary conditions and the accumulation of heat in building structures and building interiors can be taken into account. Heat transfer is treated as unsteady, which means that (i) heat flux on outer surface is not equal to heat flux on the inner surface of the building structure and the heat transfer rate through building thermal envelope cannot be determined solely with heat transfer coefficient U and the air temperature difference because the heat capacity of building structure accumulate the heat, (ii) indoor air temperature and operative temperature are not constant during the day and month (as assumed in monthly methods) and differ from the set-point temperature because of the accumulation of heat in the air, building structures inside the building, furniture, and in the inner layer of external building structures. In the simplest form, as one node balance of thermal response of building interior, indoor air temperature in the next time step is defined with equation:

$$\frac{C_m}{\Delta t} \cdot \theta_{i,t} + \sum_{j=1}^n A_j \cdot h_{c+r,j} \cdot (\theta_{i,t} - \theta_{si,j,t}) + H_V \cdot (\theta_{i,t} - \theta_{e,t}) = \frac{C_m}{\Delta t} \cdot \theta_{i,t-1} + \dot{Q}_i + \dot{Q}_{sol} + \dot{Q}_{system}$$

Labels for the equation terms:

- $\frac{C_m}{\Delta t}$: thermal capacity of buildings (J/K)
- $\theta_{i,t}$: indoor air temperature at time t ($^{\circ}\text{C}$)
- Δt : calculation time step (s)
- $\sum_{j=1}^n A_j$: area of j -th envelope building structure (m^2)
- $h_{c+r,j}$: combined (c+r) surface heat transfer coefficient on j -th building structure ($\text{W}/\text{m}^2\text{K}$)
- $\theta_{i,t}$: temperature of inner surface of j -th part of building envelope at time t ($^{\circ}\text{C}$)
- $\theta_{si,j,t}$: temperature of inner surface of j -th part of building envelope at time t ($^{\circ}\text{C}$)
- H_V : ventilation heat transfer coefficient (W/K)
- $\theta_{i,t}$: indoor air temperature at time t ($^{\circ}\text{C}$)
- $\theta_{e,t}$: outdoor air temperature at time t ($^{\circ}\text{C}$)
- $\frac{C_m}{\Delta t} \cdot \theta_{i,t-1}$: indoor air temperature in previous time step (at time $t-1$) ($^{\circ}\text{C}$)
- \dot{Q}_i : average heat flux of internal gains and solar radiation during the calculation time interval (W)
- \dot{Q}_{sol} : average heat flux that is transferred in or out of the building during calculation time step (W)
- \dot{Q}_{system} : average heat flux that is transferred in or out of the building during calculation time step (W)

If the building is free running (without heating and cooling), Q_{system} is equal to 0 and indoor air temperature $\theta_{i,t}$ is determined. If the building is thermostatted, indoor air temperature is $\theta_{i,t}$ is equal to the set-point temperature and the heat flux transferred into the building by heating system ($Q_{system} > 0$) or by cooling system ($Q_{system} < 0$) in the calculation time period is the result of the calculation. The energy needed for heating and cooling is equal to:

$$Q_H = \dot{Q}_{system} \cdot \Delta t \quad \text{if } \dot{Q}_{system} > 0 \quad \text{or} \quad Q_C = \dot{Q}_{system} \cdot \Delta t \quad \text{if } \dot{Q}_{system} < 0$$

Case Study A building has useful thermally conditioned area A_u equal to 35 m^2 and has heat capacity C_m $3500 \text{ kJ}/\text{K}$ (approximated as $100 \times A_u$). Total area of building thermal envelope $\sum A_j$ is equal to 55 m^2 . The specific ventilation heat transfer coefficient H_V is $18 \text{ W}/\text{K}$, combined convective and radiation surface heat transfer coefficient h_{c+r} $4 \text{ W}/\text{m}^2 \text{ K}$, temperatures on the inner surfaces of envelope are $T_{si,t}$ $24 \text{ }^{\circ}\text{C}$ on all surfaces, the ambient temperature $T_{e,t}$ $28 \text{ }^{\circ}\text{C}$, internal sources is 100 W (one person) and solar radiation transmitted through glazing is 450 W . The temperature of the indoor air $T_{i,t-1}$

in the previous calculation time step one hour ago (Δt is equal to 1 h) was 20 °C. Calculate the temperature in the building at the time t!

$$\frac{3,500,000}{3600} \cdot \theta_{i,t} + \sum_{j=1}^n 55 \cdot 4.0 \cdot (\theta_{i,t} - 24) + 18 \cdot (\theta_{i,t} - 28) = \frac{3,500,000}{3600} \cdot 20 + 100 + 450 + 0$$

$$\theta_{i,t} = 21.3 \text{ } ^\circ\text{C}$$

The case study is much too simple to be used in practice. First, the inner surface temperatures in time t $\theta_{si,j,t}$ are not known, and they are not equal in each building structure; gains (internal, solar and system) should be divided into convective and radiative parts. The convective part is taken into account in the air node energy balance equation (to determine $\theta_{i,t}$) and the radiative part on each surface node energy balance (to determine $\theta_{si,j,t}$). With the exception of light-weight windows and doors, for all other opaque building structures the inner surface temperature must be determined in a way that includes the heat capacity of the building structure. Consequently, indoor air node temperature and/or heating and cooling heat flux must be determined by using numerical methods for simultaneously solving the system of linear equations in iterative procedure. For the dynamic modelling of heat transfer inside opaque building structures, several methods can be implemented: the finite difference method based on the discretization of the fundamental differential equation developed from the Fourier conduction law in the form of a Fourier continuity equation using Taylor's theorem for discretization (a practical example of this method is presented in Sect. 3.1.7), electricity analogue R-C models, the response factor method or the wall transfer coefficient, which are developed in advance for pre-known compositions of building structures and enable the determination of inner surface temperature at time t , based on previous values. Additional iteration is required if, instead of air temperature, an operative temperature is chosen as the set point temperature for heating and cooling controlling (Davies 2004).

Computer simulation tools are used in engineering practice to determinate energy needs for the heating and cooling of buildings if an hourly calculation step is required.

Case Study Thermal response and heat fluxes in one week in r and technical unit of Virtual Lab.

Note: heat gains (+) and sings (−) are always equal; in the case of the living unit, because it is cooled by mechanical cooling and in the technical unit because the operative temperature reaches equilibrium at each moment of the simulation interval (Fig. 5.9).

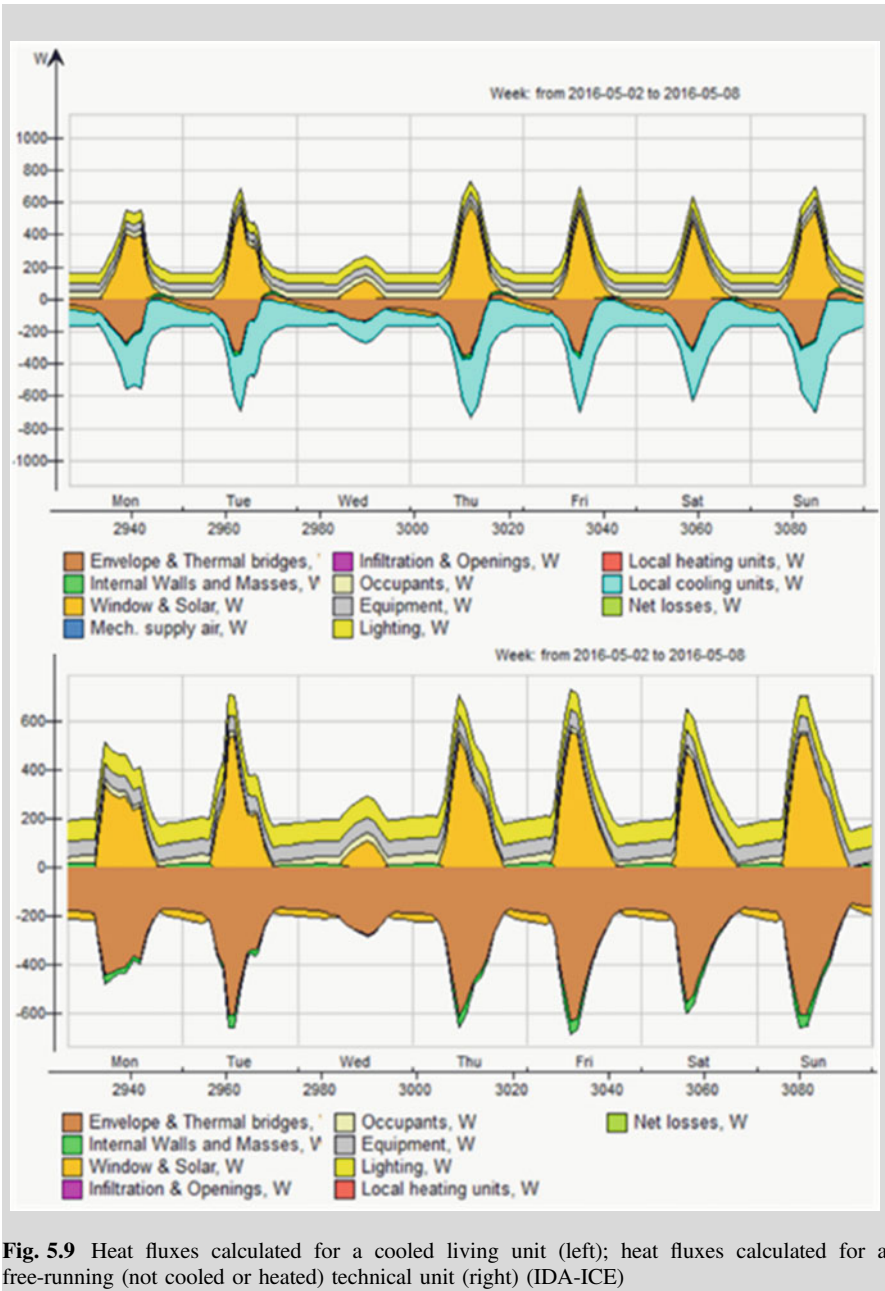


Fig. 5.9 Heat fluxes calculated for a cooled living unit (left); heat fluxes calculated for a free-running (not cooled or heated) technical unit (right) (IDA-ICE)

5.3.4 Energy Need for Ventilation Q_V

Energy needs for ventilation are not analysed separately, but as part of the energy needs for heating and cooling. It is assumed that the supplied air always has a temperature equal to the set-point temperature regardless of heating or cooling. Because of that, the description of the thermal zones in the building consists of the data of the ventilation principle (natural, mechanical with heat recovery), the amount of fresh air for ventilation (by air exchange rates n (h^{-1}) or volume (m^3/h) as well as data on the air tightness of building envelope.

5.3.5 Energy Need for Domestic Hot Water Q_W

Energy needs for domestic hot water (DHW) Q_W are defined by field studies and statistical methods and are expressed as specific values as functions of reference variables. As with other energy needs, Q_W is determined without taking into account any design data, energy losses, and auxiliary energy demand of DHW systems, and is expressed only as the heat needed to heat the required amount of hot water entering the building as cold water from the infrastructure supply to the required temperature on the outlet of the faucet or shower head. It is common that energy needs for DHW are stated in international standards (for example in EN 18599) or in relevant national regulation. Because of such an approach, no particular values are defined as the maximum allowed value of energy needs for DHW (as is common for energy needs for heating Q_{NH} and cooling Q_{NC}). Table 5.1 presents energy needs for DHW for residential buildings and some other building types as defined in EPBD-supporting standards.

Table 5.1 Guidelines for specific energy need for domestic hot water heating as presented in EN 18599; energy needs Q_W can be obtained by multiplying specific energy needs with the reference area; in the case of residential buildings, yearly energy needs are split to monthly values by the number of days (ISO 18523-1)

Building category	Reference area	Demand per usage	Demand per reference area
Single family building	Living floor area		12 kWh/m ² /year
Multifamily building	Living floor area		16 kWh/m ² /year
Office building	Office floor area	0.4 kWh/person/day	30 Wh/m ² /day
Schools with showers	Classrooms area	0.5 kWh/person/day	170 Wh/m ² /day
Hospitals	Wards and rooms area	8 kWh/bed/day	530 Wh/m ² /day
Retail shop	Sales area	1 kWh/employee/day	10 Wh/m ² /day
Hotel	Bedrooms area	1.5–7 kWh/bed/day	190–580 Wh/m ² /day
Workshops	Area of workshop	1.5 kWh/employee/day	75 Wh/m ² /day
Elderly home	Area of rooms	3.5 kWh/person/day	230 Wh/m ² /day

5.3.6 Energy Need for Humidification Q_{HU} and Dehumidification Q_{DHU} of Indoor Air

The process of humidification (needed occasionally during heating periods) or dehumidification of the indoor air (needed occasionally during cooling periods or in cases of large water vapour sources in buildings, such as evaporation of water from swimming pools) increase energy demand of buildings. Humidification of the indoor air can be done by water or steam. If, for example, water droplets are sprayed into the supply air flow for ventilation, the air must be heated to the set-point indoor air temperature after the humidification process as air is cooled because of water droplet evaporation (see Chap. 3.2). If steam is used for humidification, no additional heating is needed after humidification, but auxiliary electricity is required for producing the steam. If water vapour must be extracted from indoor by air dehumidification, the supply of ventilation air or indoor air must be cooled below the dew point temperature and heated again afterwards to avoid uncomfortable conditions. Both processes are related to energy use. The energy needs for humidification Q_{HU} and dehumidification Q_{DHU} are related to the acceptable absolute humidity of indoor air $x_{i,min}$, $x_{i,max}$ (kg/kg), the absolute humidity of the supply ventilation air x_e (kg/kg) and the water vapour source in the building G_i (kg/s). Specific moisture loads are defined by equations:

$$G_{HU} = \rho_a \cdot q_v \cdot (x_{i,min} - x_e) - G_i \quad (\text{kg/s})$$

air density
(kg/m³)
↓
 flow rate of
supply air (m³/s)

 minimum required
absolute humidity of
indoor air (kg/kg)
↓
 absolute humidity of supply
(outdoor) air (kg/kg)

 indoor water
vapour gain (kg/s)
↓
 indoor water
vapour gain (kg/s)

$$G_{DHU} = -[\rho_a \cdot q_v \cdot (x_{i,min} - x_e) - G_i] \quad (\text{kg/s})$$

maximum required
absolute humidity of
indoor air (kg/kg)
↓
 flow rate of
supply air (m³/s)

 indoor water
vapour gain (kg/s)
↓
 absolute humidity of supply
(outdoor) air (kg/kg)

If specific moisture loads G_{HU} and G_{DHU} are greater than 0 kg/s, total moisture loads for humidification and dehumidification of the indoor air are defined as:

$$\dot{Q}_{HU} = h_w \cdot G_{HU} \quad (\text{W}) \quad \dot{Q}_{DHU} = h_w \cdot G_{DHU} \quad (\text{W})$$

water evaporation heat (2466 kJ/kg)

Monthly Energy needs in form of latent heat for humidification and dehumidification are equal to:

$$Q_{HU} = \sum_{m=1}^{12} \sum_{h=1}^k \dot{Q}_{HU,h} \cdot \frac{1}{1000} \quad (\text{kWh/m})$$

sum over
months
↓
 sum over hours
per month
↓
 total moisture load
(W) in hour h
↓
 constant (Wh/kWh)

$$Q_{DHU} = \sum_{m=1}^{12} \sum_{h=1}^k \dot{Q}_{DHU,h} \cdot \frac{1}{1000} \quad (\text{kWh/m})$$

Note: As shown, energy needs for humidification and dehumidification are commonly determined by using the daily calculation method because the large fluctuation of absolute humidity of outdoor air and dynamic indoor moisture sources.

Case Study Calculate energy need for the dehumidification of an office with 10 people during a one-hour meeting. Each person emits 40 g of water vapour per hour. The airtight office is ventilated with fresh air with a density of 1.27 kg/m³. Absolute humidity of outdoor air x_e is 10 g/kg (~25 °C, 50%). To fulfil indoor thermal comfort requirements during the meeting, maximum absolute air humidity $x_{i,max}$ should not exceed 5 g/kg. To maintain IAQ 40 m³/h of fresh air is needed per person, so total ventilation air flow rate q_v is 400 m³/h or 0.111 m³/s. Water evaporation heat is equal to 2466 kJ/kg. The specific moisture load is equal to:

$$G_{DHU} = -[\rho_a \cdot q_v \cdot (x_{i,max} - x_e) - G_i] \quad (\text{kg/s})$$

$$G_{DHU} = -\left[1.27 \cdot 0.111 \cdot (0.005 - 0.010) - \frac{40 \cdot 10}{3600 \cdot 1000}\right] = 5.937 \cdot 10^{-4} \text{ kg/s}$$

and the total moisture load is equal to:

$$\dot{Q}_{HU} = h_w \cdot G_{DHU} \quad (\text{W})$$

$$\dot{Q}_{HU} = 2,466,000 \cdot 5.937 \cdot 10^{-4} = 1464 \text{ W}$$

Note: beside water vapour, each person attend at the meeting emits approximate 100 W of sensible heat. This means that beside 1464 Wh of latent heat, the people attending the meeting emit an additional 4000 Wh of sensible heat that must be extract by natural means or by a mechanical system from meeting room during the one-hour meeting.

5.3.7 Energy Need for Lighting Q_L

The method and rules for determination of energy demand for lighting are covered by standard EN 15193-1⁵ as an EPDB-supporting standard. The energy need for lighting is not defined as a separate indicator but included indirectly by LENI (Light

⁵EN 15193-1:2017 Energy performance of buildings—Energy requirements for lighting—Part 1: Specifications, Module M9.

Energy Numerical Indicator). LENI is calculated according to the installed electrical power of electrical light sources, type of controlling of the lights and the daylighting factor of observed room. The method for calculation of LENI is presented in Sect. 12.6.1. Electricity demand for lighting must be taken into account when calculating the delivered energy for building operation.

5.4 Delivered Energy for the Building Operation Q_f

In Sect. 5.3, the meaning of term “energy needs” was explained as the energy required to provide required indoor comfort conditions, not taking into account any heat losses of installed systems or losses associated with the imperfect control of systems operation or auxiliary energy needed for the operation of systems. Unlike energy needs, delivered energy is energy that must be provided to the building service systems (hereinafter, systems will be called “EPBD systems”) to cover the energy needs of the building. Once delivered energy is known (i) environmental impacts (e.g. primary energy needed, CO₂ emissions) can be evaluated, (ii) cost of energy use for building operation can be calculated, and (iii) the overall (yearly) efficiencies of particular EPBD systems can be determined.

For the determination of delivered energy for building operations, not only the total amount of energy, but amount and type of each energy carrier must be determined as well as all the technological aspects of building service systems. Quite commonly, all EPBD systems are not installed in particular building, but at a minimum heating, domestic hot water heating and lighting systems are always installed regardless of the type of the building and climate conditions. Because of heat losses and auxiliary energy use for operation of the systems, the total amount of delivered energy differs from energy needs. In most cases, part of heat losses and auxiliary energy can be recovered or transformed into useful heat. Recoverable losses are heat losses from distribution pipes inside the heated space, generator heat losses through the assembly of a heat generator if it is installed in heated space, or part (25% is assumed) of auxiliary electricity demand for operation of a fan or a pump that raises the temperature of heat transfer media inside fan or pump. Consequently, delivered energy must be calculated with an iterative procedure taking into account the interaction between buildings and EPBD systems, as shown in Fig. 5.10. There is also iteration between EPBD systems. For example, the distribution heat losses of a DHW system can be recoverable for the heating system during the heating season (but not during summer). Nevertheless, some heat losses cannot be recovered. Examples of non-recoverable energy losses are losses by flue gasses in boilers, losses due to imperfect controlling or losses from distribution pipes in unheated cellars. These losses are directly added to the energy needs and increase by same amount the delivered energy.

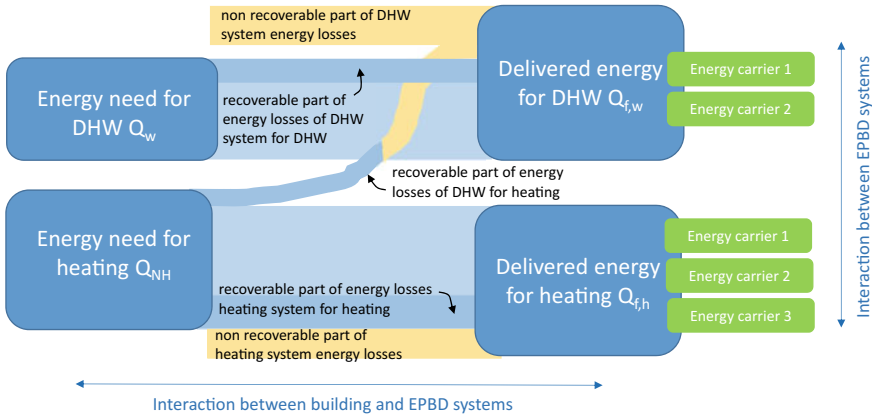


Fig. 5.10 Principle of the determination of delivered energy assuming that only a heating and DHW system are installed

Case Study Using the TRIMO Expert software examine nomenclature of energy flows in combined heating and DHW system in the Virtual Lab building. Energy needs are equal to Q_{NH} and Q_w . The hypothetical system consists of a heat pump (G1) with heat storage (H1, 50 liter per 1 kW thermal power) which is connected to a hydronic heating system, a solar system with vacuum tubes (S1) and heat storage (H2, 50 lit per 1 m² of SC aperture area); biomass boiler is used for backup DHW heating; four circulation pumps are installed: in heating distribution system (1), in solar system distribution system (2), for backup heating (3) and for circulation of DHW (4) (Fig. 5.11).

Nomenclature:

- heat fluxes (Q) are shown with orange arrows, electricity (W) with blue ones;
- energy need for heating Q_H , for domestic hot water heating Q_w ;
- indexes related to elements of systems have the following meanings: **h** heating, **w** DHW, **g** heat generator, **s** storage, **d** distribution, **l** losses **em** heat emitters in rooms, **sol** solar system, **p** pump;
- indexes related to heat fluxes have the following meanings: **rhh** recoverable energy losses “from heating system to heating system” and **rwh** recoverable energy losses “from DHW system to heating system”, **aux (=e)** auxiliary energy (electricity) and electricity for operation of heat pump and circulation pumps.

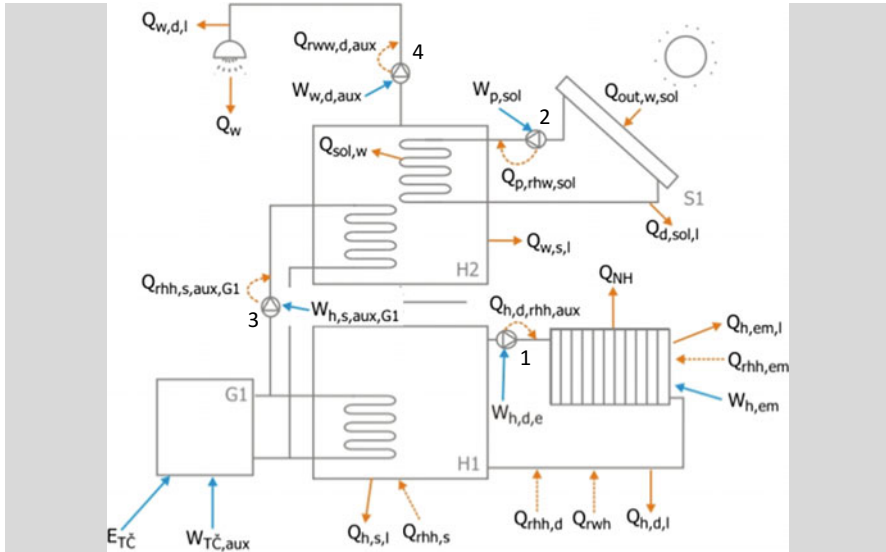


Fig. 5.11 Energy fluxes in case of combined heating and DHW system as in the Virtual Lab building

Example: $E_{T\check{c}}$ and $W_{T\check{c};aux}$ represent delivered electricity for the operation of a heat pump for heating and DHW, and $Q_{out,w,sol}$ delivered heat from solar collectors as part of DHW system. $Q_{h,s,l}$ and $Q_{w,s,l}$ represent energy losses of heating and DHW system storage. $Q_{h,d,l}$ and $Q_{w,d,l}$ shown energy losses of heating and DHW system distribution, $Q_{d,sol,l}$ energy losses of solar thermal system distribution and $Q_{em,l}$ energy losses of emitters according to inaccurate regulation of the set-point temperature. $Q_{rrh,d}$ represents recoverable losses of heating distribution system (as part of heating system distribution losses $Q_{h,d,l}$) that reduce heat for heating, Q_{rwh} shows recoverable losses of the DHW distribution system that decrease the delivered energy of the heating system (only if pipes are inside the thermal envelope of the building). $Q_{h,d,rhh,aux}$ shows part of the electricity needed for the operation of the circulation pump in a heating system that decreases the delivered energy for heating since water in the distribution system is heated because of friction and vortexes inside the pump.

Note: Examples of delivered energy determination will be shown in Chaps. 8–12, where building service systems are presented.

5.5 Primary Energy Needed for the Building Operation

Primary energy is energy that is contained in natural materials or processes that has not been subjected to any conversion or transformation. Such materials or processes can be renewable or non-renewable. For the production of energy carriers, which are available to end users, renewable and/or non-renewable natural energy sources are used. To define the primary energy needed for the operation of the building, renewable and non-renewable parts of each energy carrier must be summarised. Consequently, each energy carrier has its own renewable $f_{p,ren}$ and non-renewable $f_{p,nren}$ primary energy factor. The total primary energy factor $f_{p,tot}$ is sum of both.

Example: Solar energy has $f_{p,nren}$ 0 and $f_{p,ren}$ equal to 1 and therefore $f_{p,tot}$ 1, meanwhile natural gas has $f_{p,nren}$ 1.1, $f_{p,ren}$ 0 and $f_{p,tot}$ 1.1, wood pellets have $f_{p,nren}$ 0.2 and $f_{p,ren}$ 1 and, therefore, $f_{p,tot}$ 1.2. Electricity is an energy carrier that is produced by renewable and non-renewable energy sources. In Iceland, all electricity is produced from hydro and geothermal energy, which are renewable energy sources but in most other countries the share of non-renewable energy sources is significant. Therefore, primary energy factors for electricity differ between countries. For example, in Slovenia the $f_{p,nren}$ is equal to 2.2 and $f_{p,ren}$ equal to 0.3, and $f_{p,tot}$ equal to 2.5.

Primary energy demand is defined as total ($E_{p,tot}$), renewable ($E_{p,ren}$) or as non-renewable ($E_{p,nren}$) primary energy needed for the operation of buildings and expressed as yearly demand in kWh per year. It is determined as the weighted sum of delivered energy:

$$\begin{aligned}
 E_{p,tot} = E_{p,ren} + E_{p,nren} &= \sum_{n=1}^{12} \left(\sum_{j=1}^k Q_{f,j} \cdot f_{p,ren,j} + \sum_{j=1}^k Q_{f,j} \cdot f_{p,nren,j} \right) \quad (\text{kWh/a}) \\
 \text{renewable primary energy (kWh/y)} & \quad \text{non-renewable primary energy (kWh/y)} \\
 \text{number of months} & \quad \text{number of energy carrier used} \\
 \text{delivered energy by j-th energy carrier (kWh/m)} & \\
 \text{renewable primary energy factor of j-th energy carrier (-)} & \quad \text{non-renewable primary energy factor of j-th energy carrier (-)}
 \end{aligned}$$

As explained in the Sect. 5.2, a high share of renewable energy sources in primary energy needed for operation of buildings is required for nearly Zero Energy Buildings. Once renewable and non-renewable energy demand is established, RER can be determined by the equation:

$$RER = \frac{E_{p,ren}}{E_{p,tot}} \quad (-)$$

Case Study Determine total renewable primary energy needed for the operation of a building if 10,000 kWh heat from biomass, 5000 kWh of electricity and 2500 kWh heat from solar energy is used for operation of the building per year.

$$E_{P,tot} = E_{P,ren} + E_{P,nren} = (Q_{f,bio} \cdot f_{P,ren,bio} + E_{f,el} \cdot f_{P,ren,el} + Q_{f,sol} \cdot f_{P,ren,sol}) + (Q_{f,bio} \cdot f_{P,nren,bio} + E_{f,el} \cdot f_{P,nren,el} + Q_{f,sol} \cdot f_{P,nren,sol})$$

$$E_{P,tot} = (10,000 \cdot 1 + 5,000 \cdot 0.3 + 2,500 \cdot 1) + (10,000 \cdot 0.2 + 5,000 \cdot 2.2 + 2,500 \cdot 0)$$

$$E_{P,tot} = E_{P,ren} + E_{P,nren} = 14,000 + 13,000 = 27,000 \text{ kWh/a}$$

$$RER = \frac{E_{P,ren}}{E_{P,tot}} = \frac{14,000}{27,000} = 0.519 = 51.9\%$$

If one or more energy products are produced with technologies integrated into the building on-site, in a quantity that exceed consumption of the building on a yearly scale and are exported to near-by or to distant energy consumers, the exported energy products reduce the primary energy needs of the building. Renewable and non-renewable primary energy factors for exported energy carriers are the same as they are for the same imported energy carrier.

Note: If electricity is produced by on-site installed natural gas-driven cogeneration and electricity is exported, the primary energy factors for the imported energy carrier are $f_{P,ren}$ equal to 0 and $f_{P,nren}$ equal 1.1; meanwhile, the primary energy factors for the exported energy carrier are $f_{P,ren}$ equal to 0.3 and $f_{P,nren}$ equal to 2.2.

Case Study 1 For heating and DHW of the building with a useful floor area A_u 120 m², a heat pump with a seasonal coefficient of performance equal to 3 is used. Specific delivery heat per unit of useful floor area for heating and DHW is 37 kWh/m² per year; meanwhile, delivered electricity for the operation of all other systems and components is 35 kWh/m² per year. The primary energy factors of electricity are $f_{P,ren}$ 0.3, $f_{P,nren}$ 2.2 and $f_{P,tot}$ 2.5; for ambient heat utilized by the heat pump, they are $f_{P,ren}$ 1, $f_{P,nren}$ 0 and $f_{P,tot}$ 1. Calculate RER for the same building if a gas boiler is used for heating and DHW and a photovoltaic system is installed on the roof of the building with power 3.8 kW_p (30 m² of PV modules) that produce 4900 kWh of electricity per year. Electricity produced from solar energy by PV system has primary energy factors $f_{P,ren}$ 1, $f_{P,nren}$ 0 and $f_{P,tot}$ 1. Gas has primary energy factors $f_{P,ren}$ 0, $f_{P,nren}$ 1.1 and $f_{P,tot}$ 1.1.

Case Study 2 4400 kWh per year of heat is needed for heating and DHW (37×120 kWh/year). For that, 1480 kWh of electricity and 2960 kWh per year of ambient heat are used. For operation of other systems, 4200 kWh/year is used.

$$\begin{aligned} \text{RER}_1 &= \frac{E_{P,\text{ren}}}{E_{P,\text{tot}}} = \frac{(1480 + 4200) \cdot f_{P,\text{ren,el}} + 2960 \cdot f_{P,\text{ren,amb}}}{(1480 + 4200) \cdot f_{P,\text{tot,el}} + 2960 \cdot f_{P,\text{tot,amb}}} = \\ &= \frac{(1480 + 4200) \cdot 0.3 + 2960 \cdot 1}{(1480 + 4200) \cdot 2.5 + 2960 \cdot 0} = \frac{4664}{14200} \rightarrow 32.9\% \end{aligned}$$

Case Study 3 4400 kWh per year of gas is imported. All electricity needed for operation of the building annually is produced by the PV system; 700 (6900–4200) kWh per year is exported.

$$\begin{aligned} \text{RER}_2 &= \frac{E_{P,\text{ren,import}} + E_{P,\text{ren,on-site}} - E_{P,\text{ren,export}}}{E_{P,\text{tot,import}} + E_{P,\text{tot,on-site}} - E_{P,\text{tot,export}}} = \\ &= \frac{4400 \cdot f_{P,\text{ren,gas}} + 4900 \cdot f_{P,\text{ren,el,on-site}} - 700 \cdot f_{P,\text{ren,el,export}}}{4400 \cdot f_{P,\text{tot,gas}} + 4900 \cdot f_{P,\text{tot,el,on-site}} - 700 \cdot f_{P,\text{tot,el,export}}} = \\ &= \frac{4400 \cdot 0 + 4900 \cdot 1 - 700 \cdot 0.2}{4400 \cdot 1.1 + 4900 \cdot 1 - 700 \cdot 2.5} = \frac{4760}{9565} \rightarrow 59.6\% \end{aligned}$$

References

- Davies MG (2004) Building heat transfer. John Wiley & Sons, Ltd
- IPCC (2014) Summary for policymakers. In: Edenhofer O, Pichs-Madruga R, Sokona Y, Farahani E, Kadner S, Seyboth K, Adler A, Baum I, Brunner S, Eickemeier P, Kriemann B, Savolainen J, Schlömer S, von Stechow C, Zwickel T, Minx JC (eds) Climate change 2014: mitigation of climate change. Contribution of working group III to the fifth assessment report of the intergovernmental panel on climate change. Cambridge University Press, Cambridge, United Kingdom and New York, NY, USA

Chapter 6

Best Available Technologies (BAT) for On-Site and Near-by Generation of Heat for NZEB



Abstract In the European Union, heat is dominant form of energy needed in buildings. More than 50% of total final energy demand in EU is in form of heat and more that 80% of heat is needed at temperatures less than 250 °C. In buildings, heat is needed for space heating, domestic hot water heating, and air-conditioning and for space cooling when cold is produced by heat-driven sorption systems and, in small amounts, for cooking. Heat generators are appliances that convert the internal energy of an energy carrier and exchange heat to the heat transfer fluid at the highest energy efficiency and the lowest environmental impact as possible. In this chapter, the best available technologies for the on-site generation of the heat from fossil fuels and renewable energy sources are presented, as well as the advantages of near-by district heating systems.

In most EU countries, the heat demand in residential buildings dominates in comparison to the energy demand for space cooling. In EU-27 households, on average, energy is mainly used for space heating (70%), domestic hot water (14%), appliance and lighting (13%) and cooking (4%) (Fig. 6.1).

Note: In non-residential buildings, the final energy for lighting as well as energy demand for humidification and dehumidification in air-conditioned buildings can be dominant.

Heating systems in buildings are used to provide required indoor thermal comfort with the highest possible energy efficiency. In any heating system, one or several heat generators are installed. In addition to technical issues, the selection of heat generator is based on:

- availability and price of energy carriers,
- national or local community regulations according to environmental impacts,
- requirements regarding the share of renewable energy sources for operation of the building; this criterion is especially important for nZEB.

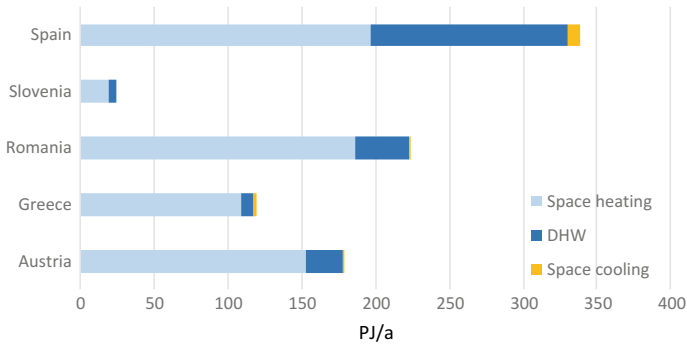


Fig. 6.1 Final energy demand for heating and cooling in residential sector in EU-27 (Pardo 2012)

Heat generators can be decentral or central. Decentral heat generators are stoves or local heaters, which are located in the rooms and provide heating mostly for a single room. Heat is transferred into the room by radiation and convection of the indoor air. Single-point temperature regulation is commonly used for controlling heat dissipation. The central heat generator is part of the central heating system that consists of, beside the heat generator, the heat transfer fluid (water or air, less often steam), the heat distribution system (consisting of pipes or channels) and heat emitters that heat the air in the rooms. More heat generators could be installed in one heating system, for example (i) to enable use of several energy carriers during the year, (ii) to provide back-up heating (e.g. in case of solar heating or use of heat pumps) or (iii) to adjust heating power to the heating load by parallel operation. The central heating system requires more complex regulation to provide that the air temperature is equal (or close) to the set-point temperature, which ensures not just higher thermal indoor comfort for residents but also higher energy efficiency of the heating system. Well-controlled central heating systems are more flexible for energy carrier switching or the use of multiple energy carriers, require less maintenance work and are often more cost effective in comparison to decentral heat generators (Fig. 6.2).

6.1 Local or Decentralized Heat Generators for Residential Buildings

6.1.1 Biomass Stoves and Furnaces

Local heat generators in the form of open fire places and stoves using coal or log wood were used for centuries as heat generators in buildings. Open fire places have low thermal efficiency (below 50%) and can cause low indoor quality (IAQ) since the oxygen for combustion of the fuel is taken directly from the indoor space. In many countries, especially in the urban regions with low quality of outdoor air,

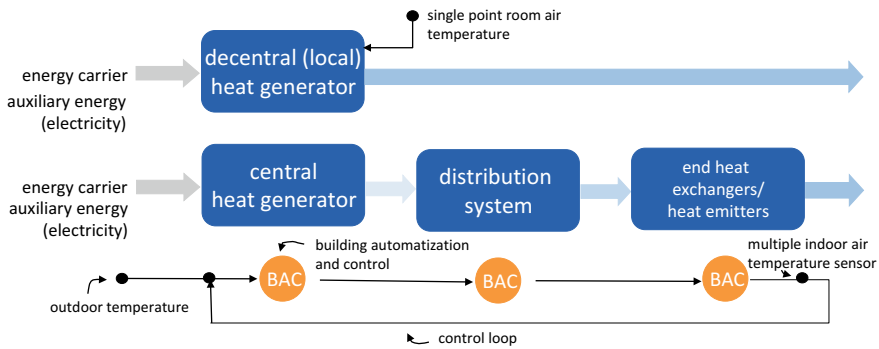


Fig. 6.2 Heat generator are essential elements of decentral and central heating systems; decentral heat generators are mostly used for single-room space heating and are controlled by single-point room thermostats, while central heating systems consist of additional distribution systems and end-heat emitters; such systems are controlled by more advance building automation and control systems, which ensures better thermal comfort and higher energy efficiency

such heat generators are not allowed for permanent heating due to high emissions of deadly carbon oxide (CO) and solid particles (PM). Due to their higher thermal efficiency and heat accumulation, clay brick stoves with hot air channels remain very popular for burning log wood in cold climate regions.

Biomass stoves with closed combustion chambers and clay brick stoves with high thermal mass are quite common for mid-season heating in low energy buildings. The main reasons are that biomass is a renewable energy source, biomass fuels can be produced locally and are treated as zero CO₂ emission fuels. To avoid low IAQ, modern biomass stoves must be equipped by external (combustion) air inlet pipe with a diameter at least 80 mm and use a fan to provide and control the supply of combustion air and the extraction of flue gasses. This improves the thermal efficiency (over 90%) and significantly reduces the emission of pollutants. Nowadays, modern appliances used pre-fabricated wood fuels, such as pellets, and advanced mechanical devices and control units to provide high thermal efficiency, low emissions of pollutants, and comfortable use. With such devices, fuel is transported from integrated or separate fuel storage by a mechanical device, combustion air is delivered by the fan, and unburnt particles are removed automatically into integrated ash storage. Because of high thermal power and intensive convection heat transfer, the temperature gradient of indoor air is high, causing a decrease in the overall efficiency of heating and making control of operation less efficient. High surface temperature can also cause unpleasant operational temperature conditions. Such an appliance is often used in combination with central heat generator for heating during the mild outdoor temperature periods (Fig. 6.3).

Note: Biomass stoves must be connected to a chimney for discharging flue gasses into the atmosphere. The material used for chimney pipe must be high temperature resistant since flue gasses have temperatures up to 200 °C. Only



Fig. 6.3 Pellet stove; small storage for pellets (20 kg) is integrated in the stove to enable operation for a day or two; a mechanical transport system for fuel load and electrical heater as fire starter and combustion air fan are integrated to enable on-demand heat supply; biomass stoves have thermal power in the range of several kW_t to several tens of kW_t, have thermal efficiency up to 94% and can be remote controlled; in most cases, pellet stoves are air heaters and the realised heat is transferred by natural or forced convection by an integrated fan; nevertheless, a water heat exchanger can be integrated together with a circulation pump and expansion vessel (www.edilkamin.com)

one stove should be connected to one chimney. An adequate grill in the outer wall or combustion air supply channel with a diameter at least of 80 mm must be installed for a single biomass stove (Fig. 6.4).

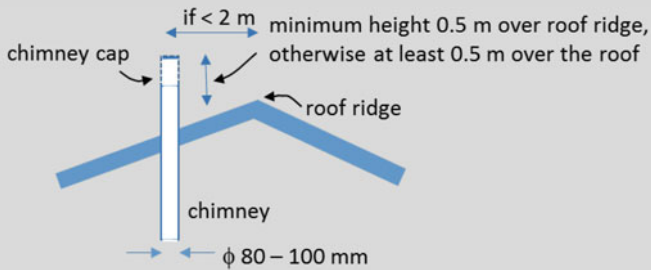


Fig. 6.4 Each biomass stove must have a separate chimney, which must be higher than the roof ridge; values are indicative; for details, the technical manual and local legislation must be checked

6.1.2 Electrical Heaters

Because of high emissions of pollutants and high primary energy needed for the production of electricity, electrical heaters are not considered suitable for permanent heating in low energy buildings. Nevertheless, if heat demand is extremely low, or indoor thermal comfort should be improved by providing higher radiant temperature, electrical heaters can be considered. Electrical resistant heaters (called also Joule heaters or ohmic heaters), which have heat power proportional to their electrical resistance and the square of electricity current, are commonly used. Such heaters can be in the form of built-in heating foil or integrated into the mechanical ventilation system that enables heating with warm air; they can be cost effective in passive buildings or built-in heating foil (Figs. 6.5 and 6.6).

High efficiency, advanced control units and quick response times are the advantages of such heat generators. Electrical resistance heaters in the form of foil of thin spiral integrated in floors or walls have high specific power (100–250 W/m²) and enable occasional rapid heating.

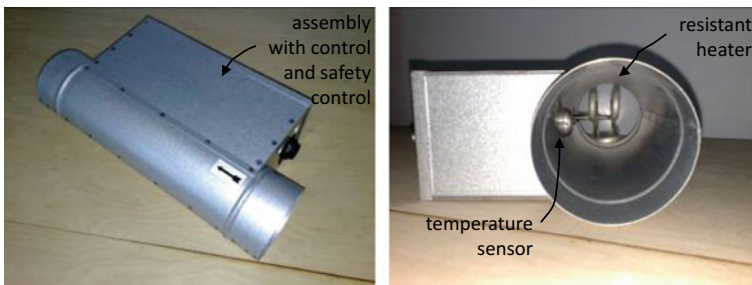
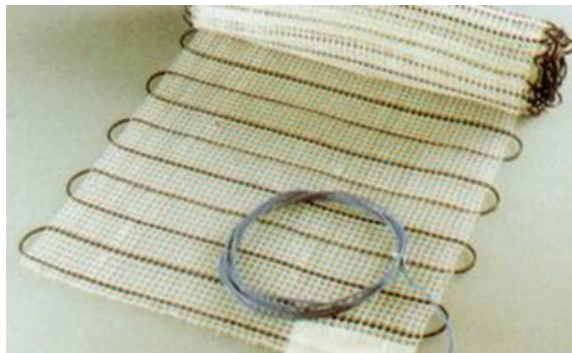


Fig. 6.5 Electrical resistance heater integrated in mechanical ventilation system. Control unit with safety operation function is included in the assembly

Fig. 6.6 Electric resistant heater designed to be built in the floor to prevent unpleasant “cold feet” effect if floor cover has high thermal effusivity



Despite the low cost of electrical heaters, designers should encourage the use of electrically driven heat pumps instead of resistance heaters. One reason is the high cost of electricity in many EU countries and the high CO₂ emission factor for this energy carrier.

6.2 Heat Generators for Central Heating Systems

6.2.1 Combustion Boilers

When fossil or biomass fuel are used, combustion boilers are most often heat generators in central heating systems. A combustion boiler consists of a burner that provides an adequate mixture of fuel and combustion air, the ignition of the mixture, a burning chamber where heat is generated, a thermally insulated heat exchanger where heat is transferred to the heat transfer media, a chimney connection for the discharge flue gasses, and a control unit. Combustion air is provided through the ventilation grill in the outer wall of the boiler room or by the air supply pipe connected to the boiler. Best available technologies (BAT) have an additional heat exchanger for the condensation of water vapour contained in the flue gasses for the use of latent heat (Figs. 6.7 and 6.8).

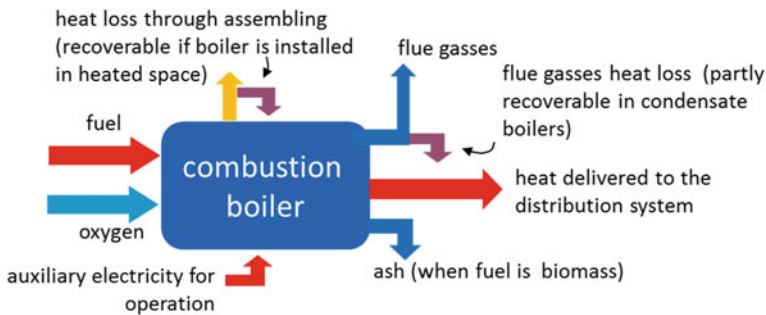


Fig. 6.7 Inlet and outlet energy and mass flows in a combustion boiler during operation. Some of heat losses are recoverable if the boiler is installed in heated space or flue gasses are cooled below the dew point temperature and the latent heat of water vapour is utilized

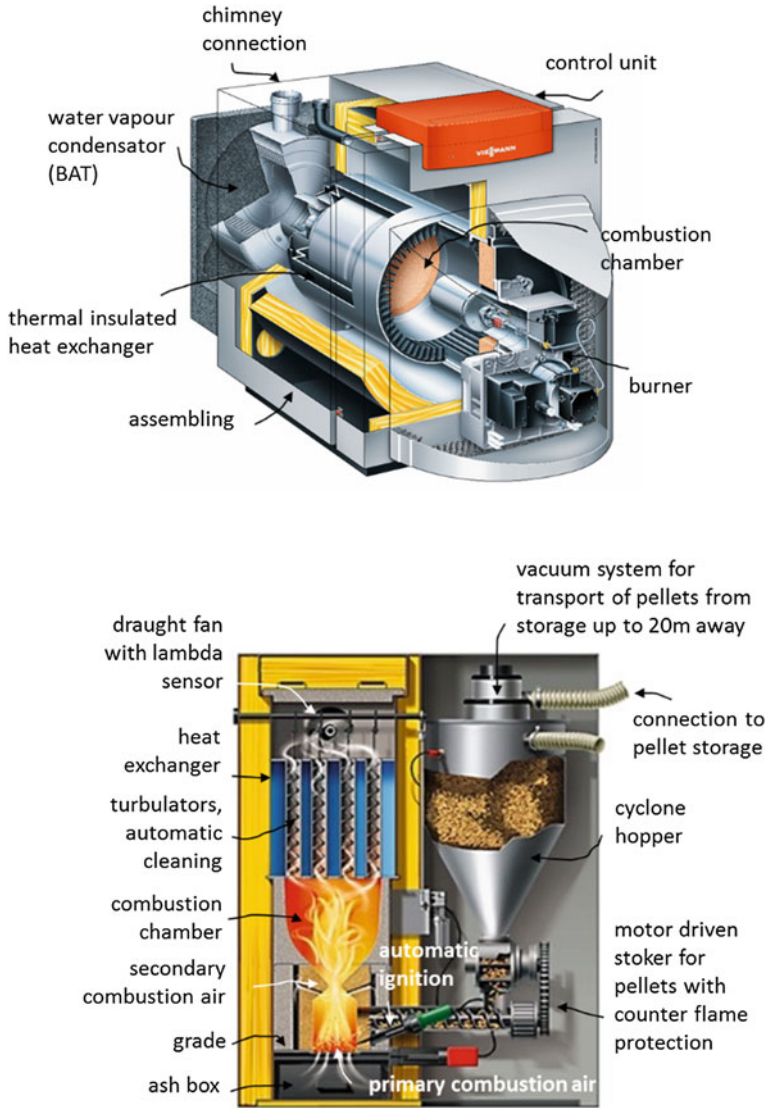


Fig. 6.8 Main elements of the condensate heating oil boiler (top) (www.viessmann.com) (Vitoladens 300-T)), elements of low temperature pellet boiler (bottom) (www.hargassner.at). A lambda sensor is used to measure the amount of oxygen in the flue gases, on the basis of which the amount of combustion air is regulated; the name follows from the ratio between the actual amount of combustion air that is supplied to the combustion process and the theoretical or stoichiometric quantity according to fuel type. The ratio is indicated by the lambda (λ); turbulators are inserts in flue gas channels that increase the convective heat transfer and are used to clean deposited particles with a mechanical drive

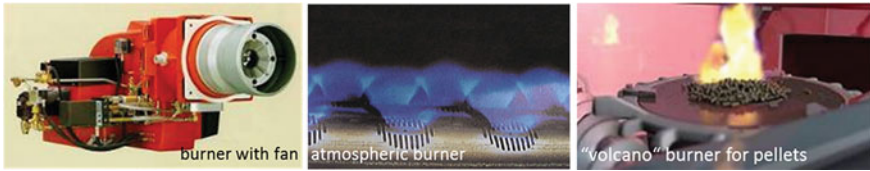
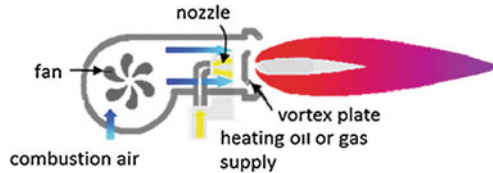


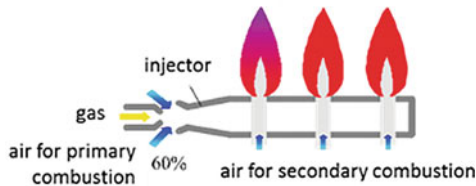
Fig. 6.9 Burners with fans, atmospheric burners, and volcano burners have a common task: to prepare the optimal mixture of fuel and combustion air; burners are equipped with high voltage devices that ignites the mixture of liquid or gaseous fuel or electrical heater for ignition of biomass fuels

To provide adequate mixture of fuel and combustion air, several burners' technologies are used:

- burners with fans are used for liquid (heating oil, bio-oil, shown on figure), gaseous fuels (NG, LPG, purified biogas) and solid (biomass pellets);



- atmospheric burners for gaseous fuels (NG, LPG);



- volcano burners for biomass fuels (biomass chips or pellets) (Fig. 6.9).

6.2.1.1 Thermal Efficiency of Combustion Boilers

The thermal efficiency of combustion boilers is determined by the quality of the combustion process (depending on how close to stoichiometric (perfect) combustion the real process is), heat losses by flue gasses, and heat transfer through the boiler assembly. Heat losses depend on the temperature of heat transfer fluid (water in most cases) that is needed for heating of the building at design and current

meteorological conditions. Regarding the operation temperature, water heating combustion boilers are divided among:

- high temperature boilers; temperature of flue gases ($\sim 180\text{ }^{\circ}\text{C}$) must be higher than the dew point temperature of water vapour in flue gases at all times during the operation to prevent the condensation of water vapour; consequently, the temperature of heating water in the boiler must be in the range between 75 and $90\text{ }^{\circ}\text{C}$;
- low temperature boilers; water vapour condensation in the boiler is allowed occasionally if the boiler is made from corrosion-resistant cast steel; the temperature of heating water could be lower ($45\text{--}65\text{ }^{\circ}\text{C}$), resulting in lower thermal losses by flue gasses ($120\text{--}140\text{ }^{\circ}\text{C}$) and assembly and, therefore, the higher thermal efficiency of boiler;
- if flue gases are cooled below the water vapour dew point temperature, additional latent heat from the gasses can be obtained. In such boilers, so-called “condensation boilers”, a drain for the water must be provided and an additional ventilator is needed to transfer flue gasses to the environment because their temperature is too low for thermal bouncy driven flow (Figs. 6.10 and 6.11).

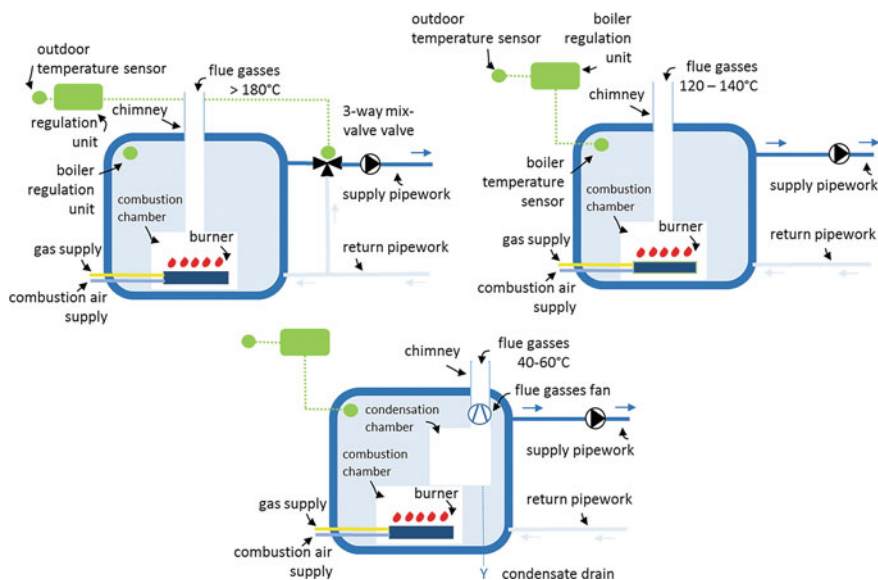


Fig. 6.10 Operating conditions of high temperature (top, left), low temperature (top, right) and condensation gas combustion boilers (bottom); in the case of high temperature boilers, the supply temperature must be regulated by a 3-way mixing valve, while in the case of low and condensation boilers, the temperature of heating water can be adjusted in the boiler itself according to current energy needs for heating of the building

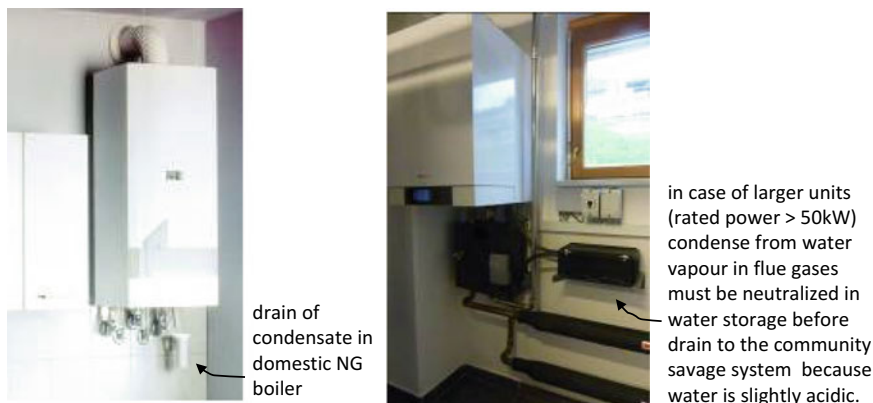
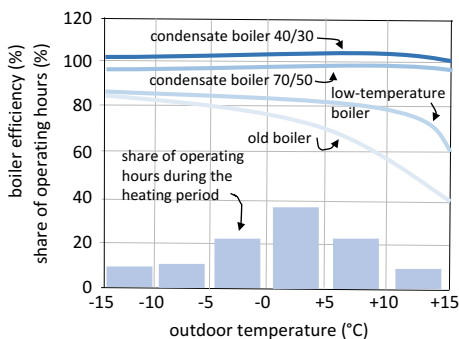


Fig. 6.11 NG condensation boilers with atmospheric burners

Note: Following the requirements on energy efficiency of the buildings, it is common that low temperature combustion boilers must be installed if liquid fossil or biomass fuels are used and condensation boilers in the case of gaseous fuels.

The thermal efficiency of high temperature boilers is in the range of 80–85%, while low temperature boilers have efficiency in the range of 90–95% because heat losses are reduced significantly. Condensation boilers utilize the latent heat of water vapour in flue gases. This means that such boilers utilize the gross calorific value (GCV) of the fuels. As amount of the latent heat depends on the share of hydrogen in the fuel, natural gas (having a ratio gross to lower calorific value GCV/LCV or H_s/H_i equal to 1.11) is the most commonly used fuel in condensate boilers followed by LG (H_s/H_i 1.09), biomass (H_s/H_i 1.08), and heating oil (H_s/H_i 1.06). In real operating conditions, natural gas boilers can reach thermal efficiency up to 105% (based on H_i) or up to 98% (based on H_s) at design-rated thermal power conditions.

Fig. 6.12 Thermal efficiency of different combustion boilers at nominal and partial heating load conditions



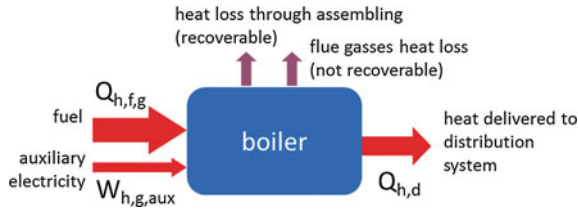


Fig. 6.13 Seasonal performance indicator SPI of combustion boiler is determine by heat delivered into the heating distribution system and final energy demand for operation of the boiler over one year of operation; weighting factor for electricity in this case is based on total primary energy factor ($f_{p,tot}$)

Condensation technology is obligatory for gas boilers in many EU countries. Another advantages of condensate boilers is that such boilers operate at full power rate only a part of time during the heating season. From Fig. 6.12, it can be seen that condensate boilers have even higher efficiency at partial load conditions, while the efficiency of high and even low temperature boilers decreases significantly at partial load operation.

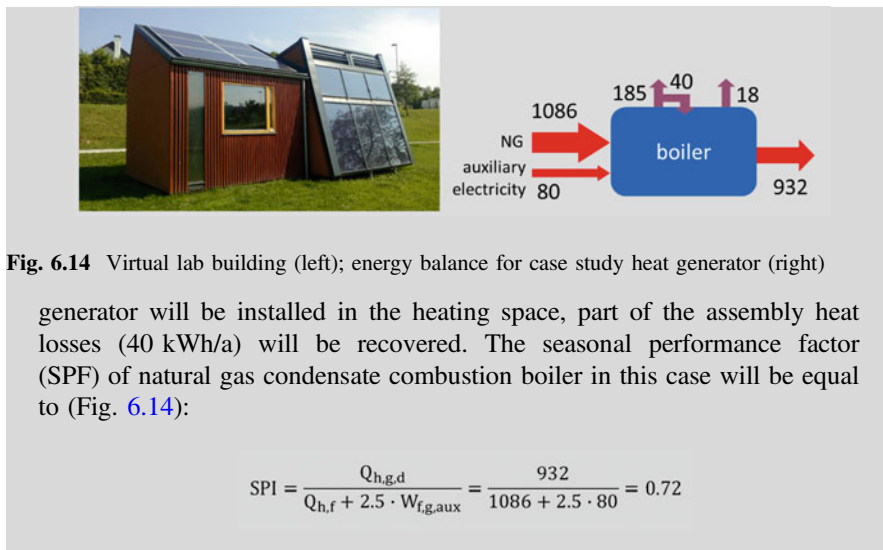
The rated auxiliary electrical power for supporting devices (e.g. for operation of transport system for wood chips or pellets, fan, and control unit) is in the range of 0.1–1% of rated thermal power for biomass and heating oil boilers and 1–1.5% for condensation gas boilers with thermal power up to 20 kW.

The efficiency of combustion boilers is defined at steady state conditions (at constant operation temperatures and rated heat extraction), the seasonal performance indicator (SPI) of boilers is defined by the ratio of the annual heat delivered in the distribution system ($Q_{h,g,d} = \text{heating.generator.delivered}$) at partial load operation on the sum of the quantity of annually consumed fuel ($Q_{h,f,g} = \text{heating.final energy.generator}$; assuming lower caloric value H_i of particular fuel) and auxiliary energy ($W_{h,g,aux} = \text{heating.generator.auxiliary}$) for operation of the boiler: (Fig. 6.13)

$$SPI = \frac{Q_{h,g,d}}{Q_{h,f} + f_p \cdot W_{h,g,aux}}$$

\uparrow
 factor related to primary factor
 of electricity (according to EN
 15316-1 suggest value is 2.5)

Case Study If the Virtual Lab building is heated by a natural gas condensate combustion boiler with partial load efficiency shown on Fig. 6.12 (operating at temperature conditions 40°/30°), 1086 kWh/a of final energy of NG and 80 kWh/a of electricity as auxiliary energy will be needed. Flue gas heat losses will be 18 kWh/a and assembly heat losses 185 kWh/a. As a heat



6.2.1.2 Environmental Impacts of Combustion Boilers

Environmental impacts are mainly related to the flue gas released to the atmosphere. Emissions of pollutants from combustion boilers include:

- carbon dioxide (CO₂) because fuels (fossil and biomass) consist of carbon,
- carbon monoxide (CO), methane (CH₄) and volatile organic compounds (VOC) because in practice the combustion of carbon is never completed (stoichiometric); VOC emissions, including very dangerous formaldehyde and benzene could be reduced at high combustion temperatures and a long residence time of high temperatures in combustion chamber;
- nitrogen oxides (NO_x, mainly in the form of nitrogen dioxide (N₂O) and nitric oxide (NO)); nitrogen oxides are formed because (i) fuels contain certain amounts of nitrogen that react at high temperatures with oxygen (called fuel NO_x), (ii) thermal dissociation of N₂ which enters the boiler as part of the combustion air (called thermal NO_x) and (iii) reaction of nitrogen, oxygen, and hydrocarbon radicals from the fuel within the flame at low temperatures (called prompt NO_x); low NO_x burners (very efficient if natural gas is used as fuel) and flue gas recirculation techniques could reduce NO_x emissions; in combination, a decrease of as much a 90% of NO_x emissions could be achieved; emissions of NO_x can be reduced if the amount of combustion air is regulated according to excess oxygen in flue gases with a sensor called a lambda-sonde in combination with combustion air fan controlling;

- sulphur oxides (SO_x , mainly in form of SO_2); occur mainly if the fuel contains sulphur or if the sulphur contains odorants (to enable the detection of gas leakage by smell): sulphur oxides emissions can be significantly reduced if sulphur-free fuel is used (e.g. NG or LPG) instead of heating oil) or in the case of large combustion boilers with wet scrubber with which up to 95% of SO_x can be removed from flue gas (Oland 1996);
- particulate matter (PM) in the form of aerosols (larger molecular weight hydrocarbons not combusted) or solid particles in size down to less than $1 \mu\text{m}$; controlled combustion and use of gaseous fuels or low-ash content fuels are measures that enable reducing PM emissions in household applications, while cyclone separators, electrostatic precipitators or fabric filters could be used cost-effectively for the removal of PM from flue gases in large units.

The amount of pollutants depends on the combustion technology and selected fuel (and, of course, on the energy requirements of the building). Use of natural gas results in the low emissions of all pollutants (comparing to other fossil fuels), with the exception of NO_x emissions. Heating oil has relative high sulphur content; therefore, high emissions of SO_2 and PM are typical, especially from old equipment. The boiler technology and quality of biomass fuel have crucial influence on emissions from biomass boilers. It has been determined that the typical emission of PM, the most crucial pollutant in this case, from a logwood boiler with natural draught is 6–10 times larger than that of a pellet boiler with forced draught (Nussbaumer 2008).

Note: This chapter deals with the emissions of pollutants which cause different health and environmental problems in nature. The size of the problem depends on the concentration of pollutants in the environment or the emissions of pollutants (concentration in environment at observed point). The most obvious harmful processes in the environment that originate from emissions of pollutants from energy transformation processes are presented in Chap. 14.

6.2.2 Heat Pumps

Buildings have become much more energy efficient in recent decades. As consequence, the heat load for space heating as well as the heat demand for heating per unit of conditioned area of buildings are much lower in comparison to the buildings from the “pre-EPBD era”. Furthermore, (i) lower rated thermal power of heat generator means that (ii) the temperature of the heat transfer fluid could also be lower as. This is most prominent reason that heat generators called heat pumps (HP) have become very popular recently. Heat pumps generate useful heat using the

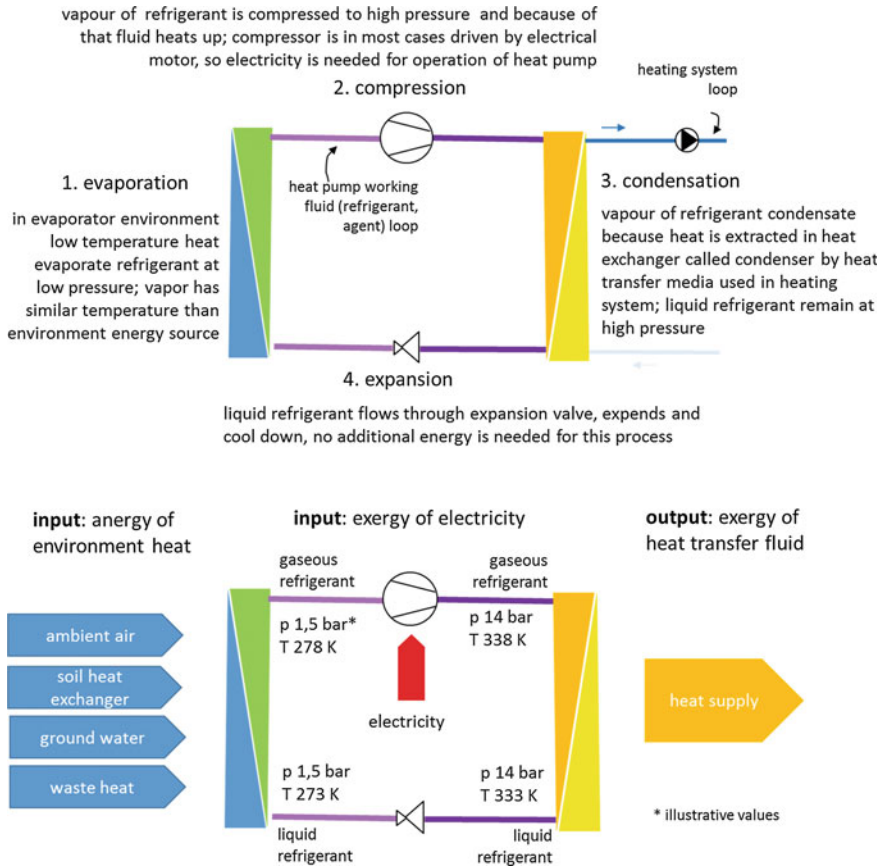


Fig. 6.15 Thermodynamic cycles in heat pump consist of processes that enable the utilisation of energy of environmental heat

environmental (renewable) heat of ambient air, soil, or underground water and transforms the energy of those sources into the energy for heating. The thermodynamic cycle in HP consists of four processes presented in Fig. 6.15.

The efficiency of a heat pump is defined by the ratio of output heat (Q_{out}) and supplied energy for the operation of the heat pump (W_{HP}) at a predefined constant operation regime (at constant temperature of heat source, constant temperature of heat sink, and constant heat removal rate). This ratio is called the coefficient of performance (COP_{HP}) of the heat pump.

$$COP_{HP} = \frac{Q_{out}}{W_{HP}} \quad (-)$$

↖ heat output
↘ electricity input

The theoretical value of $COP_{HP,th}$ depends on absolute temperature of heat sink T_{sink} (absolute temperature of heat transfer fluid entering the heating system) and absolute temperature of environmental heat source T_{source} and is expressed by equation:

$$COP_{HP,th} = \frac{T_{sink}}{T_{sink} - T_{source}} (-)$$

Case Study Calculate the theoretical value of $COP_{HP,th}$ in the case of (i) temperature of the heat transfer fluid is 55 °C, and heat is extracted from the environment at a temperature of -7 °C and (ii) if the temperature of heating fluid of 35 °C is sufficient (e.g. because of better thermal insulation of the building) and heat is extracted from environment at a temperature of 2 °C (Fig. 6.16)

It can be seen that both temperatures significantly influence the value of COP. Therefore, the rule is: to ensure high values of COP (i) the temperature of heat transfer fluid in heating system should be as low as possible (e.g. in case of thermally well-insulated building with a mechanical system with heat recovery) and (ii) the temperature of the heat source should be as high as possible and uniform during the whole heating period.

$$COP_{HP,th,a} = \frac{273+55}{(273+55)-(273-7)} = 5.3$$

$$COP_{HP,th,b} = \frac{273+35}{(273+35)-(273+2)} = 9.3$$

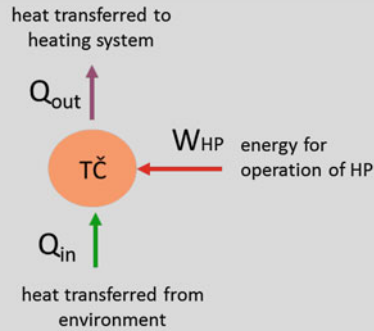


Fig. 6.16 Energy flows of heat pump

The value of COP is significantly higher than 1, which means that the amount of heat transferred to the distribution system $Q_{h,g,d}$ is larger than the energy needed for the operation $W_{h,HP}$ (and which is paid by the user). The difference in energy balance is provided by the utilization of environment renewable or waste heat $Q_{f,HP,RES}$ of ambient air, soil, groundwater or surface water. In the majority of applications, the compressor is driven by an electric motor. In a limited number of cases, the compressor is driven by an internal combustion engine. Natural gas is commonly used in this case instead of electricity. Therefore, a HP can be electrically or gas driven. As internal combustion engines have low efficiency, a gas motor-driven HP has a COP as low as 1.2–1.5.

For designers of buildings is important that HP can be used for space cooling as well, because it consists of exactly the same elements as cooling engines.

6.2.2.1 Energy Sources for Heat Pumps

Note: The type of heat pump is indicated by the source of ambient heat and fluid that transfer heat from HP to the heating system. An “A-W” HP extracts heat from the ambient air, while water is used as heat transfer fluid; an “S-W” HP extracts heat from the soil, and a “W-W” HP extract the heat from the surface of ground water. An “A-A” HP extract the heat from ambient air and in most cases heats indoor air by direct evaporation of the working fluid in an indoor unit.

Ambient air is the most common heat source for heat pumps despite the fact that such air-heat pumps have the lowest efficiency. This is mainly due to the rapid fall in capacity and performance with decreasing ambient air temperatures, the relatively high temperature difference in the evaporator, and the energy needed for occasionally defrosting the evaporator and operating the fan, which increases ambient air flow through the evaporator. In mild and humid climates, frost will accumulate on the evaporator coil surface at the ambient temperature range of 0–6°C, leading to reduced capacity and performance of the heat pump. Coil defrosting is achieved by reversing the heat pump cycle or by other, less energy-efficient means (Fig. 6.17).

Exhaust ventilation air is a fairly common heat source in commercial buildings. Continuous operation of the ventilation system is required during the heating season or throughout the year. For large buildings, exhaust air heat pumps are often used in combination with air-to-air heat recovery units installed in mechanical ventilation systems.

Ground heat source HP are used for residential and commercial applications and have similar advantages as water-source heat pumps: as with ground water, soil temperatures several meters beneath the surface are relatively high (compared to ambient air) and quite constant throughout the year. Heat is extracted by pipes laid

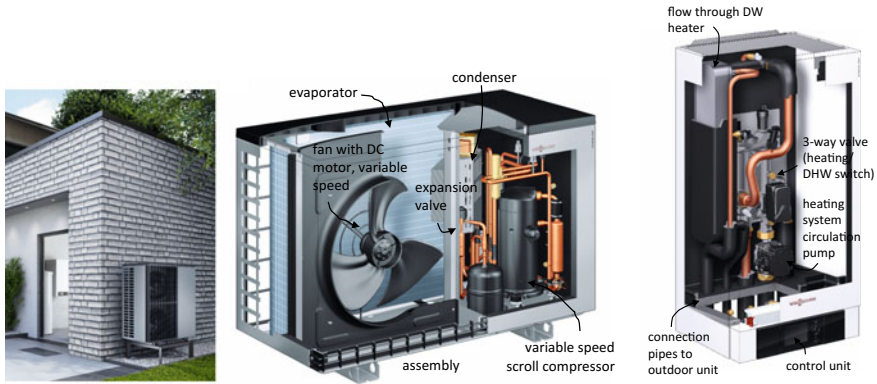
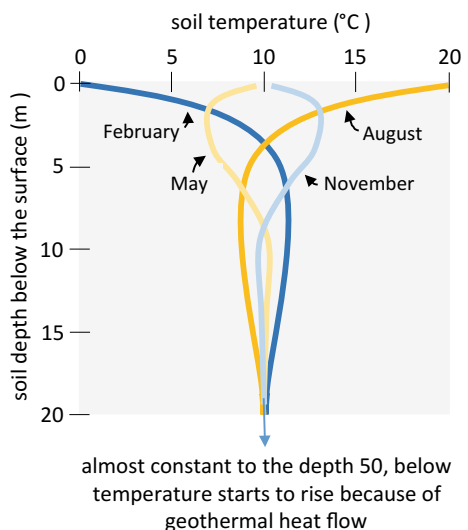


Fig. 6.17 Outdoor unit of air-water HP (left, middle), indoor unit of HP (right) (www.viessmann.com) (Vitocal 200-A))

horizontally or vertically in the soil (horizontal/vertical ground heat exchangers/coils). In most cases, brine solution (mixture of water and antifreeze fluid) is used because temperature out of the expansion valve could be below the freezing point of the water. Extracted heat from the soil varies with the soil moisture and the climatic conditions. Due to the extraction of heat, the soil temperature will fall during the heating season. In cold regions, most of the energy is extracted as latent heat when the soil freezes. However, in summer, the sun will raise the ground temperature, and complete heat (temperature) recovery is very likely. If HP is used for cooling in reverse mode operation, heat accumulated in soil is recovered more quickly, because heat is transferred from the building through the soil heat exchanger (Figs. 6.18 and 6.19).

Fig. 6.18 Temperature profile in the soil in different periods of the year; numerical model for determination of time-dependant soil temperatures is shown in Chap. 9



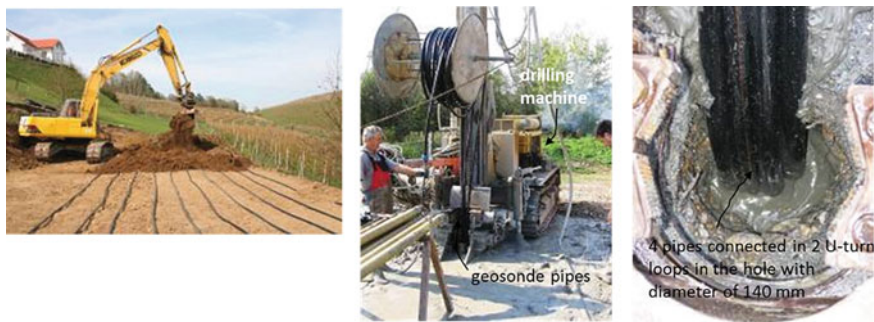


Fig. 6.19 Horizontal soil heat exchanger (left), vertical heat exchangers are up to 100 m deep and are called “geosondes” (right)

Surface and ground water are available with constant all year temperatures between 4 and 10 °C in many regions. The ground water is pumped from aquifer, cooled in HP, and then reinjected through a separate well into the aquifer. Water could be pumped from and back to surface water reservoirs, such as large rivers, lakes or the sea. The system should be carefully designed to avoid problems such as freezing, corrosion, and fouling. A major disadvantage of ground water heat pumps is their high investment cost. Additionally, local regulations may impose severe constraints regarding interference with the water table and the possibility of soil pollution. Closed systems can either be direct evaporation systems, in which working fluid evaporates in underground heat exchanger pipes, or brine loop systems. Due to the lower temperature differences between brine and soil, heat pumps have generally lower performance, but are easier to maintain.

The values of COP of market-available HP are lower than theoretical ones and are established by laboratory tests at pre-defined standardized temperature conditions. For example, test condition A2/W35 means that HP is tested using ambient air (A for air) with a constant temperature of 2 °C as a heat source and heated water (W for water) as the heat transfer fluid to the temperature of 35 °C. In a similar way, the test conditions S0/W55 (soil to water) or W10/W35 (water to water) are defined.

Case Study Calculate COP of air to water HP in case (i) the required temperature of the heat transfer media is 28 °C, and the heat is extracted from the environment (ambient air) at a temperature of -2 °C and (ii) the required temperature of heating media is 45 °C and heat is extracted from environment (ground soil) at a temperature of 7 °C (Fig. 6.20).

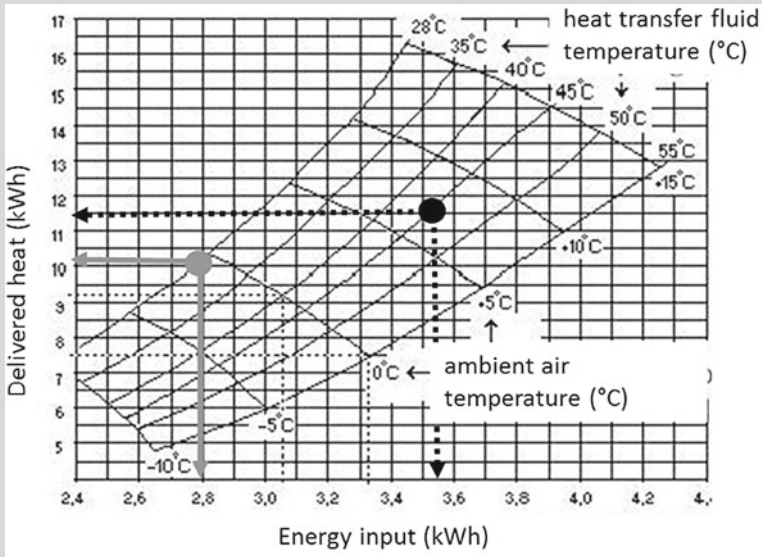


Fig. 6.20 Example of COP diagram of commercial air to water HP (Termotehnika)

$$COP_a = \frac{11.5}{3.55} = 3.24 \quad COP_b = \frac{10.1}{2.88} = 3.60$$

6.2.2.2 Efficiency and Design of HP

For the predesign and selection of HP types, the following data can be used:

- A-W HP; air flow rate 0.5 m³/s per kW of rated thermal power is needed, typical COP value: 3.1 (A2/W35), COP in real conditions is in the range between 2.2 and 4;
- S-W HP; heat flux 25 do 35 W per m of horizontal pipe length or heat flux density between 10 and 30 W/m² of ground area could be extracted; recommended distance between tubes 0.8 m and 1 m, polyethylene tube and water-glycol dilution (brine) should be used to avoid freezing; for vertical ground heat exchanger (geosonde) 50–100 m depth heat flux between 35–85 W per m of geosonde depth can be extracted (depends on thermal conductivity λ of soil); typical COP value: 4.3 (S0/W35); COP in real conditions in the range between 3 and 4.5.
- W-W HP: ground water flow rate 200–300 L/h per kW of rated thermal power is needed; ground water must be re-injected into the same aquifer, minimal distance between production and reinjection hole 25 m downstream*; typical COP value: 5.1 (W2/W35), COP in real conditions in the range between 5 and 6.

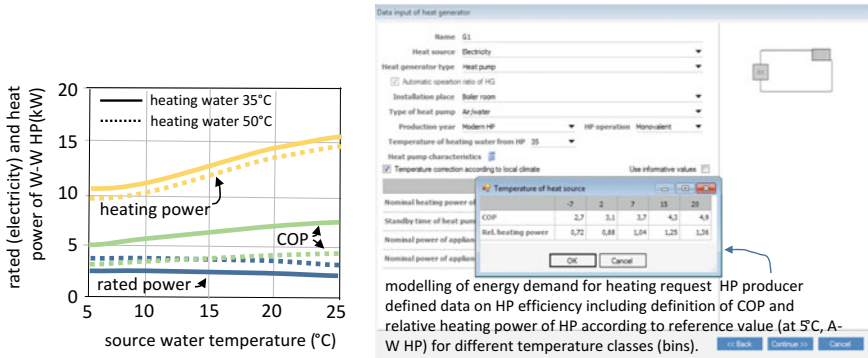
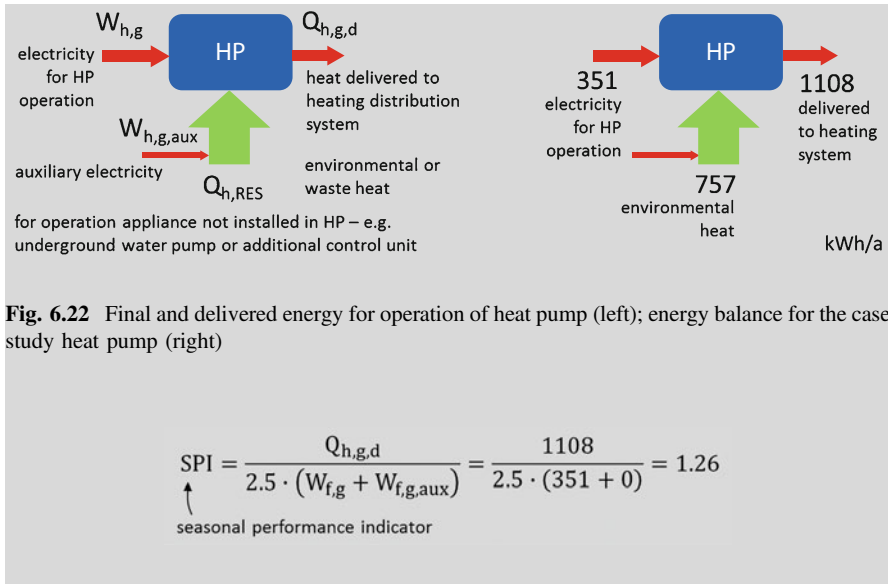


Fig. 6.21 COP, rated (electricity) power and heating power for different temperature conditions for a market-available W-W HP (left); final energy demand for heating is determined according to COP values at different ambient energy source temperature classes and the duration of those classes throughout the year (right; TRIMO Expert)

Note*: Permission criteria differ among countries regarding to the depth of the aquifer, flow rate, level of water protection area, and other legal regulations.

Because temperature conditions during HP operation are changing hourly, all-year operation COP or seasonal performance factor (SPF) is calculated on the hourly basis using test data of HP performance. In building simulation tools, the performance characteristics of HP must be defined for different temperature classes (Fig. 6.21)

Case Study If the Virtual Lab building was heated by A-W HP with COP 2.7 at an ambient air temperature of $-7\text{ }^{\circ}\text{C}$, 3.1 at $2\text{ }^{\circ}\text{C}$, 3.7 at $7\text{ }^{\circ}\text{C}$, 4.3 at $15\text{ }^{\circ}\text{C}$ and 4.9 at $20\text{ }^{\circ}\text{C}$, assuming that the heating water is heated to $35\text{ }^{\circ}\text{C}$, 1108 kWh per year will be delivered to the heating system ($Q_{h,g,d}$) using 351 kWh electricity ($W_{h,g}$) and 757 kWh of environmental heat ($Q_{h,RES}$) per year. According to energy demand and supply, average yearly COP will be 3.1 (COP_{av} 1108 kWh/351 kWh), and the seasonal performance indicator SPI will be equal to (Fig. 6.22):



6.2.2.3 Environmental Impacts of HP

Local environmental impacts of HP can be the consequences of noise emissions caused by fans in the evaporator units of A-W heat pumps, leaking of brine solution from ground heat exchanger into the ground, undercooling and soil freezing in the case of using S-W heat pumps or undercooling of surface watercourses or aquifers in the case of using W-W HP. If ground water is not reinjected, this can also lead to lowering of the aquifer level.

On the global scale, the environmental impacts of HP are mainly the consequences of electricity use for operation, because (in most countries) electricity is produced with high emissions of CO₂, which causes global warming. Emissions of greenhouse gasses because of leaking of refrigerants and maintenance of HP are not significant (<2% of greenhouse gas of HP-related life cycle emissions) (European Heat Pump Association 2005). Substances with chlorine, fluorine, or bromine (e.g., CFC-11 or CFC-12 (called freons)) were once used as refrigerants. Such fluids are ozone depletion chemicals and have a high ODP-ozone depletion potential. When escaping from HP, freons travels through the troposphere into the stratosphere and decomposes ozone molecules (O₃) in the upper layer of the stratosphere. This is harmful process, because O₃ in the stratosphere act as shield against dangerous UV

solar radiation. This process is known as the enlarging of the “ozone hole”. Since the year 2000, CFCs, as a result of several international agreement (Copenhagen, London) have been banned. However, with HP decomposition, working fluids must not be released into the atmosphere. Hydrofluorocarbons (HFCs), such as R134a, R407c and R410a, are commonly used in heat pumps and their ozone depletion potential is zero; however they have a high global warming potential GWP (on a 100-year basis) between approx. 1300 and 1700 (R134a Tetrafluorethane $C_2H_2F_4$, R407c a blend of R32/R125/R134a, R410a a blend of R32/R125). In the future, natural refrigerants, such as propane (R290), propane (R1270), ammoniac (R717), carbon dioxide (R744), or water (R718) with zero ODP and zero or low GWP shall be used.

6.3 Solar Thermal Collectors

Solar thermal collectors are devices that convert solar irradiation into the heat and transfer heat to the heat transfer fluid. The transfer fluid can be water, a mixture of water and antifreeze, or highly thermal resistant oil in liquid solar thermal collectors (LSTC) or air in air solar thermal collectors (ASTC).

Air solar thermal collectors are mainly used in open loop solar thermal systems. In such systems, ambient air enters the solar collectors, heats up, and enters the building as pre-heated ventilation air (Fig. 6.23, right). Crop drying is another application of ASTC. For heating and domestic water heating, liquid solar thermal collectors in closed loop solar heating systems prevail. Heat transfer fluid that circulates in a closed loop between solar collectors and heat storage is driven by thermal buoyancy (in thermosiphon systems) or by pump.



Fig. 6.23 Liquid flat plate solar thermal collectors (left) in close loop solar heating system; air solar thermal collector in form of perforated facade cover layer for preheating ventilation supply air (right (solarwall.com))

Depending on the design of its casing, an LSTC can be a flat plate or tubular. Flat plate solar thermal collectors are made of a casing, a thermal insulation layer at the bottom, a transparent glass cover at the top, and an absorber with integrated pipes or channels. A tubular casing made of glass is used in vacuum solar thermal collectors. In these types of LSTCs, pressure inside the casing is reduced to less than 1 Pa to increase the thermal efficiency, because convective heat losses between the absorber and casing are neglected. A heat pipe is commonly used for transporting the heat between the absorber and heat transfer fluid in vacuum STC. The heat pipe is a sealed, under-pressured, copper pipe filled with a small amount of pure water as the working fluid. In the part installed in the solar thermal collector, water in the heat pipe boils at temperatures above 30 °C, and water vapour fills whole interior of the pipe. At the top of the heat pipe, heat is extracted by heat transfer fluid and, consequently, water vapour condensates and flows back to the bottom part of heat pipe, which is in contact with the absorber. Because of the phase change process, the heat transfer is intensive and no energy is needed for the circulation of the working fluid inside the heat pipe (Fig. 6.24).

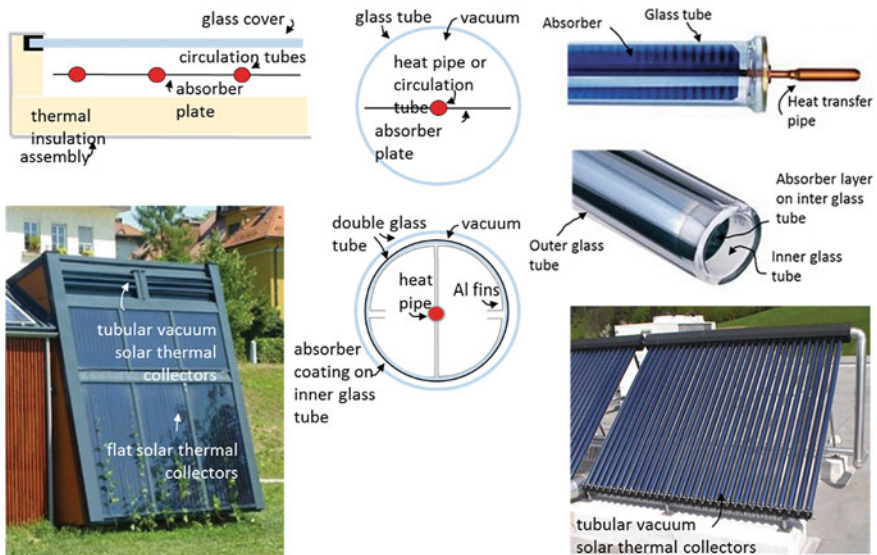


Fig. 6.24 Cross section and photo of flat plate solar thermal collectors on the Virtual Lab building (left) and vacuum solar thermal collectors—single glazed (right top) or double glazed (right middle); package of vacuum STC (right down)

6.3.1 Thermal Efficiency of Solar Thermal Collectors

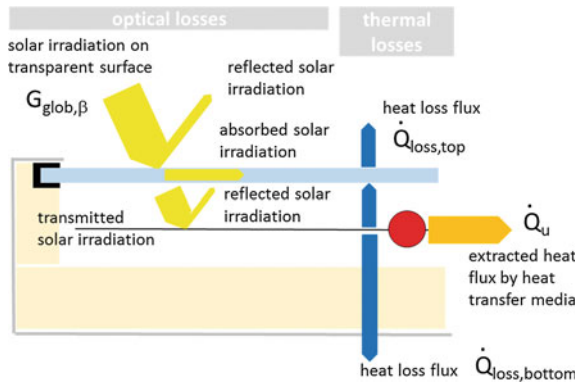
The amount of the heat flux that is transferred by the heat transfer fluid from solar thermal collector is difference between the absorbed solar irradiation and heat losses. Absorbed solar irradiation can be increased by increasing the transmissivity of the glass cover and the short wavelength absorptivity of the absorber. Heat losses are a consequence of convective and radiation heat transfer between the absorber and the glass cover and the conduction heat transfer through the STC casing. The thermal efficiency of an STC at constant operation conditions (at constant temperatures and flow rate of heat transfer fluid) or the so-called “instantaneous efficiency” η_{SC} is defined by the equation below (Fig. 6.25):

$$\eta_{SC} = \frac{\dot{Q}_u}{A_{SC} \cdot G_{glob,\beta}} \quad (-)$$

extracted heat flux (W)
aperture area (m²)
global (total) solar irradiation on the glass cover of SC (W/m²)

In engineering practice, the thermal efficiency of SC is determined by outdoor tests or indoor tests a using solar simulator at different steady state operation conditions as the instantaneous thermal efficiency of SC. During the experiment, the temperature of the heat transfer fluid is regulated to cover all the annual operating conditions of the solar thermal system. As heat losses increase when the temperature of heat transfer fluid (and absorber) increase, the thermal efficiency is defined as a function of solar irradiation $G_{glob,\beta}$ on the surface of the SC, the average temperature of heat transfer fluid $((T_{f,in} + T_{f,out})/2)$, and the ambient air temperature T_a . These influence parameters are combined in the so-called reduced temperature T^* (Fig. 6.26):

Fig. 6.25 The thermal efficiency of the solar thermal collector depends on the amount of absorbed solar irradiation and heat loss rate; the thermal efficiency of STC could be increased by decreasing optical and thermal losses



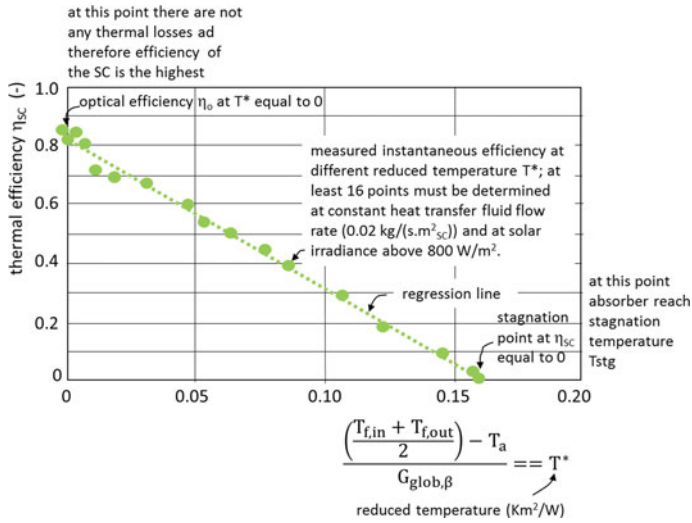


Fig. 6.26 Instantaneous thermal efficiency of STC is determined by experiments and expressed as a regression line depending on the reduced temperature T^*

On the basis of test results, the efficiency of solar thermal collectors can be approximated and presented with a regression line:

$$\eta_{sc} = \eta_0 - a_1 \cdot T^* = \eta_0 - a_1 \cdot \frac{\left(\frac{T_{f,in} + T_{f,out}}{2}\right) - T_a}{G_{glob,\beta}} \quad (1)$$

heat transfer fluid inlet temperature ($^{\circ}\text{C}$)

heat transfer fluid outlet temperature ($^{\circ}\text{C}$)

optical efficiency (-)

ambient air temperature ($^{\circ}\text{C}$)

slope coefficient ($\text{W}/\text{m}^2\text{K}$)

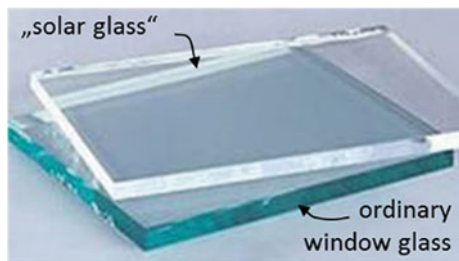
reduced temperature (Km^2/W)

global solar irradiation on SC glassing (W/m^2)

Several techniques are used to improve solar thermal collector efficiency:

- integrating solar thermal collectors into building structures; conductance heat losses through casing is lowered due to additional thermal insulation;
- replacing ordinary window glass with low-iron glass; transitivity of glass cover for solar irradiation is higher, (Fig. 6.27)

Fig. 6.27 Example of window glass and “solar glass”



- selective absorber coating; via a coating or sputtering process, the high absorptivity for (short wave) solar irradiation and simultaneously low emissivity for (long wave) thermal radiation that are emitted from the absorber reduce radiation heat losses between the absorber and cover,
- removing air molecules from interior of SC; if high vacuum (absolute pressure lower than 0.05 Pa) is established inside the casing, convection heat losses between the absorber and cover will be negligible.

Case Study What will the stagnation temperature of selective SC with low-iron glass cover be if solar irradiation on the surface of SC is 800 W/m^2 and ambient temperature equal to $30 \text{ }^\circ\text{C}$. Use the data from Table 6.1.

The stagnation temperature is maximum temperature of the absorber of SC. At the stagnation temperature, the thermal efficiency of SC will be zero, and the inlet ($T_{f,in}$) and outlet temperatures ($T_{f,out}$) will be equal and equal to the stagnation temperature T_{stg} :

$$\eta_{sc} = 0 = \eta_o - a_1 \cdot \frac{\left(\frac{2 \cdot T_{stg}}{2}\right) - T_e}{G_{glob,\beta}} \rightarrow T_{stg} = \frac{\eta_o \cdot G_{glob,\beta} + a_1 \cdot T_e}{a_1} = 227 \text{ }^\circ\text{C}$$

The seasonal performance indicator (SPI) is not applicable for solar thermal collectors but will be presented for whole solar heating system in Chap. 8. Nevertheless, the tilt angle above the horizontal plane and orientation have significant influence on heat generated by STC. In general, for optimal all-year performance, tilt angle β should be close to the geographical latitude L of the site, β equal to $L - 10^\circ$ for peak summer heat generation and equal to $L + 10^\circ$ for peak heat generation during winter season. Figure 6.28 shows the orientation performance factor that indicates the relative decrease of generated heat regarding optimum tilted and orientated SC.

Table 6.1 Typical values of optical efficiency η_o and slope coefficient a_1 of the efficiency regression line for different constructions of liquid solar thermal collectors

Type	Applications	η_o (-)	a_1 (W/ m^2K)
Un glazed	Water pool heating	0.85	20
Flat, black painted absorber	Domestic water heating	0.80–0.85	9.0
Selective coating on absorber	Domestic water heating	0.80–0.85	4.5
Selective coating with low-iron glass	Domestic water heating, solar assisted heating	0.82–0.87	3.5
Vacuum solar collectors	Domestic water heating, solar assisted heating, solar cooling	0.70–0.75	1.5

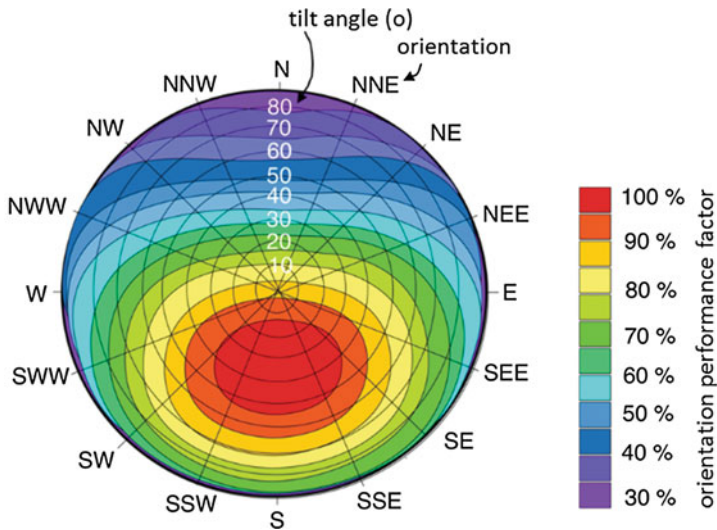


Fig. 6.28 Orientation performance factor for different tilt angles and orientations of STC; values indicate the relative decrease of heat delivery regarding the position of STC; values are determined for the mid-EU geographical latitudes

6.3.2 Production of Heat: Rule of Thumb

The amount of yearly generated heat by solar thermal collectors depends on the type of STC (Table 6.1) and operating conditions (required temperature of heat transfer fluid), but even more significantly on the heat demand itself. Therefore, the rule of thumb is: higher heat demand results in higher yearly average efficiency of STC (and solar thermal systems) and higher delivered heat. Nevertheless, at in situ conditions, at the optimum position of STC and at rated (design) heat demand, specific heat generation can be assumed as shown in Fig. 6.29.

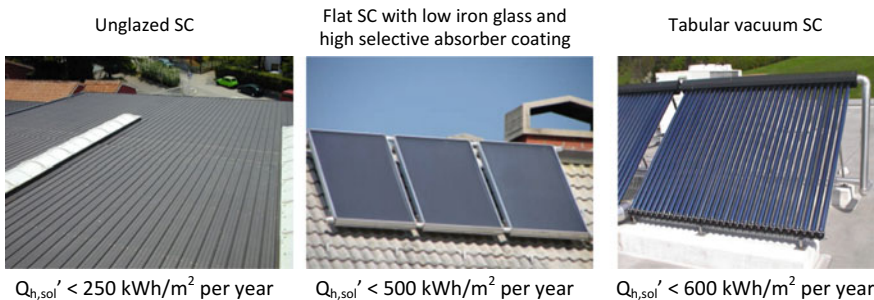


Fig. 6.29 Specific generated heat $Q_{h,sol}'$ of different types of STC; values are established for the optimum positions of STC

6.4 District Heating

District heating systems are infrastructure systems with one large heat generator and a pipeline distribution system. Buildings are connected to district heating systems via heat exchangers installed in the heat stations. Nowadays, high temperature water is predominantly used as the heat transfer media for the heating of the buildings, while steam is still used for industrial applications. The main benefits of district heating systems are:

- space needed for installation of the heating station is smaller in comparison to a boiler room,
- large combustion boilers in district heating systems have higher efficiency,
- lower cost of fuels can be achieved on the market with more flexible adjustment to suppliers,
- the flue gas cleaning devices are more efficient and cost-effective because of the large units,
- increased use of renewable energy sources, including biomass, solar energy or geothermal energy, is possible at lower investment costs,
- providing district heat is high cost effective if cogeneration of electricity and heat (CHP combine heat and power production) is applied.

Because distribution pipelines are costly, the landscape density of connected buildings should be at least 50 buildings per ha of territory. This ensures that heat demand will be at least 25 kWh per m² of territory covered by district heating per year. Due to high distribution heat losses, smaller district heating systems operate only during the heating season. In this case, additional heat generator for DHW must be installed and operate during the summer (Fig. 6.30).

Fig. 6.30 Connection of district heating pipeline and building heating system is done in technical room or heating sub-station by heat exchanger; a sub-station is much smaller in comparison to a boiler room; if district heating also enables DHW heating, a separate heat exchanger must be installed



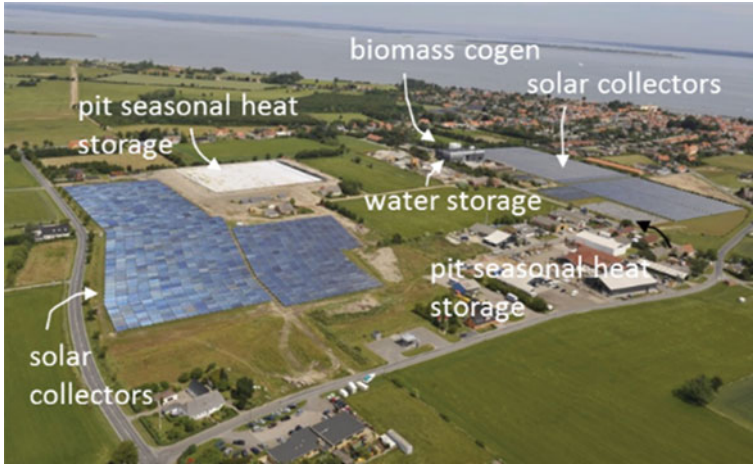


Fig. 6.31 Part of Marstal district heating plant. Flat solar collectors ($33.000 + m^2$), biomass boiler (4 MW) and heat pump (1.5 MW) are used as heat generators. Short term (daily) and seasonal (pit type, $75,000 m^3 + 10,000 m^3$ and water tank $2300 m^3$) heat storages are used to store the heat (SOLARGE 2004)

If a district heating system is characterized by buildings near the heat supply system, according to nZEB requirements, such a system increases the share of renewable energy for the operation of the building if:

- waste heat from industrial processes is used;
- waste heat from combine electricity and heat generation plants (CHP) is used;
- heat is generated using a biomass (wood or biogas) combustion boiler;
- heat is supplied by geothermal water;
- heat is generated by solar thermal collectors in combination with a backup heat generator (Fig. 6.31).

6.5 Other Heat Generators

The most common heat generators for nZEB buildings are presented in this chapter. Some other heat generators are presented in other chapters: ground heat exchangers, which are used for pre-heating of ventilation air, in Chap. 11 and cogeneration units in Chap. 7. Cogeneration units (CHP combine heat and power generation) are particularly interesting for nZEB because it is quite common in national regulations that on-site cogeneration of electricity and heat is treated as a technology that could

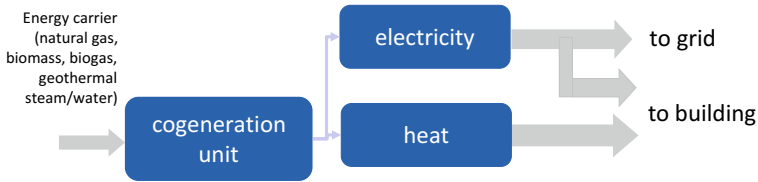


Fig. 6.32 Cogeneration units produce heat and electricity simultaneously on-site. For smaller units installed in single or multifamily residential buildings, natural gas or biomass are the most common used energy carriers; according to the national regulations in many EU Member State, CHP units, even if fossil fuel is used, ensure the required share of renewable energy sources for the operation of the building

replace other technologies for the utilization of renewable energy sources, and required share of renewable energy sources for operation of the building can be provided even if fossil fuel is used as energy carrier for CHP operation (Fig. 6.32).

References

- European Heat Pump Association (2005)
- Nussbaumer T et al (2008) Particulate emissions from biomass combustion in IEA countries. IES Task 32, Swiss Federal Office of Energy
- Oland CB (1996) Guide to low-emissions boiler and combustion equipment selection. Oak Ridge National Laboratory
- Pardo N et al (2012) Heat and cooling demand and market perspective. JRC Scientific and Policy Reports, EC Joint Research Centre, Luxembourg
- SOLARGE (2004) Enlarging solar thermal system in multi-family-houses, hotels, public and social buildings in Europe, EIALT/EIE/04/082/2004.ds

Chapter 7

Best Available Technologies (BAT) for On-Site Electricity Generation for nZEB



Abstract In addition to the large scale power plants presented in Chap. 2, there are several technologies for dispersed or in situ generation of electricity. In general these technologies use local renewable energy sources in the form of solar and wind energy or biomass. Small scale hydropower plants are a highly efficient technology with high durability and low maintenance costs; nevertheless, they will not be presented here because these devices are only useful for near-by electricity generation. Fossil or gaseous biomass fuels can be used for electricity generation on-site with the combined generation of heat and electricity. As an emerging technology, hydrogen driven fuel cells will also be presented in this chapter.

On the community level, the decentralized production of electricity is interesting because smaller units are more flexible for the production of electricity despite the fact that they transform unsteady natural sources on a short time scale. On the large scale, on-site electricity generators will be connected and controlled by smart grids. Decentral units are mainly built by private investors and, therefore, public money is spent much more rationally only for long-term subsidies. For the planners of buildings, the on-site production of electricity is interesting because in EU Member States such systems could be connected to public grid and enable the export of surplus of electricity. In this way, the primary energy needed for the operation of the building will be significantly decreased (since non-renewable electricity will be replaced by renewable electricity) and it is expected that criteria of nZEB could be more easily fulfilled by adopting on-site electricity generation. Building-integrated technologies for on-site electricity generation will be presented in the order of current market share:

- photovoltaic systems,
- small scale cogeneration,
- small scale building integrated wind turbines,
- fuel cells.

The European Union directive for promoting renewable energy use in electricity generation, established in 2001,¹ defined national targets for electricity generation from non-fossil renewable energy sources and provides the legal basis for it in all EU member states. This directive was superseded by the Renewable Energy Directive 2009/28/EC² that requires that 20% of the final energy consumed in the EU be renewable by the year 2020.

Note: The Revised Renewable energy directive³ was published in 2016, including targets of at least 27% renewables in final energy consumption in the EU by the 2030, national action plans, and promotes (among other measures) cooperation mechanisms in the form of statistical transfers of renewable energy.

According to Renewable Energy Directive, Member State must establish support schemes and actions to support investors. The three most commonly used options of support: (i) financial grants for investors; (ii) subsidies for each exported kWh of electricity on the base of so-called “feed-in tariffs”, long term (10–15 year) contracts for eligible homeowners, private and business owners of RES technologies; to stimulate investments, feed-in-tariffs differ among technologies for electricity generation from RES; (iii) Green Certificates, which indicate renewable origins of electricity and are granted per unit of produced electricity to motivate investors and can be traded between enterprises afterwards.

In recent years, small decentralized systems, especially those installed in buildings, are supported by the “net-metering” scheme; which is based on the yearly balance of exported and imported electricity. Only if the difference it is negative must it be paid by the producer of electricity.⁴

7.1 Photovoltaic (PV) Systems

Probably photovoltaic systems (PV) for the decentralized production of electricity benefit the most from the “green electricity” directive. According to Solar Power Europe, the installed power of PV systems in the EU at the end of 2015 was 97 GW

¹Directive 2001/77/EC of the European Parliament and of the Council of 27 September 2001 on the promotion of electricity produced from renewable energy sources in the internal electricity market (Official Journal of the European Union, L 283/33).

²Directive 2009/28/EC of the European Parliament and of the Council of 23 April 2009 on the promotion of the use of energy from renewable sources and amending and subsequently repealing Directives 2001/77/EC and 2003/30/EC (Official Journal of the European Union, L 140/16).

³Proposal for a Directive of the European Parliament and of the Council on the promotion of the use of energy from renewable sources (recast); COM/2016/0767 final/2-2016/0382 (COD).

⁴Uredba o samooskrbi z električno energijo iz obnovljivih virov energije (Decree on self-supply of electricity from the renewable energy sources) (Uradni list RS, št. 97/15 in 32/18).

(Note: the installed capacity of all power plants in Slovenia is 3.4 GW.), and 3.2% out of total production of 3030 TWh_e was produced by PV systems in EU. Photovoltaic systems consist of large numbers of solar cells gathered in solar panels or modules to enable the conversion of solar energy directly into electricity. There are several types of solar cells, but they are mostly made from silicon, a very common element. Despite the relative low efficiency of photovoltaic systems, (i) decreasing costs in previous decade, (ii) widely accepted support schemes in EU countries, and (iii) the fact that the areas of facades and roofs in buildings are in most cases large enough for independent electricity supply have resulted in a substantial increase of installed capacities building-integrated PV systems (Fig. 7.1).

Most commonly, PV cells are made from silicon (Si). Story of PV cell production starts with intrinsic (pure) Si, which has a low concentration of impurity atoms (<1 in 10^9) and high electrical resistivity (2500 W m). To become an electricity production device, intrinsic Si (Si is group IV chemical element) is doped by atoms with lower valence (boron, group III element) and atoms with higher valence (phosphorus, group V element). As result, positive energy carriers, called holes, in the Si layer doped with boron and negative energy carriers, called electrons, in the Si layer doped with phosphorus occur. In this way, the p-type (positively charged) and n-type (negatively charged) doped Si is made. If layers (typical n-layer is less than 1 μm thick and p-layer has thickness less than half of mm) are put together, a p-n junction or depletion region is made. As a result, an electric field occurs around the junction with a theoretical value of ~ 0.8 V (in the case of a Si cell) (Twidell and Weir 1996) (Fig. 7.2).

Photons, as solar energy carriers, can produce new pairs of electrons and holes in junction regions, generating so-called generation photocurrent. Only photons that have adequate energy, measured in electronic volts (eV), can produce new electron-hole pairs. For silicon PV cells, these photons will have energy higher than 1.18 eV (of solar irradiation with wavelength less than 1.1 μm). This limit value is called the band gap E_g . Other materials that are also used for PV cell production have different band gaps: for example, Germanium (Ge) 0.67 eV or Cadmium Telluride (CdTe) 1.49 eV. In contrast, the total energy of photons at lower wavelengths is not used for the creation of new pairs of electron-holes (meaning electricity) but is partially converted

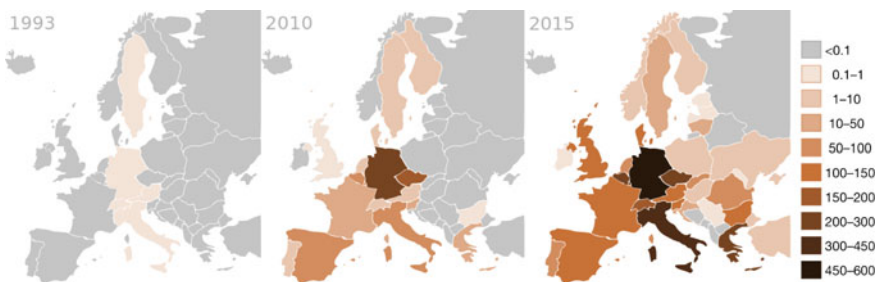


Fig. 7.1 Growth of installed PV systems in W per capita (stand alone and building integrated) (Solar energy in the European Union; www.en.m.wikipedia.org)

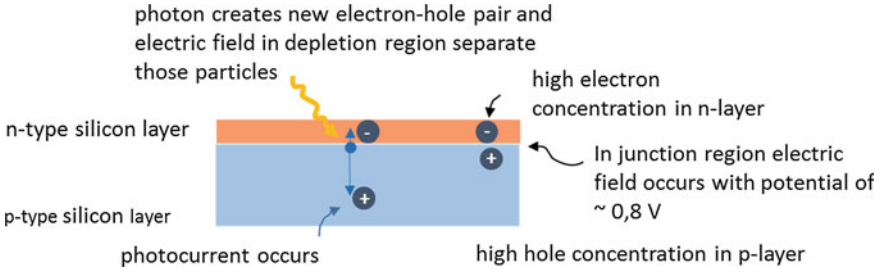


Fig. 7.2 Silicon photo-cell consists of a negatively charged n-type layer with doped P atoms and positively charged p-type layer; when put together, a junction or depletion cone occurs and an electric field is created

to heat (which is not a goal here). A third problem is the so-called recombination, which is the process of the recombination of electrons and holes caused by photons before they are permanently separated by the depletion region. As the share of produced electricity in the useful part of solar spectrum increases with increased band gap, the range of useful solar spectrum decreases simultaneously. An optimum band gap for the utilization of solar irradiation (taking into account spectral distribution of solar radiation) exists: 34% for material with band gap 1.2 eV, which is close to that of silicon. These values are valid for so-called single-junction cell that are PV cells with one p-n junction (Fig. 7.3).

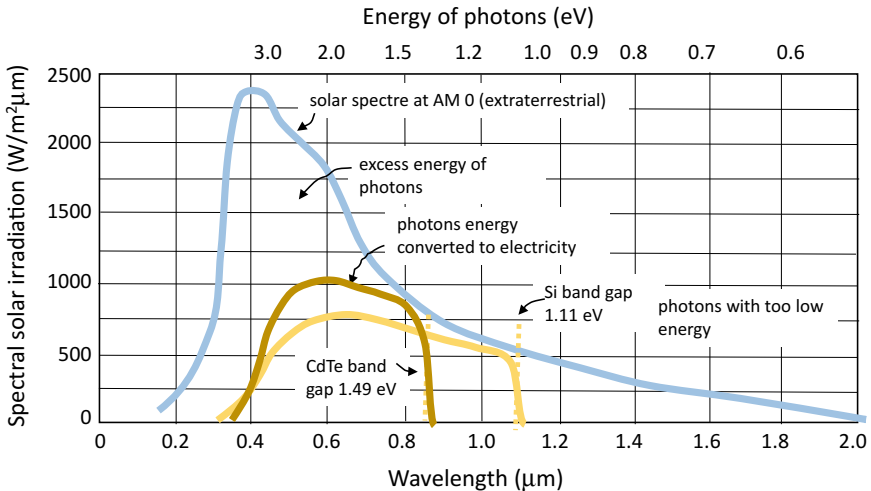
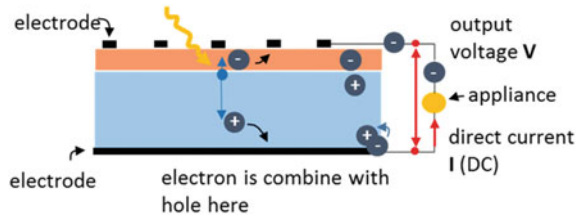


Fig. 7.3 Not all photons create new electron–hole pairs (meaning production of electricity) in a PV cell; the band gap of PV cell material defines the wavelength of useless solar irradiation ($\lambda > \lambda_g$ or $E < E_g$) and the amount of utilized solar irradiation with energy higher than the band gap at the same time

Fig. 7.4 When exposed to photons and connected to an appliance by the circuit, PV generates electricity



If electricity-conductive electrodes are added to the n-type and p-type layer, new electrons and holes produced by photons and separated by the electrical field in depletion zone are bound to the electrodes. If the electrodes are connected, the electrical current (flow of electrons) starts to flow through the circuit and enable the operation of connected devices. Generation of electron-hole pairs can be increased by several n-p junctions with different band gaps within one PV cell, using different semiconductor materials. Such PV cells are called multi-junction PV cells. PV cells with up to 4 n-p junctions have been developed with efficiency up to 42%, but this technology is currently in the laboratory research phase (Fig. 7.4).

7.1.1 Types of PV Cells

Several types of PV cells have been developed in recent decades. The main reasons for developing a wide range of PV cell technologies are the rational use of materials, the increasing efficiency of cells, decreasing the environmental impacts during production, and the cost of PV cells.

It can be seen from Fig. 7.5 that nowadays most PV cells are made as single-junction cells from silicon (Si). Such PV cells could be produced from a single crystal of Si (this type is called monocrystalline or “mc-Si” PV cell) or several crystals of Si (this type is called polycrystalline or “p-Si” PV-cell). Si PV cells are made from ingots, large blocks of pure silicon that grow from the molten raw material doped with boron atoms. Such blocks contain just one or multiple crystals of silicon. From the block, thin (~ 400 μm) slices are made with saws (leading to the waste of material). As boron atoms are added, slices are p-type layers in the PV structure. In a vacuum chamber, wafers are heated, and phosphor is doped to the surface area to create p-n junctions. An anti-reflective coating is made on the top of the cell surface to reduce the reflectance of solar irradiation (e.g. with titanium dioxide TiO_2 coating). Fingers (thin contacts) and busbars (connection contacts) are made on the top (to allow penetration of photons) and full surface rear contact on the bottom of the PV cell (Fig. 7.6).

Instead of large mono/poly crystalline blocs, thin sheet of silicon can be continuously pulled out of the molten silicon bath. In such a way, large area wafers from ribbons of thin film silicon PV cells are produced. PV cells made of Si crystals have the highest efficiency of all (single-junction) PV cells: market-available mc-Si

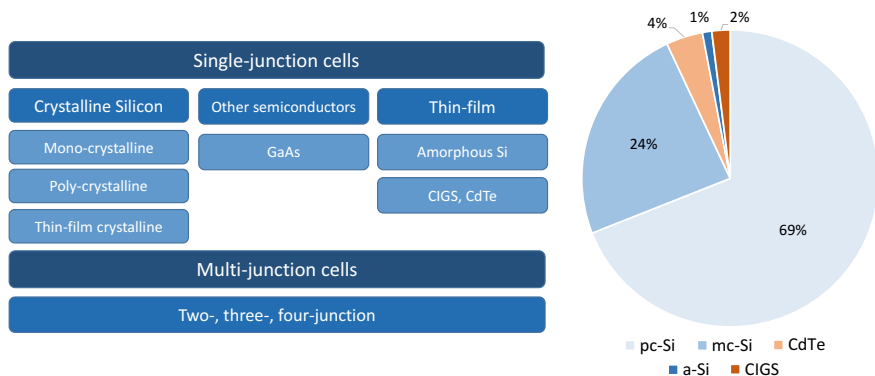


Fig. 7.5 PV cell technologies; while single-junction cell are available on the market, multi-junction cells remain at the laboratory stage and limited to applications in outer space; some emerging technologies, such a dye or organic cells, are not included because of low efficiency and time degradation (left); (National Renewable Energy Source, USA, 2017) the market share of PV cell technologies in 2015 (right), (Fraunhofer Institute for Solar Energy Systems, ISE, 2016) in the last 20 years the market share of mc-Si cells has decreased from almost 60–24% on account of polycrystalline Si cells; at the same time the share of thin film cells has remained more or less constant

PV cells have efficiencies of 18–20% (best lab efficiency: 26%), while the efficiency of pc-Si and thin-film Si cells are in the range of 16–18% (best lab efficiency: 22%). Crystalline PV cells can be produced from another semiconductor: gallium arsenide (GaAs). GaAs cells have high efficiency (up to 30% in lab conditions, highest among single-junction cells), but their high production price limits the use of GaAs cells to non-commercial applications.

Instead of making “massive” wafers from crystals, semiconductors can be deposited as thin layers (few nm to few μm) on the substrate (e.g. glass, steel, polymer) in a vacuum atmosphere. These are called thin-film PV cells and are so thin that they can be flexible. As a semiconductor, cadmium telluride (CdTe), copper indium gallium selenide (GIGS), copper indium selenide (GIS) or amorphous silicon (another type of silicon) are used in multi-layer structures. Thin-film PV cells are made at much lower energy demand for production (and therefore potentially promise lower prices), at an efficiency that is only a few percentage points lower in comparison to crystalline silicon PV cells, but they degrade faster than crystalline SI PV cells do (Fig. 7.7).

7.1.1.1 PV Cell Efficiency

Carnot’s Law, which defines the maximum efficiency of a thermal process within which heat is transformed into work, will be implemented and, taking into account that absolute temperature of Sun is 6000 K and absolute temperature of ambient is 300 K ($\eta_{\text{carnot}} = 1 - (T_{\text{amb}}/T_{\text{Sun}})$), the Carnot efficiency of PV cell could be 95%.

Fig. 7.6 Mono crystalline Si cell (fingers and busbars contacts can be seen) (top) and polycrystalline Si cell (bottom) prevails on the market

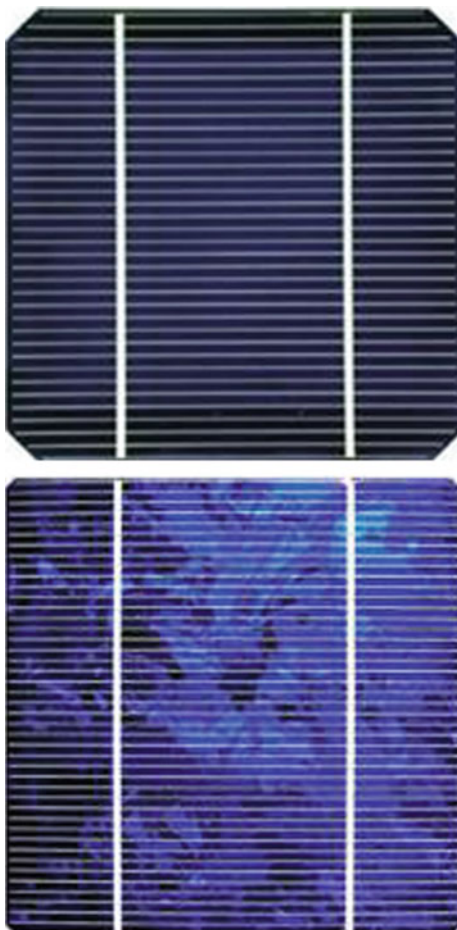


Fig. 7.7 CIS PV cell



To be more realistic and knowing the solar irradiation spectrum and optimum band gap (1.2 eV), the theoretical efficiency will be $\sim 34\%$. In reality, the efficiency of the PV cell is defined by I-U curve, which reflects the relation between direct current (DC) and voltage produced by PV cell at different electrical resistances of the circuit and at standard conditions (solar irradiation density 1000 W/m^2 , solar spectrum AM 1.5, temperature of PV cell 25°C) shown in Fig. 7.8.

I-U characteristic curve gives following data:

- U_{OC} is maximum voltage provided by PV cell if resistance of circuit is infinite (like open circuit); as a consequence of that, the electricity current is zero, and the power of the PV cell at this point is zero as well; U_{OC} depends on PV type, and for silicon cells it is $\sim 0.6 \text{ V}$;
- I_{SC} is direct current in the case of an open circuit (no electrical resistance, no load); this is the maximum current that can be generated by a PV cell, but without voltage; the power of PV cell at this point is therefore zero; I_{SC} is proportional to the area of the PV cell, at standard conditions a single PV cell in size of $150 \times 150 \text{ mm}$ will produce direct current $\sim 6 \text{ A}$;
- maximum power of PV cell which will be available at voltage U_{MP} and current I_{MP} ; in the case of BAT U_{MP} is in the range $0.8\text{--}0.9$ of U_{OC} and I_{MP} $0.85\text{--}0.95$ of I_{SC} ;
- Fill factor FF is the ratio between the actual maximum power of PV cell ($I_{MP} \times U_{MP}$) and the product of short-circuit current and open circuit voltage ($I_{SC} \times U_{OC}$); FF is a good indicator of PV cell efficiency and values of ~ 0.8 are typical for silicon cells.

Values of I_{SC} and U_{OC} depends on the density of solar irradiation and the temperature of a cell. At higher temperatures, I_{SC} slightly increases because the

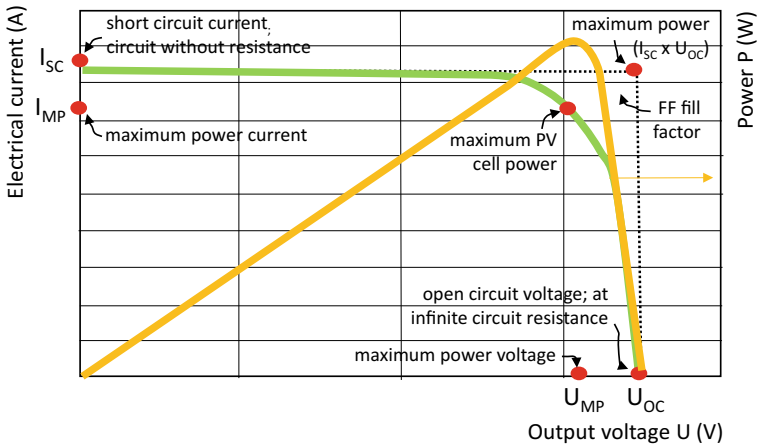


Fig. 7.8 I-U characteristic curve of single p-n junction PV cell

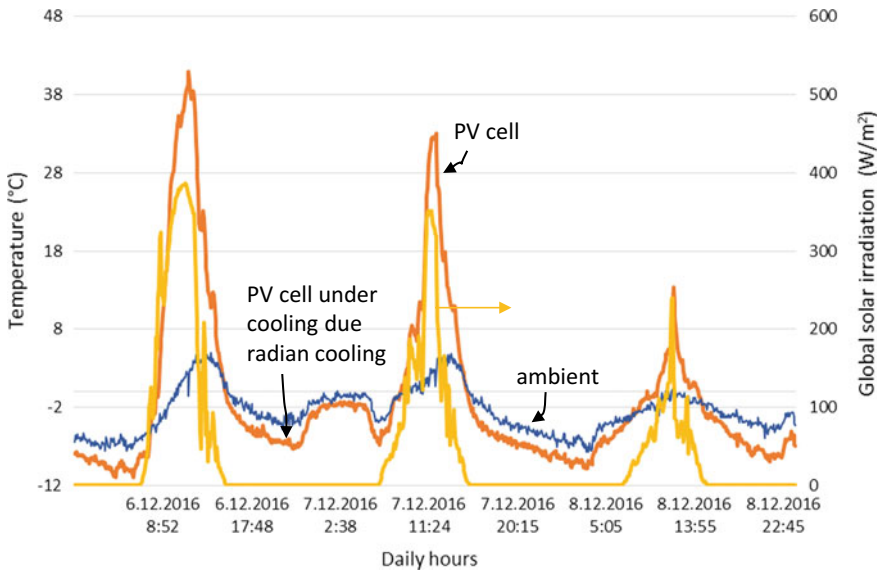


Fig. 7.9 Ambient air temperatures and temperatures of PV cells installed on the Virtual Lab building (Fig. 7.13) for three consecutive days in December

atoms in a PV cell have higher energy, and less energy is needed for creation of new electron–hole pairs. In contrast, at higher temperatures of the PV cell, U_{OC} will reduce to such an extent that the power of the PV cell will decrease. For polycrystalline cells efficiency decreases for about 0.04% per each $^{\circ}\text{C}$ above reference temperature 25°C (Fig. 7.9).

7.1.2 PV Modules

Several PV cells are connected together in a PV module. The PV cells are inserted between a cover of tempered low iron glass with a low reflectance surface (other transparent materials, such as polymers, can be used but are not common) and a supporting structure (metal or polymer sheet) and sealed by encapsulate gel (most commonly, ethyl vinyl acetate (EVA) is used). Encapsulated gel prevents water and water vapour penetration and the corrosion of contacts and ensures the long lifetime of the PV cells. Modules are in different sizes from some hundreds of cm^2 to several m^2 . Most commonly, modules in size up to $1\text{ m} \times 1.6\text{ m}$ are used in buildings (Fig. 7.10).

Another reason to build a PV module is that PV cells are connected in series to increase the voltage. A PV module with 36 (Si) PV cells has $U_{OC} \sim 21\text{ V}$ ($U_{PM} \sim 18\text{ V}$). In such a case, the electrical current is defined by single cell area

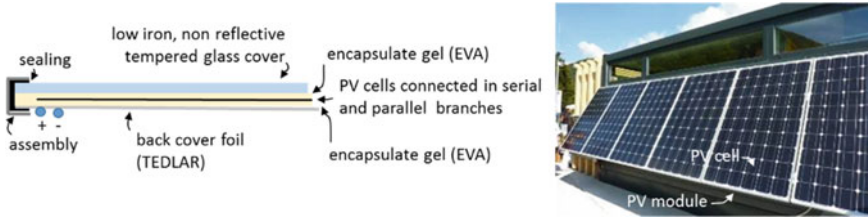


Fig. 7.10 Cross-section and installed PV modules

(typically 3–3.5 A per 100 cm² PV cell area (10 × 10 cm)). If serial strings are connected in parallel, this will increase produced direct current.

Note: The U_{OC} of PV module is proportional to number of serially connected PV cells; the I_{SC} of the PV module is proportional to the number of parallel connected PV cells.

7.1.2.1 Efficiency of PV Module

The electrical power of each module is declared to be “peak electrical power (W_p)”. This is the electrical power measured at ideal conditions: at solar irradiation with spectral distribution AM 1.5 and density 1000 W/m² and module (cell) temperature (cooled down to) 25 °C. The efficiency of a PV module at optimum and in situ operation conditions of PV module is defined by the equation:

$$\eta_{PV,p} = \frac{U_{MP} \cdot I_{MP}}{A_{PV} \cdot G_{PV}} \quad (-); \quad \eta_{PV} = \frac{FF(T) \cdot U_{OC(T)} \cdot I_{SC}}{A_{PV} \cdot G_{glob,PV}} \quad (-)$$

voltage at maximum power (V) current at maximum power (A) temperature dependent fill factor (-) temperature dependent open circuit voltage (V) short cut current (A)
 PV cell area (m²) solar irradiation 1000 W/m² AM 1,5 area of PV module (m²) global solar irradiation on the surface of PV module (W/m²)

The efficiency of PV modules built from different types of PV cells are presented in Fig. 7.11. It can be seen that efficiency significantly decreases if solar irradiation is lower than ~200 W/m², regardless of the PV cell type and, especially in case of crystalline PV cells, efficiency decreases with increased PV cell temperatures. Because of that, stand-alone PV modules have slightly higher efficiency in comparison to PV modules built into the building envelope, and this is also the reason

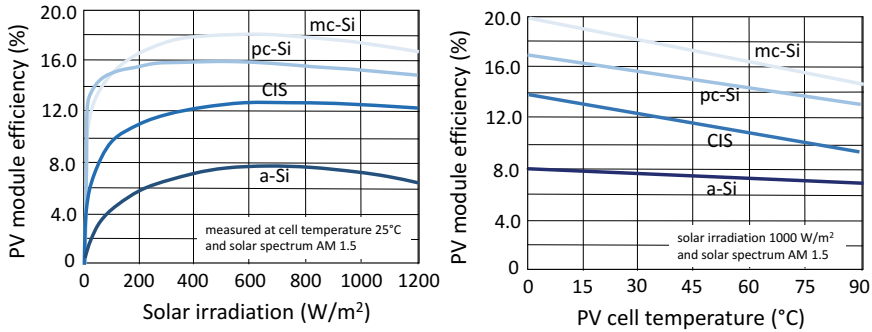


Fig. 7.11 Efficiency of BAT PV cell available on the market (Technical data of PV cell producers)

that manufacturers developed T-PV modules (thermal PV modules) that combined solar thermal collectors (that cool PV cells) with PV modules.

The performance data of PV modules includes the producers’ declared “durability factors”, which define the decrease of nominal power of the PV modules after long times of operation (typically after 25 years). Producers of BAT guaranteed that after 25 year of operation, the nominal power of PV module will not be less than 85% of the nominal power of the new product.

A decrease of electrical production can also be a result of operation conditions. Because PV cells in PV modules are connected in serial strings, the shading of just one cell by surrounding object or a fallen leaf can cause this cell to not produce electrical current. If electrical current produced by other cells in the string is more than I_{SC} of the shaded one, this cell will limit electricity production of whole string, and the shading will cause so-called “hot spot heating”, because the shaded cell will heat up. This will result in mismatch losses of PV module. This problem can be reduced by connecting a bypass diode in parallel with the PV-cell serial string inside the PV module. As the hot-spot effect can occur in serially connected PV modules, too, bypass diodes are installed in parallel with the PV modules.

7.1.3 Building Integrated PV Modules

Requirements for nearly zero energy buildings (nZEB) include the requirement for a high share of energy needed for the operation of the building to be produced on-site by the use of renewable energy sources. PV systems are one of most promising technologies to fulfil this requirement, especially if PV modules connected to the PV system are integrated into the building envelope. Such PV systems have advantages in comparison to stand-alone PV systems, such as:

- PV modules can replace facade and roof structures and decrease the cost of the building,
- PV modules are highly weather durable; therefore, maintenance of the building will be cheaper,
- PV modules can improve building envelopment properties, reducing the heat transfer coefficient (U) and providing shading of large glass areas,
- PV systems guarantee long-term benefits for the owner as the cost for electricity decreased,
- PV systems emphasizes the “green view” of the buildings,
- building integrated PV systems reduces the use of land needed for installing stand-alone PV systems.

Producers of PV modules have developed solutions that attract designers and investors. For example, PV modules can be opaque or semi-transparent, and the density of the solar cells in PV modules can be custom made and adjusted to desired visual effect, natural lighting, or shading (Fig. 7.12).



Fig. 7.12 Transparent PV modules (above) PV modules can be integrated into the building envelope and replace standard envelope structures (below) (<http://www.dansksolenergi.dk>; <http://www.concerto-sesac.eu>; <http://www.solarpv.co.uk>; <http://photovoltaic-shingles.com>; <http://drexelcorp.wordpress.com>)

7.1.4 PV Systems

Two types of PV system are common: (i) off-grid systems or island operation stand-alone systems, and (ii) grid connected systems. Off-grid systems can be low-voltage direct current (DC) (mostly 24 V) or high-voltage systems equipped with batteries. The BAT is Li-ion batteries with efficiency up to 93, and 80% of capacity after 10 years of use. In larger PV systems, an inverter is installed between the batteries and grid to produce high voltage (220 V) alternating current (AC). This allows common appliances to be supplied with electricity, reduces the cross-section of wires, and reduces system costs (Fig. 7.13).

Grid-connected systems are so-called PV power plants. These systems export electricity to the public grid. In many countries, investors in PV power plants are encourage with state incentives. The most efficient is the so-called “feed-in-tariff”, which is the price of exported electricity offered to investors in a long-term contract. Feed-in-tariffs for PV systems are normally 2–4 times greater than the regular price of electricity (between €0.10 and 0.20/kWh, depending on the country).

For several years now, another support scheme for smaller PV systems suitable for nZEB has been the net-metering policy, according to which surplus electricity (differences in the current electricity demand in building and PV system production) could be feed into the public grid, “stored” for free and used later during the same calendar year; any surplus at the end of calendar year is not paid.

Case Study In Slovenia, the nominal power of a PV system included in net metering is limited to 11 kWp. Taking into account yearly solar radiation and the BAT of PV modules, this means that $\sim 88 \text{ m}^2$ of PV modules could be installed and $\sim 16 \text{ MWh}_e$ per year would be produced and used immediately or during the calendar year. For comparison: an average of one family-home uses 4500 kWh_e per year.



Fig. 7.13 Off-grid PV system installed on the virtual lab building

7.1.5 Production of Electricity: Rule of Thumb

The yearly production of electricity by a PV system, assuming that it is grid connected and the delivered electricity therefore does not depend on demand in the building, depends on the yearly solar radiation, as well as the orientation and efficiency of PV modules. As shown in Fig. 7.14, the average yearly solar radiation depends on geographical longitude of the site. For Central Europe, a reference value 1100 kWh/m^2 per year can be assumed. If PV modules are integrated into the building envelope, they probably will not be orientated optimally. In this case, the orientation factor, shown on the graph, must be taken into account.

Case Study A PV system will be installed on a site with annual global solar radiation $1800 \text{ kWh/m}^2\text{a}$ and polycrystalline silicon PV modules with efficiency of 16% will be installed on southeast vertical facade. It can be assumed that average temperature of PV modules during the year will be 35°C . What will be yearly electricity production with 100 m^2 of PV modules?

Performance orientation factor for PV modules installed on southeast façade is 0.60 and from Fig. 7.11 it can be seen that efficiency of pc Si PV module at average temperature 35°C will be 15%.

Annually produced electricity will be $E \approx 1800 \text{ kWh/m}^2\text{a} \times 0.15 \times 0.60 \times 100 \text{ m}^2 = 16,200 \text{ MWh/a}$ and specific electricity production E' is equal to 162 kWh/m^2 .

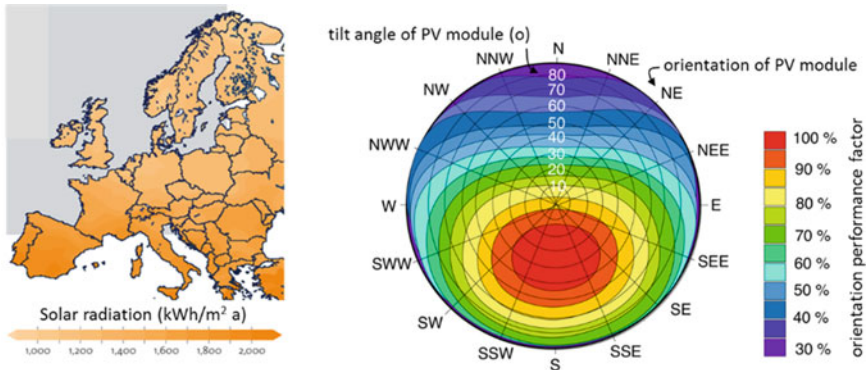


Fig. 7.14 Average yearly solar radiation (left) and orientation performance factor (right)

7.1.6 Environmental Impacts of PV Cells

While the production of electricity by PV systems is free of emissions, several indicators can be used to justify the production of PV cells regarding their environmental impact. Embodied energy is the ratio of electricity produced over the lifetime of PV modules to the energy needed for production of them. Typically, Si cells produce in their lifetime (in general, 30 years) 10–20 times more energy than it is needed for the production. Further on, the recycling of Si cells will reduce energy consumption for PV cell production up to 33%. The reduction of greenhouse gases emissions over the lifetime operation is another frequently used environmental indicator. Studies have shown that lifetime greenhouse gas emissions decreased between 60 and 90% in comparison to fossil thermal power plants. Thin film PV cells exhibited lower environmental impacts. Despite the fact that some types of PV cells contain dangerous substances (e.g. cadmium), closed loop manufacturing including the complete recycling of materials prevents harmful pollution. More complex methods for environmental impact evaluation are also available. The general method of life cycle assessment (LCA) will be presented in Chap. 14. Some focused on electricity generation technologies such as the PI (pollution index*) method. According to this method, the pollution indexes of different power plants are (note: less is better) PI equal to 885 for coal power plants, PI 52 for PV systems, PI 9 for wind turbines and PI 0.5 for hydro power plants.⁵

7.2 Small Scale Cogeneration

In thermal power plants, large amounts of the heat must be released to the environment; and consequently, the efficiency of electricity production in such power plants is low. Overall efficiency can be improved if waste heat is used, for example, for district heating systems. Such a power plant is called a cogeneration plant, and the process combines heat and power production (GHP). GHP operates efficiently in district heating systems, where power generation is adjusted to heat demand during the year. Unfortunately, heat supply during the summer causes high (50% or more) heat losses in the distribution system. The overall efficiency of CHP could be improved in the case of decentralized block-type cogeneration or microcombined heat and power units (mCHP) installed in residential buildings. In most cases, mCHP systems have power from a few kW_e to 50 kW_e (Fig. 7.15).

⁵www.envimpact.eu.

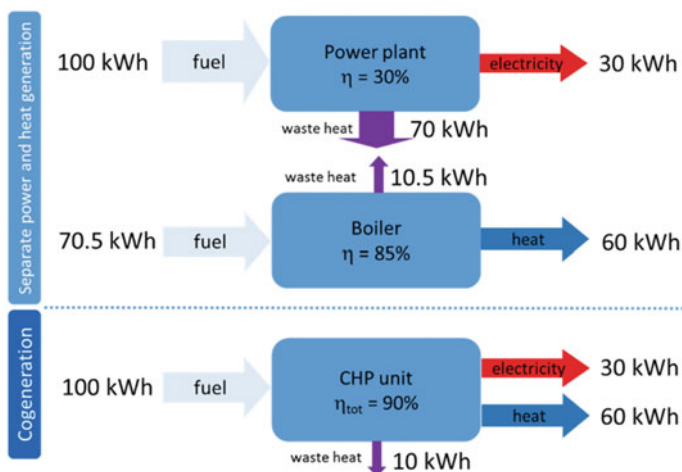


Fig. 7.15 Figure explains why the cogeneration of heat and electricity is more efficient than the separate generation of both energy carriers

Note: With the BAT of combustion boilers, heat is produced with higher efficiency than with the cogeneration units; therefore, in most cases, mCH is cost effective only if electricity is exported to the public grid and subsidized by a feed-in-tariff scheme.

Even if exported electricity is subsidized, the cost effectiveness of mCHP is highly dependent on the hour-by-hour demand of heat. In residential buildings, heat is needed for heating, domestic tap water heating, but also for cooling in absorption cooling. In this case, heat consumption over the year is much more uniform. Nevertheless, a mCHP unit should be in operation at least ~ 4000 h per year to be cost effective with heat demand of at least 20.000 kWh and electricity demand of more than 3000 kWh per year.⁶ Several units can be combined to avoid operation at lower efficiencies at partial loads. Advanced hour-by-hour computer simulation of heat demand and operation of mCHP is needed for accurate feasibility studies (Fig. 7.16).

Most commonly, electricity is produced by mCHP using natural gas or biomass as fuel in a process that consists of the production of heat by combustion and the mechanical work needed to run the electricity generator. mCHP technologies differ mainly regarding to the process of the production of mechanical work by:

- internal combustion engine (ICE; Otto or Diesel engine); natural gas or LG, biogas or liquid biofuels can be used as fuel; this technology has high efficiency

⁶www.viessmann.com.

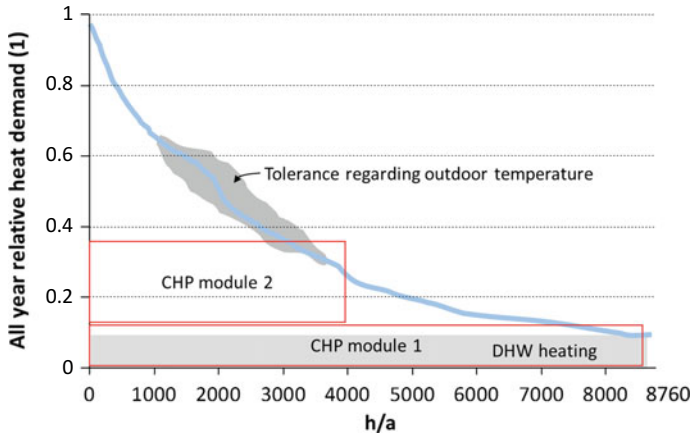


Fig. 7.16 Hour-by-hour relative heat demand for heating and DHW; uniformity of heat consumption can be improved by sorption cooling

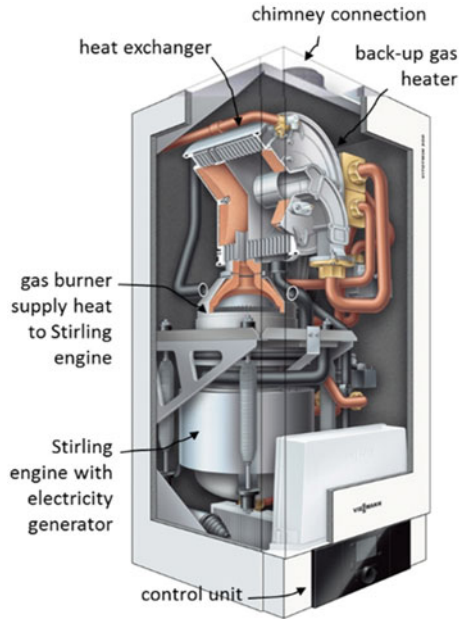
Fig. 7.17 mCHP unit with piston gas engine with rated power 6 kW_e and 15 kW_t , with efficiency of electricity production 27% and heat production 67%, total efficiency 94% (www.viessmann.com (Vitobloc 200 E-6/15))



(25–35% of electricity production, overall 85–95% if condensing technology is used); BAT with rated power output (electricity) down to 5 kW is available; a combustion engine (2 or 3 cylinder) mCHP requires frequent maintenance (after 5000–10,000 h of operation); units with rated power up to 500 kW are available on the market (Fig. 7.17);

- fuel-cell-driven cogeneration uses hydrogen for the generation of electricity and heat; since hydrogen infrastructure is not developed yet, reformers that “extract” hydrogen from natural gas (CH_4) are integrals part of mCHP units (see Sect. 7.4).

Fig. 7.18 mCHP unit with Stirling motor; Stirling engine generates up to 1 kW_e and 5 kW_t , with back up gas heater with rated power up to 26 kW_t with efficiency up to 109% (www.viessmann.com (Vitolwin 350 W))



- Stirling engine; engine that convert externally produced heat by combustion or solar radiation into mechanical work; mechanical work is produced by periodic expansion and contraction of gas (helium) sealed inside the engine; different heat sources including many renewable energy sources (e.g. biomass, solar energy and geothermal energy) can be utilized; Stirling engine-driven mCHP remain under development: pilot applications with smaller size (1–40 kW) with efficiency of electricity production 10–30% and overall efficiency up to 80% are in operation (Fig. 7.18).
- micro-turbines are gas engines with electrical power output 30–500 kW; micro-turbines have lower efficiency in comparison to ICE (25–30% for electricity production, overall up to 70%), but have better partial-load efficiency, lower maintenance cost and lower emissions of NO_x, CO, and hydrocarbons; a micro turbine driven CHP consists of high-speed generator, compressor and turbine wheels that are on the same rotating shaft, the only moving part in the engine; this enables compact size and long-term reliability; units with rated power several 100 kW_e are available for industrial applications and large buildings.

7.2.1 Cost Effectiveness

mCHP systems are more expensive per unit of size in comparison to large community scale systems. The cost of combustion driven CHP systems is between

~€1200 and €700 per kW_e (P_e 100–5000 kW) and for micro-turbine driven CHP systems between ~€2000 and €1400 per kW_e (P_e 100–5000 kW). However, the difference in price has become lower in recent years. mCHP systems are often included in subsidy schemes for energy efficient electricity production. In Slovenia, for example, the feed-in tariff for electricity produced by small CHP is €23.71 per kWh_{e1} for systems that operate not more than 4000 h per year.

7.2.2 Environmental Benefits of mCHP

Due to their high overall efficiency, mCHP produce much lower emissions in comparison to ordinary fossil fuel power plants: at least four times lower emissions of CO₂ in comparison to coal fired power plants and more than twice lower emissions in comparison to natural gas fired power plants.

7.3 Wind Turbines

Evidence of wind exploitation for water pumping and mechanical work from the Middle East and China more than 1000 years ago exists. In the middle of the 19th century, several thousand wind-driven mills, pumps, and saws operated in Europe. At the end of the 19th century, the first windmills for electricity production were built (in the UK and Denmark). From that time and especially in recent decades, electricity production by wind turbines has become a highly efficient, very reliable and cost effective technology for the production of electricity. From the year 2000, wind power in Europe has shown the largest growth among all power plant technologies as 142 GW new installations were built. This is even more than solar PV systems (101.2 GW of new installations) and noticeably more than natural gas-driven power plants (93.5 MW of new installations) (Fig. 7.19).

Note: In 2016, natural gas power plants have largest share (20.3%) among total installed power capacity in EU (887 GW), following by wind turbines (16.7%), coal power plants (16.5%), hydro power plants (14.8%), nuclear power plants (13.1%), solar PV (11.0%), and biomass (1.5%) (see Footnote 4).

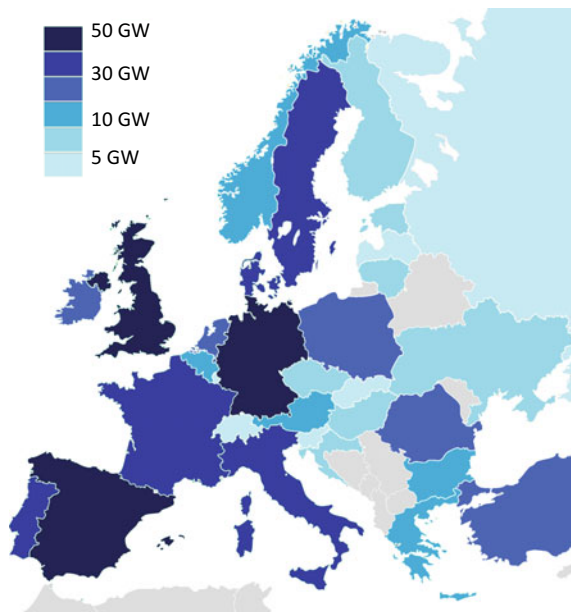


Fig. 7.19 Installed capacity of wind turbines in EU in 2016 (WindEurope, www.windeurope.org)

7.3.1 Wind Energy Potential

Wind occurs in the troposphere as a result of temperature expansion and convection of air mass heated on the surface by absorbed solar radiation. The rotation of the Earth also influences global wind patterns. Due to the friction between moving air layers, wind velocity increases from the ground level (where $w = 0$ m/s) to a maximal value at ~ 1000 m above open ground. Wind velocity at height h (m) above the ground can be calculated with the equation (Fig. 7.20):

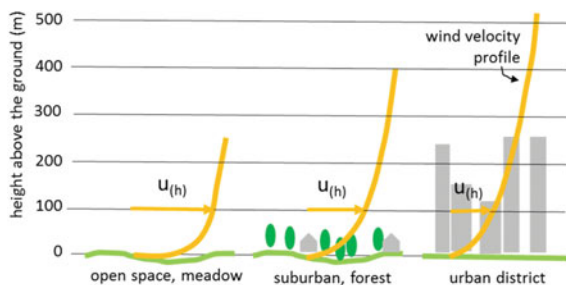


Fig. 7.20 Wind velocity increases with the height above the ground according to the ground surface roughness

α coefficient of surface roughness (0.1 for sand surface; 0.13 for pastures; 0.30 for large settlements)

wind velocity at height h (m) above the ground (m/s)

$$u_{(h)} = u_{10} \cdot \left(\frac{h}{10}\right)^\alpha \quad (\text{m/s})$$

u₁₀ wind velocity 10 m above the ground (m/s)

Wind data at specific locations are measured and year-long average values are presented as “wind rose” charts. Wind rose chart shown the average monthly or yearly wind velocity direction at a height of 10 m above the ground. As large wind turbines are much higher, data must be corrected to the height of the turbine. As geographic terrain has significant influence on local wind velocity, wind potential is measured on specific and precise locations. Hourly data on wind velocity are available in meteorological Test Reference Years, but it is common that the wind energy potential for building nearby (using nZEB nomenclature) wind turbines on specific location is analysed using measurements over a period of several years. The potential for on-site wind turbines can only be modelled by CFD tools for average boundary conditions because of intensive turbulent flow around the buildings (Fig. 7.21).

Note: Average yearly wind velocity is good indicator of wind potential for the utilization of wind turbines. If the average yearly wind velocity is more than 5 m/s, the location has adequate wind energy potential.

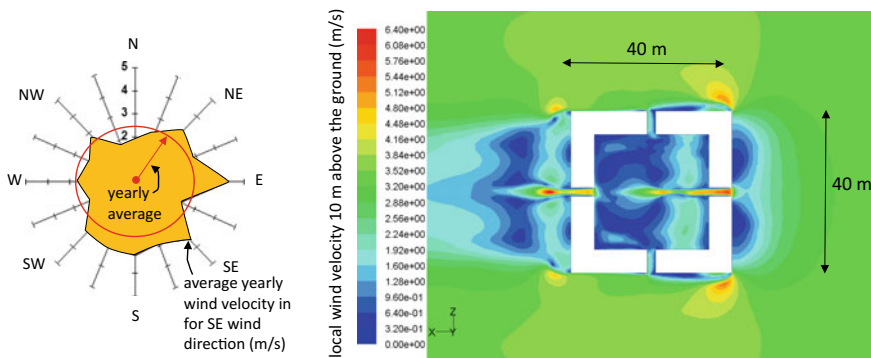


Fig. 7.21 Wind rose for City of Ljubljana (left); CFD (computational fluid dynamics) numerical solution of velocity field around the atrium type multifamily building (right)

7.3.2 Rated Power and Efficiency of Wind Turbines

Wind turbines convert the kinetic energy of an air mass into the electricity. If the equation of kinetic energy is divided by time differential (dt), the mass of the air replaced by mass flow rate, a continuity equation is introduced, and the relation for theoretical wind turbine power can be developed:

$$E_{th} = \frac{1}{2} \cdot m \cdot v^2 \quad \rightarrow \quad \frac{1}{dt} \rightarrow \frac{E_{th}}{dt} = P_{th} = \frac{1}{2} \cdot \frac{m}{dt} \cdot v^2 = \frac{1}{2} \cdot \rho \cdot A \cdot v \cdot v^2 = \frac{1}{2} \cdot \rho \cdot A \cdot v^3 \quad (W)$$

air mass flow rate (kg/s)
air density (kg/m³)
wind velocity (m/s)

air volume flow rate (m³/s)
cross-section area of wind turbine eq. (π·d_{rotor}²) (m²)

It can be seen that a wind turbine will deliver more energy at the sea level (since density of the air is 1225 kg/m³ (25 °C, 1 bar) than at higher altitudes (density of air at same conditions at altitude 600 m is 1184 kg/m³). In both cases, wind turbine power depends on the cube of velocity, which is the dominant influence factor. All wind energy cannot be transformed into mechanical work because that would mean that the wind velocity behind the turbine would be zero and, as a consequence, the air mass flow rate through the turbine cross-section area would then be zero as well. The minimum theoretical value of the ratio of the kinetic energy of outflow air to the kinetic energy of inflow air defines the theoretical maximum efficiency of the wind turbine in open space (without any wind router) and is called the “Betz coefficient”. This coefficient has value of 0.597 (59.7%). In operation, the efficiency of wind turbines is lower because of turbulent air flow and swirls that occurs along and at the tip of blades; nevertheless BAT wind turbines have power coefficient c_p in the range between 38 and 42% and the power of a wind turbine is define by the equation:

$$E = \frac{1}{2} \cdot c_p \cdot \rho \cdot A \cdot v^3 \quad (W)$$

power coefficient (-)

Wind velocity u changes in time and, therefore, the relative velocity v_r and attack angle α as shown in Fig. 7.22 also changes. As power coefficient c_p depends on the instantaneous attack angle, the increase in air velocity will cause a significant increase of attack angle and simultaneously decrease power coefficient c_p .

At low wind speeds, c_p is zero and only at wind speeds higher than the “cut-in speed” (2–4 m/s) does the wind turbine starts to produce electricity that is synchronized to connection grid. As wind speed increases, the lift force that act on turbine blade is more and more dominant over the drag force, and the wind turbine power increases as function of cube of wind speed until the rated power is reached

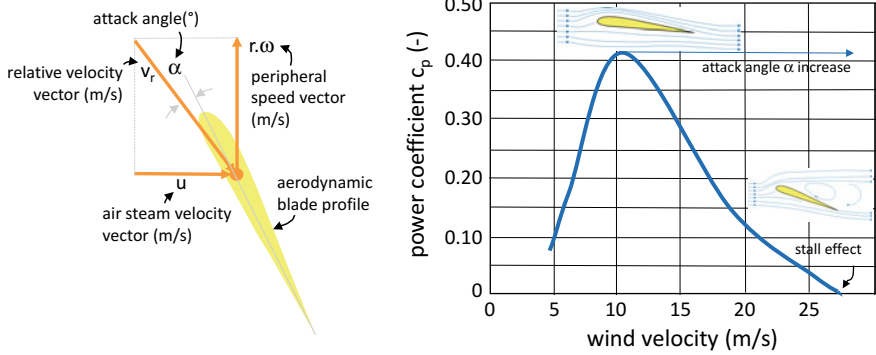
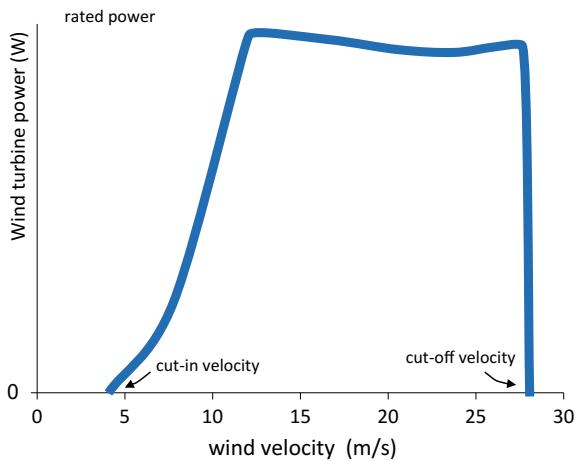


Fig. 7.22 Velocity triangle on blade of wind turbine rotor (left), power coefficient of wind turbine (right)

(at u 10–12 m/s). At these conditions, the power coefficient is maximal. The aerodynamic profile of the blade is developed in such a way that wind turbine operates at (\sim) rated power despite increased wind velocity because power coefficient c_p decreases. At “cut-off” speed (25–30 m/s), the wind turbine stops because of increased mechanical load and synchronization with grid. This could be by stall effect, the phenomena of the instant reduction of lift force that act on the blade due to the large attack angle.

Other techniques used to stop the wind turbine are (i) pitching of the blades (longitudinal rotation of blades, used during operation of the wind turbine to adjust c_p to optimal value at changing wind velocity), (ii) rotation of the wind turbine as whole out of the wind speed vector or (iii) by activating an aero brake at the end of the blade (Fig. 7.23).

Fig. 7.23 Typical power curve for wind turbines with cut-in and cut-out wind velocities; at wind velocity above ~ 10 m/s, the power of wind turbine is approximately constant because efficiency (and c_p) decrease



7.3.3 Types of Wind Turbines

Several types of wind turbines were developed in previous century. In recent decades wind, turbines are built mostly as power plant stations. Such turbines have 2 or 3 blades and operate high speed ratio turbines.

Note: Speed ratio λ is ratio of the peripheral velocity of tip (end point of blade with maximum distance to rotation axe) to wind velocity; optimal speed ratio is defined as $(4.\pi/n)$, where n is number of the blades in rotor; for a 2-blade turbine, the optimal speed ratio is ~ 6 ; for 3-blade turbines ~ 6 .

The most common division of wind turbines for near-by production of electricity (following nZEB definition) is made regarding to the position of the rotation axe. Wind turbines can be horizontal axe wind turbines (HAWT) where the wind velocity vectors are parallel to the rotation axe or vertical axe wind turbines (VAWT) where wind velocity vectors are perpetual to the rotation axe (Figs. 7.24 and 7.25).

Nowadays wind turbines are used for electricity production and are connected into grid. Regardless of the type of the rotor, all wind turbines consist of a tower

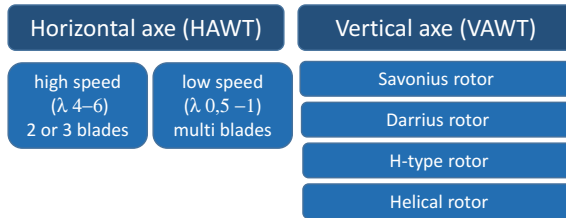


Fig. 7.24 Wind turbines are most commonly divided according to rotor rotation axe



Fig. 7.25 Vertical axe wind turbines (VAWT) for near-by electricity production: Savonius rotor, Darrius rotor, helical rotor and H-type rotor

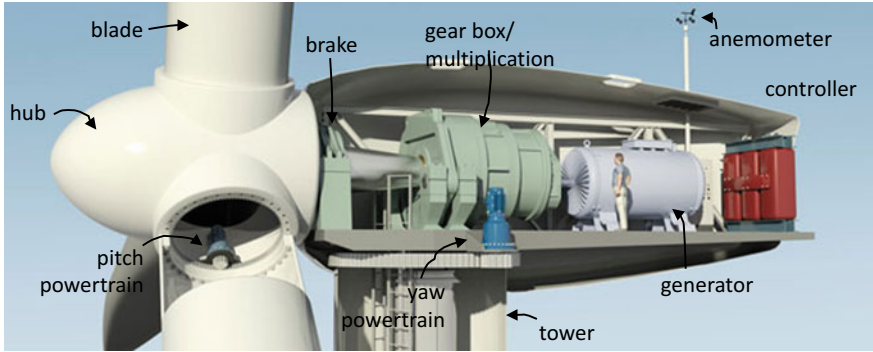


Fig. 7.26 Sub-systems of wind turbine (www.designteam-berlin.de)

(whose height is approximately equal to the diameter of the rotor), a hub, and a nacelle containing mechanical sub-systems, the electricity generator, and the controller. The nacelle is rotated with a yaw powertrain to adjust the wind turbine to the wind direction and a pitch powertrain to adjust the angle of the blades to wind speed (Fig. 7.26).

7.3.3.1 Building-Integrated Wind Turbines

Most small scale wind turbines generate direct current electricity (DC) and require an inverter to convert it to alternating current electricity (AC). In off-grid systems, a battery is needed to store the electricity for later use. BAT are available for the range of power between several hundred watts to several ten kilowatts. Potential for building-integrated wind turbines must be evaluated by detailed wind flow pattern study taking into account detailed space shape and obstacles. CFD tools are mostly used. As a rule, small scale wind turbines are much less cost effective in comparison to large scale ones (Fig. 7.27).



Fig. 7.27 Examples of small scale building-integrated wind turbines

7.3.4 Production of Electricity: Rule of Thumb

A detailed study of electricity production must be modelled on an hour-to-hour scale, taking into account local wind conditions and power curve data provided by producers. By introducing capacity factor (CF), approximate annual electricity production can be forecast. Capacity factor is the ratio of actually produced electricity to the theoretical maximal production per year. Capacity factors for best practice cases are between 33 and 48%.^{7,8,9,10} Yearly electricity production of wind turbines is defined by equation:

$$E = P \cdot CF \cdot 8760 \quad (\text{MWh/a})$$

rated power (MW) number of hours per year (h/a)
capacity factor (-)

Case Study Anholt 1, wind farm in Denmark with rated power of wind turbines 399.6 MW has CF 0.474 (in 2016). How much electricity was produced at Anholt 1 in 2016?

$$E = P \cdot CF \cdot 8760 = 399.6 \cdot 0.474 \cdot 8760 \sim 1660 \text{ GWh/a}$$

7.3.5 Environmental Impacts

On the global level, wind turbines have very low (after hydropower plants) life cycle emissions of greenhouse gases and other air pollutants. Several potential problems occurs on the local scale. Wind turbines are big (up to 150 m in high for rated power of 7.5 MW) and have visual impact on the landscape. Off-shore wind farms are a solution to that. Problems with the interference of electromagnetic waves and noise emission have been reduced by using non-metallic materials and new blade designs. Possible impacts on underground water by leaking fluid were reduced as well, since only 14% of malfunctions are reported because of mechanical problems as lighting strike and the occurrence of fire are the main reasons for breakdown. Potential problems about birds and bats colliding with blades must be mentioned. The most studies show that this is less problematic than

⁷energynumbers.info.

⁸www.ofgem.gov.uk.

⁹www.elexon.co.uk.

¹⁰ens.dk.

discussed in public; nevertheless, ornithological research must be done before permission for building is granted. Flash shading patterns of rotating blades (rotation frequency up to 10 min^{-1}) must be avoided in indoor spaces in cases of people with epilepsy.

7.4 Fuel Cells (FC)

Electrochemical energy conversion is the direct conversion of chemical energy of an energy carrier into electricity. An example of this is fuel cells that convert the chemical energy of hydrogen molecules (Fig. 7.28). Because heat is a by-product, fuel cells can be used as mCHP. In comparison to “heat-driven” CHP, fuel cells have higher efficiency of electricity production (up to 60%) and only water (if hydrogen is used as fuel) is the by-product of electricity generation. (The simplest) fuel cell is made from two electrodes (– anode and + cathode) and an intermediate electrolyte layer, capable of transferring positive ions from negative to the positive electrode (or negative ions in opposite direction), but not allowing electrons to pass through. The flow of electrons through the external circuit from the negative to positive electrode provides electrical power. All fuel cells use hydrogen (as fuel) and oxygen (as oxidant) for operation but they differ regarding the type of electrodes (solid/fluid) and electrolyte (fluid/solid). In a hydro-oxygen fuel cell, hydrogen gas is led to the porous negative electrode, allowing generated H^+ ions to diffuse through the electrolyte, meanwhile the electrons are gathered by anode and may flow through the external circuit towards the cathode. If the catalyst (platinum film on the electrode surface) is present, the H_2 dissociates at the negative electrode in reaction:

Fig. 7.28 Structure of hydrogen-oxygen fuel cell; Hydrogen-oxygen fuel cell in operation, similar to PV cell (by n-p junction), charged particle (negative electrons and positive ions) are separated inside the device

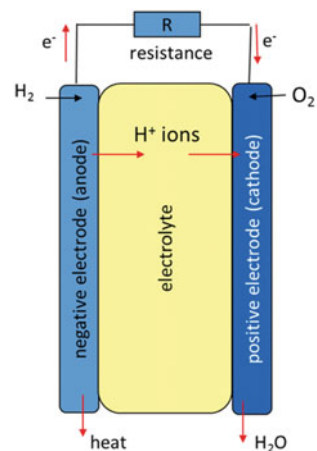
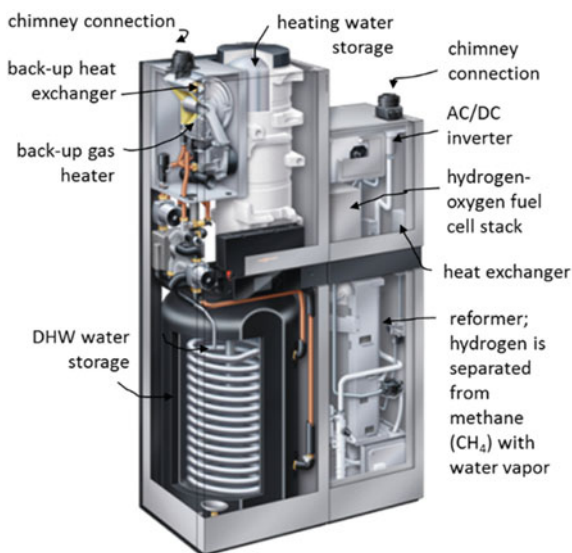
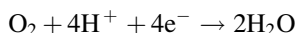


Fig. 7.29 mCHP unit with fuel cells; fuel cells with rated electricity power 750 W_e and heating power 1 kW_t with total efficiency of 90%, with back-up heater with rated power up to 19 kW with efficiency up to 109%; most times during the year the operation of fuel cells provides adequate amounts of electricity and heat for the operation of a single or double family house (www.viessmann.com (Vitovalor 300-P))



Gaseous oxygen (or air) is led to the positive electrode, where both hydrogen ions and electrons are captured:



This reaction is accompanied by the generation of the water and heat (at temperatures $50\text{--}800\text{ }^\circ\text{C}$ depending on the fuel cell type) that can be used for heating. Similar to PV cells, fuel cells produce direct current at low voltage ($\sim 0.6\text{ V}$) and are combined into the fuel cell stack to increase output voltage. For grid connection, a DC/AC inverter is needed (Fig. 7.29).

7.4.1 Types of Fuel Cells

In addition to the most simple hydrogen-oxygen fuel cells, other technologies have been developed. Proton exchange membrane fuel cells (PEMFC) are used as mobile as well as stationary units. They operate at low temperatures ($50\text{--}100\text{ }^\circ\text{C}$). In PEMFC, a polymer membrane conducts hydrogen ions (H^+) but not electrons (e^-). Solid oxide fuel cells (SOFC) use solid ceramic (zircon) as the electrolyte to conduct oxygen ions at the positive electrode. These are high temperature fuel cells (operating temperature $800\text{--}1000\text{ }^\circ\text{C}$) and have high efficiency of electricity production $\sim 50\%$, but may be up to 80% in the future. High operating temperatures



Fig. 7.30 Cogeneration units with different types of fuel cells

enable reforming of different fuels that contain hydrogen. Other FCs are also under development. For example, the phosphoric acid fuel cell (PAFC), which use phosphoric acid H_3PO_4 acid as an electrolyte or the molten carbon fuel cell (MCFC) which use molten alkaline carbonate as an electrolyte.¹¹

Hydrogen as an energy carrier for electricity production with fuel cells can be produced by hydrolysing water using electricity produced by renewable electricity from hydro and solar power plants. In the case of a building-integrated fuel cell mCHP, hydrogen is commonly produced on site by the decomposition of hydrogen from natural gas. Such a PEMFC mCHP is shown in Fig. 7.30.

References

- ENVIMPACT, Increasing the impact of Central-Eastern European environment research results through more effective dissemination and exploitation, Grant agreement n° 265275
 Twidell J, Weir T (1996) Renewable Energy Resources. TNP Cambridge

¹¹Producers' technical information.

Chapter 8

Space Heating of nZEB



Abstract Buildings in northern and continental European climates need to be heated more than the half of the year to maintain required indoor thermal comfort; even in the Mediterranean countries space heating is needed at least occasionally. The energy used for the space heating of residential buildings has the largest share in energy demand for operation of building; consequently, the determination of the building energy efficiency class, most noticeable indicator on Energy Labelling Certificate (see Chap. 12), is based on the energy needs for space heating. Even in non-residential buildings, energy demand for heating has significant impact on the overall energy efficiency indicators and on the share of renewable energy sources used for operation of buildings. It is also important to be aware that the operation of the heating system must not compromise the other aspects of indoor living quality, such as indoor air quality (IAQ) or excessive noise. A space heating system can be decentral, local or central. Decentral heating systems consist of a stove or heater as heat generator, which is located in a heated room and provided heating only for that room. Heat generated in a heat generator is transferred into the room by radiation and convection to indoor air and structures. Central heating systems are more commonly used in mild and cold climates as they provide better indoor thermal comfort conditions and have higher overall energy efficiency of the heating. In this case, heat transfer fluid, a distribution system, and end heat exchangers in heated space are needed in addition to the heat generator. In Chap. 6, local and central heat generators are presented. The current chapter presents the design of components and the assessment of the energy efficiency of central space heating systems.

8.1 Heat Load of the Building

Heat load of the building is the starting point for the determination of the designed thermal power of a heat generator at full load operation. Heat load is determined at constant design indoor and outdoor air temperatures by the transmission and ventilation heat losses of the building. If spaces are intermittently heated, additional heating-up thermal power is needed. Heating-up power depends on (i) the designed

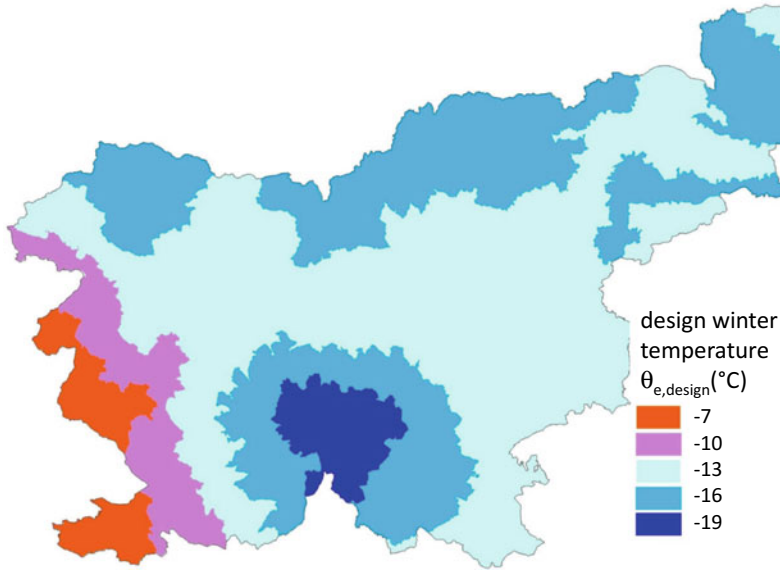


Fig. 8.1 Design winter temperatures $\theta_{e,design}$ for regions in Slovenia; because the average temperature of minimum outdoor temperature for several consecutive days is used for determination of $\theta_{e,design}$, values are in higher than the lowest actual accrued outdoor air temperatures (www.arso.si)

indoor air temperature drop (to large temperature drop increase risk of inner surface water vapour condensation and possible decrease of indoor thermal comfort), (ii) thermal accumulation of building (buildings with low thermal storage capacity are built from lightweight structures or have suspended ceilings; meanwhile, buildings with high thermal storage capacity have solid structures made of brick, concrete, or thick solid wood), (iii) design heating-up time.

Design winter outdoor air temperatures ($\theta_{e,design}$) are provided by the national climate office for the building's site location. It is common that several climate regions are defined on the national level. Design indoor air temperature ($\theta_{i,design}$) is determined according to the purpose of the building and indoor thermal comfort requirements. In very high spaces (>4 m), an air temperature gradient according to the type of heat emitters should be used for the correction of design indoor air temperature. Different methods for the determination of the design heat load of space heating can be used at different stages of building design (Fig. 8.1) (Davies 2004).

8.1.1 Rule of Thumb

For pre-design and simple feasibility studies, the rule of thumb for specific heat load in W per m² of heated area of the building with moderate internal heat gains (e.g. residential, office, schools, etc.) can be assumed as:

- 100–150 W/m² for old, non-thermal insulated buildings with non-tight windows;
- 80–100 W/m² for older buildings with some thermal insulation, well-maintained double glass windows;
- 35 W/m² for low energy buildings, buildings that fulfil contemporary criteria of energy efficiency of buildings;
- 10 W/m² for passive buildings, as defined by the PHPP Institute.

8.1.2 Steady State Heat Load

Steady state heat load calculation is commonly used in engineering practice. Heat load is determined at constant design conditions; therefore, no dynamic heat transfer processes, because of heat accumulation in building structures changing the internal heat gains during the day or week or intermittently heating are taken into account. Heat load is calculated starting with the determination of the transmission heat transfer coefficient (H_T) and ventilation heat transfer coefficient (H_V), as presented in Chap. 3. Coefficient H_T indicates heat flux (expressed in W) that is transmitted through the envelopment of the building at 1 K temperature difference between indoor and outdoor air and coefficient H_V indicates the heat flux needed to heat up infiltration and ventilation air per 1 K. Coefficients H_T and H_V are defined by equations:

weighting factor: $b < 0$ for constructions towards unheated close space, $b > 0$ for constructions with floor heating

$$H_T = \sum_{i=1}^n b_i \cdot U_i \cdot A_i + \sum_{j=1}^m \psi_j \cdot l_j + \sum_{k=1}^l \chi_k \cdot n_k \quad (W/K)$$

total number of envelope elements \downarrow n

thermal transmittance of i -th building envelope (W/m²K) \uparrow U_i

area of i -th building envelope (m²) \uparrow A_i

length of j -th thermal bridge (m) \downarrow l_j

linear (2D) thermal transmittance of j -th thermal bridge (W/mK) \uparrow ψ_j

point (3D) thermal transmittance of k -th thermal bridge (W/K) \downarrow χ_k

number of point (3D) thermal bridges in building envelope \uparrow n_k

air density and specific heat could be
replace by constant 0.34 (Wh/m³K)

$$H_V \cong b \cdot \underbrace{[\rho_a \cdot c_{p,a}]}_{\text{constant } 0.34} \cdot (\eta_{inf} \cdot V + (1 - \eta_{rec}) \cdot \dot{q}_{vent}) \quad (\text{W/K})$$

net building volume (m³)
ventilation rate (m³/h)

adjustment factor equal to 1 unless if
ventilation air is taken from unheated
space or through earth pipe heat
exchanger; in such cases $b < 1$ (-)
 infiltration air exchange
rate, approximate value
 $n_{50}/10$ to $n_{50}/20$ could be
assumed (h⁻¹)
efficiency of heat
recovery unit, 0.75
to 0.95 for BAT (-)

Additional heating-up thermal power (H'_{h-u}) is required in the case of intermittent space heating to achieve the required indoor set-point temperature after temperature setback within a given time. It is recommended that set-back temperature should not be more than 2 K (below set-point indoor air temperature) for night setback and not more than 4 K for weekend setback. To avoid oversizing the heat generator, heat-up time should be at least 1 h in the case of night-time and at least 3 h in the case of weekend setback.

Note 1: Additional specific heating-up thermal power expressed in W per m² of heated area as proposed in EN 12831-1¹ is 18 W/m² for lightweight and 21 W/m² for heavyweight buildings (night time set-back temperature drop 2 K, heating-up time: 1 h) and 14 W/m² for lightweight and 29 W/m² for heavyweight buildings for weekend setback (temperature drop 4 K, heating-up time: 3 h).

Note 2: It is common that low energy and passive residential buildings are heated at a constant temperature during the occupied days because of low heat losses and, consequently, only a slight decrease in air temperature during night-time intermittent space heating.

Heat load of the building is sum of transmission and ventilation heat losses and heating-up power:

$$\dot{Q}_{h,design} = (H_T + H_V) \cdot (\theta_{i,design} - \theta_{e,design}) + H'_{h-u} \cdot A_u \quad (\text{W})$$

transmission heat transfer
coefficient (W/K)
ventilation heat transfer
coefficient (W/K)
design outdoor temperature in
heating period (°C)

design heat load
of building
design indoor
temperature in
heating period (°C)
specific heat-up
thermal power (W/m²)
conditioned
(useful) area of
building (m²)

¹EN 12831-1:2017 Energy performance of buildings—Method for calculation of the design heat load—Part 1: Space heating load, Module M3-3.

Design thermal power of heat generator ($\dot{Q}_{h,design,g}$) must be provide sufficient heat load of the building and all unrecoverable heat losses of heat generator itself, the distribution system, heat storage and imperfect controlling of the space heating system, which results in occasional increases of indoor air temperature above the set point and vertical temperature gradient in the heated rooms.

Note 3: In the initial design phase, the approximate design thermal power of the heat generator used for the design of boiler room or a prefeasibility study can be approximated by the term:

$$\dot{Q}_{h,design,g} \approx 1.3 \cdot \dot{Q}_{h,design} \text{ (W)}$$

design thermal power of heat generator for space heating
approximation factor that includes all unrecoverable heat losses and heat-up power (-)

Case Study Determine the heat load of the Virtual Lab building, which has a heated area (A_u) of 27.7 m² to constant indoor air temperature $\theta_{i,design}$ 20 °C and is ventilated with a mechanical ventilation system with a heat recovery temperature efficiency of 90% (see Sect. 11.2.3). Thermal transmittance U and areas A of opaque and transparent building envelope structures are listed in the tables. The air tightness of the building expressed as n_{50} is equal to 0.6 h⁻¹. No heat bridges are taken into account (Fig. 8.2).

Transmission heat transfer coefficient H_T is 21.9 W/K and ventilation heat transfer coefficient H_V is 1.7 W/K (as result of high efficiency heat recovery of mechanical ventilation system). Winter design outdoor temperatures $\theta_{e,design}$ for the site is -13 °C. The heat load of the Virtual Lab building is:

$$\dot{Q}_{h,design} = (H_T + H_V) \cdot (\theta_{i,design} - \theta_{e,design}) = (21.9 + 1.7) \cdot (20 - (-13)) = 1012 \text{ W}$$

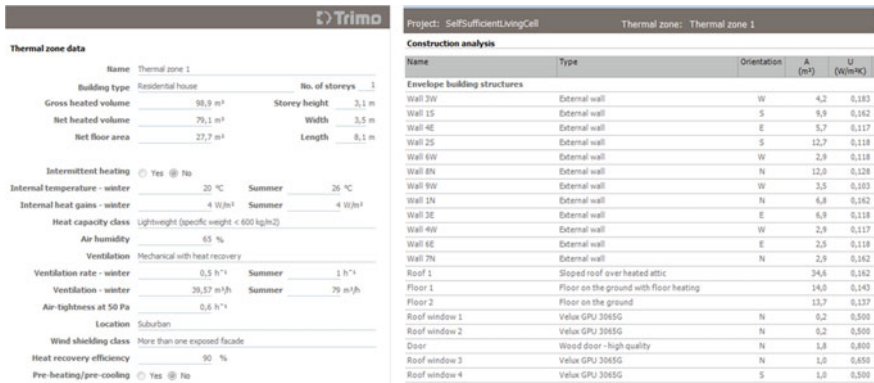


Fig. 8.2 Description of Living Unit of Virtual Lab building (left), list of envelope elements of the Living Unit; complete description of the Virtual Lab building can be fined in TRIMO Expert computer tool under Project Virtual Lab

8.1.3 Heat Load Determination by Dynamic Simulations

In this case, the heat load of the building is determined by dynamic heat transfer simulations in short time steps. Schedules for the building's use and the operation of building service systems can be analysed together with unsteady heat transfer in building structures. Hourly meteorological data is needed as are computer tools that simulate transient heat transfer in building implementing numerical methods. Heat flux at the inner surface of the building envelope elements depends on thermal mass in contact with indoor air, by the surface-absorbed short-wavelength (solar) radiation and long-wavelength (IR) radiation exchange with other surfaces in the enclosure (a building in the case of a one-zone model or rooms in the case of multi-zone model). Because analytical solutions are not possible for real cases, several numerical methods have been developed for the determination of the dynamic thermal response of the building as the result of time dependent outdoor climate conditions and indoor heat sources or sinks:

- The simplified dynamic method; regressive models are developed from steady-state models by repeating the calculation for the expected range of steady-state boundary conditions; for approximation, time series in the form of a Fourier series is favoured (Černe and Medved 2005);
- electricity analogue method; the building structure is divided into an adequate number of layers, called nodes; on each surface of a node, the temperature is set, and it is constant along this surface; between nodes, heat conduction is described by resistance R , and heat accumulation by material capacity C ; an energy balance equation is developed for each temperature node, and a set of algebraic equations are solved using a numerical method; such a method is proposed in EN ISO 52016-1 for hour-by-hour calculation of yearly energy needs for heating (Q_{NH}) and cooling (Q_{NC}) of the building (Fig. 8.3);

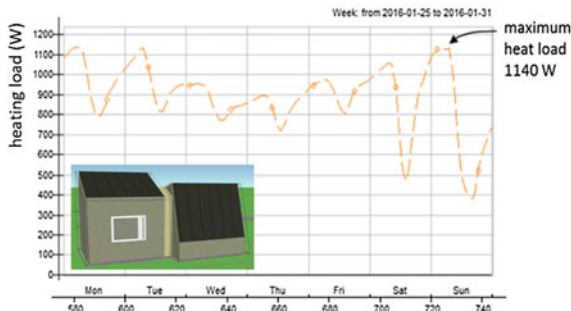


Fig. 8.3 Heat load of the Virtual Lab building calculated by dynamic hour-by-hour simulation with time step 0.25 h (IDA-ICE)

- response factor method; transient heat transfer is determined by differential equation and solved by numerical methods for the simplified time variation of boundary conditions (e.g. step, sinusoidal, exponent) or by analogy between electrical and thermal quantities by developing a so-called resistance-capacity model; the inner surface temperature and heat flux on the surface at time t are determined by the transfer coefficient, temperature, and heat flux in previous time steps ($t-1$, $t-2$); transfer coefficients are calculated for individual structures according to the material properties and thickness of the layers in advance;
- energy balance solved by CFD technique; temperatures in small parts of building structures are determined by coupling temperature, velocity, pressure fields and turbulence heat generation in the form of Navier-Stokes equations and solved with numerical methods: finite difference, finite volume or finite element method; such an approach is time consuming but no empirical expressions are needed for defining boundary conditions because the solution is based only on physical phenomena. This means that, for example, inner and outer surface convection and radiation heat transfer coefficient and infiltration air inflow are the result of numerical simulation, not required inputs.

Case Study Dynamic response of the building with a double sliding door determined by computational fluid dynamic (CFD) techniques. In Fig. 8.4, the air temperature 0.15 m above the floor in a shopping centre is shown.

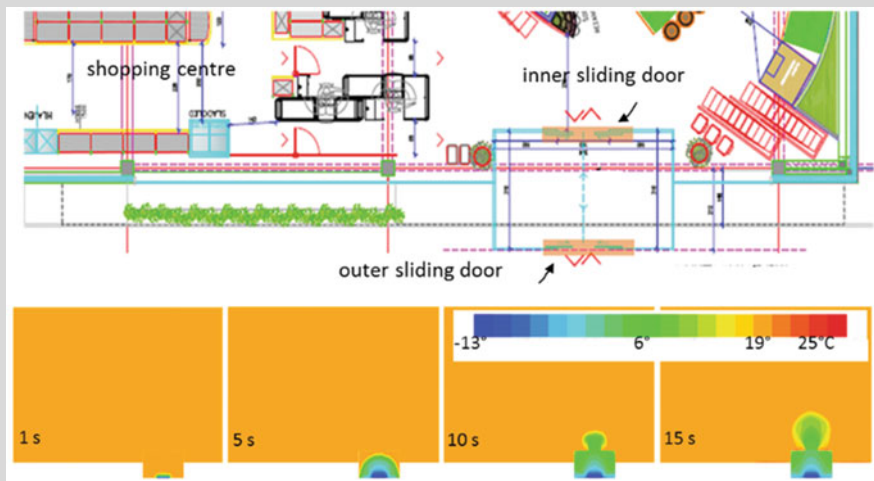


Fig. 8.4 Floor plan of entrance in shopping centre (top), air temperatures 0.15 m above the floor 1, 5, 10, and 15 s after the door is opened; calculated with PHOENICS CFD (PHOENICS, Concentration, Heat and Momentum Limited (CHAM), UK) software with the finite volume method (bottom)

8.2 Central Space Heating Systems

Central space heating systems are most often divided according to the type of heat transfer fluid. Heat transfer fluid can be water (in hydronic systems), air or (not commonly used any more) steam (Daniels and Hammann 2009).

8.2.1 *Comparative Advantages and Disadvantages of Hydronic and Hot Air Space Heating Systems*

Hydronic systems have an advantage over hot air space heating systems in higher specific thermal power per square metre of heated floor area, better indoor thermal comfort (because of higher operative temperature and low air velocity and low noise emission), utilization of low temperature (low energy) heat sources (e.g. geothermal water or solar heating), smaller distribution system, lower energy consumption for heat transfer fluid circulation, and more efficient temperature control in each of the heated spaces due to room thermostats. Water heating systems can also be upgraded simply into domestic water heating systems. Although hydronic systems have high thermal inertia and therefore they respond more slowly to rapid changes in heat demand (due to internal and solar gains), they are costlier and water can freeze in the distribution system in the case of failure or longer non-heating periods.

The most evident advantages of the air space heating systems is that such systems can be upgraded to central ventilation and air cooling systems. Hot air heating systems react more rapidly to rapid changes in heating demand, especially in low thermal inertia buildings. Nevertheless, the high air velocities caused by inlet flume of hot air and lower room radiant temperature can decrease comfort because of noise emissions and lower thermal comfort. An additional system for domestic hot water heating must be installed. In continental and central Europe climate regions, air space heating systems are rare because of the low specific thermal power (expressed in W per unit of flow rate e.g. m^3/s) and only in high energy efficient buildings with low heat load, is the air flow rate for space heating comparable to ventilation flow rate, and there is no need for significant enlarging the ventilation system.

8.2.1.1 **Relation Between Flow Rate and Temperature of Heat Transfer Fluid**

Either water or air is used as the heat transfer fluid, and the heat flux transferred at design conditions must be equal to the design heat load of space heating of the building. The transferred heat flux is proportional to transfer fluid mass flow rate,

and the differences in temperatures of the heat transfer fluid on the supply and return sites, and its thermodynamic properties:

$$\dot{Q}_{h,design} = \dot{m}_{f,design} \cdot c_{p,f} \cdot (\theta_{f,sup} - \theta_{f,ret}) = \dot{V}_{f,design} \cdot \rho_f \cdot c_{p,f} \cdot (\Delta\theta_{f,h}) \quad (W)$$

design mass flow rate of heat transfer fluid (kg/s)
temperature of heat transfer fluid on the supply (°C)
temperature of heat transfer fluid on the return (°C)
design temperature difference of heat transfer fluid for space heating (°C)

design heat load of building
specific heat (at constant pressure) of heat transfer fluid (J/kgK)
design volume flow rate of heat transfer fluid (m³/s)
density of heat transfer fluid (kg/m³)

In the case of hydronic systems design, temperature difference $\Delta\theta_{f,h}$ is defined as difference between the design supply and the return temperature of heating water measured at the inlet and outlet of the heat emitters built-in in heated spaces. In fact, the design of a space heating system begins with a choice of supply and return temperature of heating water. In high temperature systems, $\theta_{f,sup}$ is by definition 90 °C and return temperature $\theta_{f,ret}$ is 70 °C (which is indicated by 90/70), down to 75/65. In moderate temperature systems $\theta_{f,sup}$ is 55 °C and return temperature $\theta_{f,ret}$ is 45 °C (55/45), down to 50/40. In low temperature systems, $\theta_{f,sup}$ is 35 °C and return temperature $\theta_{f,ret}$ is 30 °C, down to 30/25.

Note: Due to high thermal losses in high temperature space heating systems, the maximum design temperature of heating water $\theta_{f,sup}$ 75 °C in new systems is recommended and even prescribed in some national regulations. The choice of design temperature of heating water depends on the design heat load and type of heat generator. Specific heat loads of the building 60 W/m² (per m² of heated area) require high temperatures of the supply heating water; meanwhile, the specific heat loads of a building below 25 W/m² can be covered by a low temperature space heating system. Heat pumps and solar thermal heating systems require lower temperatures of heat transfer fluid to maintain high operational efficiency.

In the case of air heating systems, the design temperature difference $\Delta\theta_{f,h}$ is defined as the difference between the temperature of supply air that enters the heated space and the air temperature in a heated space (which is also the return temperature of air). In residential buildings, the temperature of supply air $\theta_{f,sup}$ should not exceed 35–40 °C to prevent thermal discomfort and high air temperature gradient of the indoor air.

Case Study The design heat load of the Virtual Lab building is 1012 W. What will be the design volume flow rate of heat transfer fluid in hydronic

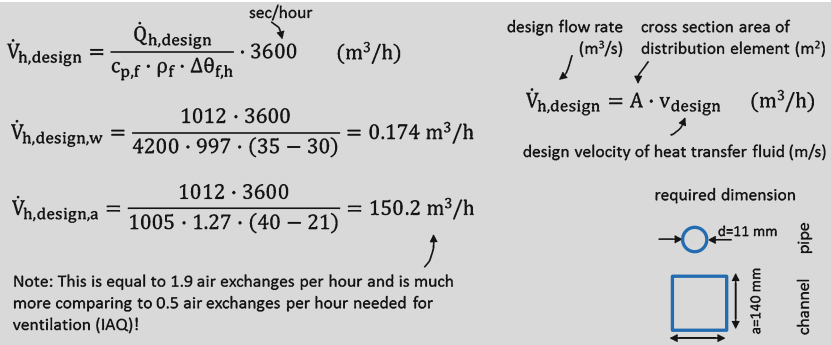


Fig. 8.5 Required dimensions of distribution pipe and channel for the case study

(type 35/30) and hot air heating systems (design supply temperature 40 °C). The specific heat of water $c_{p,f}$ is 4200 and air 1005 J/kgK. Density of water ρ_f is 997 and air 1.27 kg/m³. The design indoor air temperature θ_i is 21 °C. The net volume of the building is 79.1 m³.

To ensure low pressure drop and noise emission, the design velocity of water in distribution pipes should be 0.3–0.8 m/s (common 0.5 m/s) and the velocity of the air in distribution ducts 2–5 m/s (common in residential buildings 2 m/s). Using a continuity equation, the cross section of distribution elements can be determined (Fig. 8.5):

$$A_w = \frac{\dot{V}_{h,design}}{3600 \cdot v_{design}} = \frac{0.179}{3600 \cdot 0.5} = 9.7 \cdot 10^{-5} \text{ m}^2 \quad A_a = \frac{\dot{V}_{h,design}}{3600 \cdot v_{design}} = \frac{150.2}{3600 \cdot 2} = 2.1 \cdot 10^{-2} \text{ m}^2$$

Note 1: For transferring the equivalent heat flux, an 880 times greater volume flow rate is needed in the case of air space heating systems in comparison to hydronic heating. For the distribution of the hot air, a fan is used. The energy efficiency of the fan is classified as the Specific Power of Fan (SPF), which states the electrical power of the fan per 1 m³/s of volume flow rate generated. A minimum value SPF 3 is required in Slovenian legislation, which means that SPF must not be more than 1250 W/(m³/s). The adequate maximum specific power of pumps in a hydronic system is limited to 15 W per 1 kW of transferred heat flux. In the presented case study, this means that maximum fan power must not exceed 52 W, and the maximum pump power must be below 15 W.

8.2.2 Sub-systems of Space Heating System

Regardless of the type of heat transfer fluid, central space heating systems consist of several sub-systems:

- heat generator(s), which can be, for example, a combustion boiler, solar collectors, heat pump or heat exchanger of a district heating system. In a heat generator, the heat transfer fluid is heated by transforming the internal energy of an energy carrier into heat; the auxiliary energy (electricity) is needed for operation of a burner, a flue gas fan, or the motor of a feed-in transport device in the case of solid fuels;
- heat distribution system in the form of pipes in a hydronic system or channels if hot air is used as the heat transfer medium; auxiliary energy (electricity) is needed for the operation of the pump or fan;
- heat storage may be built-in between the heat generator and the distribution system; heat storage is mainly used in hydronic systems.
- heat emitters; in hydronic systems, heat emitters are heat exchangers that transfer heat from the transfer fluid to the room by convective and radiant heat flux; in the case of air space heating systems, inlet diffusers and outlet grills in each room must be built into enable the circulation of the hot air; auxiliary energy (electricity) is needed for the operation of the fan in the case of fan-coil heat exchangers.
- control unit consisting of appliance control units (sensors and actuators in heat generator, valves, pumps or fans and emitters) and a central control unit that controls the temperature and/or flow rate of heat transfer media with a control protocol that includes a control loop (Figs. 8.6 and 8.7).

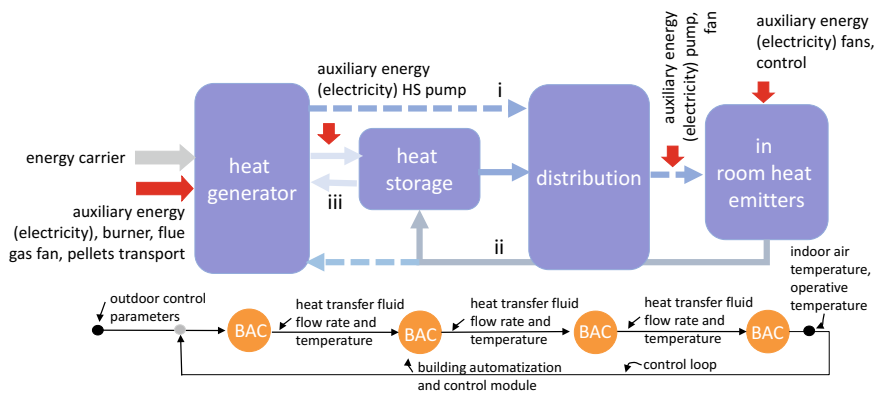


Fig. 8.6 Scheme of sub-systems in a hydronic space heating system; energy flows and operation modes are shown

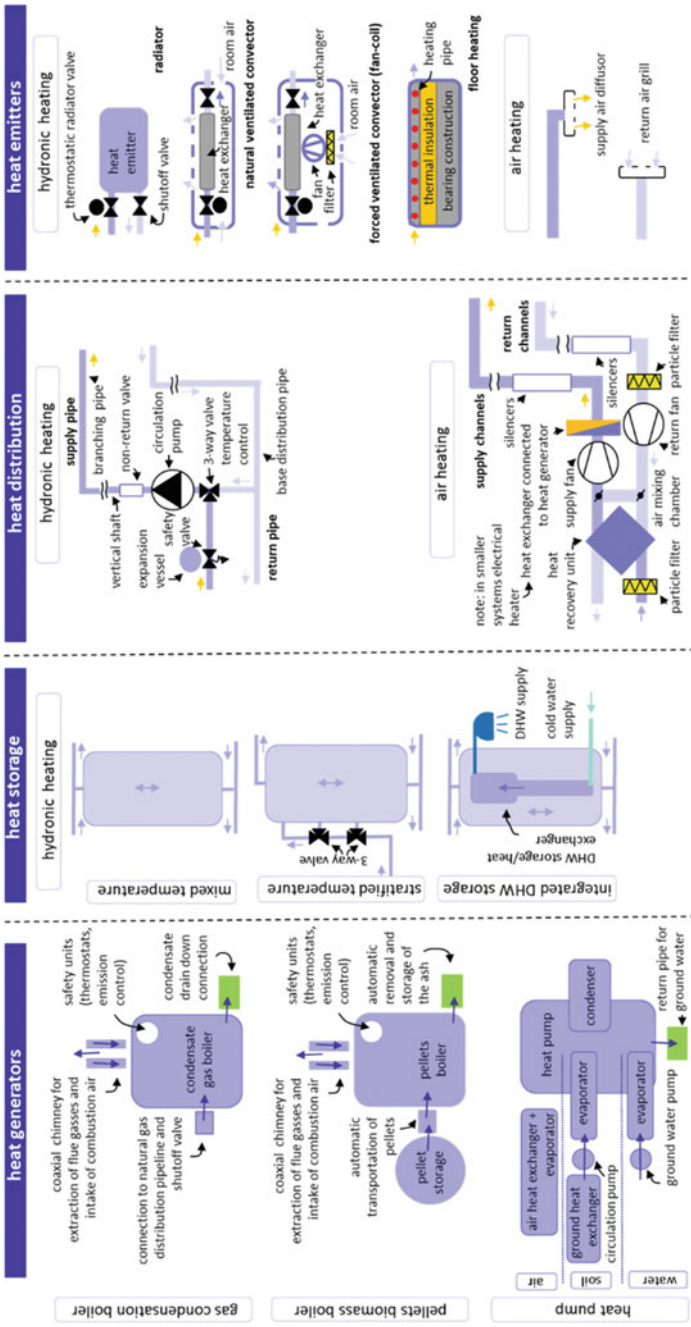


Fig. 8.7 Most common basic elements of space heating sub-systems

8.2.3 Basic Elements of Space Heating System

As heat generators are presented in the Chap. 6, other basic elements of space heating systems are presented below.

8.3 Heat Storage

Heat storage may be installed between a heat generator and the distribution system. Heat storage is mainly used in hydronic systems. The main advantages of the integration of the heat storage in the space heating systems are:

- the design thermal power of heat generator $\dot{Q}_{h,design,g}$ can be lower because heat can be stored during the low-heat demand day-time period or non-occupied hours and used later during high demand periods or if boosted heating is needed;
- heat generator efficiency is higher because it operates at constant design thermal power and excess heat is stored for later use and not wasted by flue gasses because of less efficient combustion processes (for example, when log wood is used as fuel);
- harmonizing the production and consumption of heat if unsteady energy sources are used for the production of heat (e.g. solar radiation);
- a heat generator can operate during the period of a cheaper energy carrier (e.g. during the night time if an electricity-driven heat pump is used as a heat generator) and store the heat to be used in the period of expensive energy (e.g. during the night time if an electricity-driven heat pump is used as heat generator).

Heat can be stored in a form of sensible or latent heat or within exothermic reversible chemical processes. While density, specific heat, and conductivity are the most important properties of materials for storing of sensible heat, which is done by increasing the temperature of the accumulation mass, the heat of fusion (for melting/solidification) is utilized for storing latent heat in so-called phase change materials' (PCM) latent heat. This type of heat storage is still in the pilot phase. The high cost and durability regarding the number of phase change processes without influence on the storage capacity of the heat-storing material are most indicative properties of latent heat storage. Because of the excellent thermal properties for storing sensible heat without any environment impacts and at low cost, water is most commonly used in heating systems as a heat storage medium. Water storage is commonly used if wood log biomass boilers, solar collectors, or heat pumps are chosen as heat generators, while in large solar systems so-called pit heat storage, construction pits filled with stones and water, can be used (Fig. 8.8).

The quality of heat storage is not only measured by the quantity of stored heat, but by heat losses and even more importantly, by the amount of available energy. Energy produced by a heat generator can be maintained in temperature-stratified heat storage. This means that heat is stored in heat storage at different temperatures,

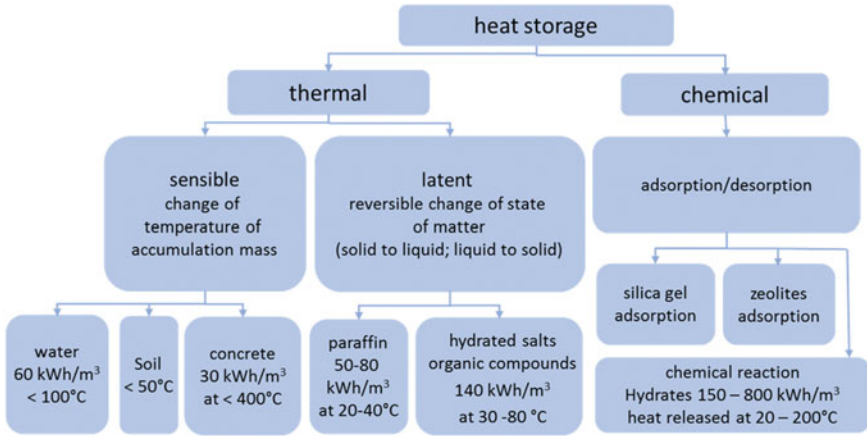


Fig. 8.8 Types of heat storage according to the process of accumulation and heat release (SOLARGE 2004)

while the entire volume of the water in mixed heat storage is heated to the approximate constant temperature leading to energy losses (Figs. 8.9 and 8.10).

The second common classification of heat storage is made according to the duration of heat accumulation. Heat storage for space heating systems can be:

- short term; such heat storage is a thermal insulated steel tank with one or two integrated heat exchangers. Two heat exchangers are common for solar heat storage, such systems that need backup heating with an additional heat generator. For backup heating in smaller systems, an electrical resistant heater can be inserted instead of a tube-type heat exchanger. They are mainly use for domestic hot water heating (DHW) (see Chap. 9).

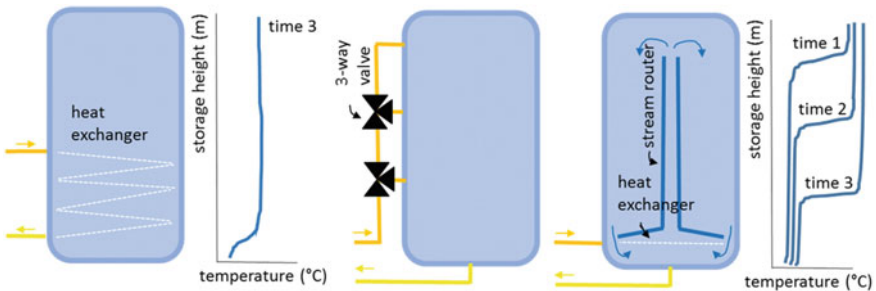


Fig. 8.9 Mixed (left) and stratified heat storage (right) for solar heating systems; temperature stratification is achieved by controlling 3-way valves (middle) or by directional buoyancy flow of heated fluid in heat storage (top) (SOLARGE 2004)

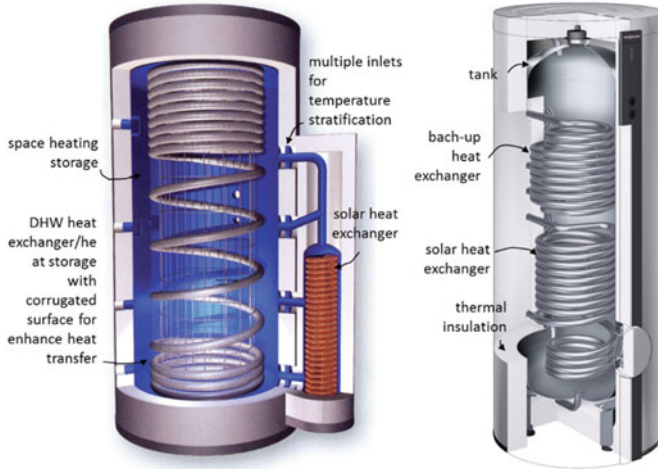


Fig. 8.10 Example of stratified heat storage with integrated domestic hot water heat exchanger, external heat exchanger connected to the heat generator, and multiple water inlets (TiSUN PC PRO-CLEAN, www.tisun.com) (left); Mid-term heat storage for solar assisted heating and DHW heating (www.viessmann.com) (right)

Note: The volume of heat storage in solar DHW systems in single family buildings should be between 50 and 100 L per m² of the installed area of solar collectors. If heat storage is connected to the log wood boiler to increase heat generator efficiency during the partial load operation periods, a volume of 50–80 L per 1 kW of thermal power of boiler is required.

- mid-term heat storage systems are larger and connected to the space heating system. Often a heat exchanger for DHW heating is built in. Heat storage can be connected with a heat generator as an open system (directly) or via a heat exchanger. Temperature stratification is an important property because of low solar irradiation during winter months and high required temperature of heating water.

Note: The volume of heat storage in solar assisted space heating systems should be between 100 and 200 L per m² of the installed area of solar collectors (Fig. 8.10).

- long term or seasonal heat storage enables the accumulation of the heat during the summer and the discharge of that heat after several months during the next heating period. In most cases, such storage is used for the solar-assisted district heating

Seasonal water storage in form of concrete underground tank with volume 1.5 to 2.5 m³ per m² of solar collector area.



Construction pit with layers of dug horizontal closed loop heat exchange pipes. Storage is consist of body of stones in fist size stones fist, filled by the water. Pipes are connected with solar collectors, meanwhile water in the storage is used for heat transfer and heat storage. Size of pit heat storage should be between 2.5 to 4 m³ per m² of solar collector area.

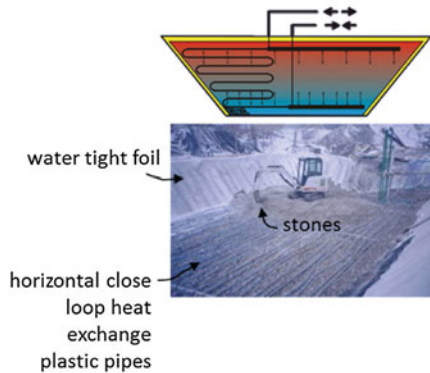


Fig. 8.11 Examples of long-term water (left) and pit-type seasonal heat storage (right) (SDHplus 2015)

systems. Two technologies are commonly used for large-scale systems: (i) a water type made in the form of large concrete wall cavities filled with water and (ii) pit type heat storage, which are cavities filled with water and fist-sized stones (Fig. 8.11);

8.4 Distribution Systems

A distribution system is grid of pipes or channels for the distribution of heat transfer fluid between heat generator(s), heat storage(s), and room heat emitters. It must be designed so that: (i) the cost of the distribution system is optimized, (ii) the cost of auxiliary energy for the transfer of heat and maintenance costs are as low as possible, (iii) heat losses from the pipes or channels are as low as possible, and (iv) the flow of the heat transfer fluid does not cause emissions of noise or other disturbing effects on living comfort. In this sub-chapter, cost issues will be analysed through the use of auxiliary energy for the operation of pump(s) or fan(s) needed for providing adequate flow rates of the heat transfer fluid.

8.4.1 Hydronic Systems

The distribution system in hydronic heating systems is designed as a grid of pipes with fittings and made of steel, or nowadays usually of copper or plastic. Such pipes can be installed quickly and have smooth surfaces with lower friction coefficients. Pumps and devices for safe operation (expansion tank, safety valves or air separators) and control devices (sensors and actuators) are also part of the distribution system.

Each pipework is divided into the sections shown in Fig. 8.12. Regarding the position, base distribution pipes can be installed below vertical shafts as a low level

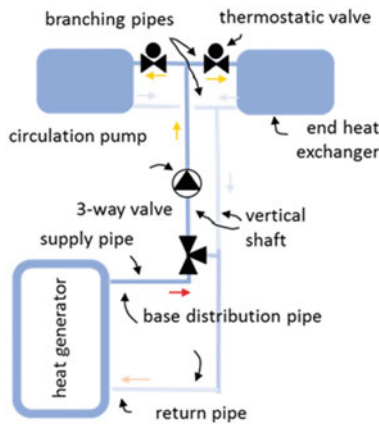


Fig. 8.12 Pipelines in hydronic space heating systems are divided into base distribution, shaft, and branching sections

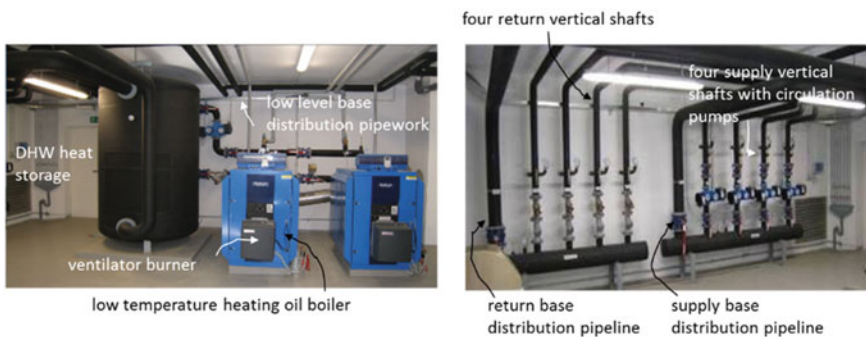


Fig. 8.13 Base distribution pipework and vertical shafts in the boiler room of office and residential building; four separated shafts enable zoning and split heating systems in south-, north- and west-orientated office thermal zones and a heating system in residential building

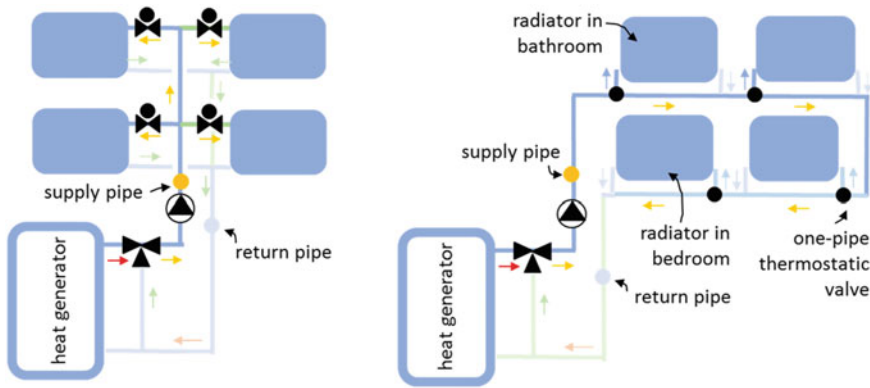


Fig. 8.14 Two-pipe distribution (left), one-pipe distribution network circulation (right) in hydronic space heating systems

supply and return pipeline (e.g. in non-heating basement) or above the vertical shafts as a high level supply and return base distribution pipeline (e.g. above the ceiling of the highest floor in the building). Several vertical shafts can be installed to enable zone heating. Heat emitters in the rooms are connected to vertical shafts by branching pipes. Heat emitters can be connected as one-pipe or two-pipe circuit types (Fig. 8.13).

In the case of a two-pipe network, water enters each heat emitters at the same temperature, while water flow splits before the heat emitter inlet and only part of the water flows through radiator in the case of a one-pipe circuit. Flows merge again at the outlet of each emitter. This means that heating water is cooler at the inlet into each of the following emitters; therefore, heat flux emitted from equal-sized emitters is lower step by step. This must be compensated by increasing the size of emitters or placing them according to required air room temperature (e.g. the first emitter in the bathroom, the last one in a bedroom). One-pipe systems were introduced because they enable easier-to-install heat counters and measure the actual heat demand in each of the flats in multifamily buildings because only one pipe enters and exits the flat. The system is limited to the connection of up to ~ 5 emitters and, because in practice there were no significant cost decrease, the one-pipe branching pipe network is not used commonly nowadays and two-pipe circuit distribution systems prevail (Fig. 8.14).

Some guidelines on how to design distribution networks in hydronic space heating systems can be found in Sect. 8.2.1.1 (Hausladen 2005).

Distribution systems and pump(s) are designed for the design heat load of the building. The pump converts electricity into the potential and kinetic energy of the working fluid. Potential energy is expressed in total pressure head and measured in meters of water column; kinetic energy is expressed as flow rate and measured as capacity in kg/s or kg/h. The operation curve of pump shows a relationship between this two quantities as presented in Fig. 8.15. During the real time operation, heat flux that must be transferred by water is changing due to the changing of ambient temperature, solar irradiation, or internal heat sources. To balance the heat flow to actual needs, either temperature or flow rate control or bought can be used. Within temperature control, the supply water temperature is adapted by changing the set-point temperature in the heat generator or by mixing it with return water by a

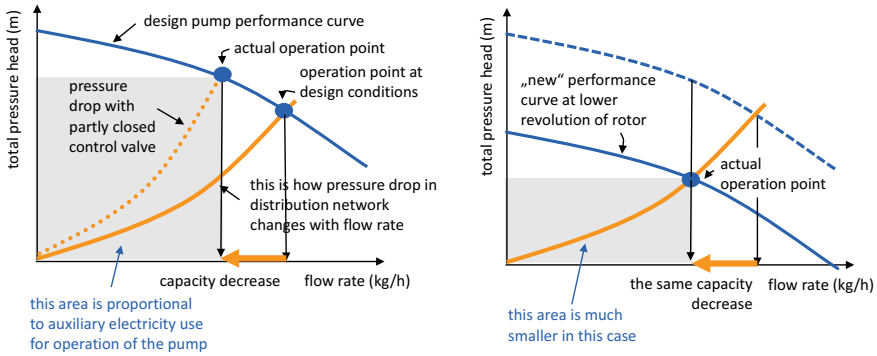


Fig. 8.15 Two-pipe distribution (left), one-pipe distribution network circulation (right) in hydronic space heating system

3-way valve. In the case of flow rate control, the flow rate of water is changed according to control parameters (outdoor temperature, indoor temperature, schedule of building use, etc.). The simplest way to do so is to adapt the flow rate by manual, motor-driven, or thermostatic valves. Pressure drop in the pipe network increases and, as a result, the flow rate also decreases. Unfortunately, the energy consumption of electricity for the operation of pump(s) will be unchanged. It is much more efficient if flow rate is decreased by lowering the number of the rotor’s revolution with a frequency-controlled electric motor. For that, a device that adjusts the frequency of the electricity current below the normal 50 Hz is needed. In this way, the motor efficiency will remain almost the same (pump efficiency is ~85%) if the capacity is decreased to 40% of the design value (at 30 Hz). If the frequency is lowered further to 20 Hz, the pump at 20% of design capacity will still have efficiency of around 75% (Fig. 8.16) (McQuiston et al. 2005).



Fig. 8.16 Old pumps that operate with constant speed (left) and modern variable speed pump with frequency control device (right)

Note: The electrical power of the pump is designed according to required total pressure head and capacity. The required total pressure head is determined by friction loss due the flow of the water, which is proportional to the length of pipeline sections, the roughness of pipe material, and the velocity of water in the pipeline. The friction losses of various valves and fittings are added to the total pressure head expressed in meters of water column. The required flow rate is defined by the heat load of the building and the design temperatures of heating water.

In some national regulations, the electrical power of a pump is limited because energy conservation. For example, in Slovenia, it is limited to 15 W per 1 kW of transferred heat flux.

8.5 End Heat Exchangers/Heat Emitters

End heat exchangers or heat emitters transfer heat flux from the heat transfer fluid to the indoor air. Heat emitters can be in the form of plate radiators, convectors, heated floors, ceilings or walls, or thermally activated building structures.

8.5.1 Radiators

Radiators are made from metals (steel or aluminium) and emit heat flux by radiation and convection (approx. with a 50:50 ratio). In the past, radiators were installed under windows to prevent the surface condensation of water vapour in the glass, to reduce the flow of downwards cold air below the window (because of cold glass and not tight windows) and to improve the mean radiant temperature. Nowadays such a position of is no longer necessary because of advanced windows' thermal properties, and radiators can be installed inner walls. In non-residential buildings, radiation panels can be installed below the ceiling. In this way, heat is transferred mainly by radiation directly to the bodies of persons beneath. The emitted heat flux from a plate radiator is approximately 1000 W per 1 m² of surface radiator at design temperature $\theta_{f,sup}/\theta_{f,ret}$ 90/70, but it is reduced to 435 W (55/45) and to 152 W (35/30) (Fig. 8.17).

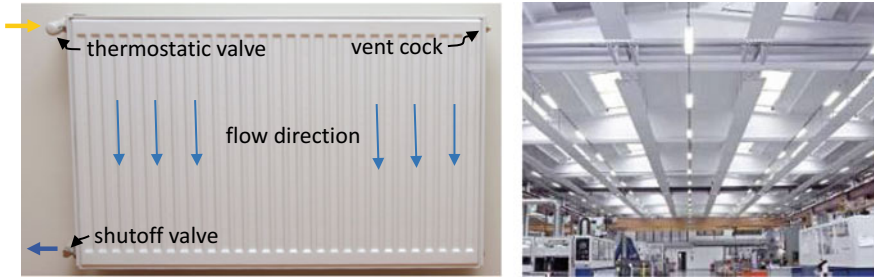


Fig. 8.17 Steel plate radiator with valves and fittings (left); ceiling radiant panels are used mainly in non-residential buildings (right)

Note 1: Emitted heat flux depends on temperature differences between temperature of supply $\theta_{f,sup}$ and return water $\theta_{f,ret}$ and is defined by equation:

$$\dot{Q} = \dot{Q}_{ref} \cdot \left(\frac{\Delta\theta}{\Delta\theta_{ref}} \right)^n$$

actual emitted heat flux (W) \dot{Q}
 reference emitted heat flux (W) \dot{Q}_{ref}
 reference temperature difference: $(\theta_{f,sup,design} + \theta_{f,ret,design})/2 - \theta_i$; $(90^\circ + 70^\circ)/2 - 20^\circ = 80^\circ\text{C}$
 reference temperature difference: $(\theta_{f,sup} + \theta_{f,ret})/2 - \theta_i$
 exponent of heat transfer: 1.2 for radiators, 1.1 for convectors, 1.0 for floor heating

Note 2: Radiators must be installed without blockage and connected to the distribution system in a way that enables counter-flow operation (Fig. 8.18).

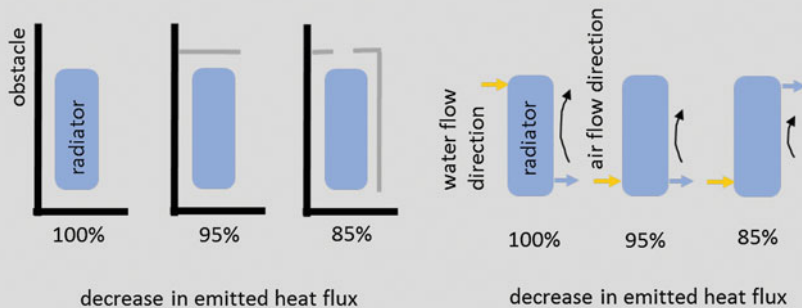


Fig. 8.18 Decrease of emitted heat flux from radiators installed by blockage (left); decrease of emitted heat flux at different flow directions of heat transfer fluid (right). Adopted from Kabele et al. (2012)

8.5.2 Convectors and Fan-Coils

Convectors have heat exchangers made from copper pipes and aluminium or copper coils. Heat flux is mainly (up to 4/5 of total emitted heat flux) transferred by natural or forced convection. Fan-coil convectors can be installed in the floor, be self-standing, or be installed below or integrated into the ceiling. The emitted heat flux of floor-type fan-coil convectors is up to 100 W per m length in the case of natural (gravitational) convection heat transfer and up to 500 W per m length in the case of forced convection heat transfer convectors caused by the built-in fan. Because of that, such emitters are called fan-coils. The heating power of fan-coils can be much higher, up to several kilowatts. While convectors based on natural convection are mainly used to compensate cold air streams from large facade glass surfaces, fan-coils are mainly used for space heating (and cooling) because of the large amount of thermal power that can be controlled by the multi-step operation of the fan (Figs. 8.19 and 8.20).



Fig. 8.19 Convectors installed into the floor below glass façade to compensate a cold air jet that descends from the glassing; draught is eliminated and thermal comfort is improved (left); (Bridge & PR Media Service Ltd.) forced convection fan-coil convector installed in a raised floor (right) (KI TDC d.o.o.)

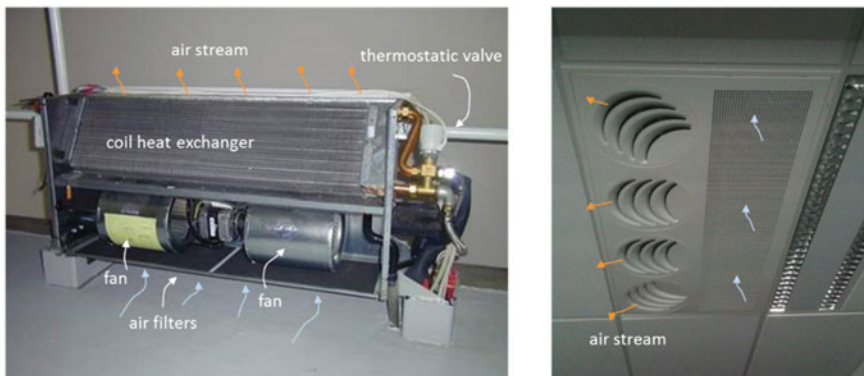


Fig. 8.20 Stand-alone fan-coil without assembly (left), fan-coil integrated in a suspended ceiling (right)

It is convenient that the same fan-coils are also used for the space cooling of the buildings. In this case, cold water cooled in a separate cold generator (with temperature 5–7 °C) enters the supply side of the fan-coil. Such fan-coils can be connected with heat and cold generators by 2- or 4-pipe distribution systems. While a 2-pipe distribution system enables only heating or cooling, and the transition between the operations is manually regulated, a 4-pipe distribution system enables the simultaneous heating of one zone(s) and the cooling of others if needed. This is often case in office and public buildings due to high solar heat gain in the rooms with south- or west-orientated glazing. In this case, the heat and cold generators must operate simultaneously. Because water vapour from the indoor air can condensate on the surface of a cold heat exchanger, an additional water drain down pipe is needed (Figs. 8.21 and 8.22).

Fan-coil convectors can be connected to the ventilation systems in such a way that fresh supply air flows into the room through a heat exchanger in a convector. Supply air must be conditioned (heated or cooled (to temperature ~20 °C throughout the year) and air pollutants should be removed in the air handling unit

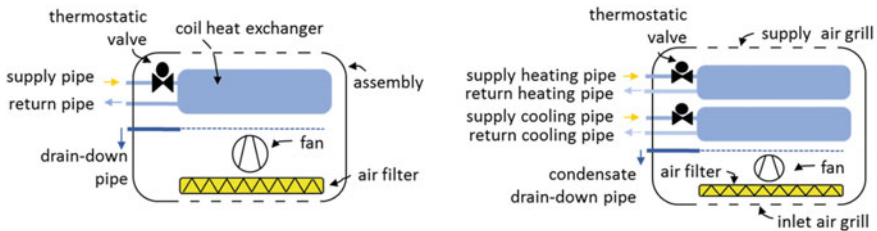


Fig. 8.21 Scheme of 2-pipe (left) and 4 pipe fan-coil (right)

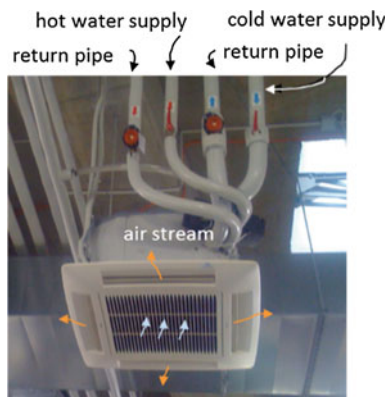


Fig. 8.22 Ceiling fan-coil convector for heating and cooling



Fig. 8.23 AHU on the roof of the office building (left); vertical channels for supply of ventilation air (right)

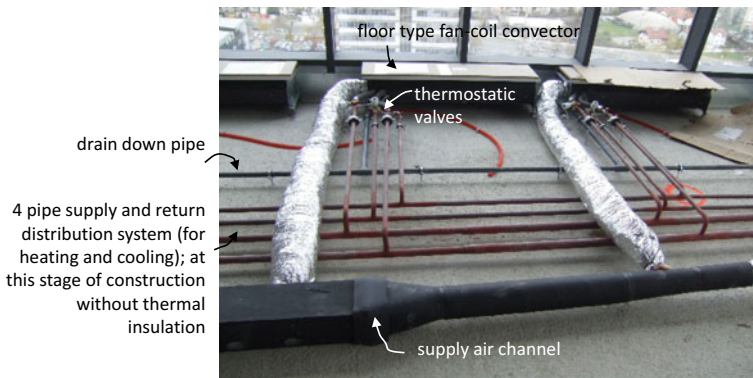


Fig. 8.24 Fan-coils for heating, cooling and ventilation in office building

(AHU) before entering the fan-coils. Because the air velocity in heat exchanger is greater, the transferred heat flux increases significantly (Figs. 8.23 and 8.24).

8.5.3 Active Beams

Instead of fan-coils, hydronic space heating/cooling and ventilation can be combined using active beam units, which are the end units of ventilations system where fresh ventilation air is supplied to the room. An active beam unit consist of a plenum where conditioned fresh air from the central AHU is supplied. Fresh air flows through a series of nozzles with high velocity and induces air from the room to flow upwards through coil heat exchanger, heat up, and mix with fresh air. In this manner, heat flux is transferred into the room completely by convection. Typically, the amount of airflow from the room is up to 4 times that of the supply air. Because

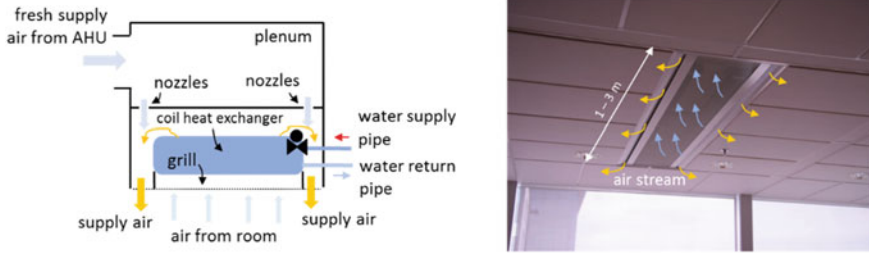


Fig. 8.25 Schematic of active beam (left), active beam installed in the ceiling of a conference room (right)

of that, a fan is not needed to enhance heat transfer from coil heat exchanger (Fig. 8.25) (Jayamaha 2007).

The flow rate of fresh supply air is designed according to IAQ requirements and not regarding space heating needs. As no fans are needed in active beam units, no auxiliary electricity is needed for the operation of active beams. Nevertheless, a ventilation system must be carefully designed to avoid increased pressure losses (and increased auxiliary electricity demand for fan operation) in comparison to air heating systems. The emitted heat flux depends on several influenced variables; heat flux of 100–150 W emitted per meter length of active beam can be used as a recommended design value.

Note: Active beams can be also be used for cooling. The temperature of the cooling water (usually in the range of 16–18 °C) is controlled in such a way that the temperature of the heat exchanger's surface is always above the dew point temperature to prevent the condensation of water vapour from the indoor air.

8.5.4 Floor and Ceiling Radiant Heat Emitters

Radiant heat emitters are parts of building structure with large surface areas that are heated to low temperatures (25 °C to maximum 35 °C). The surface temperature convective heat flux is low (<1/5 of total emitted heat flux) comparing radiation flux. Such heat emitters consist of grids (called loop or register) of pipes (with diameter 12–18 mm), which are embedded in a 6–8 cm thick layer of concrete (wet at time of build), which is deposited on the layer of thermal insulation to decrease heat losses and reduce the transmission of impact sound. In this way, wet-type floor radiant heating systems are built. Dry-type radiation emitters (floor and ceiling) are built from prefabricated thermal insulation plates (2–3 cm thick) with groves in which circulation pipes are inserted. To ensure the uniformity of the surface

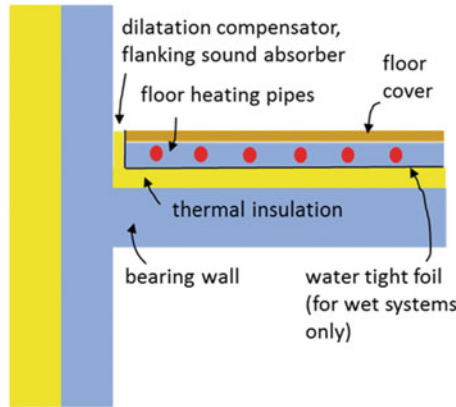


Fig. 8.26 Cross-section of structure with integrated floor heating pipe register

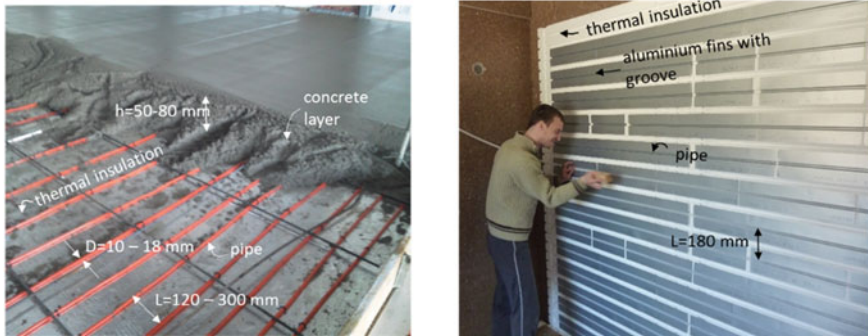


Fig. 8.27 Wet floor (left) (www.mikesheating.com) and dry wall type of radiant heat emitter (right)

temperature, aluminium fins can be used. Pipes can be inserted in the layer of plaster in the case of ceiling or wall-type radiant heat emitters (Figs. 8.26 and 8.27).

Floor radiant heat emitters emit radiant heat flux up to 50 W per m^2 of the surface area. Radiant heat emitters are divided in separate hydraulic loops or registers to enable controlling thermal comfort conditions in separate thermal zones (rooms). Usually, each register covers $20-30\text{ m}^2$ of heated room area. If several registers are installed in the room, registers are organized inside the room regarding heat losses (facade towards interior). Registers are connected with the heat generator by common supply and return pipelines inside the junction box. Each room is

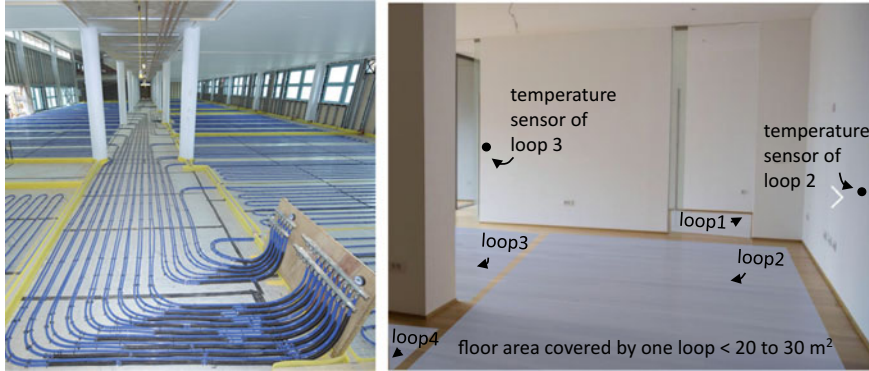


Fig. 8.28 Organization of floor heating registers in an open space office building (left) (www.thermo-floor.co.uk) and in the flat of a residential building (right)

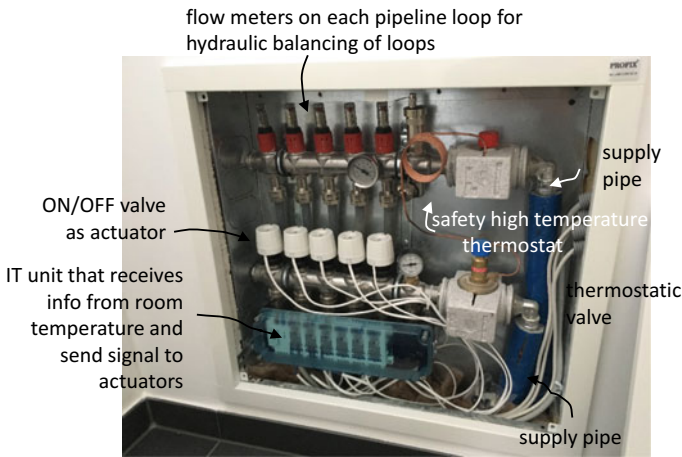


Fig. 8.29 In each floor in a residential building or in each apartment in multifamily buildings, a junction box is installed

equipped with temperature sensors that send wireless data to the IT unit in junction box. According to temperature in the monitored room, the flow of the heat transfer media is switched on or off by a thermostatic valve to maintained thermal comfort without overheating (Figs. 8.28 and 8.29).

The main advantages of radiant space heating is that the air temperature gradient (distribution of the indoor air temperatures over the height of the room) is very close to ideal (to simplify: warm legs, cold head) because heat is emitted mainly by radiation towards all walls in the room. This is the opposite in the case of local heating by stove or even by radiators as the surface temperatures of those elements

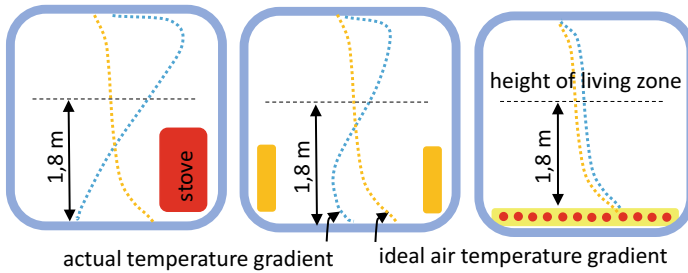


Fig. 8.30 Air temperature gradient in the rooms with different types of heat emitters: stove, radiators, and floor heat emitters

are much higher in comparison to heated floors, and convection heat flux is dominant (Fig. 8.30).

If a floor is covered by material with high thermal effusivity (e.g. tiles or stone lining), floor space heating prevents inappropriate thermal comfort conditions in the spaces where people walk barefoot. As large surface areas are heated above the set-point indoor air temperature, the operative temperature is higher, and thermal comfort conditions can be achieved at lower set-point indoor air temperatures, which means that heat losses are also lower (up to 5% in thermally well-insulated buildings with mechanical ventilation with heat recovery per 1 K of decreased air temperature). Because of the large area of heated surface, the supply temperature of heat transfer fluid can be lower (down to 28 °C), which results in lower heat losses of the heat generator and distribution system. The utilization of renewable energy sources by heat pumps, solar heating systems, or low temperature geothermal water is more efficient because a lower energy of supply heat is needed to provide the required indoor comfort conditions. A disadvantage of radiant space heating is that overboost heating after longer unheated periods cannot be provided, but such cases can be partially be compensated by electrical heaters and built-in mechanical ventilation systems. Radiant heating systems slowly adapt to rapid changes of internal heat and solar gains. Nevertheless, due to strict energy efficiency requirements, the disadvantages of radiant space heating systems are significantly lower.

8.5.5 Thermally Activated Building Structures

Thermally activated building structures (TABS) are building structures that are thermostatted throughout the year to almost constant temperature 20–24 °C by the pipes built into the core of the floor (ceiling) structure. Such structures enable low temperature radiant heating and high temperature radiant cooling if the thickness of the structure is sufficient (25–30 cm), construction material with high thermal capacity is used (e.g. concrete) and surfaces on both sides are not covered by thermal insulation layer of suspended ceiling to ensure sufficient open accumulation thermal mass. Maximum heating and cooling heat fluxes are up to 40 W/m², both for space heating and cooling. TABS enable highly efficient utilization of low



Fig. 8.31 Pipes built-in in the core of the concrete-bearing plate in office building; circulation pipes must be installed in TABS during the construction of the building (www.rehau.com)

energy sources, such as ground water, low temperature geothermal water, or heat from solar thermal systems (Fig. 8.31).

8.5.6 Other Applications of Floor Heating

The applications of ground heating for the melting the snow is used to prevent the freezing of outdoor areas and, therefore, reduces the possible injuries of pedestrians on outdoor areas and entrances to building during winter. Ground heating of open spaces decreases the cost of community services and lowers environmental impact because the salting of sidewalks can be avoided. For small areas, electrical resistant heaters are usually used because the operation time is limited only to wet conditions with freezing temperatures, while water systems are used for the heating of large outdoor areas. A mixture of water and antifreeze fluid must be used as the heat transfer fluid. With this case, the use of district heating or geothermal water prevails (Fig. 8.32).



Fig. 8.32 Stairs heated with electrical resistant heater (left); ground heating of pavement in St. Moritz; in this case, heating water must be mixed with antifreeze fluid (right)

Buildings for deep freezing and ice rinks are often built on the ground. To ensure adequate load-bearing of the soil, the foundation temperature should never be cooled below 0 °C. Consequently, the foundation of such buildings must be heated continuously with thermal activation of the foundation layer.

8.6 Control of Space Heating Systems

Space heating systems very rarely operate at design conditions; therefore, they need to be adjusted to the current thermal response of the buildings with adequate control. The control of a space heating system is done with the adjustment of one or more parameters, such as temperature, flow rate, or pressure of the heat transfer fluid in distribution system. The control system consists of devices called sensors (sensing the actual value of a variable, e.g. temperature) and actuators (that act to change something, e.g. change water flow rate through radiator in the case of thermostatic valves). For efficient control, a controlling algorithm is also needed. It can be integrated into an actuator or in a separate IT unit that connects several sensors and actuators or in central control system called BMS (building automation system).

A control system is responsible for operational safety, the restriction of the operational parameters of the heat generator and any element installed in heating system, the control of output heat produced by the heat generator according to actual heat needs, and the hydronic balancing of the flow rate of heat transfer fluid. Several techniques can be used, as shown in Figs. 8.33 and 8.34.

Central control can be done with the adaptation of supply heat transfer fluid temperature and/or its flow rate. Temperature is adapted by controlling the temperature of the supply water in the heat generator and/or by mixing return (colder)

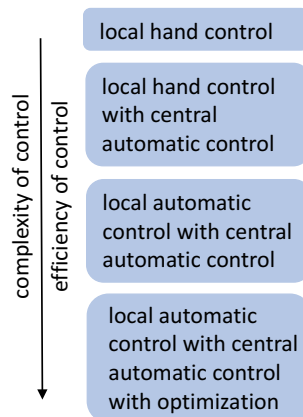


Fig. 8.33 Techniques of controlling a heating system

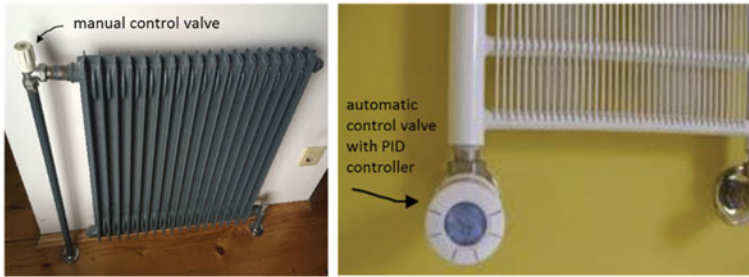


Fig. 8.34 Radiator with hand control valves (left) for local (in-room) control of air temperatures are not allowed by the law in many countries nowadays and must be replaced with thermostatic one to decrease indoor air temperature swing, overheating, and energy demand for space heating; thermostatic valves consist of temperature sensors and actuators that change the flow rate through the radiator according to the room’s air temperature. Nowadays, thermostatic valves have built-in PID microprocessor, and a PID control algorithm that enable simple programming, e.g. intermediate heating (right) and overview of temperature

heat transfer fluid using a motor-driven 3-way valve with supply (warmer) heat transfer fluid. Supply temperature is regulated according to current outdoor air temperature by the so-called equithermal curve (e.g. by the linear decrease of supply water temperature according to outdoor air temperature). For flow rate control, a throttling valve can be used; however, such a method of adjusting the flow rate is very inefficient, because the electrical power of the pump or fan remains the same throughout the operation. In contemporary systems, the pressure of supply fluid is constantly measured and a pump or a fan operates at constant total pressure head. This means that the flow rate of the heat transfer fluid is adjusted by variable flow volume (Fig. 8.35).

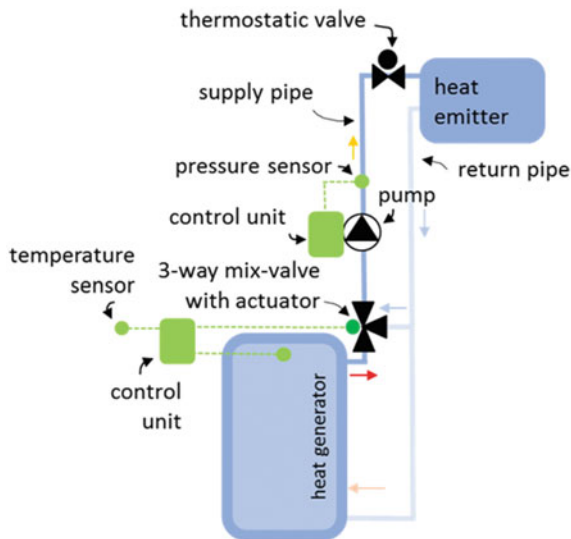


Fig. 8.35 Schematic of basic central control of supply heat flux in space heating system

With controlling algorithms inputs gathered by sensors are transformed into signals sent to actuators. The simplest algorithm is an ON/OFF one, which means that actuator has only two states (e.g. full or no flow rate through radiator). A “P” type or proportional algorithm changes the output signal to the actuator according to the current difference between the actual and set value of variables (called error; e.g. the power of an electrical heater is lowered proportionally to the decreasing of difference between the actual indoor air temperature and the set point temperature). A “PI type” or proportional-integral algorithm adapts the output signal to the controller not only according to the present difference between the actual and set values, but also analyses the value of the error in the history of controlling. A “PID type” (proportional-integral-differential) control algorithm is the most advanced and most commonly used control algorithm. It predicts future errors based on the differential of error curve at the present. The latest development of control algorithms includes weather forecast data and detailed models of the thermal response of the building.

Control devices and algorithms have significant influence on the energy demand for the space heating of the building. According to the rule of thumb, the efficiency of control with an ON/OFF controller is 0.80 (this means that the final energy for heating $Q_{f,h}$ is 1/0.8 or 25% more than the energy need for heating Q_{NH} only because of non-ideal controlling), the efficiency of controlling with a P-type controller 0.85, a PI-type controller 0.93–0.95, and efficiency of controlling with a PID-type controller 0.99.

Case Study Figures show control devices and control unit of fan-coil. Each fan-coil is controlled individually according to the thermal response of the room. Control units are connected in a central control system that controls common functions, e.g. weekend temperature set-back (Fig. 8.36).

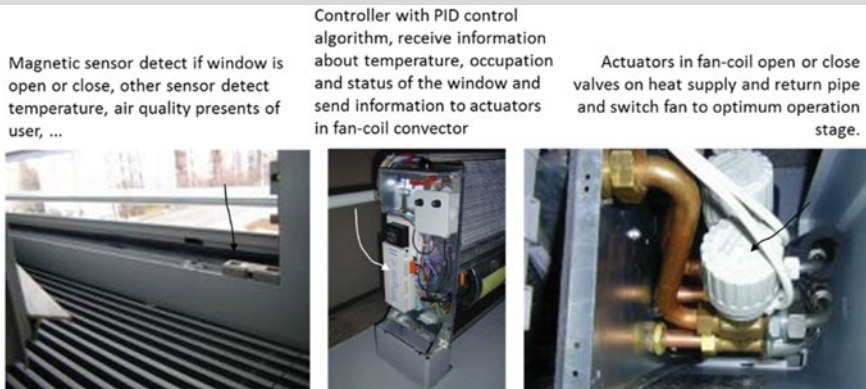


Fig. 8.36 Sensors and actuators for control of fan-coil

8.7 Energy Needs and Delivered Energy for Space Heating

In Sect. 5.3.1, energy needs (Q_{NH}) for space heating are presented. Energy needs are defined according to transmission and ventilation heat losses and solar and internal heat gains. The monthly average heat gain utilization factor in the case of the monthly method or detailed unsteady modelling of heat transfer in building structures in the case of the hourly method is used to take into account the influence of the heat accumulation in the building on the energy needs for space heating.

Delivered energy (final energy) for space heating ($Q_{h,f}$) is calculated by energy balance on monthly or hourly time steps, taking into account the energy needs and the design and thermal properties of all components/devices of space heating system, as described in Sect. 5.4. The procedure starts with the determination of energy need for space heating (Q_{NH}), the determination of heat loss of heat generator, heat storage, and distribution system, as well as heat losses of end heat exchangers due to imperfect control of the indoor air temperature. Auxiliary energy for the operation of the space heating system, including the operation of the heat generator, pump or fan, and end heat exchangers built in in the thermal zones (rooms) and control units is also calculated as well. Some of heat losses can be recovered to some extent, depending on where the devices of the space heating system are built in (in heated or unheated parts of the building). In Fig. 8.37, energy flows for a simple space heating system are presented following the nomenclature introduced in EPBD-supporting EN standards (see Sect. 5.4).

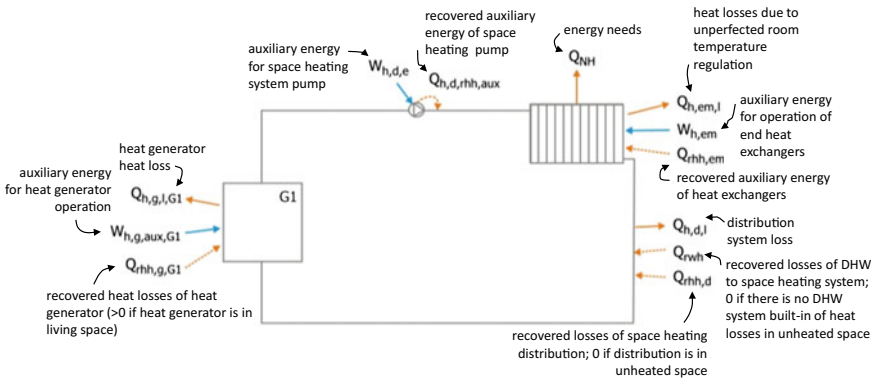


Fig. 8.37 Energy flows in a space heating system consisting of a gas boiler, two-pipe distribution system with and flat-type radiators (orange arrows indicate heat, blue arrows electricity)

Case Study 1 What will the delivered energy be for the space heating of the Virtual Lab building if the building is heated by a hydronic system consisting of a condensate gas boiler, a two-pipe distribution system, and flat-type radiators (Fig. 8.38).

The balance of energy flows is determined for each of the month of the year and then summarized to yearly delivered energy (Fig. 8.39).

Seasonal performance indicator SPI of space heating system is equal to (Fig. 8.40):

$$SPI = \frac{Q_{NH}}{Q_{h,f} + 2.5 \cdot W_{f,aux}} = \frac{1980}{2214 + 2.5 \cdot (129 + 32)} = 0.76$$

Note: Weighting factor 2.5² for electricity is defined according to environment impact as a mixture of technologies used for electricity production in EU.

Heat generators configuration:

- Name: Space heating of VirtualLab building } gas boiler
- Heat source: Natural gas
- Heat generator type: Condensing boiler
- Automatic operation ratio of HG:
- Installation place: Heated space
- Boiler control: Temperature control

	Informative	Project
Nominal power of heat generator [kW]	1	1,3
Power of heat generator at 30% load [kW]	0,3	0,39
Efficiency of heat generator at nominal power [-]	0,91	0,91
Efficiency of heat generator at 30% load [-]	0,97	0,97
Heat loss in standby operation [kW]	0,02	0,02
Power of auxiliary appliances at full load [kW]	0,05	0,05
Power of auxiliary appliances at 30% load [kW]	0,02	0,02
Power of auxiliary appliances in standby operation [kW]	0,02	0,02

Pipes configuration:

- Thermal zone: Thermal zone 1 - Living unit, Thermal zone 2 - Technical unit
- Name: Space heating system distributor
- Piping system type: Double pipe
- Pumps in heated space: Yes No
- Thermally insulated pipes: Yes No
- Pipes mainly in: Internal walls

	Informative	Project	#
Circulation pump power [W]	15	15	1
Pipe length between heat generator and supply pipe L _v [m]	29	29	
Main supply pipe length [m]	3	3	
Branching pipe length [m]	25	25	
Heat transfer coefficient of pipes between generator and supply pipe [W/m ² K]	0,200	0,2	
Heat transfer coefficient of main supply pipe [W/m ² K]	0,255	0,255	
Heat transfer coefficient of branching pipe [W/m ² K]	0,255	0,255	
Share of pipes in unheated space [%]			0

Emitters configuration:

- Thermal zone: Thermal zone 1 - Living unit, Thermal zone 2 - Technical unit
- Name: Emittor
- % of delivered energy by selected emitter: 100
- Actuators inside heated space: Yes No
- Emitter type: Radiant panel 40/30
- Control unit type: Electrothermal actuator
- Indoor temperature: Reference room
- Installation of emitters: With thermal insulation
- System: Dry with the flooring

	Informative	Project	#
Nominal power of controller [W]	1	2	0

Fig. 8.38 Characteristics of the system and devices (TRIMO Expert)

²EN 15316-1:2017 Energy performance of buildings—Method for calculation of system energy requirements and system efficiencies—Part 1: General and Energy performance expression.

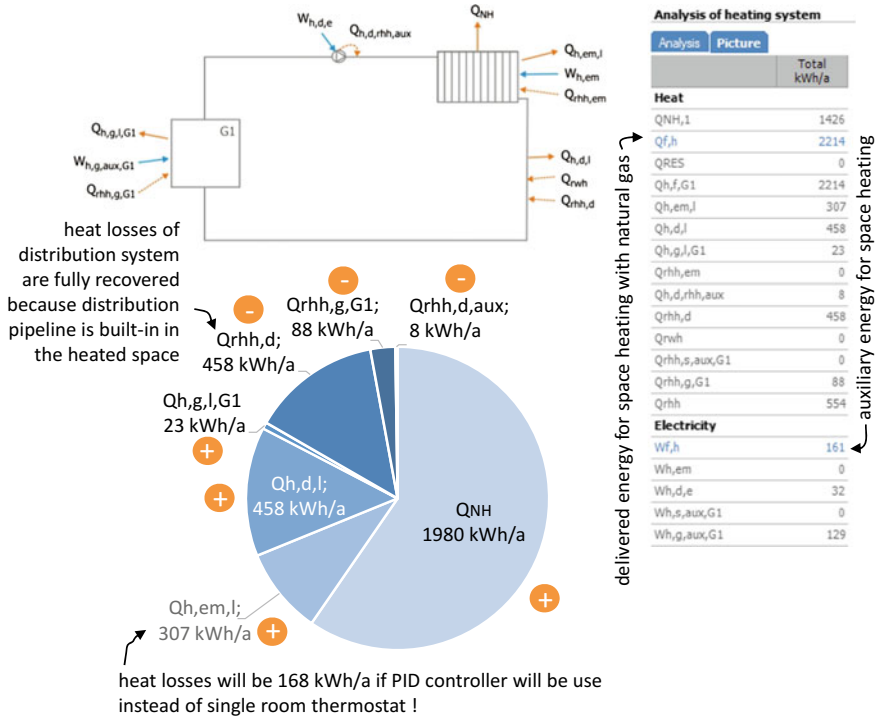


Fig. 8.39 Yearly heat demand for space heating system (TRIMO Expert)

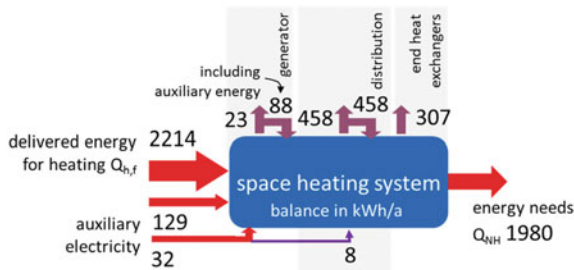


Fig. 8.40 Energy balance for the case study space heating

Case Study 2 The Virtual Lab building is heated with a solar thermal system (A_{sc} 10.8 m²) and a resistant electrical backup heater installed in heat storage (V_s 950 l). A schematic of the system and the yearly energy requirement for space heating is presented below. The energy needs for heating Q_{NH} of the Virtual Lab is 1980 kWh/a (Figs. 8.41 and 8.42).

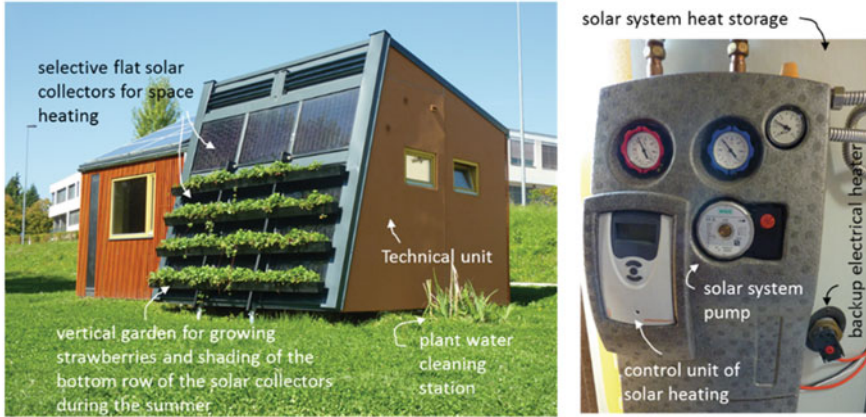


Fig. 8.41 Solar thermal collectors and heat storage of solar space heating system

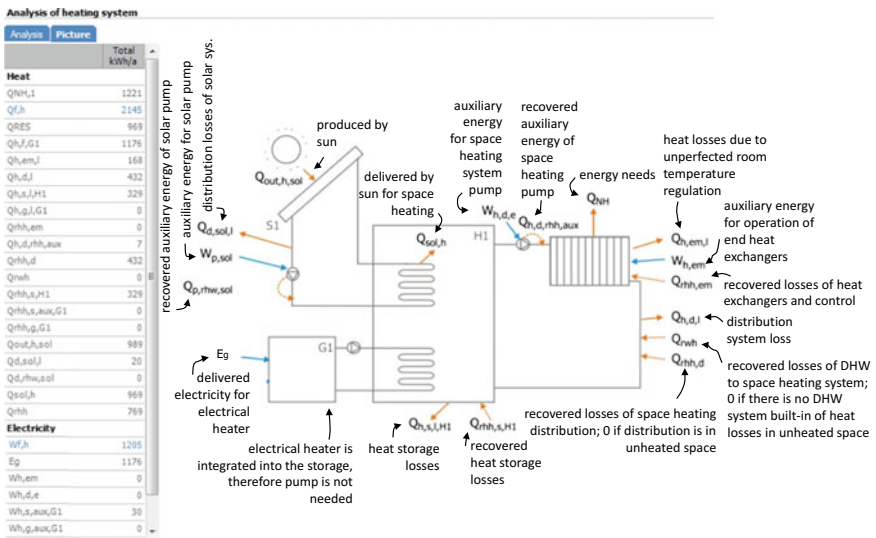


Fig. 8.42 Schematic and energy fluxes of the space heating system in the Virtual Lab building (TRIMO Expert)

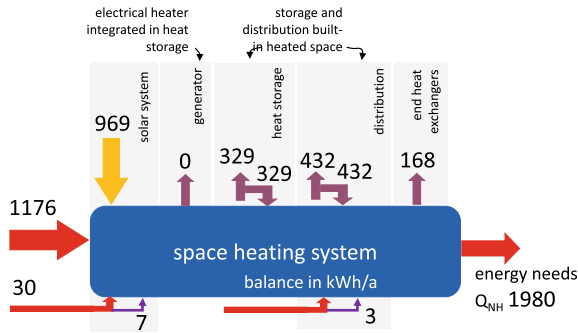


Fig. 8.43 Energy balance of the space heating system in the Virtual Lab building

Seasonal performance indicator SPI_h of space heating system and ration of renewable energy REN_h in delivered energy for space heating are equal to (Fig. 8.43):

$$SPI_h = \frac{Q_{NH}}{2.5 \cdot (Q_{h,f,G1} + W_{f,aux})} = \frac{1980}{2.5 \cdot (1176 + 30)} = 0.66$$

$$REN_h = \frac{Q_{sol,h}}{Q_{h,f,G1} + W_{h,aux} + Q_{sol,h}} = \frac{969}{(1176 + 30 + 969)} = 44.6\%$$

Case Study 3 In the case that an air-water type heat pump would be used for backup space heating instead of a resistant electrical heater, the electricity demand for the operation of the heat pump would be 378 and 798 kWh/a of the environmental heat would be utilized by the heat pump. SPI_h and REN_h in this case will be equal to:

$$SPI_h = \frac{Q_{NH}}{2.5 \cdot (Q_{h,f,G1} + W_{h,aux})} = \frac{1980}{2.5 \cdot (378 + 30)} = 1.94$$

$$REN_{sol+HP,h} = \frac{Q_{sol,h} + Q_{HP,env}}{Q_{h,f,G1} + W_{h,aux} + Q_{sol,h} + Q_{HP,env}} = \frac{969 + 798}{(378 + 30 + 969 + 798)} = 81.2\%$$

Note: The renewable energy share (REN) indicates share of renewable energy sources in the delivered energy for space heating. It differs from the renewable energy ratio (RER), which is used as a criterion for nearly zero energy buildings. RER is defined by the primary energy needed for the operation of the building (see Sect. 5.5).

8.8 Principles of Rational Use of Energy for Space Heating

Energy demand for space heating and the energy efficiency of space heating systems depend on the design, operation control, and maintenance of the system and the durability of the components and devices throughout the life cycle of the system. In the design phase, several factors, including climate, architectural design, the design of the space heating system according to available energy sources, and the heat load of the building and the quality of components and devices, should be considered.

The local climate must be studied carefully; using bioclimatic diagrams is a common approach. Such diagrams shown hour-by-hour outdoor air temperatures, humidity, sunshine duration and other meteorological variables typical for the site for the course of a year. In the context of space heating, bioclimatic diagrams show the length of heating period, the period when a building can be heated by natural (passive) solar heating or the period of potential overheating, during which a shading device should be activated, which will result in lower solar energy stored in the building structure for later use during the day (Fig. 8.44).

Architectural design must lead to a building with small shape factor, the ratio between the total building envelope area, and the volume of the building. Together with the design of envelope structures with low thermal transmittance (see Sect. 3.1), such planning will result in decreased transmission heat losses. The building envelope should be tight to decrease air infiltration and, therefore, part of the ventilation heat losses. Thermal zoning of the indoor spaces (positioning the indoor spaces according to the time of the day during which will be occupied), the thermal capacity of building structures and the positioning and sizing of transparent envelope elements (windows) should also be considered. The prompt determination of energy performance of building as part of the building information modelling (BIM) process enables an immediate overview of the consequences of changes in planning without significant time/cost increases.

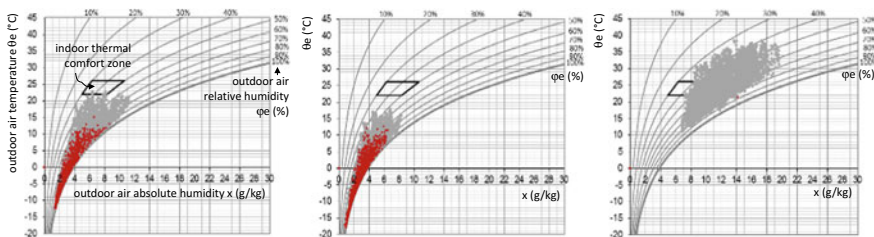


Fig. 8.44 Bioclimatic diagrams for Ljubljana, Stockholm and Dubai; hour-by-hour outdoor temperatures, absolute and relative humidity for the cold half of the year are shown with grey dots, hours during which building must be heated are indicated by red dots; the number of heating hours and outdoor temperatures at which a building must be heated can be seen; note: red dots are constructed for a specific office building and are not general



Fig. 8.45 Renovation of district heating station decrease heat consumption in multi-family buildings up to 20%

A number of technical measures can also be taken to improve the overall efficiency of space heating systems. Some examples:

- low temperature space heating systems will have lower heat losses in general and enable the use of renewable energy, especially solar and environmental energy, with higher efficiency;
- best available technologies of combustion condensate boilers operate with equal or even higher efficiency at partial load and thermal power could be adjusted in wide range (e.g. between 100 and 350 kW) with unchanged efficiency; the yearly energy efficiency of heat pumps (SPF) can be improved up to 10% with variable speed controlling of the compressor motor (Karlsson 2007).
- renovation of district heating stations including replacement of the heat exchanger, replacement of the circulation pumps, thermal insulation of the pipe network, multi-point controlling and installing of heat counters can lead to 20% decreased energy consumption for space and DHW heating³; (Fig. 8.45)
- pumps or fans should operate with variable flow rate adjusted to actual energy needs by using a frequency-controlled motor. It is assumed that up to 30% of auxiliary energy can be saved in this way. Such pumps or fans are driven by modern electric motors that have 5–10% lower consumption in comparison to older ones;

³Pravilnik o metodah za določanje prihrankov energije (Rules on the methods for determining energy savings) (Uradni list RS, št. 67/15 in 14/17).

- distribution pipes and channel networks should be as short as possible; lower heat transfer fluid velocity by a factor of 2 will reduce pressure drop by a factor of 8; a larger distribution network will be costly, and the decrease in the temperature of the distribution fluid will be higher due to heat losses; pipes and channel materials with low friction factors (copper or plastic) should be used instead steel, concrete or flexible ones; pipes should be insulated with the thermal insulation with a thickness equal to the inner diameter of pipe; regular maintenance of air filters in air space heating system will decrease yearly electricity consumption for fan operation by up to 10%;
- vertical shafts must be hydraulically balanced; this means that the flow in each vertical branch will be adjusted to the current pressure drop in the network and end heat exchangers; this can be done by differential pressure regulators and constant pump total heat within the variable flow; a decrease of heat demand of up to 30% was reported in multifamily buildings (Harvey 2006).⁴

References

- Černe B, Medved S (2005) The dynamic thermal characteristic of lightweight building elements with a forced ventilated cavity and radiation barriers. *Energy Build* 37(9):972–981
- Daniels K, Hammann RE (2009) *Energy design for tomorrow, energy design fur morgen*. Edition Axel Menges, Stuttgart
- Davies MG (2004) *Building heat transfer*. Wiley Ltd.
- Harvey LDD (2006) *A handbook on low-energy buildings and district-energy systems, fundamentals, techniques and examples*. Earthscan, London
- Hausladen G et al (2005) *ClimaDesign, Losungen fur Gebaude die mit weniger Technik mehr konnen*. Verlag G. D. W. Callwey GmbH
- Jayamaha L (2007) *Energy-efficient building systems, green strategies for operation and maintenance*. McGraw-Hill, New York
- Kabele K et al (2012) *Heating and cooling. Educational Package, IDES-EDU Master and Post graduate education and training in multi-disciplinary teams implementing EPBD and Beyond, IEE/09/631/SI12.558225*
- Karlsson F (2007) *Capacity control of residential heat pump heating system*. Chalmers University of Technology, Department of Energy and Environment
- McQuiston FC, Parker JD, Spitler JD (2005) *Heating, ventilating, and air conditioning, analysis and design*. Wiley Inc, United States
- SDHplus (2015) *New business opportunities for solar district heating and cooling, IEE/11/803/SI2.616372*
- SOLARGE (2004) *Enlarging solar thermal system in multi-family-houses, hotels, public and social buildings in Europe, EIALT/EIE/04/082/2004*

⁴EcopAgent, www.ecopagent.si.

Chapter 9

Space Cooling of nZEB



Abstract The International Energy Agency (IEA) predicts that the final energy demand for cooling worldwide will increase from current 4 to 9 EJ per year by the year 2050. There are several reasons for increased energy demand. The contemporary architecture trend of “all-glass” architecture is a significant reason for the increased energy need for cooling of the buildings. An increase number of domestic appliances cause increased use of electricity and, therefore internal heat gains that must be removed by cooling systems. The EU population is getting older, and it is estimated that in the year 2030 almost one third of population in EU will be older than 65 years; elderly people are more vulnerable to heat stress. As a consequence, more cooling systems will be installed. During the last century, cities become larger and built with low albedo materials (low reflection of shortwave solar irradiation) with limited green areas. As a result, urban and street canyon heat islands are more intense. It has been calculated that in a mid-size city, an urban island could cause increase the need for cold for 10 kWh/m² of building area per year. Climate change is another reason for the increased energy demand for the cooling of buildings. The United States Environment Protection Agency (EPA) predicts that in hot climate regions the demand for energy for cooling will increase due to global warming by 5–20%. *Note* An urban heat island is defined by the difference in the maximal daily outdoor air temperature in the built environment and surrounding countryside; a street canyon heat island is defined by the difference in maximal daily outdoor air temperature in the particular street canyon and in the city. In cities with more than one million inhabitants, the intensity of the urban heat island could be as high as 6–10 °C; the intensity of the street canyon heat island in tall streets without trees could be 1–3 °C in non-windy conditions.

A cooling system in a building is not obligatory, as heating DHW and lighting systems are, as thermal comfort requirements can be fulfilled by extend thermal insulation, green building structures, effective shading of windows and other

IEA Technology Roadmap Solar Heating and Cooling, 2012.
www.eea.europa.eu.

© Springer Nature Switzerland AG 2019
S. Medved et al., *Sustainable Technologies for Nearly Zero Energy Buildings*,
Springer Tracts in Civil Engineering, https://doi.org/10.1007/978-3-030-02822-0_9

transparent structures, by increased indoor thermal accumulation mass or/and intensive night-time natural ventilation. Nevertheless, if thermal comfort must be provided at any outdoor and indoor conditions, mechanical cooling system must be installed. In such cases, the energy demand for the operation of a cooling system must be included in the energy performance indicators of the building. In this chapter, different techniques for the cooling of buildings will be presented, including natural cooling, free cooling, and mechanical cooling as well as methods for the determination of the cooling load of the building and examples of delivered (final) energy use for the mechanical cooling of buildings.

9.1 Cooling Load of Buildings

9.1.1 Rule of Thumb

The cooling load of a building is determined by building architecture and thermal properties, thermal comfort requirements, the type of cooling system, operation strategies, and climate conditions (Kabele et al. 2012). The following rule of thumb can be used in the pre-designing phase and for simple feasibility studies to predict specific cooling load and a cooling system's annual operation time:

- specific cooling load of residential buildings in the range between 25–35 W/m² of useful area (A_u) and time of operation 500 h per year;
- 40–80 W/m² in public and office buildings and time of operation 1500–2000 h per year;
- 60–100 W/m² in retail buildings and time of operation 1500–2000 h/a.

The indicated values have been determined for warmer climate in southern EU countries. In the ECOHEATCOOL project, the European Cooling Index (ECI) is introduced to present how climate conditions affect the energy demand for cooling. Values are relative and normalized to average European climate conditions (ECI 100), meaning that twice higher ECI will result in doubled energy demand for mechanical cooling (Fig. 9.1).

9.1.2 Steady State Cooling Load

Steady state cooling load calculation is commonly used in engineering practice for the design of the cooling system's thermal power at reference conditions. Cooling load is determined at reference heat gains (solar and internal heat gains) and reference sinks: heat losses due heat transmission and ventilation. The design indoor temperature for cooled spaces is defined by the set-point indoor air temperature and the maximum permitted indoor air temperature:

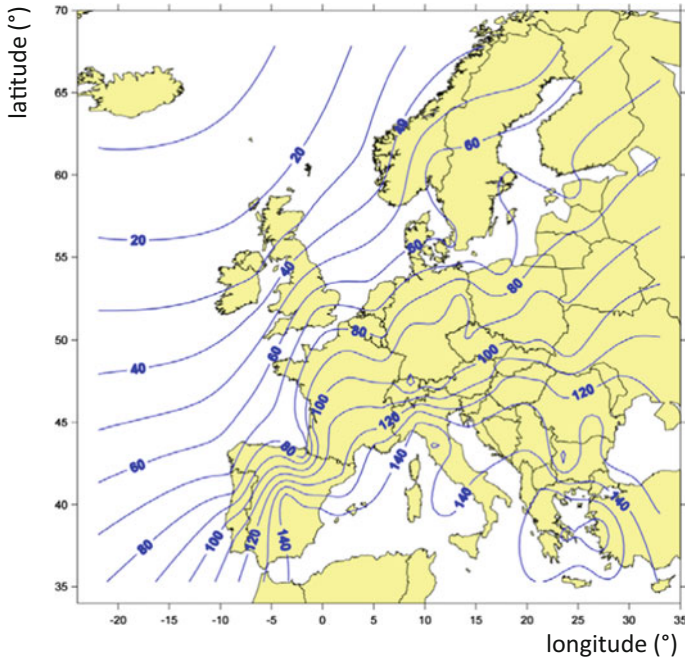


Fig. 9.1 European cooling index (ECI); regions with ECI higher than 120 have high needs for cooling of the buildings (ECOHEATCOOL; A Euroheat & Power 2006, www.euroheat.org)

$$\theta_{i,c,design} = \overset{\substack{\text{indoor air set-point temperature for cooling (}^\circ\text{C)}}{\downarrow}}{\theta_{i,c,set-point}} - 1\text{K (}^\circ\text{C)}$$

Reference design conditions are defined by the daily average outdoor air temperature for the hottest day and the maximum hourly solar irradiance on the reference day in the summer months between July and September. Climate data for the reference day are defined on the national level, values from Table 9.1 can be used in early design phase.

Note: Values should be adapted to local conditions for advance design.

Cooling load calculation starts with determination of transmission heat transfer coefficient H_T and ventilation heat transfer coefficient H_V , as presented in Chap. 3. H_T indicates heat flux that is transmitted through the envelopment of the building at 1 K temperature difference between indoor and outdoor air, and H_V indicates the heat flux needed to cool down air entering the building (coefficients are expressed in W/K). Design $H_{T,c,design}$ is equal to:

Table 9.1 Suggested average daily outdoor temperatures for different climate regions

Climate	Average daily outdoor air temperature in the design reference day $\theta_{e,max}$ (°C)								
Alpine	23.0								
Central Europe	28.5								
Mediterranean	31.0								
Orientation of the receiving plane	Maximal solar irradiation on the design reference day $G_{glob,max}$ (W/m ²)								
	S	SW	W	NW	N	NE	E	SE	Horizontal
Vertical plane	490	550	670	510	200	430	590	560	900
South slope plane (45°)	910	940	840	680	300	670	840	890	

Note different values could be defined on the national level or locally
 Medved S., et al., KI Energija 2017, Version: 7.2.0.0., KnaufInsulation d.o.o., Škofja Loka, Slovenia

weighting factor: $b < 0$ for constructions towards unheated close space, $b > 0$ for constructions with floor heating

$$H_{T,c,design} = \sum_{i=1}^n b_i \cdot U_i \cdot A_i + \sum_{j=1}^m \psi_j \cdot l_j + \sum_{k=1}^l \chi_k \cdot n_k \quad (W/K)$$

total number of envelope elements n

linear (2D) thermal transmittance of j -th thermal bridge (W/mK)

length of j -th thermal bridge (m)

point (3D) thermal transmittance of k -th thermal bridge (W/K)

thermal transmittance of i -th building envelope (W/m²K)

area of i -th building envelope (m²)

number of point (3D) thermal bridges in building envelope

According to the method given in EN 13370, $H_{v,c,design}$ is determined taking into account infiltration and natural ventilation with air exchange rate 0.1 h^{-1} . The impact of mechanical ventilation is ignored because supply air temperature is close to the design indoor air temperature $\theta_{i,c,set-point}$ because air is cooled in an AHU heat exchanger during the daytime operation. Design $H_{v,c,design}$ is defined by equation:

air density and specific heat could be replace by constant $0.34 \text{ (Wh/m}^3\text{K)}$

$$H_{v,c,design} \cong \rho_a \cdot c_{p,a} \cdot (n_{inf} \cdot V + 0.1 \cdot V) \quad (W/K)$$

net building volume (m³)

infiltration air exchange rate, approximate value $n_{50}/10$ to $n_{50}/20$ could be assumed (h⁻¹)

air exchange rate 0.1 h^{-1} is assume due to the window airing net building volume (h⁻¹)

Note: $H_{v,c,design}$ is defined for the determination of the cooling load of the building. For the evaluation of energy needs for cooling, heat recovery and/or night time bypass operation of mechanical ventilation system as well pre-cooling by ground heat exchanger could be taken into consideration.

Beside heat transfer coefficients, time constant building or building zones, daily operating time of cooling system and permitted daily indoor air temperature variation must also be defined. Building time constant τ depends on the internal heat capacity and heat transfer coefficients:

$$\tau = \frac{C}{(H_{T,c,design} + H_{V,c,design})} \cdot \frac{1}{3600} \text{ (h)}$$

internal heat capacity of zone/building (J/K) $\leftarrow C$
 transmission heat transfer coefficient at design conditions (W/K) $\leftarrow H_{T,c,design}$
 ventilation heat transfer coefficient at design conditions (W/K) $\leftarrow H_{V,c,design}$
 constant $\leftarrow 3600$ (s/h)

Internal heat capacity is determined by the area of all building structures in contact with indoor air and the thermal properties of the materials (density and heat capacity). Because dynamic heat transfer in buildings is periodic, heat penetration thickness into the building structures during the daily period is assumed to be 0.1 m, and only structure’s layers to this thickness contribute to the accumulation of cold. In the predesign phase, when all details about the building structures are not known, default values of specific internal heat capacity can be used, as proposed in EN ISO 13790, according to the conditioned (useful) area A_u of the building (Table 9.2).

According to methodology presented in EN ISO 13790, estimated cooling load $\dot{Q}_{c,design}$ is equal to:

$$\dot{Q}_{c,design} \text{ (W)} = 0.8 \cdot (\dot{Q}_{c,source} - \dot{Q}_{c,T+V}) \cdot \left(1 + 0.3 \cdot e^{-\frac{\tau}{120}}\right) - \frac{C}{60} \cdot (\Delta\theta - 2K) + \frac{C}{40} \cdot \left(\frac{12}{t_{c,op,d}} - 1\right)$$

sum of all heat sources (W) $\leftarrow \dot{Q}_{c,source}$
 sum of all heat transmission and ventilation heat fluxes (W), negative value represent thermal gains, positive value thermal losses $\leftarrow \dot{Q}_{c,T+V}$
 time constant of building zone (h) $\leftarrow \tau$
 permitted variation of indoor air temperature during the day (K), 2 K are reasonable, higher value decrease design cooling load $\leftarrow \Delta\theta - 2K$
 internal heat capacity of building zone (Wh/K) $\leftarrow C$
 daily operation time of cooling system (h/day), 12 h/day is reasonable, lower value increase design cooling load $\leftarrow \frac{12}{t_{c,op,d}}$

Table 9.2 Reference specific heat capacity of buildings according to EN ISO 13790 and DIN V 18559-2

Building structures	Internal specific heat capacity C of building zone (Wh/K); A_u (m ²)
Light (wood cavity walls, light metal insulated panels, structures with inner close gap layer) mass 200–400 kg/m ² of A_u	$50 \times A_u$
Medium (bearing walls made by; hollow brick, solid wood walls) mass 400–600 kg/m ² of A_u	$90 \times A_u$
Heavy (bearing walls made by solid brick, concrete) mass > 600 kg/m ² of A_u	$130 \times A_u$

DIN V 18559-2: 2016 energy efficiency of buildings—calculation of the net, final and primary energy demand for heating, cooling, ventilation, domestic hot water and lighting—part 2: net energy demand for heating and cooling of building zones

While heat source $\dot{Q}_{c,source}$ is always positive, transmission and ventilation heat fluxes can be negative (as heat sources increase the cooling load) or positive (as heat losses decrease the cooling load) depending on the temperature difference between design outdoor $\theta_{e,max}$ and indoor $\theta_{i,c,design}$ air temperature. Heat sources are consequences of solar irradiation transfer through transparent parts of the envelope and internal heat gains' flux, which are emitted by people, appliances, and systems:

$$\dot{Q}_{c,source} = \dot{Q}_{c,sol} + \dot{Q}_{c,int} = \left(\sum_{i=1}^j A_i \cdot g_i \cdot F_F \cdot F_S \cdot F_W \cdot G_{glob,\beta,max,i} \right) + \dot{Q}'_{c,int} \cdot A_u \quad (W)$$

solar gain heat flux (W)
 number transparent envelope elements, e.g. windows
 frame factor, ration of frame area to window area; default 0.7; (-)
 solar radiation incident angle factor, default value 0.9 (-)
 maximum solar irradiation on the outer surface of the window on reference day (W/m²)
 specific internal heat gains of inhabitants, appliance and lighting (W/m²)
 internal heat gains (W)
 area of i-th transparent element (m²)
 total solar irradiation transmittance (-)
 shading factor, equal to 1 if window is not shaded by surround buildings, overhangs or fins or shades are not installed (-)
 useful area of zone (m²)

If internal heat gains flux are not specified in the national legislation, values proposed in ISO 18523-1 could be used.

Note: Each occupant emits 80–120 W of heat flux, data on electricity consumption can be used for determination of appliance heat gains and heat gains of illumination. Data varies in the range between 20 and 80 W/m² of A_u according to type of the building.

The sum of transmission and ventilation heat flux at design conditions is determined by transmission heat transfer coefficient $H_{T,c,design}$, ventilation heat transfer coefficient $H_{V,c,design}$ and reference temperature for the case of cooling of the building:

$$\dot{Q}_{c,T+V} = (H_{T,c,design} + H_{V,c,design}) \cdot (\theta_{e,max} - \theta_{i,c,design}) \quad (W)$$

transmission heat transfer coefficient for design conditions (W/K)
 ventilation heat transfer coefficient for design conditions (W/K)
 average daily outdoor air temperature in the design reference day (°C)
 design indoor temperature in cooling period (°C)

Case Study Determine cooling load of Virtual Lab building. Building has heated area (A_u) of 27.7 m², medium accumulation mass, design transmission heat transfer coefficient $H_{T,c,design}$ 29.1 W/K and ventilation heat transfer coefficient $H_{V,c,design}$ 15.3 W/K. Internal heat gain flux is 10 W/m². Building is in a location with a Central European climate ($\theta_{e,max} = 28.5$ °C). The set point indoor air temperature is 26 °C. Windows are not equipped with shading devices (Table 9.3).

$$\begin{aligned} \dot{Q}_{c,source} &= \dot{Q}_{c,sol} + \dot{Q}'_{c,int} \cdot A_u = 742 + 10 \cdot 27.7 = 1019 \text{ W} \\ \dot{Q}_{c,T+v} &= (H_{T,c,design} + H_{V,c,design}) \cdot (\theta_{e,max} - \theta_{i,c,design}) = \\ &= (29.1 + 15.3) \cdot (28.5 - (26 - 1)) = 155 \text{ W} \\ \tau &= \frac{C}{(H_{T,c,design} + H_{V,c,design})} = \frac{80 \cdot 27.7}{(29.1 + 15.3)} = 49.9 \text{ h} \\ \dot{Q}_{c,design} &= 0.8 \cdot (\dot{Q}_{c,source} + \dot{Q}_{c,T+v}) \cdot \left(1 + 0.3 \cdot e^{-\frac{\tau}{120}}\right) - \frac{C}{60} \cdot (\Delta\theta - 2K) + \frac{C}{40} \cdot \left(\frac{12}{t_{c,op,d}} - 1\right) \\ &\text{(W)} \\ \dot{Q}_{c,design} &= 0.8 \cdot (1091 + 155) \cdot \left(1 + 0.3 \cdot e^{-\frac{49.9}{120}}\right) - \frac{80 \cdot 27.7}{60} \cdot (2K - 2K) + \frac{80 \cdot 27.7}{40} \cdot \left(\frac{12}{12} - 1\right) = \\ &= 1194 \text{ W} \sim 1.2 \text{ kW} \end{aligned}$$

Table 9.3 Cooling load of transparent structures of Virtual Lab building

		A_i (m ²)	$G_{glob,\beta,max,i}$ (W/m ²)	g_i (-)	F_f (-)	F_w (-)	F_s (-)	$Q_{c,sol}$ (W)
Living unit	Roof window	0.79	695 (average north, horizontal)	0.49	0.70	0.9	1	169
	South window	2.1	490	0.55	0.63	0.9	1	320
Technical unit	Roof windows	0.72	695	0.49	0.9	0.9	1	202
	East windows	1.02	590	0.55	0.5	0.9	1	51

9.1.3 Cooling Load Determination by Dynamic Simulations

Methods for dynamic heat transfer simulations in building structures and spaces are presented in Chap. 8. The same methods are used for the determination of cooling load and energy needs for cooling of the building as well.

Case Study Cooling load of Virtual Lab building at set point temperature $q_{i,c,\text{set-point}} 26\text{ }^{\circ}\text{C}$ ($\theta_{i,c,\text{design}}$) determined by dynamic modelling. All input data are equal to the previous case with exception of meteorological data. Instead of a reference day, hourly data in the form of Test Reference Year (for Ljubljana) were used in dynamic simulation of the building's thermal response. Cooling load was determined for a constantly open and controlled shading screen installed in the front of the south-orientated window in the living unit (Fig. 9.2).

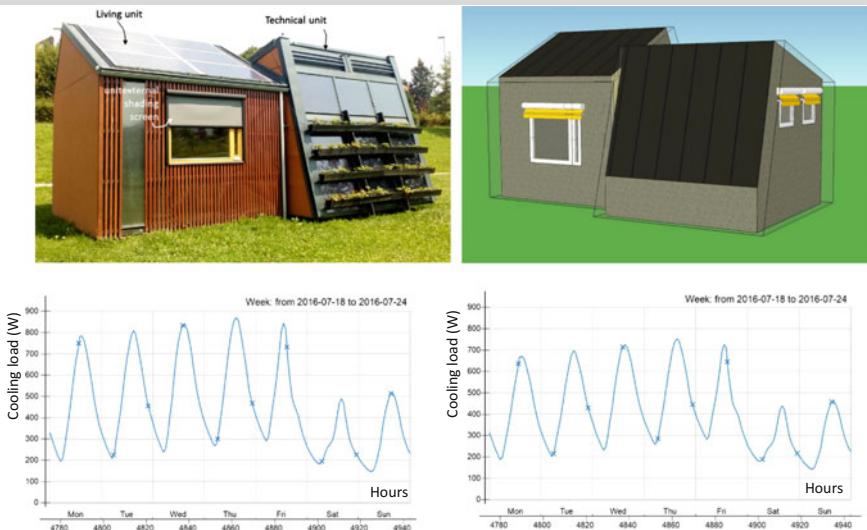


Fig. 9.2 Virtual Lab building with half closed external shading screen in front of the south window in the living unit; the shading screen is controlled, in situ and in computer simulation, according to solar irradiation (fully closed at solar irradiation higher than 300 W/m^2); cooling load in the case of unshaded (left) and shaded (right) south window; the IDA-ICE simulation tool was used for dynamic modelling

9.2 Techniques for Cooling of the Buildings

Cooling of the building is process of the transfer of the heat flux from the building to the outdoor environment to maintain the required indoor thermal comfort. Three main types of cooling techniques can be implemented: natural cooling,

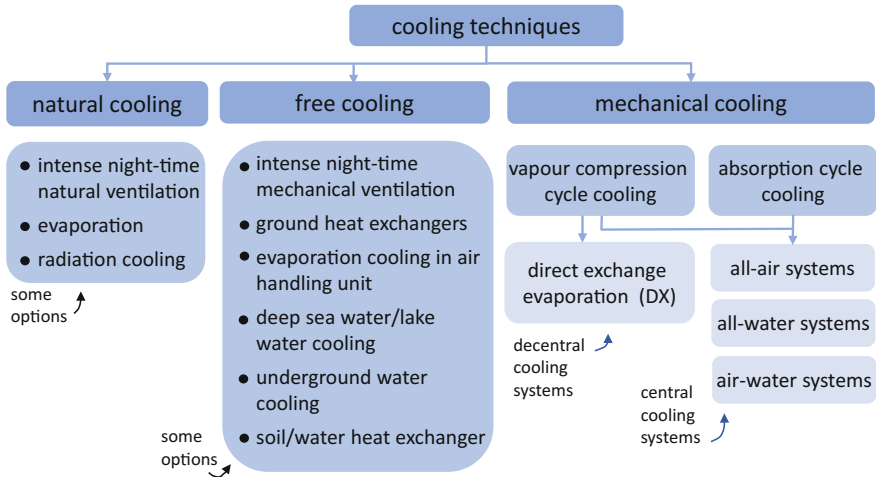


Fig. 9.3 Techniques for cooling of buildings

free-cooling, and mechanical cooling. The first two techniques are related to decreasing energy used for cooling as indoor thermal comfort cannot be provided full-time. Because of that, overheating hours (yearly sum of hours of indoor air temperature over cooling set-point air temperature) are used for the evaluation of natural and free cooling efficiency. If thermal comfort requirements are mandatorily without any deviation, mechanical cooling is necessary, particularly in buildings in Central and Mediterranean climates and with high internal heat gains (Fig. 9.3).

Natural cooling can be implemented with architectural design of the building. No technological systems are needed (with the exception of controlled ventilation openings). Natural cooling can be achieved by increasing the ventilation heat losses and heat transfer through envelope building structures. Natural ventilation cooling is possible at outdoor air temperatures that are 5–10 K below the indoor temperature. This ensures high air exchange rates, but it is efficient only if a sufficient amount of cold can be stored in the mass of building structures and furnishings during the night time. Increased transmission of heat losses through envelope building structures can be achieved by the use of the specific coatings on the outdoor surfaces of structures so that the atmospheric window property can be fully utilized, resulting in the night-time surface temperatures 10–15 K below the outdoor air temperature.

Note: Atmospheric window is phenomena of high transitivity of the Earth’s atmosphere for IR radiation with wavelengths 8–12 μm, which allows direct radiation heat exchange between outdoor surface of the building structure and the space (at temperature ~ 1 K).

Another way to decrease the indoor air temperature is the evaporation of water from indoor plants and wet textile membranes (see Sect. 3.2). Unfortunately, such techniques of natural cooling result in increased absolute humidity of the indoor air, which may be disruptive for residents.

Free cooling can be achieved by mechanical systems that transport the cold from outdoor air into the buildings by mechanical ventilation systems during the night-time. Ground heat exchangers can be used for pre-cooling of ventilation air during the day-time operation (see Sect. 11.4). Cold can be supplied into the buildings by pumping the ground water and, in the case of larger building or district cooling, the seawater or deep lake water from below thermocline zone into the close loop heat exchanger connected with fan-coils, floor heating registers or thermal activated structures (TABS) (see Sect. 8.5).

Note: Applications show that seawater at temperature 7 °C or colder can be reached at sea depth of 700 m and at temperature 5 °C or below at the depth of 1000 m.¹

Another free-cooling technique is evaporative cooling of the supply (direct evaporative cooling) or extract air (indirect evaporative cooling) before it flows into the recovery heat exchanger (which will be the cold exchanger in this case) inside the air handling unit (AHU) of the ventilation system. Some mechanical cooling system can operate in free-cooling mode, such as cooling towers in mechanical cooling systems, heat pumps that use ground water as an environmental heat source if ground water is pumped directly (with temperature in the range 10–14 °C) into the building's water cooling system or heat pumps with vertical ground heat exchangers (geosondes). In this case, heat can be transferred from indoor to the ground through geosondes by operation of the circulation pump only. Another advantage of such a free-cooling technique is that heat in the soil is regenerated quickly and, because of that, the efficiency of the heat pump is (slightly) higher in the first two or three months of next heating season.

In the following section, we will focus on mechanical cooling systems. The natural and free cooling techniques will be presented in Sect. 9.1 as technologies for the improving energy efficiency of buildings.

9.3 Mechanical Cooling of nZEB

Mechanical cooling system must transfer the heat from colder spaces of the building to the warmer outdoors. Because such heat transfer process is not possible with respect to 2nd law of thermodynamics, a refrigeration thermodynamic cycle

¹www.makai.com.

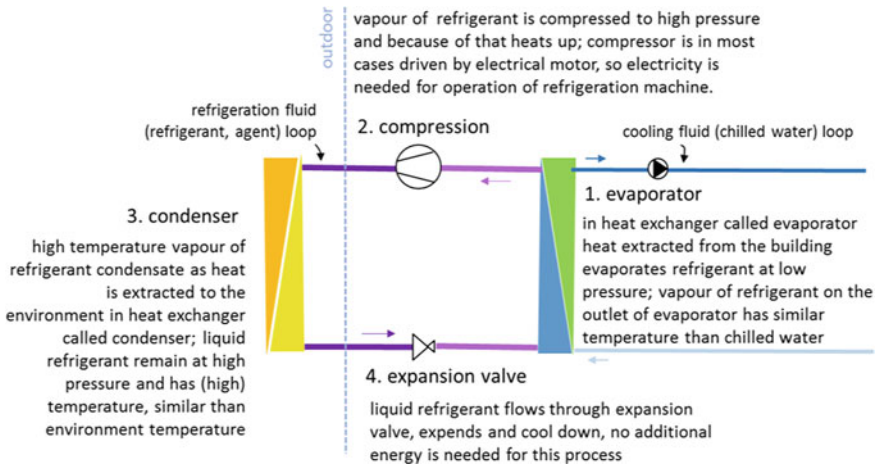


Fig. 9.4 Refrigeration vapour compression cycle is most commonly used for the mechanical cooling of buildings; in engineering practice, such a machine is known as a chiller

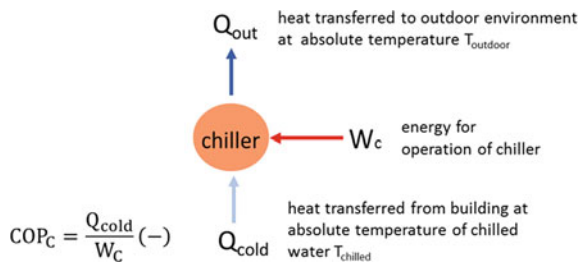
must be implemented. Most commonly, a vapour compression refrigeration cycle is used. Figure 9.4 shows how this process is occurs and the main components of a refrigeration machine known as a chiller.

Note: A refrigeration vapour compression cycle is similar to a heat pump cycle with the difference in the direction of the refrigerant flow. That is why a heat pump can operate as a refrigeration machine with quite simple adjustment of the refrigerant flow direction. In this case, COP is defined as shown in Fig. 9.5.

Chiller efficiency is defined by the ratio of extracted heat from the building (Q_{cold}) to the input of energy for the operation of the machine (W). This ratio is called the coefficient of performance (COP_c) of the chiller.

The theoretical value of $COP_{C,th}$, known as Carnot efficiency, depends on the absolute temperature of the outdoor environment where excess heat is removed

Fig. 9.5 Definition of vapour compressor chiller coefficient of performance COP_c



from the building and the absolute temperature of the chilled water needed to cool the building.

$$COP_{C,th} = \frac{T_{outdoor}}{T_{outdoor} - T_{chilled}} \quad (-)$$

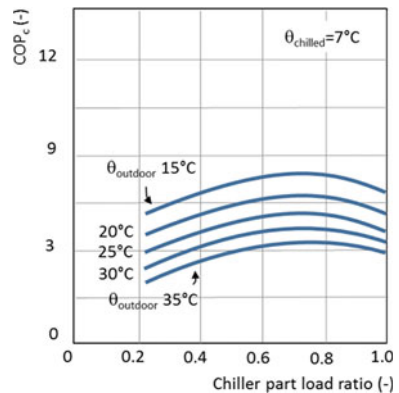
↙ absolute temperature of outdoor environment (K)
↘ absolute temperature of chilled water (K)

Note: If chilled water is used to cool the building at an outdoor environment temperature of 35 °C (308 K) with thermally activated building structures (TABS) instead of fan-coils, the temperature of chilled water could be as high as 15 °C (288 K) instead of 7 °C (280 K); the theoretical COP of a chiller will 15.4 be instead of 11. In practice, COPs are significantly lower (3–5 times), but the difference will still be noticeable; COPs are much higher than 1, meaning that more heat is removed from the building than energy (electricity) is consumed.

In practice, COP is lower than in theory and is determined experimentally in laboratories under constant operation conditions ($\theta_{chilled}$ 7 °C, $\theta_{outdoor}$ 30 °C and at full load operation). From Fig. 9.2, it can be seen that the cooling load of the building changes significantly over time (daily and seasonally) because of variation in solar irradiation and in internal heat gains; therefore, chillers operate most of the operation time at partial load. Chillers can operate at a wide range of the cooling part load ratio (ratio between actual and maximum-rated cooling power). At partial load operation of a chiller, COP is not constant, as it shown in Fig. 9.6.

If the actual time-dependant cooling load profile is not known, the Integrated Part Load Value (IPLV) can be used to evaluate the chillers’ all-year performance. The IPLV is calculated according to ASHRAE Standards using the efficiency of the chillers operating at 100, 75, 50 and 25% and weighted with assumed operation

Fig. 9.6 COP_c of refrigeration vapour compressor machine at part load operation



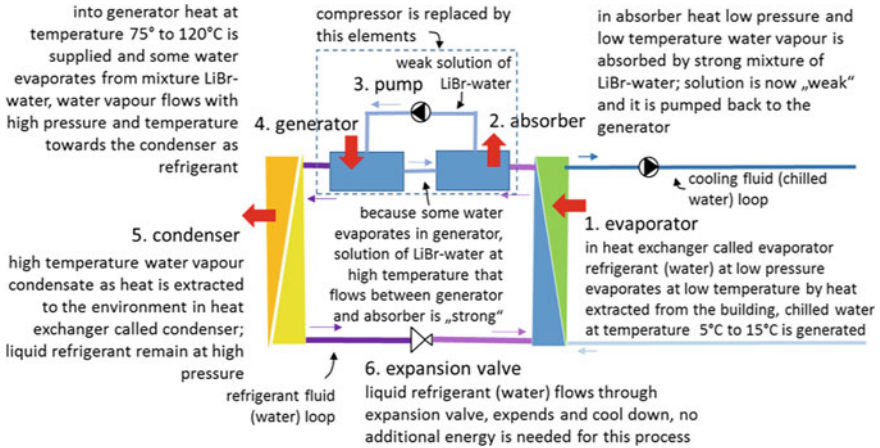


Fig. 9.7 Absorption refrigeration cycle in which homogeneous mixture of water and lithium bromide (water-LiBr) is used as refrigerant and absorbent; the main components of absorption refrigeration machine is shown

time at that part load. Similar to IPLV, the European Seasonal Energy Efficiency Ratio (ESEER) can be used for the same purpose.

Note: The rated cooling load of chiller is sometimes expressed in tons of refrigeration (RT); the rated cooling load in kW can be calculated as $3.517 \times RT$.^{2,3}

If waste heat, heat produced by cogeneration unit during the summer, heat produced by solar thermal system or geothermal heat is available at low cost, the absorption refrigerant cycle can be used instead of the vapour compression cycle. The main idea is to replace the compressor with a circulation pump that uses much less electricity and replaces a major part of the electricity needed for operation of the compressor with the heat. As environment impact of electricity production is much higher in comparison to that of heat, more sustainable cooling of the buildings can be provided. In the absorption cycle, a homogeneous mixture of two fluids is involved. One is called the absorbent, another the refrigerant. The most common mixture used in absorption cooling machines is mixture of water (as refrigerant) and lithium bromide (as absorbent). Such a process of absorption cooling is presented in Fig. 9.7.

²EUROVENT—Europe’s Industry Association for Indoor Climate (HVAC), Process Cooling, and Food Cold Chain Technologies, www.eurovent.eu.

³ASHRAE, www.ashrae.org.

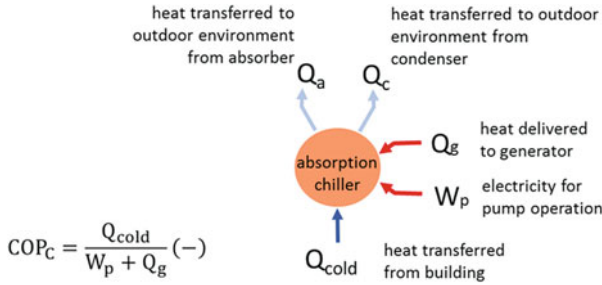


Fig. 9.8 Definition of absorption chiller coefficient of performance (COP_c)

Note 1: Instead of a water-LiBr mixture, ammonia-water is another mixture used in absorption refrigeration machines. In this case, ammonia (NH_3) is the refrigerant and water is absorbent. The most obvious advantage of such refrigeration machines is possibility of freezing (cooling below $0\text{ }^\circ\text{C}$), which is not possible if water is used as refrigerant because of possible freezing in the condenser.

Note 2: Instead of a liquid mixture of refrigerant-absorbent, a solid sorbent that adsorbs the refrigerant in during the sorption process, while releasing the refrigerant at the input of heat is used in adsorption refrigeration machines. Most commonly, water as refrigerant and silica gel or zeolites as sorbents are used.

Absorption and adsorption chiller efficiency is defined by the ratio of extracted heat from the building (Q_{cold}) to input of energy for the operation of the machine ($W_p + Q_g$). This ratio is called the coefficient of performance (COP_c) of the absorption/adsorption chiller (Fig. 9.8).

The theoretical or Carnot efficiency of absorption/adsorption refrigeration cycle $COP_{C,th}$ depends on the absolute temperature of delivered heat in a generator (T_g), the absolute temperature of the outdoor environment where heat from the absorber and condenser is rejected ($T_{outdoor}$), and the absolute temperature of the chilled water needed to cool the building ($T_{chilled}$):

$$COP_{C,th} = \frac{T_{chilled}}{T_g} \cdot \frac{(T_g - T_{outdoor})}{(T_{outdoor} - T_{chilled})} (-)$$

absolute temperature of chilled water (K) absolute temperature of outdoor environment (K)
 absolute temperature of heat delivered to generator (K)

Compared to absorption chillers, adsorption runs at lower driving temperatures ($T_g > 350\text{ K}$; $\theta_c 75\text{ }^\circ\text{C}$) but has lower coefficient of performance. Absorption and adsorption refrigeration cycle machines are significantly less efficient than the vapour compressor cycle because they have COP in the range 0.5–0.7.

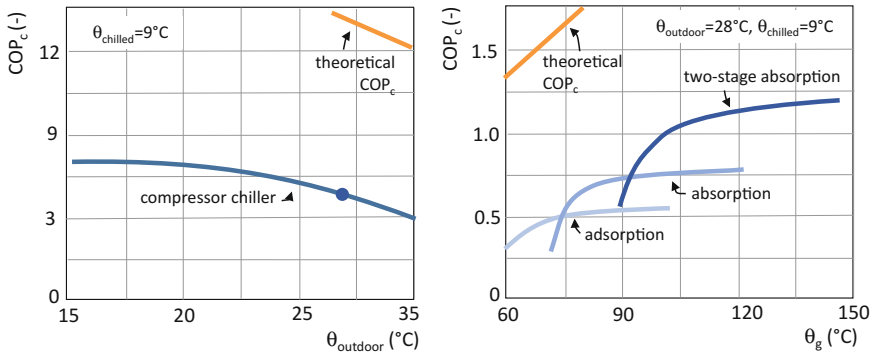


Fig. 9.9 Theoretical—Carnot and actual efficiency of vapour compressor and absorption refrigeration machine

Nevertheless, especially large units with design cooling power from several hundred kW up to several MWs are cost effective if heat is available at low cost and because they run at lower maintenance costs (Fig. 9.9).

Note: COPs of absorption chillers can be increased with a double stage absorption process in which the process runs at two temperature levels with additional pair generators/condensers. In this case, heat must be provided at temperatures above 150 °C, commonly by water steam. Solar energy can be utilized with concentrating solar concentrators (CSC). Water steam can be generated in the flasher, i.e. a pressure vessel in which the pressure of hot water (~ 180 °C) decreases and water evaporates, or in a heat exchanger in which oil heated in CSC as heat transfer fluid boils the water. Market-available double-stage absorption solar refrigeration machines have rated cooling power between 16 kW (driven by parabolic CSC with area of 32 m²) up to 580 kW (CSC area of 1024 m²) (Fig. 9.10).



Fig. 9.10 Parabolic CSC with area 32 m² that drives double stage absorption chiller with rated cooling power of 16 kW (left), (Broad Technology Centre, China) 180 m² CSC array of the double-stage chiller with cooling power of 116 kW [middle, right; Lokurly 2010]

9.4 Mechanical Space Cooling Systems for nZEB

As shown in Fig. 9.3, mechanical space cooling of buildings can be implemented through direct evaporation (DX) or chilled water systems. Chilled water systems that have either compressors or heat (absorption/adsorption)-driven chillers are divided by the type of the cold transfer fluid inside the building into all-air, all-water, or mixed systems.

While DX systems can be decentral (cooling of one room only) or central (cooling of multiple rooms at the same time) and the refrigerant itself is cold transfer fluid in the whole cooling system, chilled water cooling systems are always central, and water as heat transfer fluid is commonly cooled to 5–7 °C in the chiller. Chilled water is then pumped into air handling units (AHU) in the case of all-air cooling systems or into end heat exchangers in rooms through a distribution system in case of all-water system. Chilled water cooling systems can only provide cooling of the building, while DX systems can be transformed into air heating systems as they can operate as heat pump in a reverse cooling cycle operation. The important difference between DX and chilled water systems is in the element by which heat from building is transferred to the outdoor environment. In DX systems, the condenser of the chiller perform this task; in chilled water cooling systems, an additional component called cooling tower is needed; it can be designed as dry or wet type. Mixed chilled water cooling systems are used for the air conditioning of the buildings because such systems must provide other tasks, such as fresh air supply and humidification/dehumidification of the indoor air as well. In this case, cold is transferred into the building by the AHU-cooled air and chilled water distribution system.

9.4.1 Direct Evaporation (DX) Cooling Systems

The label DX indicates that there is direct heat exchange between the refrigerant in the evaporator and the indoor air. Most commonly, DX systems are designed as split ones, which means that an evaporator is installed in the cooled space (room), while the rest of the chiller components [compressor, condenser and expansion device (thermostatic expansion valve or capillary tube in smaller systems)] are installed outdoors. In the case of multi-split systems, several evaporators are connected to one external unit. This enables the adaptive controlling of indoor air temperature in each room. Indoor and outdoor units are connected with pipes, forming the refrigerant loop in which the refrigerant (as liquid towards and gas backwards) circulates (Figs. 9.11 and 9.12).

The advantages of DX systems are (i) efficient controlling of required air temperature in separate rooms, (ii) removal of indoor air pollutants (dust particles) by filter built-in in indoor units, (iii) compact refrigerant loop piping that could be long (several hundred metres) with high vertical distance (up to 50 m) (Bhatia 2012), (iv) refrigerant pre-filled components, (v) large number of indoor units that can be connected to one outdoor unit (100+) and (vi) operation as heat pump when heating is needed. Such systems are easy to install in renovated buildings. The best available technologies (BAT) have COP up to 4.5. Advanced technologies utilize

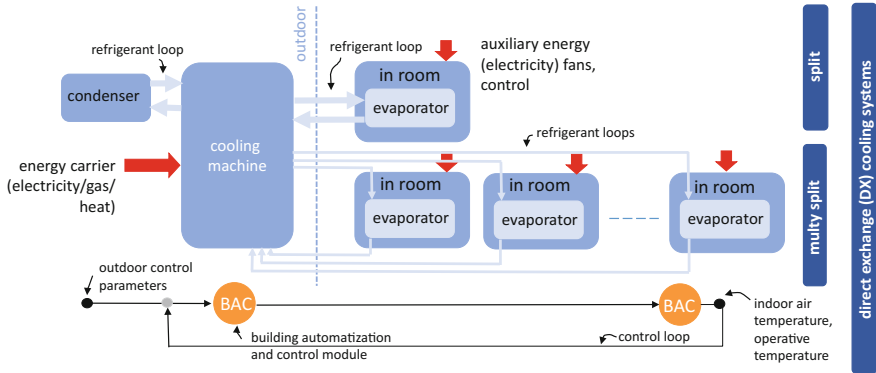


Fig. 9.11 Schematic of direct exchange (DX) space cooling system

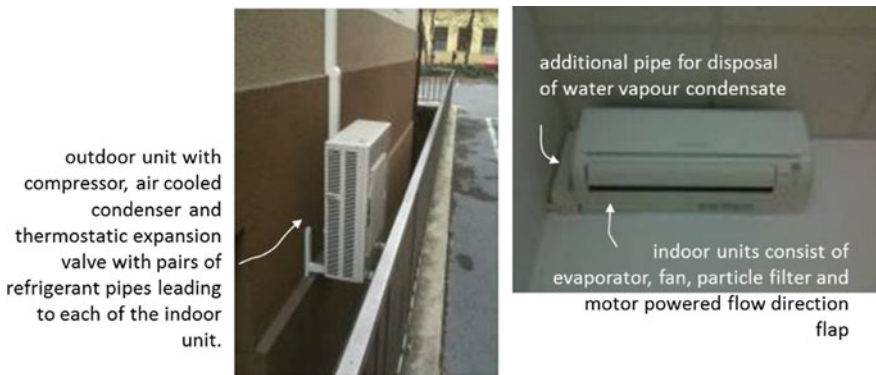


Fig. 9.12 Multi-split DX space cooling system in renovated office building

heat from cooling by recovery units instead to expelling it to the environment. The COP of such a chiller is 7 or higher.⁴

9.4.2 Chilled Water Space Cooling Systems

Chilled water space-cooling systems consist of several components, such as chiller (s) that generate chilled water, cooling water loops that connect the chiller to the cooling tower needed for rejecting the heat from the building to the outdoor environment, a chilled water distribution system in the form of supply and return pipe networks, water-to-air heat exchangers for cooling the supply air in the air handling unit (AHU) in the case of all-air systems or end heat exchangers built in

⁴Daikin Industries, Ltd., www.daikin.com.

cooled spaces to extract heat by convective and radiant heat flux in the case of all-water systems and control units consisting of sensors and actuators to adapt the mass flow rate and temperature of chilled water to the actual cooling load of the building and separate thermal zones (e.g. rooms). Cold storage may be built-in optionally between the chiller and chilled water distribution system.

The main advantages of chilled water space cooling systems over DX systems are (i) higher cooling capacity and longer durability of refrigeration machine, (ii) lower cost in the case of cooling of large buildings, (iii) distribution of cold over long distances in multi-storey buildings is possible, (iv) use of low cost and non-toxic cold transfer fluid, (v) free cooling can be implemented by direct cooling of chilled water with cooling water from during the mid-season, and (vi) use of cold storage. In contrast, additional components, like cooling towers, are needed and circulation pumps must be installed in cooling and chilled water loops resulting in the increase use of auxiliary energy. COPs of chillers depend on temperature conditions (temperature of cooling water on the inlet of chiller condenser and temperature of chilled water at outlet of chiller evaporator), type of compressor and cooling tower. The best available technologies (BAT) of chillers have COP in the range between 4.5 (for chillers with screw compressor and dry cooling tower) and 7 (for chillers with centrifugal compressor and wet cooling towers) (Fig. 9.13).

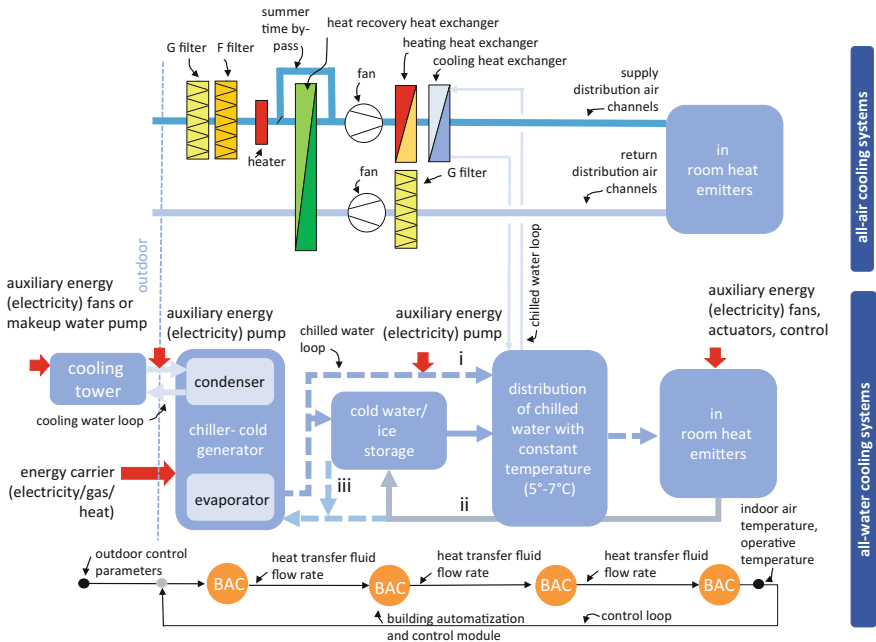


Fig. 9.13 Schematic of all-air and all-water space cooling systems; options i–iii indicate flow directions of chilled water in the case of all-water system with integrated cold storage; *note* most commonly, chilled water is cooled to 5–7 °C, but can be as high as 15 °C if a building is cooled by thermal activated building structures (TABS) or floor-or-ceiling cooling loops; in this case, a chiller will operate at higher COP

9.4.2.1 Major Components of Chilled Water Space Cooling Systems

Chillers

Chillers in chilled water space cooling systems are compact units with a compressor, expansion valve and water-cooled condenser and evaporator in the form of shell and tube heat exchangers. Tubes in an evaporator heat exchanger are connected with chilled water loop and provide heat transfer from return chilled water to the refrigerant. Tubes in a condenser heat exchanger are connected with cooling tower by cooling water loop. Heat is transferred in condenser from refrigerant to cooling water, which is pumped into the cooling tower where heat is released to the outdoor environment. Most commonly, chillers are installed in technical rooms inside buildings and, therefore, are



Fig. 9.14 Water-cooled vapour compressor refrigeration machine or chiller, full cooling capacity 123 MW_c (350 ton), motor electrical power 250 kW_e, rated COP 4.933 (Carrier, Evergreen 19 XR, Hermetic centrifugal water chiller)



Fig. 9.15 Packed chiller and cooling tower unit on the top of the roof of shopping centre (left) and office building (right). To prevent freezing of water in the outdoor section of a chilled water loop (i) antifreeze fluid (glycol) could be added to chilled water, (ii) pipeline could be heated by a wire electrical resistance heater installed on the pipes’ outer surface, (iii) a chilled water pipeline can be drained manually until next cooling season

protected against weather impact. If they are designed as packed units, they consist of a chiller, cooling tower and circulation pumps in one assembly and can be installed outside of the building, most often on the flat roof of the building (Figs. 9.14 and 9.15).

Compressors

Compressors are mechanical devices that increase the pressure of the refrigerant by reducing the refrigerant volume in reciprocating, scroll, or screw type compressors or by the conversion of the angular momentum of the rotating impeller to the pressure energy of the refrigerant vapour in centrifugal compressors. Compressors are most commonly driven by electrical motors and rarely by piston gas engines.

In the reciprocating or piston compressor, the vapour of the refrigerant enters the piston chamber and is compressed as the piston rises. Due to the pressure losses through the partial open valve, full-load efficiency is lower in comparison to other types of compressors, but the decreasing of efficiency at partial load is the lowest. Such compressors are common in small and medium-sized chillers with cooling capacity up to $100 + \text{kW}_c$. Scroll compressors consists of two spiral-shaped scroll assemblies, one scroll assembly rotates, while the other is stationary. The vapour of refrigerant is compressed between the scrolls. Such compressors are used in applications with cooling capacity from several kW_c to several hundreds of kW_c . Screw compressors consists of male and female helically grooved rotors. The vapour of the refrigerant is compressed between the screw teeth during rotation. Screw compressors are used in all sizes of chillers. Centrifugal compressors consist of a single impeller or a number of impellers mounted on the shaft that rotates at high speed inside the housing. Refrigerant enters the impeller in the axial direction and is discharged radially. Such compressors are used in large capacity chillers with cooling capacity up to several tenths of MW_c .

The best available compressor technologies have inverter-driven electrical motors. This is technology of frequency-controlled electricity supply to the compressor's electric motor that improves the control of cooling power and the temperature of the refrigerant. In DX systems, inverter technology can be implemented in outdoor units (condenser fan motor) and indoor units (evaporator fan motors) to provide more precise control of indoor air temperatures and improve the efficiency of cooling system (Fig. 9.16).

Note: Compressors can have open drives or can be semi-hermetic or hermetic. In the case of open drives, the compressor motor is separated from the assembly. In semi-hermetic compressors, the compressor and motor drive are in the same assembly, but the motor can be disconnected in the case of malfunction; in hermetic compressors, the compressor and motor are sealed in the one assembly, and the whole unit must be replaced in the case of malfunction.

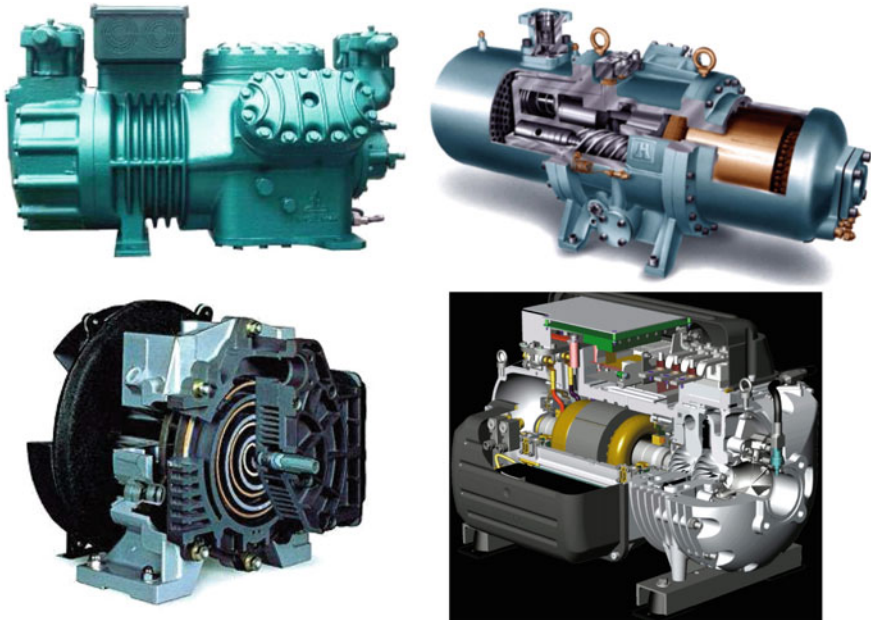


Fig. 9.16 Types of compressors commonly used in vapour compression chillers; top left (www.danfoss.com): reciprocating; top right (www.bitzer.de): screw; bottom left (www.daikin.com): scroll; bottom right (www.smardt.com): centrifugal

Cooling Towers

A cooling tower is an essential component of a chilled water space cooling system because it provides transfer of the heat released in the condenser of the chiller to the outdoor environment: to the atmosphere. The quantity of heat that must be rejected in the cooling tower is equal to the sum of heat extracted from the building and the energy used for operation of the chiller. A cooling tower can be closed loop or dry (air cooled) or open loop or wet (water cooled) one.

A dry cooling tower consists of a finned pipe heat exchanger and a fan that increases the air velocity inside the heat exchanger and, therefore, the heat transfer coefficient. Heat is transferred by sensible heat flux and, therefore, cooling water can be cooled only to few degrees above dry-bulb temperature (=outdoor air temperature). Because the cooling water circulates in the close loop, there is no need for occasional refilling and treatment of the cooling water. In a wet cooling tower, heat is released to atmosphere mainly as latent heat. Warm cooling water from the chiller condenser is pumped into the cooling tower and sprayed on the surface of the filling structure. At the same time, outdoor air is flowing above the wet surface of the filling structure with the aid of the fan, causing some of the water to evaporate and cool. Cold cooling water is captured in a water basin at the bottom of the cooling tower and pumped back into the condenser. Because some cooling

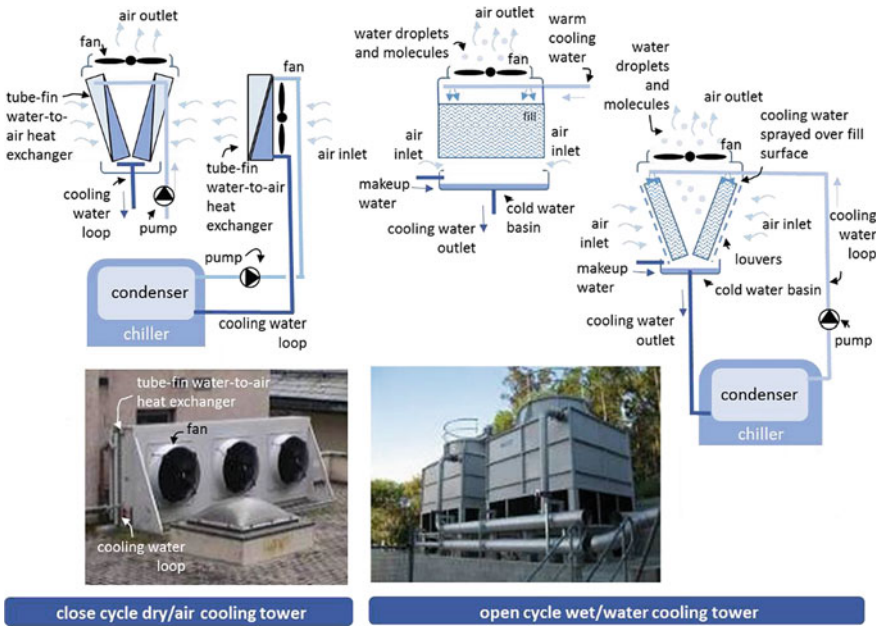


Fig. 9.17 Schematics of operation and examples of dry and wet cooling towers of chilled water space cooling systems; designers must carefully study possible local environmental impacts of cooling towers because of noise caused by fans and air pollution by microorganisms in aerosols in the case of wet cooling towers; noise barriers and regular maintenance can be effective solutions

water evaporates, an additional amount of makeup water must be constantly added. This increases the cost of cooling because of the cost of the makeup water and water treatment. A wet cooling tower operates in an open loop and pollutants (e.g. particles) must be removed from water basin occasionally. All this makes a wet cooling tower costly for the initial investment and ongoing maintenance, especially at locations with limited fresh water supply. Nevertheless, a major advantage of wet cooling towers is in the higher efficiency of chiller operation because temperatures in the condenser are lower in comparison to dry cooling towers. As heat is transferred in wet cooling towers mainly by evaporation, cooling water can be cooled to few degrees over the wet-bulb temperature of outdoor air, which is significantly lower than dry-bulb outdoor temperature, most of the time (Fig. 9.17).

Cold Storage

Cold storage may be installed between the chiller and chilled water distribution system. The main advantages of cold storage in the space cooling system are:

- design cooling capacity of chiller $\dot{Q}_{c,design,g}$ can be lower because cold can be stored during the low cold demand night-time period or non-occupied hours and used later during high demand periods;
- electrically driven chillers can operate during the night-time period of cheaper electricity;
- in the case of solar-driven chillers (e.g. photovoltaic-driven vapour compressor chillers or solar thermal absorption chillers), sufficient cold can be provided during the evening and night time.

Most commonly, water is used for storing cold in form of sensible or latent cold. Regardless of the type, storage operates as short-time storage because cold is stored only for approximately half a day of cooling of the building. In sensible storage, water is cooled to 4–5 °C and at average operation conditions ~ 10 kWh of cold can be stored in 1 m³ of water. In the ice, 80 times more latent cold can be stored in a cubic metre in comparison to sensible cold in water. However, the design of latent (ice) cold storages is more complicated, because heat inside the ice layer is transferred by conduction only, and ice is a poor heat conductor. Because of that, cold is stored in thin layers, not more than 2–4 cm tick, which requires a large area of heat

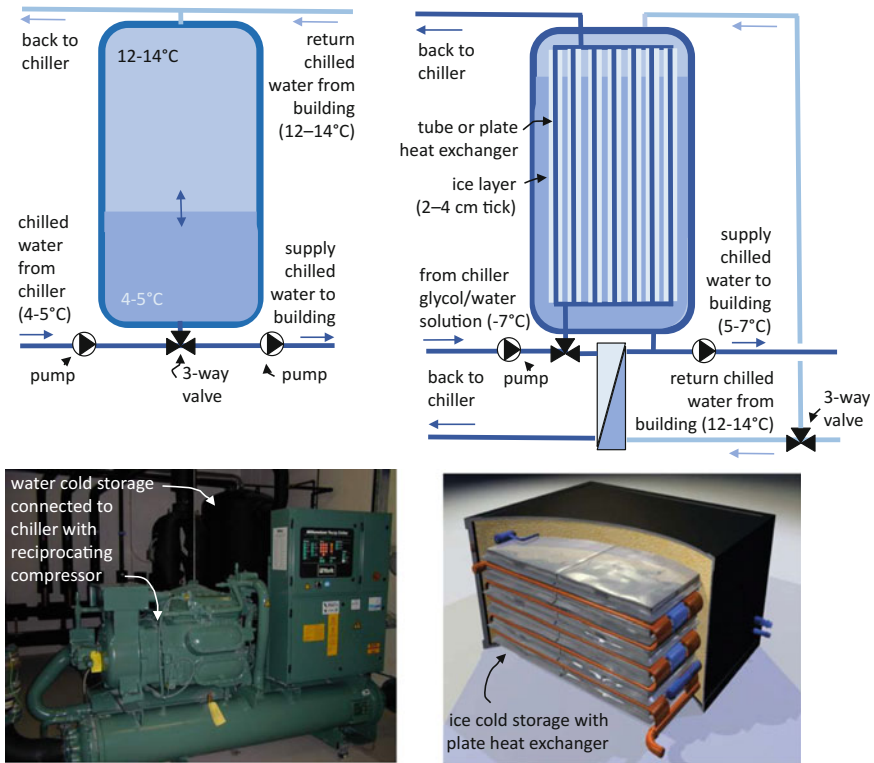


Fig. 9.18 Sensible water and latent ice cold storages which are mostly used in chilled water space cooling systems (Omega Thermo Products, www.omegathermoproducts.nl)

exchanger that is submerged in the storage vessel. Another disadvantages of ice cold storage is that the chiller must operate at lower evaporator temperature (~ -7 °C) and a mixture of glycol and water must be used in chilled fluid loop. Under such operating conditions, efficiency of chillers is up to 40% lower; the cost effectiveness of ice cold storage must be studied carefully (Fig. 9.18) (Kosi 2015).

Chilled Water Distribution Pipe Network

A chilled water distribution pipe network connects the chiller with a water-to-air heat exchanger in AHU or/and end heat exchangers installed inside the cooled building spaces. The distribution system should be designed similarly to the distribution network in hydronic space-heating systems (see Sect. 8.4). Two-pipe networks are common. All elements of chilled water distribution must be insulated with vapour-tight insulation to prevent condensation on the outer surface of pipes. As the temperature difference between chilled water and indoor air temperature is smaller than in the case of space heating, the thermal insulation can be thinner (up to several cm). Operation with variable flow rate (see Sect. 8.8) improves space air temperature controlling and decreases auxiliary electricity demand for operation of pumps.

End Heat Exchangers

End heat exchangers are needed for transfer heat flux out of the cooled space. Several types of end heat exchangers that are used for hydronic space heating can be used for space cooling as well. While use of fan-coils (see Sect. 8.5.2) prevails, active beams (see Sect. 8.5.3), floor and ceiling radiant heat panels (see Sect. 8.5.4) and thermal activated building structures (TABS, see Sect. 8.5.5) can be used for extract heat from indoor cooled spaces.

As the temperature difference between the average chilled water temperature circulated through end heat exchange and indoor air temperature is lower in comparison to space heating, lower heat flux transfer per unit of end heat exchanger size can be achieved. This must be compensated by increasing the size of heat exchanger and/or increased flow rate of cold transfer fluid.

Control of Chilled Water Space Cooling Systems

Controlling of space cooling systems should follow the measures described in Sect. 8.6 for the space heating of a building. As cooling systems mostly operate at partial load conditions and the range of chilled water temperature adjustment is small (\sim between 5 and 18 °C), the variable mass flow rate operation is essential for controlling the amount of the cold delivered into the building at high chiller

efficiency. BAT are frequency controlled electro-motors (inverter drives) for compressors, circulation pumps, and fans in fan-coil end heat exchangers.^{5,6}

9.5 Environmental Impacts of Space Cooling

The cooling of the buildings has environmental impacts related to global climate change and health issues because it affects the global warming and stratospheric ozone depletion. Environmental impacts can be reduced by decreasing the use of electricity for operation of chillers and cooling systems, the energy carrier that has the highest environmental impacts (see Sect. 2.3) among non-renewable energy carriers. Solar cooling is another measure to reduce the contribution of space cooling to global warming. The second major measure to protect the environment is the use of refrigerants with lower global warming potential (GWP100) and ozone depletion potential (ODP). These properties of refrigerants are presented in detail in Sects. 6.2.2.3 and 14.4.

Case Study Daikin, a manufacture of chillers uses refrigerant R32 instead of the currently most commonly used refrigerant R410A. Both refrigerants have ozone depletion potential ODP equal to 0, but R32 has global warming potential GWP₁₀₀ equal to 675 CO_{2,eq} while R401A has GWP₁₀₀ equal to 2090 CO_{2,eq}.⁷

9.6 Energy Needs and Delivered Energy for Space Cooling

In Sect. 5.3.2, the energy needs for space cooling (Q_{NC}) are presented. Energy needs are defined according to solar and internal heat gains, as well as transmission and ventilation heat losses. The monthly average cold gain utilization factor in the case of the monthly method or detailed unsteady modelling of heat transfer in building structures in the case of the hourly method is used to take into account the influence of the heat accumulation in the building on the energy needed for space cooling.

Delivered energy (final energy) for space cooling ($Q_{h,c}$) is calculated by energy balance on monthly or hourly time steps, taking into account energy needs and the design and thermal properties of all components/devices of a space cooling system, as

⁵Report on Application of High Efficient Chillers, www.emsd.gov.hk/filemanager/en/content_764/Aplctn-Hgh-Efcny_Chtrs.pdf, 2015.

⁶Mitsubishi Electric Cooling & Heating, www.mitsubishicomfort.com/technology, 2018.

⁷Daikin; R-32, next-generation refrigerant, 2018.

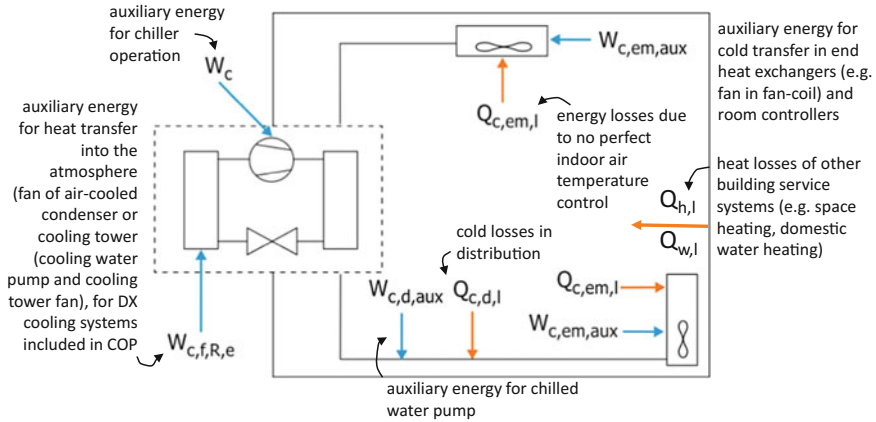


Fig. 9.19 Energy flows in chilled water cooling system (orange arrows indicate heat, blue arrows electricity)

described in Sect. 5.4. The procedure starts with the determination of the energy needed for space cooling (Q_{NC}), the determination of chiller, the heat storage and distribution system as well as heat losses of end heat exchangers due to imperfect controlling of the indoor air temperature. Auxiliary energy for the operation of the space cooling system, including operation of the chiller, pumps (all-water) or fans (all-air) in distribution subsystems and the cooling tower (chilled water cooling systems) or the fan and end heat exchangers built in the thermal zones (rooms) and control units.

Because of the low temperature difference between heat transfer fluid and indoor air temperatures, heat losses of the cold storage and distribution system are not taken into account in all-air or in all-water cooling systems. In Fig. 9.19, energy flows for a chilled water space cooling system are presented following the nomenclature introduced in EPBD-supporting EN standards (see Sect. 5.4).

Case Study What will the delivered energy be for chilled water space cooling of the Virtual Lab building? The set point indoor air temperature in the technical and living units is 26 °C. Internal heat gains in the living unit are constant 27.1 W/m² (from 2 persons and appliances) and 13.3 W/m² due to the heat losses of the solar heating system heat storage and piping in the technical unit. Characteristics of the chiller and distribution system and devices are shown in the tables below. The balance of energy flows is determined for each of the month of the year and then summarized to yearly delivered energy (Fig. 9.20).

Seasonal performance indicator (SPI) of the space cooling system is equal to (Fig. 9.21):

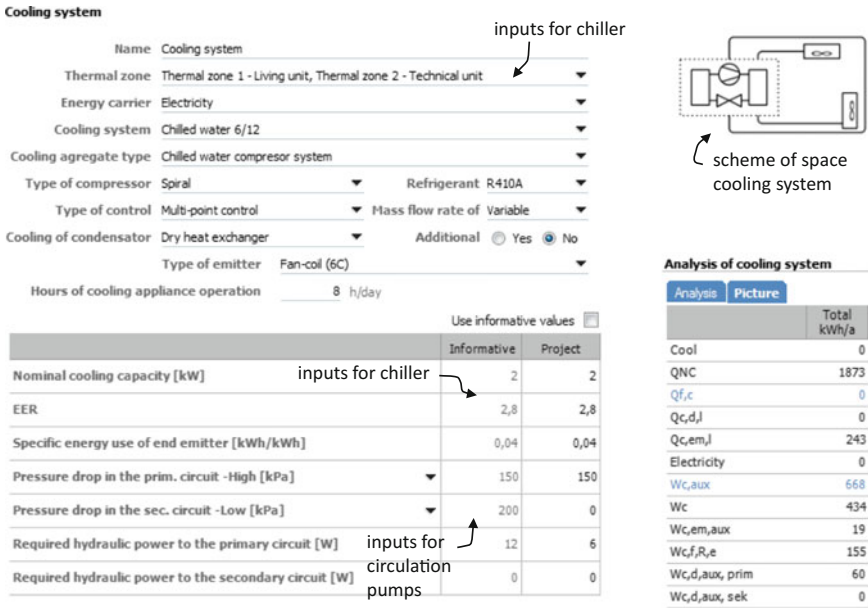
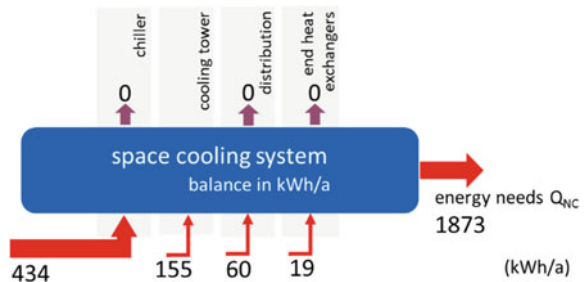


Fig. 9.20 Final energy use for space cooling of the Virtual Lab building

Fig. 9.21 Energy balance of the virtual space cooling system in the Virtual Lab building



$$SPI_c = \frac{Q_{NC}}{2.5 \cdot (W_c + W_{c,f,R,e} + W_{c,d,aux} + W_{h,aux})} = \frac{1873}{2.5 \cdot (434 + 155 + 60 + 19)} = 1.12$$

Note: Weighting factor 2.5 for electricity is defined according to environment impact as the mix of technologies used for electricity production in the EU.

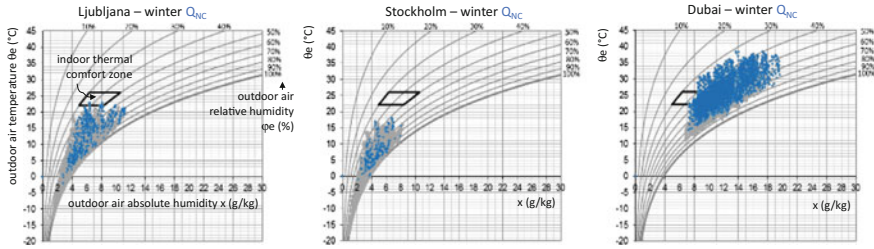


Fig. 9.22 Bioclimatic diagrams for Ljubljana, Stockholm and Dubai; hour-by-hour outdoor air temperature, absolute and relative humidity in the period between October to March are shown with grey dots, while blue dots show the hours when space cooling is needed; *note* hours of space cooling are shown for an office building with an all-glass envelope and high internal heat source; values were determined using dynamic thermal response modelling

9.7 Principles of Rational Use of Energy for Space Cooling

The energy demand for space cooling and the energy efficiency of space cooling systems depend on architectural design of the building, the design, operation control, the maintenance of the system and the durability of the components and devices in whole life cycle of the space cooling system. As presented in Sect. 8.8, the local climate should be studied using bioclimatic diagrams to determine the risk of overheating, the length of the space cooling period, and the potential of natural cooling techniques (Fig. 9.22).

9.7.1 Architecture Design

The adoption of vernacular architecture principles including the use of locally available construction materials, the implementation of local building traditions, and the thermal zoning of the indoor space are the most effective ways of reducing the need for space cooling of the buildings. Technology aspects of architecture design that lead to the reduction of problems related with overheating and increased use of energy for space cooling will be discussed in this chapter (Santamouris 2006).

9.7.1.1 Reducing the Solar Gains Through Transparent Envelope Structures

Solar gains through transparent building envelope structures, most likely the glazing of the windows, are determined by total solar energy transmittance g (see Sect. 3.1.9). With the respect of the overheating and in general, the g -value should be below 0.25 if total area of glazing is up to 1/5 of the zone floor area and below 0.10 in case of all-glass buildings. Such a low g -value can only be achieved by installing high solar radiation reflective external shading devices, as shown in Fig. 3.16.

Note: Selection of glazing according to the total solar energy transmittance must be based on the holistic study of the solar gains during heating period and daylight study.

9.7.1.2 Reducing the Solar Heat Gains Through Opaque Structures

The outdoor surface of the building structures absorb shortwave solar irradiation and exchange longwave (IR) irradiation with the sky and surroundings. As a result, structures heat up above the outdoor air temperature during the daytime. As a consequence, heat flow towards the building's interior is driven by the outdoor envelope building structure's surface temperature, rather than the outdoor air temperature; as a result, the process of heat transfer becomes dynamic. That is why the heat transfer coefficient of the building structure, the U-value, as a static parameter that is determined at constant outdoor and indoor air temperatures, cannot be used for the modelling of dynamic heat transfer in opaque envelope building structures. In dynamic modelling of heat transfer in opaque envelope building structures, the U-value is replaced by two dynamic indicators: decrement factor f and time delay ϕ (Medved 2014; Davies 2004).

Decrement factor f is defined as the ratio of the daily maximum rate of heat flow at the indoor surface of the structure that is caused by the variation of outdoor air temperature by ± 1 K around the daily average value during 24 h period, while indoor air temperature is kept constant at a value equal to the average daily outdoor air temperature. Decrement factor f is in the range between 0 and 1. Value 1 indicates that heat flux at the indoor surface of structure responds immediately to the changes of outdoor conditions (with time delay 0 h), while value 0 indicates that the building structure is adiabatic and outdoor conditions have no influence on the interior of the building (with infinity time delay). Heavy building structures have decrement factor f below the 0.25 (and time delay > 8 h), while light weight building structures have decrement factor f above the 0.75 (with time delay 1–2 h). To minimize cooling load caused by dynamic heat transfer through opaque building structures, they should be designed so that their decrement factor f is below 0.3.

Case Study Two opaque envelope building structures consist of three layers. The lightweight structure consists of inner gypsum plasterboard (1.5 cm thick), thermal insulation layer (25 cm, density 33 kg/m^3) and polyethylene foil (0.1 cm), while the heavyweight structure consists of inner gypsum plasterboard (1.5 cm thick), concrete layer (15 cm, density 2200 kg/m^3) and thermal insulation layer (22 cm, density 80 kg/m^3). Both building structures have equal heat transfer coefficients ($U 0.15 \text{ W/m}^2\text{K}$) but have significantly different dynamic heat transfer properties (f , ϕ) (Fig. 9.23).

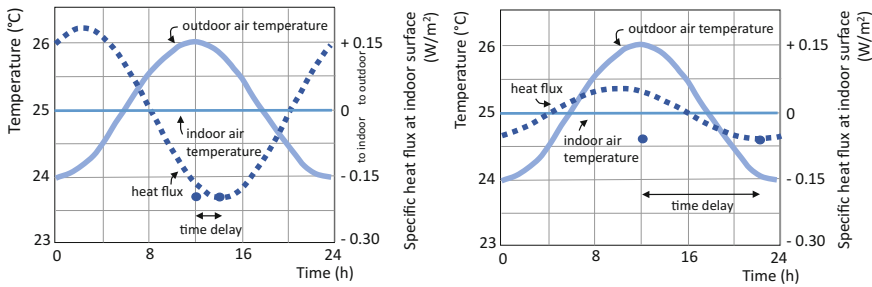


Fig. 9.23 Dynamic thermal response of two roof structures with the same heat transfer coefficient U equal to $0.15 \text{ W/m}^2\text{K}$; lightweight (left), heavyweight (right)

Decrement factor f of the lightweight building structure is equal to 0.938 (–) and time delay ϕ is equal to 2:22 h, while the heavyweight structure with the same heat transfer coefficient U has a decrement factor f 0.30 (–) and time delay ϕ 10:01 h (Medved et al. 2004).

Another measure for reducing the solar gains through opaque building envelope structures is the use of high solar irradiation reflective colour coatings called cool colours. A bright white outer surface coating reflects visible (wavelengths 0.38–0.76 μm) as well as near infrared (wavelengths 0.78 to 3+ μm) parts of solar irradiation and has high emittance for the longwave infrared irradiation that is emitted from outer surface of the structure (Synneta et al. 2007). Cool colour coatings are most effective on flat roofs. For example, in comparison to a dark grey bitumen outer layer, the surface temperature of a cool colour coating could be as much as 40 °C lower on a clear summer day. If architects design dark-coloured building envelope structures, selective coatings can be used to decrease the temperature of the outer surface of the building envelope at times of high solar irradiation. Such a coating absorbs and reflects pre-designed wavelengths of the visible solar irradiation (to achieve the desired colour of building envelope), but has high reflectance of all other wavelengths of solar irradiation that have no influence on the colour of the structure and have high emissivity for all wavelengths of thermal irradiation emitted by the envelope surface towards surrounding. An example of such a selective coating is presented in Fig. 9.24. Research shows that a decrease of surface temperature up to 15 °C can be achieved in case of dark green, dark grey, or black surfaces in comparison to non-selective coatings.

9.7.1.3 Greening of Building Structures

Greening of facades and roofs of buildings not only (i) decreases heat flow toward the interior, but (ii) absorbs air pollutants, (iii) retaining precipitation water, thus relieving the urban drainage network and reducing the use of water for irrigation of

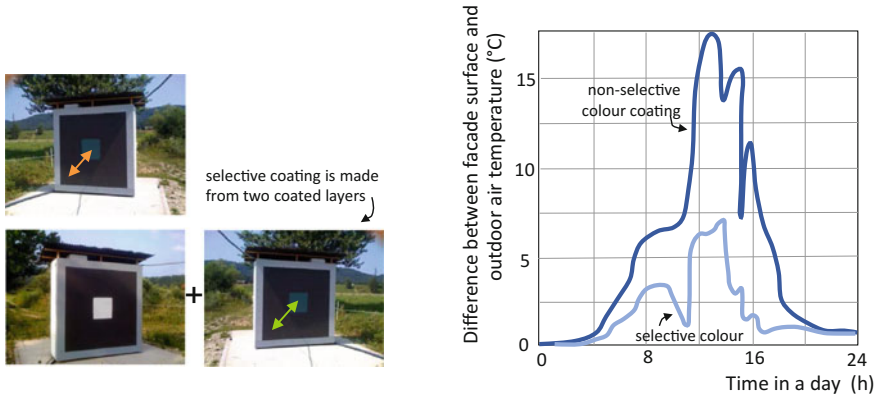


Fig. 9.24 Example of thermal response of the façade with non-selective and selective dark green coating in a selected sunny day; the surface of the façade with selective coating is up to 10 °C cooler in comparison to ordinary (non-selective) façade coating

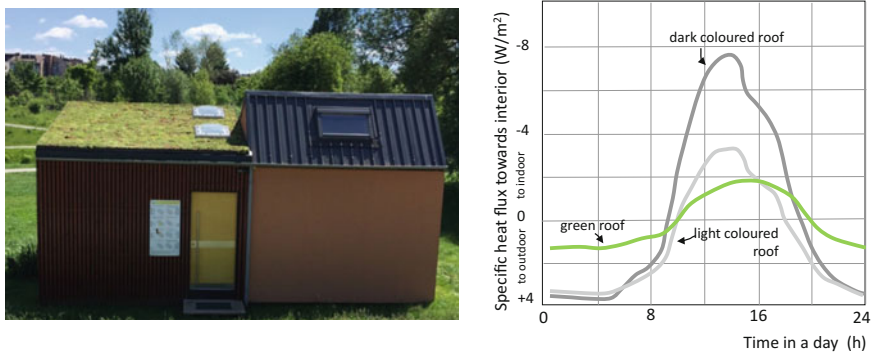


Fig. 9.25 Green roof on the technical unit of the Virtual Lab building (left), heat flow rate towards interior of the building with ordinary and green roof (right); *note* lower heat flux through the green roof during the night time is due to respiration, a process opposite to the photosynthesis that occurs in the plants during the dark part of the day

plants and (iv) decreases outdoor air temperature, as well as redirecting air currents and improving outdoor air quality. All these advantages of greened structures are especially important in the urban environment. Most of these advantages are the consequence of the evapotranspiration, transportation of water from earth by roots towards the plant leaves where water droplets evaporate and cool both the plant and the surrounding air (Fig. 9.25) (Arkar 2018; Vidrih and Medved 2013).

9.7.2 Natural Cooling and Free Cooling of the Buildings

Natural or passive cooling of the nZEB is most commonly achieved by intense night-time natural ventilation. This technique is presented in Sect. 11.4.2. Natural cooling by ventilation can only be effective if high air exchange rates are achieved. Numerical models for the determination of air exchange rates in the case of large and small ventilation openings are presented in Sect. 11.1.3.

9.7.3 Free Cooling

Principles of free cooling are presented in Sect. 9.3. As explained, free cooling can be implemented, for example, by intensive mechanical ventilation, by cooling the supply air in the ground heat exchanger that operates in bypass mode enable that supply air flows directly into the building or by evaporative cooling. Evaporative cooling is the most commonly implemented free cooling technique because it has the highest coefficient of performance (COP). In some states (e.g. Slovenia) evaporative cooling is obligatory in the case of large buildings with mechanical ventilation. With free cooling, fresh supply air is cooled in the AHU with a water evaporative cooling process (see Sect. 3.2). As result of small water droplet evaporation in the stream of the air, the air cools and become more humid. The lowest temperature that can be achieved in this way is equal to the wet-bulb temperature of the air, which can be significantly lower than the temperature of outdoor supply air. Such a cooling process needs no auxiliary energy with the exception of a small amount of energy required for the pumping of the water through spray nozzles. The process itself is adiabatic, as the internal energy (enthalpy) of the supply air does not change.

Evaporative cooling can be direct or indirect. In the case of the direct evaporate cooling process, water droplets are sprayed directly into the flow of supply air. This means that air with lower temperature but higher humidity enters into the living spaces. As a consequence, indoor living comfort can deteriorate. The direct free cooling process is efficient in the climates with high summer outdoor temperatures at low air humidity. To avoid additional humidification of the supply air, extracted air can be cooled by an evaporation process before entering the heat recovery heat exchanger in the AHU. Supply air is cooled in the heat exchanger at constant absolute humidity (without increasing the amount of the water vapour in the supply air). This principle is commonly used in climates with high summer outdoor air temperatures at moderate air humidity (Figs. 9.26 and 9.27) (SOLAIR 2007).

The efficiency of evaporative cooling must be evaluated for local climate conditions and by hour-by-hour modelling; COP up to 100 are commonly achieved.

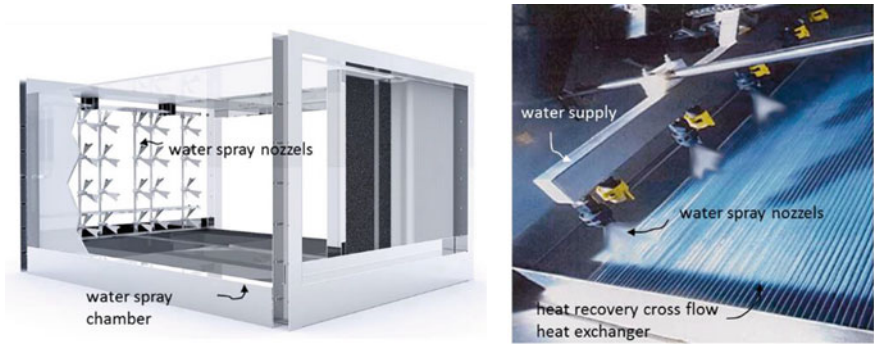


Fig. 9.26 Water spray chamber for direct evaporative cooling of supplied air; cross section of water spray chamber designed to maintain the air velocity in the range 2–4 m/s and is 1.5–2 m long to enable high efficiency evaporative cooling (left) (Klingenburg, www.klingenburg-usa.com); indirect evaporative cooling can be implemented by spraying the water into the air stream and on the surface of heat recovery heat exchanger (right)

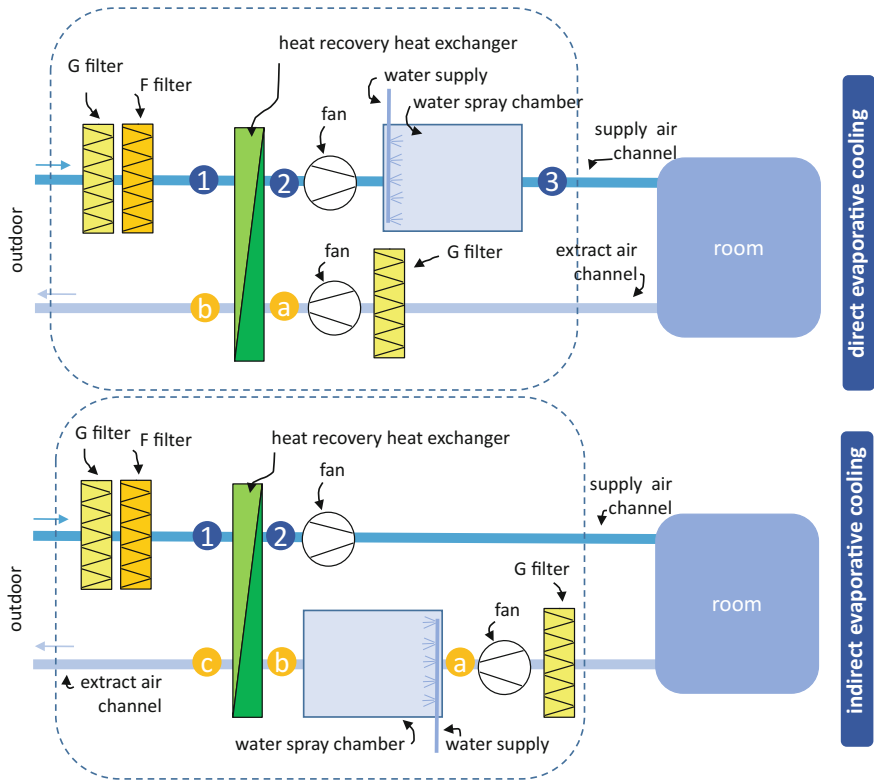


Fig. 9.27 Schematic of AHUs with direct and indirect evaporative cooling process

Note: Free cooling can be provided in chilled water space cooling systems if the chiller is switch off and heat from return chilled water is transferred in by-pass directly into the cooling tower and back to the evaporator of the chiller. In air space cooling systems, free cooling can be implemented if the chiller compressor is switched off and the refrigerant flows between the evaporator and condenser and back in the heat pipe, because the outdoor air temperature is low enough to enable condensation of the refrigerant at lower pressures. Both techniques can be used during the period of low outdoor air temperature (during spring and autumn) only.

9.7.4 Solar Cooling

Solar assistant space heating of the buildings requires the size of solar collectors (SC) array in the range between $1/6$ and $1/3$ m^2 of SC per m^2 of heated floor area to achieve a solar fraction between 0.5 and 0.75. Such a large area of solar collector array is rarely needed for heat supply during the off-heating season and heat can be at zero investment and operation cost used for solar cooling. Absorption and adsorption refrigeration cycles that utilize heat instead of electricity in the case of vapour compressor refrigeration systems are described in the Sect. 9.3. If the building is mechanically ventilated, and nZEB are because the heat recovery of ventilation heat losses is commonly required, another type of solar cooling, called desiccant evaporative cooling (DEC) can be implemented as well. Such systems are known as open cycle solar cooling systems.

Solar-assisted DEC is based on a combination of air dehumidification by a desiccant mater followed by evaporative cooling by spraying water droplets into the supply and extract air stream. Air dehumidification is necessary in locations with high outdoor air temperatures and humid climate (in most parts of Central and Southern Europe) to enable highly efficient evaporative cooling without increasing the supply air humidity above acceptable levels regarding indoor comfort. Dehumidification by sorption is the opposite process to the evaporation cooling process; air is heated during this process. Either solid or liquid hygroscopic material can be used for air dehumidification. The DEC cycle most commonly applied today, using a rotating desiccant wheel with silica gel or plate heat exchanger sprayed with lithium–chloride (Li–Cl) as sorption material. Solar energy is used for heating the air to the temperature above 70 °C, which is needed for the continuous drying of the rotating desiccant wheel. After supply air is dried by the desiccant wheel, air is cooled in a heat recovery heat exchanger by indirect evaporation by spraying water droplets in extract air stream and later by direct evaporation by spraying water droplets in the supply air stream. The DEC process is presented in Mollier's T-x psychometric diagram in Fig. 9.28 (Oprešnik 1987).

See Figs. 9.29, 9.30 and 9.31 (Moran and Shapiro 1998).

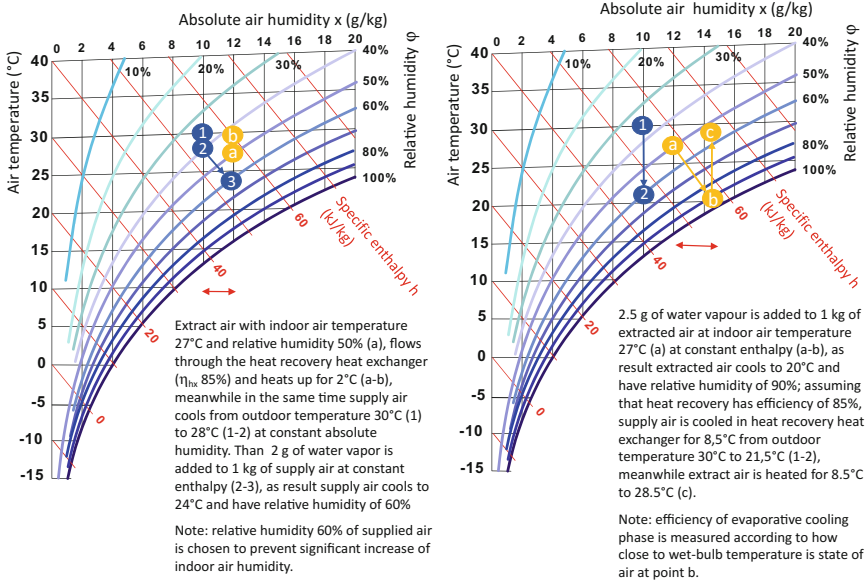


Fig. 9.28 Presentation of direct (left) and indirect (right) evaporative cooling in Mollier’s T-x psychrometric diagrams; comparing the specific enthalpy of indoor air (a) and supply air (3), it can be concluded that 5 kJ per kg of air (Δh a-3) of cold is transferred into the indoor by the supply air in case of direct evaporative cooling and 11 kJ/kg of supply air in case of indirect evaporative cooling (Δh a-2) (right)

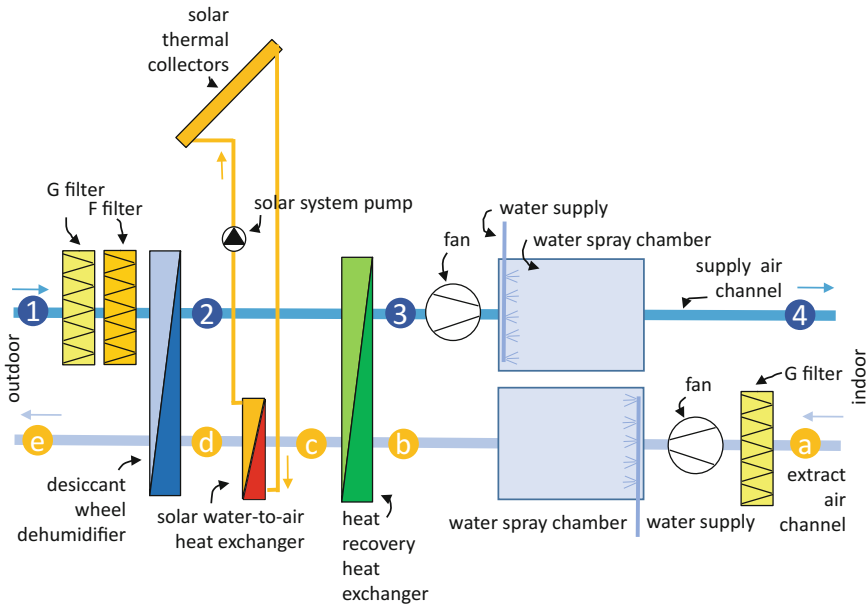


Fig. 9.29 Schematic of desiccant evaporative cooling (DEC) solar cooling process

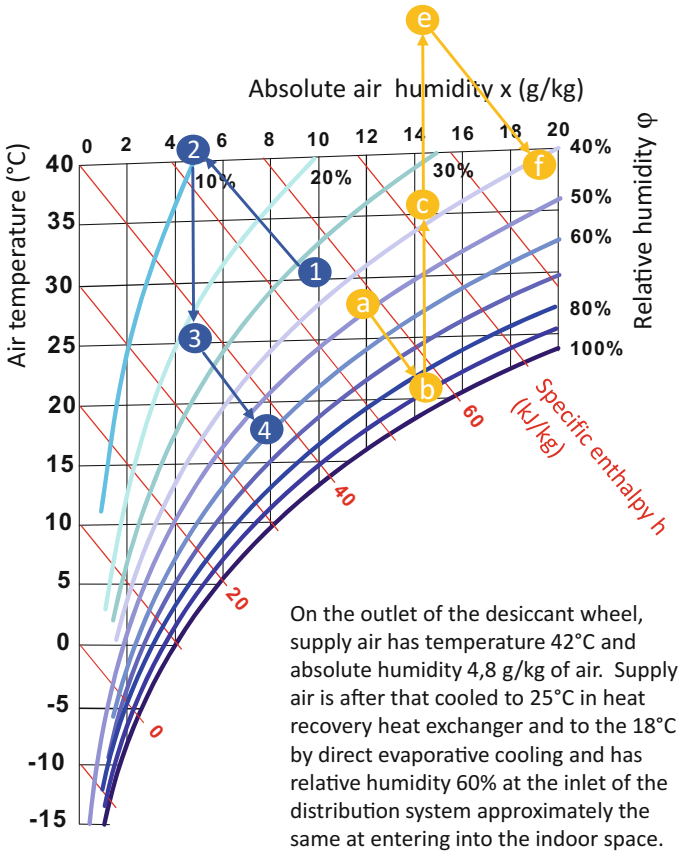


Fig. 9.30 Presentation of DEC solar space cooling in Mollier's T-x psychrometric diagrams; comparing the specific enthalpy of indoor air (a) and supply air (4) it can be seen that 20.5 kJ/kg of supply air (Δh a-4) of cold is transferred into the indoor by the supply air; this is significantly more in comparison the direct and indirect evaporative cooling, as shown in Fig. 9.28



Fig. 9.31 DEC solar cooling system for space cooling of office building; AHU has rated capacity of 6000 m³/h and rated DEC cooling power is 30 kWc; heat for dehumidification of the desiccant wheel is delivered by vacuum solar collectors array with area of 12 m²; DEC system produce $10,000$ kWh of cold at seasonal coefficient of performance 0.6 . (www.oekoplan-hartberg.at)

Note: A survey of existing solar cooling systems in EU made as part of the SOLAIR project (SOLAIR) research shown that average specific solar collector array area 2.77 m² in the case of solar adsorption cooling, 3.5 m² of SC in the case of solar absorption cooling, and 1.8 m² of SC in the case of a DEC built-in in operating solar cooling systems per 1 kWc of rated cooling power. It can be concluded that no additional SC area is needed if the solar collector area is designed to provide a high solar fraction for space heating.

9.7.5 Other Measures for Increasing Energy Efficiency of Space Cooling Systems

Several technical measures can be taken to improve the overall efficiency of space cooling systems. Some examples:

- compressors, pumps, or fans in space cooling systems operate in such a way that the cold transfer fluid flow rate is adjusted to actual cooling needs; this can be done with high efficacy frequency controlled drive motors (inverters). It is assumed that up to 30% of auxiliary energy can be saved in this way. Such pumps or fans are driven by highly efficient electric motors that have 5–10% lower energy demand in comparison to older ones; these measures are even more important in the case of space cooling in comparison to space heating as the temperature range of heat transfer fluid is narrower and adaptation to partial load operation of the space cooling system is mostly done by adjustment of cold transfer fluid mass flow rate;
- distribution pipes and channels network should be as short as possible; lower cold transfer fluid velocity by a factor of 2 will reduce pressure drop by a factor of 8; however, larger distribution network will be costly and cause the increase in the temperature of cold transfer fluid because of distribution network heat gains;
- vertical shafts must be hydraulically balanced; this means that flow in each vertical branch will be adjusted to the current pressure drop in network and end heat exchangers/emitters; this can be done by differential pressure regulators and constant pump total head operation by adjustment of the heat transfer fluid flow rate;
- because cooling systems must respond quickly to changes of the cooling load, the control algorithm should be upgraded by (i) a control algorithm that follows the history of thermal response of the building and adjusts the control protocol to the specifics of the particular building and (ii) a control algorithm that predicts future thermal response of the building by including weather forecasts into the predictive controlling.

References

- Arkar C, Domjan S, Medved S (2018) Raziskava toplotnih in hidroloških lastnosti ozelenjenih streh URBANSCAPE (Survey of thermal and hydrological properties of URBANSCAPE green roofs). University of Ljubljana, faculty of Mechanical Engineering
- Bhatia A (2012) HVAC variable refrigerant flow systems. Continuing Education and Development Inc, USA
- Davies MG (2004) Building heat transfer. Wiley, Hoboken
- Kabele K et al (2012) Heating and cooling. Educational package, IDES-EDU master and post graduate education and training in multi-disciplinary teams implementing EPBD and beyond, IEE/09/631/Si12.558225
- Kosi FF et al (2015) Cold thermal energy storage. In: Handbook of research on advances and applications in refrigeration systems and technologies. Engineering science reference
- Lokurlu A (2010) Integration of renewable energy systems in Mediterranean countries based on SOLITEM parabolic trough collectors. SOLITEM Group Aachen, Germany
- Medved S (2014) Gradbena fizika II (Building physics II. Faculty of Architecture, University of Ljubljana, Ljubljana
- Medved S et al (2004) Termo enciklopedija 2 = Termo encyclopedia 2. Termo, Škofja Loka
- Moran JM, Shapiro NH (1998) Fundamentals of engineering thermodynamics. Wiley, UK
- Oprešnik M (1987) Termodinamika (Thermodynamics). Faculty of Mechanical Engineering, University of Ljubljana, Ljubljana
- Santamouris M (ed) (2006) Environmental design of urban buildings. Earthscan
- SOLAIR (2007) Increasing the market implementation of solar air-conditioning systems for small and medium applications in residential and commerce buildings, EISAS/EIE/06/034/2006
- Synnefa A, Santamouris V, Apostolakis K (2007) On the development, optical properties and thermal performance of cool coloured coatings for the urban environment. Sol Energy 81 (4):488–497
- Vidrih B, Medved S (2013) Multiparametric model of urban park cooling island. Urban Forest Urban Green 12(2):220–229

Chapter 10

Domestic Hot Water Heating in nZEB



Abstract Domestic hot water (DHW) is needed for personal hygiene and washing. In low-energy and passive buildings, energy consumption for DHW water heating can exceed the amount of energy used for heating the building. DHW systems are included in the energy use assessment of the buildings as one of the so-called EPBD (Energy Performance of Building Directive) systems. Since DHW is needed throughout the year, solar energy or ambient heat can be utilized with high efficiency and with significant impact on the share of renewable energy sources in energy for the operation of the building. The rational use of DHW has a major influence not only on the rational use of energy but also on environment protection. Lower DHW consumption decreases drinkable water use, which is pumped from natural reservoirs or treated in water-cleaning systems and transported to the buildings. Lower DHW consumption reduces the drain of waste water that must be treated in central water cleaning utility systems. *Note 1* Despite the fact that water covers 70% of our planet, only 2.5% is not salty. Of this amount, only 0.3% is drinkable (Water in the city, European Environment Agency, 2012). *Note 2* In the City of Ljubljana (population: 300,000), overall fresh water consumption is approx. 200 L per inhabitant per day. The majority is used in households (68%), trade and shopping centres (10%), and industry (4%). The water supply system is continuously refurbished to decrease network leakage. Water losses in network were over 100% of the supplied water in 1991; were decreased to ~ 30% in 2011 (Municipality of Ljubljana, VO-KA, 2017).

10.1 Demand for DHW

The demand for DHW depends on the building category. Data should be obtained by measurements in local environment since lifestyles and cultural habits have significant influence on DHW demand. Statistical methods or data on a national

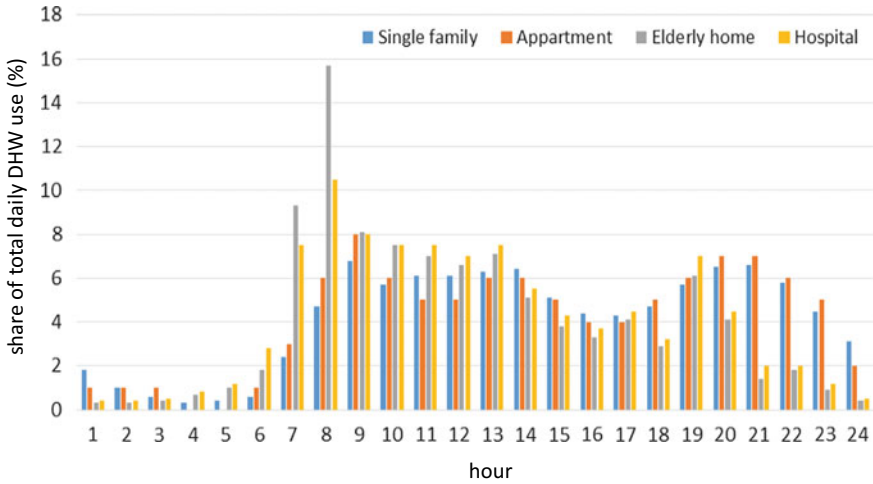


Fig. 10.1 Share of DHW total daily use for four building categories as proposed in standard EN 12831-3

Table 10.1 Daily DHW use for different building categories according to standard EN 12831-3

Type of the building	Daily DHW l/d/unit	Reference unit
Simple residential building	26–60	Person
Single family dwellings	60–100	Person
Apartment dwellings	40–70	Person
Schools	5–15	Person
Student residence	25–35	Person
Gym	5–15	User
Restaurants	15	Meal
	2	Breakfast
Hospitals	55–90	Bed
Laundry	6	Kg

basis can be used. Load profiles of DHW use can be defined for hourly, daily, or seasonal periods. Hourly profiles of DHW daily use proposed in EN 12831-3¹ for different building categories are shown in Fig. 10.1.

In standard EN 12831-3, daily demand of DHW for different building categories is defined according to reference unit (Table 10.1).

¹EN 12831-3:2017 Energy performance of buildings—Method for calculation of the design heat load—Part 3: Domestic hot water systems heat load and characterisation of needs, Module M8-2, M8-3.

10.2 DHW Heating Load

Heating load of DHW systems, which defines the heat capacity of a heat generator, is defined by the design draw-off flow rate \dot{V}_D , the temperature of cold water entering from the infrastructure supply system ($\theta_{w,c}$), and the design temperature of hot water ($\theta_{w,draw-off}$). The empirical equation for determination of design DHW flow rate:

$$\dot{V}_D = a \cdot \left(\sum_i \dot{V}_{a,i} \right)^b - c$$

design DHW flow rate (l/s)
draw-off flow rate at i-th draw-off point (l/s)
 \dot{V}_D
 $\dot{V}_{a,i}$
constant (-)
number of draw-off points (-)

If values for \dot{V}_a are not defined on a national basis, they can be obtained from standard EN 806-3.² The draw-off flow rates for selected draw-off points are shown in Table 10.2.

Constants a, b, and c take into account the simultaneity of DHW use at different draw-off points. Values of constants are defined in EN 12831-3 for different building categories (Table 10.3).

In the case of tank-less DHW systems, the heat generator consists of a flow-through heat exchanger for heating of DHW only when the draw-off point is activated (Fig. 10.2).

Table 10.2 Draw-off flow rate \dot{V}_a for some draw-off points (EN 806-3)

Draw-off points	\dot{V}_a (l/s)
Bath	0.15
Shower	0.15
Basin	0.07
Bide	0.07

²EN 806-3:2006 Specifications for installations inside buildings conveying water for human consumption—Part 3: Pipe sizing—Simplified method.

Table 10.3 Constants for determination of the DHW design flow rate (EN 12831-3)

	a	b	c
Residential buildings	1.48	0.19	0.94
Office buildings	0.91	0.31	0.38
Schools	0.91	0.31	0.38
Nursing homes	1.48	0.19	0.94
Hotels	0.70	0.48	0.13
Hospitals	0.75	0.44	0.18

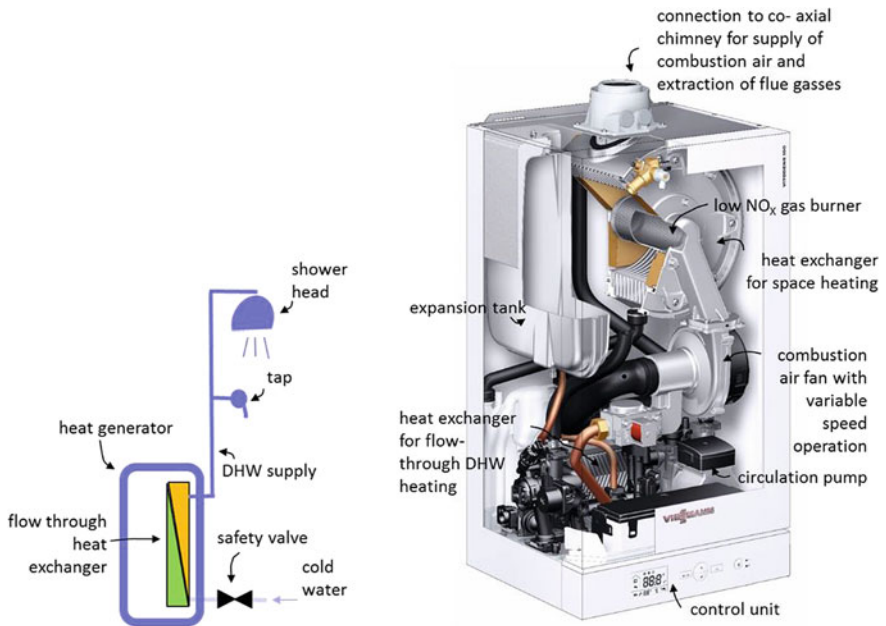


Fig. 10.2 Tank-less DHW heating system (left); condensate gas boiler for space heating and DHW heating with integrated flow through heat exchanger with heat capacity 35 kW and efficiency 109% (Hi)/98% (Hs) (right) (www.viessmann.com (Vitodens 100-W))

Heat capacity of heat generator can be determined with the equation:

$$\dot{Q}_W = \dot{V}_D \cdot \rho_W \cdot c_{p,W} \cdot (\theta_{w,\text{draw-off}} - \theta_{w,c}) \cdot \frac{1}{1000} \quad (\text{W})$$

design DHW flow rate (l/s) temperature of draw-off water (°C);
 default value 42°C
 density of water (~998 kg/m³) specific heat of water (~4200 J/kgK) cold water temperature (°C); default value 10°C

Because the heat generator must cover additional heat losses of the distribution system, it is recommended that the design heat load of the heat generator is increased by a factor of 1.1–1.3.

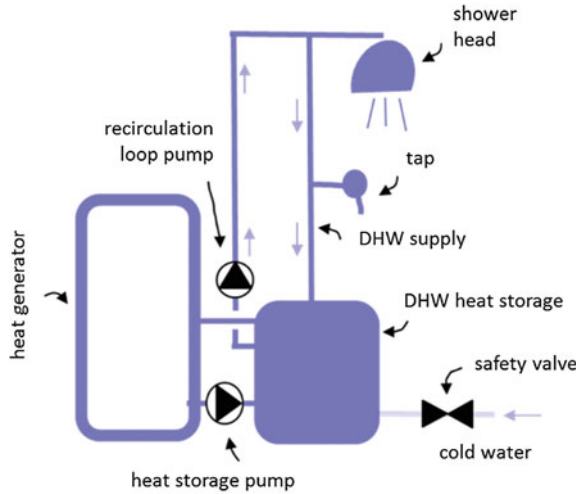
Case Study Calculate the heat capacity of a DHW tank-less system in a residential building with three basin taps and a shower for the reference conditions.

$$\dot{V}_D = a \cdot \left(\sum \dot{V}_a \right)^b - c = 1.48 \cdot (3 \cdot 0.07 + 0.15)^{0.19} - 0.94 = 0.27 \text{ l/s}$$

$$\begin{aligned} \dot{Q}_W &= \dot{V}_D \cdot \rho_W \cdot c_{p,W} \cdot (\theta_{w,\text{draw-off}} - \theta_{w,c}) \cdot \frac{1}{1000} = \\ &= 0.27 \cdot \frac{998 \cdot 4200 \cdot (42 - 10)}{1000} \cdot 1.1 \doteq 39.8 \text{ kW} \end{aligned}$$

The case study shows that the heat capacity of a DHW heat generator in a tank-less system is usually much higher than the heat capacity needed for space heating. In residential buildings, tank-less DHW heating systems are used only in combination with space heating system to reduce stand-by heat losses of the heat generator. Gas is a commonly used fuel in this case. In other building types, electrical heaters can be used to decrease the heat losses in long supply pipes. In addition to the high required heat capacity of the heat generator, another disadvantage of tank-less DHW heating systems is that a recirculation loop cannot be installed. Consequently, the waiting time for hot water arriving at the draw-off point can be quite long. In practice, the waiting time depends on the length of the pipes between the heat generator and draw-off point, the size (diameter) of the pipes, and the duration of non-use periods. It was determined that heat losses due to the cooling of hot water standing still in distribution pipes are up to 30% in the case of high use and up to 50% of energy needs in the case of long non-use daily periods (Harvey 2006). Larger waiting times also increase demand of the water. It can be assumed that 20–40 L of water is wasted per day per faucet if a DHW system operates with long non-use periods.

Fig. 10.3 DHW system with heat storage and recirculation; in such systems, hot water is almost immediately available to users, which in turn reduces water consumption; to ensure the high energy efficiency of a DHW system, heat storage and pipes must have good thermal insulation and the recirculation pump must be controlled



The heat capacity of a heat generator in a DHW system can be lowered by incorporation of heat storage. In single family buildings, small units with volumes of ~ 50 to 150 L are sufficient. Such heat storage can be built into the heat generator. Recirculation pipes that connect the heat storage and draw-off decrease waiting time and reduce the amount of wasted water by up to 80%. Nevertheless, recalculation pipes significantly increase the heat losses if recirculation is not controlled. This can be done with timers and temperature sensors that control the circulation pump (Figs. 10.3 and 10.4).

In multifamily buildings and in buildings with high demand of DHW, heat storage has even greater influence on the design heat capacity of DHW heat generators. The design heat capacity of heat the generator and the volume of the heat storage depend on the number of flats (n), the simultaneous factor (because all of the faucets are not in use in the same time; φ), and time needed for the heat generator to heat the water in heat storage (Z_A , value of 2 h is common). Guidelines for design DHW system in multifamily buildings are shown in Table 10.4 (Recknagel et al. 1995).

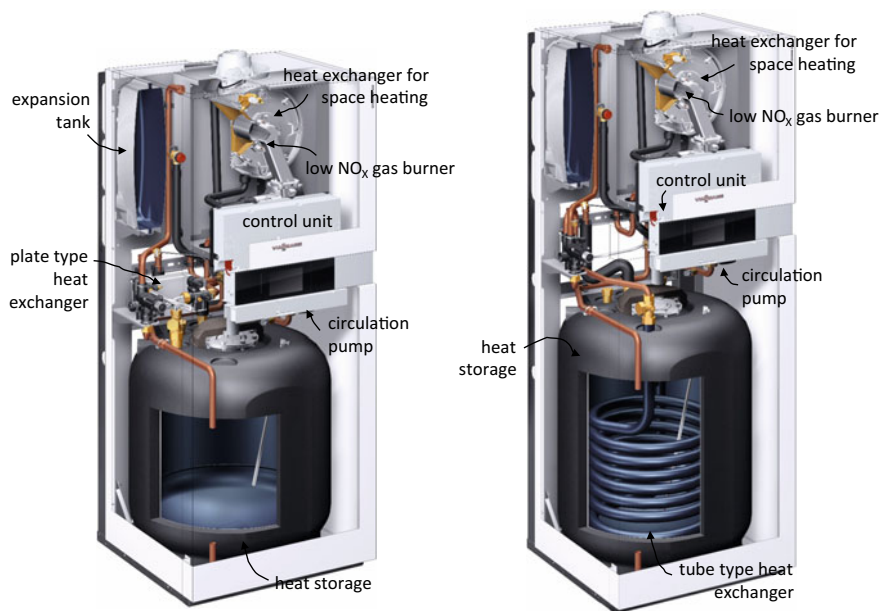


Fig. 10.4 Gas condensation boiler with integrated heat storage with volume of 86 L (left) (www.viessmann.com (Vitodens 222-F B2TB)). Heat storage is heated by a plate heat exchanger integrated in the boiler. An additional pump is needed to pump water through the heat exchanger. Such solutions are suitable for locations where the cold supply water has low amounts of dissolved salts of calcium and magnesium (see Sect. 10.5) because this substance deposits at high temperatures in heat exchangers and could cause malfunctioning of the DHW system or the increase maintenance cost of DHW system operation. A gas condensation boiler with integrated heat storage with volume of 130 L and a tube heat exchanger should be designed if cold water in the infrastructure supply system has more than 12 °dH (German degree of hardness, see explanation in Sect. 10.5) (right) (www.viessmann.com (Vitodens 222-F B2SB)). Because heating water in the boiler is separated from cold water, the accumulation of minerals in the boiler could be avoided

Table 10.4 Heat capacity of heat generator and heat storage volume for DHW heating system in multifamily buildings

No of flats (<i>n</i>)	Simultaneous factor (φ)	Heat capacity of heat generator without DHW heat storage (kW)	Heat capacity of heat generator with DHW heat storage (kW)	Volume of DHW heat storage (L)
1	1.25	8	4	200
2	0.86	12	6	300
4	0.65	18	9	450
8	0.50	28	12	690
20	0.40	56	28	1400
40	0.33	93	46	2300
60	0.31	130	65	3200
80	0.29	160	80	4000
100	0.28	190	100	5000

Case Study In a multifamily building with 40 flats, a light heating oil boiler with a heat load of 50 kW and heat storage with a volume of 2.5 m³ are installed for DHW heating. Note that all connection pipes and heat storage are thermally insulated. Pipes are insulated with thermal insulation thickness equal to the pipe diameter, and heat storage with 80 mm of thermal insulation (Fig. 10.5).



Fig. 10.5 Space heating and DHW boiler in a multifamily building

10.3 Energy Needs and Delivered Energy for DHW

In Chap. 5.3.5, the energy needs (Q_w) for the heating of domestic hot water are presented. Energy needs are defined as empirical values expressed as specific values per square metre of a building's useful area or reference unit (e.g. number of persons, number of beds). If the usage profile of DHW is known, energy needs can be determined for such specific cases; nevertheless, it is common that specific values are prescribed in national legislation that covers EPBD implementation.

The delivered energy (final energy) for DHW heating ($Q_{w,f}$) is calculated by the energy balance on hourly or monthly time steps, taking into account energy needs and the design and thermal properties of all components of the DHW heating system, as described in Chap. 5.4. The procedure starts with the declaration of energy need (Q_w), the determination of the heat loss of heat storage and the distribution system, as well as heat losses regarding imperfect control. The auxiliary energy for the operation of DHW heating system is also calculated. This includes electricity use for the operation of the heat generator, circulation pumps, and control units. Some energy flows can be recovered to some extent in DHW systems (auxiliary energy for circulation pumps); in other systems, the distribution losses of the DHW system, and the heat generator and heat storage heat losses decrease energy use for space heating. In Fig. 10.6, energy flows for a DHW system with a gas boiler and heat storage are presented, following the nomenclature introduced in EPBD-supporting EN standards (see Chap. 5.4).

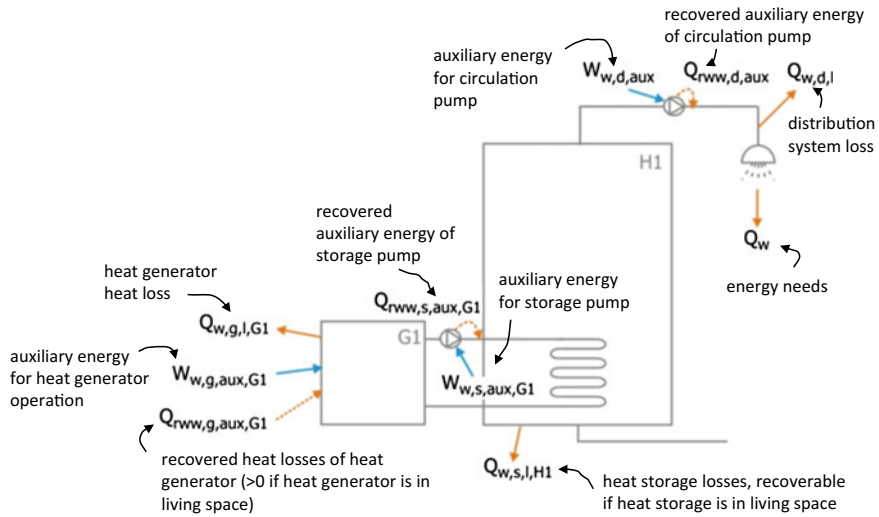


Fig. 10.6 Energy flows in a DHW system consisting of a gas boiler and stand-alone heat storage and DHW circulation (orange arrows indicate heat, blue arrows electricity)

Case Study Delivered energy for DHW heating in the system with gas boiler and heat storage (Figs. 10.7 and 10.8).

Seasonal performance indicator SPI of such DHW heating system is equal (Fig. 10.9).

Note: It is clear how important it is to reduce all kinds of heat losses of DHW system components.

The screenshot shows the TRIMO Expert software interface for configuring a DHW system. It includes a schematic of the DHW system and several input tables.

energy needs and DHW temperatures

Required heat for domestic water heating	Unit	Informative	Project	days/year
Zone 1: Residential house	kWh/m ² a	12	12	365

inputs for distribution system

	Informative	Project	#
Pipe length between heat generator and supply pipe L_v [m]	15	15	
Main supply pipe length [m]	18	18	
Branching pipe length [m]	12	12	
Heat transfer coefficient of pipes between generator and supply pipe [W/mK]	0,200	0,2	
Heat transfer coefficient of main supply pipe [W/mK]	0,255	0,255	
Heat transfer coefficient of branching pipe [W/mK]	0,255	0,255	
Share of pipes in unheated space [%]			0

inputs for heat generator

	Informative	Project
Nominal power of heat generator [W]	3	15
Efficiency of heat generator at nominal power [-]	0,915	0,922
Power of auxiliary appliance at full load [kW]	0,076	0,165
Power of auxiliary appliance in standby operation [kW]	0,015	0,015
Nominal power of pump for storage heating [W]		40

inputs for heat storage

	Informative	Project
Heat storage volume [l]		120
Daily heat loss of heat storage [kWh/day]	1,6	1,6

Fig. 10.7 Input parameters for the case study (TRIMO Expert)

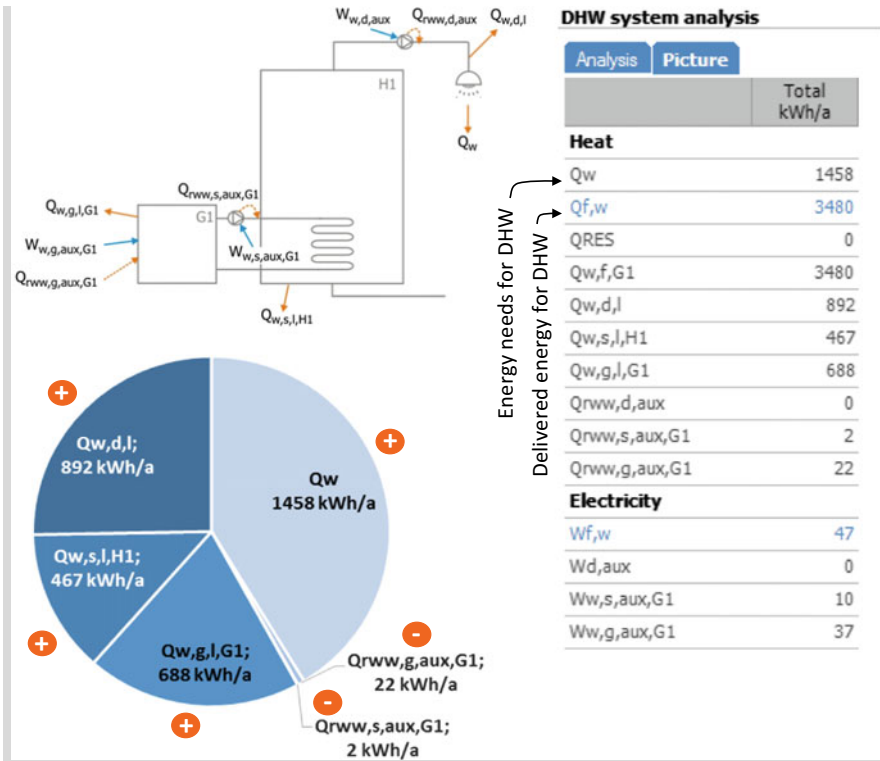


Fig. 10.8 Balance of energy flows is determined for each of the month of the year and then summarized to yearly delivered energy (TRIMO Expert)

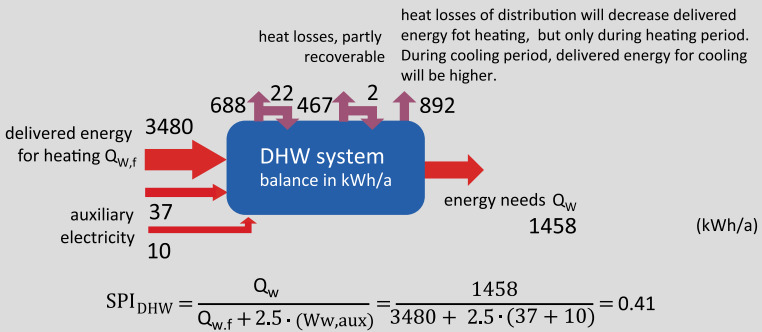


Fig. 10.9 Schematic of energy flows

10.4 Principles of Rational Use of Energy for DHW Heating

The most important measure of the rational use of energy in DHW systems is reducing the amount of consumed hot water. This can be done by raising awareness among the residents, as well as the implementation of technologies, such as low-flow showerheads and faucets and more efficient washing and dishwashing machines. As already mentioned, decreased DHW consumption also has a large impact on environmental protection. It is also important to reduce standby, distribution, and parasitic losses of DHW systems. Standby by and distribution losses are the results of heat transfer from heat storage and pipes and can be reduced by placing the supply systems, the kitchen, and the bathroom close together and by well-insulated heat storage (with thermal insulation thickness at least 80 mm) and pipes (thickness of thermal insulation at least equal to inner pipe diameter). Parasitic losses are related to electricity consumption of circulation pump (Fig. 10.10).

10.4.1 DHW Solar Heating

The use of energy for preparation of DHW is unlike space heating, extended throughout the whole year. The consequence is that DHW solar heating systems significantly improve two of the nZEB indicators: decrease of primary energy demand for the operation of the building and an increased share of renewable energy sources. At present, in some countries or cities, solar DHW heating is required and in most EU countries such systems are financially supported.^{3,4}

Fig. 10.10 Aerated shower head reduces water flow rate from 15 L per minute to 5–7.5 L per minute



³Barcelona Solar Hot Water Ordinance, C04 Cities, www.c40.org.

⁴Best practice regulations for solar thermal, EIE/04/240/S07.38607, ESTIF European Solar Thermal Industry Federation, 2007.



Fig. 10.11 Thermo-syphon DHW solar heating systems (SOLARGE 2004)

Note: 6 m² of installed solar thermal collectors for DHW heating is required to fulfil the criteria of minimum renewable energy source share in the delivered energy for whole-year operation of single family buildings in Slovenia.⁵

The simplest and most cost effective DHW solar heating systems are thermos-syphon ones. Such systems consist of solar thermal collector(s) and heat storage installed above. Such a design is required to prevent counter flow of the hot water from the storage back to solar thermal collectors during the night. In the presence of solar radiation, heat from solar collectors is transferred by the natural convection of heat transfer fluid into the heat storage. No additional element, such as pump or control unit, is needed. As water is the heat transfer fluid in most cases, such systems can be only used in mild climate regions or during part of the year to prevent the freezing of the water (Fig. 10.11).

In continental climate regions closed loop solar heating systems are common. In such systems, solar thermal collectors and heat storage are connected by a circulation pipeline, and pump and control units are installed to ensure the circulation of heat transfer fluid. In most cases, this is a mixture of water and freezing protection fluid. The control unit detects the temperature in the solar thermal collectors and in the heat storage and switches pump on in the case of positive temperature difference. In small DHW solar heating systems (with solar thermal collectors up to

⁵Pravilnik o učinkoviti rabi energije v stavbah (Rules on efficient use of energy in buildings with a technical guideline). (Uradni list RS, št. 52/10 in 61/17—GZ).

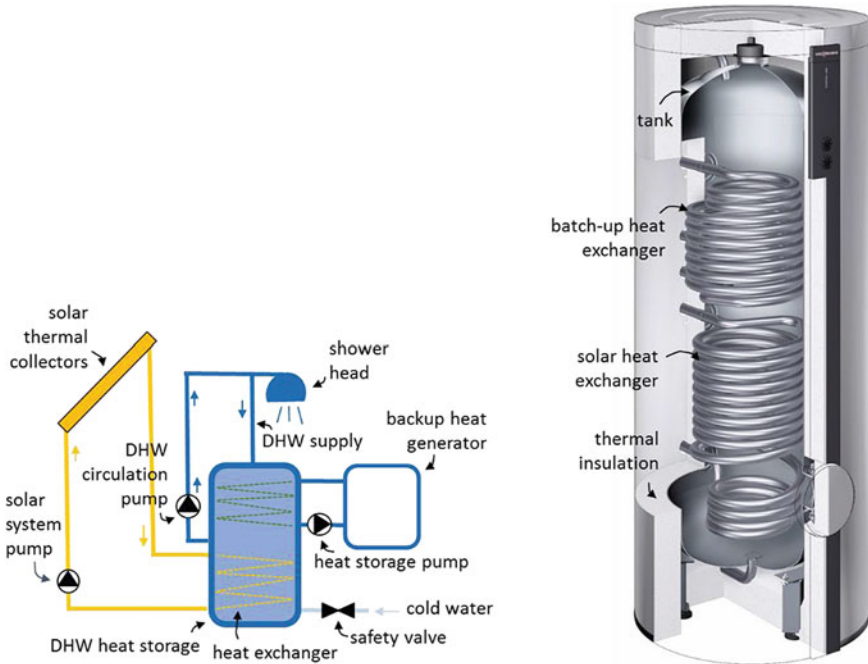


Fig. 10.12 Closed loop DHW solar heating system with backup heating (left); heat storage with integrated solar and backup heat exchanger (right) (www.viessmann.com (Vitocell 300-B))

12 m²), one heat storage unit is installed, and tube heat exchangers are integrated into the storage; the lower one is connected to the solar collector’s loop, and the top one with the backup auxiliary heat generator. An additional built-in electrical heater could also be used (Fig. 10.12).

Note: As a rule of thumb, 1.5 m² of flat or 1.2 m² of vacuum solar collectors are needed for single family DHW heating per resident and 50–75 L of heat storage volume should be installed per 1 m² of solar collectors. Such a system provides a solar fraction of between 65 and 75% of DHW heating during the year. The solar fraction depends on local meteorological conditions, shading, placement of solar collectors, and DHW consumption. For the precise determination of the solar fraction, software must be used, as presented in previous chapter.

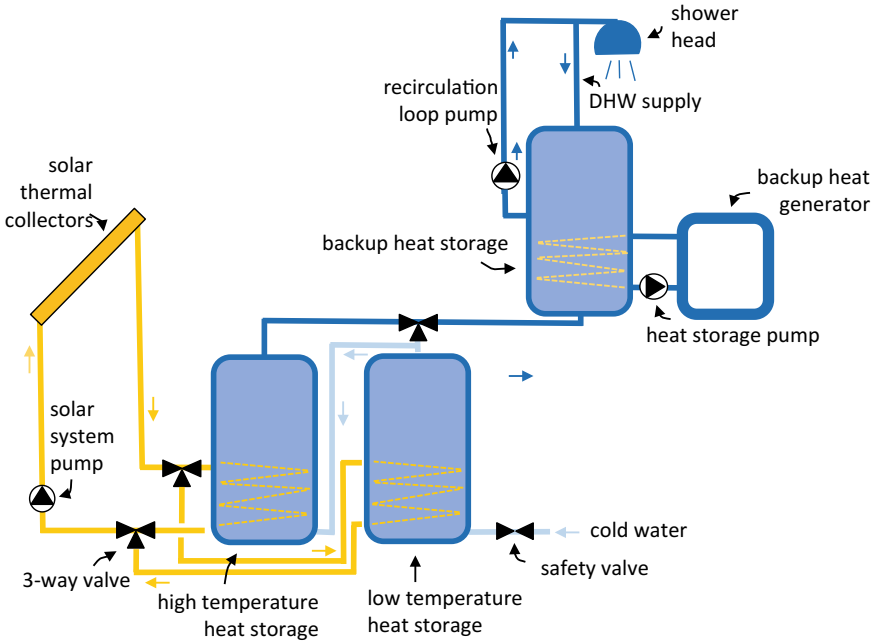


Fig. 10.13 Large DHW solar heating system with multiple heat storage units provide high exergy efficiency because heat is stored at different temperature levels

In the case of multifamily buildings or in buildings with high DHW demand, several heat storage units are installed and connected to solar thermal collectors. In this case, not only is more heat stored, but heat storage can also be connected to maintain high quantity of exergy because heat is stored at different temperature levels. As solar irradiance is not a constant energy source, separate heat storage for backup heating must be installed. Such a system enables a high level of microorganism protection because DHW can be heated to temperature 65–70 °C in backup heat storage the by backup heat generator (Fig. 10.13).

Case Study Example of large DHW solar heating system with multiple solar heat storage units and backup heat storage connected to gas a boiler. The solar systems provide $\sim 30,000$ kWh_t per year and 6 t of CO₂ emissions per year are avoided (Fig. 10.14).



10.4.2 Waste Heat Recovery from Drain-Water

Heat from consumed DHW can be utilized for preheating the cold water supply. This can be done with a flow-through counter flow heat exchanger installed between the drainage and cold supply water distribution pipeline (Fig. 10.15). The efficiency of heat recovery is in the range between of 30% in the case of shower drain integrated heat exchangers, and up to 60% if waste heat is stored in water storage with integrated heat exchanger (Fig. 10.16). In the case of a flow-through heat exchanger, supply water is heated to 19–22 °C and up to 740 kWh_t per year can be recovered in a flat with 5 people (Amo and Lopez 2015).

10.4.3 Heat Recovery from Utility Sewage Systems

Waste heat can be utilized in utility sewer systems. The constant volume flow rate of sewage water at least 10 l/s and a minimum temperature 10 °C are requested. Heat exchangers with varying cross-section geometries are built modularly (2–6 m length) and can be installed in new or existing sewers. Heat flux in the range between 3 and 5 kW per metre of heat exchanger length can be gained (pipe diameter 1200 mm, sewage water temperature 13 °C). Waste heat can only be utilized by heat pumps in these applications. Such systems can also be used for the passive cooling of buildings (Fig. 10.17).

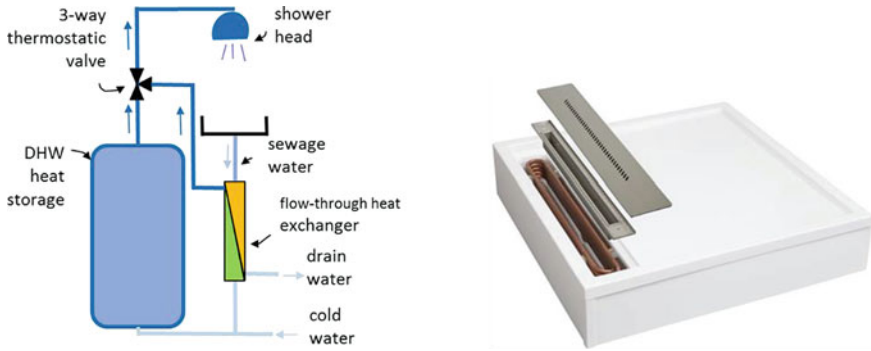


Fig. 10.15 DHW waste heat recovery system with flow-through heat exchanger (left); heat exchanger integrated in shower drain (right) (www.heatsnagger.com)

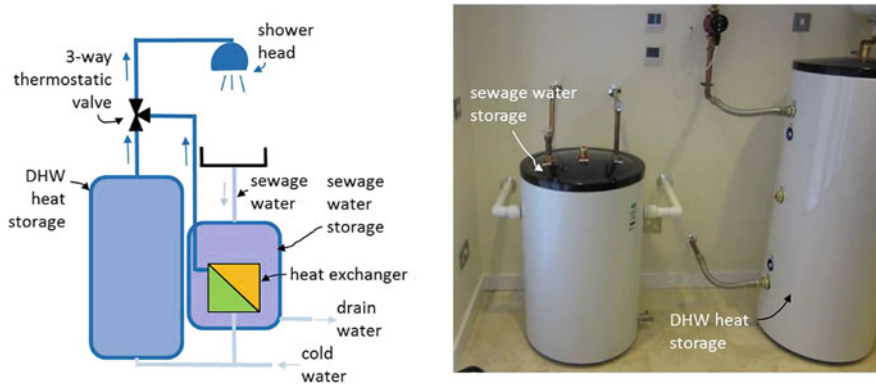


Fig. 10.16 Heat exchanger integrated in sewage water storage (www.silverspray.co.uk)

10.5 Treatment of DHW for Reliable and Healthy Operation of DHW Heating System

To ensure reliable operation of DHW heating systems and the supply of safe water, domestic hot water is treated in two steps: first, substances that can cause unreliable supply and increased cost of DHW heating system operation must be eliminated before entering the heat generator or heat storage; second, the growth of legionella microorganisms in heat storage and pipelines must be prevented (Viessman and Hammer 1985).

Fig. 10.17 Double jacket stainless steel heat exchanger installed on the entire pipe circumference in pressurized sewage pipes (top); double jacket stainless steel heat exchanger installed on 1/3 (120°) pipe circumference: such systems can be adapted to sewage water levels determined by the natural gradient of sewage water level (middle); double jacket stainless steel heat exchanger with integrated cooling pipes (bottom) (www.kasag.ch)

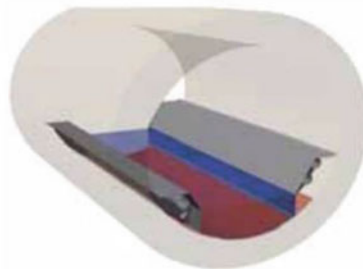
KASAG Pressurepipe



KASAG Gravitytube



KASAG Sewer



The most harmful substances that should be eliminated from supply water are:

- coarse particles; these can be inorganic or organic; using back-washing filters, the large particles (>100 µm) are retained; filters should be cleaned by hand or automatically by back-flushing at least once per month using the ball-valve at the bottom of the filter case;
- colloidal solutions originate from small particles of 1–100 µm dispersed in the water; such particles can be grease, silica, iron and manganese compounds and can be removed by fine filters;
- chlorine, nitrates, pesticides and very small particles can be removed by active carbon filters;

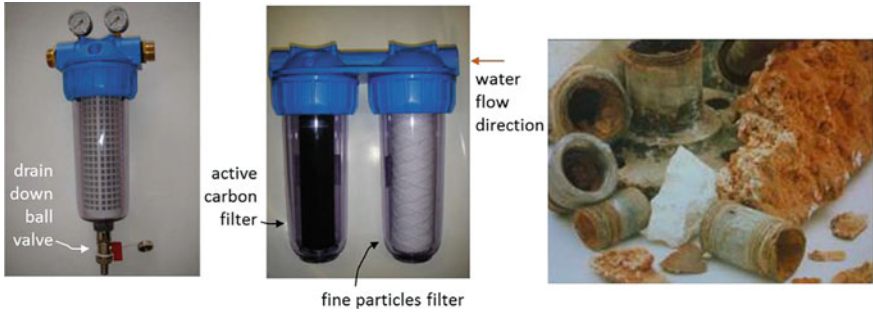


Fig. 10.18 Coarse particles filter with drain down valve (left); fine particles filter and active carbon filter (middle); decomposition of dissolved salts can cause unreliable supply of DHW and increased energy demand and costs of DHW heating (right)

- dissolved salts of calcium (Ca) and magnesium (Mg); the amount of dissolved salts (CaCO_3 , MgCO_3 , etc.) and other materials that increase the hardness of water;
- dissolved gas (e.g. CO_2 and O_2) should be removed because they are highly aggressive and cause corrosion of pipelines (Fig. 10.18).

Note: Total permanent hardness of the water is expressed and classified by amount of calcium and magnesium ions as equivalent of calcium carbonate CaCO_3 or as the German degree of hardness ($^\circ\text{dH}$).

		German degree of hardness ($^\circ\text{dH}$)
soft water	0 to 60 mg/lit (0 – 4 $^\circ\text{dH}$)	↙
moderately hard water	60 to 120 mg/lit (4 – 8 $^\circ\text{dH}$)	
water	120 to 180 mg/lit (8 – 18 $^\circ\text{dH}$)	hard
very hard water	180 mg/lit (18 – 30 $^\circ\text{dH}$)	

In contrast to the solubility of most salts, CaCO_3 becomes less soluble as the temperature of the water increases. From hard water 130 mg CaCO_3 deposits per litre of water, if such water is heated from 30 to 80 $^\circ\text{C}$. Deposits can cause malfunctioning and additional energy losses of water heaters. To avoid problems with the decomposition of salts, the temperature of water should be lowered, heat exchangers made from titanium should be used, or water softening devices should be installed at the beginning of the pipeline.

10.6 Avoiding the Presence of Harmful Microorganisms in Domestic Hot Water

In DHW systems at certain conditions, the rapid growth of undesirable microorganisms called legionella can occur. The following measures must be implemented to reduce the risk of the occurrence of legionella microorganisms in the heat storage units and distribution loops of DHW systems:

- temperature of the cold water supply in the pipeline should be below 20 °C;
- the hot water temperature at all (even the most remote) faucets and showers should be at least 50 °C;
- temperature of the water in the whole volume of the heat storage should be more than 60 °C at least 1 h per day;
- meshes on the taps and shower heads must be cleaned (from sediment, dirt, stone) at least 4 times per year;
- regular inspection and cleaning of heat storage once per year;
- chlorine shock treatment for disinfection must be done after each intervention in DHW network system.⁶

For the prevention from legionella microorganisms in large DHW systems in hotels or multi-family buildings with central DHW heating system, implementing the so-called “temperature shock” disinfection on daily or weekly basis is recommended. This is done by heating hot water to 70 °C and circulating high temperature water throughout the DHW system for at least of one hour. In addition to the temperature shock, protection against the growth of undesirable microorganisms

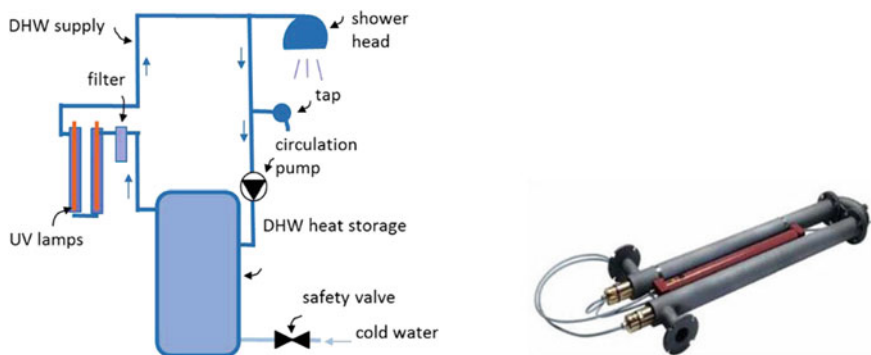


Fig. 10.19 UV lamp eliminates microorganisms in DHW heating system

⁶Pravilnik o pitni vodi (Rules on drinking water) (Uradni list RS, št. 19/04, 35/04, 26/06, 92/06, 25/09, 74/15 in 51/17); Requirements to be met for drinking water in order to protect human health from the adverse effects of any contamination of drinking water.

can be achieved with UV disinfection using a UV lamp. UV radiation in the water generates hydroxyl radicals (-OH). They are highly aggressive and rapidly react with microorganisms. The life time of microorganisms is reduced to the few nanoseconds. The maintenance of the system includes regular (annual) replacement of lamps and cleaning of the particle filter. UV disinfection is always used in addition not instead of temperature shock protection (Fig. 10.19).

References

- Amo AG, Lopez AA (2015) Drain water heat recovery in a residential building. Faculty of Engineering and Sustainable Development, University of Gavle
- Harvey LDD (2006) A handbook on low-energy buildings and district-energy systems, fundamentals, techniques and examples. Earthscan, London
- Recknagel H, Sprenger E, Hönmann W (1995) Taschenbuch für Heizung + Klimatechnik. R. R. Oldenbourg Verlag GmbH
- SOLARGE (2004) Enlarging solar thermal system in multi-family-houses, hotels, public and social buildings in Europe, EIALT/EIE/04/082/2004
- Viessman W, Hammer MJ (1985) Water supply and pollution control. Harper International Edition

Chapter 11

Ventilation of nZEB



Abstract Ventilation is the process of the dilution of indoor air pollutants by exchanging the indoor air with the exterior air. This can be done because, in general, outdoor air is less polluted than indoor air. With ventilation, the amount of indoor air pollutants must be lowered to a level that does not affect the perceived quality of the indoor environment, decrease the productivity or influence the health of residents. Several hundreds of pollutants can be found in indoor air because they are emitted from human bodies, animals, plants, as well as building materials and processes. Water vapour, CO₂, CO, solid particles and odours are the most indicative pollutants in residential buildings. Requirements and methods for the determination of amount of supply fresh air needed to reach the desired category of indoor air quality (IAQ) are presented in Chap. 1. In this chapter, the principles and types of ventilation, design of ventilation systems, energy performance indicators and measures for increasing energy efficiency of ventilation systems are presented. When determining the energy needs for ventilation, as described in Sect. 5.3, it is assumed that supply air is delivered into the building at the indoor air set-point temperature (during heating and cooling periods). Consequently, energy needs for ventilation are included in the energy needs for heating (Q_{NH}) and cooling (Q_{NC}) and the final energy demand for ventilation is only related to the energy use of electricity for the operation of the fans in the case of mechanical ventilation. Ventilation systems can be extended to air-heating or air-cooling systems. In such systems, heat is delivered or extracted by air that is supplied into the building (rooms) at higher (up to ~ 40 °C) or lower temperatures (down to ~ 18 °C) in comparison to the indoor air set-point temperature. Air-conditioning systems are another type of extended ventilation systems using air as a heat transfer fluid for heating and cooling. In contrast to air-heating and air-cooling systems, such systems also regulate the humidity of the indoor air. Besides providing the required indoor air quality, the process of ventilation can be used for the removal of the heat of internal sources and solar radiation to cooling the building's thermal mass during summer nights to avoid overheating and decrease the energy needs for cooling the building. It is common for all those processes that a much larger quantity of supply air is required in comparison to IAQ requirements. Only "pure" ventilation systems will be presented in this chapter.

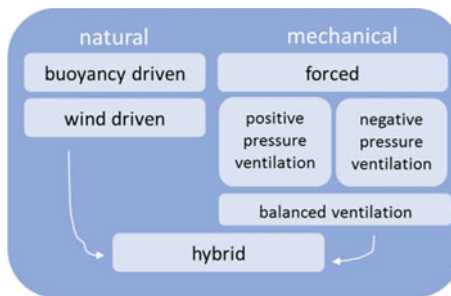
In nature, fluids flow if there is a difference in pressure between two regions: in the case of buildings, this is between a building's interior and outdoor. A difference in the air pressure can be due to natural phenomena that can be exploited for natural ventilation of the building or energy input by the fan, in the case of mechanical ventilation (Fig. 11.1). In this case, pressure inside the buildings can be adjusted by fan(s) that either supply (positive pressure) or extract air (negative pressure) from the building to control the spread of pollutants. In the case of balanced ventilation, fans are used to supply and extract the air in the same time. Balanced ventilation is compulsory to recovery the heat (during the heating period) or cold (during the cooling period) from extracted air to the fresh air to decrease ventilation heat losses or gains. Hybrid ventilation is a controlled combination of both principles, and it is used to decrease energy demand for the operation of fans and to reduce the over-heating of the buildings.

11.1 Natural Ventilation

11.1.1 Advantages and Disadvantages of Natural Ventilation

Natural ventilation is highly appreciated by occupants, especially if ventilation can be controlled, for example, by opening and closing windows. Such ventilation can be cost effective if ventilation openings are regulated regarding to actual indoor air pollution. Natural ventilation is silent and maintenance of technology system is not needed. Intensive natural ventilation through open windows and grills can significantly decrease energy demand for cooling and reduce the length of overheated periods during the summer.

Fig. 11.1 Principles of ventilation of the buildings



High air velocity can cause the sensation of draught but does provide cooling sensation during the summer because of increased indoor air velocities. The requirements of energy efficient buildings are one reason that windows (and whole building envelope as well) must be built very air tight, and adequate natural ventilation regarding to IAQ requirements (see Sect. 1.2.1) can be achieved only if windows are open or additional ventilation openings are installed. Natural ventilation is not preferred in urban environments, because some outdoor pollutants cannot be removed by filtering. In noisy outdoor environments, ventilation opening can cause high indoor sound pressure levels. Probably the most important disadvantages of natural ventilation are high energy losses because heat recovery cannot be implemented as it can in the case of mechanical ventilation.

11.1.2 How Natural Ventilation Works

Natural ventilation can be buoyancy driven or wind driven. Buoyancy-driven ventilation occurs as a consequence of differences in density of warm and cold air and, therefore, differences in the hydrostatic air pressure. Hydrostatic air pressure is the consequence of the force of the mass of air column that acts in a perpendicular direction on the observed plane:

$$p = \frac{F}{A} = \frac{g \cdot \rho(\theta) \cdot H}{A} \quad (\text{Pa})$$

The diagram shows the equation $p = \frac{F}{A} = \frac{g \cdot \rho(\theta) \cdot H}{A}$ with arrows pointing from descriptive labels to the corresponding terms in the equation. The labels are: 'hydrostatic air pressure (Pa)' pointing to 'p', 'gravity acceleration (m/s²)' pointing to 'g', 'air density as function of air temperature (kg/m³)' pointing to 'ρ(θ)', 'height of air column (m)' pointing to 'H', and 'area (m²)' pointing to 'A'.

Figure 11.2 shows the distribution of hydrostatic air pressure at outer and inner surfaces of the building envelope, assuming that indoor θ_i and outdoor θ_e air temperatures are constant and $\theta_i > \theta_e$. If the envelope of the building is not tight or ventilation openings exist, differences in hydrostatic air pressure cause the air mass to flow in and out of the building in the direction from the region with higher to that with the lower hydrostatic air pressure. The level in the room at which outdoor and indoor hydrostatic air pressure are equal is called the pressure neutral level.

Hydrostatic air pressure differences at inlet Δp_{in} and at outlet opening Δp_{out} , as presented in Fig. 11.2, are equal to:

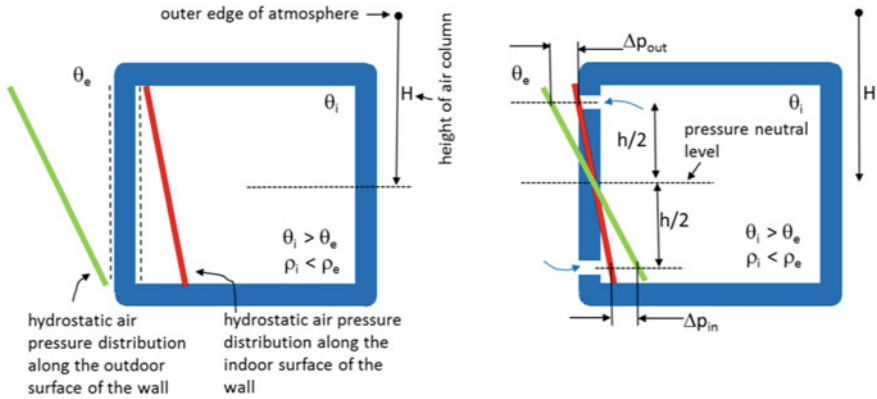


Fig. 11.2 Distribution of hydrostatic air pressure at outer and inner surfaces of the building ($\theta_i > \theta_e$) (left); if the envelope of the building is not tight or ventilation openings exist, differences in hydrostatic air pressure cause air mass flow in and out of the building (right)

$$\Delta p_{in} = g \cdot (\rho_e - \rho_i) \cdot \left(H + \frac{h}{2} \right)$$

$$\Delta p_{out} = g \cdot (\rho_i - \rho_e) \cdot \left(H - \frac{h}{2} \right) \xrightarrow{\times(-1)} -\Delta p_{out} = g \cdot (\rho_e - \rho_i) \cdot \left(-H + \frac{h}{2} \right)$$

and total hydrostatic air pressure difference between the room and ambient environment is:

$$\Delta p_t = \Delta p_i - \Delta p_o = g \cdot (\rho_e - \rho_i) \cdot \left(H - H + \frac{h}{2} + \frac{h}{2} \right) = g \cdot (\rho_e - \rho_i) \cdot h \text{ (Pa)}$$

If air is assumed as ideal gas, air density can be expressed by absolute temperature, and Δp_t is equal to:

$$\rho_i = \rho_e \cdot \left(\frac{T_e}{T_i} \right) \rightarrow \Delta p_t = g \cdot (\rho_e - \rho_i) \cdot h = g \cdot \left(\rho_e - \rho_e \cdot \left(\frac{T_e}{T_i} \right) \right) \cdot h = g \cdot \rho_e \cdot \left(\frac{T_i - T_e}{T_i} \right) \cdot h \text{ (Pa)}$$

absolute temperature of outdoor air (K) density of outdoor air (kg/m³)
 absolute temperature of indoor air (K) density of indoor air (kg/m³)

It can be seen that natural ventilation intensity depends on temperature differences and vertical distance between ventilation openings. The influence of temperature difference is larger, and deep spaces' natural ventilation is more effective if ventilation openings are installed on the opposite facades to enable cross flow ventilation. Stack ventilation is another technique to increase natural ventilation intensity because the height between inlet and outlet opening can be much higher than the floor height (Fig. 11.3).



Fig. 11.3 Examples of natural ventilated buildings with stack enhance natural ventilation; Library and Resource Centre Coventry University (left) (Limam et al. 2011), BRE Office building (right) (Kleiven 2004)

If the facade is exposed to the wind, pressure at the wall surface increases because the wind slows down and part of the kinetic energy of the air is converted to the pressure, because, as defined by the Bernoulli equation, the total energy content of the small air volume at isothermal conditions remains constant along the streamline:

$$\begin{array}{ccc}
 \text{pressure} & \text{kinetic energy} & \text{potential energy} \\
 \downarrow & \downarrow & \downarrow \\
 p_1 + \frac{1}{2} \cdot \rho_1 \cdot v_1^2 + \rho_1 \cdot g \cdot \underbrace{z_1}_{=z_2} = p_2 + \frac{1}{2} \cdot \rho_2 \cdot \underbrace{v_2^2}_0 + \rho_1 \cdot g \cdot z_2 \rightarrow p_2 - p_1 = \Delta p_w = \frac{1}{2} \cdot \rho_1 \cdot v_1^2
 \end{array}$$

Note: Assuming that in theory the wind stops at the wall (v_2 is equal to zero). Assuming that p_1 is the reference pressure equal to 10^5 Pa and the density of the air at 20 °C equal to 1.2 kg/m^3 , pressure at the outdoor surface of the wall increases by $\sim 258 \text{ Pa}$ if wind velocity v_1 in open space is 20 m/s. This is much higher comparing to buoyancy pressure difference. As wind velocity increases with height over the terrain, the upper floors in high rise buildings are even more intensely naturally ventilated.

In real environmental conditions, wind causes the formation of positive (windward) and negative (leeward) air pressure fields around the building, as shown in Fig. 11.4. Pressure differences Δp_w between the environment and the building exposed to the wind is determined by pressure coefficient c_p :

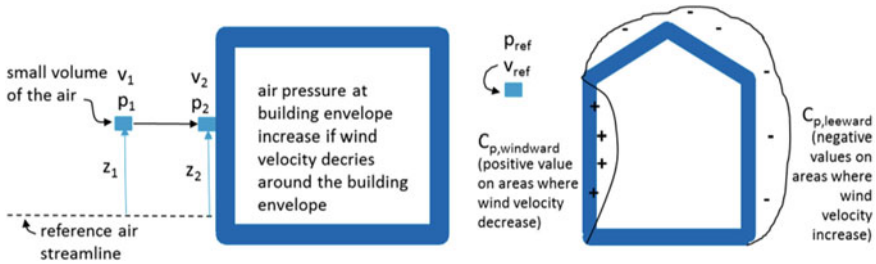


Fig. 11.4 Air pressure increased at surface of the façade exposed to the wind as kinetic energy is transformed to pressure (left); wind causes the formation of positive and negative pressure around the building, which increases air flow through the building (right)

$$\Delta p_w = \frac{1}{2} \cdot c_p \cdot \rho_{ref} \cdot v_{ref}^2 = (c_{p,windward} - c_{p,leeward}) \cdot \frac{1}{2} \cdot \rho_{ref} \cdot v_{ref}^2$$

pressure coefficient (-) reference air density and velocity in open space (kg/m³, m/s)

Pressure coefficient c_p (with value between -1 and $+1$) depends on wind direction and velocity and the shape of the building. Values are positive on the windward-exposed envelope of the building and negative on the leeward-exposed envelope. Pressure differences Δp_w between the environment and a building exposed to the wind can be increased if ventilation openings are placed on both windward and leeward areas. Typical design values are $+0.65$ for $c_{p,windward}$ and -0.65 for $c_{p,leeward}$. For detailed research, pressure coefficients can be evaluated by experiments on small-scale models in wind tunnels or by computational fluid dynamics simulation tools.¹

11.1.3 Determination of Ventilation Air Flow Rate in Case of Natural Ventilation

Empirical models for the determination of air flow rate by natural ventilation are the simplest way to design natural ventilation. For single side ventilation, empirical models have been developed for ventilation through large opening (window) and for stack ventilation through ventilation openings. Limam et al. (2011) proposed the following empirical models²:

¹ASHRAE Fundamentals, 2009.

²EN 15242:2007 Ventilation for buildings—Calculation methods for the determination of air flow rates in buildings including infiltration.

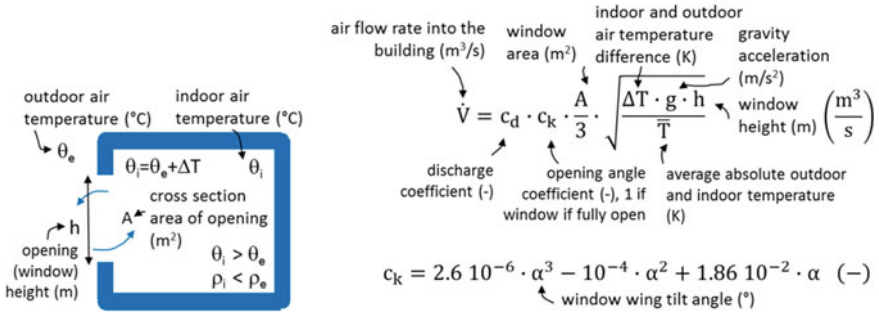


Fig. 11.5 Model of buoyancy-driven ventilation through large opening

- Buoyancy-driven ventilation through large opening; a large opening is area through which air flows simultaneously in and out of the building. Both areas are separated by a pressure neutral level (Fig. 11.5). The discharge coefficient of the opening indicate decreasing of the air flow rate through the opening because of the pressure drop at the contraction and turbulent flow. The value of the discharge coefficient is between 0 and 1 with a typical value of 0.65 for large opening.

Case study: Calculate air flow rate \dot{V} through an open window with height h 1.2 m and cross section area A 0.3 m^2 if θ_i is 20 °C and θ_e -5 °C. Discharge coefficient c_d of fully open window is 0.65. What will the air flow rate be if the window wing will be rotated (in the vertical plane) at 15°?

$$c_k = 2.6 \cdot 10^{-6} \cdot 15^3 - 10^{-4} \cdot 15^2 + 1.86 \cdot 10^{-2} \cdot 15 = 0.265$$

$$\dot{V} = 0.65 \cdot 0.265 \cdot \frac{0.3}{3} \cdot \sqrt{\frac{25 \cdot 9.81 \cdot 1.2}{\left(\frac{(293 + 268)}{2}\right)}} = 0.0176 \frac{\text{m}^3}{\text{s}} = 63.4 \frac{\text{m}^3}{\text{h}}$$

- Wind driven ventilation through large openings (Fig. 11.6):
- Single side stack buoyancy-driven ventilation; in this case, the inlet and outlet openings are separated, and the air flows only in one direction (in or out of the building) through each opening. As in the previous cases, ventilation is single sided as the window and ventilation openings are installed in the same facade. Because of that, rooms are efficiently ventilated to a depth not more than approximately 2.5 that of the room height (Fig. 11.7).

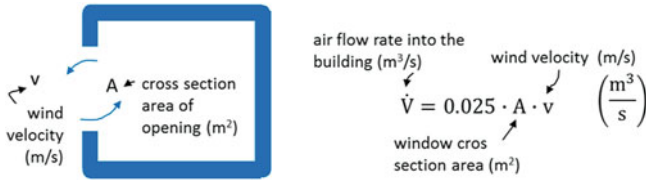


Fig. 11.6 Model of wind-driven ventilation through large opening

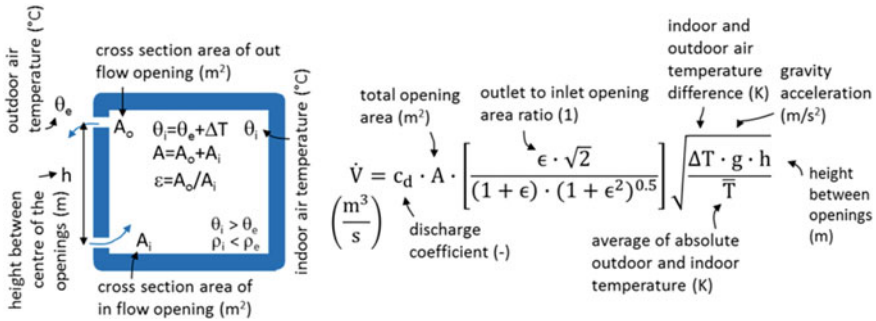


Fig. 11.7 Model of single side stack-buoyancy driven ventilation

Case study: Calculate air flow V into the building through single side ventilation openings with cross section area A_o and A_i equal to 0.015 m^2 ($5 \times 30 \text{ cm}$) at outdoor temperature $15, 10, 5,$ and $0 \text{ }^\circ\text{C}$. Vertical distance between ventilation openings h is 1.8 m , θ_i is $20 \text{ }^\circ\text{C}$ Discharge coefficient c_d of openings is 0.65 .

$$\dot{V}_{15^\circ\text{C}} = 0.65 \cdot (0.015 + 0.015) \cdot \left[\frac{1 \cdot \sqrt{2}}{(1 + 1) \cdot (1 + 1^2)^{0.5}} \right] \cdot \sqrt{\frac{5 \cdot 9.81 \cdot 1.8}{290.5}} = 0.0054 \frac{\text{m}^3}{\text{s}} = 19.6 \frac{\text{m}^3}{\text{h}}$$

$\theta_i = 15^\circ\text{C}$	$\theta_i = 10^\circ\text{C}$	$\theta_i = 5^\circ\text{C}$	$\theta_i = 0^\circ\text{C}$
$V = 19.6 \text{ m}^3/\text{h}$	$V = 27.5 \text{ m}^3/\text{h}$	$V = 33.8 \text{ m}^3/\text{h}$	$V = 39.2 \text{ m}^3/\text{h}$

Cross natural ventilation occurs when windows or ventilation openings are installed on the opposite facade. Because of the higher pressure difference in general, natural ventilation is more intense, and deeper rooms can be naturally ventilated. For cross ventilation Limam et al. (2011) proposed the following empirical models:

- Buoyancy-driven ventilation through small openings (Fig. 11.8)
- Wind-driven ventilation through small openings (Fig. 11.9)

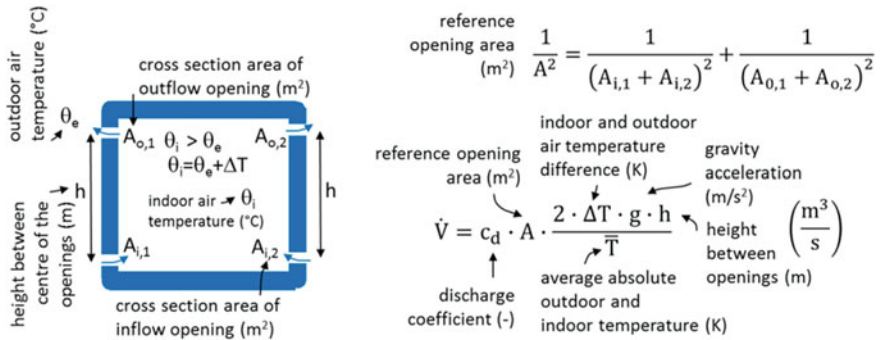


Fig. 11.8 Model of buoyancy-driven ventilation through small openings

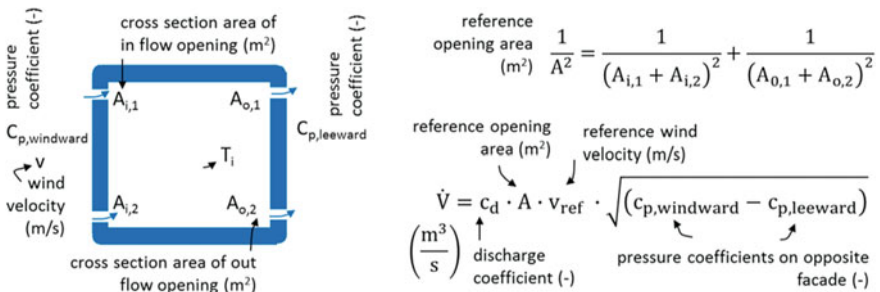


Fig. 11.9 Model of wind-driven ventilation through small openings

Case study: Compare air flow rate \dot{V} into the building from the previous case if ventilation openings with cross section area $A_{i,1}$ and $A_{o,2}$ are equal to 0.015 m^2 ($5 \times 30 \text{ cm}$) and installed in the opposite facade. Outdoor temperature θ_e is $0 \text{ }^\circ\text{C}$. Vertical distance between ventilation openings h is 1.8 m and θ_i is $20 \text{ }^\circ\text{C}$ the discharge coefficient c_d of openings is 0.65 .

$$\frac{1}{A^2} = \frac{1}{(A_{i,1} + A_{i,2})^2} + \frac{1}{(A_{o,1} + A_{o,2})^2} = \frac{1}{0.015^2} + \frac{1}{0.015^2} = 0.0106 \text{ m}^2$$

$$\dot{V} = c_d \cdot A \cdot \frac{2 \cdot \Delta T \cdot g \cdot h}{\bar{T}} = 0.65 \cdot 0.0106 \cdot \frac{2 \cdot 20 \cdot 9.81 \cdot 1.8}{283} = 0.0172 \frac{\text{m}^3}{\text{s}} = 61.9 \frac{\text{m}^3}{\text{h}}$$

This shows that cross ventilation is more efficient than a single-sided ventilation. Apart from the higher ventilation air flow rate, the uniformity of pollutant dilution is higher because of cross-building air flow.

The presented empirical models are suitable for the early design phase; for more precise determination of natural ventilation, computational fluid dynamics (CFD) techniques should be used. Some dynamic modelling software tools use such models for the prediction of natural ventilation (see case study in Sect. 11.4).

11.1.4 Controlling of Natural Ventilation

Natural ventilation can be demand-controlled in a way that the ventilation air flow rate is adjusted to the value to meet occupants' needs. This can be done according to indoor air humidity, the presence of occupants, and CO₂ or VOC concentration sensing. As water vapour in indoor air is one of the most noticeable pollutants, natural ventilation can be effectively controlled by adjusting the area of ventilation opening according to the indoor air humidity. Polyamide, a material that lengthen when humidity increase and shortens when humidity is lower, can be used as an activator in ventilation grills (Fig. 11.10).

Ventilation grills could be upgraded with self-regulating flap that adapt its position according to wind velocity and ensures that the air flow rate remains constant despite increasing outdoor air pressure. Such a device ensures the same natural ventilation intensity of flats in multi-storey buildings and reduces the negative impact of wind-driven ventilation at high wind velocity (Fig. 11.11).

It is important that ventilation openings consist of sound-damping material that absorbs outdoor noise. Some products also have dust and pollen filter membranes (Fig. 11.12).

11.2 Mechanical Ventilation

11.2.1 Advantages and Disadvantages of Mechanical Ventilation

In the case of mechanical ventilation, differences in air pressure are produced by one or several fans. Mechanical ventilation can be more precisely adjusted to the actual needs of occupants in comparison to natural ventilation. The air exchange rate, in the case of mechanical ventilation, is not influenced by the current outdoor air temperature and wind velocity. Such ventilation is more suitable for noisy and polluted outdoor environments because pollutants can be removed by integrated

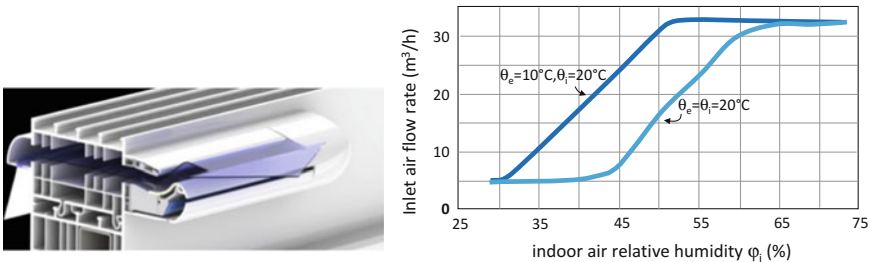


Fig. 11.10 Humidity sensitive air inlet grill (Aereco EHA²), (left); inflow air flow rate at pressure difference 10 Pa and different temperature conditions. Adapted from www.aereco.co.uk

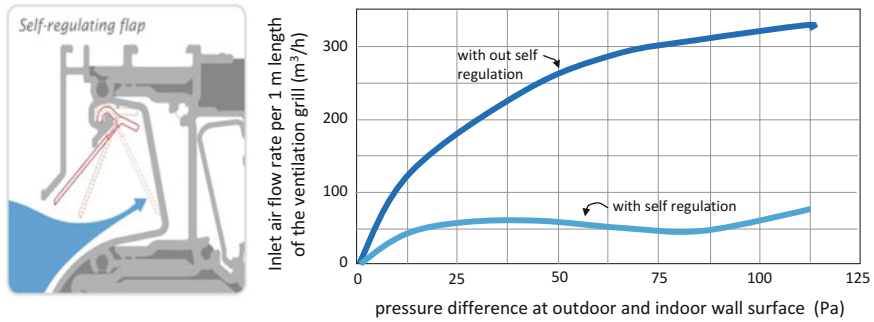


Fig. 11.11 Window air inlet with pressure sensitive self-regulating flap (www.renson.eu)



Fig. 11.12 Air inlet with self-regulating flap with sound absorbing foam integrated in window frame (Omega Thermo Products, www.omegathermoproducts.nl)

filters, and outdoor noise transmission can be reduced by silencers. If balanced ventilation is used, and an air-to-air heat exchanger is installed between the extract and supply air ducts, heat losses by ventilation can be significantly reduced because of heat recovery (up to 90%+). If a heat exchanger is made from vapour-permeable material, the supply air is humidified, and the latent heat of water vapour increases heat recovery efficiency.

Mechanical ventilations system must be designed carefully to avoid draught in ventilated rooms and noise generation by ventilators and turbulent air flow swirls in ducts. As pressure drop and therefore air velocity in distribution ducts must be low, mechanical ventilation systems need quite large distribution systems and space for AHU. Mechanical ventilation systems use electricity for operation and must be carefully designed to ensure low electricity demand. Air filters must be regularly replaced or cleaned, and the whole system must be regularly maintained. Beside high initial cost, electricity demand and maintenance costs increase the operating costs of the building.

11.2.2 Mechanical Ventilation Systems

Mechanical ventilation systems can be designed as extract, supply, or balanced ventilation systems.

Mechanical extract ventilation systems can be designed as single point (Fig. 11.13, top) or multi-point (Fig. 11.13, bottom) systems. Operation of such systems can be controlled manually, by timers or air quality sensors. These systems are easy to install and operate silently. Negative relative air pressure in the building and the extraction of moist air prevents the condensation of water vapour and mould growth. In the case of multi-point systems, indoor pollutants can be efficiently removed from each of the rooms without contaminating other spaces. Such systems are easy to install. Fresh air flows directly into the room(s) and, therefore, cannot be temperate, and filtering the pollutants in outdoor air cannot be highly effective. In case of single point extraction, air is extracted from more polluted rooms (kitchen, toilet) and living spaces is not equally ventilated. Flood ventilation openings must be installed between rooms and must have sufficient cross-section areas. In most cases, a 1–2 cm high slot under the wing of the door is sufficient.

Mechanical supply ventilation is most often designed as multi-point ventilation. Each room receives a pre-designed amount of fresh air. Outdoor air can be filtered and preheated or precooled. Energy efficiency can be increased by solar collectors, ground heat exchangers, and use of waste heat or evaporative cooling of supply air. Such systems can be used in polluted and noisy environments.

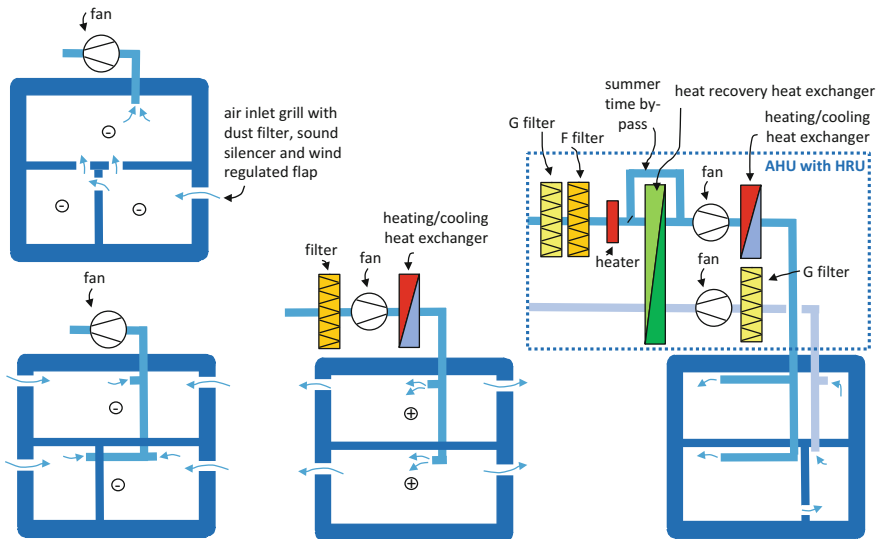


Fig. 11.13 Mechanical ventilation systems can be designed as extract (left, top and bottom), supply (middle) or as pressure-balanced system (right) according to pressure differences between ventilated space, neighbouring spaces, and the outdoor environment

The airtightness of the building envelope has no significant influence on the ventilation efficiency as indoor air pressure is higher than air pressure in the outdoor environment. The quantity of fresh air can be controlled by on/off switches or air quality sensors. The electricity demand for operation is higher because of pressure drop in the filter and heat exchanger but can be decreased with a frequency-controlled fan motor. The main disadvantage of such systems is that heat recovery cannot be implemented.

In mechanically balanced ventilation systems, supply fans and extract fans are installed to provide similar air flow in and out of the rooms. Such systems enable heat transfer between polluted extracted air and fresh air. In this case, ventilation systems consist of air handling units (AHU) with air-to-air heat exchangers (heat recovery unit (HRU)), supply and exhaust fans, filters, and assemblies. As extracted air during the winter has high water vapour content and is cooled in the heat exchanger, condensation of water vapour can occur. This can cause growth of mould and bacteria in the HRU and AHU. To prevent the condensation of water vapour (i) additional (electrical) heater can be installed to heat cold supply air before it enters the heat exchanger, (ii) additional ground heat exchanger could be used to preheat fresh supply air or (iii) the flow rate of supply air is stopped if sensors detect that the air humidity of the extract air is greater than $\sim 70\%$. To enable summer night-time cooling by ventilation, a bypass is integrated into the AHU to prevent air heating in the heat exchanger. Mechanical ventilation systems with HRU are obligatory in passive and nZEB buildings and in places with highly polluted and noisy outdoor environments.

11.2.3 Types of Heat Recovery Units (HRU) in Air Handling Units (AHU)

Air-to-air heat exchangers are used for heat recovery in AHU. Such appliances can be designed as direct cross flow, counter flow, rotary wheel, flip-flop or indirect closed water loop HRU.

11.2.3.1 Temperature Efficiency and Enthalpy Efficiency of Heat Recovery

The temperature efficiency of heat recovery η_{rec} is defined as the ratio between the actual temperature differences of supply air to the maximum possible temperature differences of supply air, as presented in Fig. 11.14. The value indicates the amount of sensible heat that is transferred between extract and supply air during the observed time interval.

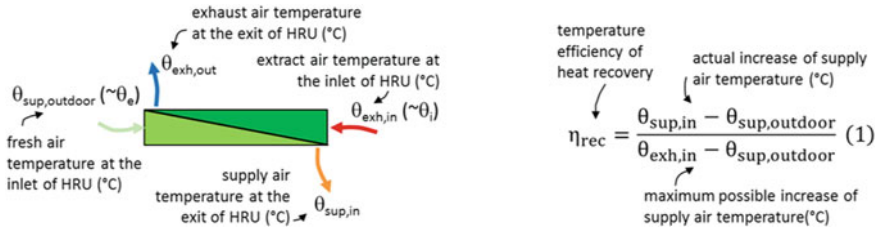


Fig. 11.14 Temperature efficiency of heat recovery is defined by the temperatures of extract and supply air at the inlet and outlet of HRU

The temperature efficiency of heat recovery depends on the construction of HRU and the air flow rates of supply and extract air. The maximum temperature efficiency can be reached if flows are equal.

If HRU is produced from water vapour permeable material, in addition to sensible heat, the latent heat of water vapour is transferred between the extract and supply air. Because the absolute humidity of indoor air is higher than that of outdoor air during the heating season, the latent heat of water vapour is transferred from exhaust to supply air, which lead to increased heat recovery efficiency (see Sect. 3.2). In this case, the efficiency of heat recovery is defined as enthalpy efficiency $\eta_{rec,x}$ by the enthalpies of the air instead of air temperatures:

$$\eta_{rec,x} = \frac{H_{sup,in} - H_{sup,outdoor}}{H_{exh,in} - H_{sup,outdoor}} \quad (1)$$

energy efficiency of heat recovery
actual increase of supply air enthalpy (J)
maximum possible increase of supply air enthalpy (J)

11.2.3.2 Cross-Flow HRU

In cross-flow heat exchangers, the direction of exhaust and supply air flows are perpendicular to each other. Such heat exchangers are more compact (shorter), but the theoretical limit of heat recovery is 75%; in practice, heat recovery between 60 and 65% can be achieved. Because of the relative low efficiency, the risk of water vapour condensation inside the assembly is also low (Fig. 11.15).

11.2.3.3 Counter-Flow HRU

In counter-flow heat exchangers, the exhaust and supply air flows in the opposite direction. Such a structure requires longer units, which results in higher pressure drop, which increases energy demand for the operation of fans. In theory, such heat exchangers can have temperature efficiency up to 100%; the best available

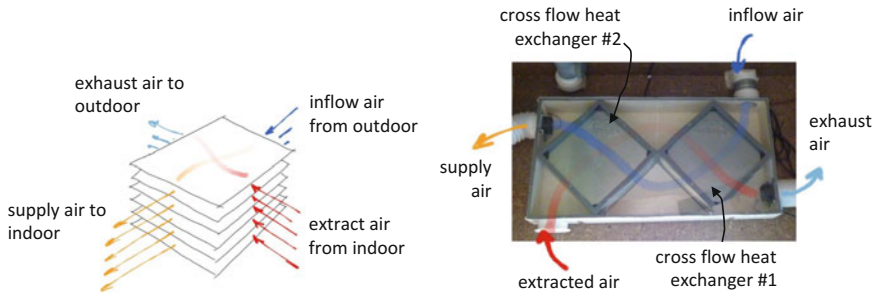
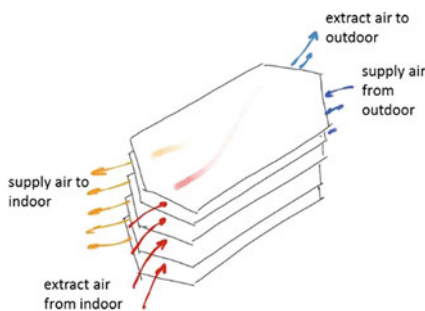


Fig. 11.15 Cross-flow heat exchangers are compact and have low pressure drop, which decreases the use of electricity for fan operation (left); two consecutive cross-flow heat exchangers are installed in the mechanical ventilation system in the technical unit of the Virtual lab (right) to increase the efficiency of heat recovery up to 90%

technologies have between 90 and 95% efficiency. The AHU must be equipped with a supply air by-pass (“around the heat exchanger”) channel, to enable cooling of the building by ventilation during summer nights.

Instead of metal (aluminium is used most common), heat exchanger plates can be made from pore-structured polymer. In this manner, enthalpy heat exchangers are built. In addition to sensible heat, water vapour molecules are transferred by osmosis between two air flows: extract and supply. The latent heat of water vapour improves energy efficiency (up to 120% in comparison to regular HRU) and improves indoor thermal comfort conditions because water vapour molecules transfer from extract to supply air during the winter and in the opposite direction during the summer (Figs. 11.16 and 11.17).

Fig. 11.16 Counterflow heat exchangers are larger and have high efficiency of heat recovery in comparison to other HRU technologies



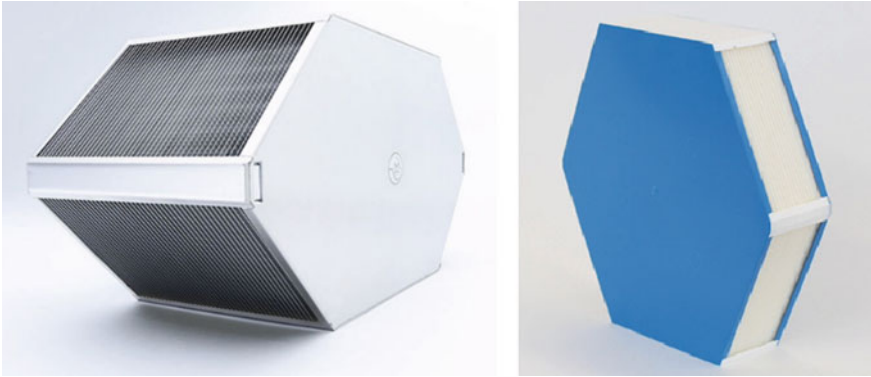


Fig. 11.17 Counter-flow heat exchanger (left); (www.klingenburg-usa.com) the polymer foil used in this enthalpy counter-flow heat exchanger is coated with an antimicrobial layer that prevents the transport of microbes to supply air (right) (paul-lueftung.de)

11.2.3.4 Rotary Wheel HRU

Rotary wheel heat exchangers are made from honeycomb like structures in the form of wheels placed in and rotating between of supply and exhaust air channels. Rotation is made by an integrated motor. The honeycomb structure, made from aluminium or plastic, heats up and accumulate heat in the exhaust air channel (winter-time operation) and cools the supply air channel down when turned into the supply channel. Rotary wheel heat exchangers are so-called regenerative heat exchangers because heat is regenerated in the accumulative mass every time that part of the wheel is turned into the warm extract air channel. Approximately 10 revolutions per minute is needed to reach of heat recovery efficiency of 85% (Fig. 11.18).

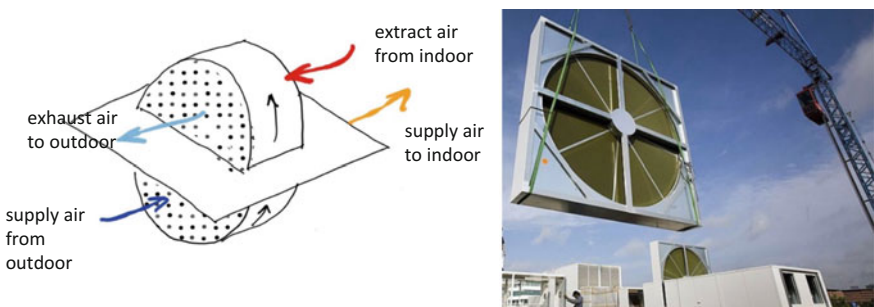


Fig. 11.18 Rotary regenerative heat exchangers have diameter ranging from 300 to +8000 mm and are suitable for high capacity ventilation systems. (www.klingenburg-usa.com)

Fig. 11.19 Air handling unit installed in ventilation system with rotary wheel HRU; the rotary wheel is designed for an air flow rate $5000 \text{ m}^3/\text{h}$ and is driven by a 100 W electric motor



Rotary wheel heat exchangers are compact and can be used in high capacity ventilation systems because of the low pressure drop and simple production technology. Instead of by-pass operation, wheel rotation can simply be switched off during summer nights. These heat exchangers have limitations if noxious pollutants are present in the exhaust air because such heat exchangers are not air tight. Nevertheless, these heat exchangers can be used for general building ventilation as well as in hospitals (Fig. 11.19).

The surface of the honeycomb structure in a rotary wheel heat exchanger can be coated with sorption material, such as Silica Gel or zeolite that collects and accumulates water vapour molecules. In this way, moisture is transferred by sorption and desorption between the supply and extract air. If zeolite is used as the sorption material, the very miniscule porous structure of zeolite collects only water vapour molecules and not bacteria or odour molecules; high air hygiene is thus maintained.

Note: Sorption is called adsorption if solid mater catches the water vapour molecules and absorption if water vapour molecules penetrate the liquid mater.

11.2.3.5 Flip-Flop HRU

Flip-flop heat exchangers are regenerative HRU. Unlike rotary wheels, two porous thermal accumulation masses acting as regenerative heat exchangers are still; supply and extract air are periodically (duration of period is ~ 60 to 90 s) redirected by a flap or valve through one of the heat exchangers. In the first half period, extract air flows through the first regenerator, while supply air flows in the opposite direction through the second one. During the second half period, air flow directions are reversed, supply air cools the first regenerator, meanwhile extract air heat up the

Fig. 11.20 Principle of flip-flop regenerative HRU with continuous air supply

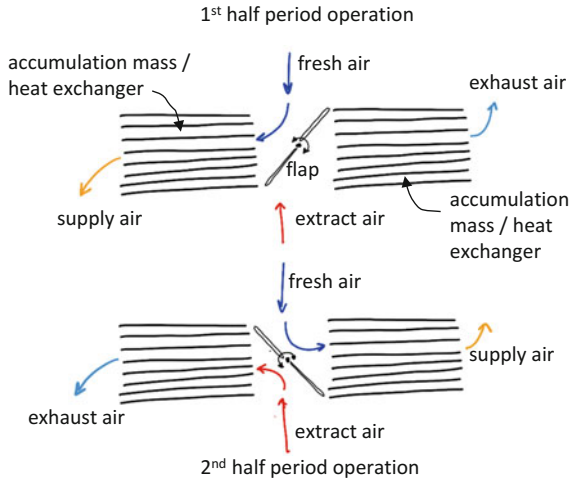
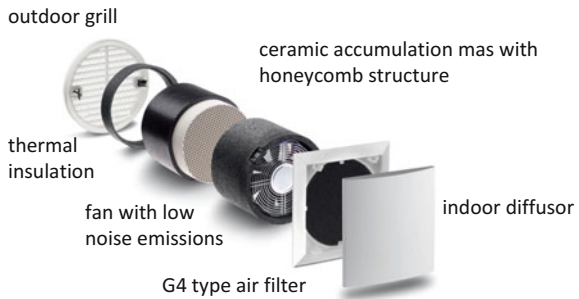


Fig. 11.21 Compact HRU with regenerator and reversible air flow (www.lunos.si)



second one. This process continues throughout the operation of the ventilation system. Such heat recovery units have efficiency up to 95% (Fig. 11.20).

Instead of one HRU with two regenerative heat exchangers and flaps, two HRU units with one regenerator and reversible fan operation could be used for ventilation in smaller apartments. In this case, units must operate simultaneously with air flow in the opposite direction. Each 60–90 s, the air flow directions in both HRU are reversed (Fig. 11.21).

11.2.3.6 Indirect HRU

An indirect HRU consist of two air-to-water heat exchangers integrated separately in the supply and exhaust air channels. Heat exchangers are connected by pipes filled by water with and an antifreeze solution, as well as a circulation pump. Heat recovery efficiency is ~50%; therefore, such recuperation systems are only suitable for renovation if the supply air system is far away from the extract air channels or if the extract air is highly contaminated and any mixing of extract and supply air must

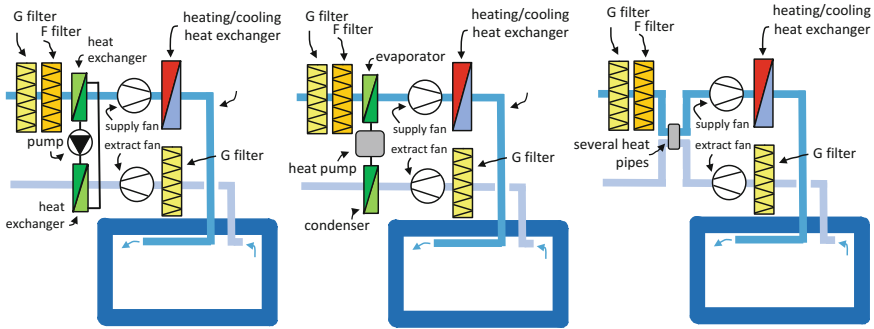


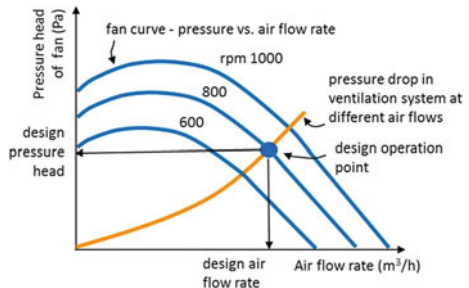
Fig. 11.22 Indirect HRU with closed water loop, heat pump or heat pipe heat transfer system

be prevented. Recovery efficiency could be increased by heat pipes installed between tight extract and supply air channels. The higher efficiency of heat recovery, operation without auxiliary energy, and the lack of frost problems are the main advantages of such HRU. Another way to increase heat recovery efficiency is to use a heat pump instead of a circulation pump with an evaporator in the extract channel and a condenser in supply air channel (Fig. 11.22).

11.2.4 Fans

Energy demand for mechanical ventilation systems' operation depends on the type of the fan, the efficiency of the fan's motor, the volume of the air that must be transferred, and the pressure drop that occurs in the duct system, as well as elements, such as flaps, filters, grills, or diffusers. The performance of the fan is expressed by the fan curve. It shows the relation between the air flow rate and the pressure increased by the fan at a constant fan speed (revolutions per minute) (Fig. 11.23).

Fig. 11.23 Fan-generated pressure head versus air flow rate at different revolutions per minute of the impeller; the shape of the curves depends on the type of impeller: the curves shown are typical for centrifugal fans with for back-curved blades



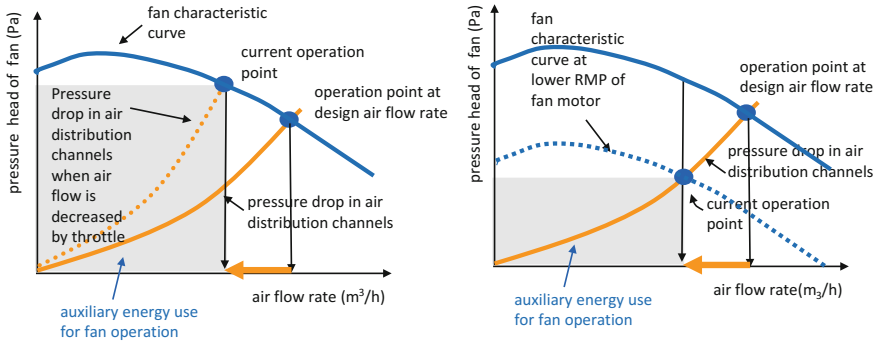


Fig. 11.24 Energy efficiency of ventilation systems can be improved by adjustment (decreasing) of the supply air flow rate to the actual number of persons and the concentration of pollutants in the ventilated room or building; if the throttle is used (left) for reducing the air flow rate, the energy for fan operation increases because of the increased pressure drop. In large ventilation systems in which AC motors are used, the air flow rate can be reduced by lowering the fan motor RMP by frequency regulation (right) or by electronic commutation when DC motors are used. This enables the connection of DC motors to high AC voltage

Ventilation systems are controlled to provide either (i) constant flow rate required to maintain indoor air quality regardless of the changing of pressure drop in distribution system, or (ii) constant pressure difference to adjust the supply air flow rate to the actual demand needed for diluting the pollutants in indoor air. In energy efficient ventilation systems, this is done by adapting the fan speed. Two techniques are used: frequency inverters that adapt the frequency of electricity voltage in the range between 0 and ~ 100 Hz (in this way, 1- or 3-phase alternating current (AC) motors are controlled) or by electronically commutated brushless DC motors with permanent magnets. In this case, the electronic circuit itself converts AC to DC. Such motors have almost constant efficiency in a wide range of speed rates and, therefore, the overall efficiency of such drives can be increased up to 30% (Fig. 11.24) (Harvey 2006; Jayamaha 2007; McQuiston et al. 2005).

11.2.5 Filters in AHU

Filters are installed in ventilation systems to remove particles of different sizes, bio-organisms, and aerosols. In ventilation systems, mostly fibrous media is used. Filters are classified regarding the size of particles separated from air flow. G class filters (short label G4) remove 90% of particles that are larger in diameter than $10\ \mu\text{m}$. F filters (F7–F9) remove 95% of particles larger than $5\ \mu\text{m}$ (class F7) or larger than $0.1\ \mu\text{m}$ (class F9). This means that pollen is removed from supply ventilation air. For ventilation of clean spaces (surgery room, pharmacy plants or spaces where electronic components are manufactured, food industry) very small

particles must be removed from the air. In this case, HEPA (high performance class H10–H14) or ULPA (ultra-high performance class U15–U17) filters are used. Such filters remove 99.99+% of particles in sizes from 0.1 to 0.001 μm . This includes bacteria and viruses. ULPA filters remove aerosols, radioactive aerosols, and mist. For the elimination of volatile organic compounds (VOC) and odours, active carbon filters should be installed in ventilation systems. Such filters remove particles (molecules) and aerosols with sizes down to 0.0001 μm . If filters are not regularly maintained, they do not function well and pressure drop increases. Consequently, air flow decreases and/or energy use for fan operation increases. To prolong the maintenance period, filters are installed in a cascade from lower class to higher class.³

11.2.6 Design of Mechanical Systems with Balanced Ventilation and Heat Recovery

Mechanical ventilation systems for balanced ventilation can be designed as central or decentral systems.

11.2.6.1 Centralized Ventilation Systems

Centralized systems have one air handling unit (AHU) with an integrated heat recovery unit (HRU) and a system of channels or ducts for the distribution of supply and exhaust air. In smaller buildings, fresh supply air is delivered into living spaces and extracted from utility spaces, such as kitchens, corridors and toilets. Free air flow between spaces must be provided by ventilation openings. In non-residential buildings, supply air is delivered, and polluted air is extracted from each room (Fig. 11.25).

The distribution duct system in centralized ventilation systems can be designed as an octopus type or loop type. The octopus distribution type is mostly used in small house or in apartment ventilation. Supply distribution ducts are connected to the air distributor chamber of the AHU and distributed to room in suspended ceilings in most cases. Indoor air is extracted from polluted rooms, such as bathrooms, corridors, and kitchens. Equal air flow rate is designed for supply and extract air. To avoid high pressure drop and noise emissions, designed air velocity in ducts should be below 2 m/s (Figs. 11.26 and 11.27).

Loop-type distribution is more suitable for the ventilation of large buildings, because very long ducts to supply fresh air to distant rooms will be needed otherwise. One duct is led through rooms and part of the supply air flows into each room. The size (area of cross section) of the ducts decreases from connection with

³www.fischer-luftfilter.de.

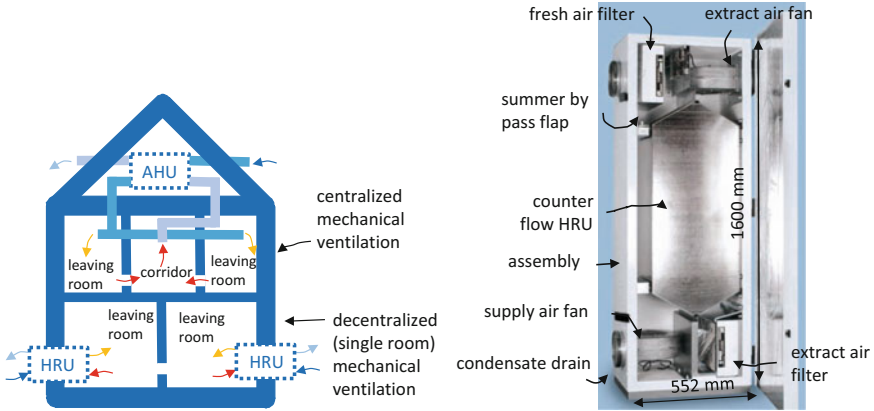


Fig. 11.25 Centralized and decentralized mechanical ventilation with heat recovery in a residential building (left); air handling unit with heat recovery unit; supply (and extract) air flow rate can be controlled in 7 steps between 70 and 300 m³/h (right) (paul-lueftung.de (Atmos 175 DC))

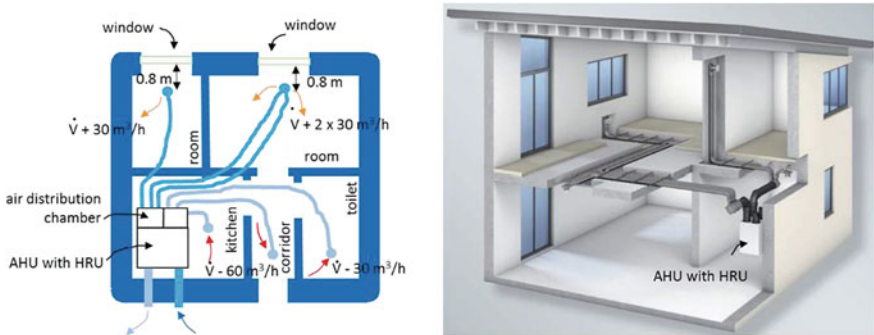


Fig. 11.26 Schematic of central mechanical ventilation system with octopus type distribution duct system (www.viessmann.com)

AHU to the farthest outlet. In this way, equal pressure drop in each part of the duct system is maintained. In multi-storey buildings, loop distribution systems are connected with AHU by vertical distribution branches (Fig. 11.28).

Supply air is delivered into the room through diffusor(s) that distribute supply air into the room without any draught. Some examples are presented in Fig. 11.29.

11.2.6.2 Design of Distribution Duct System

The design procedure of a mechanical ventilation system starts with the precise design of the required supply air flow rate, continues with the sizing of the



Fig. 11.27 Octopus type of distribution duct system in apartment; each tube has diameter of 80 mm and air flow rate is designed to 30–40 m³/h per duct; this corresponds to the physiological needs of one person. If two persons are expected to be in the room, two ducts are connected to the assembly of inlet diffuser

distribution network branches on the basis of pressure losses. Pressure losses increase with the square of the air flow rate, and electricity consumption for fan operation increases with the third power of the air flow rate. To reduce the pressure losses, air velocity should be kept in the range between 4 m/s (near AHU) to 2 m/s (in the end sections of the duct), and the air velocity in the inlet diffuser should be around 1 m/s to avoid draught, high pressure losses, and noise emission. Alternatively, constant design pressure drop per unit of duct length (typical 0.4 Pa/m in households and up to 1 Pa/m in industrial buildings) can be used for the design of the duct size. When air velocity is determined, the cross-section area of duct can be determined using the continuity equation:

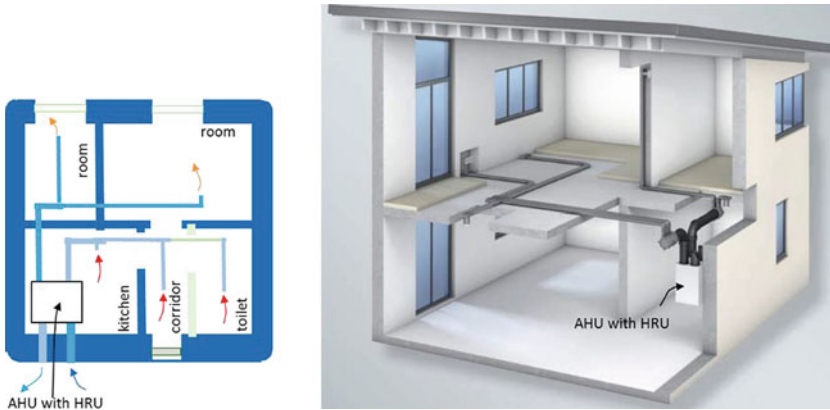


Fig. 11.28 Schematic of a central mechanical ventilation system with loop type distribution duct system (www.viessmann.com)

$$\begin{aligned} \text{design air flow rate (m}^3/\text{s)} \quad \dot{V} &= A_{\text{duct}} \cdot v \left(\frac{\text{m}^3}{\text{s}} \right) \rightarrow A_{\text{duct}} = \frac{\dot{V}}{v} \text{ (m}^2\text{)} \\ \text{duct cross section area (m}^2\text{)} \quad \uparrow & \quad \uparrow \\ & \quad \text{air velocity in duct (m/s)} \end{aligned}$$

Case study: Air flow rate 60 m³/h should be delivered into the bedroom. The required duct diameter is:

$$A_{\text{duct}} = \frac{\dot{V}}{v} = \frac{60}{\frac{3600}{2.5}} = 0.0067 \text{ (m}^2\text{)} \rightarrow d_{\text{in,duct}} \doteq 90 \text{ mm}$$

inner diameter of round duct

Note: Instead of round ducts, rectangular channels can be used with a width-to-height ratio of not more than 5:1.

11.2.6.3 Decentralized Ventilation Systems

Decentralized ventilation is most suitable for the renovation of existing flats or buildings because such HRU are compact and can be built into the outer walls. No duct system is needed. Such systems have low capacity of fresh supply air (<45 m³/h) to ensure high heat recovery efficiency (up to 90%), low energy demand for operation, and low noise emissions. The last factor is the most critical performance indicator if such units are installed in bedrooms or working spaces. The best



Fig. 11.29 Examples of diffusers and grill (Lindab IMP Klima)

available technologies cause noise pressure levels below 20 dB at air flow rate $\sim 30 \text{ m}^3/\text{h}$ in laboratory conditions at 1 m distance.

For heat recovery, two types of heat exchangers are used: counter flow or regenerative. A ventilation unit with a counter-flow heat exchanger is similar to the AHU in central ventilation systems as they provide a constant supply of fresh air. In regenerative types of HRU, the heat exchanger is made from honeycomb-structured ceramic acting as heat storage, and heat is charged and discharged by the

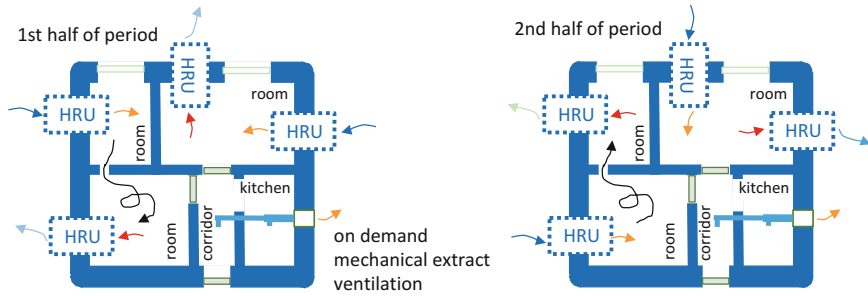


Fig. 11.30 Decentral ventilation system with regenerative heat recovery must work in pairs

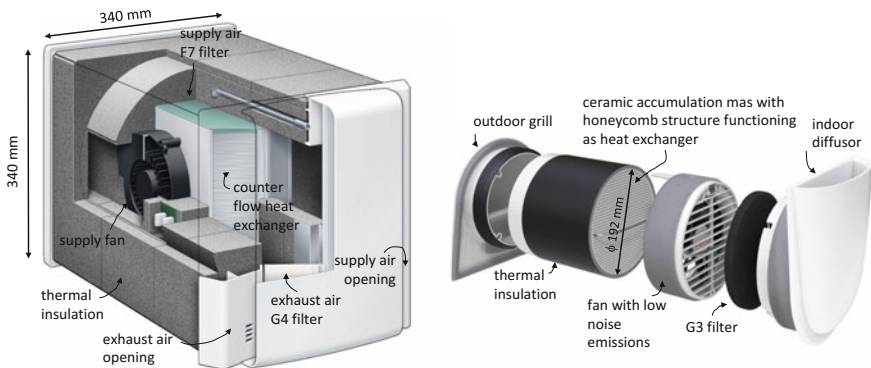


Fig. 11.31 Example of decentral ventilation unit with counter flow heat exchanger (left) (www.viessmann.com) (Vitovent 200-D)) with supply air capacity up to $55 \text{ m}^3/\text{h}$, heat recovery efficiency $>90\%$ and electricity power 25 W (at air flow rate $55 \text{ m}^3/\text{h}$ including control unit), noise level 38 dB ; regenerative decentral ventilation unit (right) (www.viessmann.com) (Vitovent 100-D)) with supply air capacity up to $46 \text{ m}^3/\text{h}$, heat recovery efficiency 90% and electricity power 6.1 W (at air flow rate $46 \text{ m}^3/\text{h}$ including control unit)

periodically changing air flow direction. At least two units must be installed and must work as a pair. Indoor air circulation between those units must be enabled. Every $\sim 60 \text{ s}$ (period depends on air flow rate; typical step air flow rates for room ventilation units are $15, 30$ and $40 \text{ m}^3/\text{h}$),⁴ the air flow direction through two paired HRU changes, and the heat accumulation mass is cooled in one and heated in the other HRU. To avoid the dispersion of odours, kitchens and toilets should be ventilated by additional time-controlled extract ventilation systems (Figs. 11.30 and 11.31).

⁴www.lunos.si.

11.3 Energy Efficiency Indicators of Mechanical Ventilation Systems with HRU

Mechanical ventilation with HRU is effective only if buildings are properly air tight to avoid undesirable air infiltration. The energy efficiency requirements of mechanical ventilation systems are covered in national legislation acts, EN standards and European Commission regulation No 1253/2014.⁵ Energy efficiency indicators could be expressed as:

- design temperature efficiency of heat recovery unit; design temperature efficiency is determined by experiments in conditions of dry air, design air flow rate (in m^3/s or m^3/h), equal air flow rate of supply and extract air, without corrections of heat gains from fan motors and at temperature difference of indoor and outdoor air $13\text{ }^\circ\text{C}$;

Note: Minimum requested temperature efficiency η_{rec} of HRU is in Slovenia 65%, minimum requested η_{rec} 75% for units in passive buildings (according to the Passive house Institute in Darmstadt) and η_{rec} 73% according to Eco-design guidelines.⁶

- specific fan power (SFP) of each of installed fan in W per air flow one m^3/s ($\text{W}/(\text{m}^3/\text{s})$) or specific total electricity power of AHU in $\text{W}/(\text{m}^3/\text{h})$; for example, in passive houses only AHU with specific electrical power (including control units) below $0.45\text{ W}/(\text{m}^3/\text{h})$ at operating pressure differences 100 Pa could be installed;

Note: In EN 16798-3 classification of specific fan power SFP is shown. It is based on design fan motor power and expressed in W per m^3/s of air flow rate. Class 0 corresponds to $\text{SFP} < 300\text{ W}/(\text{m}^3/\text{s})$, $\text{SFP} 1 \leq 500\text{ W}/(\text{m}^3/\text{s})$, $\text{SFP} 2 \leq 750\text{ W}/(\text{m}^3/\text{s})$, $\text{SFP} 3 \leq 1250\text{ W}/(\text{m}^3/\text{s})$, $\text{SFP} 4$ to $\leq 2000\text{ W}/(\text{m}^3/\text{s})$, $\text{SFP} 5$ to $\leq 3000\text{ W}/(\text{m}^3/\text{s})$ and last class $\text{SFP} 7$ to $>4500\text{ W}/(\text{m}^3/\text{s})$.⁷

⁵Commission Regulation (EU) No 1253/2014 of 7 July 2014 implementing Directive 2009/125/EC of the European Parliament and of the Council with regard to ecodesign requirements for ventilation units (Official Journal of the European Union, L 337/8).

⁶International Passive House Association, www.passivehouse-international.org.

⁷EN 16789-3:2017 Energy Performance of buildings—Ventilation for buildings—Part 3: For non-residential buildings—Performance requirements for ventilation and room-conditioning systems (Module M5-1, M5-4).

- specific energy consumption (SEC; defined according Eco-design guidelines); indicator represents the difference between the primary energy use of mechanical ventilation system operation and decreased primary energy demand for heating during a one-year period expressed as a specific value per m² of heated floor area; SEC 0 kWh/m² a is set as target value, but it will be lowered to -20 kWh/m² per year after 2018. SEC is defined by equations (Commission Regulation No 1253/2014):

$$SEC = \frac{E_{p,ven} - E_{p,avoid,h}}{A_u} \quad \left(\frac{kWh}{m^2 a} \right)$$

needed primary energy for operation of ventilation system (kWh/a) avoided primary energy for heating because HRU (kWh/a)

specific energy consumption heated floor area (m²)

$$E_{p,ven} = t_{v,a} \cdot \dot{V}' \cdot SFP \cdot CTRL^x \cdot MISC \cdot f_{p,v} \quad \left(\frac{kWh}{m^2 a} \right)$$

specific supply air flow rate(m³/(h. m²)) primary energy factor of electricity (for ventilation system operation) (-)

annual operating hours of ventilation system (h/a) specific fan power (kW/(m³/h)) ventilation control factor (-), x non-linearity coefficient (-)

duct factor (-)

$$E_{p,avoid,h} = t_{h,a} \cdot (\Delta\theta_h - 3) \cdot c_{p,air} \cdot ((1 - \eta_{rec}) \cdot \dot{V}' \cdot CTRL \cdot MISC) \cdot \frac{1}{\eta_h} \cdot f_{p,h} + Q'_{defr} \cdot f_{p,v}$$

solar and internal gains correction factor(°C) air specific heat capacity (kWh/m³K); 0,000344 kWh/m³K

annual operating hours of heating system (h/a) average difference in indoor and outdoor temperature (°C) HRU efficiency (-)

primary energy factor, energy carrier for heating system operation (-) annual average efficiency of heating system (-)

primary energy carrier for defrosting (-) specific energy for defrosting of HRU (kW/m²a) (at temperatures of environment air below -4°C (kWh/m²a))

Instead of the second term ($E_{p,avoid,h}$), the decrease of final energy use for heating as consequence of mechanical ventilation with heat recovery can be calculated with software and multiplied with the primary energy factor of energy carrier(s) used for heating.

Note: According to Commission Regulation No 1253/2014, the following factors are proposed:

- MISC: ventilation system with ducts 1.1, without ducts 1.21;
- CTRL: manual control 1, timer control 0.95, central system 0.85, local demand control 0.65;
- x: on/off operation, single speed 1, 2 speed fan 1.2, multi speed fan 1,5, variable speed 2;
- specific energy for defrosting Q'_{defr} for $t_{h,a}$ 5000 h/a 0.45 kWh/m² a, for $t_{h,a}$ 6500 5.82 kWh/m² a;
- $t_{v,a}$ 8760 h/a;
- η_{rec} 0.75.

- seasonal coefficient of performance COP is the ratio between annual the decrease of ventilation heat losses in comparison to a naturally ventilated building and the annual total electricity use for operation of the ventilation system;

$$\text{COP} = \frac{Q_{v,\text{nat}} - Q_{v,\text{HRU}}}{W_{v,f}} (-)$$

ventilation heat losses for natural ventilated building (kWh/a) ventilation heat losses for mechanical ventilated building with HRU (kWh/a)
 ↘ ↙
 ↙ ↘
 energy demand for operation of ventilation system (kWh/a)

- minimum supply air temperature to maintain indoor thermal comfort requirements is an additional criterion posted by the Passive House Institute; at an outdoor temperature of $-15\text{ }^{\circ}\text{C}$, supply air temperature must be warmer than $16.5\text{ }^{\circ}\text{C}$; in practice, this criterion can be fulfilled by an additional air heater or if air is preheated in ground heat exchanger.

Case study: SEC of mechanical ventilation system with heat recovery installed in the living unit of the Virtual Lab building (Fig. 11.32).

Energy need Q_{NH} (see Sect. 5.3.1) for heating of natural ventilated living unit of Virtual laboratory building ($V\ 56\ \text{m}^3$, $A_u\ 16\ \text{m}^2$, $V_{\text{supply}}\ 30\ \text{m}^3/\text{h}$) is equal to $991\ \text{kWh/a}$ ($61.9\ \text{kWh/m}^2\text{a}$). Energy use for heating $Q_{f,h}$ is $1002\ \text{kWh/a}$ (electrical heater) and electricity use for operation of the heating



Fig. 11.32 HRU* is integrated into south-orientated wall and has a transparent cover to utilize solar energy by additional heating of the fresh supply air; in the present calculation, only heat transfer between the exhaust and fresh air is taken into account

system $W_{f,h}$ is equal to 13 kWh/a. Primary energy factor for electricity is $f_{p,h} = 2.5$ (kWh/kWh). Electricity is the only energy carrier that is used.

Because ventilation of living unit with mechanical ventilation with HRU ($\eta_{rec} 0.85$) and a supply air flow rate of 30 m³/h, Q_{NH} is equal to 414 kWh/m²a (25.9 kWh/m²a). Supply and extract fans with power of 7 W (class SPF 4) are installed in AHU, and the control unit has electrical power of 1.2 W. The system has no duct distribution system (MISC 1.21), and is controlled by local demand control (CTRL 0.65); motors of the fans operate at a constant speed ($x = 1$), and no defrosting is provided. Energy use for heating $Q_{f,h}$ is this case equal to 417 kWh/a (electrical heater), electricity use for operation of the heating system $W_{f,h}$ is equal to 9 kWh/a and electricity use for a year operation of the ventilation system is 134 kWh/a.

$$E_{p,avoid,h} = (Q_{f,h,natural} \cdot f_{p,e} + W_{f,h} \cdot f_{p,e} + \underbrace{W_{f,v}}_0 \cdot f_{p,e}) - (Q_{f,h,mec} \cdot f_{p,e} + W_{f,h} \cdot f_{p,e} + W_{f,v} \cdot f_{p,e}) =$$

$$E_{p,avoid,h} = (1002 \cdot 2.5 + 13 \cdot 2.5) - (417 \cdot 2.5 + (9 + 134) \cdot f_{p,e}) = 2537.5 - 1400 = 2537.5 - 1400 = 1137.5 \frac{kWh}{m^2a}$$

$$E_{p,ven} = \underset{\substack{\text{hours per year} \\ \downarrow}}{8760} \cdot \underset{\substack{\text{air flow rate} \\ \text{(m}^3\text{/h)} \\ \downarrow}}{\frac{30}{16}} \cdot \underset{\substack{\text{total electrical power of} \\ \text{HRU(W)} \\ \downarrow}}{\frac{(7 + 7 + 1.2)}{1000}} \cdot \underset{\substack{\text{conversion factor (W/kWh)} \\ \uparrow}}{0.65^1} \cdot 1.21 \cdot 2.5 = 16.4 \frac{kWh}{m^2a}$$

$$SEC = 16.4 - 71.1 = -54.7 \frac{kWh}{m^2a}$$

Ventilation heat losses of the living unit of the Virtual Lab building decreased from 736 kWh/a in the case of the naturally ventilated unit to 113 kWh/a for the mechanically ventilated unit with heat recovery $\eta_{rec} 0.85$. Electricity demand for the operation of AHU is 134 kWh/a. Seasonal coefficient of performance of ventilation system is equal to:

$$COP = \frac{Q_{v,nat} - Q_{v,HRU}}{W_{v,f}} = \frac{736 - 113}{134} = 4.67$$

If the mechanical ventilation system operates only during the heating season, electricity use for operation of the AHU will decrease to 84 kWh/a and seasonal COP will increase to 7.4.

11.3.1 Energy Needs and Delivered Energy for Mechanical Ventilation

As prescribed by the Energy Performance of Buildings Directive, energy needs for ventilation of the buildings and the use of energy (electricity) for the operation of mechanical ventilation systems are included in the assessment of energy efficiency indicators. In Sect. 5.3.4, energy need for ventilation is explained. The use of energy for the operation of a ventilation system is defined by the total electricity use of the fan and control unit operation. As a ventilation system usually operates with a variable air flow rate according to the quality of the indoor air or the presence of residents, this must be taken into account in the calculation of annual energy consumption (Fig. 11.33).

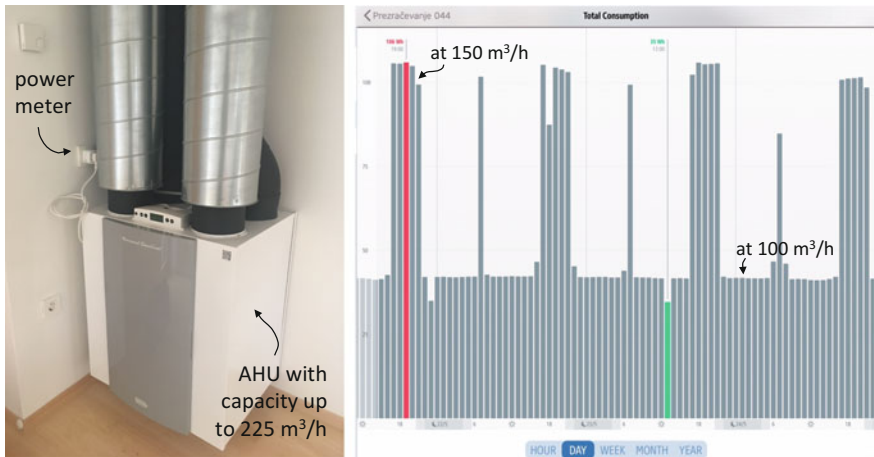


Fig. 11.33 Central apartment AHU (left) and electricity use for operation presented as average hourly power of AHU including fans and control unit (right) (Elgato Eve, Eve Systems GmbH, 2016)

11.4 Techniques for Improving Energy Efficiency of Ventilation

11.4.1 Increasing Heat Recovery Efficiency by Ground Heat Exchanger (GHX)

Supply air can be preheated (or precooled) in a ground heat exchanger. Such earth-to-air duct heat exchangers use the ambient heat of soil and, therefore, increase the share of renewable energy sources for the operation of the building. An increase of the supply air temperature by ~ 5 to $10\text{ }^\circ\text{C}$ can be achieved. If mechanical ventilation with a high efficiency HRU is used for building ventilation, ground heat exchangers are mainly used to prevent water vapour condensation from exhaust air in the HRU heat exchanger. In the summer time, during the daytime, supply air can be precooled in GHX if HRU operates in by-pass mode; during the night time, a GHX by-pass operation is needed to prevent preheating of the supply air. Increase (or decrease in case of cooling) of supply air temperature depends on outdoor air (θ_e) and soil temperature (θ_{soil}), supply air flow rate (V), length (L) and diameter (D) of the duct, the depth of the duct below the surface (Z) and conductivity (λ_{soil}) and specific heat of soil ($c_{p,soil}$), as shown in Fig. 11.34.

Average daily soil temperature $\theta_{soil,Z,n}$ at distance Z (m) below the surface for n -th day of the year can be determined by equation:

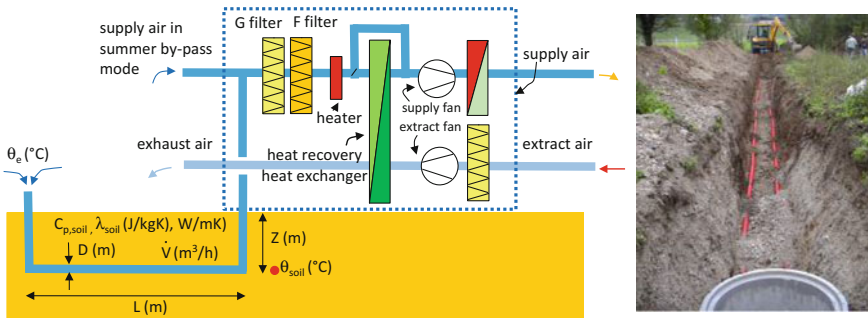


Fig. 11.34 Ground-to-air duct heat exchanger GHX for preheating of supply ventilation air; parameters that influence the supply air temperature are shown (left); building phase of GHX with design capacity $150\text{ m}^3/\text{h}$ (right)

Table 11.1 Thermal diffusivity of selected soil materials

	a_{soil} (m ² /s)
Sand	9.57×10^{-7}
Limestone	10.92×10^{-7}
Clay	7.30×10^{-7}
Granite	9.13×10^{-7}

$$\theta_{soil,Z,n} = \theta_{e,av} - A_e \cdot e^K \cdot \cos \left[\frac{2 \cdot \pi}{365} (n - \Delta n) - \frac{Z}{2} \left(\frac{365}{\pi \cdot a_{soil}^*} \right)^{\frac{1}{2}} \right]$$

average yearly ambient air temperature (°C) → $\theta_{e,av}$
 exponent (-) → K
 depth of pipe (m) → Z
 average yearly amplitude of ambient air temperature (°C) → A_e
 n^{th} day of the year → n
 n^{th} day of extreme low θ_{soil} after the 1st of January (for continental climate Δn is equal to 35) → Δn
 reduced thermal diffusivity of soil (m²/day) → a_{soil}^*

Exponent K and reduced thermal diffusivity a_{soil}^* are defined by equations (Table 11.1):

$$K = -Z \cdot \left(\frac{\pi}{365 \cdot a_{soil}^*} \right)^{1/2} \quad (1)$$

$$a_{soil}^* = a_{soil} \cdot 60 \cdot 60 \cdot 24 \left(\frac{m^2}{day} \right)$$

↑
 thermal diffusivity of soil (m²/s)

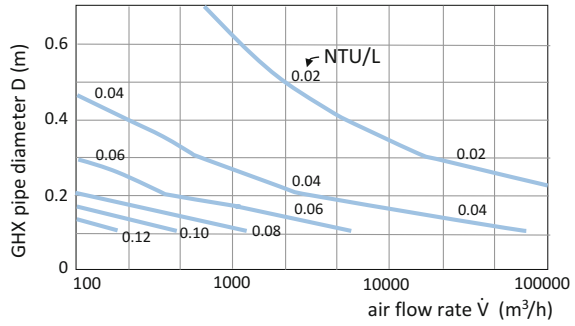
Supply air temperature at the exit of ground heat exchanger $\theta_{GHX,out}$ is defined by equation according to number of heat transfer units (NTU):

$$\theta_{GHX,out} = \theta_e + (1 - e^{-NTU}) \cdot (\theta_{soil,Z,n} - \theta_e) \quad (°C)$$

↖ number of heat transfer unit

Numerical modelling is needed for the determination of NTU. For the first design stage, the empirical model developed by Cucumo et al. (2008) can be used to determine normalized NTU per 1 m of GHX according to design air flow rate V (m³/h) and GHX inner pipe diameter D_{in} (m) as independent variables. The empirical model is presented in Fig. 11.35.

Fig. 11.35 Normalized number of heat transfer units (NTU/L) for earth-to-air duct heat exchanger (Cucumo et al. 2008)



Case study: What will average supply air temperature be at the exit of the U-shaped ground heat exchanger presented in the figure on 15 February? The design air flow rate \dot{V} is 120 m³/h and average daily outdoor air temperature $\theta_{e,av}$ on location is $-1.8\text{ }^\circ\text{C}$ (Fig. 11.36).

The limestone soil temperature θ_{soil} 2.5 m beneath the surface on 15 February (46th day of the year) on a site with a continental climate ($\theta_{e,avg}$ equal to $9.2\text{ }^\circ\text{C}$ and A_e equal to $11.0\text{ }^\circ\text{C}$ and Δn equal to 35) is equal to:



Fig. 11.36 U-shaped ground heat exchanger

$$K = -Z \cdot \left(\frac{\pi}{365 \cdot a_{\text{soil}}^*} \right)^{\frac{1}{2}} = -2.5 \cdot \left(\frac{\pi}{365 \cdot 0.103} \right)^{1/2} = -0.722$$

$$a_{\text{soil}}^* = a_{\text{soil}} \cdot 60 \cdot 60 \cdot 24 = 10.94 \cdot 10^{-7} \cdot 60 \cdot 60 \cdot 24 = 0.103 \frac{\text{m}^2}{\text{day}}$$

$$\theta_{\text{soil},Z,n} = \theta_{e,\text{av}} - A_e \cdot e^K \cdot \cos \left[\frac{2 \cdot \pi}{365} (n - \Delta n) - \frac{Z}{2} \left(\frac{365}{\pi \cdot a_{\text{soil}}^*} \right)^{\frac{1}{2}} \right]$$

$$\theta_{\text{soil},2.5,46} = 9.2 - 11.0 \cdot e^{-0.722} \cdot \cos \left[\frac{2 \cdot \pi}{365} (46 - 35) - \frac{2.5}{2} \left(\frac{365}{\pi \cdot 0.103} \right)^{\frac{1}{2}} \right] = 5.2^\circ\text{C}$$

$$D = 0.2 \text{ m}, \dot{V} = 120 \frac{\text{m}^3}{\text{h}} \rightarrow \frac{\text{NTU}}{L} = 0.08 \rightarrow \text{NTU} = 4.8$$

$$\theta_{\text{GHX,out}} = \theta_e + (1 - e^{-\text{NTU}}) \cdot (\theta_{\text{soil},Z,n} - \theta_e) \text{ (}^\circ\text{C)}$$

$$\theta_{\text{GHX,out}} = -1.8 + (1 - e^{-4.8}) \cdot (5.2 - (-1.8)) = 5.1 \text{ }^\circ\text{C}$$

Note: To ensure high efficiency of GHX and moderate pressure drop, the air velocity should be kept below 2 m/s and the specific heat transfer area (outer surface of pipe) should be at least 0.04 m² per 1 m³/h of air flow rate. In the presented ground heat exchanger, the designed air velocity is 1.1 m/s and the specific heat transfer area is equal to 0.165 m²/m³/h.

11.4.2 Increasing Energy Efficiency of Buildings with Passive Cooling with Night-Time Natural Ventilation

If average the daily outdoor air temperature $\theta_{e,\text{av}}$ is not higher than the indoor cooling set-point air temperature and the daily amplitude of the outdoor air is high enough ($A_e > 5 \text{ K}$), building structures can be cooled with intense natural ventilation during the night time. This enables the building structures to accumulate the heat of solar radiation and internal gains during following day without overheating. Cooling with night-time natural ventilation can be effective in the case of cross or stack ventilation if at least 5 h⁻¹ air exchanges per hour are achieved. In this case, the thermal response of the buildings must be observed as a transient process using software. Two groups of software are available: one that uses empirical tools (see Sect. 11.1.3) and the other that solves differential equations as a set of finite difference equations using computational fluid dynamics (CFD) techniques.

Case study: IDA-ICE computer code was used for the prediction of indoor air temperatures and the air exchange rates (ACH) of the natural cross-ventilated free run living unit of the Virtual Lab building during a selected summer week. From simulation results, it can be seen that passive cooling decreases the maximum indoor air temperatures by as much as 3 °C. Indoor thermal comfort significantly increased because night-time air temperatures are significantly lower (by as much as 8 °C). AHC up to 4.9 h⁻¹ was achieved during the nights (Figs. 11.37 and 11.38).

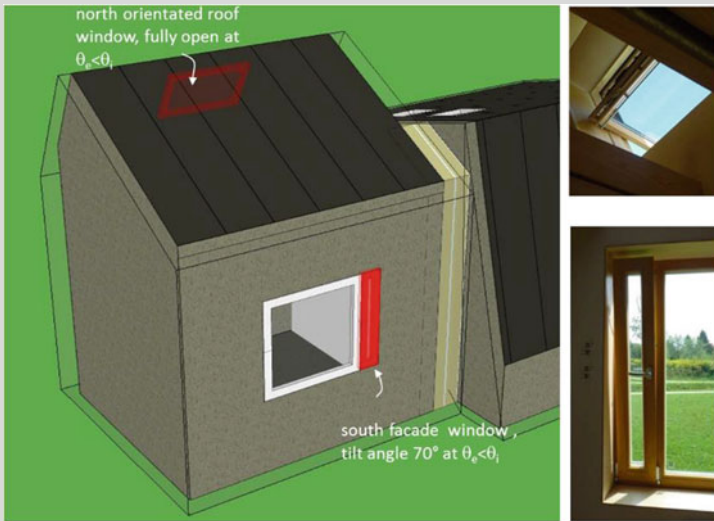


Fig. 11.37 Model of Virtual Lab building in IDA-ICE computer simulation tool (left); windows in the living unit of the Virtual Lab building (right)

11.4.3 Increasing Energy Efficiency of Buildings with Integration of Building Service Systems

If exhaust ventilation system is installed, heat recovery can be done by integrating a heat pump evaporator into the exhaust air channel. In smaller systems, heat is most likely to be used for (pre)heating of domestic hot water, and in large buildings for space heating. To avoid condensation and freezing on evaporator, exhaust air should not be cooled below ~ 5 °C. This means that heat flux of not more than 6 W can be extracted from 1 m³/h exhaust air flow rate or that the electricity power of the heat pump of 2.5 W per 1 m³/h of exhaust air flow rate can be installed. Heat can be transferred to the other building systems, such as the system for domestic

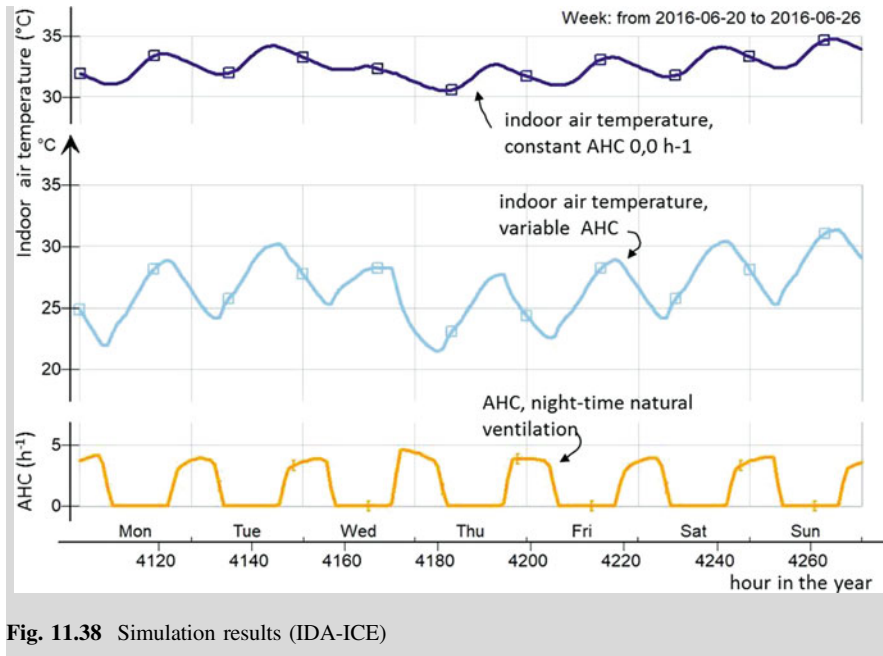
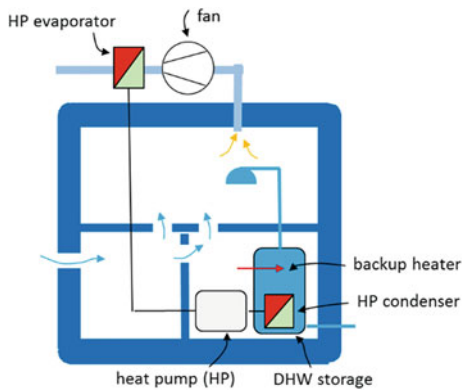


Fig. 11.38 Simulation results (IDA-ICE)

Fig. 11.39 Heat recovery in mechanical exhaust ventilation system by heat pump



water heating (DWH). Backup heating of DWH is needed in this case. A heat pump can also be installed in a mechanical ventilation system with balance ventilation, but only if supply air is preheated in the ground heat exchanger (Fig. 11.39).

References

- Cucumo M et al (2008) A one-dimensional transient analytical model for earth-to-air heat exchangers, taking into account condensation phenomena and thermal perturbation from the upper free surface as well as around the buried pipes. *Int J Heat Mass Transf* 51(3–4):506–516
- Harvey LDD (2006) A handbook on low-energy buildings and district-energy systems, fundamentals, techniques and examples. Earthscan, London
- Jayamaha L (2007) Energy-efficient building systems green strategies for operation and maintenance. McGraw-Hill
- Kleiven T (2004) Natural ventilation in buildings—architecture concept, consequences and possibilities. EuroSun
- Limam K et al (2011) Education package ventilation, Lecture 2: Natural ventilation. Master and post graduate education and training in multi-disciplinary teams implementing EPBD and beyond—IDES-EDU, IEE/09/631/SI2.558225
- Mc Quiston FC, Parker JD, Spitler JD (2005) Heating, ventilating, and air conditioning—analysis and design. Wiley

Chapter 12

Energy Efficient Lighting of nZEB



Abstract Human beings gather more than 80% of their information about their surroundings by visual perception. The information that we receive is influenced by the characteristics of the light source, the optical properties of objects reflecting the incoming light into the surrounding space, and the way we perceive light by sight and visualise “what we see” in our brain. Light is electromagnetic radiation with wavelengths that can be perceived by human vision. Such radiation is emitted from the emitter with sufficiently high temperature in the case of daylight or incandescent lamps, by electricity-excited gas atoms and molecules in the case of low and high pressure discharge lamps, by photoluminescence (the process of emission of light after absorption of nonvisible electromagnetic radiation in the case of fluorescent lamps or by electroluminescence), of the process of the emission of light after the recombination of electrons and electron holes in light-emitting diode (LED). LED technology has proven to be so efficient, so long lasting, and with such large possibilities of adaptation to users and daylight that almost no other electricity source of light is in use for lighting of buildings nowadays. While light has great influence on our health, wellbeing and productivity, this chapter focuses on the energy aspect of indoor lighting. Although extraordinary increases in the energy efficiency of artificial light sources has been achieved, the goal of designers should be focused on daylighting, which is the most acceptable and pleasant way of illumination for people. As up to 30% of delivered energy for the operation of the office and commercial buildings is still needed for lighting, the efficient combination with daylighting and advanced controlling of artificial lighting must be provided in nZEB. Additionally, visual comfort indicators are included in building assessment schemes, such as BREEM or DGNB (see Chap. 14).

12.1 Light

Light, as treated in this chapter, is electromagnetic radiation with wavelength in the range between 380 and 730 nm (Dubois 2011) that can be detected by the human eye. The eye, which has the function of detecting and transforming the luminous

flux into electrical signals, is characterized by high accommodation (it can focus picture of object from several centimetres distant to infinity in less than 350 ms) and adaptation to the luminance of observed surface (we can observe surfaces with luminance in the range between few thousandths to several hundred thousand candelas per square metre of emitter area). Electrical signals are transferred by the optic nerve to the visual cortex in the brain where interpretation of what we see is made.

Note: Values could differ according to reference source.

The sensitivity of human vision depends on wavelength of the light and brightness of observed environment. It is expressed as the luminous efficiency function $V(\lambda)$ as relative sensitivity with a value of 1 at light wavelengths that differ for photopic vision in bright environment through mesotopic to scotopic vision in dark environments (Fig. 12.1).

The spectral sensitivity of human vision is the reason that light sources and visual comfort are characterized by photometric quantities and not by physical ones. For example, a source's total emitted light flux is expressed in lumens not in watts; the received light flux per unit of receiver area is expressed in lumens per square metre or lux not in watts per square metre.

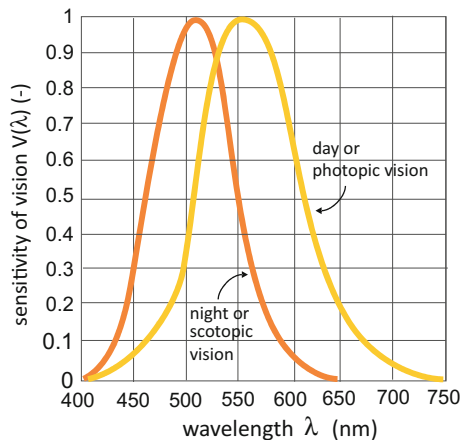


Fig. 12.1 Human perception of light depends on the light wavelength and brightness of environment; relative ability to detect different wavelengths of light is presented as luminous efficiency function $V(\lambda)$ according to the light conditions; photopic, mesotopic, and scotopic curves are standardized by CIE (CIE—Commission Internationale de l’Eclairage, www.cie.co.at)

12.2 Visual Comfort

Visual comfort is not related only to the ability to perform visual tasks, but to the psychological and health aspects of lighting as well. Considering the psychological aspect of lighting, the inhabitants of a building must be provided with appropriate natural and/or artificial light to be able to orient themselves in the space, to discern the significance of visual information, to stimulate human internal sense of time, to provide sense of individuality by creating different illuminated areas in the larger rooms, and to eliminate the sense of fear in an environment that may otherwise appear to be dangerous, for example in long hallways if the other end is not illuminated. Studies have shown that the quality of lighting also has significant influence on the market value of a property. Visual comfort is related to the health of inhabitants because daylight enables the synthesis of vitamins in our bodies, influences well-being, mental health and vitality, fills us with contentment, optimism and confidence and protect inhabitants against psychosomatic disorders, such as depression, lack of concentration, tiredness and insomnia.

The modern way of life requires that the natural sources of light be supplemented with artificial sources of light. Consequently, visual comfort indicators are divided into daylight and artificial lighting requirements.

12.3 Sources of Light

12.3.1 Daylight

There are several natural sources of daylight: the Sun, the Moon that reflects received sunlight from its surface and fires, volcanic eruptions and other processes in the nature, such as lightning or bioluminescence.

The temperature of the Sun's photosphere is approximately 6000 K and, as a black body, it emits thermal radiation in wide range of wavelengths: from ultraviolet (UV-C λ 100–280 nm, UV-B λ 280–320 nm and UV-A λ 320–400 nm; the division is made according to absorption by the stratospheric ozone), visible (λ 400–700 nm) to infrared (near IR-A λ 700–3000 nm, mid-infrared IR-B λ 3–5 μ m, far-infrared IR-C λ 50–1000 μ m). The share of light in the total thermal radiation emitted by the Sun is largest among all thermal emitters. Of course, bodies with higher temperature emit higher heat flux per unit of area, but the share of light in the radiation spectre is lower in comparison to the Sun's. Because of that, the Sun is a highly efficient source of light with an average luminous efficacy of 95 lm/W of emitted heat flux, which is five times more than that of incandescent bulbs per watt of electrical power. Only recently, has LED technology become more efficient, emitting up to 160 lm/W. However, daylight remains the best way of lighting buildings.

When travelling through the atmosphere, a part of the solar radiation is scattered. The surface of the Earth is therefore illuminated by the direct light coming from the

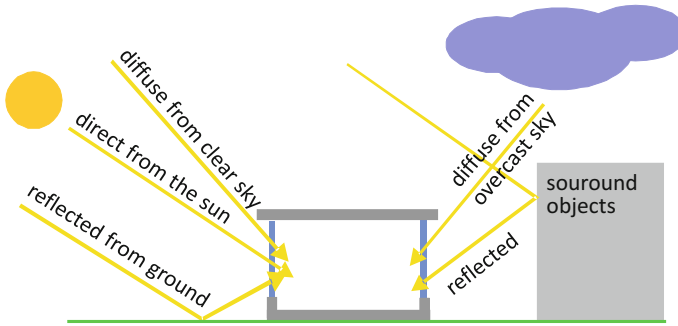


Fig. 12.2 Indoor spaces are illuminated by the direct, diffuse and reflected daylight

Sun, and by the scattered diffuse light from the sky. A surface can also be illuminated by the light reflected from the nearby natural or artificial surfaces (Fig. 12.2).

Light conditions in nature rapidly change, predominantly on whether the sky is clear or covered with clouds. For the design of daylighting in the buildings, transient natural conditions are simplified to static models used for the determination of the sky's luminance at any time during the day. Luminance (L_v in candelas per m^2 , cd/m^2) is defined as luminous flux (Φ_v in lumens, lm) emitted from sky into the solid angle of space (in candelas, cd) from one square metre of sky. Such models are:

- uniform overcast sky luminance model; the sky is isotropic, which means that the luminance of any patch in the sky is equal and independent of the elevation above horizon and the direction; the luminance of the zenith, highest point in the sky, is equal to the luminance of the horizon;
- CIE overcast sky luminance model; the luminance of the patches increases in the ratio of 1:3 between the horizon and zenith, but are independent of direction; this type of the sky luminance model is used for the design of the daylighting of interior spaces in the buildings;
- clear sky luminance model; as there are no clouds in the sky, a only small part of direct light flux is converted into a diffuse one; the solar corona is the brightest area on the sky; the area opposite to the sun is the darkest patch in the sky.
- intermediate sky luminance model; the most realistic model used for determination of the energy consumption of electric lighting, used to complement the daylight (Fig. 12.3).

Modelling the sky's luminance begins with the definition of the Sun's altitude and azimuth angle: the altitude angle (α_s) is the angle between the sunrays and the horizontal plane, and the sun's azimuth angle (γ_s) is the angle between the projection of the sunrays to the horizontal plane and the direction of south (Fig. 12.4).

The Sun's altitude and azimuth angles change through the day according to time and declination (δ), the relative Earth's axis tilt. The declination is the angle



Fig. 12.3 Uniform overcast sky (left), clear sky (middle), and intermediate sky luminance model (right)

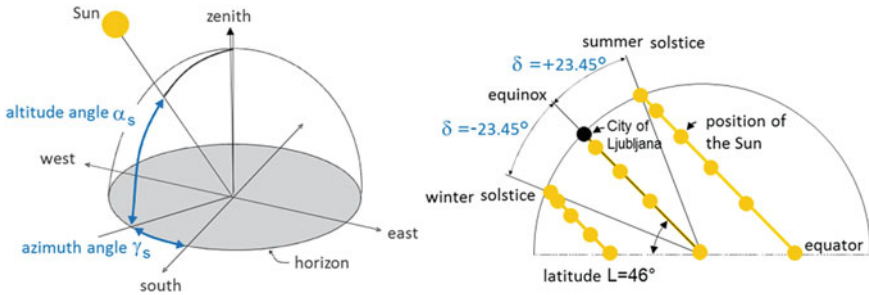


Fig. 12.4 Definition of sun altitude α_s and azimuth γ_s angle (left); the latitude (L) of a site influences the minimum and the maximum sun altitude angle at sun noon over the year. For sites at latitude $L = 46^\circ$, the minimum solar altitude angle at sun noon is 20.6° at the winter solstice and the maximum solar altitude angle 67.5° at the summer solstice (right)

between the sun’s rays and the equatorial plane, changing over a period of one year. The declination at equinox is 0° . The declination on the Northern Hemisphere in the time of the winter solstice (the shortest day of the year) is -23.45° , and at the time of the summer solstice (the longest day of the year) it is $+23.45^\circ$. The declination at any given day of the year is defined by equation:

$$\delta = 23.45 \cdot \sin \left(\frac{360}{365} (284 + n) \right) \quad (^\circ)$$

running day in the year; (15th of February is 46th day of the year)

While the declination is the same at the same time for any geographical location on the Earth, the Sun’s altitude and azimuth angle depend on the location of observation point, which is defined by its latitude (L) and longitude (λ). The latitude is the angle between the equatorial plane and the observation point on the surface measured from the centre of the Earth, and the longitude is the angle between the prime (Greenwich) meridian ($\lambda = 0^\circ$) and the local meridian towards the West or East. The latitude of locations on the Northern Hemisphere is in the range between 0° (on the equator) and $+90^\circ$ (on the North Pole). The sun’s altitude (α_s) and azimuth (γ_s) angles are defined by equations:

$$\alpha_s = \sin^{-1} \cdot (\sin L \cdot \sin \delta + \cos L \cdot \cos \delta \cdot \cos \omega) \quad (^\circ)$$

site latitude
declination
hour angle

$$\gamma_s = \sin^{-1} \frac{\cos \delta \cdot \sin \omega}{\cos \alpha_s} \quad (^\circ)$$

The hour angle ω defines the time in the day. The hour angle changes every hour by 15° . By definition, the hour angle at solar noon (12 o'clock apparent solar time) is 0° , -15° at 11 o'clock, -30° at 10 o'clock and $+45^\circ$ at 3 pm.

Example: Determine the sun's altitude and azimuth angle on 15th April in Ljubljana ($L = 46^\circ$) at 10:30. April 15th is the 105th ($31 + 28 + 31 + 15$) running day of the year. The hour angle ω at 10:30 is equal to:

$$\omega = (10.5 - 12) \cdot 15^\circ = -22.5^\circ$$

The declination δ , and the sun's altitude α and azimuth γ are:

$$\delta = 23.45 \cdot \sin \left(\frac{360}{365} (284 + n) \right) = 23.45 \cdot \sin \left(\frac{360}{365} (284 + 105) \right) = 9.4^\circ$$

$$\alpha_s = \sin^{-1} \cdot (\sin L \cdot \sin \delta + \cos L \cdot \cos \delta \cdot \cos \omega) =$$

$$= \sin^{-1} \cdot (\sin 46 \cdot \sin 9.4 + \cos 46 \cdot \cos 9.4 \cdot \cos(-22.5)) = 48.6^\circ$$

$$\gamma_s = \sin^{-1} \frac{\cos \delta \cdot \sin \omega}{\cos \alpha_s} = \sin^{-1} \frac{\cos 9.4 \cdot \sin(-22.5)}{\cos 48.6} = -34.8^\circ$$

12.3.2 The Luminance of the Clear Sky

The luminance of the clear sky depends on a number of geographical and meteorological parameters. The brightest area in the clear sky by far is the zone around the Sun ($L_v > 50,000 \text{ cd/m}^2$), while the darkest point in the sky ($L_v < 1000 \text{ cd/m}^2$) lies opposite the Sun. In engineering practice, software is used to determine the luminance of the clear sky on an hourly time scale. This is used in glare risk studies (Fig. 12.5).

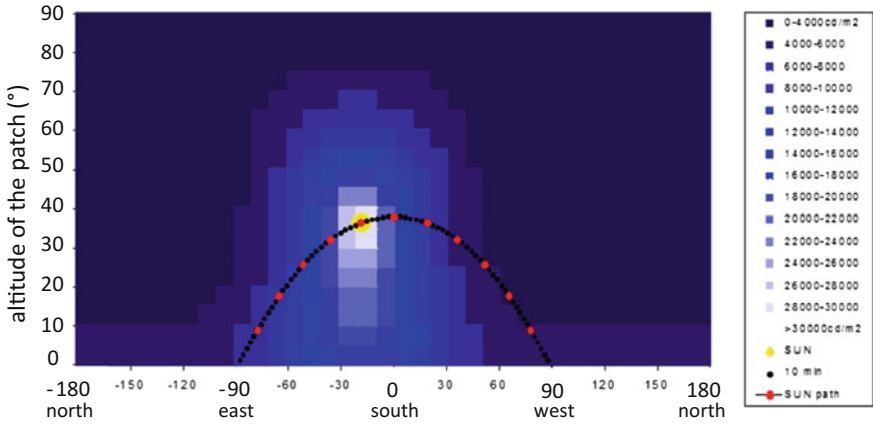


Fig. 12.5 A polar diagram shows the luminance of patches on a clear sky for a location with latitude $L = 46^\circ$, on 21th March at 11.00 (Medved and Arkar 2006)

12.3.3 The Luminance of the Overcast Sky and the CIE Overcast Sky

In the overcast sky luminance model, it is assumed that the luminance of each patch in the sky at certain moment in a day is equal, including the luminance of the zenith, highest point in the sky. Throughout the day, the luminance of the overcast sky varies depending on the solar altitude angle:

$$L_z = \frac{9}{7 \cdot \pi} \cdot (300 + 21000 \cdot \sin \alpha_s) \left(\frac{\text{cd}}{\text{m}^2} \right)$$

luminance of zenith
sun altitude angle ($^\circ$)
patch azimuth angle ($^\circ$)
patch elevation angle ($^\circ$)

$$L_z = L_{v(\phi, \alpha_p)} = L_v$$

In a CIE standard overcast sky luminance model, it is assumed that zenith is the brightest point in the sky, and the patches on the horizon are darkest. The luminance (L_v) of a particular point depends on the angle between the patch and the horizon (α_p) and on the luminance of the zenith, determined at the current solar altitude angle. The luminance of a particular sky patch according to the CIE standard overcast sky is equal to (Fig. 12.6):

$$L_{v(\alpha_p)} = L_z \left(\frac{1 + 2 \cdot \sin \alpha_p}{3} \right)$$

patch elevation angle ($^\circ$)

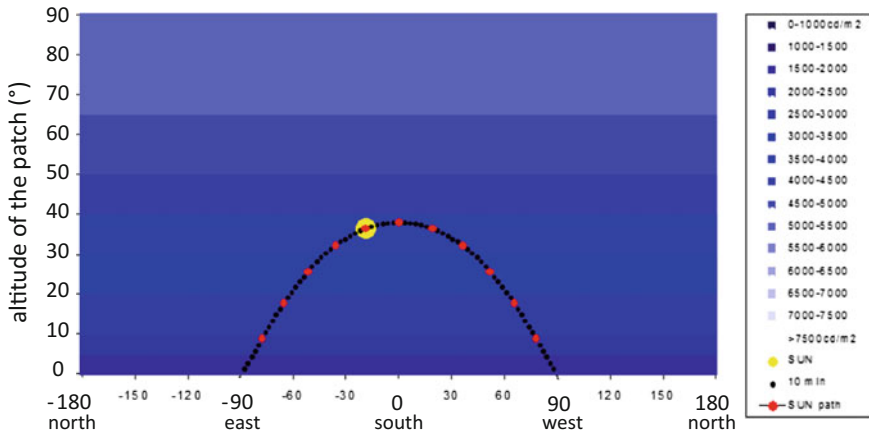


Fig. 12.6 The luminance of patches in the sky L_p as defined by CIE overcast sky luminance model for the location with latitude $L = 46^\circ$, on 21 March at 11.00; the sun path is shown, although sun is behind the clouds (Medved and Arkar 2006)

12.3.4 Luminous Efficacy of the Direct and the Diffuse Solar Radiation

The presented sky luminance models are simplified, because real time cloud cover and atmospheric pollution are not taken into account. The results of the models are difficult to compare with real conditions as long term data of sky luminance are usually not available because they are not monitored by meteorologists. Data about solar irradiation are more commonly available. Using statistical methods, long-term measurements of global solar irradiance (G_{glob} , W/m^2) can be used to convert solar irradiance into illuminance, introducing luminous efficacy factors $K_{s, glob}$ (Littlefair 1998; Medved and Arkar 2006):

$$E_{glob} = K_{s, glob} \cdot G_{glob} \quad \left(\frac{lm}{W} \frac{W}{m^2} = lux \right)$$

illuminance of the surface ($lm/m^2 = lux$)
 luminous efficacy factor (lm/W)
 global solar irradiation on the surface (W/m^2)

In the same way, luminous efficacy has also been determined for the other forms of solar irradiation, direct and diffuse, as $K_{s, dir}$ and $K_{s, dif}$. The typical values are presented in Table 12.1.

Table 12.1 Typical luminous efficacy of solar irradiation in case of overcast and clear sky; luminous efficacy of global and direct solar irradiation depends on sun altitude angle α_s

	Luminous efficacy factor K_s (lm/W)
Overcast sky	$K_{s,dif} = 107$
Clear sky, global solar irradiance data	$K_{s,glob} = 91.2 + 0.272\alpha_s - 0.00063 \alpha_s^2$
Clear sky, direct solar irradiance	$K_{s,dir} = 51.8 + 1.646\alpha_s - 0.01513 \alpha_s^2$
Clear sky, diffuse solar irradiance	$K_{s,dif} = 144$

Case Study: Calculate the illuminance of a horizontal surface E_H in Ljubljana on 15th April at 8.00. At that time, the sun's altitude angle is 30° , the global irradiance of a horizontal surface G_{glob} is 380 W/m^2 of which the direct irradiance G_{dir} is 210 W/m^2 and the diffuse irradiance G_{dif} is 170 W/m^2 .

$$K_{s,dir} = 51.8 + 1.646 \cdot 30 - 0.01513 \cdot 30^2 = 87.6 \left(\frac{\text{lm}}{\text{W}} \right) \quad K_{s,dif} = 144 \left(\frac{\text{lm}}{\text{W}} \right)$$

$$E_H = K_{s,dir} \cdot G_{dir} + K_{s,dif} \cdot G_{dif} = 87.6 \cdot 210 + 144 \cdot 170 = 42876 \left(\frac{\text{lm W}}{\text{W m}^2} = \text{lux} \right)$$

12.3.5 Availability of Daylight

The quality of daylight can be measured by the period during which the daylight is sufficient to illuminate indoor space. This daylight time period is then compared to the period of occupation of the building, e.g. between 8.00 and 17.00 in office buildings. The daylight availability can be expressed as the percentage of the yearly indoor space occupation period during which no artificial lighting is needed. Daylight availability can be expressed as a function of outdoor illumination as shown in Fig. 12.7 derived from average long-term solar irradiation data for the City of Ljubljana.

12.4 Artificial Sources of Light

Daylight is not available whenever the building is in use. For this reason, daylighting is complemented with artificial (electric) lighting. Because the properties of emitted light differ from daylight, electric light sources are characterized by the following properties:

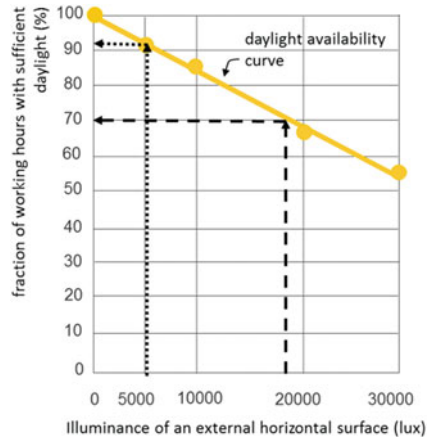


Fig. 12.7 Daylight availability developed for the typical office building and using hourly solar irradiation data for City of Ljubljana; it can be seen that if daylight requirements are fulfilled at outdoor illumination of horizontal surface 5000 lx, this will enable sufficient daylighting of 92% of the working hours; in contrast, if because of poor architecture design, indoor daylight requirements are fulfilled at outdoor horizontal surface illumination 18,000 lx, the daylight will be sufficient only during 70% of the working hours (working time 8:00–17:00, without weekends was assumed for determination of daylight availability curve)

- luminous efficacy K_j ; this is the ratio of the emitted luminous flux Φ to the electric power of a light source expressed in lm/W; a monochromatic light source emitting light at 550 nm wavelength will have the greatest luminous efficacy of 683 lm/W; electric light sources have a lower luminous efficacy—incandescent light bulbs up to 20 lm/W, compact fluorescent lamp up to 90 lm/W, and LED lamps up to 140 lm/W (Hausleden et al. 2005);
- luminous efficiency E_l ; is the ratio of a light source's luminous efficacy K_s to the maximum luminous efficacy of a monochromatic light source (683 lm/W); E_l is given in as a percentage; a thermal emitter at 3000 K has $E_l = 4\%$, for a radiator at temperature 4000 K $E_l = 7\%$, and for the Sun's photosphere at 5700 K $E_l = 34\%$;
- colour temperature T_C ; is defined by comparing the spectrum of light emitted by light source and the spectrum of light emitted by an ideal thermal emitter, i.e. black body and expressed in Kelvins. A thermal emitter with higher temperature emits more light at shorter wavelengths (light is bluish and rated as cold), while emitters at a lower temperatures emit longer wavelengths (light is reddish and rated as warm); for electrical light sources that emit light without being thermal emitters (fluorescence lamps, LED), a correlated colour temperature CCT is used instead of colour temperature T_C (Table 12.2).
- the colour rendering index CRI is a measure of the faithfulness of surface colours illuminated by an artificial source of light compared to an ideal natural

Table 12.2 Electrical sources of light emit light with different apparent colours

Colour of light	T_c (K)
Warm	<3300
Neutral white	3300–5000
Cold daylight	>5000

The wavelengths of emitted light are compared to ideal black body at temperature T_c

Table 12.3 The required classes and colour rendering indexes CRI

Class	CRI	Intended use
1A	>90	Galleries
1B	80–90	Apartments, hotels, restaurants, hospitals, schools
2A	70–80	Industrial buildings
2B	60–70	Industrial buildings
3	40–60	Spaces where the colour detection is less important
4	20–40	Spaces where the colour detection is not important

source of light: the sunlight at a solar noon; the value of CRI is between 0 and 100. A higher colour rendering index is required in galleries and residential buildings (Table 12.3).

- the luminous intensity distribution diagram or candela diagram; the diagram is used to calculate the illuminance of surfaces in a space according to the position of the luminaire; the luminaires are divided into five categories according to the shape of the luminous intensity distribution diagram; the boundary cases are the direct lighting fixtures, sending the light straight downward in a narrow angle, and indirect lighting fixtures directing the light up to the ceiling.

In the last one hundred years, several technologies for transforming electrical energy into light were developed. Incandescent light bulbs have an element that produces visible electromagnetic radiation when the electric current is run through it. In halogen incandescent lamps, the glass enclosure is filled with an inert gas (argon or krypton) with added atoms of halogen elements such as iodine or bromine. The service life of such light bulb is 2500–3500 h. Because of poor luminous efficacy (the ratio between emitted light flux in lumens per one watt of electrical power), less than 15 lm/W, this light source is not in use in energy efficient buildings nowadays. Fluorescent lamps are gas-discharge lamps, in which the electrical energy is used to excite molecules of gas, which in turn emit energy in the form of invisible radiation. This radiation is then converted into light in a special coating on the inside surface of the lamp assembly. The lamps are equipped with a ballast and a starting switch. The ballast regulates the voltage in the lamp during operation, while the starter provides the high voltage necessary for the initial ionization of mercury atoms. High-frequency electronic ballasts are integrated into



Fig. 12.8 Halogen incandescent bulb, fluorescent lamp, compact fluorescent lamp, LED (from left to right)

modern lamps, also known as compact fluorescent lamps. The fluorescent lamps have a service life between 12,000 and 15,000 h and luminous efficacy up to 90 lm/W (Fig. 12.8).

Note: Fluorescent lamps contain mercury vapour, which requires special disposal and recycling; the presence of mercury must be marked on the lamp.

Light-emitting diodes (LED) are the latest achievement in electric lighting technology. They utilize the principle of electroluminescence, a phenomenon causing some substances emit electromagnetic radiation when electric current is passing through them. LED are made of semiconducting materials, in which the added electrons and gaps form a band gap. LED-diodes emit monochromatic light at wavelengths (colours) depending on the size of the band gap. LEDs emitting white light can be made of three individual LEDs emitting the primary monochromatic colours (red, green and blue). The other possibility is to use a LED emitting monochromatic blue light or ultraviolet radiation and coat it with phosphor. The light-emitting diodes have long service life, which is independent of number of switching cycles: from 75,000 to 100,000 h and high and luminous efficacy up to 140 lm/W.

12.5 Requirements and Criteria of Visual Comfort

The main engineering criteria used in designing and verifying the visual comfort are presented in Sect. 1.3. Two requirements that are closely connected to energy demand for lighting will be present hereinafter.

12.5.1 Illuminance

Adequate illumination is required for distinguishing objects and performing various tasks. The illumination level is measured by the luminous flux per square meter of illuminated surface E (lm/m^2 or lux). To recognize a human face, it must be

Table 12.4 Minimum illuminance of objects regarding to the complexity of visual tasks (Baker et al. 1993)

Illuminance E (lx)	Complexity of visual task
50	Discerning of details is not required, safe walking is guaranteed; warehouses, corridors
100	Occasionally occupied spaces, correct object recognition, sanitary facilities, corridors
200	Lengthy work, discerning of large details, serving counters
300	Lengthy work, easier visual tasks, discerning of details larger than 10 arc minutes with high contrast, meeting spaces
500	Visual tasks of medium complexity, discerning details between 5 and 10 arc minutes with low contrast; meeting spaces, classrooms, offices, dining rooms, restrooms
750	Exacting visual tasks, discerning details between 3 and 5 arc minutes, good perception of colours, supermarkets, offices, drafting rooms
1000	Very exacting visual tasks, discerning details between 2 and 3 arc minutes; low contrast; accurate colour perception; assembly rooms, colour verification
>1500	Very exacting tasks, discerning details smaller than 1 arc minute, optical accessories recommended, precision engineering work, colour control

illuminated with approximately 10 lx, which corresponds to 20 lx for a horizontal surface. To distinguish facial details, the illuminance must be considerably higher: at least 200 lx. The illumination level required depends on the difficulty of visual tasks. The recommended illumination levels for visual tasks of different complexity, requiring the recognition of details, are given in Table 12.4.

Illuminance is in most often designed and in situ evaluated at working plane 0.85 m above the floor and 1 m away from the internal walls or furniture bought for daylight and electrical lighting. Software tools are used to calculate the illumination of surfaces in scope of indoor visual comfort design. The results are represented graphically with isolux lines, i.e. curves connecting all points in space of equal illumination (Hausleden et al. 2006).

12.5.2 Daylight Factor

The daylight factor (DF) is an indicator of quality of daylight. It is defined as the ratio of illuminance at a selected point in the space $E_{p,H}$ to the illuminance on an external horizontal unshaded plane E_H , expressed as a percentage (Fig. 12.9):

$$DF = \frac{E_{p,H}}{E_H} \cdot 100(\%)$$

Fig. 12.9 The daylight factor definition

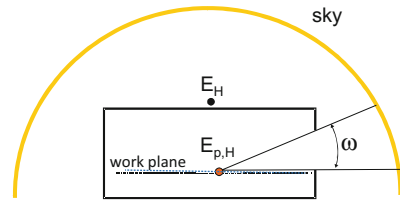


Table 12.5 Recommended average (DF_{av}) and minimum daylight factor (DF_{min}) (Baker et al. 1993)

	DF_{av} (%)	DF_{min} (%)
Office	5	2
Classroom	5	2
Living room	1.5	0.5
Bedroom	1	0.3
Kitchen	2	0.6

The CIE overcast sky lamination model is used for the determination of the daylight factor on a work plan at conditions of external horizontal unshaded surface illuminance of $E_H = 5000$ lx. In the case of one side window, the daylight factor decreases towards the space interior, especially in the second half of the room. Because of that, DF is evaluated as average value (DF_{av}) and point with the lower value (DF_{min}) is also determined. Values of daylight factor are more often referred as recommendations rather than as minimum requirements. Typical values for are shown in Table 12.5.

Trezenga and Loe defined the perception of space illumination according to the average daylight factor. They propose minimum DF_{av} of 2%. They recommend a value of 5% so that the inhabitants will perceive the space as pleasantly bright and caution that DF_{av} above 10% requires a glare risk check and adequate shading (Trezenga and Loe 2004) (Table 12.6).

Table 12.6 Perception of space brightness with regard to the average daylight factor DF_{av} (Trezenga and Loe 2004)

DF_{av} (%)	Perception of space
<1	Space feels too dark
2	Minimum at the centre of the space
5	Optimal to perceive the space as pleasantly bright
>10	Risk of glare and overheating; adjustable shading must be installed

12.6 Principles of Rational Use of Energy for Lighting

Lighting accounts for 5–10% of total electricity consumption in residential buildings and up to 60% in office buildings. Energy efficient lighting of buildings can be achieved through a series of architectural and technological measures, among others by:

- not designing the spaces with one-sided natural illumination with depths greater than approximately 2.5 times the height of the upper edge windows; keep the window-to-wall area ratio to 25–30%; * spaces should have high diffuse reflectance ceilings (Keller 2001);
- windows with high light transmittance τ_{vis} glazing (e.g. the minimum value of τ_{vis} 0.5) are defined in national regulation on energy efficiency of the buildings in Slovenia;
- spaces should be designed to provide high daylight factor; research has shown that daylighting does not affect the electricity consumption for lighting if the average daylighting factor DF_{av} is less than 2%; the energy demand is reduced by up to 50% if $DF_{\text{av}} = 5\%$ and by up to 80% if $DF_{\text{av}} = 12\%$ (Keller 2001);
- LED lamps with high luminous efficacy should be installed; further 15–20% decrease of electricity demand can be achieved by using optimally shaped and high reflectivity mirrors in luminaire; regular maintenance is required to maintain the optical properties of mirrors;
- groups of lamps installed in deep spaces should be controlled according to distance from the window;
- energy savings can only be achieved if the electric lighting is controlled; the lamps should be dimmed according to the space occupancy and the quantity of daylight; modern electronic devices can reduce the luminous flux of fluorescent lamps down to 3% of the design luminous flux at 90% decrease of electricity consumption and yearly electricity consumption for lighting can be reduced by up to one third;
- smart controlling device in the spaces and connection of lamps with central control system should be established (Harvey 2006).

Note*: General recommendation must be check by case-to-case evolution.

12.6.1 Energy Needs and Delivered Energy for Lighting of nZEB

Lighting is one of so called EPBD systems. This means that according to Energy Performance of Buildings Directive,¹ energy use for lighting must be included in building energy performance indicators. The method for determination of energy demand for lighting is defined in EN 15193-1. The standard introduces the LENI (lighting energy numerical indicator) for the specific annual delivered energy for lighting per square metre of useful building floor area. LENI is defined by the following expression:

$$\text{LENI} = \frac{Q_l}{A_u} = \frac{P_n \cdot F_c \cdot F_o \cdot (t_d \cdot F_d + t_n) + W_{pe} + W_{pc}}{1000 \cdot A_u} \left(\frac{\text{kWh}}{\text{m}^2 \cdot \text{a}} \right)$$

The diagram illustrates the components of the LENI equation with arrows pointing to the variables in the formula:

- Q_l : energy needs for lighting
- A_u : conditioned (useful) area of building (m²)
- P_n : power of installed lighting system (W)
- F_c : constant illuminance dependency factor (-)
- F_o : occupancy dependency factor (-)
- t_d : daytime operation of lighting system (h/a)
- F_d : daylight dependency factor (-)
- t_n : night-time operation of lighting system (h/a)
- W_{pe} : standby energy for automatic lighting controls (kWh/a)
- W_{pc} : battery charging of emergency luminaires (kWh/a)

Note: The presented method is most simplified method proposed in EN 15193-1. More precise data on electricity demand for lighting can be evaluated with hour-by-hour simulations.

Total installed power of the lighting system P_n shall be calculated by summation of the power of the specified luminaires as they are predicted in lighting design plan. In case there are no available design data, the maximum allowed specific installed power (in W/m² of conditioned area) as defined in national regulations or data from ISO 18523-1² and ISO 18523-2³ can be used. In Table 12.7, the maximum allowed installed specific power of lighting systems as defined in the national regulation on energy efficient buildings as adapted in Slovenia is shown.

¹Directive 2010/31/EU of the European Parliament and of the Council on the energy performance of buildings (recast) (Official Journal of the European Union L 153/13).

²ISO 18523-1:2016 Energy performance of buildings—Schedule and condition of building, zone and space usage for energy calculation—Part 1: Non-residential buildings.

³ISO 18523-2:2018 Energy performance of buildings—Schedule and condition of building, zone and space usage for energy calculation—Part 2: Residential buildings.

Table 12.7 Maximum allowed specific installed power of electric lights $P_{n,spec}$ in different buildings according to national regulation adapted in Slovenia

Building type	Maximum allowed installed specific electric power of lamps (W/m^2)
Garages, parking lots	3
Residential buildings, general residential buildings, predominant use of CFL or LED	8 2.5
Supermarkets, shopping centres	9
Community health care centres, hotels, offices	11
Gyms, museum, sports halls	12
Congress centres, hospitals, schools	13
Restaurants, libraries, industrial buildings	14
Theatres	17

Table 12.8 Electric light source correction factor (ISO 18523-1)

Lamp type	F_L
Incandescent	6.38
Halogen incandescent	4.49
Compact fluorescent lamp (FCL)	1.56
T8 linear fluorescent lamp	0.95
T5 linear fluorescent lamp	0.90
Light emitting diode (LED)	0.86

The maximum allowed specific installed power of electric lighting system defined in national regulations or data from ISO 18523-1 assume that energy efficient luminaires are used. If particular lamp types are installed, the correction factor F_L accounting for the lighting technology should be introduced. Values of F_L are shown in Table 12.8.

Case study: If LED lamps are used instead of tungsten halogen lamps for the lighting of an office. Taking into account the fact that the maximum allowed specific installed power according to national regulation is $11 W/m^2$, adequate installed power of lighting system P_n for the calculation of LENI will be reduced from $49.4 W/m^2$ (for incandescent luminaires) to $9.5 W/m^2$ (for LED luminaires).

Time interval t_d and t_n are the numbers of operating hours in the daytime (t_d) and night time (t_n). Typical values as proposed in standard EN 15193-1 for different building types are given in Table 12.9.

Occupancy dependency factor F_O is equal to 1 when the lighting system is switched on in more than one space at once or in the case of spaces larger than

Table 12.9 Number of building occupancy hours per year during the daytime (t_d) and the night time (t_n) for different types of building (EN 15193-1)

Building type	Daytime operating hours t_d (h/a)	Night-time operating hours t_n (h/a)
Residential buildings	1820	1680
Offices	2250	250
Education buildings	1800	200
Hospitals, hotels, retail service	3000	2000
Restaurants	1250	1250
Sports facilities	2000	2000
Industrial buildings	2500	1500

30 m² if the luminaires are switched on together. In other cases, F_O is less than 1 and depends on absence factor F_A and control function factor F_{OC} (Table 12.10). The value of absence factor F_A depends on the building type and on the zoning of the building (overall or space by space approach). The suggested value according to standard EN 15193-1 for domestic buildings for overall calculation F_A is 0 and 0.3 for living room, 0.4 for bedroom, 0.7 for dining room, 0.6 for kitchen, 0.7 for corridors, etc. in a room-by-room approach. For office buildings and overall calculation, F_A is assumed equal to 0.2 and 0.4 for a one-person office, 0.3 for an open plan office, 0.2 for a large open plan office, etc. in the case of a room-by-room approach.

Constant illuminance dependency factor F_C is defined as the ratio of the average input power at a specified time to the initial installed input power of a luminaire. Typical values of F_C are equal to 1 for any building with non-dimmable lighting system, 0.9 for linear fluorescent lamps in a clean environment and 0.85 for LED light sources (life time 30,000 h) if luminaires are cleaned annually or 0.80 for luminaires in dirty environments cleaned biannually.

The daylight dependency factor F_D shall be calculated for a zone and can be evaluated according to average daylight factor DF_{av} and classification of daylight availability for a particular building zone. Daylight availability is defined as “strong” (if $DF_{av} \geq 6\%$), “medium” ($4\% \leq DF_{av} < 6\%$), “low” ($2\% \leq DF_{av} < 4\%$) and “none” ($DF_{av} < 2\%$).

Yearly standby energy use for lighting control W_{pc} and emergency luminaires battery charging W_{pc} are assumed to be zero for residential buildings and as proposed in standard EN 15193-1; equal to 1 kWh/m² a for battery charging of emergency luminaires (W_{pc}) and 1.5 kWh/m² a for standby operation of lighting controls (W_{pc}) per m² of conditioned area.

Case study: Determine the delivered energy lighting of the Virtual Lab Living unit (Fig. 12.10).

Table 12.10 Occupancy dependency factor F_O (EN 15193-1)

Occupancy dependency factor F_O	Absence factor F_A										
	0.0	0.1	0.2	0.3	0.4	0.5	0.6	0.7	0.8	0.9	1.0
Manual on/off switch	1.0	1.0	1.0	0.900	0.800	0.700	0.600	0.500	0.400	0.300	0.0
Manual on/off switch + additional automatic sweeping	1.0	0.975	0.950	0.850	0.750	0.650	0.550	0.450	0.350	0.250	0.0
Auto on/dimmed	1.0	0.975	0.950	0.850	0.750	0.650	0.550	0.450	0.350	0.250	0.0
Auto on/auto off	1.0	0.950	0.900	0.800	0.700	0.600	0.500	0.400	0.300	0.200	0.0
Manual on/dimmed	1.0	0.950	0.900	0.800	0.700	0.600	0.500	0.400	0.300	0.200	0.0
Manual on/auto off	1.0	0.900	0.800	0.700	0.600	0.500	0.400	0.300	0.200	0.100	0.0



Fig. 12.10 Photo of Virtual Lab building (left), LED luminaires in living unit (right)

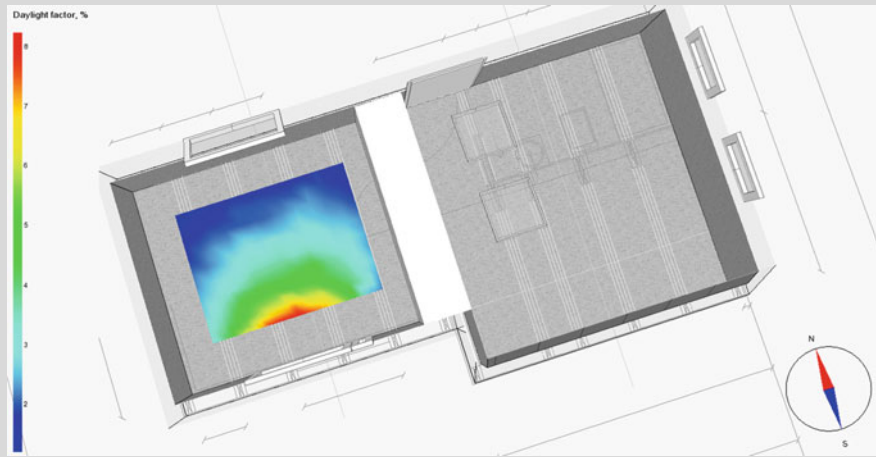


Fig. 12.11 Daylight factor DF on working plane (IDA ICE)

Luminaires in Living unit with living area A_u 12 m^2 consist of LED which emits the light with colour 6000 K with Illuminance efficiency 100 lm/W . The specific installed electricity power of LED luminaires is 9 W/m^2 (in total 108 W). Lights are controlled with “auto on/auto off” control. The daylight factor is determined for the working plane 0.8 m above the floor and 0.5 m aside from walls. The average daylight factor DF_{av} is 3.17% (Fig. 12.11).

In case of permanent use and data from EN 15193-1, it is assumed that the Living Unit is used during daytime 1820 h per year (t_d) and 1680 h per year during the night-time (t_n). The constant illuminance dependency factor for LED F_C is 0.85 . Absence factor F_A is equal to 0.3 (domestic buildings, living

room) and occupancy dependency factor F_O is taken from the Table 12.10. Daylight dependency factor F_D is taken from Table 12.11, taking into account pre-calculated average daylight factor DF_{av} .

$$LENI = \frac{Q_l}{A_u} = \frac{P_n \cdot F_C \cdot F_O \cdot (t_d \cdot F_D + t_n) + W_{pe} + W_{pc}}{1000 \cdot A_u}$$

$$LENI = \frac{108 \cdot 0.85 \cdot 0.80 \cdot (1820 \cdot 0.44 + 1680)}{1000 \cdot 12} = 15.2 \frac{kWh}{m^2 a}$$

Table 12.11 Daylight dependency factor F_D for spaces with vertical windows; for more detailed evaluation of F_D (EN 15193-1)

Daylight dependency factor F_D									
	DF_{av} (%)								
	0.13	0.5	1.0	1.5	2.0	3.0	5.0	8.0	12.0
Windows in south orientated facades with shading	0.92	0.84	0.61	0.52	0.50	0.44	0.40	0.34	0.33
Windows in E, W or N orientated facades of sought orientated façade without shading	0.83	0.75	0.70	0.66	0.65	0.62	0.60	0.56	0.56

References

Baker NV, Fanchiotti A, Steemers K (1993) Daylighting in architecture: a European reference book. James & James

Dubois MC (2011) Education package lighting. Master and post graduate education and training in multi-disciplinary teams implementing EPBD and Beyond—IDES-EDU, IEE/09/631/SI2.558225

Harvey LDD (2006) A handbook on low-energy buildings and district-energy systems, fundamentals, techniques and examples. Earthscan, London

Hausleden G et al (2005) ClimaDesign Lösungen für Gebäude die mit weniger Technik mehr können. Verlag Georg D.W. Callwey GmbH

Hausleden G et al (2006) ClimaSkin Konzepte für Gebäudehüllen die mit weniger Energie mehr können. Verlag Georg D.W. Callwey GmbH

- Keller B (2001) Bautechnologie II, Bauphysik, Teil 1: Stadtebaulich relevante Factoren. ETH Eidgenossische Technische Hochschule Zurich
- Littlefair PJ (1988 Dec) Measurements of the luminous efficacy of daylight. *Light Res Technol* 20 (4):177–188
- Medved S, Arkar C (2006) Applied lighting technologies for urban buildings. In: Santamouris M (ed) *Environmental design of urban buildings*. Earthscan
- Trezenga P, Loe D (2004) *The design of light*. E & FN Spon, London

Chapter 13

Energy Labelling of Buildings



Abstract According to official EU data, about 35% of buildings in EU are more than 50 years old and, as a consequence, extremely poorly energy efficient. It is assumed that if the overall energy efficiency of the buildings in EU were to be improved, the final energy consumption could be decreased by as much as 6%, resulting in a 6% decrease of CO₂ emissions. Two key documents were published to increase energy efficiency of the buildings: the Energy Performance of Building Directive (EPBD 2010) and the Energy Efficiency Directive (EED 2012 [Directive 2012/27/EU of the European Parliament and of the Council of 25 October 2012 on energy efficiency, amending Directives 2009/125/EC and 2010/30/EU and repealing Directives 2004/8/EC and 2006/32/EC (Official Journal of the European Union L 315/1)]). This chapter focuses on the presentation of energy performance certificates of building, which is one of the most recognizable outcome of directives (ec.europa.eu/energy/en/topics/energy-efficiency/buildings).

Directive 2010/31/EU of the European Parliament and of the Council on the Energy Performance of the Buildings (known as EPBD recast), an updated version of first EPBD published in 2002, is key document regarding the energy efficiency of the buildings. According to the EPBD, each of Member State must (among others):

- introduce national a methodology (based on EN standards) for the calculation of energy performance indicators of buildings;
- provide education and examination of independent accredited experts who will create energy performance certificates;
- define the minimum requirements for the energy efficiency of buildings [maximum values of indicators—for example specific energy need for heating (kWh/m² a) or specific primary energy demand (kWh/m² a)] on the basis of cost-optimal levels; indicators must indicate quality of building envelope (including air tightness), and system for (i) heating and (ii) domestic water heating, (iii) mechanical ventilation, (iv) cooling, (v) air-conditioning and (vi) lighting (if in the building) and must be developed for different building categories: for houses and apartment blocks, offices, education buildings, hospitals, hotels and restaurants, sports facilities,

commercial buildings; it is expected that types of EPBD buildings will increase in the future (EN ISO 52000-1);

- establish a national register and means of independent verification of energy certificates;
- ensure that energy performance certificated is included in all advertisements for the sale or rental of buildings;
- draw up an action plan for increasing the number of nearly-zero energy buildings.

EPBD as well as EED were updated in 2016 and 2018. EED was updated by extension of the energy savings requirement by 30% to 2030. The updated EPBD emphasizes long-term building renovation strategies, inspections of heating and air-conditioning systems, enhances the use of building automation and control, promotes e-mobility, and introduces smartness indicator that assesses the technological ability of the building to interact with occupants and with grid (infrastructure systems). Updated energy efficiency legislation aims for huge yearly energy savings through Ecodesign (requirements for minimum energy efficiency of new product) and Energy labelling.

13.1 Energy Performance Certificates of Buildings

According to the EPBD, an energy performance certificate must be assigned for new and significantly renovated buildings and must include proposals for improving the energy efficiency of buildings and buildings service systems. For specific buildings, for example public buildings like schools, kindergartens, hospitals and public administration buildings, the energy certificate must be presented visibly to the public.

Two types of energy certificates are introduced: calculated and measured. A calculated energy certificate is made by calculations only. The procedure is described in Chap. 3. The measured energy certificate is made on the base of measured consumption of all energy carriers needed for operation of buildings in the (calendar) year. More consecutive annual data could be requested (in Slovenia, the data on energy consumption in three consecutive year is required).

Depending on national regulations, it is quite common that calculated energy certificates are assigned for households, while measured energy certificates assigned to public non-residential buildings. Nevertheless, if no data for measured energy carriers' consumption is available, a calculated energy certificate is assigned to public and non-residential buildings.

The design of energy certificates differ between EU Member States, but must include reference values regarding the minimum national criteria in the way that is easy to understand by consumers. Criteria must be ordered in classes and cost-effective measures of rational use of energy and utilization of renewable energy sources must also be presented. Environmental impacts are most often

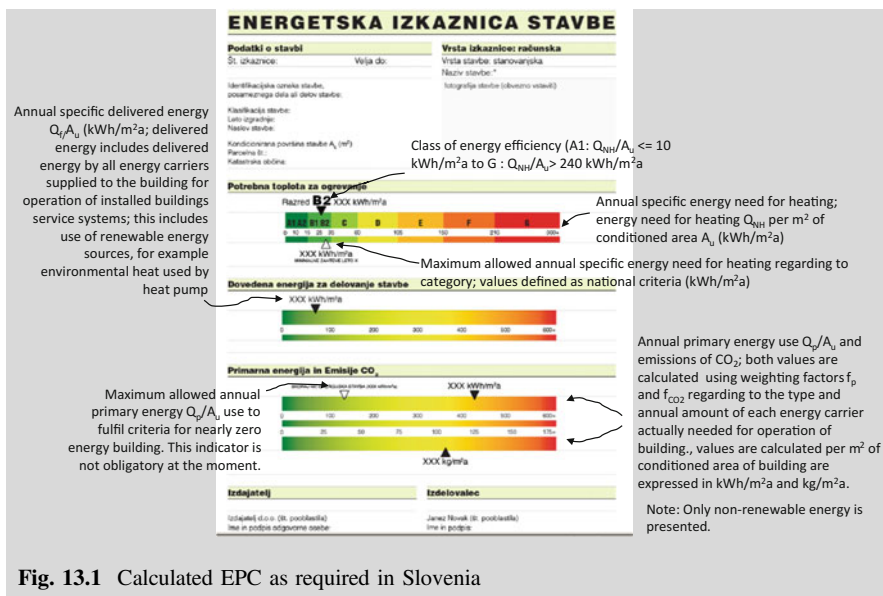


Fig. 13.1 Calculated EPC as required in Slovenia

expressed by CO₂ emissions. All indicators are presented as specific values, commonly per square metre of useful area and year. Energy efficiency indicators are based on physical quantities, such as specific energy needs for heating, specific final energy for operation of the buildings, specific primary energy needed for the operation of the buildings or expressed as ratings (0–100). In this case, the rating of a reference building or potential rating after implementing proposed energy efficiency measures are presented. Measures can be shown in estimating cost savings (Bio Intelligence Service, Ronan Lyons and IEEP 2013).

13.1.1 Calculated Energy Performance Certificate of Building (cEPC)

Note: Sections 13.1.1 and 13.1.2 present the display of energy performance certificate (EPC) of buildings as required by national legislation in Slovenia.¹ This is the first page of an EPC, which is followed by detailed description of energy demand and proposals for increasing energy efficiency. In buildings of public administration, schools, and hospitals, this page must be visibly displayed. The design of certificates differs among the EU countries, but the

¹Pravilnik o metodologiji izdelave in izdaji energetskih izkaznic stavb (Rules on the methodology for the production and issuance of energy performance certificates for buildings) (Uradni list RS, št. 92/14).

methods are the most commonly expressed indicators (Q_{NH} , Q_f and Q_p) of energy performance; they are calculated as described in Chap. 5.

Case Study Display of energy certificate of building for cEPC as requested in Slovenia (Fig. 13.1):

Case Study Calculated energy performance certificate of Virtual Lab building. Building is heated by solar thermal system and electrical heater inserted in the solar heat storage. Floor- and wall-integrated dry heating panels are installed. A mechanical ventilation system has double cross heat exchanger and efficiency up to 80%. It is assumed that all generated electricity by PV system is utilized (Figs. 13.2, 13.3).



Fig. 13.2 Photo of Virtual Lab building

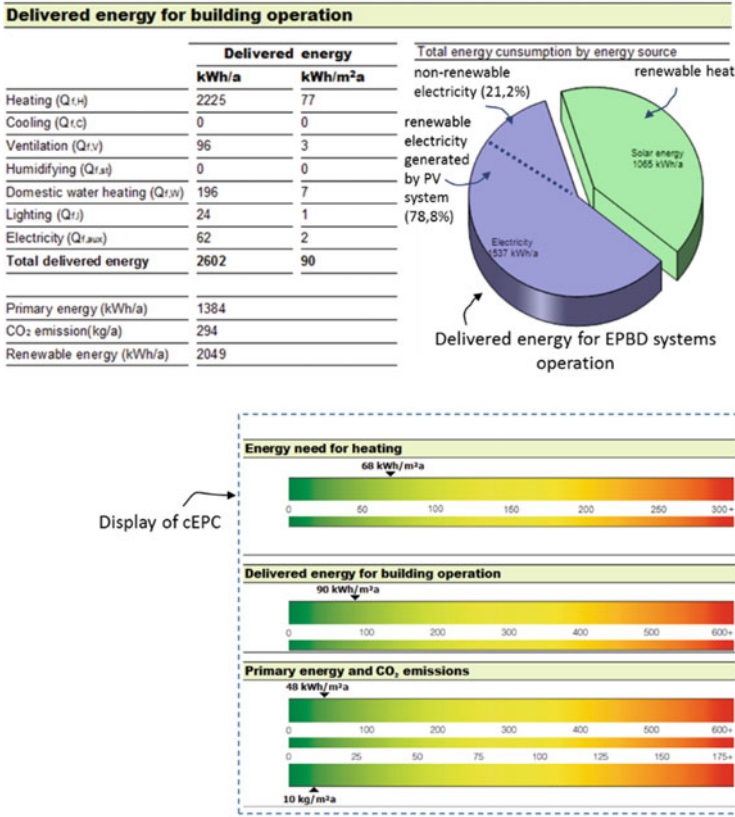


Fig. 13.3 Calculated EPC of Virtual Lab building

13.1.2 Measured Energy Performance Certificate (mEPC)

Indicators presented on the measured energy performance certificate of building are determined by the measured consumption of each energy carrier (district heat, electricity, fuels, etc.) and evaluated as an average yearly value during the last three full calendar years. Data must be provided by the client, who is also responsible for the accuracy of the data as well. While annual data are sufficient to finalize mEPC, monthly or even hourly data on energy demand are very useful in the phase of preparing recommendations for improving the energy efficiency of the building and building systems.

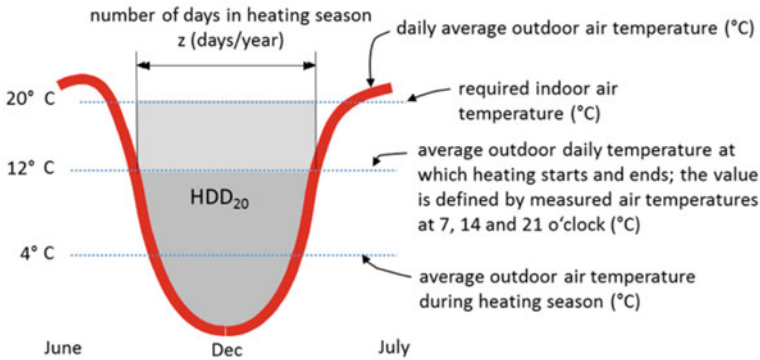


Fig. 13.4 Definition of heating degree-days (HDD); HDD, presented by grey area, are determined for specific indoor air temperature thresholds

With known quantity of energy carriers or/and fuels needed for operation of the buildings, delivered energy is calculated using the calculation factor (equal to 1 kWh/kWh for electricity or distant heat) or by the lower calorific value LCV of fuels. LCV of the most commonly used fuels are presented in Chap. 2. It is recommended to collect data on the actual measured consumption of all energy carriers for last three full calendar years. If complete sets of data are not available, the heating degree-days (HDD) method could be used to supplement data for energy carriers intended for heating the building. Heating degree-days are dependent on the local climate and are part of national meteorological databases. HDD are available as long-term climate averages and as monthly values for particular previous years. Using HDD missing data on energy demand for heating can be approximated. HDD are defined with equation (Fig. 13.4):

$$HDD_{20} = z \cdot ((20 - 12) + (12 - \bar{T}_e)) \quad (\text{K.day/a})$$

number of days in heating season (days/year) \rightarrow z
 average outdoor daily temperature at which heating starts and ends (local defined, value for defined for Ljubljana, Slovenia) \rightarrow \bar{T}_e
 indoor air temperature as defined for indoor thermal comfort (°C) \rightarrow 12
 average ambient air temperature during heating season (°C) \rightarrow \bar{T}_e
 Indicate that indoor air temperature 20°C is assumed as set-point \rightarrow 20

If some form of energy (in practice, heat or electricity) is generated by on-site technologies (photovoltaic system, wind turbine, solar heating system, or cogeneration) and exported to the public electricity grid or district heating system, this amount should be deducted from delivered energy.

Fig. 13.5 Hospital building in Ljubljana, Slovenia (gis. arso.gov.si/atlasokolja)



Case Study Data of energy demand for full calendar year 2012 were provided by energy manager of the building with conditioned area of 8349 m². The yearly delivered district heat for heating $Q_{f,h}$ was 1159.9 MWh/a, delivered district heat for district domestic water heating was $Q_{f,w}$ 146.6 MWh/a and delivered electricity E_f for operation of the building was 820.6 MWh/a. HDD for location of the hospital were 2776 Kday/a in 2012, 2856 Kday/a for 2013 and 2181 Kday/a for 2014. Data were retrieved from the web service of ARSO (National Agency for Environment) (Fig. 13.5).

Predicted delivered heat for heating in 2013 and 2014 are equal to:

$$Q_{f,h,2013} = Q_{f,h,2012} \frac{\text{heating degree-days for year 2013 (Kday/a)}}{\text{measured consumption in the year 2012 (MWh/a)}} = 1160 \frac{2856}{2776} = 1193 \frac{\text{MWh}}{\text{a}}$$

$$Q_{f,h,2014} = Q_{f,h,2012} \frac{\text{heating degree-days for year 2014 (Kday/a)}}{\text{measured consumption in the year 2012 (MWh/a)}} = 1160 \frac{2181}{2776} = 911 \frac{\text{MWh}}{\text{a}}$$

Case Study Display of energy certificate of building made on the basis of delivered energy (mEPC) as required in Slovenia. The mEPC can be made only for non-residential buildings if reliable data on the actual delivered energy are known for the least of one calendar year (Fig. 13.6).

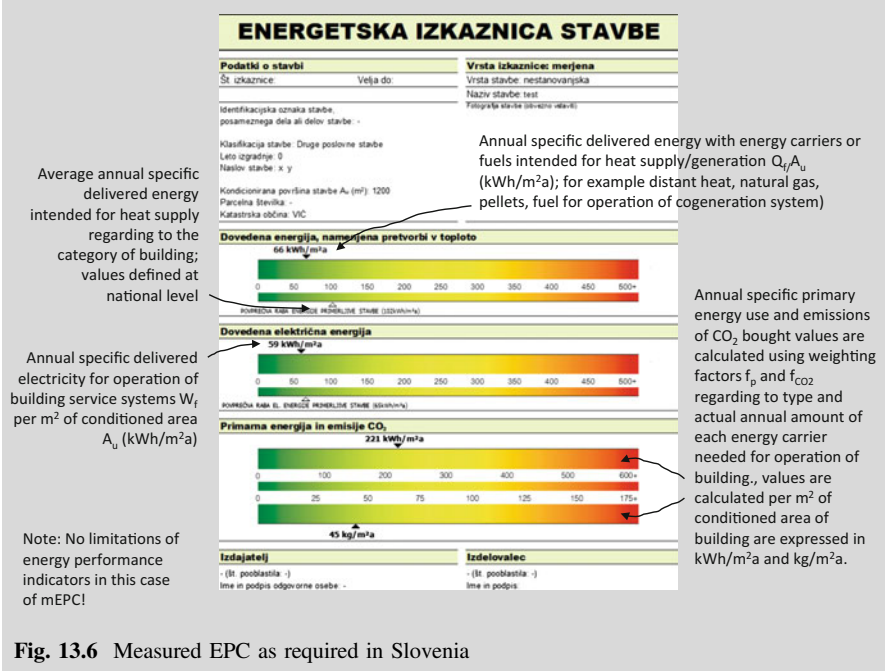


Fig. 13.6 Measured EPC as required in Slovenia

Reference

Bio Intelligence Service, Ronan Lyons and IEEP (2013) Energy performance certificates in buildings and their impact on transaction prices and rents in selected EU countries. Final report prepared for European Commission (DG Energy)

Chapter 14

Environmental Labelling of Buildings



Abstract Actions and goals towards sustainable societies should address the design, construction and use of buildings. The building sector has significant impact on the use of natural resources and the quality of the environment. Recent studies shown that half of natural resources used are related to the building sector. At the same time, the construction and operation of buildings are responsible for the largest share of greenhouse gas emissions. The European Commission has adopted several directives regarding improved energy efficiency, the wider use of renewable energy, and the use of sustainable materials and products to guide designers and evaluate the impact of buildings in all stages of their life cycle. In this chapter, the most widespread methods for the environmental labelling of products based on the life cycle assessment approach and methods for the holistic certification of buildings' environmental impact are presented.

14.1 Sustainable Development and Environmental Impacts of Buildings

The current understanding of sustainable development is based on the conclusions of the report “The Limits to Growth”, which was published by “Club of Rome” in 1972, and the report of the World Commission on Environment and Development, also known as the Brundtland Commission “Our Common Future” from 1987. Both documents underline the need for economic development based on the simultaneous protection of the environment and natural sources. On the basis of the conclusions of the United Nations Conference on Environment and Development UNCED (1992), the European Commission developed a strategy of sustainable development that emphasized the great importance of sustainability in the building sector. The construction industry contributes significantly to the use of natural resources, while it contributes 50% to usage of all natural resources in the world, the buildings sector contributes 60% to the total amount of generated waste, and 50% of the overall total energy consumption is related with buildings (40% for operation and 10% for the production of materials) (Meadows et al. 1972).

While the energy performance assessment of nearly zero energy buildings includes some environmental indicators, for example, primary energy needed for operation of the building and emissions of CO₂ greenhouse gas responsible for global climate changes, two major weaknesses regarding to environmental impact assessment can be highlighted: (i) the pollutants that are responsible for pollution of the environment at the local scale, such as tropospheric ozone forming or acidification of precipitation, are not included in the assessment and (ii) environmental impacts are not analysed during the whole life time, including extraction of raw materials, manufacturing, maintenance, decommissioning and disposal of product (e.g. thermal insulation layer) or technology (e.g. heat pump) but only during the operation of the building.

Therefore, for a comprehensive evaluation of the building environmental impacts, methods that are based on the life cycle assessment (LCA) should be used. Such methods are developed in a three-step approach:

- defining of the damage categories with respect to typical environmental phenomena (e.g. change in atmospheric greenhouse effect, acidification of precipitation, occurrence of winter and summer smog) and consequential impacts on human health (e.g. respiratory diseases, cardiovascular diseases, cancers), loss of biodiversity, and decrease of available natural sources;
- determination of the weighted quantity of emitted pollutants that contribute to a particular damage category; the impact of each pollutant is weighted according to a reference pollutant by factors such as greenhouse gas warming potential (GWP) or stratosphere ozone depletion potential (ODP) and then summarized as the equivalent of the emission of a reference pollutant (e.g. CO_{2,eq} for greenhouse gasses or PO_{4,eq} for pollutants that cause eutrophication); values of weighing factors are defined, taking into account period of pollutants' impact (typically 50, 100, or 500 years);
- defining the observation boundaries of the LCA; the widest range extends from the extraction of raw material to disposal of waste (cradle-to-grave), while the narrowest observation boundary takes into account only the production of the product (gate-to-gate); typical limits that could be used in engineering according to practice for environmental impact assessment are shown in Fig. 14.1.

The results of the LCA impact assessment can be presented in different forms and levels of complexity. The impact on one only or several damage categories can be shown or an assessment can be a "mid-point" assessment in which only impacts to damage categories are presented or at the "end point" where consequences to human health, biodiversity, or natural resources are shown. Some examples of life cycle impact assessment (LCIA) methods are presented further on.

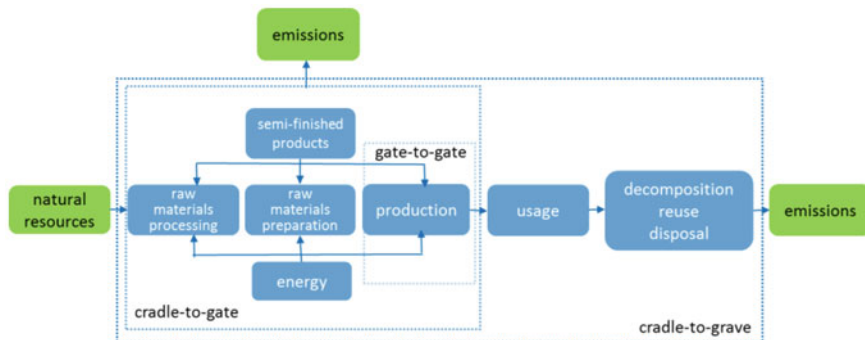


Fig. 14.1 Boundaries of the LCA assessment (ISO 14044:2006 environmental management—life cycle assessment—requirements and guidelines)

14.2 Ecodesign and Energy Labelling of Energy Related Products

The environmental impact of the buildings is strongly dependant on the properties of the installed appliances and systems. To ensure that more energy efficient household products come to the market, the Ecodesign Directive for Energy-related Products (ErP) 2009/125/EC¹ was introduced in European Union as a legislative framework. This directive provides specific minimum requirements for the energy efficiency and environmental parameters of pre-defined products. If these products fulfil the requirements, they receive a “CE Mark” as a conformity label. The Ecodesign Directive is implemented through the Ecodesign Working Plan,² a document that is published for the next three years including the list of new energy related product groups for which Ecodesign guidelines will be adopted. That list of depends on the impact on the environment (including energy demand) and market potential, as well as the improvement potential of particular product group (called Lot). Three successive working plans were published: Ecodesign Working Plan 2009–2011, 2012–2014 and 2016–2019.

Case Study Environmental requirements in Ecodesign consist of (among others) energy performance, stand-by energy use, water consumption (e.g. washing machines, dishwashers), noise emissions (air conditioning, heat

¹Directive 2009/125/EC of the European Parliament and the Council of 21 October 2009 establishing a framework for the setting of eco-design requirements for energy-related products (recast) (Official Journal of the European Union L 285/10).

²Communication from the Commission, Ecodesign Working Plan 2016–2019, COM(2016) 773 final.

pumps), NO_x emissions (heaters), CO, VOC emissions (solid fuel boilers), minimum lifetime (lamps), GWP of refrigerants in air conditioners, disassembly, recycling and disposal (vacuum cleaners, fans, space heaters, etc.).

While the Ecodesign Directive defines the minimum requirements that manufacturers must take into account, Energy Labelling Directive 2010/30/EU³ is a legislative framework that defines the way to present energy efficiency and environmental impacts for users (buyers). The layout of the energy label is adjusted to the product and shows not only efficiency at design conditions, but energy demand for all-year operation of the product at three pre-defined climate conditions (in the case of a heat generator like a heat pumps). According to the energy use for the operation, products are classified in one of the energy efficiency classes from A (or A+++ for some products types) to G. The data that must be shown on Energy Label are also defined in framework of the Energy Labelling Directive and are adjusted to the particular type of product.

Case Study According to Ecodesign ErP Lot 1 heat pump (HP) are space heaters for which the minimum seasonal space heating efficiency for low temperature HP (temperature of heat emitters 35 °C) based on primary energy is not less than 110% and for high temperature HP (temperature of heat emitters 55 °C) not less than 100%. According to Energy Labelling regulation, HP for low temperature applications are classified into the energy efficiency class A+++ with seasonal space heating efficiency equal or above 175% and into Class B if seasonal space heating efficiency of HP are in the range between 107 and 115%. This indicates that only HPs classified in Class B or a higher energy efficiency class will receive CE mark as they are in conformity with the Ecodesign Directive.^{4,5}

Note: Seasonal energy use for operation of heat pump is determine by pre-design climate conditions according to outdoor temperature range and heating load (in kW) at specified outdoor air temperatures. The EU is divided

³Directive 2010/30/EU of the European Parliament and the Council of 19 May 2010 on the indication by labelling and standard product information of the consumption of energy and other resources by energy-related products (recast) (Official Journal of the European Union L 153/1).

⁴Commission Regulation (EU) No 813/2013 of 2 August 2013 implementing Directive 2009/125/EC of the European Parliament and of the Council with regard to ecodesign requirements for space heaters and combination heaters (Official Journal of the European Union L 239/136).

⁵Commission Delegated Regulation (EU) No 811/2013 of 18 February 2013 supplementing Directive 2010/30/EU of the European Parliament and of the Council with regard to the energy labelling of space heaters, combination heaters, packages of space heater, temperature control and solar device and packages of combination heater, temperature control and solar device (Official Journal of the European Union L 239/1).

into three climate zones: warm, moderate, and cold. Seasonal efficiency is determined using Primary Energy Factors (PEF). The PEF equal to 2.5 for electricity shall be taken into account.

14.3 Environmental Labels

Although Ecodesign guidelines were developed based on a life cycle environment impact assessment approach, the indicators are strongly related to energy demand during the operation and intended only for pre-selected types of products.

There are several other voluntary methods of environmental performance certification and labelling methods that follow life cycle assessment principle more consistently. The aim of ecolabels is to increase consumer awareness of the environmental impacts of the products. As consequence, producers improve their public image and increase market share of the product awarded with an ecolabel. In accordance with ISO 14020,⁶ a series of standard environmental labels are divided into Type I, Type II, and Type III (ISO 2012; UNOPS 2009).

Type I environmental labelling leads to the award of an ecolabel in form of a mark or a logo, based on the fulfilment of criteria proposed by an independent certification organization according to requirements of the ISO 14024 standard.⁷ The certification procedure includes the selection of products, the definition of products' environmental criteria, function characteristics, and the procedure for awarding the ecolabel; the requirements for the ecolabelling scheme's operation are defined in the standard. The eco labelling should be voluntary, based on compliance with relevant legislation, and must include the consideration of each life cycle phase (e.g. extraction of materials, manufacturing, distribution, use and disposal). Examples of ecolabels are: EU Ecolabel (54.511 products and services in 29 product groups were awarded from the start in 1992), EKOenergy (label for electricity produced from renewable energy sources), Blue Angel (German label for environmentally friendly products and services), FSC (Forest Stewardship Council, an international label for responsible forest management). Such labels present technical data about the environmental impacts of the product in simplified way to the public (Fig 14.2).

⁶ISO 14020:2000 Environmental labels and declarations—General principles.

⁷ISO 14024:1999 Environmental labels and declarations—Type I environmental labelling—Principles and procedures.



Fig. 14.2 Examples of Type I ecolabels (from left to right: European Flower (ec.europa.eu/environment/ecolabel), EKOenergy (www.ekoenergy.org), Blue Angel (www.blauer-engel.de), and FSC (ic.fsc.org)); detailed data on Type I ecolabel certification schemes worldwide are provided by Global Ecolabelling Network (GEN) (www.globalecolabelling.net)

Type II ecolabels are self-declared claims made by producers. As such, they are not awarded by independent organizations. As regulated by the ISO 14021 standard,⁸ such ecolabels shall be accurate and not misleading, verified, and presented in such a way as to avoid misinterpretation. Claims such as “biodegradable”, “recyclable”, “reduced energy and water consumption”, “containing recycled materials” can be used, but non-specific claims such as “environment friendly”, and “green” shall not. Recognized testing methods must be used for claim verification, and test results must be available to anyone if required. In 2011, the standard was supplemented by the terms, definitions, and evaluation methods for “renewable materials”, “renewable energy”, “sustainable” and arguments related to greenhouse gas emissions (carbon footprint and carbon neutral). Type II ecolabels may be in graphical or textual form.

Case Study Environmental impacts of three technologies of lamp production: compact fluorescent lamp (CFL) and light-emitting diode (LED) produced by technologies available in 2012 and 2015, as claimed by producer to show the environmental benefits of BAT for the production of LED lamps. This Type II ecolabel show impacts (less is better) on specific environmental areas⁹ (Fig. 14.3).

⁸ISO 14021:2016 Environmental labels and declarations—Self-declared environmental claims (Type II environmental labelling).

⁹www.eere.energy.gov/eere.

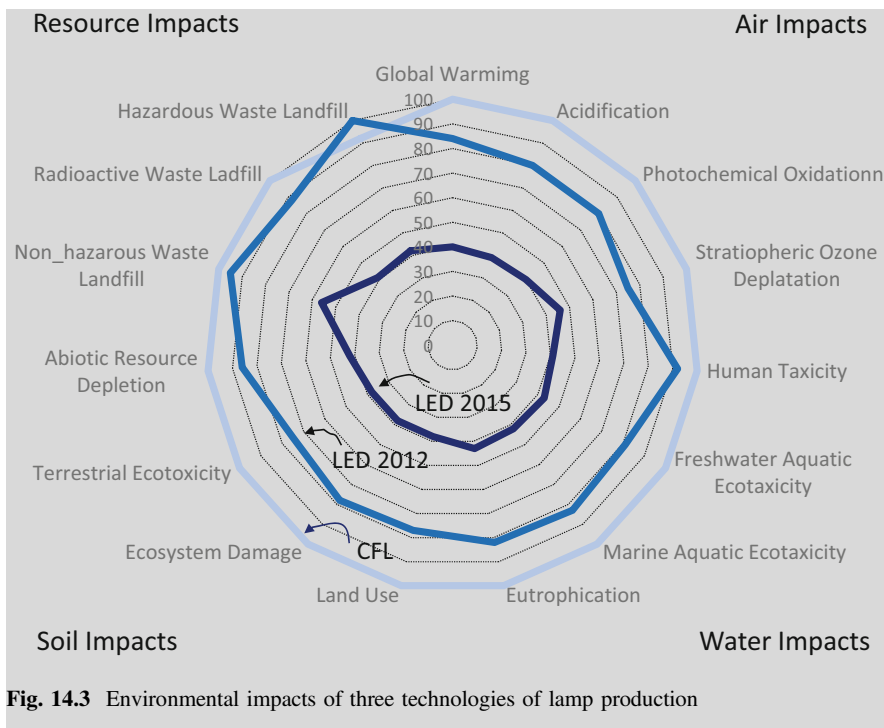


Fig. 14.3 Environmental impacts of three technologies of lamp production

Type III environmental declarations are quantitative and allow the direct comparison of individual products. They are prepared on the basis of predetermined groups of criteria defined in ISO 14040.¹⁰ Principles and procedures are defined in the ISO 14025 standard.¹¹ Environment declarations are published by independent institutions on the basis of data obtained from producers in form of life cycle inventory analysis (LCI), which provide information on the material and energy flows. LCI data are used for the determination of life-cycle impact assessment (LCIA). Environmental impacts are presented in the form of pre-defined parameters, which are specified using common methodology and, therefore, enable direct comparison between similar products. ISO standards were the basis for the standard EN 15804, published in 2012 and updated in 2013.¹² The standard defines the phases that must be included in the environmental assessment of products in the

¹⁰ISO 14040:2006 Environmental management—Life cycle assessment—Principles and framework.

¹¹ISO 14025:2006 Environmental labels and declarations—Type III environmental declarations—Principles and procedures.

¹²EN 15804:2012/FprA1 Sustainability of construction works—Environmental product declarations—Core rules for the product category of construction products.

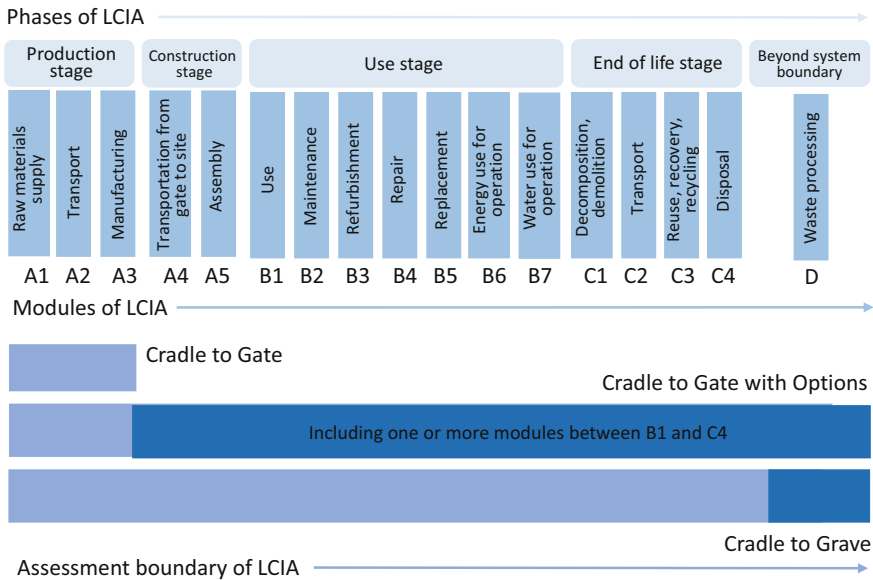


Fig. 14.4 Environmental declarations consist of several phases of environmental LCIA and modules A1 to D that describe stages in the life cycle of the product. In EN 15804, the borders of environmental LCIA are proposed as Cradle to Gate (LCIA consist of modules A1–A3), Cradle to Gate with options (A1–A3 + module(s) from use stage (B1–B7) and/or module(s) from end of life stage (C1–C4)) or Cradle to Grave. In this case, only module D is not obligatory

form of modules and minimum requirements for the number of included modules. As with other environmental labels, Type III environmental declarations are voluntary (Fig 14.4).

14.4 Environment Product Declaration—EPD

In standard EN 15804 25, sustainability indicators are provided and classified into four groups: environmental impact indicators (7), indicators of rational use of natural resources (energy, materials, water, 10), waste treatment indicators (4), and recycling and reuse indicators (4). The LCIA survey leads to the environment declaration presented as Environment Product Declaration (EPB). In most cases, publicly accessible EPDs contain environmental impact indicators, which are also the most recognizable in global society. Environmental impact indicators are determined based on the life cycle inventory assessment of mass and energy flows (LCIA) and evaluated by characterization factors (CF) in seven pre-defined damage categories. Characterization factors represent the relative impact of the individual

pollutants according to reference substances and are determined according to the expected retention time in the environment, i.e. 20, 100, or 500 years. The following damage categories are covered by seven environmental indicators in the EPD:

- global climate changes; the indicator is Global Warming Potential (GWP) of the product or system, expressed as equivalent of CO₂ emissions (short notation kg eqCO₂ or kg CO_{2,eq}),
- decomposition of stratospheric ozone; the indicator is Depletion Potential of the Stratospheric Ozone layer (ODP), expressed as the equivalent of trichlorofluoromethane CCl₃F emissions (short notation kg eqCFC-11),
- acidification of land and water; the indicator is Acidification Potential (AP), expressed as equivalent of SO₂ emissions,
- eutrophication; the indicator is Eutrophication Potential (EP), expressed in kg eqPO₄³⁻,
- creation of photochemical tropospheric ozone; the indicator is Photochemical Ozone Creation Potential POCP or Tropospheric Ozone Forming Potential TOFP, indicator is expressed as equivalent of ethene emissions (in kg eqC₂H₄),
- use of abiotic sources (materials); the indicator is Abiotic Depletion Potential Elements (ADPE) expressed as antimony equivalent (in kg eqSb),
- use of abiotic sources (energy); the indicator is Abiotic Depletion Potential—Fossil (ADPF) expressed in MJ.

All indicators are expressed per unit of product (unit, mass (kg) or volume (m³)) or per time period (year, life cycle period).

Case Study 1 How equivalents are developed—case of eqCO₂

Global warming is phenomena of the rapid increase of planetary temperature in the last 150 year caused by anthropogenic emissions of so-called greenhouse gasses. Most anthropogenic greenhouse gasses originate from the combustion of fossil fuels. Greenhouse gasses in the atmosphere absorb longwave thermal radiation emitted from Earth's surface toward to the space. As consequence, the troposphere is heated. According to the methodology proposed by the Intergovernmental Panel on Climate Changes (IPCC),¹³ the following gasses are treated as greenhouse gasses: carbon dioxide CO₂, methane CH₄, di-nitrous oxide (N₂O), F-gasses (partially fluorinated hydrocarbons HFC), fully fluorinated hydrocarbons (PFC) in sulphur hexafluoride SF₆. While each greenhouse gas retains the Earth's long-wave thermal radiation differently, the total environmental impact of emissions of greenhouse gases is determined as the sum of the weighted emissions of the greenhouse gases (CO₂, CH₄, N₂O, etc.). Weighting factors, called

¹³www.ipcc.ch.

← Similar products made from gypsum →

Rigidur gypsum fibre boards		Rigidur gypsum fibre flooring elements	
Primary energy, non-renewable (MJ)	4.90	Primary energy, non-renewable (MJ)	4.89
Primary energy (MJ)	0.06	Primary energy (MJ)	0.06
Global warming potential (GWP 100) (kg CO ₂ -eq.)	0.308	Global warming potential (GWP 100) (kg CO ₂ -eq.)	0.303
Ozone depletion potential (ODP) (kg R 11-eq.)	12.4E-09	Ozone depletion potential (ODP) (kg R 11-eq.)	12.4E-09
Acidification potential (AP) (kg SO ₂ -eq.)	0.39E-03	Acidification potential (AP) (kg SO ₂ -eq.)	0.38E-03
Eutrophication potential (EP)(kg PO ₄ -eq.)	6.55E-05	Eutrophication potential (EP)(kg PO ₄ -eq.)	6.33E-05
Photochemical ozone creation potential (POCP)(kg C ₂ H ₄ -eq.)	3.70E-05	Photochemical ozone creation potential (POCP)(kg C ₂ H ₄ -eq.)	3.76E-05

Fig. 14.5 Comparison of seven indicators of two similar gypsum products

greenhouse warming potential (GWP), for the retention time 100 years are as follows: 1 for CO₂, 21 for CH₄, 310 for N₂O, 23,900 for SF₆, 1300 for HFC-134a, 6500 for CF₄ and 9200 for C₂F₆. Total weighted greenhouse gases emissions are expressed in kilogram of CO₂ equivalent (kg eqCO₂).

Case Study 2 Seven environmental indicators of two similar products can be compared. Among other sources, the EPD of building products can be found at enivondec.com¹⁴ and oekobaudat.de¹⁵ (Fig 14.5).

14.4.1 Single Issue Type III Environmental Declarations

Type III environmental declarations are developed so that only one indicator is shown for a particular product or process. For example, the Eutrophication Declaration of the agriculture or farming product emphasizes environmental impacts related to enriching the land and water with nutrients. The most widespread single issue environment declarations are Climate Declarations, which show upstream (modules A1–A3 and A4), core (A5), and downstream (B1–B7, C1–C4) emissions of greenhouse gases expressed as equivalent of CO₂ (Fig 14.6).

The equivalent of CO₂ emissions is also used as an independent indicator for the evaluation of the cost efficiency of the rational energy use measures and renewable energy technologies.

¹⁴www.environdec.com.

¹⁵oekobaudat.de.

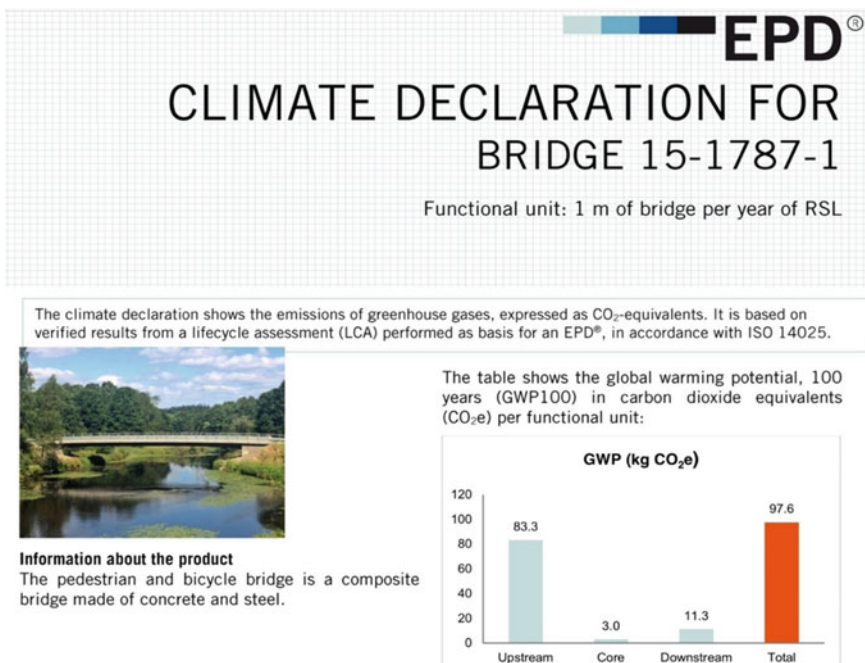


Fig. 14.6 Example of climate declaration showing emitted greenhouse gases expressed as equivalent of CO₂ for the unit (1 m length) of the bridge; in addition to the climate declaration, the EPD for the same product is available as well (www.environdec.com)

Case Study The equivalent of CO₂ emissions could be used as a single issue indicator for the evaluation of cost efficiency of the rational energy use measures and renewable energy technologies in the building sector. As an example, Mc Kinsley’s greenhouse gas abatement cost curve for global emissions into building sector for the period to 2030 is shown. The diagram shows how much the abatement of 1 ton of eqCO₂ will cost according to implemented measure. Negative values indicate that specific measures will not only decrease the emissions of greenhouse gases but also running costs. The cost of €60 per ton of reduced tonne of eqCO₂ emissions is used as limit cost value in presented case (McKinsey and Company 2009) (Fig 14.7).

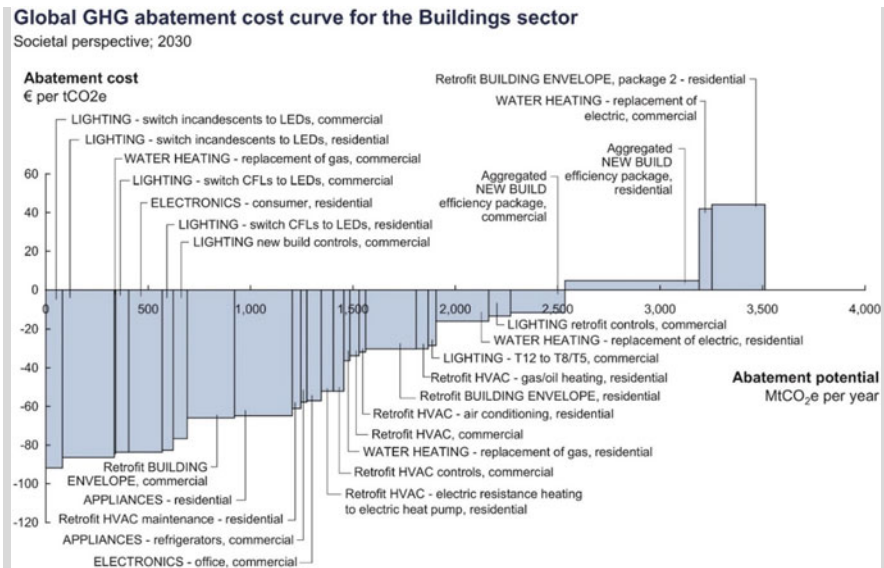


Fig. 14.7 Mc Kinsley's greenhouse gas abatement cost curve for global emissions in building sector for the period up to 2030 (McKinsey and Company 2009)

14.5 Life Cycle Impact Assessment (LCIA)

Several life cycle impact assessment methods and tool have been developed since the 1990s and are increasingly used in practice nowadays to reduce environmental problems, and to avoid shifting the environmental impacts from one part of the product life cycle to another, from one environment problem to another, or from our generation to the next one. Methods were developed according to the ISO 14040 and ISO 14044 international standards along the following four main steps:

- definition of the objective and purpose of the environmental assessment by defining the life-cycle phases that will be included in the assessment (cradle to gate, gate to gate, gate to grave, cradle to grave) and functional units (1 kWh, 1 m³, 1 piece, etc.);
- determination of life cycle inventory (Life Cycle Inventory (LCI)) of all (i) energy flows, (ii) amount of substances entering the process, and (iii) emitted solid, liquid, or gaseous pollutants released into the air, water, or soil during all phases of product life-cycle; LCI is prepared by the manufacturer or supplier and verified by an independent authority using a recognized database, for example, the Ecoinvent v3 database (Swiss Centre for Life Cycle Inventories 2013);
- determination of environmental impacts (Life Cycle Impact Assessment LCIA) as mid-point or end-point assessment approaches; mid-point assessment includes definition of impact categories (such as climate changes, stratospheric

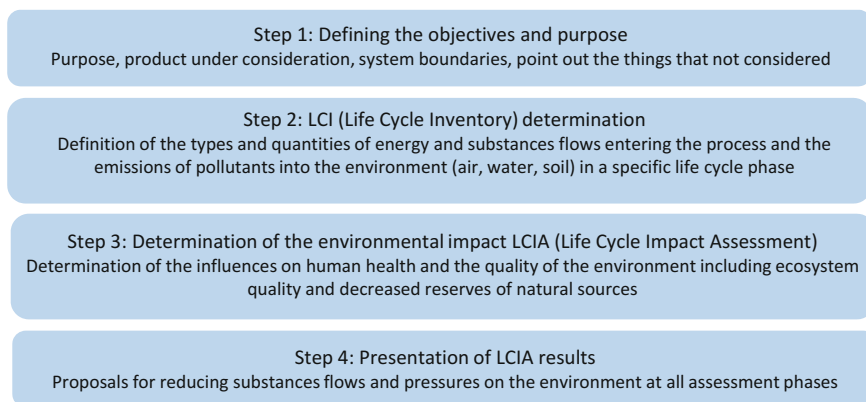


Fig. 14.8 Methodological steps in life cycle impact assessment methods as defined in the standard ISO 14040

ozone depletion or land use, etc.) and evaluation of environmental stress causes by each energy or material flow and emitted pollutant from product LCI on particular impact category. End-point assessment includes definitions of damage categories (such as damage to human health or damage to natural resources) and assessment of damage in particular damage categories caused by relevant impact categories. Damage in the separate categories can be weighted and summarized into a “single-score” LCIA result. For LCA practitioners, methods are integrated into LCA software, such as SimaPro¹⁶ or Gabi¹⁷ (EC JRC, IES 2010);

- presentation of LCIA results with proposals for reducing environmental impact (Fig 14.8).

14.5.1 Classification, Characterization, Normalization, and Weighting in LCIA Methodologies

As pointed out in Sect. 14.4, several methods are available for LCA practitioners. In this chapter, three of them (mid-point TRACI, end-point ReCePi, and IMPACT 2002+) will be presented. The TRACI (Tool for Reduction and Assessment of Chemicals and other Environment Impacts) methodology was developed as a Microsoft Excel tool for mid-point assessment, by the U Environmental Protection Agency. First published in 2002 was adapted in 2011. TRACI 2.1 consists of 10 mid-point impact categories (EPA 2012). The ReCiPe methodology was developed in 2009 as an upgrade and fusion of the CML 2001 (as mid-point) and Ecoindicator 99 (as end-point) methods (Goedkoop et al. 2009; Huijbregts et al. 2016). It consists

¹⁶SimaPro, simapro.com, PRé Sustainability, Amersfoort, The Netherlands.

¹⁷GaBi, www.gabi-software.com, Thinkstep, Leinfelden-Echterdingen, Germany.

of 18 mid-point impact and 3 end-point damage categories. The IMPACT 2002+ method was developed by the Swiss Federal Institute of Technology in 2003 as an end-point method. Method consists of 14 impact and 4 damage categories (Humbert et al. 2012).

Note: Some pollutants contribute in more than one impact categories (e.g. refrigerants increase global warming and cause depletion of stratospheric ozone) and some impact categories have impact on more than one damage category (e.g. depletion of stratospheric ozone impacts human health and ecosystem quality).

Common to all LCIA methodologies are the use of calculation factors in the process of classification, characterization, normalization and weighting, as shown in Fig. 14.9.

The “Classification phase” is the process in which each pollutant emitted and each resource used in the life cycle of the product is assigned into one of the environment impact categories. Impact categories differ according to the method, as shown in Fig. 14.10.

The classification phase is followed by the two-stage “Characterization phase”. In the first part, which is mandatory, the environmental stress of each pollutant emitted and each resource used is compared to reference material or unit-using characterization factors (CF). Some of characterization factors were already presented in Sect. 14.3. The total amount of characterized pollutants or resources in a particular impact category is expressed as the equivalent of reference matter. Equivalent can differ among the methods. For example, in the IMPACT 2002+ method (IMPACT 2002+, 2010), mineral depletion is characterized comparing total world reserves and yearly extraction of particular mineral and expressed as Antimony equivalent (Sb), while Iron equivalent (Fe) is used as mid-point indicator in same impact category in the ReCiPe method.

Case Study During the life cycle of product A, emissions of 0.5 kg CO₂, 0.1 kg of methane CH₄ and 0.02 kg of dinitrogen oxide N₂O occur. All pollutants are classified in the climate change impact category. Characterization factors CF are determined according to reference material, which is, in this case, CO₂ and are: CF_{CO₂} equal to 1 kg CO₂ per 1 kg CO₂, CF_{CH₄} equal to 23 kg CO₂ per 1 kg of CH₄ and equal to 310 kg CO₂ per 1 kg of emitted N₂O. Therefore, the total environmental burden caused by product A in the impact category climate change is equal to $0.5 \text{ kg} \times \text{CF}_{\text{CO}_2} + 0.1 \text{ kg} \times \text{CF}_{\text{CH}_4} + 0.02 \text{ kg} \times \text{CF}_{\text{N}_2\text{O}} = 0.5 \text{ kg} \times 1 \text{ kg/kg} + 0.1 \text{ kg} \times 23 \text{ kg/kg} + 0.02 \text{ kg} \times 310 \text{ kg/kg} = 9 \text{ kg CO}_{2\text{eq}}$.

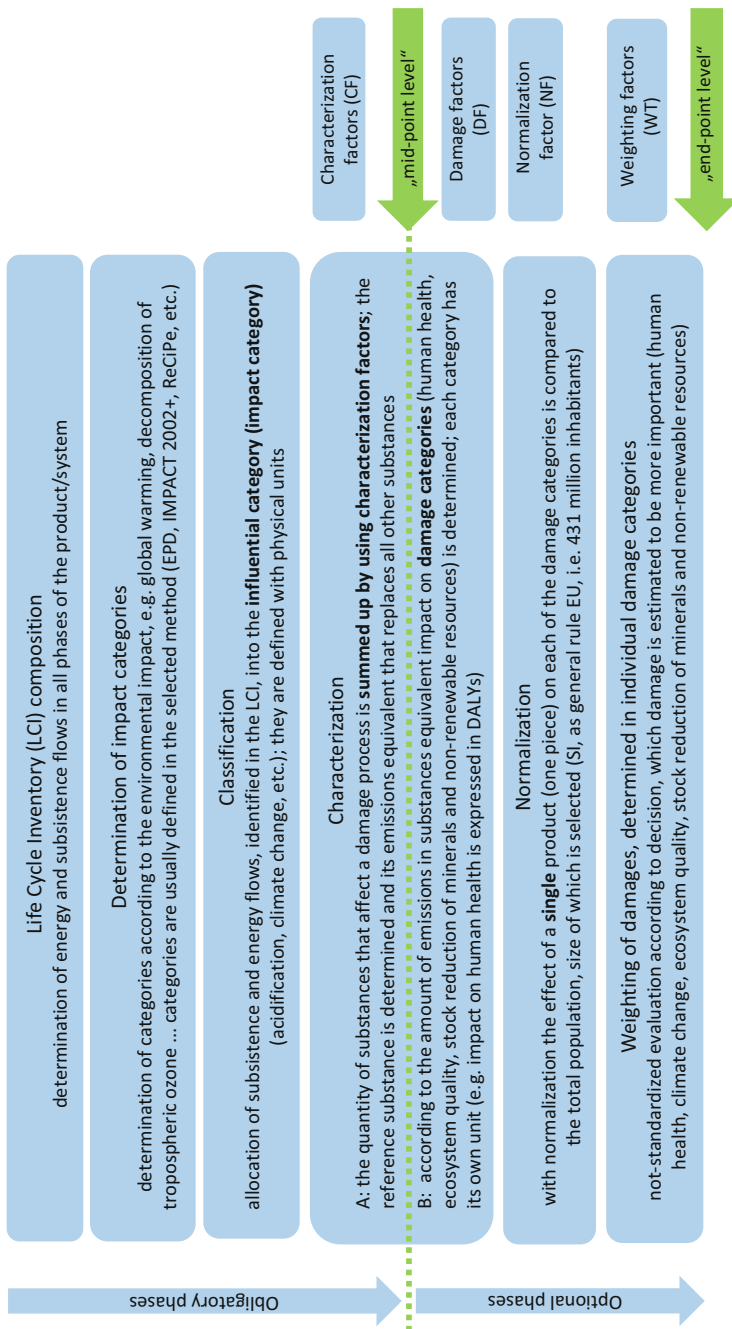


Fig. 14.9 Methodological steps in life cycle impact assessment methods as defined in the ISO 14040 standard

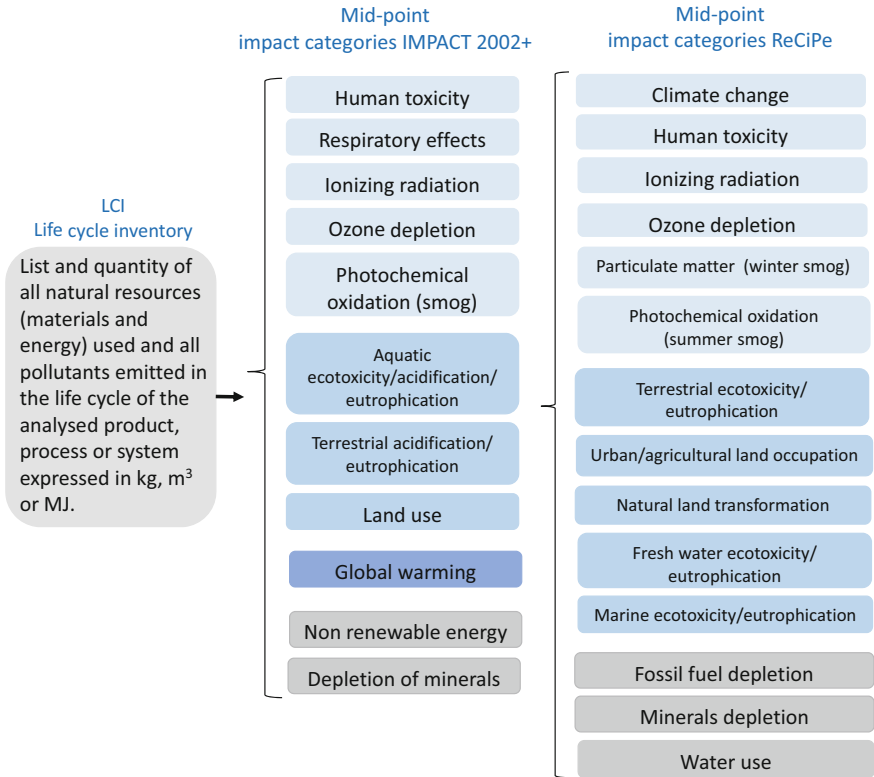


Fig. 14.10 Mid-point impact category in IMPACT 2002+ and ReCiPe LCIA method

Apart from the difference in the number of mid-point and end-point assessment categories, the ReCiPe method differs from IMPACT 2002+ because the characterization factors (needed for mid-point characterization) are developed from three perspectives: I (individualist), H (hierarchical) and E (egalitarian). Perspective I is based on the assumption that technology development as well as human adaptation will reduce environmental damage in the future, while perspective E is the most precautionary and take into account the largest time horizons: instead of the 20-year time horizon in perspective I, a 500-year time horizon for climate change damage category is used in perspective E.

In the second stage of characterization, which is optional, environmental damage cause by equivalents of pollutants are determined using damage factors (DF). The number of damage categories varies between methods; for example, the IMPACT 2002 + method evaluates four damage categories: human health, ecosystems quality, climate change, and the stock reduction of minerals and non-renewable resources; in contrast, the ReCiPe method evaluates only three: human health, ecosystems quality, and the stock reduction of minerals and non-renewable resources, while the equivalent of CO₂ emissions is taken into account within the human health category (Fig 14.11).

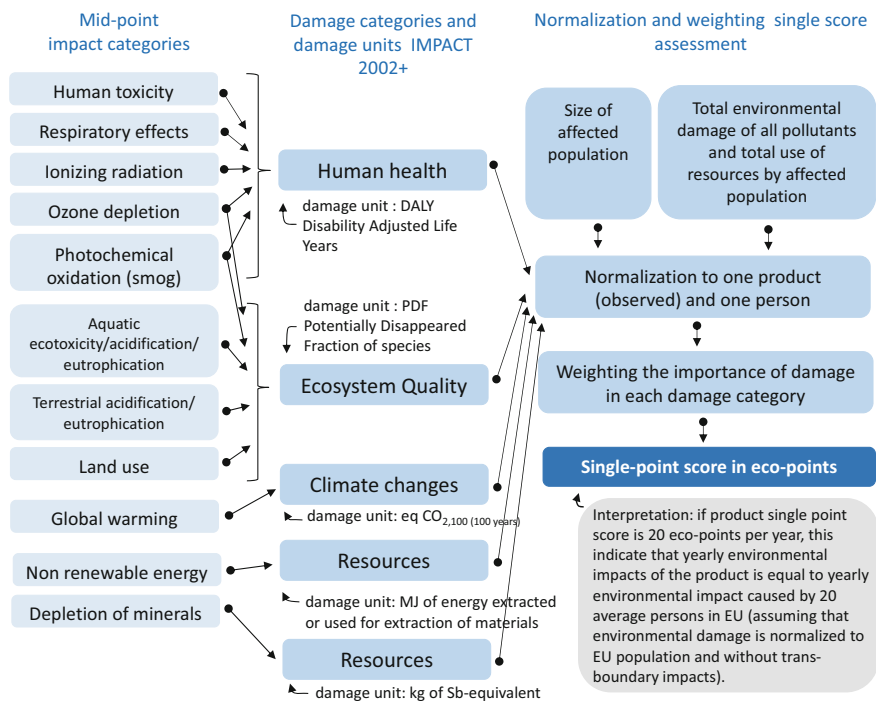


Fig. 14.11 Mid-point and damage categories included in IMPACT 2002+ LCIA method

Each of the damage categories is expressed by a different quantity. For the evaluation of the impact in the damage category of human health, that quantity DALY (Disability Adjusted Life Years) is used, which defines the total number of years in which a reference population is affected by diseases, injuries, and premature death per year. DALYs are calculated as a cumulative value, taking into account all human health-related emissions of pollutants caused by the observed systems (Fig 14.12).

Case Study Total emissions of greenhouse gasses expressed in eqCO₂ in EU are 4.99×10^{12} kg per year. The damage factor for human health in the climate change damage category is equal to 1.19×10^{-6} DALY per kg of eqCO₂ emissions in the ReCiPe perspective I and 1.40×10^{-6} DALY per kg of eqCO₂ emissions in perspectives H and E. The total impact on human health of the EU population because of climate changes is equal to 5.94×10^6 DALY per year (4.99×10^{12} kg/year \times 1.19×10^{-6} DALY/kg) (I) and 6.99×10^6 DALY per year (H, E).¹⁸

¹⁸ www.sph.umich.edu/riskcenter/jolliet/impact2002+.

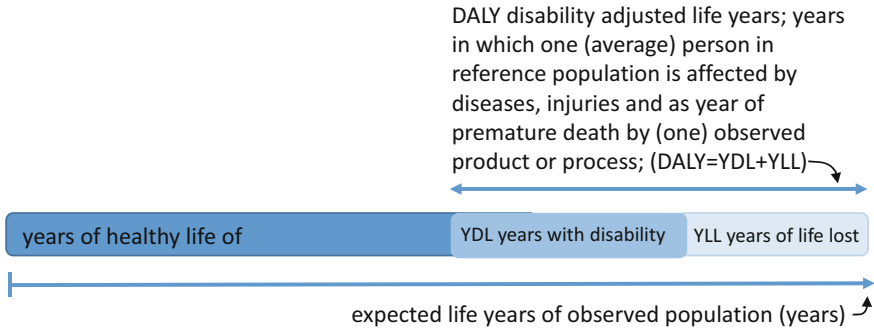


Fig. 14.12 In IMPACT 2002+ and ReCiPe method, damage in human health damage category is expressed in DALYs, the year of disability adjusted life years

In the Ecosystem Quality damage category, the environmental impacts of acidification and eutrophication of the soil, marine, and fresh water systems because of the transfer of phosphorus and nitrogen compounds and the loss of fertile land are taken into account. Damage caused by acidification and eutrophication is evaluated as a potential loss of ecosystems (Potentially Disappeared Fraction, PDF) per m^2 of land, caused by 1 kg of an individual pollutant's emissions per year. Therefore, the indicator is measured in $(PDF \times m^2 \times year)$ per kg of pollutant. Damage caused by emissions into the hydrosphere deal with potentially affected water ecosystems (Potentially Affected Fraction, PAF) per m^3 of water, caused by 1 kg of individual pollutant's emissions per year. This indicator is measured by $(PAF \times m^3 \times year)$ per kg of pollutant. PAF is converted to the PDF by a weighting factor of 0.1.

Environmental damage in the resources damage category caused by the use of resources (separated on biotic and abiotic) is assessed differently in the assessment methods. In EPD and IMPACT 2002+, such damage is expressed with reference material antimony, referred in kg Sb eq. In Eco-Indicator 99, it is expressed as an increased amount of energy that will be needed in the future for the extraction of 1 kg of the substance referred in MJ/kg. In ReCiPe, it is referred to as an additional cost of society for exploitation of the substance referred in \$ per kg of resource. Decreasing of the non-renewable energy source stock, i.e. fossil and nuclear fuels, is calculated by caloric value in MJ per kg of energy carrier. Use of water, if included in the assessment, is measured in m^3 per product unit.

In the normalization phase, environmental damage caused by an assessed product or process is compared to the total damage in a particular damage category and distributed among all members of population. Normalization factors (NF) can be determined for example for a particular country, the EU, or the World. Normalization factors enable evaluation of environmental impacts as single score value. Single score result is expressed in person years or Ecopoints (Pt).

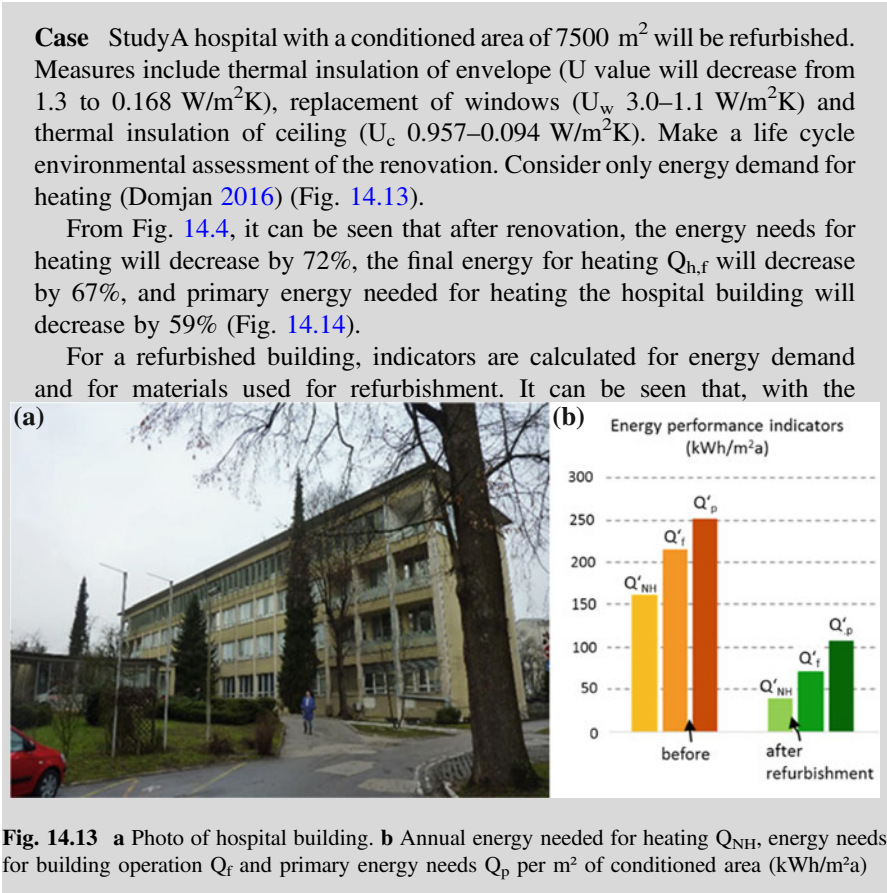
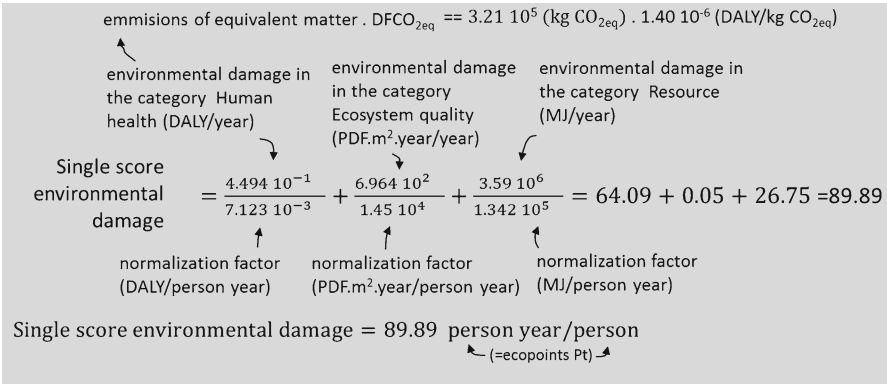
Case Study Characterized emissions of all pollutants that cause damage in the human health damage category in the EU are equal 3.07×10^6 DALY per year (3.02×10^6 DALY per year is due to emissions of pollutants into the air). Total emissions of greenhouse gasses in EU are 4.99×10^{12} kg CO_{2eq} per year. The EU population is 431×10^6 . The normalization factor for the damage category human health NF_{DALY} is equal to 7.123×10^{-3} DALY per year per person (3.07×10^6 DALY per year/ 431×10^6 person) and the normalization factor for the damage category climate change NF_{CO2} is equal to 1.158×10^4 kg CO_{2eq} per person per year (4.99×10^{12} kg per year/ 431×10^6 person).

Before the determination of a single score end-point assessment result, normalized damage can be weighted to give greater importance to one of the categories by weighting factors (WF). However, the authors of assessment methods mainly suggest that WF equal to 1 should be used for each damage category.

Case Study During the production and operation in the life cycle period of product A, emissions of 3.21×10^5 kg of CO_{2eq} per year and 6.69×10^2 kg of SO_{2eq} per year occur. Energy consumption for the operation of the product is 3.59×10^6 MJ per year. Determine a single score environmental impact product A, using the ReCePi methodology (greenhouse gas emissions are included in damage category for human health).¹⁹

Damage category	Damage factors (DF)	Damage	Normalization factors (NF)
Human health	1.4×10^{-6} DALY per kg CO _{2eq}	4.494×10^{-1} DALY per year	7.123×10^{-3} DALY per (person year)
Ecosystem quality	1.041 PDF.m ² .year per kg of SO _{2eq}	6.964×10^2 PDF m ² year per year	1.45×10^4 (PDF.m ² .year) per (person year)
Resources	1 MJ per year per MJ per year	3.59×10^6 MJ per year	1.342×10^5 MJ per (person year)

¹⁹ www.sph.umich.edu/riskcenter/jolliet/impact2002+.



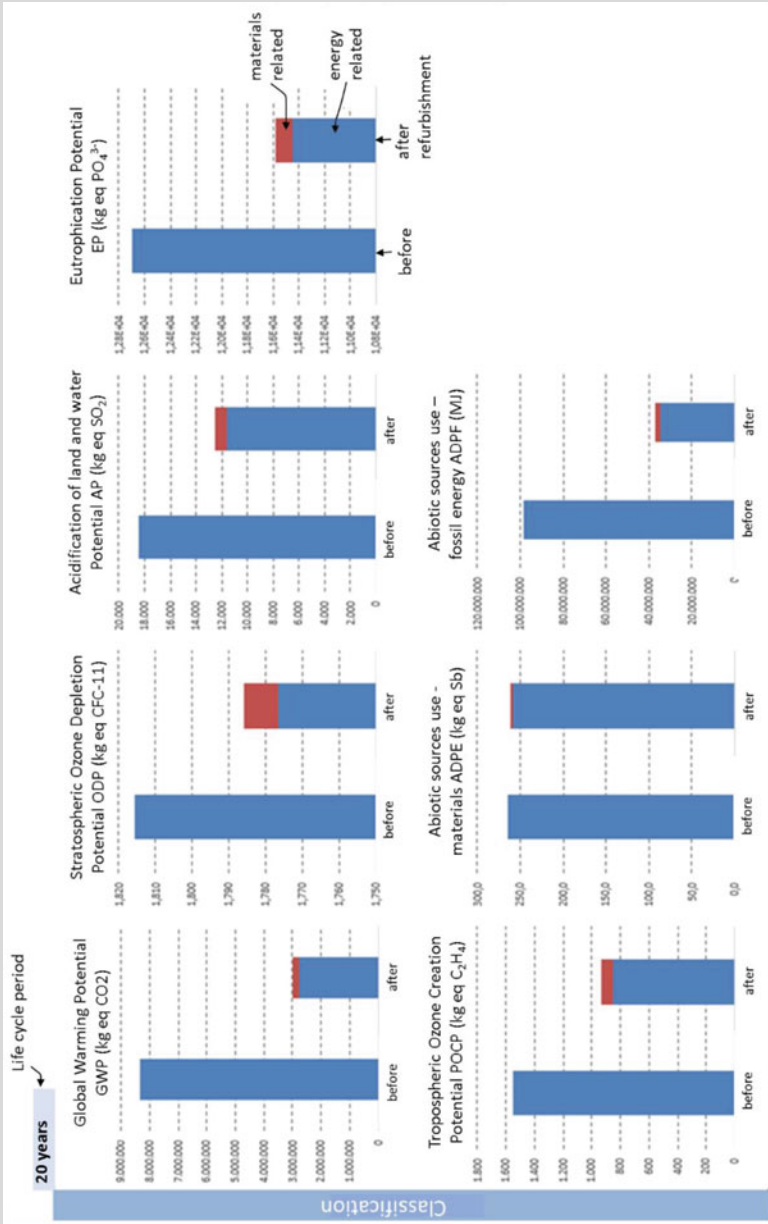


Fig. 14.14 Mid-point environment impact indicators calculated for life cycle period of 20 years as required in EPBD

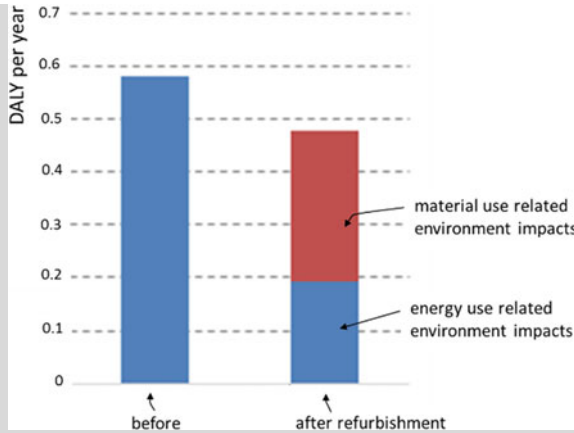


Fig. 14.15 End-point characterization in DALY per year for the current building and for the first year of operation of building after refurbishment. Influence of building’s materials on human health is comparable to the impact of energy use. After the first year, DALY will be only 1/3 of current value

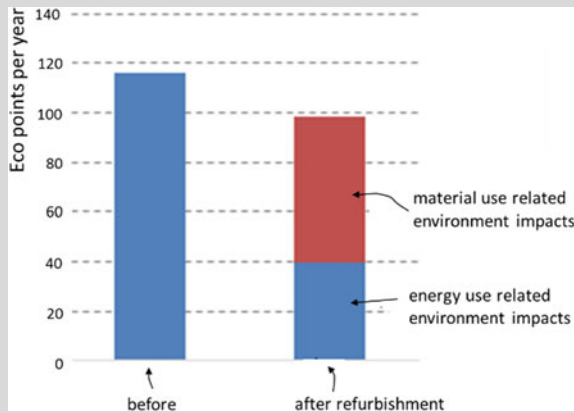


Fig. 14.16 Eco points are calculated after normalization of three end-point indicators (DALY, PDF and MJ). Damage was normalized according to pollutant emissions in the EU, use of resources and EU population. Pt will decrease after renovation from 115 to 99 Pt in the first year after renovation and to 40 Pt per year during following years

exception of ADPE, all other environment impact indicators are decreased approximately by approximately one half (Figs. 14.15 and 14.16).

Note: Environmental impacts of current building is equal to environmental impacts caused by 115 average EU citizens and will be reduced to environmental impacts caused by 40 EU citizens in the second year after the renovation and afterwards.

14.6 Environmental Impact Assessment of Buildings

Sustainable development is continuous process that includes economic, ecological, and social aspects of human actions and related consequences in the future. Buildings are systems that have significant impact on the use of natural sources and the quality of the environment. Energy and other resource use related to the buildings are related to one third of all greenhouse gasses emissions, almost 40% of energy use and almost a half of total use of natural resources. Therefore, the sustainability of the buildings is indispensable for the establishment of sustainable development in general (Fig 14.17).

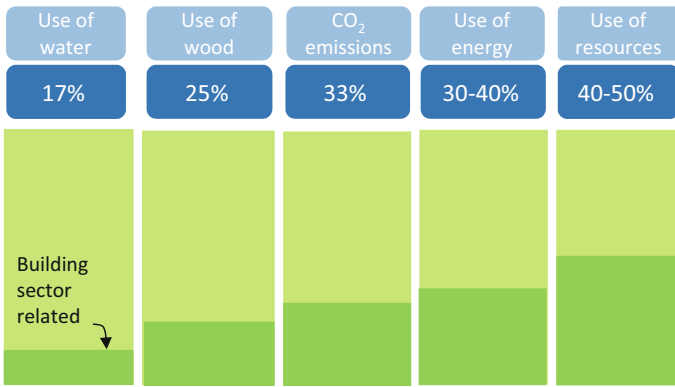


Fig. 14.17 Global use of resources and environmental load in the buildings sector (UNEP information note, DGNB, 2006)

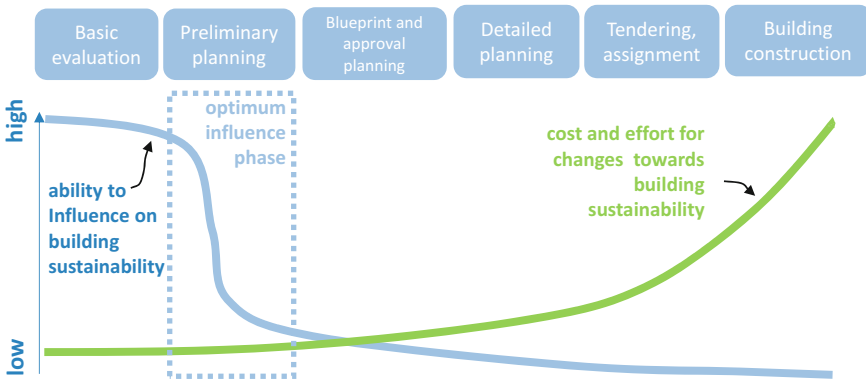


Fig. 14.18 Planning phases of building; during preliminary planning phase, building designers can contribute the most to the sustainability of a building, and this can be achieved with the lowest relative cost for investors

Among building planning phases, there are different opportunities for implementing sustainability, but during preliminary planning phase a significant effect on sustainability can be attained with the lowest amount of expenses. The success of this phase greatly depends on the professional knowledge of the planners and their awareness of necessity of holistic assessment approach. To verify the sustainability of solutions, holistic assessment methods must be used. In this chapter, such methods will be presented (Fig 14.18) (Allen et al. 2016).

Several certification schemes have been developed, taking into account regional requirements and engineering practice. More than 20 schemes are used in EU, and methods have several common features. For example, all schemes take into account national legislative frameworks, are voluntary and include life cycle assessment with environmental, cost and social criteria. Assessment is done through several categories (e.g. management, health, energy, transport, etc.), each consisting of various criteria (e.g. commissioning, daylighting, thermal comfort, IAQ, etc.). Indicators of criteria are weighted and results are summarized in single a score rating. Most methods are developed for different building types (e.g. residential, commercial, sport facilities, etc.) with the building type adapted by weighting and score steps. BREEAM, LEED, and DGNB are the main voluntary certification schemes currently used in the EU^{20,21} (Ebert et al. 2011).

14.6.1 BREEAM

The Building Research Establishment Environmental Assessment Method (BREEAM) was the first certification system for the assessment of buildings' sustainability. It was developed in the UK in 1980s and become widely used after 1990. After several revisions, the current version was published in 2008 and is used in more than 20 countries in the EU-28. The method was originally developed for the assessment of residential and office buildings, but now any building type can be assessed. Assessment is divided into ten BREEAM sections with different weighting factors. Each section consists of criteria, and the maximum credit for each criterion is defined. The following BREEAM sections are evaluated²² (Fig. 14.19).

A BREEAM certificate is awarded if the minimum criteria in selected categories are met (for example, 6 credits out of 13 must be awarded for the energy performance criteria to score the highest level of certificate) as well as on overall scoring. At least 30% of total score must be reached to get a certificate (Pass), and more than 85% of total score for highest (Outstanding) level (BREEAM UK 2018) (Figs. 14.20 and 14.21).

²⁰ec.europa.eu/energy/en/content/introduction-0.

²¹National Institute of Building Science, WBDG Whole Building Design Guide.

²²www.bre.co.uk.

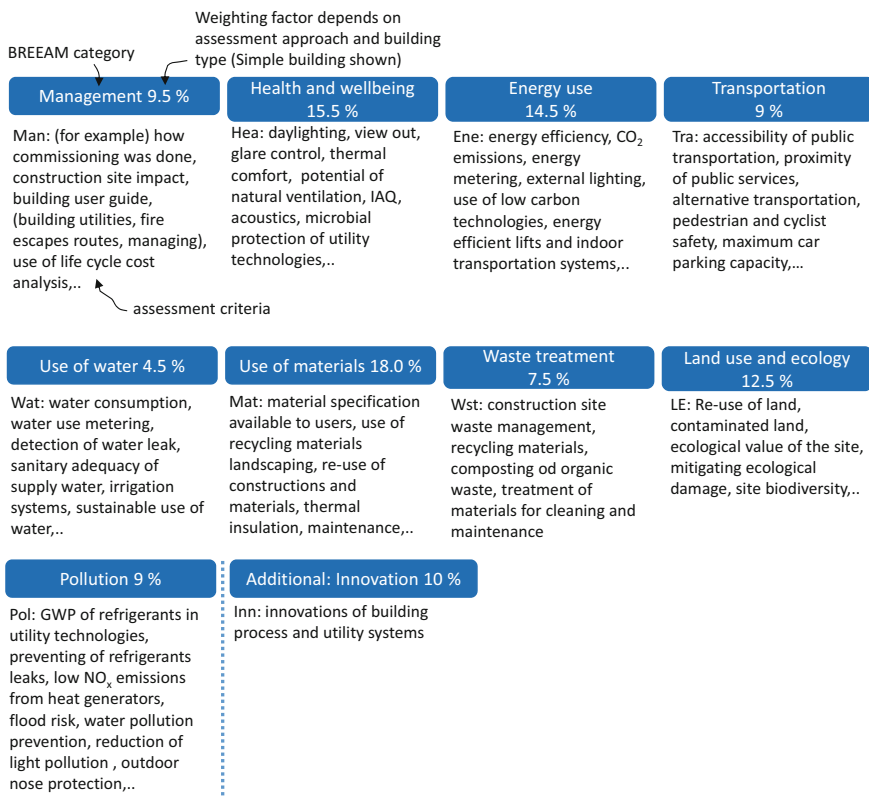


Fig. 14.19 BREEAM sections and categories

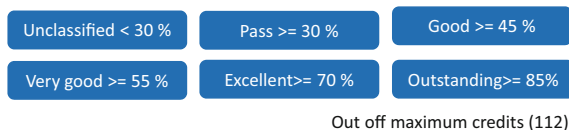


Fig. 14.20 BREEAM certificate classification of building sustainability is based on awarded percentage of total credits

14.6.2 LEED

The certificate Leadership in Energy and Environmental Design (LEED) was developed by the U.S. Green Building Council in the early 1990s and has been used worldwide in its current version since the year 2000. The LEED certification scheme enables the certification of different building types (new construction, buildings after major renovation, homes, schools, healthcare, commercial buildings, as well as neighbourhood development). LEED certification is based on points

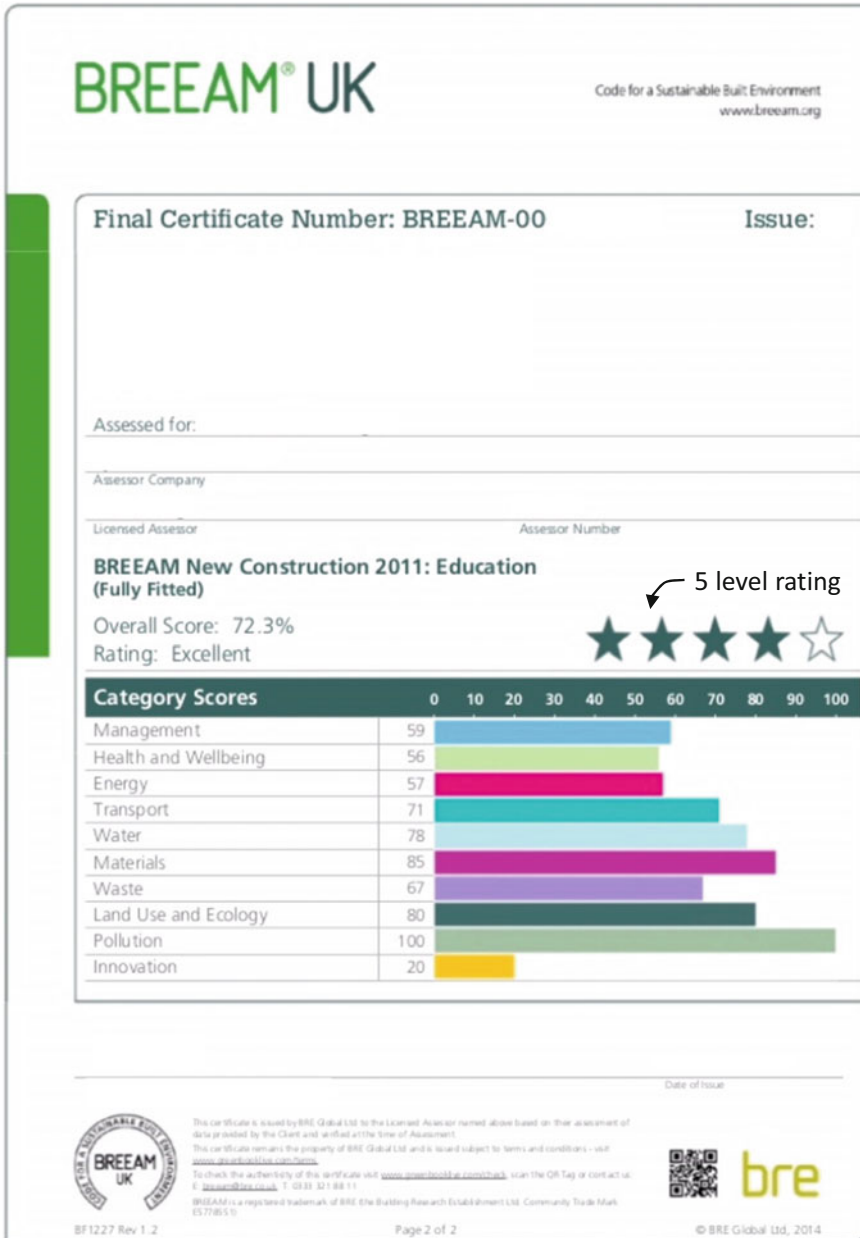


Fig. 14.21 Example of BREEAM certificate (www.slideshare.net)

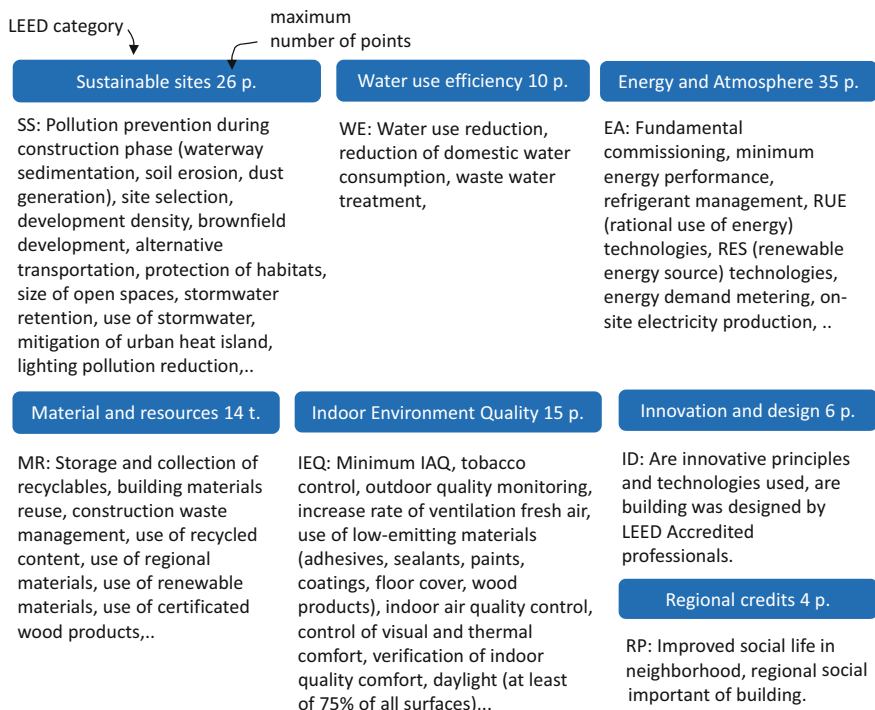


Fig. 14.22 LEED categories and indicators

awarded according to credits of 64 indicators included in the seven assessment categories presented in Fig. 14.22. For all building types, the same assessment category is used; only weighting factors are adapted. For example, schools have highest weighting factor for the criterion of indoor environment quality, while for commercial buildings the weighting factor for the criterion of energy and atmosphere is the highest.

14.6.2.1 Rating and Certificates

A LEED certificate is awarded regarding to minimum number of points required for one of the four levels of LEED certification, shown in Fig. 14.23. Furthermore, some pre-requirements are needed as well: reduce environmental impact during construction, at least 20% of water use reduction, commissioning of building service systems, compliance with minimum energy efficiency requirements, zero use of CFC refrigerants, storage of recyclables (paper, glass, metal, plastics waste), and fulfilment of minimum IEQ requirements etc. LEED for new construction and major renovation is divided into two phases: design and construction. The design



Fig. 14.23 LEED certificate’s logo; classification of building sustainability is based on awarded total point score out of maximum 110 points (www.usgbc.org)

phase assessment can be done before construction starts, and the final certificate is awarded after competition and review of the building.

14.6.3 DGNB

Die Deutsche Gesellschaft für Nachhaltiges Bauen (DGNB, German Sustainable Building Council) is the latest method, first introduced in 2007. It was developed on the basis of Germany’s national energy efficiency requirements. It is a so-called second generation assessment method because ecological, economics and social indicators, as well as technical and functionality indicators are included. A DGNB certificate can be awarded for numerous building types according to the occupancy profiles (different for residential buildings, new and existing office and administration buildings, education buildings, hotels, etc.). A certificate can be awarded as pre-certificate (at the end of design phase) or as an actual certificate (permanent, full) after an audit of the completed building (Fig 14.24).

Assessment according to the DGNB scheme is based on 61 criteria, which are included in 6 categories, as shown in Fig. 14.25.

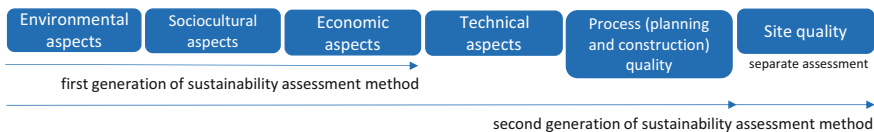


Fig. 14.24 DGNB is a so-called second generation assessment method; beside common sustainability indicators, technical processes and site quality are assessed (www.dgnb.de)

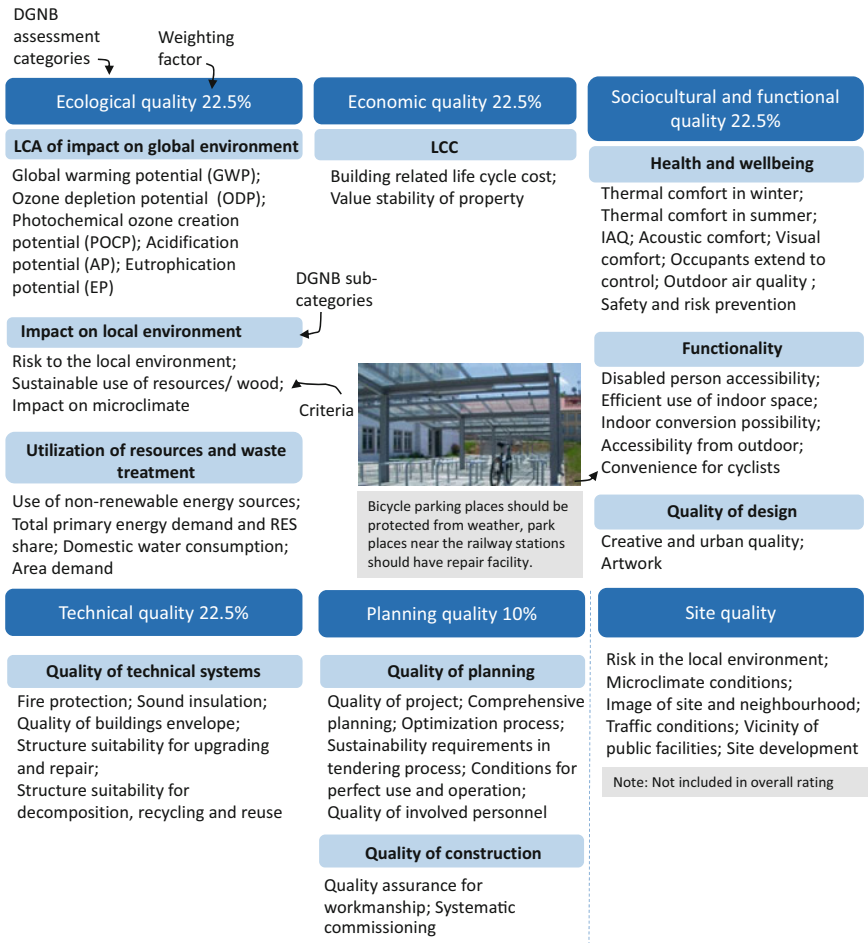


Fig. 14.25 Assessment categories and criteria of DGNB certification method

14.6.3.1 Rating and Certificates

A DGNB certificate is awarded regarding the degree of fulfilment of sustainability measured by 51 obligatory and 10 additional indicators (from the assessment’s site quality category). A certificate can be awarded as a pre-certificate after the design phase, allowing the designers to improve concepts to reach a higher level of rating. An actual certificate is awarded after an audit of the finished building. Both assessment categories and criteria are weighted (design factors are 1, 2, 3) and can be adjusted to national or local building aspects. The assessment is awarded with bronze, silver or gold certificates on the basis of the total score. A minimum 50% of the weighted maximum possible points must be achieved to attain the bronze

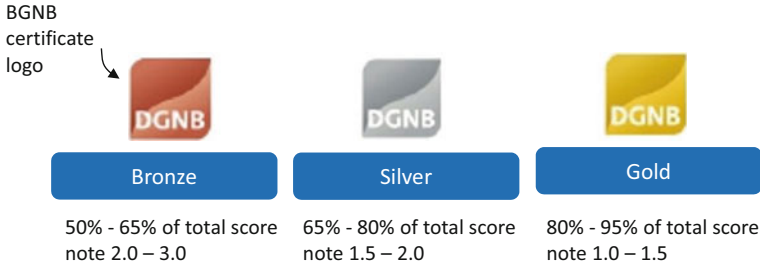


Fig. 14.26 DGNB certificates results can be classified, bronze, silver or gold depending on total score achieved; final result of DGNB assessment can be shown by note (lower is better)

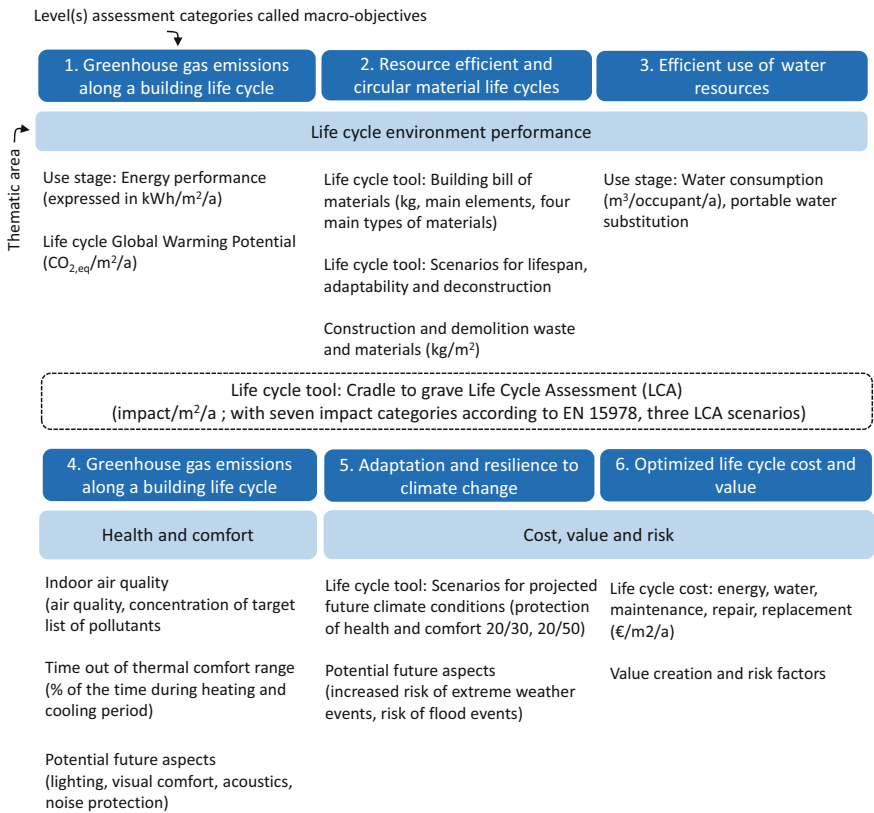


Fig. 14.27 Level(s) consists of six assessment categories, called macro-objectives, which cover three thematic area

certificate, as shown in Fig. 14.26. The DGNB method will soon be extended for the evaluation of towns and regional areas.

14.6.4 *Level(s)*

Level(s) is the latest introduced LCA method for the assessment of a building's sustainability. The method was developed by the European Commission in close cooperation with industry as a common European certification method. The name of the method originates from the three levels of assessment depending on the complexity of approach. Level 1 is the common, simplest level of assessment. Level 2 is comparative and designed for professionals, and required more demanding evaluation. Energy-related indicators are calculated by standardized methods and tools. Level 3 is performance-optimized and the most advanced assessment. It is based on hour-to-hour calculations of energy demand. It contains future cost and environmental risk models for the period of building's life time. The assessment includes six macro objectives: greenhouse gas emissions, resource efficient and circular material, efficient use of water, healthy and comfortable spaces, adaptation and resilience to climate change, and optimised life cost and value. For each of the macro objectives several indicators have been developed. The method is currently in the pilot phase (European Commission 2018) (Fig. 14.27).

References

- Allen JG et al (2016) The 9 foundations of a healthy building. Harvard T.H. Chan, School of Public Health
- BREEAM UK (2018) Technical manual SD5078: BREEAM UK new constructions 2018. Non-domestic Buildings, United Kingdom
- Domjan S (2016) Parametric models for multi-criteria analysis of nearly zero-energy buildings. Master thesis, Faculty of Mechanical Engineering, University of Ljubljana, Ljubljana
- Ebert T, Essig N, Hauser G (2011) Green building certification systems. Detail Green Books
- EC JRC, IES (2010) ILCS (International Reference Life Cycle Data System) handbook, analysis of existing environmental impact assessment methodologies for use in life cycle assessment. EC Joint Research Centre & Institute for Environment and Sustainability
- EPA (2012) TRACI 2.1. (Tool for Reduction and Assessment of Chemicals and other Environment Impacts). EPA Environmental Protection Agency, USA
- European Commission (2018) Level(s): a guide to Europe's new reporting framework for sustainable buildings. European Commission
- Goedkoop M et al (2009) ReCiPe 2008. A life cycle impact assessment method which comprises harmonised category indicators at the midpoint and the endpoint level. Ministrie van Volkshuisvesting, Ruimtelijke Ordening en Milieubeheer (Ministry of VROM)

- Huijbregts MAJ et al (2016) ReCiPe 2016 v 1.1: a harmonized life cycle impact assessment method at midpoint and endpoint level. RIVM report 2016-0104a. Bilthoven, The Netherlands
- Humbert S et al (2012) IMPACT 2002+: user guide. Life Cycle Assessment Expert, Quantis, Lausanne
- IMPACT 2002+ (2010) Implementation of life cycle impact assessment methods. Swiss Centre for Life Cycle Inventories
- ISO (2012) Environmental labels and declarations, how ISO standards help. ISO Central Secretariat
- McKinsey and Company (2009) Pathways to a low-carbon economy, V2 of the global greenhouse gas abatement cost curve. McKinsey and Company
- Meadows DH, Meadows DL, Behrens III JRWW (1972) The limits of growth. The Club of Rome
- Swiss Centre for Life Cycle Inventories (2013) Overview and methodology. Swiss Centre for Life Cycle Inventories, St. Gallen
- UNCED (1992) Agenda 21
- UNOPS (2009) A guide to environmental labels—for procurement practitioners of the United Nation system
- World Commission on Environment and Development (1987) Our common future